eCAM Evidence-Based Complementary and Alternative Medicine

Complementary/Alternative Medicine in Cardiovascular Diseases 2014

Guest Editors: Ke-Ji Chen, Myeong Soo Lee, Hao Xu, and Qunhao Zhang

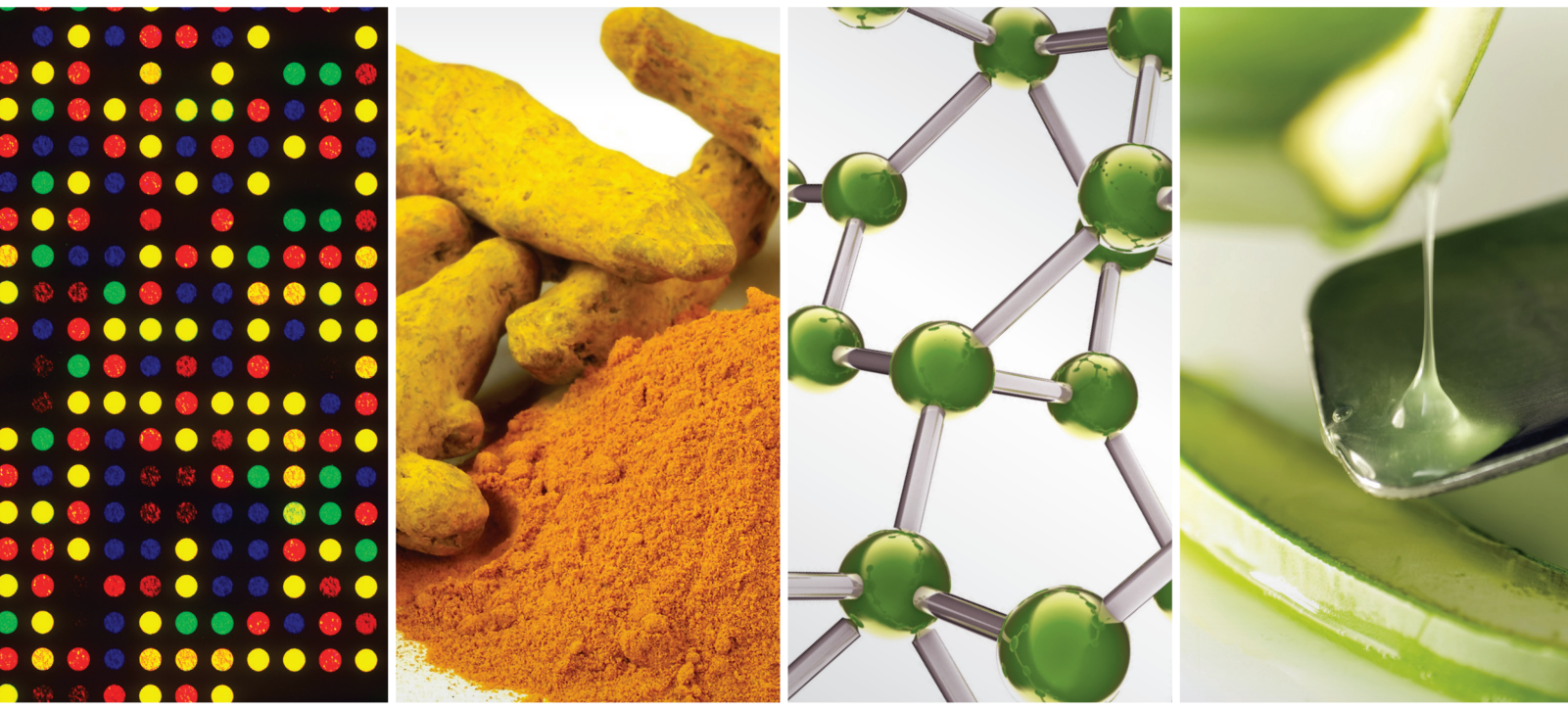

Complementary/Alternative Medicine in Cardiovascular Diseases 2014

Evidence-Based Complementary and Alternative Medicine

Complementary/Alternative Medicine in Cardiovascular Diseases 2014

Guest Editors: Ke-Ji Chen, Myeong Soo Lee, Hao Xu, and Qunhao Zhang

Editorial Board

Contents

Hindawi Publishing Corporation
Evidence-Based Complementary and Alternative Medicine
Volume 2015, Article ID 349375, 2 pages
http://dx.doi.org/10.1155/2015/349375

Editorial

Complementary/Alternative Medicine in Cardiovascular Diseases 2014

Ke-Ji Chen,[1] Myeong Soo Lee,[2] Hao Xu,[1] and Qunhao Zhang[3]

[1]*Cardiovascular Center, Xiyuan Hospital, China Academy of Chinese Medical Sciences, Beijing 100091, China*
[2]*Clinical Research Division, Korea Institute of Oriental Medicine, Daejeon 305-811, Republic of Korea*
[3]*Department of Medicine, Massachusetts General Hospital, Harvard Medical School, Boston, MA 02114, USA*

Correspondence should be addressed to Ke-Ji Chen; kjchenvip@163.com

Received 22 March 2015; Accepted 22 March 2015

Cardiovascular diseases (CVDs) are the leading cause of long-term morbidity and mortality worldwide and are on an alarming rise in populations. According to the report of World Health Organization (WHO) in 2012, an estimated 17.5 million people died of CVDs, accounting for 31% of global deaths. As the increasing significance is attached to CVDs globally, the urgency to respond to CVDs with stronger and more effective therapies is widely recognized. Despite enormous efforts, revascularization, and secondary prevention, to prevent CVDs in the past, major challenges remain to cope with repeated recurrent acute cardiovascular events, readmission to the hospital and improvement of the long-term prognosis and quality of life. In this case, complementary and alternative medicine (CAM) therapies have the potential to provide a major public health benefit.

In this special issue, papers from different parts of the world like China, Republic of Korea, Malaysia, Columbia, Chile, and so forth, are presented. These articles provide a review of this field and make original contributions towards the mechanism of action and the clinical application of CAM for CVDs. In these studies, antiatherogenesis effects of some CAM products were highlighted, including the extracts of herbal plants such as paeonol (Pae), polysaccharide of *Polygonatum sibiricum* (PPGS), or fermented mung bean and fermented red yeast rice. Their cardioprotective role in hypolipidemic, antioxidant, and antiatherogenesis was introduced. In addition, a study on the consumption of apple peel with rich phenolic compounds concluded that it reduced several metabolic syndrome parameters and the atherogenic progression in mice.

Attention was also paid to treatment of ischemia/reperfusion (I/R) injury. Increasing evidence has indicated that traditional Chinese medicine (TCM) could significantly prevent myocardial apoptosis and provide alternative options for protection of myocardial I/R injury. *Huangzhi oral liquid* was an effective treatment for arrhythmias by increasing caspase-3 and apoptosis network proteins. *Shuang Shen Ning Xin* played an important antiapoptotic role by blocking the mitochondrial apoptotic pathway. Neuroprotection of *Sanhua decoction* against focal cerebral ischemia/reperfusion injury was demonstrated in rats through a mechanism targeting aquaporin 4. Two papers about ginsenoside Rb1 (GS-Rb1) discussed how to protect hypoxia- and ischemia-induced cardiomyocytes by regulating expression of miRNAs and inhibition of the mitochondrial apoptotic pathway, respectively.

The roles of Chinese medicine and other CAM therapies in relieving symptoms of hypertension, angina pectoris, and chronic heart failure were reviewed in several articles. A systematic review of randomized controlled trials showed that Chinese herbal medicine (CHM) combined with conventional therapies was effective in controlling blood pressure variability and symptoms of hypertension. Two other papers also highlighted the roles of integrative medicine therapy, for instance, *Xuefu Zhuyu decoction* functioning together with traditional antianginal medications could relieve the clinical symptoms of angina pectoris; *Wenxin Keli* and sotalol could effectively facilitate sinus rhythm reversion from hyperthyroidism related paroxysmal atrial fibrillation. In addition, the advantage of *Dangguijagyagsan*, a Korean traditional herbal

prescription, on the treatment for cardiovascular diseases of menopausal women was referred to in a study. Another three-stage, multicenter, clinical trial evaluated the efficacy, safety, feasibility, compliance, and universality of CHM in the treatment of chronic heart failure.

A variety of functional readouts of CAM may reveal new therapeutic strategies to manipulate cardioprotection, which could be transferred into application of treating CVDs. However, despite the growing utility of CAM, rigorous evidence-based studies with high quality are required to reinforce the application of CAM among CVD patients, especially its clinical benefit, prognostic impact, and potential interaction when used in combination with prescription medicines. It is widely acknowledged that there should be great potential in developing CAM use based on open dialogue between mainstream medicine doctors and CAM practitioners, healthcare professionals and patients.

Ke-Ji Chen
Myeong Soo Lee
Hao Xu
Qunhao Zhang

Hindawi Publishing Corporation
Evidence-Based Complementary and Alternative Medicine
Volume 2015, Article ID 752610, 15 pages
http://dx.doi.org/10.1155/2015/752610

Review Article

Chinese Herbal Compounds for the Prevention and Treatment of Atherosclerosis: Experimental Evidence and Mechanisms

Qing Liu,[1,2] Jianping Li,[1] Adam Hartstone-Rose,[1] Jing Wang,[2] Jiqiang Li,[2] Joseph S. Janicki,[1] and Daping Fan[1]

[1] *Department of Cell Biology and Anatomy, University of South Carolina School of Medicine, 6439 Garners Ferry Road, Columbia, SC 29208, USA*
[2] *Guangdong Provincial Hospital of Chinese Medicine, The Second Clinical School of Medicine, Guangzhou University of Chinese Medicine, Guangzhou 510405, China*

Correspondence should be addressed to Daping Fan; daping.fan@uscmed.sc.edu

Received 19 August 2014; Accepted 15 October 2014

Academic Editor: Qunhao Zhang

Atherosclerosis is a leading cause of disability and death worldwide. Research into the disease has led to many compelling hypotheses regarding the pathophysiology of atherosclerotic lesion formation and the resulting complications such as myocardial infarction and stroke. Herbal medicine has been widely used in China as well as other Asian countries for the treatment of cardiovascular diseases for hundreds of years; however, the mechanisms of action of Chinese herbal medicine in the prevention and treatment of atherosclerosis have not been well studied. In this review, we briefly describe the mechanisms of atherogenesis and then summarize the research that has been performed in recent years regarding the effectiveness and mechanisms of antiatherogenic Chinese herbal compounds in an attempt to build a bridge between traditional Chinese medicine and cellular and molecular cardiovascular medicine.

1. Introduction

Atherosclerosis is a disease of the arterial wall that occurs at susceptible sites in major arteries. It is initiated by endothelial injury and subsequent lipid retention and oxidation in the intima which then provokes chronic inflammation and ultimately causes stenosis or thrombosis [1]. During this progression, residential arterial wall cells including endothelial cells (ECs) and vascular smooth muscle cells (VSMCs), as well as circulating leukocytes, especially monocytes/macrophages, are mainly involved. Atherosclerotic lesions can cause stenosis with potentially lethal distal ischemia or, if ruptured, can trigger thrombotic occlusion of major arteries to the heart, brain, legs, and other organs [2]. A variety of risk factors may intensify or provoke atherosclerosis through their effects on endothelial function, low-density lipoprotein (LDL) concentration and modification, and vascular wall inflammation. These risk factors include hypertension, smoking, diabetes mellitus, obesity, and bacterial infection [3].

Traditional Chinese medicine (TCM), especially herbal medicine, has been used for the treatment of cardiovascular diseases for hundreds of years as documented in *Inner Canon of Yellow Emperor* and *Synopsis of Golden Chamber*. Also, the effectiveness of several extracts derived from Chinese herbs has been evaluated in recent years. However, the cellular and molecular details regarding the underlying efficacious mechanisms of Chinese herbal medicine in treating atherosclerosis have just begun to be understood. Therefore, the purpose of this review is to first provide a brief description of the mechanisms of atherogenesis and then to summarize the recent research results regarding the effectiveness and mechanisms of antiatherogenic Chinese herbal compounds.

2. Mechanisms of Atherogenesis

Atherogenesis is an inflammatory process, initiated by the retention of lipids in the subendothelial space of the vascular wall and encompasses a complex interaction among the

modified lipoproteins, residential vascular cells, and immune system [4]. The schematic in Figure 1 depicts the main steps of atherogenesis. In the following section, the main elements involved in the pathogenesis of atherosclerosis will be briefly described.

2.1. Hyperlipidemia. Dyslipidemia is one of the main risk factors leading to atherosclerosis [5]. The lipid hypothesis of atherogenesis states that abnormally elevated levels of plasma LDL and low levels of plasma high density lipoproteins (HDL) are the primary causes of atherosclerosis [6–8]. This hypothesis has been strongly supported by the success of statin drug therapy, which has significantly reduced coronary artery disease mortality through lowering plasma LDL levels during the past 40 years [9]. However, the HDL wing of the hypothesis remains to be confirmed by successful HDL-targeting approaches. A common mechanism through which hyperlipidemia causes atherosclerosis involves the accumulation of cholesteryl esters in macrophages of the arterial wall [10].

2.2. Endothelial Injury. The response-to-injury hypothesis of atherogenesis states that endothelial injury triggers subsequent interactions among all of the cells found in the atherosclerosis lesions [11]. Injured endothelium allows lipoproteins to migrate into subendothelial space. This, together with the discovery of adhesion molecules expressed by endothelial cells (e.g., vascular cell adhesion molecule-1), provides important insight into the initiation of atherosclerotic lesions [12]. That is, increased expression of adhesion molecules favors monocyte adhesion and penetration, which results in accumulation of macrophages within the subendothelial space where they encounter lipoprotein particles [13].

2.3. LDL Subendothelial Retention and Oxidation. Subendothelial retention of lipoproteins is a key early step in atherosclerosis, provoking a cascade of adverse events to the pathogenic response [14]. High levels of plasma lipids, particularly LDL and very-low density lipoproteins (VLDL), are among the pathophysiologic stimuli that induce endothelial dysfunction. Retention and modification of apolipoprotein B (apoB) containing lipoproteins, LDL, intermediate density lipoprotein (IDL), and lipoprotein (a) [Lp(a)] in the arterial intima extracellular matrix (ECM) represent early events of plaque development, which is referred to as the "response-to-retention" hypothesis [15].

The oxidation hypothesis of atherosclerosis suggests that an early event in the development of atherosclerosis is an oxidative modification of LDL that significantly increases its uptake into the arterial intima [16, 17]. Moreover, lipid overload may increase lipopolysaccharide (LPS) circulating levels and oxidative stress. In particular, the oxidation of lipoproteins that results from an imbalance of the pro- and antioxidant equilibrium is involved in the pathologic process of atherosclerotic alterations of cellular function. Lipid oxidation, induced by leukocyte-derived reactive oxygen species, not only promotes the growth and migration of smooth muscle cells, monocytes/macrophages, and fibroblasts, but also amplifies foam cell formation through oxidized LDL (oxLDL) formation and uptake [18].

2.4. Monocyte Migration and Activation. The overexpression of inducible adhesion molecules results in the adherence of mononuclear cells to the endothelial surface whereupon they receive chemoattractant signals that beckon them to enter the intima. With regard to the mechanisms that mediate monocyte-derived macrophage maturation, it has been reported that macrophage colony-stimulating factor (M-CSF) induces scavenger receptors and promotes the proliferation of monocytes in early atherosclerotic lesions [19]. Macrophages also contribute to the thrombotic complications of atherosclerosis in pivotal ways. These phagocytes furnish the bulk of the enzymes (i.e., matrix metalloproteinases, MMPs) that catabolize collagen, a key constituent of the fibrous cap of the plaque, which when activated predisposes the plaque to rupture [20].

2.5. Vascular Smooth Muscle Cell (VSMC) Migration and Proliferation. In response to atherogenic stimuli, VSMCs undergo a phenotypic switch from contractile phenotype to synthetic and inflammatory phenotype; the inflammatory VSMCs migrate into intima and proliferate, contributing to the atherogenesis [21, 22]. VSMCs are the major producers of ECM within the vessel wall [23] and can modify the type of matrix proteins produced. In turn, the type of matrix present can affect the lipid content of the developing plaques and the proliferative index of the cells that are adherent to them. Like endothelial cells, VSMCs can also express a variety of adhesion molecules such as vascular cell adhesion molecule-1 (VCAM-1) and intercellular adhesion molecule-1 (ICAM-1) to which monocytes and lymphocytes can adhere and migrate into the vessel wall [24]. Like macrophages, VSMCs can also express a variety of receptors for lipid uptake and can form foam-like cells, thereby participating in the early accumulation of plaque lipid [25].

2.6. Foam Cell Formation. Foam cells mainly arise from mononuclear phagocytes, although smooth muscle and endothelial cells can also become engorged with lipids. Within the plaque, the mononuclear phagocytes express scavenger receptors (SRs), including CD36, SR-A, and SR-BI. These scavenger receptors mediate the engulfment of modified LDL particles that contribute to macrophage foam cell formation [26]. Other receptors for native lipoprotein particles, including LDLR, VLDLR, and LRP1, also contribute to foam cell formation. As mentioned above, VSMCs, which acquire a synthetic and inflammatory phenotype in the plaque, can also take up lipoproteins and transform into foam cells [27]. Death of foam cells leads to formation of a necrotic core, which serves as a depot for cellular debris and lipids [28].

2.7. Apoptosis and Efferocytosis and Unresolved Inflammation. As atherosclerotic lesions evolve, both the macrophage-derived and smooth muscle-derived foam cells can undergo programmed cell death or apoptosis [29]. The death of foam

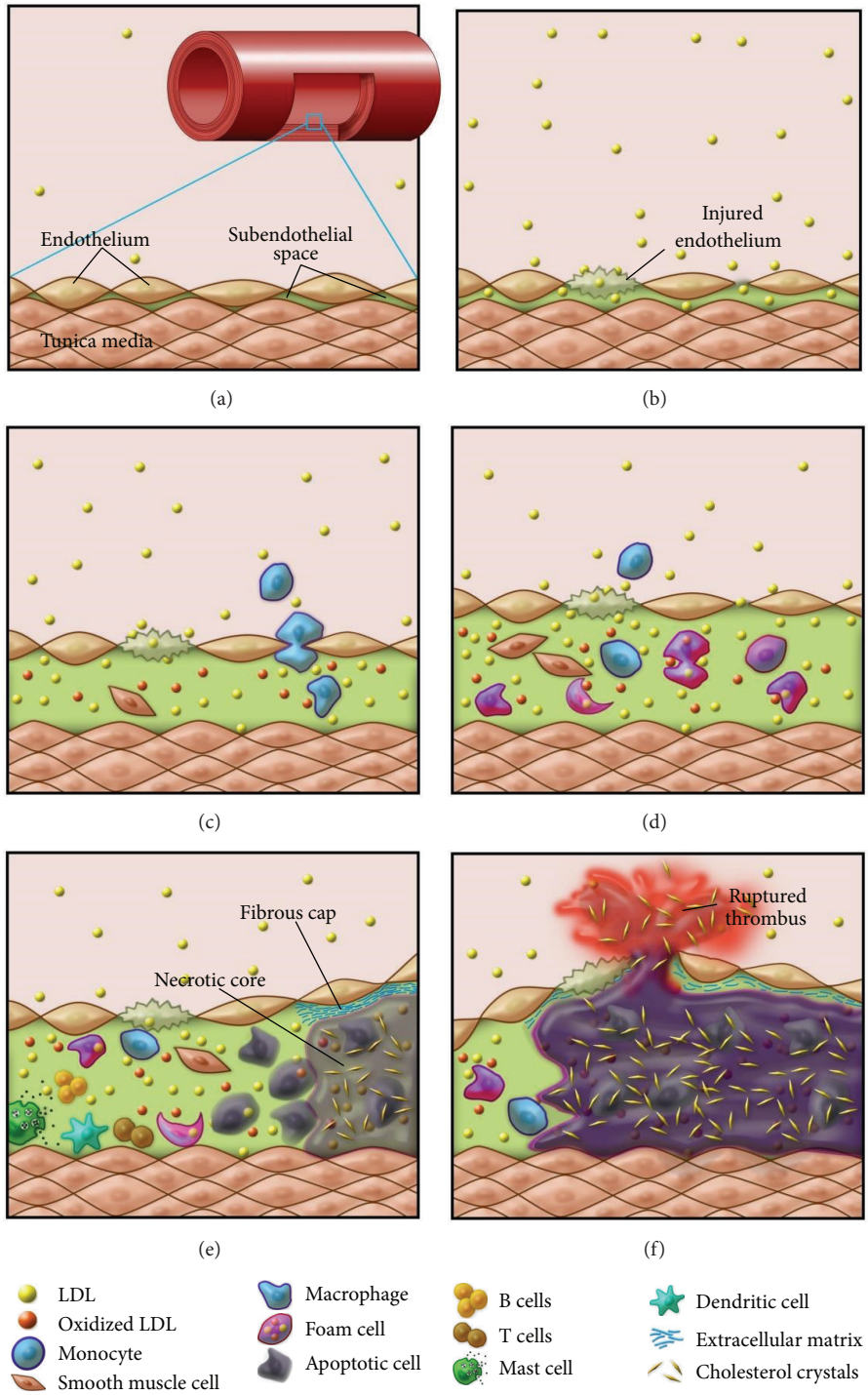

Figure 1: A schematic drawing depicting the formation of atherosclerotic plaques. (a) In the wall of a normal artery, there is a very small subendothelial space in the intima between the endothelium and the smooth muscle cell layer in tunica media. (b) Hyperlipidemia and endothelial injury lead to the infiltration of LDL particles into the subendothelial space. (c) A large number of LDL particles are retained and subsequently oxidized in the subendothelial space, followed by monocyte infiltration (from lumen) and smooth muscle cell migration (from tunica media). (d) Monocytes and smooth muscle cells differentiate into macrophages, which engulf LDL and turn into foam cells, and are activated by oxidized LDL. SMCs are also activated, proliferate, and transform into lipid-laden foam cells. (e) Macrophage and smooth muscle foam cells undergo apoptosis; unbalanced apoptosis/efferocytosis results in necrotic core formation and unresolved inflammation. Other immune cell types also participate in the arterial wall inflammation. (f) Erosion of the fibrous cap caused by the matrix degrading enzymes secreted by the macrophages leads to unstable plaques, which eventually rupture and result in thrombus formation and adverse clinical events.

cells may not be a random event or the result of bursting like an overinflated balloon due to lipid overload. Rather, it may be due in part to gradients of concentration of factors such as macrophage colony-stimulating factor (M-CSF) required for survival of human monocytes [20]. However, some apoptotic cells may not disappear from the atherosclerotic lesions but instead accumulate in a "mummified" state [20]. The elegant studies of Ira Tabas have elaborated upon this concept of impaired clearance, or "efferocytosis," of apoptotic cells in plaques, which leads to unresolved inflammation [30]. The apoptotic foam cells that escape efferocytosis release their lipid content to the extracellular space and contribute to lipid core formation.

Over the last dozen years, appreciation of the role of inflammation in atherosclerosis has burgeoned. Intralesional or extralesional inflammation may hasten atheroma evolution and precipitate acute events. Circulating acute-phase reactants elicited by inflammation not only may serve as a biomarker for increased risk of vascular events, but also in some cases may contribute to their pathogenesis [31]. Advances stemming from basic research have established a fundamental role for inflammation in mediating all stages of this disease from initiation through progression and, ultimately, to the thrombotic complications of atherosclerosis.

The basic science of inflammatory biology applied to atherosclerosis has provided considerable insight into the mechanisms underlying the recruitment of leukocytes. Early after the initiation of atherogenesis, arterial endothelial cells begin to express on their surface selective adhesion molecules that bind various classes of leukocytes [12]. In particular, VCAM-1 binds precisely the types of leukocytes involved in early atheroma, the monocyte and T lymphocyte. Not only does VCAM-1 expression increase on endothelial cells overlying nascent atheroma, but defective VCAM-1 shows interrupted lesion development [32]. Once adhered to the endothelium, leukocytes penetrate into the intima in response to chemoattractant molecules. For example, monocyte chemoattractant protein-1 (MCP-1) appears responsible for the direct migration of monocytes into the intima at sites of lesion formation [33]. Once resident in the arterial wall, the blood-derived inflammatory cells participate in and perpetuate a local inflammatory response. The macrophages express scavenger receptors for modified lipoproteins, permitting them to ingest lipid and become foam cells. In addition to MCP-1, macrophage colony-stimulating factor (M-CSF) contributes to the differentiation of the blood monocyte into the macrophage foam cell [34]. T cells likewise encounter signals that cause them to elaborate inflammatory cytokines such as tumor necrosis factor-α (TNF-α) that in turn can stimulate macrophages as well as vascular endothelial cells and SMCs [35]. As this inflammatory process continues, the activated leukocytes and intrinsic arterial cells can release fibrogenic mediators including a variety of peptide growth factors that can promote replication of SMCs and contribute to elaboration by these cells of a dense ECM characteristic of a more advanced atherosclerosis lesion. Inflammatory processes not only promote initiation and evolution of atheroma, but also contribute decisively to precipitating the acute thrombotic complications of atheroma [3]. The activated macrophages abundant in atheroma can produce proteolytic enzymes capable of degrading the collagen that lends strength to the plaque's protective fibrous cap, rendering the cap thin, weak, and susceptible to rupture. Inflammatory mediators regulate tissue factor expression by plaque macrophages, demonstrating an essential link between arterial inflammation and thrombosis [36].

Both innate and adaptive immunity are involved in atherosclerosis. Inflammation per se can drive arterial hyperplasia, even in the absence of traditional risk factors [37]. Cytokines as inflammatory messengers provide a mechanism whereby risk factors for atherosclerosis can alter arterial biology. Inflammation regulates aspects of plaque biology that trigger the thrombotic complications of atherosclerosis [38]. Overall, inflammatory mediators participate in all phases of atherogenesis, from lesion initiation through progression and ultimately to the clinical complications of this disease. The fact that all types of immune cells have been found in atherosclerotic plaques indicates that all immune components may participate in atherogenesis. All of these factors form the basis of the "inflammatory hypothesis."

3. Effects and Mechanisms of Chinese Herb Compounds in the Attenuation of Atherosclerosis

An early description of the clinical manifestations and treatment of atherosclerosis can be found in the classic traditional Chinese medicine book *Inner Canon of Yellow Emperor*, which was completed around 500 BC. In the theory of traditional Chinese medicine, atherosclerosis is usually referred to as "*MaiBi*," a vascular problem that is caused by *Qi* stagnation, *Blood* stasis, and/or coagulated *Phlegm*, in which *Qi* stands for the energy, *Blood* stands for the material, and *Phlegm* stands for a kind of pathological product. For over two thousand years, atherosclerosis and its resulting heart disease have been treated with numerous herbal remedies. While somewhat effective, these herbal remedies have not been well studied using evidence-based approaches or using modern cellular and molecular techniques. Recently, however, investigations to examine the effects and mechanisms of single herbal compounds in the modulation of atherogenesis have occurred. A summary of these studies is presented in the following section wherein the compounds are discussed according to their site of activity.

3.1. Chinese Herbal Compounds with Endothelial Protective Activity (Table 1). The study by Lee et al. demonstrated that pretreatment of human umbilical vein endothelial cells (HUVEC) with *Buddleja Officinalis* (BO, 1–10 microg/mL) for 18 hrs dose-dependently inhibited TNF-α-induced adhesion U937 monocytic cells as well as mRNA and protein expressions of VCAM-1 and ICAM-1. Pretreatment with BO also blocked TNF-α-induced reactive oxygen species (ROS) formation. Nuclear factor-kappa B (NF-kappa B) is required for the transcription of these adhesion molecule genes [43]. Wan et al. found that *Panax notoginseng saponins* (PNS), derived from the Chinese herb *Panax notoginseng*,

Table 1: Chinese herbal compounds with endothelial protective activity.

Compound	Herb	Target or indicator	Type of study	Reference
Resveratrol	*Rhizoma polygonum cuspidatum*	cav-1, VEGF, KDR	In vitro	[39]
Cynanchum wilfordii	*Cynanchum wilfordii*	LDL, HDL, NO, E-selectin, VCAM-1, ICAM-1, ET-1	In vivo	[40]
Protocatechuic aldehyde	*Salvia miltiorrhiza* Bunge	Caspase-3, caspase-2, Bcl-2/Bax, cytochrome c, caspase-9, granzyme B	In vitro	[41]
Cryptotanshinone	*Salvia miltiorrhiza* Bunge	oxLDL, NO, ICAM-1, VCAM-1; monocyte adhesion	In vitro	[42]
Aqueous extract of *Buddleja officinalis*	*Buddleja officinalis*	VCAM-1, ICAM-1; ROS; NF-κB	In vitro	[43]
Tribulus terrestris extract	*Tribulus terrestris*	TC, HDL, LDL, TG	In vivo	[44]
Panax notoginseng	*Panax notoginseng saponins*	ICAM-1 and VCAM-1	In vivo	[45]
Ginkgo biloba extract	*Ginkgo biloba*	VCAM-1, ICAM-1, E-selectin; ROS, RSTF	Both	[46, 47]
Salvia miltiorrhiza	*Salvia miltiorrhiza* Bunge	eNOS, NO, NADPH oxidase subunit Nox4	In vitro	[48]
Bisacurone	*Curcuma longa* Linne (Zingiberaceae)	VCAM-1, NF-κB p65, Akt, PKC	In vitro	[49]
Magnolol	*Magnolia officinalis*	IL-6, STAT3, Tyr705 and Ser727, ICAM-1, IREs, monocyte adhesion, cyclin D1, MCP-1, NF-kB, VCAM-1	Both	[50, 51]
Aqueous extract of *Salvia miltiorrhiza*	*Salvia miltiorrhiza* Bunge	ICAM-1, VCAM-1, GSH, NF-κB	In vitro	[52]
Salvianolic acid B	*Salvia miltiorrhiza* Bunge	ICAM-1, E-selectin, NF-κB	In vitro	[53]

dose-dependently inhibited monocyte adhesion to activated endothelium, as well as the expression of TNF-α-induced endothelial adhesion molecules, such as ICAM-1 and VCAM-1 [45]. Recent findings reported by Tian et al. indicated that *Resveratrol*, a compound derived from the Chinese herb *Rhizoma polygonum cuspidatum*, downregulated the increased expressions of vascular endothelial growth factor (VEGF) and kinase insert domain receptor (KDR or VEGF receptor-2) [39]. Results from Choi et al. showed that *extract from Cynanchum wilfordii* (ECW) treatment significantly decreased vascular inflammation through an inhibition of cellular adhesion molecules such as E-selectin, VCAM-1, and ICAM-1 as well as endothelin-1 (ET-1) expression [40].

3.2. Chinese Herbal Compounds That Lower Lipids and Anti-oxidation (Tables 2 and 3). Zhang et al. [54] using a plasma lipid analysis approach found *Celastrus orbiculatus Thunb Extract* (COT), a compound derived from the Chinese herb *Celastrus orbiculatus Thunb*, to decrease total cholesterol (TC), non-high-density lipoprotein cholesterol (non-HDL-C), triglyceride (TG), apolipoprotein B100 (apoB100), and apolipoprotein E (apoE) levels and to increase the level of HDL cholesterol (HDL-C). Quantitative real-time PCR revealed that COT upregulated the mRNA abundance of LDL receptor (LDL-R), scavenger receptor class B type 1 (SR-B1), cholesterol 7α-hydroxylase A1 (CYP7A1), and 3-hydroxy-3-methyl-glutaryl-CoA reductase (HMGCR) [54]. Choi et al. reported that extract from the herb *Cynanchum wilfordii treatment* in HFCD-fed rats lessened LDL cholesterol and triglyceride levels and elevated HDL cholesterol [40]. Results from Subramaniam et al. indicated that the ethanolic fraction of the herb *T. arjuna* significantly decreased TC, LDL, and TG levels, increased HDL, and lessened the number of aortic atherosclerotic lesions [57]. Dinani et al. demonstrated the ability of the extract from the Chinese herb *Artemisia aucheri* to significantly reduce the levels of TC, LDL cholesterol, and TG and to increase HDL cholesterol [58].

Li et al. discovered that *Farrerol,* an extract from the Chinese herb *Rhododendron dauricum L.*, significantly inhibited the H_2O_2-induced loss of cell viability and enhanced superoxide dismutase (SOD) and glutathione peroxidase (GSH-Px) activities in EA.hy926 cells. In addition, *Farrerol* inhibited the H_2O_2-induced elevation in the levels of intracellular malondialdehyde (MDA) and reactive oxygen species (ROS) [63]. Chen et al. reported that treatment with *Salvianolic acid B* (Sal B), a main compound derived from the herb *Salvia miltiorrhiza* Bunge, suppressed ERK1/2 and JNK phosphorylation and attenuated the increase in prostaglandin E2 production and NADPH oxidase activity in LPS-treated human aortic smooth muscle cells (HASMCs), indicating that

Table 2: Chinese herbal compounds that lower lipids.

Compound	Herb	Target or indicator	Type of study	Reference
Celastrus orbiculatus Thunb.	*Celastrus orbiculatus* Thunb.	TC, non-HDL, TG, apoB100, apoE, HDL; LDL receptor, SR-B1, CYP7A1, HMGCR, CRP, MDA	In vivo	[54]
Salvianolic acid B	*Salvia Miltiorrhiza* Bunge	mLDL, CD36	In vitro	[55]
Cynanchum wilfordii	*Cynanchum wilfordii*	LDL, HDL, NO; Akt,	In vivo	[56]
Ethanolic fraction of *T. arjuna*	*Terminalia arjuna*	LDL, TG, VLDL, HDL	In vivo	[57]
Artemisia aucheri	*Artemisia aucheri*	Total cholesterol, LDL cholesterol, triglycerides, HDL cholesterol	In vivo	[58]
Tribulus terrestris extract	*Tribulus terrestris*	TC, HDL, LDL, TG	In vivo	[44]
Ginsenosides	*Panax spp.*	PPARs, total cholesterol, triglyceride	In vivo	[59]
Ocimum basilicum	*Ocimum basilicum*	Total cholesterol, triglycerides, LDL-cholesterol, HDL-cholesterol	In vivo	[60]

Sal B has antioxidant properties [71]. Jia et al. showed that Tanshinone IIA (TSN IIA), another main compound derived from the Chinese herb *Salvia Miltiorrhiza* Bunge, markedly inhibited the elevation of ROS evoked by H_2O_2. Real time RT-PCR and Western blotting analysis demonstrated the ability of TSN IIA to significantly decrease the H_2O_2-induced expression of proapoptotic proteins Bax and caspase-3 and to significantly increase the expression of antiapoptotic protein Bcl-2 in EA.hy926 cells [64].

Results from Xu et al. showed that the Lectin-like oxidized LDL (oxLDL) receptor-1 (LOX-1), a novel scavenger receptor highly expressed in human and experimental atherosclerotic lesions, is responsible for the uptake of oxLDL in vascular cells. oxLDL induced LOX-1 expression at the mRNA and protein levels, which was abrogated by the addition of Tanshinone IIA or a widely used inhibitor of NF-κB, suggesting the involvement of NF-κB [65]. Hung et al. described that a low dose (0.015 mg/mL) of *S. miltiorrhiza* aqueous extract (SMAE), derived from the Chinese herb *Salvia miltiorrhiza* Bunge, significantly inhibited the growth of a rat smooth muscle cell line (A10) under Hcy stimulation, and the intracellular ROS concentration decreased after SMAE treatment in terms of reducing p47 (phox) translocation and increasing catalase activity. The signaling profile suggests that SMAE inhibited Hcy-induced A10 cell growth via the PKC/MAPK-dependent pathway [68].

3.3. Chinese Herbal Compounds That Suppress Monocyte Migration and Activation (Table 4). Within plaque formation, activated endothelial cells increase the expression of adhesion molecules and inflammatory genes and circulating monocytes migrate into subendothelial space and differentiate into macrophages. In support of this concept, Chen et al. found that extract from *Ginkgo biloba*, a Chinese herb with antioxidant activity, could significantly suppress inflammatory cytokine-stimulated endothelial adhesiveness to human monocytic cells by attenuating intracellular ROS formation, redox-sensitive transcription factor activation, and VCAM-1 as well as ICAM-1 expression in human aortic endothelial cells [46]. Wan et al. found that *Panax notoginseng saponins* (PNS) dose-dependently inhibited monocyte adhesion on activated endothelium, as well as the expression of TNF-α-induced endothelial adhesion molecules, such as ICAM-1 and VCAM-1 [45]. According to the report by Park, *Prunella vulgaris ethanol* extract inhibited adhesion of monocyte/macrophage-like THP-1 cells to the activated HASMCs [91]. The role of *Curcumin*, derived from the Chinese herb Curcuma longa, was shown by Wang et al. to have a sonodynamic effect on THP-1-derived macrophages and, therefore, to be a promising treatment for atherosclerosis [92]. Finally, Duan et al. identified *Phyllanthus emblica extract* as being able to prevent ECV-304 cells from adhering to monocytes [79].

3.4. Chinese Herbal Compounds That Suppress VSMC Migration and Proliferation (Table 5). Several lines of evidence exist to indicate the effectiveness of Chinese herbs on VSMC migration and proliferation. Moon et al. observed that *Protocatechuic aldehyde* (PCA), a compound derived from the Chinese herb *Salvia miltiorrhiza Bunge*, significantly attenuated PDGF-induced VSMC proliferation and migration at a pharmacologically relevant concentration (100 μM). On a molecular level, they observed downregulation of the phosphatidylinositol 3-kinase (PI3 K)/Akt and the mitogen-activated protein kinase (MAPK) pathways, both of which are known to regulate key enzymes associated with migration and proliferation. Moreover, they found that PCA arrested the S-phase of the VSMC cell cycle and suppressed cyclin D2 expression [93]. Results from Kim et al. indicated that *Corynoxeine*, derived from the Chinese herb *Hook of*

Table 3: Chinese herbal compounds with antioxidation activity.

Compound	Herb	Target or indicator	Type of study	Reference
Arisaema tortuosum tuber extract	*Arisaema tortuosum* Schott	β-Glucuronidase; FRAP	In vitro	[61]
Andrographolide derivatives	Andrographolide	VLDL-C, LDL-C, HDL-C; superoxide anions, hydroxyl radicals	In vivo	[62]
Farrerol	*Rhododendron dauricum* L. (ManShanHong)	SOD, GSH-Px; caspase-3, p38 MAPK, Bcl-2	In vitro	[63]
Celastrus orbiculatus Thunb.	*Celastrus orbiculatus* Thunb.	TC, non-HDL, TG, apoB100, apoE, HDL; LDL receptor, SR-B1, CYP7A1, HMGCR, CRP, MDA	In vivo	[54]
Tanshinone IIA	*Salvia miltiorrhiza* Bunge	ROS, Bax/Bcl-2, caspase-3, LOX-1, NF-κB, oxLDL, monocyte adhesion, VSMC migration and proliferation, macrophage cholesterol accumulation, TNF-α, TGF-β1, platelet aggregation, GPx	Both	[64–67]
Cryptotanshinone	*Salvia miltiorrhiza* Bunge	oxLDL, NO, ICAM-1, VCAM-1; monocyte adhesion	In vitro	[42]
Ethanolic fraction of *T. arjuna*	*Terminalia arjuna*	LDL, TG, VLDL, HDL	In vivo	[57]
Salvia miltiorrhiza aqueous extract	*Salvia miltiorrhiza* Bunge	Hcy, ROS; PKC/MAPK	In vivo	[68]
Chlorophytum borivilianum root extract	*Chlorophytum borivilianum*	LDL oxidation, lipid hydroperoxides, thiobarbituric acid	In vitro	[69]
Aqueous extract of *Buddleja officinalis*	*Buddleja officinalis*	VCAM-1, ICAM-1; ROS; NF-κB	In vitro	[43]
Salvianolic acid B	*Salvia miltiorrhiza* Bunge	oxLDL, ROS, COX, ERK1/2, JNK, MAPK; prostaglandin E2, NADPH oxidase, MMP-2, MMP-9	Both	[70–73]
Caffeoylquinic acids (CQs)	Chwinamul	ROS	Both	[74]
Epimedium (Berberidaceae)	*Epimedium spp.*	ROS	Both	[75]
Goji	*Lycium barbarum* and *L. chinense*	SOD, MDA; JNK	Both	[76]
Ginkgo biloba extract	*Ginkgo biloba*	VCAM-1, ICAM-1, E-selectin; ROS, RSTF	Both	[46]
Salvia miltiorrhiza	*Salvia miltiorrhiza* Bunge	eNOS, NO, NADPH oxidase subunit Nox4	In vitro	[48]
Scutellaria baicalensis Georgi flavonoids	*Scutellaria baicalensis* Georgi	SOD	Both	[77]
Emodin	*Rheum rhabarbarum*	ApoE, PPAR-γ, GM-CSF, MMP-9	In vivo	[78]
Bisacurone	*Curcuma longa* Linne (Zingiberaceae)	VCAM-1, NF-κB p65, Akt, PKC	In vitro	[49]
Phyllanthus emblica extract	*Phyllanthus emblica*	ox-LDL, MDA	In vitro	[79]
Ethanol extract of *Glossogyne tenuifolia*	*Glossogyne tenuifolia*	oxLDL, ROS	In vitro	[80]
Ocimum basilicum	*Ocimum basilicum*	total cholesterol, triglycerides, LDL, HDL	In vivo	[60]
Paeonol	*Paeonia lactiflora* Pallas	ICAM-1, NF-κB p65 translocation, ERK, p38	In vitro	[81]
Water extracts of Achyrocline satureoides	*Achyrocline satureoides*	LDL oxidation	In vitro	[82]
Alaternin	*Cassia tora*	NO, Peroxynitrite	In vitro	[83]
Aqueous extract of *Salvia miltiorrhiza*	*Salvia miltiorrhiza* Bunge	Hcy	In vitro	[84]

Table 3: Continued.

Compound	Herb	Target or indicator	Type of study	Reference
Gypenosides Saponins	*Gynostemma pentaphyllum*	mitochondrial enzyme	In vitro	[85]
baicalein, baicalin and wogonin	*Scutellaria baicalensis*	VSMC proliferation	In vitro	[86]
Scoparone	*Artemisia scoparia*	monocyte adhesion, lipid laden foam cells	In vivo	[87]
Trilinolein	*Panax pseudoginseng*	OFR	In vitro	[88]
Celastrol	*Tripterygium wilfordii* Hook F.	oxLDL, LOX-1, ROS, iNOS, NO, TNF-a, IL-6	In vivo	[89]
Phenolic Rye (*Secale cereale* L.)	Ferulic acid	oxLDL	In vitro	[90]

Table 4: Chinese herbal compounds that suppress monocyte migration and activation.

Compound	Herb	Target or indicator	Type of study	Reference
Prunella vulgaris ethanol extract	*Prunella vulgaris*	VCAM-1, ICAM-1, E-selectin, ROS; p38 MAPK, ERK	In vitro	[91]
Curcumin	*Curcuma longa*	Macrophage morphological changes	In vitro	[92]
Panaxnotoginseng	*Panax notoginseng* saponins	ICAM-1 and VCAM-1	In vivo	[45]
Ginkgo biloba extract	*Ginkgo biloba*	VCAM-1, ICAM-1, E-selectin; ROS, RSTF	Both	[46]
Phyllanthus emblica extract	*Phyllanthus emblica*	oxLDL, MDA	In vitro	[79]

Table 5: Chinese herbal compounds that suppress VSMC migration and proliferation.

Compound	Herb	Target or indicator	Type of study	Reference
Protocatechuic aldehyde	*Salvia miltiorrhiza* Bunge	PI3K/Akt, MAPK, cyclin D2	In vitro	[93]
Gleditsia sinensis thorn extract	*Gleditsia sinensis* thorns	MMP-9; p21WAF1, cyclinB1, Cdc2 and Cdc25c; ERK1/2, p38 MAPK, JNK; NF-κB, AP-1	In vitro	[94]
Corynoxeine	Hook of *Uncaria rhynchophylla*	DNA synthesis of VSMCs, ERK1/2	In vivo	[95]
Phyllanthus emblica extract	*Phyllanthus emblica*	ox-LDL, MDA	In vitro	[79]
Berberine	*Coptis chinensis*	MAPK1/2, ERK, Egr-1, PDGF, c-Fos, Cyclin D1	In vitro	[96]
Nucifera leaf extract	*Nelumbo nucifera* GAERTN	JNK, MAPK, FAK/PI 3-kinase/small G protein	In vitro	[97]
Hibiscus sabdariffa Extract	*Hibiscus sabdariffa* L.	triglyceride, LDL, foam cell formation, VSMC migration	In vivo	[98]
Panax notoginseng saponins	*Panax notoginseng*	integrin, FAK, NF-κB	In vivo	[99]
Astragalus polysaccharide	*Astragalus membranaceus*	ABCA1, NF-κB	In vitro	[100]
Scoparone	*Artemisia scoparia*	monocyte adhesion, lipid laden foam cells	In vivo	[87]
Hibiscus sabdariffa Extract	*Hibiscus sabdariffa* L.	TC, LDL-C; foam cell formation, VSMC migration	In vivo	[98]

Table 6: Chinese herbal compounds that suppress foam cell formation.

Compound	Herb	Target or indicator	Type of study	Reference
Panax notoginseng saponins	*Panax notoginseng*	integrin, FAK, NF-κB	In vivo	[99]
Astragalus polysaccharide	*Astragalus membranaceus*	ABCA1, NF-κB	In vitro	[100]
Scoparone (6,7-dimethoxycoumarin)	*Artemisia scoparia*	monocyte adhesion, lipid laden foam cells	In vivo	[87]
Hibiscus sabdariffa Extract	*Hibiscus sabdariffa* L.	TC, LDL-C; foam cell formation, VSMC migration	In vivo	[98]

Uncaria rhynchophylla, significantly inhibited the PDGF-BB-induced DNA synthesis of VSMCs in a concentration-dependent manner without causing any cytotoxicity. Preincubation of VSMCs with corynoxeine significantly inhibited PDGF-BB-induced extracellular signal-regulated kinase 1/2 (ERK1/2) activation [95]. Liang et al. showed that *Berberine*, a compound from the Chinese herb *Coptis chinensis*, inhibited serum-stimulated rat aortic VSMC growth in a concentration-dependent manner. Berberine blocked injury-induced VSMC regrowth by inactivation of the ERK/Egr-1 signaling pathway thereby preventing the early signaling induced by injury in vitro [96].

3.5. Chinese Herb Compounds That Suppress Foam Cell Formation (Table 6). In the studies reported by Yuan et al., the formation of foam cells was inhibited by *Panax notoginseng saponins* (PNS) via its ability to inhibit the phosphorylation of FAK on threonine 397 and the translocation of NF-κB. Wang et al. discovered that TNF-α could enhance the activity of NF-kappa B in the foam cells, and this effect could be attenuated by *Astragalus polysaccharide* (APS), a compound derived from the Chinese herb *Astragalus membranaceus* [99]. In a study by Chen et al., large numbers of monocytes were found adherent to the luminal surface and a markedly thickened intima filled with many lipid laden foam cells was apparent. However when treated with *Scoparone*, a compound derived from the Chinese herb *Artemisia scoparia*, atherosclerosis was less advanced and the plasma cholesterol was lower [87]. Interestingly, Chen et al. reported that upon histopathological examination *Hibiscus sabdariffa Extract* (HSE) was noted to reduce foam cell formation and inhibit smooth muscle cell migration and calcification in the blood vessel of rabbits. These results clearly indicate that Chinese herb-derived extracts can be used to lower serum lipids and produce antiatherosclerotic activity [98].

3.6. Anti-Inflammatory Chinese Herb Compounds (Table 7). Intralesional or extralesional inflammation may hasten atheroma evolution and precipitate acute adverse events. Hence, herb-associated treatment targeting inflammation is beneficial. From the findings of Jia et al., real time RT-PCR and Western blotting analysis revealed that *Tanshinone IIA* (TSN IIA) significantly decreased the expressions of the proapoptotic proteins Bax and caspase-3, significantly increased the expression of antiapoptotic protein Bcl-2, and resulted in the reduction of the Bax/Bcl-2 ratio in EA.hy926 cells induced by H_2O_2 [64]. Li et al. reported that *Farrerol* inhibited H_2O_2-induced elevation in the levels of intracellular malondialdehyde and ROS, as well as cell apoptosis [63]. Xing et al. found that LPS (15 μg/mL) stimulation for 30 hr resulted in significant HUVEC apoptosis, as detected by Hoechst 33258 staining and Annexin V analysis and that *Protocatechuic aldehyde* (PCA, 0.25–1.0 mmol/L, 12 h) inhibited the apoptosis in a dose-dependent manner [41].

Recently, the research of Napagoda et al. indicated that the ethnopharmacological use of *Plectranthus zeylanicus extract* constituted an anti-inflammatory remedy [101]. Zhang et al. found that *Celastrus orbiculatus Thunb* (COT) lowered the levels of C-reactive protein (CRP), interleukin-6 (IL-6), and TNF-α in plasma [54]. Wang et al. discovered that *Artemisinin*, a compound derived from the Chinese herb *Artemisia annua*, inhibited the secretion and mRNA levels of TNF-α, interleukin (IL)-1β, and IL-6 in a dose-dependent manner in THP-1 human monocytes. They also found that the NF-κB pathway may be involved in a decreased cytokine release [107]. Chen and Cheng reported that the extract from Chinese herb *Feverfew* effectively reduced LPS-mediated TNF-α and CCL2 (MCP-1) release by THP-1 cells [109].

4. Summary and Perspective

Herein, we have reviewed most of the Chinese herbal compounds recently reported to have antiatherogenic properties either in vitro or in vivo. Chinese herbal medicine has the potential to provide a major public health benefit by reducing morbidity and mortality secondary to cardiovascular disease. Recent experimental prevention and treatment studies using Chinese medicine clearly demonstrate the benefits of lowering LDL retention and LDL oxidant, protecting endothelium, inhibiting monocyte/macrophage/VSMC proliferation and migration, and preventing foam cell formation as well as the accompanying inflammation. While the promise of Chinese herb-derived compounds as effective therapies for atherosclerotic cardiovascular diseases has been indicated in the literature, the published studies have severe limitations and apparently more research is required. Firstly, most of the clinical studies are of limited value because of the small sample size and/or incomplete data and most experimental studies have focused mainly on single compounds extracted from Chinese herbs. Studies of Chinese

Table 7: Anti-inflammatory Chinese herbal compounds.

Compound	Herb	Target or indicator	Type of study	Reference
Plectranthus zeylanicus extracts	*Plectranthus zeylanicus* Benth	5-LO	In vitro	[101]
Arisaema tortuosum tuber extract	*Arisaema tortuosum* Schott	β-Glucuronidase; FRAP	In vitro	[61]
Prunella vulgaris ethanol extract	*Prunella vulgaris*	VCAM-1, ICAM-1, E-selectin, ROS; p38 MAPK, ERK	In vitro	[91]
Celastrus orbiculatus Thunb.	*Celastrus orbiculatus* Thunb.	TC, non-HDL, TG, apoB100, apoE, HDL; LDL receptor, SR-B1, CYP7A1, HMGCR, CRP, MDA	In vivo	[54]
2,3,5,4′-Tetrahydroxystilbene-2-O-β-D-glucoside (TSG)	*Polygonum multiflorum*	HSP 70, lipocortin 1, Apo A-I; calreticulin, vimentin;	In vivo	[102]
Salvianolic acid B	*Salvia miltiorrhiza* Bunge	JAK2 (Tyr 1007/1008), STAT1 (Tyr701 and Ser727); CXC chemokines' IP-10, Mig, I-TAC; monocyte adhesion; PIAS1, SOCS1	In vitro	[103]
Cynanchum wilfordii	*Cynanchum wilfordii*	LDL, HDL, NO, E-selectin, VCAM-1, ICAM-1, ET-1	In vivo	[40]
Panax notoginseng extract	*Panax notoginseng*	TNF-α, IL-6, TGF-β, IL-1β	In vivo	[104]
Cryptotanshinone	*Salvia miltiorrhiza* Bunge	oxLDL, NO, ICAM-1, VCAM-1; monocyte adhesion	In vitro	[42]
Salvianolic acid B	*Salvia miltiorrhiza* Bunge	CD40, CD86, CD1a, HLA-DR; IL-12, IL-10, TNF-α; TLR4; PPARγ; p38-MAPK, PAI-1, JNK, NF-κB, COX, ERK1/2, prostaglandin E2, NADPH oxidase, MMP-2, MMP-9, oxLDL, ICAM-1, E-selectin	Both	[53, 71, 72, 105, 106]
Tanshinone IIA	*Salvia miltiorrhiza* Bunge	oxLDL, monocyte adhesion, VSMC migration and proliferation, macrophage cholesterol accumulation, TNF-α, TGF-β1, platelet aggregation, GPx	Both	[66, 67]
Aqueous extract of *Buddleja officinalis*	*Buddleja officinalis*	VCAM-1, ICAM-1; ROS; NF-κB	In vitro	[43]
Artemisinin	*Artemisia annua*	TNF-α, IL-1ß, IL-6; NF-κB, IKKα/ß, IκBα	In vitro	[107]
Evodiamine	*Evodia rutaecarpa*	COX-2, iNOS, prostaglandin E2; HIF-1a; Akt, p70S6K, 4E-BP	In vitro	[108]
Panax notoginseng	*Panax notoginseng* saponins	ICAM-1, VCAM-1	In vivo	[45]
Goji	*Lycium barbarum and L. chinense*	SOD, MDA; JNK	Both	[76]
Ginkgo biloba extract	*Ginkgo biloba*	VCAM-1, ICAM-1, E-selectin; ROS, RSTF	Both	[46]
Scutellaria baicalensis Georgi flavonoids	*Scutellaria baicalensis* Georgi	SOD	Both	[77]
Emodin	*Rheum rhabarbarum*	ApoE, PPAR-γ, GM-CSF, MMP-9	In vivo	[78]
Bisacurone	*Curcuma longa* Linne (Zingiberaceae)	VCAM-1, NF-κB p65, Akt, PKC	In vitro	[49]
Feverfew extract	*Tanacetum parthenium*	TNF-α, CCL2	In vitro	[109]
Magnolol	*Magnolia officinalis*	IL-6, STAT3, Tyr705 and Ser727, ICAM-1, IREs, monocyte adhesion, cyclin D1, MCP-1	In vitro	[50]

Table 7: Continued.

Compound	Herb	Target or indicator	Type of study	Reference
Paeonol	*Paeonia lactiflora* Pallas	ICAM-1, NF-kB p65 translocation, ERK, p38	In vitro	[81]
Aqueous extract of *Salvia miltiorrhiza*	*Salvia miltiorrhiza* Bunge	ICAM-1, VCAM-1, GSH, NF-kB	In vitro	[52]
Magnolol	*Magnolia officinalis*	MCP-1, NF-κB, VCAM-1	In vivo	[51]
Ginkgo biloba extract	*Ginkgo biloba*	VCAM-1, ICAM-1	In vitro	[47]
Scoparone	*Artemisia scoparia*	monocyte adhesion, lipid laden foam cells	In vivo	[87]
Celastrol	*Tripterygium wilfordii* Hook F.	oxLDL, LOX-1, ROS, iNOS, NO, TNF-α, IL-6	In vivo	[89]

decoctions or formulations are scarce, although decoction and formulations are the main forms of therapy in traditional Chinese medicine practice. Capitalization of the interactions between the different components and herbs is the essence of traditional Chinese medicine whereby herbs are combined to attenuate toxicity as well as to enhance efficacy. Secondly, like other therapies, Chinese herbs and the compounds derived from them are expected to have side effects. However, published in vivo studies seldom mention whether adverse effects occurred. In future studies, including animal studies and clinical studies, systemic and organ-specific side effects of Chinese herb medicine should be carefully examined. Thirdly, in modern medical practice, it is unlikely that Chinese herbal medicine will be used as a sole treatment for cardiovascular disease; instead, they will more likely be used in combination with other proven drugs. Therefore, the herb-drug interaction should be carefully evaluated in future studies where Chinese herbs or compounds are used in addition to traditional proven therapies. Fourth, atherosclerosis is a multiple-staged and multifaceted disease; most published studies are focused on examining the effects of Chinese herb medicine on one or only a few aspects of the disease. In future studies, a more systemic evaluation of the effects of Chinese herbal medicine on all aspects of atherosclerosis should be performed, including lipoprotein metabolism, endothelial injury, systemic and arterial local inflammation, as well as cell apoptosis and efferocytosis dynamics/balance in the plaques.

Abbreviations

5-LO: 5-Lipoxygenase
ABCA1: ATP-binding cassette transporter A1
AP-1: Activator protein-1
ApoB100: Apolipoprotein B100
ApoE: Apolipoprotein E
Cav-1: Caveolin-1
CDC6: Cell division cycle 6
COX: Cyclooxygenase
CRP: C-Reactive protein
CYP7A1: Cholesterol 7α-hydroxylase A1
Egr-1: Early growth response protein 1
ERK: Extracellular-signal-regulated kinase
E-selectin: Endothelial cell selectin
ET-1: Endothelin-1
FRAP: Ferric reducing antioxidant power
GM-CSF: Granulocyte-macrophage colony-stimulating factor
GPx: Glutathione peroxidase
GSH: Intracellular glutathione
Hcy: Homocysteine
HGL: High density lipoprotein
HIF-1α: Hypoxia-inducible factor 1alpha
HMGCR: 3-Hydroxy-3-methyl-glutaryl-CoA reductase
ICAM-1: Intercellular cell adhesion molecule-1
IL: Interleukin
iNOS: Inducible nitric oxide synthase
IREs: IL-6 response elements
JNK: c-Jun NH2-terminal kinase
KDR, or VEGF receptor-2: Kinase insert domain receptor
LDL: Low density lipoprotein
LOX-1: Oxidized low density lipoprotein receptor-1
MAPK: p38 mitogen-activated protein kinase
MCP-1: Monocyte chemotactic protein-1
MDA: Malondialdehyde
mLDL: Modified low density lipoprotein
MMP: Matrix metalloproteinase
NF-κB: Nuclear factor kappa B
NO: Nitric oxide
non-HDL: Non-high-density lipoprotein
OFR: Oxygen-derived free radicals
oxLDL: Oxidized low-density lipoprotein
PAI-1: Plasminogen activator inhibitor type 1
PDGF: Platelet-derived growth factor
PI3K: Phosphatidylinositol 3-kinase
PPARs: Peroxisome proliferator-activated receptors
ROS: Reactive oxygen species
RSTF: Redox-sensitive transcription factor
SOD: Superoxide dismutase

SR-B1:	Scavenger receptor class B type 1
STAT3:	Signal transducer and activator of transcription protein 3
TC:	Total cholesterol
TG:	Triglycerides
TNF-α:	Tumor necrosis factor-α
VCAM-1:	Vascular cell adhesion molecule-1
VEGF:	Vascular endothelial growth factor
VLDL:	Very low density lipoprotein
VSMC:	Vascular smooth muscle cell.

Conflict of Interests

The authors declare that they have no conflict of interests regarding the publication of this paper.

Acknowledgment

This work was supported by Grants from the National Institute of Health nos. R21AT006767 and R01HL116626 (to Daping Fan).

References

[1] W. Insull Jr., "The pathology of atherosclerosis: plaque development and plaque responses to medical treatment," *The American Journal of Medicine*, vol. 122, no. 1, pp. S3–S14, 2009.

[2] M. B. Furie and R. N. Mitchell, "Plaque attack: one hundred years of atherosclerosis in the American Journal of Pathology," *The American Journal of Pathology*, vol. 180, no. 6, pp. 2184–2187, 2012.

[3] P. Libby, P. M. Ridker, and A. Maseri, "Inflammation and atherosclerosis," *Circulation*, vol. 105, no. 9, pp. 1135–1143, 2002.

[4] N. Foin, P. Evans, and R. Krams, "Atherosclerosis: cell biology and lipoproteins—new developments in imaging of inflammation of the vulnerable plaque," *Current Opinion in Lipidology*, vol. 19, no. 1, pp. 98–100, 2008.

[5] A. Tavridou and V. G. Manolopoulos, "Novel molecules targeting dyslipidemia and atherosclerosis," *Current Medicinal Chemistry*, vol. 15, no. 8, pp. 792–802, 2008.

[6] D. Steinberg, "Thematic review series: the pathogenesis of atherosclerosis: an interpretive history of the cholesterol controversy, part III: mechanistically defining the role of hyperlipidemia," *Journal of Lipid Research*, vol. 46, no. 10, pp. 2037–2051, 2005.

[7] S. Omoigui, "Cholesterol synthesis is the trigger and isoprenoid dependent interleukin-6 mediated inflammation is the common causative factor and therapeutic target for atherosclerotic vascular disease and age-related disorders including osteoporosis and type 2 diabetes," *Medical Hypotheses*, vol. 65, no. 3, pp. 559–569, 2005.

[8] K. J. Williams and I. Tabas, "Atherosclerosis and inflammation," *Science*, vol. 297, no. 5581, pp. 521–522, 2002.

[9] D. Steinberg, "An interpretive history of the cholesterol controversy. Part V. The discovery of the statins and the end of the controversy," *Journal of Lipid Research*, vol. 47, no. 7, pp. 1339–1351, 2006.

[10] R. B. Singh, S. A. Mengi, Y.-J. Xu, A. S. Arneja, and N. S. Dhalla, "Pathogenesis of atherosclerosis: a multifactorial process," *Experimental and Clinical Cardiology*, vol. 7, no. 1, pp. 40–53, 2002.

[11] R. Ross, "Mechanisms of atherosclerosis—a review," *Advances in Nephrology from the Necker Hospital*, vol. 19, pp. 79–86, 1990.

[12] D. B. Cines, E. S. Pollak, C. A. Buck et al., "Endothelial cells in physiology and in the pathophysiology of vascular disorders," *Blood*, vol. 91, no. 10, pp. 3527–3561, 1998.

[13] P. Rajendran, T. Rengarajan, J. Thangavel et al., "The vascular endothelium and human diseases," *International Journal of Biological Sciences*, vol. 9, no. 10, pp. 1057–1069, 2013.

[14] L. Badimon, J. Martinez-Gonzalez, V. Llorente-Cortes, C. Rodriguez, and T. Padro, "Cell biology and lipoproteins in atherosclerosis," *Current Molecular Medicine*, vol. 6, no. 5, pp. 439–456, 2006.

[15] K. J. Williams and I. Tabas, "The response-to-retention hypothesis of early atherogenesis," *Arteriosclerosis, Thrombosis, and Vascular Biology*, vol. 15, no. 5, pp. 551–562, 1995.

[16] I. Peluso, G. Morabito, L. Urban, F. Ioannone, and M. Serafini, "Oxidative stress in atherosclerosis development: the central role of LDL and oxidative burst," *Endocrine, Metabolic and Immune Disorders: Drug Targets*, vol. 12, no. 4, pp. 351–360, 2012.

[17] J. Steinberger, S. R. Daniels, R. H. Eckel et al., "Progress and challenges in metabolic syndrome in children and adolescents: a scientific statement from the American Heart Association Atherosclerosis, Hypertension, and Obesity in the Young Committee of the Council on Cardiovascular Disease in the Young; Council on Cardiovascular Nursing; and Council on Nutrition, Physical Activity, and Metabolism," *Circulation*, vol. 119, no. 4, pp. 628–647, 2009.

[18] L. Badimón, G. Vilahur, and T. Padró, "Lipoproteins, platelets and atherothrombosis," *Revista Espanola de Cardiologia*, vol. 62, no. 10, pp. 1161–1178, 2009.

[19] K. Ley, Y. I. Miller, and C. C. Hedrick, "Monocyte and macrophage dynamics during atherogenesis," *Arteriosclerosis, Thrombosis, and Vascular Biology*, vol. 31, no. 7, pp. 1506–1516, 2011.

[20] P. Libby, "Inflammation in atherosclerosis," *Arteriosclerosis, Thrombosis, and Vascular Biology*, vol. 32, no. 9, pp. 2045–2051, 2012.

[21] D. Gomez and G. K. Owens, "Smooth muscle cell phenotypic switching in atherosclerosis," *Cardiovascular Research*, vol. 95, no. 2, pp. 156–164, 2012.

[22] P. Lacolley, V. Regnault, A. Nicoletti, Z. Li, and J.-B. Michel, "The vascular smooth muscle cell in arterial pathology: a cell that can take on multiple roles," *Cardiovascular Research*, vol. 95, no. 2, pp. 194–204, 2012.

[23] A. C. Doran, N. Meller, and C. A. McNamara, "Role of smooth muscle cells in the initiation and early progression of atherosclerosis," *Arteriosclerosis, Thrombosis, and Vascular Biology*, vol. 28, no. 5, pp. 812–819, 2008.

[24] M. Braun, P. Pietsch, K. Schrör, G. Baumann, and S. B. Felix, "Cellular adhesion molecules on vascular smooth muscle cells," *Cardiovascular Research*, vol. 41, no. 2, pp. 395–401, 1999.

[25] S. Ma, D. Yang, D. Li, B. Tang, and Y. Yang, "Oleic acid induces smooth muscle foam cell formation and enhances atherosclerotic lesion development via CD36," *Lipids in Health and Disease*, vol. 10, article 53, 2011.

[26] N. Platt, R. Haworth, L. Darley, and S. Gordon, "The many roles of the class A macrophage scavenger receptor," *International Review of Cytology*, vol. 212, pp. 1–40, 2002.

[27] R. E. Clempus and K. K. Griendling, "Reactive oxygen species signaling in vascular smooth muscle cells," *Cardiovascular Research*, vol. 71, no. 2, pp. 216–225, 2006.

[28] L. Hegyi, J. N. Skepper, N. R. Cary, and M. J. Mitchinson, "Foam cell apoptosis and the development of the lipid core of human atherosclerosis," *The Journal of Pathology*, vol. 180, no. 4, pp. 423–429, 1996.

[29] B. L. Gerber, "In vivo evaluation of atherosclerotic plaque inflammation and of anti-inflammatory effects of statins by 18F-fluorodeoxyglucose positron emission tomography," *Journal of the American College of Cardiology*, vol. 62, no. 10, pp. 918–920, 2013.

[30] E. Thorp and I. Tabas, "Mechanisms and consequences of efferocytosis in advanced atherosclerosis," *Journal of Leukocyte Biology*, vol. 86, no. 5, pp. 1089–1095, 2009.

[31] R. R. S. Packard and P. Libby, "Inflammation in atherosclerosis: from vascular biology to biomarker discovery and risk prediction," *Clinical Chemistry*, vol. 54, no. 1, pp. 24–38, 2008.

[32] F. Grover-Paez and A. B. Zavalza-Gomez, "Endothelial dysfunction and cardiovascular risk factors," *Diabetes Research and Clinical Practice*, vol. 84, no. 1, pp. 1–10, 2009.

[33] R. Natarajan and Q. Cai, "Monocyte retention in the pathology of atherosclerosis," *Future Cardiology*, vol. 1, no. 3, pp. 331–340, 2005.

[34] H. Kanda, S. Tateya, Y. Tamori et al., "MCP-1 contributes to macrophage infiltration into adipose tissue, insulin resistance, and hepatic steatosis in obesity," *The Journal of Clinical Investigation*, vol. 116, no. 6, pp. 1494–1505, 2006.

[35] C. Zhang, "The role of inflammatory cytokines in endothelial dysfunction," *Basic Research in Cardiology*, vol. 103, no. 5, pp. 398–406, 2008.

[36] E. Galkina and K. Ley, "Immune and inflammatory mechanisms of atherosclerosis," *Annual Review of Immunology*, vol. 27, pp. 165–197, 2009.

[37] P. Libby, "Inflammation in atherosclerosis," *Nature*, vol. 420, no. 6917, pp. 868–874, 2002.

[38] P. Libby, "Molecular and cellular mechanisms of the thrombotic complications of atherosclerosis," *The Journal of Lipid Research*, vol. 50, pp. S352–S357, 2009.

[39] C. Tian, R. Zhang, X. Ye et al., "Resveratrol ameliorates high-glucose-induced hyperpermeability mediated by caveolae via VEGF/KDR pathway," *Genes and Nutrition*, vol. 8, no. 2, pp. 231–239, 2013.

[40] D. H. Choi, Y. J. Lee, H. C. Oh et al., "Improved endothelial dysfunction by *Cynanchum wilfordii* in *Apolipoprotein* $E^{-/-}$ mice fed a high fat/cholesterol diet," *Journal of Medicinal Food*, vol. 15, no. 2, pp. 169–179, 2012.

[41] Y.-L. Xing, Z. Zhou, Z.-Y. Zhong et al., "Protocatechuic aldehyde inhibits lipopolysaccharide-induced human umbilical vein endothelial cell apoptosis via regulation of caspase-3," *Phytotherapy Research*, vol. 26, no. 9, pp. 1334–1341, 2012.

[42] K.-P. Ang, H.-K. Tan, M. Selvaraja et al., "Cryptotanshinone attenuates *in vitro* oxLDL-induced pre-lesional atherosclerotic events," *Planta Medica*, vol. 77, no. 16, pp. 1782–1787, 2011.

[43] Y. J. Lee, M. K. Moon, S. M. Hwang et al., "Anti-inflammatory effect of buddleja officinalis on vascular inflammation in human umbilical vein endothelial cells," *The American Journal of Chinese Medicine*, vol. 38, no. 3, pp. 585–598, 2010.

[44] M. A. Altug Tuncer, B. Yaymaci, L. Sati et al., "Influence of *Tribulus terrestris* extract on lipid profile and endothelial structure in developing atherosclerotic lesions in the aorta of rabbits on a high-cholesterol diet," *Acta Histochemica*, vol. 111, no. 6, pp. 488–500, 2009.

[45] J.-B. Wan, S. M.-Y. Lee, J.-D. Wang et al., "*Panax notoginseng* reduces atherosclerotic lesions in ApoE-deficient mice and inhibits TNF-α-induced endothelial adhesion molecule expression and monocyte adhesion," *Journal of Agricultural and Food Chemistry*, vol. 57, no. 15, pp. 6692–6697, 2009.

[46] Y.-H. Chen, S.-J. Lin, Y.-L. Chen, P.-L. Liu, and J.-W. Chen, "Anti-inflammatory effects of different drugs/agents with antioxidant property on endothelial expression of adhesion molecules," *Cardiovascular and Hematological Disorders—Drug Targets*, vol. 6, no. 4, pp. 279–304, 2006.

[47] J.-W. Chen, Y.-H. Chen, F.-Y. Lin, Y.-L. Chen, and S.-J. Lin, "*Ginkgo biloba* extract inhibits tumor necrosis factor-α-induced reactive oxygen species generation, transcription factor activation, and cell adhesion molecule expression in human aortic endothelial cells," *Arteriosclerosis, Thrombosis, and Vascular Biology*, vol. 23, no. 9, pp. 1559–1566, 2003.

[48] K. Steinkamp-Fenske, L. Bollinger, N. Völler et al., "Ursolic acid from the Chinese herb Danshen (*Salvia miltiorrhiza* L.) upregulates eNOS and downregulates Nox4 expression in human endothelial cells," *Atherosclerosis*, vol. 195, no. 1, pp. e104–e111, 2007.

[49] D.-I. Sun, I. T. Nizamutdinova, Y. M. Kim et al., "Bisacurone inhibits adhesion of inflammatory monocytes or cancer cells to endothelial cells through down-regulation of VCAM-1 expression," *International Immunopharmacology*, vol. 8, no. 9, pp. 1272–1281, 2008.

[50] S.-C. Chen, Y.-L. Chang, D. L. Wang, and J.-J. Cheng, "Herbal remedy magnolol suppresses IL-6-induced STAT3 activation and gene expression in endothelial cells," *British Journal of Pharmacology*, vol. 148, no. 2, pp. 226–232, 2006.

[51] Y.-H. Chen, S.-J. Lin, J.-W. Chen, H.-H. Ku, and Y.-L. Chen, "Magnolol attenuates VCAM-1 expression in vitro in TNF-α-treated human aortic endothelial cells and in vivo in the aorta of cholesterol-fed rabbits," *British Journal of Pharmacology*, vol. 135, no. 1, pp. 37–47, 2002.

[52] M. Ding, G.-R. Zhao, Y.-J. Yuan, and Z.-X. Guo, "Aqueous extract of Salvia miltiorrhoza regulates adhesion molecule expression of tumor necrosis factor α-induced endothelial cells by blocking activation of nuclear factor κB," *Journal of Cardiovascular Pharmacology*, vol. 45, no. 6, pp. 516–524, 2005.

[53] Y.-H. Chen, S.-J. Lin, H.-H. Ku et al., "Salvianolic acid B attenuates VCAM-1 and ICAM-1 expression in TNF-α-treated human aortic endothelial cells," *Journal of Cellular Biochemistry*, vol. 82, no. 3, pp. 512–521, 2001.

[54] Y. Zhang, Y. Si, S. Yao et al., "*Celastrus orbiculatus* thunb. decreases athero-susceptibility in lipoproteins and the aorta of Guinea pigs fed high fat diet," *Lipids*, vol. 48, no. 6, pp. 619–631, 2013.

[55] Y. Bao, L. Wang, Y. Xu et al., "Salvianolic acid B inhibits macrophage uptake of modified low density lipoprotein (mLDL) in a scavenger receptor CD36-dependent manner," *Atherosclerosis*, vol. 223, no. 1, pp. 152–159, 2012.

[56] D. H. Choi, Y. J. Lee, J. S. Kim, D. G. Kang, and H. S. Lee, "Cynanchum wilfordii ameliorates hypertension and endothelial dysfunction in rats fed with high fat/cholesterol diets," *Immunopharmacology and Immunotoxicology*, vol. 34, no. 1, pp. 4–11, 2012.

[57] S. Subramaniam, R. Subramaniam, S. Rajapandian, S. Uthrapathi, V. R. Gnanamanickam, and G. P. Dubey, "Anti-atherogenic activity of ethanolic fraction of terminalia arjuna bark on

hypercholesterolemic rabbits," *Evidence-Based Complementary and Alternative Medicine*, vol. 2011, Article ID 487916, 8 pages, 2011.

[58] N. J. Dinani, S. Asgary, H. Madani, G. H. Naderi, and P. Mahzoni, "Hypocholesterolemic and antiatherosclerotic effect of Artemisia aucheri in hypercholesterolemic rabbits," *Pakistan Journal of Pharmaceutical Sciences*, vol. 23, no. 3, pp. 321–325, 2010.

[59] H.-X. Ni, N.-J. Yu, and X.-H. Yang, "The study of ginsenoside on PPARγ expression of mononuclear macrophage in type 2 diabetes," *Molecular Biology Reports*, vol. 37, no. 6, pp. 2975–2979, 2010.

[60] S. Amrani, H. Harnafi, N. E. H. Bouanani et al., "Hypolipidaemic activity of aqueous Ocimum basilicum extract in acute hyperlipidaemia induced by triton WR-1339 in rats and its antioxidant property," *Phytotherapy Research*, vol. 20, no. 12, pp. 1040–1045, 2006.

[61] S. H. Nile and S. W. Park, "HPTLC analysis, antioxidant, anti-inflammatory and antiproliferative activities of *Arisaema tortuosum* tuber extract," *Pharmaceutical Biology*, vol. 52, no. 2, pp. 221–227, 2014.

[62] S. Pandeti, R. Sonkar, A. Shukla, G. Bhatia, and N. Tadigoppula, "Synthesis of new andrographolide derivatives and evaluation of their antidyslipidemic, LDL-oxidation and antioxidant activity," *European Journal of Medicinal Chemistry*, vol. 69, pp. 439–448, 2013.

[63] J.-K. Li, R. Ge, L. Tang, and Q.-S. Li, "Protective effects of farrerol against hydrogen-peroxide-induced apoptosis in human endothelium-derived EA.hy926 cells," *Canadian Journal of Physiology and Pharmacology*, vol. 91, no. 9, pp. 733–740, 2013.

[64] L.-Q. Jia, G.-L. Yang, L. Ren et al., "Tanshinone IIA reduces apoptosis induced by hydrogen peroxide in the human endothelium-derived EA.hy926 cells," *Journal of Ethnopharmacology*, vol. 143, no. 1, pp. 100–108, 2012.

[65] S. Xu, Z. Liu, Y. Huang et al., "Tanshinone II-A inhibits oxidized LDL-induced LOX-1 expression in macrophages by reducing intracellular superoxide radical generation and NF-κB activation," *Translational Research*, vol. 160, no. 2, pp. 114–124, 2012.

[66] S. Gao, Z. Liu, H. Li, P. J. Little, P. Liu, and S. Xu, "Cardiovascular actions and therapeutic potential of tanshinone IIA," *Atherosclerosis*, vol. 220, no. 1, pp. 3–10, 2012.

[67] Y.-I. Li, G. Elmer, and R. C. LeBoeuf, "Tanshinone IIA reduces macrophage death induced by hydrogen peroxide by upregulating glutathione peroxidase," *Life Sciences*, vol. 83, no. 15-16, pp. 557–562, 2008.

[68] Y.-C. Hung, P.-W. Wang, and T.-L. Pan, "Functional proteomics reveal the effect of *Salvia miltiorrhiza* aqueous extract against vascular atherosclerotic lesions," *Biochimica et Biophysica Acta: Proteins and Proteomics*, vol. 1804, no. 6, pp. 1310–1321, 2010.

[69] N. P. Visavadiya, B. Soni, N. Dalwadi, and D. Madamwar, "Chlorophytum borivilianum as potential terminator of free radicals in various in vitro oxidation systems," *Drug and Chemical Toxicology*, vol. 33, no. 2, pp. 173–182, 2010.

[70] T.-L. Yang, F.-Y. Lin, Y.-H. Chen et al., "Salvianolic acid B inhibits low-density lipoprotein oxidation and neointimal hyperplasia in endothelium-denuded hypercholesterolaemic rabbits," *Journal of the Science of Food and Agriculture*, vol. 91, no. 1, pp. 134–141, 2011.

[71] Y.-L. Chen, C.-S. Hu, F.-Y. Lin et al., "Salvianolic acid B attenuates cyclooxygenase-2 expression in vitro in LPS-treated human aortic smooth muscle cells and in vivo in the apolipoprotein-E-deficient mouse aorta," *Journal of Cellular Biochemistry*, vol. 98, no. 3, pp. 618–631, 2006.

[72] S. J. Lin, I. T. Lee, Y. H. Chen et al., "Salvianolic acid B attenuates MMP-2 and MMP-9 expression in vivo in apolipoprotein-E-deficient mouse aorta and in vitro in LPS-treated human aortic smooth muscle cells," *Journal of Cellular Biochemistry*, vol. 100, no. 2, pp. 372–384, 2007.

[73] Y.-J. Wu, C.-Y. Hong, S.-J. Lin, P. Wu, and M.-S. Shiao, "Increase of vitamin e content in LDL and reduction of atherosclerosis in cholesterol-fed rabbits by a water-soluble antioxidant-rich fraction of Salvia miltiorrhiza," *Arteriosclerosis, Thrombosis, and Vascular Biology*, vol. 18, no. 3, pp. 481–486, 1998.

[74] H.-J. Park, "Chemistry and pharmacological action of caffeoylquinic acid derivatives and pharmaceutical utilization of chwinamul (Korean Mountainous Vegetable)," *Archives of Pharmacal Research*, vol. 33, no. 11, pp. 1703–1720, 2010.

[75] H. Ma, X. He, Y. Yang, M. Li, D. Hao, and Z. Jia, "The genus Epimedium: an ethnopharmacological and phytochemical review," *Journal of Ethnopharmacology*, vol. 134, no. 3, pp. 519–541, 2011.

[76] O. Potterat, "Goji (*Lycium barbarum* and *L. chinense*): phytochemistry, pharmacology and safety in the perspective of traditional uses and recent popularity," *Planta Medica*, vol. 76, no. 1, pp. 7–19, 2010.

[77] M. Broncel, "Antiatherosclerotic properties of flavones from the roots of *Scutellaria baicalensis* Georgi," *Wiadomości Lekarskie*, vol. 60, no. 5-6, pp. 294–297, 2007.

[78] M. Zhou, H. Xu, L. Pan, J. Wen, Y. Guo, and K. Chen, "Emodin promotes atherosclerotic plaque stability in fat-fed apolipoprotein E-deficient mice," *Tohoku Journal of Experimental Medicine*, vol. 215, no. 1, pp. 61–69, 2008.

[79] W. Duan, Y. Yu, and L. Zhang, "Antiatherogenic effects of *Phyllanthus Emblica* associated with corilagin and its analogue," *Yakugaku Zasshi*, vol. 125, no. 7, pp. 587–591, 2005.

[80] M.-J. Wu, C.-L. Huang, T.-W. Lian, M.-C. Kou, and L. Wang, "Antioxidant activity of *Glossogyne tenuifolia*," *Journal of Agricultural and Food Chemistry*, vol. 53, no. 16, pp. 6305–6312, 2005.

[81] I. T. Nizamutdinova, H. M. Oh, Y. N. Min et al., "Paeonol suppresses intercellular adhesion molecule-1 expression in tumor necrosis factor-α-stimulated human umbilical vein endothelial cells by blocking p38, ERK and nuclear factor-κB signaling pathways," *International Immunopharmacology*, vol. 7, no. 3, pp. 343–350, 2007.

[82] A. Gugliucci and T. Menini, "Three different pathways for human LDL oxidation are inhibited in vitro by water extracts of the medicinal herb *Achyrocline satureoides*," *Life Sciences*, vol. 71, no. 6, pp. 693–705, 2002.

[83] T. H. Park, D. H. Kim, C. H. Kim et al., "Peroxynitrite scavenging mode of alaternin isolated from *Cassia tora*," *Journal of Pharmacy and Pharmacology*, vol. 56, no. 10, pp. 1315–1321, 2004.

[84] K. Chan, S. H. Chui, D. Y. L. Wong, W. Y. Ha, C. L. Chan, and R. N. S. Wong, "Protective effects of Danshensu from the aqueous extract of *Salvia miltiorrhiza* (Danshen) against homocysteine-induced endothelial dysfunction," *Life Sciences*, vol. 75, no. 26, pp. 3157–3171, 2004.

[85] L. Li, L.-P. Jiao, and B. H. Lau, "Protective effect of gypenosides against oxidative stress in phagocytes, vascular endothelial cells and liver microsomes," *Cancer Biotherapy*, vol. 8, no. 3, pp. 263–272, 1993.

[86] H.-C. Huang, H.-R. Wang, and L.-M. Hsieh, "Antiproliferative effect of baicalein, a flavonoid from a Chinese herb, on vascular smooth muscle cell," *European Journal of Pharmacology*, vol. 251, no. 1, pp. 91–93, 1994.

[87] Y.-L. Chen, H.-C. Huang, Y.-I. Weng, Y.-J. Yu, and Y.-T. Lee, "Morphological evidence for the antiatherogenic effect of scoparone in hyperlipidaemic diabetic rabbits," *Cardiovascular Research*, vol. 28, no. 11, pp. 1679–1685, 1994.

[88] P. Chan and B. Tomlinson, "Antioxidant effects of Chinese traditional medicine: focus on trilinolein isolated from the Chinese herb sanchi (*Panax pseudoginseng*)," *The Journal of Clinical Pharmacology*, vol. 40, no. 5, pp. 457–461, 2000.

[89] L. Gu, W. Bai, S. Li et al., "Celastrol prevents atherosclerosis via inhibiting LOX-1 and oxidative stress," *PLoS ONE*, vol. 8, no. 6, Article ID e65477, 2013.

[90] M. F. Andreasen, A.-K. Landbo, L. P. Christensen, A. Hansen, and A. S. Meyer, "Antioxidant effects of phenolic rye (*Secale cereale* L.) extracts, monomeric hydroxycinnamates, and ferulic acid dehydrodimers on human low-density lipoproteins," *Journal of Agricultural and Food Chemistry*, vol. 49, no. 8, pp. 4090–4096, 2001.

[91] S. H. Park, H. J. Koo, Y. Y. Sung, and H. K. Kim, "The protective effect of *Prunella vulgaris* ethanol extract against vascular inflammation in TNF-α-stimulated human aortic smooth muscle cells," *BMB Reports*, vol. 46, no. 7, pp. 352–357, 2013.

[92] F. Wang, Q. Gao, S. Guo et al., "The sonodynamic effect of curcumin on THP-1 cell-derived macrophages," *BioMed Research International*, vol. 2013, Article ID 737264, 9 pages, 2013.

[93] C. Y. Moon, C. R. Ku, Y. H. Cho, and E. J. Lee, "Protocatechuic aldehyde inhibits migration and proliferation of vascular smooth muscle cells and intravascular thrombosis," *Biochemical and Biophysical Research Communications*, vol. 423, no. 1, pp. 116–121, 2012.

[94] S.-J. Lee, S.-S. Park, W.-J. Kim, and S.-K. Moon, "*Gleditsia sinensis* thorn extract inhibits proliferation and TNF-α-induced MMP-9 expression in vascular smooth muscle cells," *The American Journal of Chinese Medicine*, vol. 40, no. 2, pp. 373–386, 2012.

[95] T.-J. Kim, J.-H. Lee, J.-J. Lee et al., "Corynoxeine isolated from the hook of Uncaria *rhynchophylla* inhibits rat aortic vascular smooth muscle cell proliferation through the blocking of extracellular signal regulated kinase 1/2 phosphorylation," *Biological and Pharmaceutical Bulletin*, vol. 31, no. 11, pp. 2073–2078, 2008.

[96] K.-W. Liang, C.-T. Ting, S.-C. Yin et al., "Berberine suppresses MEK/ERK-dependent Egr-1 signaling pathway and inhibits vascular smooth muscle cell regrowth after in vitro mechanical injury," *Biochemical Pharmacology*, vol. 71, no. 6, pp. 806–817, 2006.

[97] H. H. Ho, L. S. Hsu, K. C. Chan, H. M. Chen, C. H. Wu, and C. J. Wang, "Extract from the leaf of nucifera reduced the development of atherosclerosis via inhibition of vascular smooth muscle cell proliferation and migration," *Food and Chemical Toxicology*, vol. 48, no. 1, pp. 159–168, 2010.

[98] C.-C. Chen, J.-D. Hsu, S.-F. Wang et al., "*Hibiscus sabdariffa* extract inhibits the development of atherosclerosis in cholesterol-fed rabbits," *Journal of Agricultural and Food Chemistry*, vol. 51, no. 18, pp. 5472–5477, 2003.

[99] Z. Yuan, Y. Liao, G. Tian et al., "Panax notoginseng saponins inhibit Zymosan A induced atherosclerosis by suppressing integrin expression, FAK activation and NF-κB translocation," *Journal of Ethnopharmacology*, vol. 138, no. 1, pp. 150–155, 2011.

[100] Y.-F. Wang, X.-F. Yang, B. Cheng et al., "Protective effect of astragalus polysaccharides on ATP binding cassette transporter A1 in THP-1 derived foam cells exposed to tumor necrosis factor-alpha," *Phytotherapy Research*, vol. 24, no. 3, pp. 393–398, 2010.

[101] M. Napagoda, J. Gerstmeier, S. Wesely et al., "Inhibition of 5-lipoxygenase as anti-inflammatory mode of action of *Plectranthus zeylanicus* Benth and chemical characterization of ingredients by a mass spectrometric approach," *Journal of Ethnopharmacology*, vol. 151, no. 2, pp. 800–809, 2014.

[102] W. Yao, W. Fan, C. Huang, H. Zhong, X. Chen, and W. Zhang, "Proteomic analysis for anti-atherosclerotic effect of tetrahydroxystilbene glucoside in rats," *Biomedicine & Pharmacotherapy*, vol. 67, no. 2, pp. 140–145, 2013.

[103] S. C. Chen, Y. L. Lin, B. Huang, D. L. Wang, and J. J. Cheng, "Salvianolic acid B suppresses IFN-γ-induced JAK/STAT1 activation in endothelial cells," *Thrombosis Research*, vol. 128, no. 6, pp. 560–564, 2011.

[104] K. D. Tsai, S. M. Yang, J. C. Lee et al., "Panax notoginseng attenuates bleomycin-induced pulmonary fibrosis in mice," *Evidence-Based Complementary and Alternative Medicine*, vol. 2011, Article ID 404761, 7 pages, 2011.

[105] A. Sun, H. Liu, S. Wang et al., "Salvianolic acid B suppresses maturation of human monocyte-derived dendritic cells by activating PPARγ," *British Journal of Pharmacology*, vol. 164, no. 8, pp. 2042–2053, 2011.

[106] Z. Zhou, Y. Liu, A.-D. Miao, and S.-Q. Wang, "Salvianolic acid B attenuates plasminogen activator inhibitor type 1 production in TNF-α treated human umbilical vein endothelial cells," *Journal of Cellular Biochemistry*, vol. 96, no. 1, pp. 109–116, 2005.

[107] Y. Wang, Z. Huang, L. Wang et al., "The anti-malarial artemisinin inhibits pro-inflammatory cytokines via the NF-κB canonical signaling pathway in PMA-induced THP-1 monocytes," *International Journal of Molecular Medicine*, vol. 27, no. 2, pp. 233–241, 2011.

[108] Y.-N. Liu, S.-L. Pan, C.-H. Liao et al., "Evodiamine represses hypoxia-induced inflammatory proteins expression and hypoxia-inducible factor 1α accumulation in RAW264.7," *Shock*, vol. 32, no. 3, pp. 263–269, 2009.

[109] C.-F. Chen and C.-H. Cheng, "Regulation of cellular metabolism and cytokines by the medicinal herb feverfew in the human monocytic THP-1 cells," *Evidence-Based Complementary and Alternative Medicine*, vol. 6, no. 1, pp. 91–98, 2009.

Hindawi Publishing Corporation
Evidence-Based Complementary and Alternative Medicine
Volume 2015, Article ID 582751, 16 pages
http://dx.doi.org/10.1155/2015/582751

Research Article

Chinese Herbal Medicine Combined with Conventional Therapy for Blood Pressure Variability in Hypertension Patients: A Systematic Review of Randomized Controlled Trials

Zhuo Chen,[1] Liqiong Wang,[2] Guoyan Yang,[2] Hao Xu,[3] and Jianping Liu[2]

[1]*Graduate School, Beijing University of Chinese Medicine, Beijing 100029, China*
[2]*Centre for Evidence-Based Chinese Medicine, Beijing University of Chinese Medicine, Beijing 100029, China*
[3]*Cardiovascular Diseases Center, Xiyuan Hospital, China Academy of Chinese Medical Sciences, Beijing 100091, China*

Correspondence should be addressed to Hao Xu; xuhaotcm@hotmail.com and Jianping Liu; jianping_l@hotmail.com

Received 21 August 2014; Revised 24 September 2014; Accepted 24 September 2014

Academic Editor: Myeong Soo Lee

Objective. The aim of this systematic review is to evaluate effect of Chinese medicine combined with conventional therapy on blood pressure variability (BPV) in hypertension patients. *Methods*. All randomized clinical trials (RCTs) comparing Chinese medicine with no intervention or placebo on the basis of conventional therapy were included. Data extraction, analyses, and quality assessment were performed according to the Cochrane standards. *Results*. We included 13 RCTs and assessed risk of bias for all the trials. Chinese medicine has a significant effect in lowering blood pressure (BP), reducing BPV in the form of standard deviation (SD) or coefficient of variability (CV), improving nighttime BP decreased rate, and reversing abnormal rhythm of BP. *Conclusions*. Chinese medicine was safe and showed beneficial effects on BPV in hypertension patients. However, more rigorous trials with high quality are warranted to give high level of evidence before recommending Chinese medicine as an alternative or complementary medicine to improve BPV in hypertension patients.

1. Background

It is estimated that there are nearly one billion people suffering from hypertension worldwide, and the number of patients will increase to 1.5 billion by 2050 [1]. Blood pressure variability (BPV) means the degree of blood pressure (BP) fluctuations in a certain period of time. BPV is regarded as a separate index which is different from the BP reflecting cardiovascular activities. Many studies have confirmed that BPV could impact on hypertensive target organ damage and overall prognosis of patients [1–5]. An important factor to improve the prognosis of hypertensive patients is to reduce the BPV effectively. Clinicians pay close attention to lowering pressure steadily nowadays. There have been many studies that elucidated the relationship between western medicine and BPV. Although the results are inconclusive, most studies have shown that calcium channel blockers (CCB) are the most effective to reduce the BPV, especially amlodipine. Amlodipine in combination with other drugs may be more effective [6–8].

Short-term BPV within the 24-hour period is easier to obtain measured results. Ambulatory blood pressure monitoring (ABPM) is a way to assess the short-term BPV at present. By ABPM, a large amount of cross-sectional studies confirmed the increased BPV indicating the aggravated target organ damage [9]. A quantitative analysis of 155 Chinese people's ABPM results showed that BPV of hypertensive patients was higher than that of healthy people [10].

Western medicine puts emphasis on quickly and effectively lowering BP and helps patients reach target BP as soon as possible. But even effective long-term control of BP by western medicine may not fully achieve goals of

protecting target organs against damage, because reversing the target organ damage is a long process. Chinese medicine highlights the overall concept, self-regulation mechanism, and multitargets action and often plays an important role in the protection of target organ of hypertensive patients [11]. However, whether Chinese medicine is effective on BPV remains unclear. So, we design this systematic review to evaluate effect of Chinese medicine on BPV by ABPM in hypertension patients.

2. Methods

2.1. Search Strategy. Two reviewers (Z. Chen and L. Q. Wang) searched the following databases from their inception to April 15, 2014, for the identification of randomized clinical trials (RCTs) assessing Chinese herbal medicine for BPV: The Cochrane Library, Pubmed, China National Knowledge Infrastructure (CNKI), Chinese Scientific Journal Database (VIP), Wanfang Databases, and Sino-Med Database. There was no limitation in languages. We also searched references of included reviews, just in case eligible trials were missed. We searched using the following searching terms: "blood pressure variability," "BPV," "essential hypertension," "standard deviation," "coefficient of variability," "traditional Chinese medicine," "Chinese herbal medicine," and "randomized controlled trial." Chinese pinyin of these terms were "xue ya bian yi," "xue ya bo dong," "xue ya bian yi xing," "xue ya bo dong xing," "zhong yao," "zhong chengyao," "zhong cao yao," "zhong xi yi," "ke li," "zhong yi yao," "zhong yi," and "sui ji." Based on different characteristics of literature databases, we adapted the search strategies appropriately which are shown in Table 1.

2.2. Inclusion Criteria

2.2.1. Study Design. RCTs were included regardless of blind method and language.

2.2.2. Participants. Patients with BPV regardless of age and race were included, who were diagnosed by one of the following diagnostic criteria: WHO/ISH Hypertension Prevention Guide (1999 [12]/2003 [13]) or Chinese Hypertension Prevention Guide (2005 [14]/2010 [15]). Patients with severe liver and kidney dysfunction and serious complications were excluded.

2.2.3. Interventions. Chinese herbal medicine was used as intervention in at least one group of the study, form of which can be decoction, granule, and Chinese patent medicine (capsule/tablet). The method of application was restricted to orally taken; therefore, injections were excluded. Control groups were no treatment, placebo, or conventional medicines. Trials of Chinese herbal medicine in combination of conventional medicine compared to conventional medicine alone were also included, if the conventional medicine applied in both groups was the same. Trials with a treatment course of less than four weeks were excluded. Trials with more than one kind of Chinese herbal medicine as intervention were also excluded.

2.2.4. Outcome Measures. Primary outcome measures were BPV (measured by standard deviation (SD) and coefficient of variability (CV), at three different time points: 24 hours, day, and night), BP (24 hours, day, and night), and symptom improvement rate which had uniform criteria, that is, clinical guideline of new drugs for traditional Chinese medicine. Among all these indicators, BPV and ambulatory BP are both indispensable. Secondary outcome measures were adverse events, quality of life (QOL), the abnormal rhythm of BP reverse rate, and nighttime BP decrease rate.

2.3. Data Extraction and Quality Assessment. Two authors (Z. Chen and L. Q. Wang) performed data extraction (Figure 1) independently according to a predesigned form. Disagreements during cross-checking of the data extraction form were resolved by consensus or consultation from a third author (J. P. Liu). We assessed the methodological quality of these trials by risk of bias tool which was recommended by Cochrane Handbook [16]. Specific items of the risk of bias tool were as follows: selection bias (random sequence generation, allocation concealment), performance bias (blinding of participants and personnel), detection bias (blinding of outcome assessment), attrition bias (incomplete outcome data), reporting bias (selective outcome reporting), and other biases. Each item for all included trials was judged into "high risk," "unclear," and "low risk."

2.4. Data Analysis and Synthesis. Revman 5.2 software provided by the Cochrane Collaboration was used for data analyses. We expressed dichotomous data as risk ratio (RR) and its 95% confidence intervals (CI) and continuous outcome as mean difference (MD) and its 95% CI. Since all included trials applied different interventions, we did not pool the data due to the clinical heterogeneity. We performed qualitative description of the data synthesis.

We also failed to conduct a funnel plot to explore publication bias, because the number of included studies was less than nine for each outcome.

3. Results

3.1. Description of Included Trials. 474 trials were identified from six databases. Among them, 96 records were removed because of duplicates. By screening titles and abstracts, we excluded 263 records for reasons of animal experiment, traditional review, improper comparison, or nonprimary hypertension. By browsing full-text article, we excluded 102 records for reasons of improper comparison, nonprimary hypertension, complications, uncorrelated outcomes, or duplicate publication. At last, a total of 13 articles [17–29] that met inclusion criteria were included into this systematic review. (Basic characteristics of included studies are presented in Table 2.)

3.1.1. Study Characteristics. The 13 trials were published in Chinese from 2007 to 2013, of which seven [17–20, 27–29] were academic dissertations, five [21–25] were journal articles, and one [26] was conference paper. All trials were carried

Table 1: Search strategy.

(1) Cochrane Central Register of Controlled Trials (CENTRAL) on The Cochrane Library
#1 MeSH descriptor: [Medicine, Chinese Traditional] explode all trees
#2 MeSH descriptor: [Drugs, Chinese Herbal] explode all trees
#3 #1 or #2
#4 MeSH descriptor: [Hypertension] explode all trees
#5 "standard deviation" or SD
#6 "coefficient of variability" or CV
#7 #5 or #6
#8 #4 and #7
#9 "blood pressure variability" or "BPV" or "blood pressure fluctuation"
#10 "Randomized Controlled Trial" or "RCT"
#11 #8 or #9
#12 #3 and #10 and #11
(2) PubMed
#1 "Hypertension" [MeSH]
#2 "medicine, Chinese traditional" [MeSH Terms]
#3 "drugs, Chinese herbal" [MeSH Terms]
#4 #2 OR #3
#5 "randomized controlled trial" [All Fields] or RCT [All Fields]
#6 BPV [All Fields] OR "blood pressure variability" [Title/Abstract] OR "blood pressure fluctuation" [Title/Abstract]
#7 "standard deviation" [Title/Abstract] or SD [All Fields]
#8 "coefficient of variability" [Title/Abstract] or CV [All Fields]
#9 #7 OR #8
#10 #1 AND #9
#11 #6 OR #10
#12 #4 AND #11
#13 choose filter "Randomized Controlled Trial"
(3) CBM
((("blood pressure variability" [Common fields: intelligence]) OR ("fluctuation of blood pressure" [Common fields: intelligence]) OR ("BPV" [Common fields: intelligence]) OR ("blood pressure variability" [Common fields: intelligence])) AND ("randomized" [All: intelligence]) AND (("Chinese medicine" [All: intelligence]) OR ("Chinese patent medicine" [All: intelligence]) OR ("integrated Chinese and western medicine" [All: intelligence]) OR ("granule" [All: intelligence]) OR ("Chinese herbal medicine" [All: intelligence]) OR ("traditional Chinese medicine" [All: intelligence])))
(4) CNKI
(SU = "blood pressure variability" OR SU = "fluctuation of blood pressure" OR SU = "BPV") AND (FT = "traditional Chinese medicine" OR FT = "Chinese patent medicine" OR FT = "integrated Chinese and western medicine" OR FT = "granule" OR FT = "Chinese herbal medicine" OR FT = "Chinese medicine") AND (FT = "randomized")
(5) VIP
(Title or key word = blood pressure variability + fluctuation of blood pressure + BPV) and (Any Field = traditional Chinese medicine + integrated Chinese and western medicine + granule + Chinese patent medicine + Chinese herbal medicine + Chinese medicine) and (Any Field = randomized) and (Professional = pharmaceutical and health care) and (Range = all journals)
(6) WanFang database
(title or key word: (blood pressure variability) + title or key word: (fluctuation of blood pressure) + title or key word: (BPV)) ∗ (Chinese medicine + Chinese patent medicine + integrated Chinese and western medicine + granule + Chinese herbal medicine + traditional Chinese medicine) ∗ randomized

out in mainland China. One article [21] was funded by Shandong province science and technology development project.

3.1.2. Population Characteristics. 1103 patients were included, with an average of 85 cases per trial (range from 40 cases to 160 cases). Eight trials [17–21, 25–27] included both inpatients and outpatients, three trials [21, 23, 29] only contained outpatients, and two trials [24, 28] did not report whether outpatients or inpatients. All trials claimed baseline characteristics were comparable between the groups. Five trials

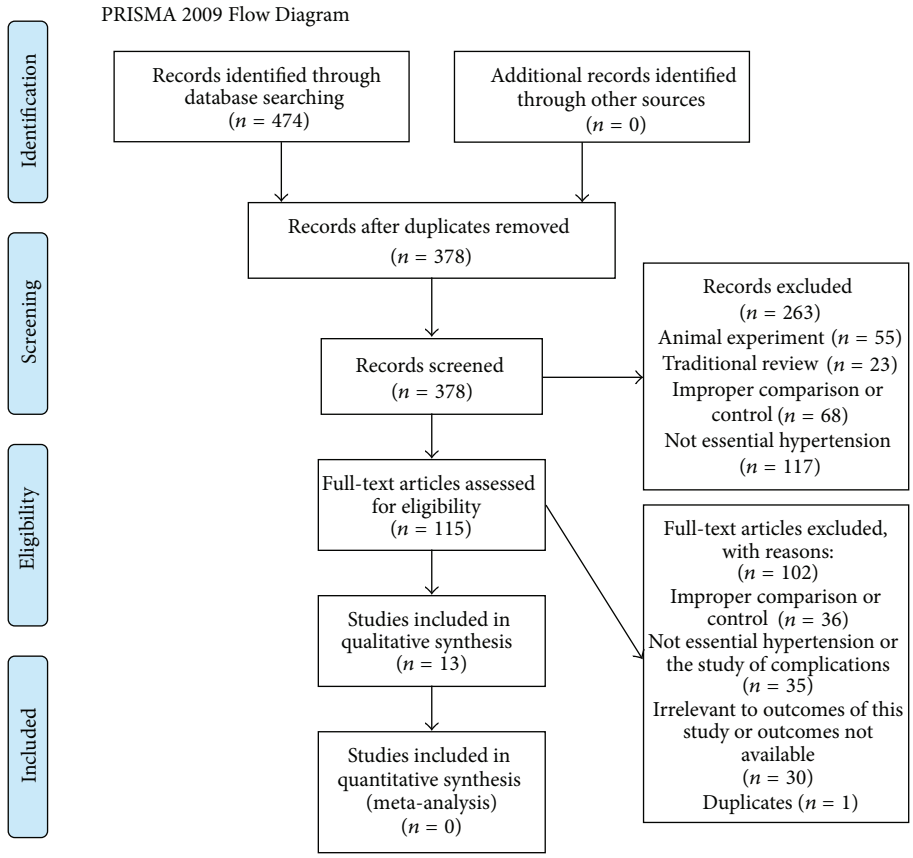

Figure 1: Flow chart of study selection.

[17, 23, 24, 26, 29] did not report male/female ratio in different groups, three trials [24, 26, 28] did not report distribution of age, and five [21, 23, 24, 26, 29] papers did not report disease duration between the groups. The remaining trials clearly reported these items. High BP classification was limited to first and second degree, except two trials (one [24] did not report high BP classification and one [25] was not limited classification). One trial [17] explicitly mentioned complications, but there was no significant difference in the distribution and two groups can be comparable. Remaining trials did not report complications.

3.1.3. Comparisons. There were two types of comparisons: (1) Chinese medicine combined with conventional therapy versus conventional therapy alone (twelve trials) and (2) Chinese medicine combined with conventional therapy versus placebo and conventional therapy (one trial). Conventional therapy of six trials [17, 20–22, 26, 29] was amlodipine besylate tablet 5 mg per day. One trial was levamlodipine [28]. One trial was nifedipine controlled released tablet [27]. Two trials [18, 24] were CCB combined with ACEI. Two trials were ACEI [19, 23]. One trial did not report the ingredients of Chinese medicine [25]. There were four dosage forms: decoction, capsule, granule, and tablet. (Herbal medicines and adverse effects in the included trials are presented in Table 4.)

3.1.4. Outcome Measures. Nine trials [17, 19, 22, 24–29] reported adverse events. Two trials [20, 23] clearly reported there was no adverse drug reaction. Two trials [23, 29] reported QOL. No trial reported health-economic indicators or follow-up visit. All trials reported BPV in the form of SD or CV, symptom improvement rate (antihypertensive effect) of which diagnostic criterion was Clinical Research Guideline of New Drugs for Traditional Chinese Medicine. Antihypertensive effect is divided into three levels according to the BP value: markedly effective, effective, and invalid.

3.2. Methodological Quality. Five trials [17, 19, 26, 27, 29] used random number table to generate the random sequence. Two trials [17, 29] referred to opaque sealed envelopes. Blinding of participants and personnel was mentioned in only one trial [29] which was double-blinding. No trial blinded the outcome assessors. There was not sufficient information to judge whether outcome assessors were blinded or not. Eleven trials did not miss outcome data, among which two trials [17, 26] clearly claimed no drop-out patient. All trials reported their prespecified primary outcomes except one trial. All trials declared baseline characteristics were comparable. One trial [21] was lack of the inclusion and exclusion criteria. Unfortunately, no trial reported sample size calculation. (Risk of bias summaries are presented in Figure 2.)

Table 2: Basic characteristics of included studies.

Study ID	Source of participants	Sample size (I/C)	Age (years, I/C)	Sex (M/F)	Intervention	Control	Treatment duration (week or month)	Outcomes
Pan 2012 [17]	Outpatients and inpatients	I: 30 C: 30	I: 66.5 ± 4.5 (skewed distribution) C: 67 ± 6.25 (Skewed distribution)	NR	Tian ma shu xin granule, 150 mL bid	Amlodipine besylate tablet, 5 mg qd	4 w	24 hCV, dCV, nCV 24 hSD, dSD, nSD 24 hBP, dBP, nBP
Ma 2013 [18]	Outpatients and inpatients	I: 20 C: 20	I: 49.00 ± 11.82 C: 55.10 ± 10.44	21/19	Qian yang yu yin granule, 10 g tid	Combined felodipine with enalapril to control blood pressure below 140/90 mmHg. felodipine, 5 mg/d, enalapril 10 mg/d, dose adjustment if blood pressure is above 140/90 mmHg	8 w	24 hSD, dSD, nSD 24 hBP, dBP, nBP
Liang 2007 [19]	Outpatients and inpatients	I: 31 C: 30	I: 50.39 ± 8.00 C: 51.60 ± 7.07	36/25	Qin dan capsule, 1.75 g tid	Enalapril maleate tablet, 5 mg bid group	8 w	dSD, nSD 24 hBP The nighttime blood pressure decrease rate
Shi 2011 [20]	Outpatients and inpatients	I: 20 C: 20	I: 74.25 ± 8.42 C: 73.05 ± 9.32	33/7	Sang ji wen dan decoction, one packet, bid	Amlodipine besylate tablet, 5 mg qd, group	4 w	24 hSD, dSD, nSD 24 hBP, dBP, nBP
Wang 2011 [21]	Outpatients	I: 70 C: 68	I: 52.1 ± 9.3 C: 50.3 ± 8.9	73/65	Songling Xuemaikang capsule, 1.5 g, tid	Amlodipine besylate tablet, 5 mg qd	4 w	dSD, nSD 24 hBP,
Kang and Fan 2013 [22]	Outpatients and inpatients	I: 60 C: 58	I: 67 ± 10 C: 66 ± 9	72/46	Xian dan tong mai decoction, one packet, bid	Amlodipine besylate tablet, 5 mg qd	4 w	24 hSD, dSD, nSD 24 hBP, dBP, nBP
Ma et al. 2013 [23]	Outpatients	I: 41 C: 37	I: 50.42 ± 4.34 C: 51.45 ± 4.70	NR	Xiang tian ma decoction, one packet, bid	Benazepril, 10 mg qd	8 w	24 hSD, dSD, nSD 24 hBP, dBP, nBP
Li 2012 [24]	NR	I: 54 C: 56	I: NR C: NR	NR	Xuezhikang capsule 600 mg, bid	A combination of ACEI and CCB as basic treatment, drug adjustment according to the circumstances	6 m	24 hSD 24 hBP
Ji and Han 2011 [25]	Outpatients and patients in hospital	I: 80 C: 80	I: 53.3 ± 11.08 C: 56.7 ± 11.61	90/70	Yang xue qing nao granule, one packet, tid	Conventional antihypertensive drugs	12 w	dSD, nSD 24 hBP, dBP, nBP, Circadian rhythm of blood pressure
Zhang et al. 2012 [26]	Outpatients and patients in hospital	I: 40 C: 40	I: NR C: NR	NR	Yin gan jing decoction, one packet, bid	Amlodipine besylate tablet, 5 mg qd, group	1 m	24 hSD, 24 hBP, dBP, nBP, trough-to-peak ratios, 24 h smoothness index (SI) The nighttime blood pressure decreased rate
Yan 2008 [27]	Outpatients and patients in hospital	I: 30 C: 28	I: 61.54 ± 6.53 C: 60.94 ± 8.01	30/28	Tiao ping kang tablet 4 tablets, tid	Nifedipine controlled released Tablets, 30 mg, qd	4 w	24 hSD, dSD, nSD 24 hBP, dBP, nBP, trough-to-peak ratios, Circadian rhythm of blood pressure, lowering blood pressure load value, morning blood pressure, stationarity index pulse pressure, pulse pressure drop rate

Table 2: Continued.

Study ID	Source of participants	Sample size (I/C)	Age (years, I/C)	Sex (M/F)	Intervention	Control	Treatment duration (week or month)	Outcomes
Liang 2011 [28]	NR	I: 35 C: 35	I: 61.3 ± 5.38 C: 61.7 ± 4.76	32/38	Gou teng si wu decoction, one packet, bid	Levamlodipine besylate tablets, 2.5 mg, qd	4 w	24 hSD, 24 hBP, 24 h blood pressure load, 24 h trough-to-peak ratios the nighttime blood pressure decrease rate
Chen 2012 [29]	Outpatients	I: 45 C: 45	I: NR C: NR	NR	Qing xuan granule, one packet, bid	Amlodipine besylate tablet, 5 mg qd, group	8 w	24 hCV, dCV, nCV 24 hSD, dSD, nSD 24 hBP, dBP, nBP

Notes: I: intervention group; C: control group; NR: not reported, that is, no related information is reported in the articles.
RCT: randomized controlled trial; qd: once a day; bid: twice a day; tid: three times a day; w: week; m: month; CV: coefficient of variability; SD: standard deviation; BP: blood pressure; h: hour; d: day; n: night.

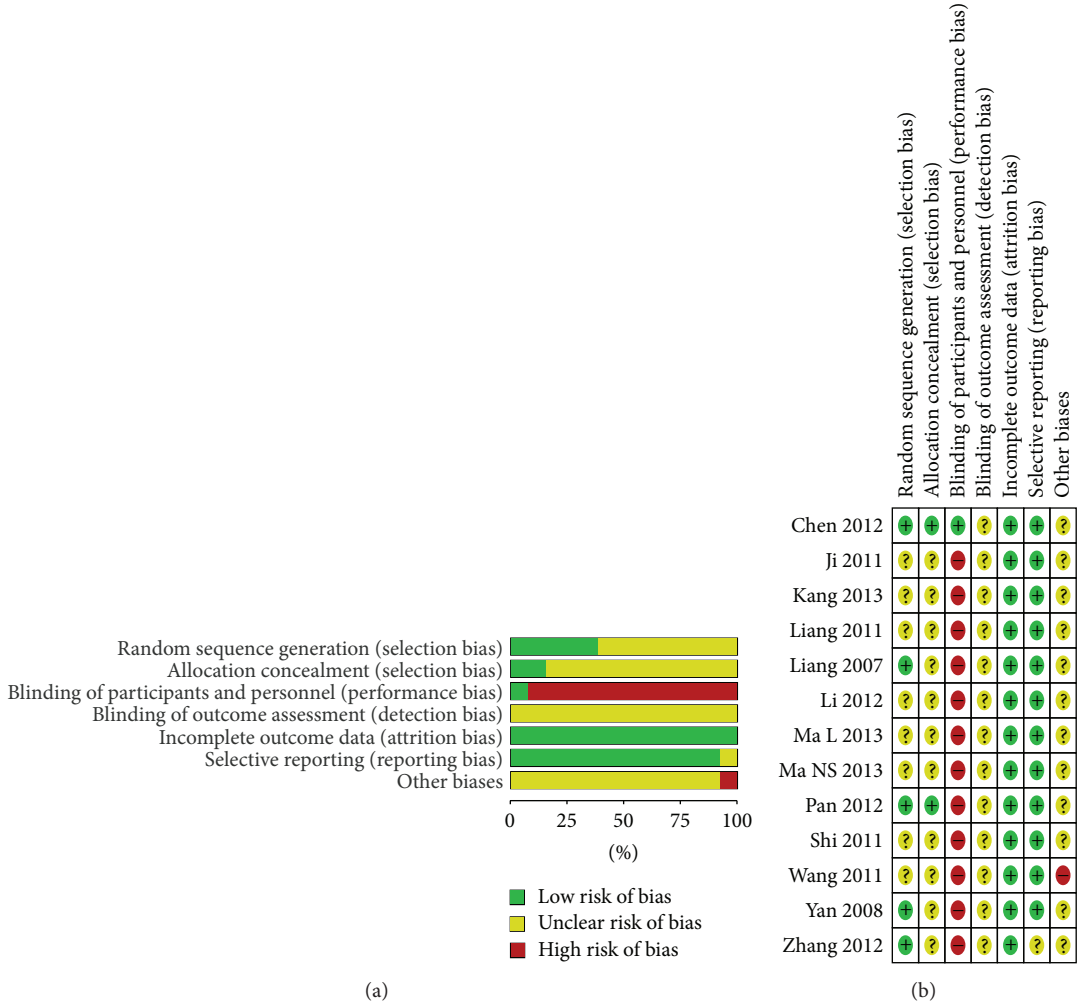

FIGURE 2: (a) Risk of bias graph: review authors' judgments about each risk of bias item presented as percentages across all included studies. (b) Risk of bias summary: review authors' judgments about each risk of bias item for each included study. "+": low risk of bias; "?": unclear risk of bias; or "–" high risk of bias.

3.3. Effects of Interventions. Since every trial had different Chinese herbal medicines as treatment, none of trials could be analyzed by meta-analysis, because of clinical heterogeneity. We presented the effects of interventions by qualitative description, according to the two types of comparisons: Chinese medicine combined with conventional therapy versus the same conventional therapy and Chinese medicine combined with conventional therapy versus placebo combined with the same conventional therapy. All BPV were measured by ambulatory BP meter. BPV mainly was expressed in two forms: SD and CV. (Effect estimate of outcomes is presented in Table 3.)

3.3.1. Chinese Medicine Combined with Conventional Therapy versus the Same Conventional Therapy

(1) SD after Treatment. There were nine trials [17, 18, 20, 22–24, 26–29] reporting 24 h systolic SD. Five trials [20, 22–24, 26] found statistical difference between groups. The results have shown that combination therapy is superior to conventional treatment. For traditional Chinese medicine (TCM) combined with amlodipine besylate tablet, three trials showed a reduction of 24 h systolic SD: Sangji Wendan decoction (MD −2.44; 95% CI −4.38 to −0.50; $n = 40$), Xiandan Tongmai decoction (MD −2.40; 95% CI −3.50 to −1.30; $n = 118$), and Yin gan jing decoction (MD −0.90; 95% CI −1.45 to −0.35; $n = 80$). Xiang tian ma decoction combined with benazepril also reduced 24 h systolic SD (MD −5.20; 95% CI −6.37 to −4.03; $n = 78$). Xuezhikang capsule was integrated with angiotensin converting enzyme inhibitors (ACEI) and calcium channel blockers (CCB) (MD −1.79; 95% CI −2.79 to −0.79; $n = 110$). There were no significant differences in the other four trials; they were Tianma Shuxin granule combined with amlodipine besylate tablet, Qianyang Yuyin granule combined with felodipine and enalapril, Tiao ping kang tablet combined with nifedipine controlled released tablets, and Gouteng Siwu decoction combined with levamlodipine besylate tablet.

Table 3: Effect estimate of Chinese herbal medicines for blood pressure variability in randomized clinical trials.

(a)

Intervention versus control	Effect estimate of outcomes (RR or MD (95% CI))											
	24 hsSD	24 hdSD	dsSD	ddSD	nsSD	ndSD	2 hsCV	24 hdCV	dsCV	ddCV	nsCV	ndCV
(1) Chinese medicine combined with conventional therapy versus the same conventional therapy												
Xiandan tongmai decoction [22]	−2.40 [−3.50, −1.30]	−1.60 [−3.12, −0.08]	−1.40 [−2.63, −0.17]	−1.90 [−3.28, −0.52]	−1.40 [−2.63, −0.17]	0.50 [−1.10, 2.10]	NR	NR	NR	NR	NR	NR
Xuezhikang capsule [24]	−1.79 [−2.79, −0.79]	−0.72 [−1.97, 0.53]	NR	NR	NR	NR	NR	NR	NR	NR	NR	NR
Gouteng siwu decoction [28]	0.28 [−1.31, 1.88]	−0.21 [−1.31, 0.89]	NR	NR	NR	NR	NR	NR	NR	NR	NR	NR
Xiang tian ma decoction [23]	−5.20 [−6.37, −4.03]	−0.67 [−1.59, 0.25]	−4.56 [−5.85, −3.27]	−1.14 [−2.09, −0.19]	−6.18 [−7.74, −4.62]	−1.19 [−2.14, −0.24]	NR	NR	NR	NR	NR	NR
Qianyang yuyin granule [18]	−1.04 [−2.74, 0.66]	−0.40 [−1.64, 0.84]	−1.47 [−3.39, 0.45]	−0.54 [−1.96, 0.88]	−0.89 [−3.85, 2.07]	−0.84 [−2.69, 1.01]	NR	NR	NR	NR	NR	NR
Tianma shuxin granule [17]	−1.24 [−2.65, 0.17]	−0.04 [−1.11, 1.03]	−1.06 [−2.30, 0.18]	−0.43 [−1.64, 0.78]	−0.37 [−2.27, 1.52]	−1.29 [−3.18, 0.60]	−0.00 [−0.01, 0.01]	0.03 [0.02, 0.04]	−0.01 [−0.02, −0.00]	−0.01 [−0.02, 0.01]	−0.01 [−0.02, 0.01]	−0.01 [−0.03, 0.01]
Sangji wendan decoction [20]	−2.44 [−4.38, −0.50]	−2.13 [−4.34, 0.08]	−0.02 [−2.21, 2.17]	−1.74 [−4.14, 0.66]	−1.00 [−3.33, 1.33]	−1.78 [−4.34, 0.78]	NR	NR	NR	NR	NR	NR
Tiao ping kang tablet [27]	−0.40 [−3.30, 2.50]	−0.62 [−3.72, 2.48]	−3.87 [−6.16, −1.58]	−4.95 [−7.10, −2.80]	−5.29 [−7.40, −3.18]	−1.82 [−4.09, 0.45]	NR	NR	NR	NR	NR	NR
Yin gan jing decoction [26]	−0.90 [−1.45, −0.35]	−0.24 [−0.46, −0.02]	NR	NR	NR	NR	NR	NR	NR	NR	NR	NR
Yangxue qingnao granule [25]	NR	NR	−0.50 [−0.81, −0.19]	−0.15 [−0.50, 0.20]	−0.39 [−0.60, −0.18]	−0.21 [−0.36, −0.06]	NR	NR	NR	NR	NR	NR
Qin dan capsule [19]	NR	NR	−2.15 [−3.39, −0.91]	−2.20 [−3.26, −1.14]	−1.15 [−2.21, −0.09]	−1.40 [−2.51, −0.29]	NR	NR	NR	NR	NR	NR
Songling Xuemaikang capsule [21]	NR	NR	−0.70 [−1.48, 0.08]	−0.60 [−1.08, −0.12]	−1.60 [−2.19, −1.01]	−0.10 [−0.59, 0.39]	NR	NR	NR	NR	NR	NR

(a) Continued.

Intervention versus control	Effect estimate of outcomes (RR or MD (95% CI))											
	24 hsSD	24 hdSD	dsSD	ddSD	nsSD	ndSD	2 hsCV	24 hdCV	dsCV	ddCV	nsCV	ndCV
(2) Chinese medicine combined with conventional therapy versus placebo combined with the same conventional therapy												
Qing xuan granule [29]	−1.47 [−2.52, −0.42]	−1.26 [−1.93, −0.59]	−1.60 [−2.65, −0.55]	−1.02 [−1.70, −0.34]	−2.02 [−3.45, −0.59]	−1.54 [−2.62, −0.46]	0.00 [−0.01, 0.01]	−0.01 [−0.07, 0.05]	0.00 [−0.01, 0.02]	0.00 [−0.01, 0.01]	−0.01 [−0.02, 0.01]	−0.01 [−0.03, 0.01]

(b)

Intervention versus control	Effect estimate of outcomes (RR or MD (95% CI))											
	24 hsBP	24 hdBP	dsBP	ddBP	nsBP	ndBP	AE*	Adverse effect*	Quality of life	NSBPDR	NDBPDR	RARBPR*
(1) Chinese medicine combined with conventional therapy versus the same conventional therapy												
Xiandan tongmai decoction [22]	−0.20 [−3.23, 2.83]	0.10 [−2.66, 2.86]	−1.70 [−4.93, 1.53]	−0.40 [−3.40, 2.60]	1.10 [−1.99, 4.19]	0.10 [−2.66, 2.86]	0.59 [0.22, 1.57]	NR	NR	NR	NR	NR
Xuezhikang capsule [24]	−5.00 [−8.80, −1.20]	−1.00 [−3.07, 1.07]	NR	NR	NR	NR	NR	0.80 [0.29, 2.21]	NR	NR	NR	NR
Gouteng siwu decoction [28]	−14.65 [−20.29, −9.01]	−4.05 [−8.09, −0.01]	NR	NR	NR	NR	0.32 [0.10, 1.04]	3.09 [0.12, 78.41]	NR	NR	NR	NR
Xiang tian ma decoction [23]	−2.90 [−6.27, 0.47]	−4.05 [−7.23, −0.87]	3.50 [0.42, 6.58]	−3.72 [−5.23, −2.21]	−6.80 [−12.85, −0.75]	−0.75 [−3.29, 1.79]	NR	0.25 [0.05, 1.26]	NR	NR	NR	NR
Qianyang yuyin granule [18]	−9.60 [−13.49, −5.71]	−6.45 [−10.58, −2.32]	−9.85 [−14.14, −5.56]	−0.84 [−2.69, 1.01]	−7.80 [−13.04, −2.56]	−6.40 [−10.72, −2.08]	NR	NR	NR	NR	NR	NR
Tianma shuxin granule [17]	−0.20 [−3.67, 3.27]	1.73 [−2.83, 6.29]	2.00 [−1.73, 5.73]	0.73 [−3.08, 4.54]	−5.84 [−15.76, 4.08]	1.46 [−2.37, 5.29]	NR	1.00 [0.19, 5.40]	NR	−0.01 [−0.02, 0.01]	−0.01 [−0.03, 0.01]	NR
Sangji wendan decoction [20]	0.52 [−6.65, 7.69]	0.16 [−4.47, 4.79]	−0.35 [−8.01, 7.31]	−0.42 [−5.50, 4.66]	1.46 [−7.06, 9.98]	0.63 [−4.75, 6.01]	0.32 [0.01, 8.26]	NR	NR	NR	NR	NR
Tiao ping kang tablet [27]	−0.10 [−4.47, 4.27]	−1.00 [−4.95, 2.95]	−3.40 [−7.38, 0.58]	−2.90 [−5.73, −0.07]	−8.70 [−13.18, −4.22]	−4.00 [−6.81, −1.19]	0.93 [0.17, 5.02]	0.09 [0.00, 1.74]	NR	NR	NR	0.17 [0.04, 0.66]
Yin gan jing decoction [26]	−2.92 [−5.51, −0.33]	−2.57 [−4.68, −0.46]	−3.15 [−5.66, −0.64]	−2.40 [−4.39, −0.41]	−3.77 [−6.39, −1.15]	−3.52 [−5.85, −1.19]	0.30 [0.09, 0.93]	0.19 [0.01, 4.09]	NR	NR	NR	NR
Yangxue qingnao granule [25]	−4.90 [−7.10, −2.70]	−2.11 [−3.60, −0.62]	−3.55 [−5.65, −1.45]	−1.20 [−2.14, −0.26]	−4.76 [−7.77, −1.75]	−2.68 [−4.82, −0.54]	NR	5.13 [0.24, 108.51]	NR	NR	NR	0.37 [0.15, 0.94]

(b) Continued.

Intervention versus control	Effect estimate of outcomes (RR or MD (95% CI))											
	24 hsBP	24 hdBP	dsBP	ddBP	nsBP	ndBP	AE*	adverse effect*	Quality of life	NSBPDR	NDBPDR	RARBPR*
Qin dan capsule [19]	−4.61 [−8.88, −0.34]	−0.34 [−3.05, 2.37]	NR	NR	NR	NR	0.45 [0.08, 2.65]	0.62 [0.10, 4.00]	NR	NR	NR	NR
Songling Xuemaikang capsule [21]	−6.10 [−9.73, −2.47]	−9.80 [−12.62, −6.98]	NR	NR	NR	NR	NR	NR	NR	NR	NR	NR
(2) Chinese medicine combined with conventional therapy versus placebo combined with the same conventional therapy												
Qing xuan granule [29]	−1.15 [−6.17, 3.87]	−2.24 [−6.66, 2.18]	−0.91 [−6.33, 4.51]	−2.11 [−6.76, 2.54]	0.53 [−4.83, 5.89]	−1.69 [−5.92, 2.54]	0.51 [0.18, 1.44]	NR	−34.07 [−55.89, −12.25]	NR	NR	NR

AE: antihypertensive effect.
NSBPDR: nighttime systolic blood pressure decreased rate.
NDBPDR: nighttime diastolic blood pressure decreased rate.
RARBPR: reversed abnormal rhythm of blood pressure rate.
NR: not reported, the article did not report any information about this item.
NO: not observed, the article reported that no adverse effects were observed in the studies.
Outcomes marked ∗ were MD; others were RR.

Table 4: Herbal medicines and adverse effects in the included trials.

Name of herbal medicines	Formulation	Compositions	Adverse events	Study ID
Xiandan tongmai	Decoction	Herba Epimedii Brevicornus 15 g, Rumulus Ginnamomi 10 g, Radix Salviae Miltiorrhizae 15 g, Fructus Macrocarpii 10 g, Fructus Lycii 10 g, Herba Taxilli Chinensis 10 g, Cortex Eucommiae 10 g, Radix Notoginseng 3 g, Radix Angelicae Sinensis 10 g, Rhizoma Chanxiong 10 g, Rhizoma Anemarrhenae 6 g, Cortex Phellodendri Amurensis 6 g, Radix Achyranthis Bidentatae 10 g	Two patients felt gastrointestinal discomfort and sick in treatment group, but symptoms disappeared with medication after meal instead	Kang and Fan 2013 [22]
Xuezhikang	Capsule	Ultivarietas Oryzae Sativae et Monasci (dosage not available)	Not reported	Li 2012 [24]
Gouteng siwu	Decoction	Herba Taxilli Chinensis 12 g, Radix Achyranthis Bidentatae 12 g, Ramulus Uncariae Rhynchophyllae cum Uncis 30 g, Concha Haliotidis 20 g, Rhizoma Gastrodiae 15 g, Rhizoma Chanxiong 15 g, Rhizoma et Radix Notopterygii 6 g, Radix Rehmanniae 15 g, Radix Paeoniae Alba 15 g	One patient had mild nausea and felt epigastric discomfort for two days, but symptoms were relieved by themselves without treatment or stopping medication	Liang 2011 [28]
Xiang tian ma	Decoction	Ziziphora Clinopodioides Lam 12 g, Radix et Rhizoma Rhodiolae Kirilowii 12 g, Radix Rehmanniae 12 g, Flos Rosae Rugosae 12 g, Apocynum venetum L 20 g, and so on	Not observed	Ma et al. 2013 [23]
Qianyang yuyin	Decoction	Herba Bidentis Bipinnatae, Radix Scrophulariae, Fructus Macrocarpii, Radix Polygoni Multiflori, Rhizoma Alismatis, Radix Achyranthis Bidentatae (dosage not available)	Not reported	Ma 2013 [18]
Tianma shuxin	Granule	Rhizoma Gastrodiae, Radix Achyranthis Bidentatae, Concha Ostreae, Radix Paeoniae Rubra, Cocculus orbiculatus (L.) DC, Rhizoma Alismatis, Radix Scrophulariae, Hirudo (dosage not available)	In treatment group, one had mild nausea, one had epigastric fullness, and one had increased stool frequency, but symptoms disappeared after 3-4 days without drug withdrawal	Pan 2012 [17]
Sangji wendan	Decoction	Folium Mori 10 g, Fructus Tribuli 10 g, Rhizoma Gastrodiae 10 g, Dendranthema lavandulifolium (Fisch. ex Trautv.) Ling et Shih 10 g, Ramulus Uncariae Rhynchophyllae cum Uncis 12 g, Concha Haliotidis 30 g, Pericarpium Citri Reticulatae 6 g, Rhizoma Pinelliae (processed with ginger) 10 g, Fructus Aurantii Immaturus 10 g, poria 12 g, Fructus et Semen Trichosanthis Kirilowii 12 g, Caulis Bambusae in Taeniam 6 g	Not observed	Shi 2011 [20]
Tiao ping kang	Tablet	Fructus Ligustri Lucidui, Herba Epimedii Brevicornus, Caulis et Folium Polygoni Multiflori, Herba Leonuri Japonici, ilex pubescens hook. et arn. and so on (dosage not available)	Not reported	Yan 2008 [27]
Yin gan jing	Decoction	Ramulus Uncariae Rhynchophyllae cum Uncis 20 g, Fructus Evodiae Rutaecarpae 15 g	Not reported	Zhang et al. 2012 [26]
Yangxue qingnao	Granule	Radix Angelicae Sinensis, Rhizoma Chanxiong, Ramulus Uncariae Rhynchophyllae cum Uncis, Radix Paeoniae Alba, Concha Margaritifera Usta, Spica Prunellae Vulgaris, Radix Rehmanniae preparata, Semen Cassiae Obtusifoliae, and so on (dosage not available)	Two patients felt stomach discomfort: symptoms disappeared after medication after meal	Ji and Han 2011 [25]

Table 4: Continued.

Name of herbal medicines	Formulation	Compositions	Adverse events	Study ID
Qin dan	Capsule	Radix Scutellariae Baicalensis, Rhizoma Coptidis, Ramulus Uncariae Rhynchophyllae cum Uncis, Radix Salviae Miltiorrhizae, Rhizoma Chanxiong, Pheretima Aspergillum, Herba Leonuri Japonici, Herba Taxilli Chinensis (dosage not available)	Not reported	Liang 2007 [19]
Songling Xuemaikang	Capsule	Radix Puerariae Lobatae, Margarita, Folium Pini Massonianae (dosage not available)	Not reported	Wang 2011 [21]
Qing xuan	Granule	Rhizoma Gastrodiae 30 g, Folium Ilicis Cornutae Immaturum 30 g, Cortex Eucommiae 30 g, Radix Scutellariae Baicalensis 15 g, Folium Ilicis Cornutae Immaturum 15 g	Two patients complained of dizziness and then stopped taking this drug. One had lobar pneumonia and then took other medicines. Four cases were lost to follow-up	Chen 2012 [29]

Not reported: the article did not report any information about adverse effects. Not observed: the article reported that no adverse effects were observed in the studies.

Nine trials [17, 18, 20, 22–24, 26–29] reported 24 h diastolic SD. Two of them which used amlodipine besylate tablet as control group found a significant effect in lowering 24 h diastolic SD in the experimental group superior to that in the control group, that is Sangji Wendan decoction (MD −2.13; 95% CI −4.34 to 0.08; $n = 40$) and Yin gan jing decoction (MD −0.24; 95% CI −0.46 to −0.02; $n = 80$). The other seven trials did not find significant difference between groups: Xiandan Tongmai decoction combined with amlodipine besylate tablet, Tianma Shuxin granule combined with amlodipine besylate tablet, Xiang tian ma decoction combined with benazepril, Xuezhikang capsule integrated with ACEI and CCB, Qianyang Yuyin granule combined with felodipine and enalapril, Tiao ping kang tablet combined with nifedipine controlled released tablets, and Gouteng Siwu decoction combined with levamlodipine besylate tablet.

Day systolic SD was reported by nine trials. Five trials [17–23, 25, 27] significantly lowered this outcome in experimental group superior to that in control group. They were Qin dan capsule plus enalapril maleate tablet (MD −2.15; 95% CI −3.39 to −0.91; $n = 61$), Xiandan Tongmai decoction plus amlodipine besylate tablet (MD −1.40; 95% CI −2.63 to −0.17; $n = 118$), Xiang tian ma decoction plus benazepril (MD −4.56; 95% CI −5.85, −3.27; $n = 78$), Yangxue Qingnao granule plus conventional antihypertensive drugs (MD −0.50; 95% CI −0.81 to −0.19; $n = 160$), and Tiao ping kang tablet plus nifedipine controlled released tablets (MD −3.87; 95% CI −6.16 to −1.58; $n = 58$). The other four trials did not find significant difference between groups, one trial about Qianyang Yuyin granule plus felodipine with enalapril and three trials compared amlodipine besylate tablets, that were Tianma Shuxin granule, Sangji Wendan decoction, and Songling Xuemaikang capsule.

Day diastolic SD was reported by nine trials [17–23, 25–27]. Five trials found the effect of lowering this outcome in experimental group superior to that in control group. They were Qin dan capsule combined with enalapril maleate tablet (MD −2.20; 95% CI −3.26 to −1.14; $n = 61$), Songling Xuemaikang capsule combined with amlodipine besylate tablet (MD −0.60; 95% CI −1.08 to −0.12; $n = 138$), Xiandan Tongmai decoction combined with amlodipine besylate tablet (MD −1.90; 95% CI −3.28 to −0.52; $n = 118$), Xiang tian ma decoction combined with benazepril (MD −1.14; 95% CI −2.09 to −0.19; $n = 78$), and Tiao ping kang tablet combined with nifedipine controlled released Tablets (MD −4.95; 95% CI −7.10 to −2.80; $n = 58$). Although the other four trials had reported this outcome too, there was no statistically significant difference. The four trials were Tianma Shuxin granule combined with amlodipine besylate tablet, Qianyang Yuyin granule combined with felodipine and enalapril, Yangxue Qingnao granule combined with conventional antihypertensive drugs, and Sangji Wendan decoction combined with amlodipine besylate tablet.

Nine trials [17–23, 25, 27] reported night systolic SD. Six trials showed a reduction of night systolic SD. Two of them are compared with amlodipine besylate tablet; they were Songling Xuemaikang capsule (MD −0.60; 95% CI −1.08 to −0.12; $n = 138$) and Xiandan Tongmai decoction (MD −1.90; 95% CI −3.28 to −0.52; $n = 118$), besides, Xiang tian ma decoction combined with benazepril (MD −1.14; 95% CI −2.09 to −0.19; $n = 78$), Qin dan capsule combined with enalapril maleate tablet (MD −2.20; 95% CI −3.26 to −1.14; $n = 61$), Tiao ping kang tablet combined with nifedipine controlled released tablets (MD −4.95; 95% CI −7.10 to −2.80; $n = 58$), and Yangxue Qingnao granule combined with conventional antihypertensive drugs (MD −0.39; 95% CI −0.60 to −0.18; $n = 160$). Three trials showed no significant difference, that is, Tianma Shuxin granule combined with amlodipine besylate tablet, Qianyang Yuyin granule combined with felodipine and enalapril, and Sangji Wendan decoction combined with amlodipine besylate tablet.

There were nine trials [17–23, 25, 27] reporting night diastolic SD. Three trials showed significant reduction of this outcome: Xiang tian ma decoction combined with benazepril (MD −1.19; 95% CI −2.14 to −0.24; $n = 78$), Yangxue Qingnao granule combined with conventional antihypertensive drugs (MD −0.21; 95% CI −0.36 to −0.06; $n = 160$), and Qin dan capsule combined with enalapril maleate tablet (MD −1.40; 95% CI −2.51 to −0.29; $n = 61$). Results of the remaining six trials had no statistical differences.

(2) CV after Treatment. Only one trial (Tianma Shuxin granule combined with amlodipine besylate tablet) reported CV. There were statistically significant differences in two outcomes. There was a reduction in day systolic CV in experimental group superior to that in control group (MD −0.01; 95% CI −0.02 to −0.00; $n = 60$). There was a reduction in 24 h diastolic CV in experimental group inferior to that in control group (MD 0.03; 95% CI 0.02 to 0.04; $n = 60$). Nevertheless, there was a reduction in day systolic CV in control group inferior to that in experimental group (MD −0.01; 95% CI −0.02 to −0.00; $n = 60$). There was no statistically significant advantage in reducing CV in experimental group in terms of 24 h systolic CV, day diastolic CV, night systolic CV and night diastolic CV.

(3) BP after Treatment. Seven trials [18, 19, 21, 24–26, 28] presented that integrative medicine had the advantage in reducing 24 h systolic BP. Six trials [18, 21, 23, 25, 26, 28] presented that integrative medicine had the advantage in reducing 24 h diastolic BP. There were three trials [18, 25, 26] showing that integrative medicine had the advantage in reducing day systolic BP; however, one trial [23] had the opposite result. Four trials [23, 25–27] presented that integrative medicine had the advantage in reducing day diastolic BP. There were five trials [18, 23, 25–27] showing that integrative medicine had the advantage in reducing night systolic BP. Four trials [18, 25–27] presented that integrative medicine had the advantage in reducing night diastolic BP.

(4) Antihypertensive Effect. Antihypertensive effect was measured taking clinical guideline of new drugs for TCM as standard. Only one trial [26] showed treatment group superior to control group in improving antihypertensive effect.

(5) QOL. One trial [23] referred to QOL but did not report which specific test scale it used.

(6) Nighttime BP Decreased Rate. Three trials [19, 26, 28] reported this outcome. Only one trial [26] presented that

combination therapy is superior to conventional treatment in nighttime BP decreased rate of both systolic BP and diastolic BP.

(7) Frequency of Reversed Abnormal Rhythm of BP. Two trials [25, 27] showed treatment group superior to control group in increasing frequency of reversed abnormal rhythm of BP.

3.3.2. Chinese Medicine Combined with Conventional Therapy versus Placebo Combined with the Same Conventional Therapy. There was only one trial [29] under this category, that is, Qing xuan granule combined with amlodipine besylate tablet versus placebo combined with amlodipine besylate tablet.

(1) SD after Treatment. All the outcomes about SD of this trial were of significant statistical heterogeneity. Qing xuan granule combined with amlodipine besylate tablet had a better efficacy than the control in terms of lowering 24 h systolic SD (MD −1.47; 95% CI −2.52 to −0.42; $n = 90$), 24 h diastolic SD (MD −1.26; 95% CI −1.93 to −0.59; $n = 90$), day systolic SD (MD −1.60; 95% CI −2.65 to −0.55; $n = 90$), day diastolic SD (MD −1.02; 95% CI −1.70 to −0.34; $n = 90$), night systolic SD (MD −2.02; 95% CI −3.45 to −0.59; $n = 90$), and night diastolic SD (MD −1.54; 95% CI −2.62 to −0.46; $n = 90$).

(2) CV after Treatment. No noteworthy statistical differences of this endpoint in any of the trials were noted.

(3) BP after Treatment. There was no significant difference between the experimental and the control groups regarding this outcome which contained 24 h systolic BP, 24 h diastolic BP, day systolic BP, day diastolic BP, night systolic BP, and night diastolic BP.

(4) Antihypertensive Effect. There was no significant difference between the experimental and the control groups regarding this outcome.

(5) QOL. There was also no significant difference between the experimental and the control groups regarding this outcome which was measured by SF-36 health related QOL scale.

(6) Nighttime BP Decreased Rate. It was not reported in this trial.

(7) Frequency of Reversed Abnormal Rhythm of BP. It was not reported in this trial.

3.4. Safety. There were 9 trials reporting 50 cases of adverse events. The experimental groups had 18 patients with side reactions, and the control groups had 29 patients with side reactions. Three patients had adverse events but with no specific group information. No significant difference about adverse events was found between two groups. The most commonly reported adverse events in the 9 trials were intestinal disturbance (abdominal distension, nausea, and constipation) [17, 22, 25, 28], ankle edema [17, 27], dizziness [22, 27, 29], palpitation [22], facial flushing [26], and dry cough [19, 24].

4. Discussion

There are thirteen RCTs including 1103 participants that were included in this systematic review. From this review, we may be able to speculate that both the TCM and combination therapy have a significant effect in lowering BP, lowering BPV, and adjusting the circadian rhythm. As we known, efficacy of amlodipine besylate tablets in lowering BP variation is better than other western medicines. Most of trials in this paper selected amlodipine besylate tablets as conventional therapy in the compare group of Chinese medicine combined with conventional therapy versus the same conventional therapy. One trial took placebo combined with conventional therapy as control group. According to TCM theories, the treatment is based on syndrome differentiation, and even the same disease could have a variety of syndromes; therefore, the treatments could be modified with different Chinese herbal medicines. Although the differences in TCM prescription, forms, course of treatment, and control drugs prevent us from performing meta-analysis which could provide precise effect estimate of intervention, from Table 4 we gladly found that there were two kinds of TCM (Ramulus Uncariae Rhynchophyllae cum Uncis and Radix Achyranthis Bidentatae) that appeared most. The most TCM syndromes were yin deficiency and yang excess. This is also consistent with the theory of TCM. It was confirmed that the integrative medicine based on syndrome differentiation, a person-centered and balanced medicine [30], was safer and more effective than western medicine alone in the treatment of hypertension [31]. Adverse reaction related to Chinese medicine to reduce BPV is relatively rare. Only a few patients had ankle edema, dizziness, and nausea during the treatment.

It is too early to recommend this conclusion to clinical practitioners considering the limitations of this review. Firstly, the methodological quality of included trials in the review generally needs to be improved. Studies have shown that the degree of rigorous design and quality of methodology of the study have a direct impact on the effectiveness of intervention [32, 33]. The randomization was unclear in most of trials. Only five RCTs described random allocation in detail, and two RCTs mentioned random hidden method. Blinding is an effective way to control measurement bias; however, only one trial mentioned double-blind; no trial reported estimation of sample size. Moreover, this review focuses on short-term BPV and all of the included trials did not have follow-up research, so we cannot evaluate long-term effect of Chinese herbal medicine for BPV. In addition, all the trials did not publish their protocols, so we can only judge their reporting bias by a compromise method, which is comparing whether the outcomes mentioned in method and results are consistent. Two trials reported QOL, but only one trial evaluated QOL by certain scale. Fifth, due to the clinical features of hypertension, hypertensive patients commonly also suffered from other diseases, such as coronary heart disease or hyperlipidemia, but only a small number of clinical trials on the baseline data reported these accompanied diseases. Most of the other tests did not report this information, but we cannot rule out the possibility of patients with accompanied disease. Sixth, we only included

13 trials with a relative small sample size in this review, and we failed to perform meta-analysis. Therefore, further rigorously designed RCTs are needed before recommending TCM to patients with hypertension. Moreover, we suggest that the design and reporting of RCTs on TCM strictly comply with both CONSORT statement [34] and that for herbal interventions [35].

5. Conclusion

TCM showed potentially short-term beneficial effects on BPV. However, because of small sample size and potential bias of most trials, this result should be interpreted with caution. More high quality trials, safety evidence, and long-term effects are warranted before TCM is recommended as an alternative or complementary medicine for BPV in hypertension patients. Information of QOL and economic effectiveness should also be paid more attention in future clinical trials.

Conflict of Interests

The authors declare that there is no conflict of interests regarding the publication of this paper.

Authors' Contribution

Hao Xu conceived, designed, and revised this systematic review; Jianping Liu designed and revised this systematic review and provided methodological guidance; Zhuo Chen developed the search strategy, did the literature selection, data extraction, and analysis, and wrote the paper; Liqiong Wang helped to develop the search strategy, did literature selection and data extraction, and offered many suggestions; Guoyan Yang assisted to correct mistakes in the paper and checked interpretation.

References

[1] P. M. Rothwell, S. C. Howard, E. Dolan et al., "Prognostic significance of visit-to-visit variability, maximum systolic blood pressure, and episodic hypertension," *The Lancet*, vol. 375, no. 9718, pp. 895–905, 2010.

[2] C. Tsioufis, I. Andrikou, C. Thomopoulos, D. Petras, A. Manolis, and C. Stefanadis, "Comparative prognostic role of nighttime blood pressure and nondipping profile on renal outcomes," *American Journal of Nephrology*, vol. 33, no. 3, pp. 277–288, 2011.

[3] G. Parati, X. Liu, and J. E. Ochoa, "Clinical relevance of visit-to-visit blood pressure variability: impact on renal outcomes," *Journal of Human Hypertension*, vol. 28, pp. 403–409, 2014.

[4] P. Muntner, D. Shimbo, M. Tonelli, K. Reynolds, D. K. Arnett, and S. Oparil, "The relationship between visit-to-visit variability in systolic blood pressure and all-cause mortality in the general population: findings from NHANES III, 1988 to 1994," *Hypertension*, vol. 57, no. 2, pp. 160–166, 2011.

[5] G. Mancia, G. Parati, M. Hennig et al., "Relation between blood pressure variability and carotid artery damage in hypertension: Baseline data from the European Lacidipine Study on Atherosclerosis (ELSA)," *Journal of Hypertension*, vol. 19, no. 11, pp. 1981–1989, 2001.

[6] A. J. Webb, U. Fischer, Z. Mehta, and P. M. Rothwell, "Effects of antihypertensive-drug class on interindividual variation in blood pressure and risk of stroke: a systematic review and meta-analysis," *The Lancet*, vol. 375, no. 9718, pp. 906–915, 2010.

[7] ALLHAT Officers and Coordinators for the ALLHAT Collaborative Research Group, "The Antihypertensive and Lipid-Lowering Treatment to Prevent Heart Attack Trial. Major outcomes in high-risk hypertensive patients randomized to angiotensin-converting enzyme inhibitor or calcium channel blocker vs diuretic: The Antihypertensive and Lipid-Lowering Treatment to Prevent Heart Attack Trial (ALLHAT)," *The Journal of the American Medical Association*, vol. 288, no. 23, pp. 2981–2997, 2002.

[8] H.-H. Xie, F.-M. Shen, L.-P. Xu, P. Han, C.-Y. Miao, and D.-F. Su, "Reduction of blood pressure variability by combination therapy in spontaneously hypertensive rats," *Journal of Hypertension*, vol. 25, no. 11, pp. 2334–2344, 2007.

[9] R. Sega, G. Corrao, M. Bombelli et al., "Blood pressure variability and organ damage in a general population: results from the PAMELA study," *Hypertension*, vol. 39, no. 2, pp. 710–714, 2002.

[10] Z. Y. Zhao, Z. Y. Zhao, Y. Q. Wang, Z. H. Yan, J. Cui, and Y. Y. Li, "Quantitative study of circadian variations of ambulatory blood pressure in Chinese healthy, hypertensive, and diabetes subjects," *Clinical and Experimental Hypertension*, vol. 27, no. 2-3, pp. 187–194, 2005.

[11] Y. Liu, J. C. Zhang, D. Z. Shi et al., "Fluctuant hypertension and platelet activation: current situations and control strategies with integrative medicine," *Zhongguo Zhong Xi Yi Jie He Za Zhi*, vol. 33, no. 7, pp. 869–872, 2013.

[12] World Health Organization and International Society of Hypertension Writing Group, "2003 World Health Organization (WHO)/International Society of Hypertension (ISH) statement on management of hypertension," *Clinical and Experimental Hypertension*, vol. 21, no. 5-6, pp. 1009–1060, 1999.

[13] World Health Organization and International Society of Hypertension Writing Group, "2003 World Health Organization (WHO)/International Society of Hypertension (ISH) statement on management of hypertension," *Journal of Hypertension*, vol. 21, no. 11, pp. 1983–1992, 2003.

[14] Chinese Hypertension Prevention Guide Revision Committee, *Chinese Hypertension Prevention Guide (2005 Revision)*, People's Health Publishing House, Beijing, China, 2006.

[15] Chinese Hypertension Prevention Guide Revision Committee, "Chinese hypertension prevention guide 2010," *Chinese Jounal of Hypertension*, vol. 19, no. 8, pp. 701–708, 2011.

[16] J. P. T. Higgins and S. Green, *Cochrane Handbook for Systematic Reviews of Interventions. Version 5.1.0*, The Cochrane Collaboration, Oxford, UK, 2011, http://handbook.cochrane.org/.

[17] L. M. Pan, *The Study of TCM Syndromes in Elderly Hypertensive Patients and Evaluation between Syndromes and Blood Pressure Variability and Treatment with TCM*, China Academy of Chinese Medical Sciences, Beijing, China, 2012.

[18] N. S. Ma, *Study on Influence of Qian Yang Yu Yin Granules on Blood Pressure Variability of the Patients with Hypertension*, Nanjing University of Chinese Medicine, Nanjing, China, 2013.

[19] L. Liang, *Clinic Study on the Effects of Qin Dan Capsule in Treating Essential Hypertension Patients of "Liver Fire and Blood Stagnation"*, Shandong University, Jinan, China, 2007.

[20] M. Shi, *The Clinical Study of Sang Ji Wen Dan Decoction Treatment on Hypertension in Old Patients with Liver Yang Hyper Activity and Phlegm-Fire Syndrome*, Nanjing University of Chinese Medicine, Nanjing, China, 2011.

[21] F. Q. Wang, "Efficacy observation of Song ling xue mai kang combined with amlodipine in treating essential hypertension patients," *Jilin Journal of Traditional Chinese Medicine*, vol. 31, no. 2, pp. 149–150, 2011.

[22] X. X. Kang and P. Fan, "The treatment of Xian Dan Tong Mai decoction in elderly hypertension patients," *Shandong Journal of Traditional Chinese Medcine*, vol. 32, no. 10, pp. 723–725, 2013.

[23] L. Ma, J. He, and H. B. Li, "The impact of Xiang Tian Ma decoction on blood pressure variability in patients of deficiency of Yin and internal dry," *Xinjiang Journal of Traditional Chinese Medicine*, vol. 31, no. 1, pp. 11–13, 2013.

[24] Y. L. Li, "Effects of combined application of xuezhikang capsule with hypotensive drug on ambulatory blood pressure and blood pressure Variability," *Guide of China Medicine*, vol. 10, no. 6, pp. 41–43, 2012.

[25] R. L. Ji and Q. H. Han, "Efficacy research on Yang xue qing nao particles in patients with hypertension," *Chinese Journal of Integrative Medicine on Cardio-cerebrovascular Disease*, vol. 9, no. 3, pp. 263–265, 2011.

[26] W. N. Zhang, H. F. Huang, and X. Z. Tang, "Influence of medicine leading to the liver channel in antihypertensive efficacy of amlodipine in the elderly hypertensive patients," in *The Tenth TCM Academic Communication of Prevention and Treatment of Senile Diseases*, Xianmen, China, 2012.

[27] Z. Q. Yan, *The Effect of Tiao Ping Kang Discus in Diurnal Rhythm and the Clinical Therapeutic Effect in Essential Hypertension Patients*, Guangzhou University of Chinese Medicine, Guangzhou, China, 2008.

[28] C. G. Liang, *The Study on the "Gou Teng Si Wu Tang" Treating Level 1,2 Elderly Hypertension*, Shandong University of Chinese Medicine, Jinan, China, 2011.

[29] J. Chen, *The Intervention Effects of Qingxuan Granule on Endothelial Injury Induced by Inflammatory Reaction of Hypertensive Patients*, China Academy of Chinese Medical Sciences, Beijing, China, 2012.

[30] X.-G. Sun, W.-K. Wu, and Z.-P. Lu, "Chinese integrative medicine: translation toward person-centered and balanced medicine," *Chinese Journal of Integrative Medicine*, vol. 18, no. 1, pp. 3–6, 2012.

[31] S.-L. Chen, X.-Y. Liu, W.-M. Xu, W.-Y. Mei, and X.-L. Chen, "Clinical study of Western medicine combined with Chinese medicine based on syndrome differentiation in the patients with polarized hypertension," *Chinese Journal of Integrative Medicine*, vol. 18, no. 10, pp. 746–751, 2012.

[32] N. Freemantle, M. Calvert, J. Wood, J. Eastaugh, and C. Griffin, "Composite outcomes in randomized trials: greater precision but with greater uncertainty?" *The Journal of the American Medical Association*, vol. 289, no. 19, pp. 2554–2559, 2003.

[33] L. L. Kjaergard, J. Villumsen, and C. Gluud, "Reported methodologic quality and discrepancies between large and small randomized trials in meta-analyses," *Annals of Internal Medicine*, vol. 135, no. 11, pp. 982–989, 2001.

[34] K. F. Schulz, D. G. Altman, and D. Moher, "CONSORT 2010 statement: updated guidelines for reporting parallel group randomized trials," *Annals of Internal Medicine*, vol. 152, no. 11, pp. 726–732, 2010.

[35] J. J. Gagnier, H. Boon, P. Rochon, D. Moher, J. Barnes, and C. Bombardier, "Reporting randomized, controlled trials of herbal interventions: an elaborated CONSORT statement," *Annals of Internal Medicine*, vol. 144, no. 5, pp. 364–367, 2006.

Hindawi Publishing Corporation
Evidence-Based Complementary and Alternative Medicine
Volume 2015, Article ID 391065, 6 pages
http://dx.doi.org/10.1155/2015/391065

Research Article

Hypolipidemic Activity and Antiatherosclerotic Effect of Polysaccharide of *Polygonatum sibiricum* in Rabbit Model and Related Cellular Mechanisms

Jun-xuan Yang,[1] Shen Wu,[2] Xi-liang Huang,[3] Xiao-quan Hu,[4] and Yi Zhang[5]

[1]*School of Traditional Chinese Medicine, Chongqing Medical University, Chongqing 400016, China*
[2]*Department of Laboratory Medicine, Guiyang Medical College, Guiyang, Guizhou 550004, China*
[3]*Department of Cardiology, Fuzhou City First People's Hospital, Fuzhou, Jiangxi 344000, China*
[4]*Department of Urology, Ningbo Zhenhai People's Hospital, Ningbo, Zhejiang 315202, China*
[5]*Chongqing Institute for Food and Drug Control, Chongqing Engineering Center for Pharmaceutical Process and Quality Control, China*

Correspondence should be addressed to Yi Zhang; liuy02004@163.com

Received 28 June 2014; Revised 11 August 2014; Accepted 19 August 2014

Academic Editor: Qunhao Zhang

Objective. To evaluate the hypolipidemic activity and antiatherosclerotic effect of polysaccharide of *Polygonatum sibiricum* (PPGS), which is a kind of Chinese herbal medicine using the rhizome part of the whole herb. *Materials and Methods*. Thirty rabbits were divided into normal control group, model control group, and PPGS subgroups of 0.8, 1.6, and 3.2 mL/kg/day under random selection. In atherosclerosis model, the effects of PPGS on diverse blood lipids, foam cells number, and aortic morphology were evaluated. In the primary culture of endothelial cells (ECs), the activities of PPGS on both ECs proliferation and ECs injury were studied as well. *Results*. In atherosclerosis model, the hypolipidemic activities of PPGS were mainly focused on TC, LDL-C, and Lp(a). All changes on these factors were statistically significant compared with model group ($P < 0.01$), except TG and HDL-C. The intimal foam cell number of PPGS subgroups (0.8, 1.6, and 3.2 mL/kg/day) was significantly reduced than model control ($P < 0.01$). In the primary culture of endothelial cells (ECs), PPGS showed no effect on cell proliferation but preferred to protect EC from injury and apoptosis induced by H_2O_2 and lipopolysaccharide (LPS). *Discussion and Conclusion*. The antiatherosclerotic effect of PPGS may be supported by its hypolipidemic activities, improving aortic morphology, and reducing foam cells number and ECs injury.

1. Introduction

Plenty of studies showed that polysaccharide of *Polygonatum sibiricum* (PPGS), a popular Chinese herbal medicine in China, performed variety of medical effects such as anti-inflammation [1], antioxidation, and antiaging [2]. In Chinese database, there were only a few studies reporting the antiatherosclerotic effect of single dose of PPGS with no cellular mechanisms in detail [3, 4]. Therefore, the aims of this paper were to evaluate the possible cellular mechanism of PPGS on antiatherosclerosis based on endothelial cells (ECs) and smooth muscle cells (SMCs) and finally to further clarify the possible role of PPGS in the development of atherosclerosis process.

2. Materials and Methods

2.1. Animals. Thirty healthy male New Zealand rabbits in general grade with body mass of 1.9–2.4 kg were from Experimental Animal Center of Chongqing in China. Rabbits were kept in the cages with the condition of natural light, room temperature, relative humidity of (50 ± 3)%, and automatic ventilation. They were fed fixed dose of food with free access to drinking water. After the adaptive feeding for 7 d, animals were randomly divided into five groups (normal control group and model subgroups: model control group and PPGS subgroups (0.8, 1.6, and 3.2 mL/kg/day)). This study received the approval of Local Animal Ethics Advisory Committee.

2.2. Drugs, Chemicals, and Instruments. The PPGS extract (content of polysaccharide ≥90%) was purchased from Department of Preparation of Chongqing Chinese Medicine Hospital (Chongqing, China). The other reagents also included M199 medium and fetal bovine serum (Hyclone Co., Ltd., Utah, USA), II collagenase and trypsin (Invitrogen Corporation, Grand Island, USA), CCK-8 kit (Dojindo Laboratories, Kyushu, Japan), crystal violet (Sigma Chemical Co., St. Louis, USA), saline (for infusion, Kelun Co., Ltd., Sichuan, China), and neonatal umbilical cord (The Affiliated Hospital of Harbin Medical University, Harbin, China). The rabbit basal diet and relative high cholesterol diet were prepared from Experimental Animal Center of Chongqing Medical University (Chongqing, China) according to the reference study [5].

2.3. Hypolipidemic Activity and Antiatherosclerotic Effect in High Fat Diet-Induced Rabbit Model. Normal control group was fed with basal diet, while model subgroups were fed with high cholesterol diet. Each rabbit was given quantitative diet of 120 g/d, in which all were basal diet for normal control group and it was composed of 40 g/d high cholesterol diet and 80 g/d basic diet in model subgroups. The PPGS subgroups were also fed with different concentrations of PPGS (0.8, 1.6, and 3.2 mL/kg/day). The dose for animal model was converted from clinical dosage. During the feeding, high cholesterol diet was given firstly, and basal diet was supplemented with free access to water for 8 weeks.

After expiration of 8-week feeding with 10 h fasting, the venous blood was obtained for lipid levels testing (total cholesterol (TC), total triglycerides (TG), high-density lipoprotein (HDL-C), low-density lipoprotein (LDL-C), and lipoprotein (a) (Lp(a))). Then rabbits were sacrificed for study. In the experiments of HE staining, after conventional dehydration, paraffin sections were prepared for HE staining. Associated pathological changes of intima and adventitia under optical microscopy were recorded. Under certain magnification (20 × 10), eyepiece micrometer and hand control counters were applied to count foam cells number on 5 small lattices, taking the mean value of all slices to get cell number on each 1 mm^2, which was seen as foam cell number per unit area of intima.

2.4. The Effects of PPGS on ECs and SMCs. Human umbilical vein endothelial cells (HUVECs) from umbilical cord were isolated by enzymatic digestion according to the method mentioned before [6]. Human umbilical artery smooth muscle cells (HUASMCs) were obtained by tissue adherent method [7, 8]. The digestion solution of 0.25% trypsin was prepared and added to serum medium. The supernatant was discarded after centrifugation; culture fluid was added to mix the cells and finally put them into culture flasks for cells growing at 37°C with 5% CO_2. The third generations were used for the following experiments.

200 μL of ECs or SMCs was seeded in 96-well plates according to the condition of 5×10^3 cells/hole. After 24 h incubation, adherent cells were randomly divided into four groups: (1) control group, the culture medium (containing 20% fetal bovine serum), and (2) subgroups with different concentrations intervention of PPGS (25, 50, and 100 μg/mL) in cultured cells. EC was cultured in drug-containing medium for 12, 24, and 48 h, while HUASMC was for 12, 18, and 24 h. Each dose subgroup was given five subholes. 10 μL CCK-8 reagent was added into each hole for 2 h before the termination of culture. The absorbance of cell supernatant was detected at the wavelength of 450 nm, and cell culture medium was used as blank control of zero absorbance. In addition, the migration ability of HUASMC was determined by transwell migration chamber (8 μm pore size) following the previous study [9]. The migration abilities of HUASMC in each group were estimated after the cells were fixed by 4% paraformaldehyde for 10 min, stained by crystal violet, and randomly selected under a fluorescence microscope with the magnification of 200x to count the number of cells migrating to the bottom of porous membrane.

2.5. The Effect on H_2O_2-Induced EC Injury. 100 μmol/L of H_2O_2 was selected as testing concentration. The main process was introduced in another study [10]. Each treatment group was given drug into medium with the final concentration of 10%. The normal control group was only administrated with medium. The model control group contained medium plus 100 μmol/L of H_2O_2. The low dose treatment group was 0.3 mg/kg PPGS in cell medium plus 100 μmol/L H_2O_2. The concentrations of PPGS in middle and high dose treatment group were 0.6 and 1.2 mg/kg, respectively. The cytokines (malondialdehyde (MDA) and superoxide dismutase (SOD)) were tested by related testing kits.

2.6. The Effect on Lipopolysaccharide- (LPS-) Induced EC Injury. After 24 h incubation, ECs were fused in adherent monolayer way [11]. The adherent cells were randomly divided into five groups the same as mentioned above. The suspension was abandoned and renewed; related drug was added into each group at the same time. After cell culture for 24 h at 37°C with 5% CO_2, the old medium was abandoned. And 3 mL serum medium containing 5 μg/mL of LPS was added into each group. The cells in each group were washed with PBS for 3 times 24 h later. Then 4% formaldehyde was used to fix them for 30 min. After washing for 3 times again with PBS solution, Hoechst 33258 fluorescent staining with the final concentration of 0.5 μg/mL was done for 10 min in the dark at room temperature. The residual staining solution was discarded. The cellular washing was repeated again for 3 times. The fluorescence in the dark was observed in microscope at the wavelength of 350 nm. The cells in five different fields of picture view and cell apoptosis were calculated for each hole.

2.7. Statistical Analysis. Results were expressed in the form of mean ± SEM. Data were analyzed by one-way ANOVA, followed by Student's two-tailed t-test for comparison between two groups. $P < 0.05$ means statistically significant.

3. Result

3.1. Hypolipidemic Activity. After the treatment, the serum level of HDL-C and TG did not change basically. From

Table 1: The hypolipidemic effects of PPGS in atherosclerosis rabbit model ($n = 6$).

Groups	TC		LDL-C		Lp(a)	
	Before	After	Before	After	Before	After
Normal control	1.26 ± 0.25	1.40 ± 0.33	1.18 ± 0.26	1.26 ± 0.17	50.41 ± 10.33	67.32 ± 15.13
Model control	1.24 ± 0.31	12.18 ± 2.40	1.17 ± 0.24	10.46 ± 1.53	47.35 ± 15.16	643.72 ± 151.69
PPGS (0.8 mL/kg/day)	1.31 ± 0.40	7.82 ± 4.13**	1.20 ± 0.31	6.42 ± 3.48**	49.52 ± 8.82	81.40 ± 26.73**
PPGS (1.6 mL/kg/day)	1.38 ± 0.41	5.81 ± 1.92**	1.25 ± 0.27	4.61 ± 1.56**	51.9 ± 14.83	47.36 ± 15.39**
PPGS (3.2 mL/kg/day)	1.32 ± 0.37	4.5 ± 2.11**	1.22 ± 0.25	3.45 ± 0.73**	46.68 ± 14.81	33.52 ± 12.68**

Note: compared with model control group, $^{**}P < 0.01$.

Table 2: The effects of PPGS on HUASMCs proliferation and migration ($n = 6$).

Groups	OD values			Cells migration number 24 h later ($n = 3$)
	12 h	24 h	48 h	
Normal control	0.186 ± 0.024	0.202 ± 0.022	0.215 ± 0.027	39.1 ± 4.2
PPGS (0.3 mg/kg)	0.172 ± 0.020	0.171 ± 0.024*	0.177 ± 0.019*	35.8 ± 4.6
PPGS (0.6 mg/kg)	0.159 ± 0.022*	0.162 ± 0.017**	0.169 ± 0.015**	33.2 ± 4.3*
PPGS (1.2 mg/kg)	0.138 ± 0.015*	0.141 ± 0.015**	0.155 ± 0.018**	30.6 ± 4.1**

Note: compared with model control group, $^{*}P < 0.05$ and $^{**}P < 0.01$.

Table 1, the results of other parameters were showed. All concentrations of PPGS were markedly effective on blood lipids control ($P < 0.01$).

3.2. The Results of HE Staining in Atherosclerotic Model. Aortic elastic membrane in normal diet group was integral. Endothelium was close to the internal elastic membrane arranged in neat rows, with smooth muscle and middle elastic membrane arranged in parallel. In model control group, aortic intima was significantly thickening with a large accumulation of foam cells. ECs were falling off or loosely attached to the membrane surface. Intimal lesions had extensively pathological changes with collagen fiber glass. Elastic fiber was ruptured and disappeared as well. In PPGS subgroups, compared with the thickening degree of aortic intima in model control group, subendothelial gap was increased with visible foam cells aggregation, but foam cells number was significantly less than model control group. The structure of medial membrane was basically integral with SMCs in the same pole, as shown in Figure 1 (200x).

3.3. The Effects of PPGS on Foam Cell Number in Atherosclerotic Model. As shown in Figure 2, PPGS could significantly reduce the foam cells number in atherosclerosis model.

3.4. The Effect of PPGS on EC Proliferation. ECs were cultured in drug-containing medium for 12, 24, and 48 h. After that, the OD values of culture supernatants in each group were recorded. The results demonstrated that, compared with control group, there was no obvious effect on ECs proliferation for PPGS subgroups (no data shown).

3.5. The Effect of PPGS on H_2O_2-Induced EC Injury. The concentration of cytokines (MDA and SOD) expressed by EC can indirectly respond to the injury degree of EC induced by H_2O_2. Therefore, Figure 3 showed some data in detail to prove the protection effect of PPGS on EC injury. MDA rising meant that EC was damaged under the condition of H_2O_2 oxidation. Meanwhile, the activity of SOD was also decreased. PPGS had the protection effect to reverse oxidative injury.

3.6. The Effect on LPS-Induced EC Injury. After Hoechst 33258 fluorescent staining, the cell apoptosis could be identified with different color. Figure 4 identified that PPGS had protection effect on LPS-induced cell apoptosis.

3.7. The Effect of PPGS on SMCs Proliferation. SMCs were cultured in drug-containing medium for 12, 18, and 24 h. The OD values of culture supernatants in each group were tested (Table 2). The results demonstrated that, compared with control group, there was obvious inhibition effect on SMCs proliferation for PPGS subgroups (0.6 and 1.2 mg/kg), which also showed significant prevention activity on SMCs migration ($P < 0.05$) (Table 2 and Figure 5).

4. Discussion

Inflammatory mediators may play an important role in the occurrence and development process of atherosclerosis. This study evaluated the effect of PPGS on high cholesterol-bearing atherosclerosis model. The results showed that, after the administration of PPGS, the blood levels of TC, LDL-C, and Lp(a) were decreased but not TG or HDL-C. It might mean that the hypolipidemic activities of PPGS mainly focused on hypercholesterolemia. The LDL-C was also a kind of lipoprotein composed of protein and cholesterol and was sensitive to the concentration of cholesterol in blood.

For the ECs, there was no evidence showing that PPGS had an effect directly on the ECs proliferation. But it had some positive interaction with the ECs apoptosis and injury.

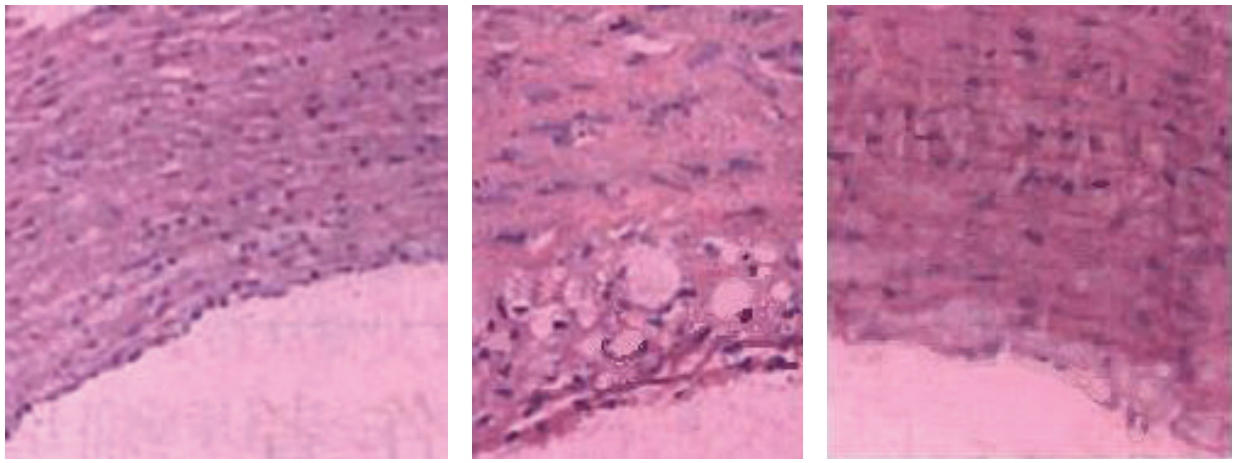

(a) (b) (c)

Figure 1: Microscope camera drawing of HE staining on rabbit thoracic aorta (200x): (a) normal group; (b) model control group; (c) 3.2 mL/kg/day PPGS group.

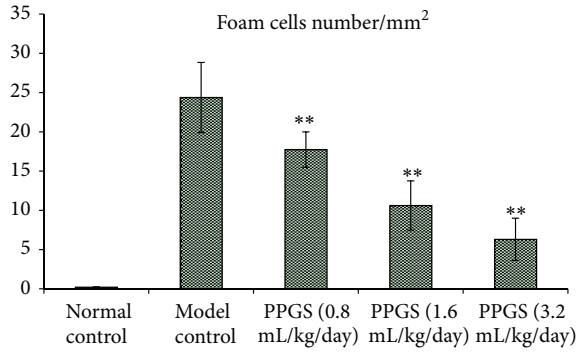

Note: compared with model control group,
$^{*}P < 0.05$ and $^{**}P < 0.01$

Figure 2: The effects of PPGS after being administered continuously for 8 weeks on foam cells number in atherosclerosis rabbit model ($n = 6$).

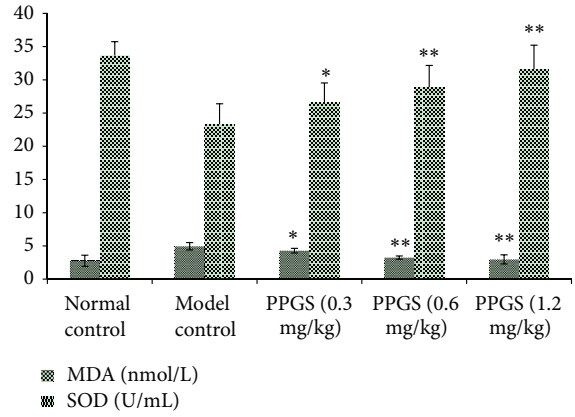

Note: compared with model control group,
$^{*}P < 0.05$ and $^{**}P < 0.01$

Figure 3: The impact of PPGS on EC injury and related cytokines releasing ($n = 6$).

The H_2O_2-induced cell injury may result into necrosis based on strong oxidation reaction. And LPS was more focused on cell apoptosis by inhibiting NOS activity and NO content both inside and outside of cell, but increasing the intracellular ROS level [12]. For another distinction based on physiological response, H_2O_2-induced cell injury may lead to inflammation and thrombosis for its acute oxidation. But the chronic oxidation effect of LPS may finally lead to atherosclerosis and plaque instability [13]. So the protection effects of PPGS on both apoptosis and necrosis of ECs were really impressive, which also indicated the primary mechanism of PPGS on atherosclerosis for the first time.

It was learnt that PPGS was composed of single monosaccharide fructose with the relative molecular mass (Mr) of 7247 [14]. In this study, the purity of PPGS was up to 90% and was good enough to evaluate the hypolipidemic activity and antiatherosclerotic effect of PPGS initially. However,

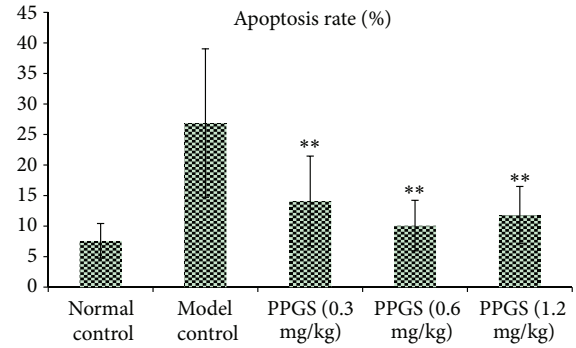

Note: compared with model control group,
$^{*}P < 0.05$ and $^{**}P < 0.01$

Figure 4: The impact of PPGS on EC injury and apoptotic condition ($n = 6$).

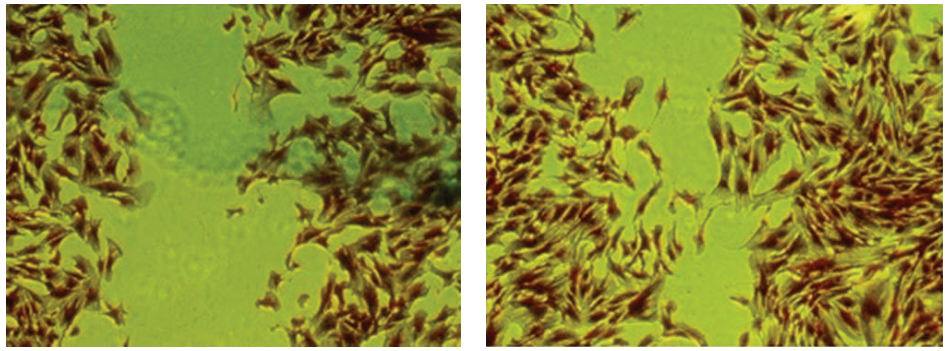

(a) (b)

Figure 5: The crystal violet staining of HUASMCs on each group: (a) 1.2 mg/kg PPGS subgroup and (b) control group (200x).

these activities in long-term period were still unknown, which might be more beneficial for clinical recommendation. Besides, further studies on more animal models with different injury degree of blood vessels were still needed.

Therefore, PPGS might play important roles on antiatherosclerosis in two different levels: (1) one is suppressing the level of blood lipids directly, (2) and another is to protect ECs from apoptosis and necrosis indirectly in cellular level . Thereafter, its activities on smooth muscle cells or other cytokines were also warranted. In one word, they all resulted into the antiatherosclerosis effect of PPGS in cellular level and animal model.

Conflict of Interests

There is no of conflict of interests. The authors alone are responsible for the content and writing of the paper.

Acknowledgment

This work was supported by finances from the Scientific and Technological Research Program of Chongqing Science & Technology Commission (Grant no. cstc2014yykfa110020).

References

[1] F. Y. Chang, "Polygonatum sibiricum Red.Anti-aging regimen and facial make-up role in interpreting," *Chinese Archives of Traditional Chinese Medicine*, vol. 29, no. 3, pp. 593–594, 2011 (Chinese).

[2] T. Debnath, S. R. Park, D. H. Kim, J. E. Jo, and B. O. Lim, "Antioxidant and anti-inflammatory activity of *Polygonatum sibiricum* rhizome extracts," *Asian Pacific Journal of Tropical Disease*, vol. 3, no. 4, pp. 308–313, 2013.

[3] S.-R. Wu, Y.-Y. Li, and X. Wu, "Effect of polygonapolysaccharose on atheromatous plaque: experiment with rabbits," *National Medical Journal of China*, vol. 88, no. 2, pp. 127–130, 2008.

[4] P. Zhang, D. Liu, and Y. Y. Li, "The influence of *Polygonatum sibiricum* polysaccharides on the expressing of IL-6 and CRP in atherosclerotic rabbits," *Journal of Clinical Research*, vol. 23, no. 7, pp. 1100–1101, 2006.

[5] J. Balkan, O. Kanbağli, A. Hatipoğlu et al., "Improving effect of dietary taurine supplementation on the oxidative stress and lipid levels in the plasma, liver and aorta of rabbits fed on a high-cholesterol diet," *Bioscience, Biotechnology, and Biochemistry*, vol. 66, no. 8, pp. 1755–1758, 2002.

[6] T. Wakabayashi, H. Naito, K. Takara et al., "Identification of vascular endothelial side population cells in the choroidal vessels and their potential role in age-related macular degeneration," *Investigative Ophthalmology & Visual Science*, vol. 54, no. 10, pp. 6686–6693, 2013.

[7] M. Artwohl, A. Lindenmair, M. Roden et al., "Fatty acids induce apoptosis in human smooth muscle cells depending on chain length, saturation, and duration of exposure," *Atherosclerosis*, vol. 202, no. 2, pp. 351–362, 2009.

[8] B. G. Ilagan and B. G. Amsden, "Surface modifications of photocrosslinked biodegradable elastomers and their influence on smooth muscle cell adhesion and proliferation," *Acta Biomaterialia*, vol. 5, no. 7, pp. 2429–2440, 2009.

[9] H. Chaulet, C. Desgranges, M.-A. Renault et al., "Extracellular nucleotides induce arterial smooth muscle cell migration via osteopontin," *Circulation Research*, vol. 89, no. 9, pp. 772–778, 2001.

[10] G. Chen and S. H. Yan, "The protection effect of Polygonatum sibiricum polysaccharides on H2O2-induced vascular endothelial cell injury," *Lishizhen Medicine and Materia Medica Research*, vol. 22, no. 3, pp. 623–624, 2011 (Chinese).

[11] W. P. Ni, X. X. Zhu, H. D. Wang, Q. Y. Li, and M. Wan, "Research of polygonatum polysaccharide on the protective mechanism of LPS-induced HUVEC injury," *Chinese Archives of Traditional Chinese Medicine*, vol. 30, no. 12, pp. 2644–2646, 2012 (Chinese).

[12] T. H. Lee, J. Chang, and B. M. Kim, "Saikosaponin C inhibits lipopolysaccharide-induced apoptosis by suppressing caspase-3 activation and subsequent degradation of focal adhesion kinase in human umbilical vein endothelial cells," *Biochemical and Biophysical Research Communications*, vol. 445, no. 3, pp. 615–621, 2014.

[13] J. F. Li, S. Chen, J. D. Feng, M. Y. Zhang, and X. X. Liu, "Probucol via inhibition of NHE1 attenuates LPS-accelerated atherosclero-

sis and promotes plaque instability in vivo," *Experimental and Molecular Pathology*, 2014.

[14] X. Zhang, G. Borjihan, and N. Zhaorigetu, "Determination of relative molecular mass and composition for Polygonatum sibiricum polysaccharide by high performance liquid chromatography," *Chinese Journal of Chromatography*, vol. 23, no. 4, pp. 394–396, 2005 (Chinese).

Hindawi Publishing Corporation
Evidence-Based Complementary and Alternative Medicine
Volume 2015, Article ID 584245, 7 pages
http://dx.doi.org/10.1155/2015/584245

Research Article

Neuroprotection of Sanhua Decoction against Focal Cerebral Ischemia/Reperfusion Injury in Rats through a Mechanism Targeting Aquaporin 4

Lin Lu, Hui-qin Li, Ji-huang Li, Ai-ju Liu, and Guo-qing Zheng

Department of Neurology, The Second Affiliated Hospital & Yuying Children's Hospital of Wenzhou Medical University, Wenzhou 325027, China

Correspondence should be addressed to Guo-qing Zheng; gq_zheng@sohu.com

Received 9 July 2014; Accepted 18 August 2014

Academic Editor: Hao Xu

Sanhua decoction (SHD) is a famous classic Chinese herbal prescription for ischemic stroke, and aquaporin 4 (AQP4) is reported to play a key role in ischemic brain edema. This study aimed to investigate neuroprotection of SHD against focal cerebral ischemia/reperfusion (I/R) injury in rats and explore the hypothesis that AQP4 probably is the target of SHD neuroprotection against I/R rats. Lentiviral-mediated AQP4-siRNA was inducted into adult male Sprague-Dawley rats via intracerebroventricular injection. The focal cerebral ischemia/reperfusion model was established by occluding middle cerebral artery. Neurological examinations were performed according to Longa Scale. Brain water content, was determined by wet and dry weight measurement. Western blot was adopted to test the AQP4 expression in ipsilateral hippocampus. After the treatment, SHD alleviated neurological deficits, reduced brain water content and downregulated the expression of AQP4 at different time points following I/R injury. Furthermore, neurobehavioral function and brain edema after I/R were significantly attenuated via downregulation of AQP4 expression when combined with AQP4-siRNA technology. In conclusion, SHD exerted neuroprotection against focal cerebral I/R injury in rats mainly through a mechanism targeting AQP4.

1. Introduction

Stroke is the second leading cause of death worldwide, and the absolute number of stroke patients and the overall global burden of stroke are great and increasing in the past decades [1]. Ischemic stroke is the most common type of stroke, accounting for 60–80% of all types of strokes. However, intravenous rt-PA is the only Food and Drug Administration approved pharmacological therapy for acute ischemic stroke within 4.5 h after stroke onset [2]. Thus, the short therapeutic window [2], low usage rate [3], and safety concerns [4] have prompted a quest for additional therapeutic approaches to acute ischemic stroke.

In China, where the population is 1.4 billion, stroke is already the leading cause of death and adult disability [5]. Fortunately, the important distinction of China's national medical system and Western medicine is that traditional Chinese medicine (TCM) can be responsible for the health care of Chinese people [6]. TCM practitioners use herbal medicines and various mind and body practices, such as acupuncture and tai chi, to treat or prevent health disorders. Sanhua decoction (SHD), a classic Chinese herbal prescription for stroke, was first recorded in *Suwen Bingji Qiyi Baomingji (Plain Questions: Discourse on Mechanism for Preserving Life)* written by Liu Wansu during the periods of Jin and Yuan Dynasties (1115-1368). In modern times, SHD is still used continuously and widely for treatment of stroke [7, 8]. However, the therapeutic mechanism of SHD against acute ischemic stroke still remains unclear.

The water channel protein aquaporin 4 (AQP4), which is the most abundant water channel in mammalian central nervous system, is widely expressed in the ependymal cells and glial membranes bordering the subarachnoidal space, ventricles, and blood vessels [9]. Since it is the structure

foundation of water homeostasis and transfer between glial cells, cerebrospinal fluid, and blood vessels, AQP4 plays a key role in maintaining brain water in equilibrium when under physiological conditions, formation of brain edema, and clearance of edema liquid when under pathological conditions [10, 11]. For ischemic stroke, genetic deletion of AQP4 ameliorated brain edema following focal ischemic stroke [12]. Thus, modulating the expression of AQP4 after ischemia stoke is a potential target for the treatment of cerebral ischemic edema.

We proposed a hypothesis that downregulation of AQP4 probably is the target of SHD neuroprotection against I/R injured rats. This study aims to investigate whether SHD could alleviate neurological deficit and provide neuroprotective effects in MCAO induced rat model of focal cerebral I/R injury mainly through a mechanism targeting AQP4.

2. Materials and Methods

2.1. Experimental Animals. Adult male Sprague-Dawley rats weighing 230–280 g were provided by Shanghai Laboratory Animal Center, CAS (SLACCAS) (NO., SCXK, Shanghai, 2010-0002). Animals were housed in the room with temperature of 21–23°C, relative humidity of 30–70%, and a 12 h light/12 h dark cycle (lights on at 08:00 h). They had free access to common forage and water. All experimental protocols and animal handling procedures were approved by the local ethical committee for animal research and in accordance with the Guide for the Care and Use of Laboratory Animals issued by the National Academy of Sciences, Institute of Laboratory Animal Resources, Commission on Life Sciences, and National Research Council.

2.2. Preparation of SHD. SHD is composed of four kinds of CHMs: (A) Radix et Rhizoma Rhei; rhubarb root and rhizome (*dahuang*), the dried root of *Rheum officinale* Baill; (B) Rhizoma et Radix Notopterygii; incised Notopterygium Rhizome and root (*qianghuo*), the dried root of *Notopterygium incisum* Ting ex H. T. Chang; (C) Fructus Aurantii Immaturus; immature orange fruit (*zhishi*), the dried fruitlet of *Citrus aurantium* L.; and (D) Cortex *Magnolia officinalis*; officinal magnolia bark (*houpu*), the dried barks of *Magnolia officinalis* Rehd. et Wils. in the ratio of 4 : 2 : 1.5 : 2 on a dry weight basis, respectively. All the CHMs are recorded in the Chinese Pharmacopoeia. Firstly essential oils are extracted and then decocted with water, extracted thrice, filtered, and concentrated; the raw herbs were made into 1 g·mL^{-1} stock solution. The stock solution was stored at 4°C until use.

2.3. Experimental Design. A total of 280 rats were randomly divided into seven groups: sham-operation (Sham) group, cerebral ischemia/reperfusion (I/R) group, Sanhua decoction (SHD) group, Vector group, AQP4-siRNA (RNAi) group, Sanhua decoction + vector (SHD + Vec) group, and Sanhua decoction + AQP4-siRNA (SHD + RNAi) group. Each group was further divided into five subgroups based on different time points. Three days before I/R model establishment, SHD were given to the rats in the three SHD-treated groups by intragastric administration at a dose of 10 g·kg^{-1}·d^{-1}, once a day till the rats were sacrificed. The other four groups were given the same volume of normal saline. The experimental design of the present study was summarized in a flow diagram (Figure 1).

2.4. Focal Cerebral Ischemia/Reperfusion. The focal cerebral ischemia was induced by middle cerebral artery occlusion (MCAO) [13] as described previously in our group [14]. Briefly, the rats were anesthetized by intraperitoneal (i.p.) injection with 10% chloral hydrate at a dose of 350 mg·kg^{-1} after 12 h fasting. After cervical skin preparation and incision, the left common carotid artery (CCA), as well as the external carotid artery (ECA) and internal carotid artery (ICA), was exposed and carefully separated from nerve and tissues. The ECA was clipped and a nylon filament was inserted from it into the lumen of ICA until the blunt tip reached the origin of the MCA. The length of the inserted thread was about 18.5 mm ± 0.5 mm from the CCA bifurcation. Reperfusion was initiated by withdrawal of the occluding filament after 120 min of ischemia. The rats in the Sham group were subjected to the same surgical procedure without suture insertion. Heating pads were used to keep the operated rats warm. A trained operator blinded to the experimental design performed the reversible ischemic injury in animal experiments.

2.5. Intracerebroventricular Injection. The lentivirus-mediated aquaporin 4-small interfering RNA (AQP4-siRNA, LV3-Aqp4-rat-543) and its vector were both obtained from GenePharma (Shanghai, China). The target sequence of AQP4-siRNA was 5′-GCTCCTGGTGGAGCTAATAAT-3′. Two days before I/R surgery, AQP4-siRNA was injected into the lateral ventricle of the ischemic side by intracerebroventricular injection: after being anesthetized by intraperitoneal injection of 10% chloral hydrate at a dosage of 350 mg·kg^{-1}, the rats were mounted in a stereotactic frame (Huaibei Zhenghua Biological Instrument Equipment Co., LTD) and injected with AQP4-siRNA at the rate of 1 μL·min^{-1} with the volume of 10 μL containing 5 μg AQP4-siRNA using the following stereotaxic coordinates [15]: 0.8 mm posterior to the bregma, 1.5 mm left/right to the midline, and 4.5 mm ventral to the bregma. After the injection, the needle remained in the target location for 5 min to avoid the tracer reflux along the needle tract. The corresponding control groups were given the same volume of vector by intracerebroventricular injection.

2.6. Neurological Deficits Scores. Neurological deficits examination was conducted at 6 h, 1 d, 3 d, 7 d, and 14 d after reperfusion by an investigator who was blind to the experiment design according to the five-point scale described previously by Longa et al. [13] as follows: 0 indicated no neurological deficit; 1 mild focal neurological deficit (contralateral forelimb flexion upon lifting the animal tail); 2 moderate focal neurological deficit (circling to the contralateral side when crawling forward); 3 severe focal deficit (falling into the contralateral side when crawling forward); 4 no spontaneous

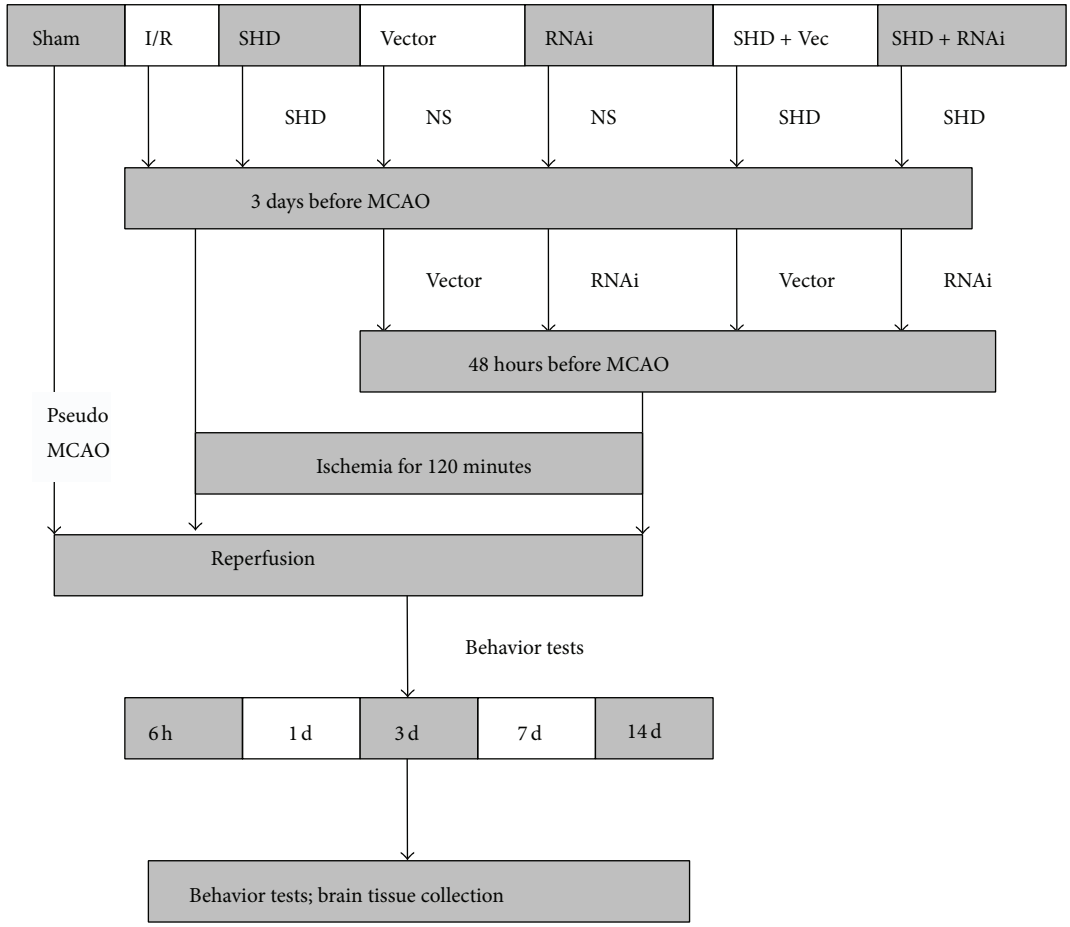

Figure 1: Flow diagram of the experimental protocols. Rats were randomly divided into seven groups. The focal cerebral ischemia/reperfusion model was established in rats by occluding middle cerebral artery (MCAO) with suture for two hours and then extracting the suture. Sham-operated group had the same operation but without suture insertion. In the SHD-treated group, the rats were administered with SHD for 3 days prior to MCAO. In some cases, rats were received by intracerebroventricular injection of either lentiviral-mediated AQP4-siRNA or vehicle 48 hours before ischemic induction. As shown in this figure, neurological functions were observed and brains were collected at indicated time points after reperfusion for brain water content, immunohistochemistry, and western blot analyses. I/R, ischemia/reperfusion group; MCAO, middle cerebral artery occlusion; NS, normal saline; Sham, sham-operated group; SHD, Sanhua decoction-treated group; SHD + RNAi, Sanhua decoction plus AQP4-siRNA-treated group; SHD + Vec, Sanhua decoction plus vector-treated group; RNAi, AQP4-siRNA-treated group; Vector, vector-treated group.

crawling with a depressed level of consciousness or death. Only rats with neurological scores of 1 to 3 were considered successful models and used in the current study.

2.7. Calculation of Brain Water Content. Brain water content was measured by the wet/dry method [16]. Briefly, at each indicated time point after reperfusion, the brains were removed after terminal anesthesia and then divided into ipsilateral and contralateral hemispheres. The two hemispheres were weighed, respectively, both before and after drying at 65°C for 48 h. The brain water content was calculated using the formula: brain water content = (wet weight − dry weight)/wet weight × 100%.

2.8. Western Blotting Analysis. Western blot was adopted to evaluate the expression level of AQP4 in ipsilateral hippocampus. Whole cells of samples were lysed with RIPA lysis buffer (P0013B, Beyotime Institute of Biotechnology, Jiangsu, China) and the protein was determined with a BCA kit (Beyotime Institute of Biotechnology, Jiangsu, China). Equal amount of protein was separated by 10% Tris-glycine SDS-PAGE polyacrylamide gel and transferred to polyvinylidene fluoride membranes (Invitrogen, USA). After blocking for 1.5 h with a 5% solution of skim milk (232100, BD-Difco, USA), the membranes were incubated with the primary antibodies polyclonal rabbit anti-AQP4 (1 : 1000; ab46182, Abcam, USA) or polyclonal rabbit anti-GAPDH (1 : 1000; AP0063, Bioworld Technology, USA) at 4°C overnight, followed by the horseradish peroxidase- (HRP-) linked anti-goat antibody (1 : 10000; Boyun Biotech, Shanghai, China) for 30–60 min at room temperature. After washing with Tris-buffered saline with 0.1% Tween-20 (Beyotime Institute of Biotechnology, Jiangsu, China), the relative intensity of

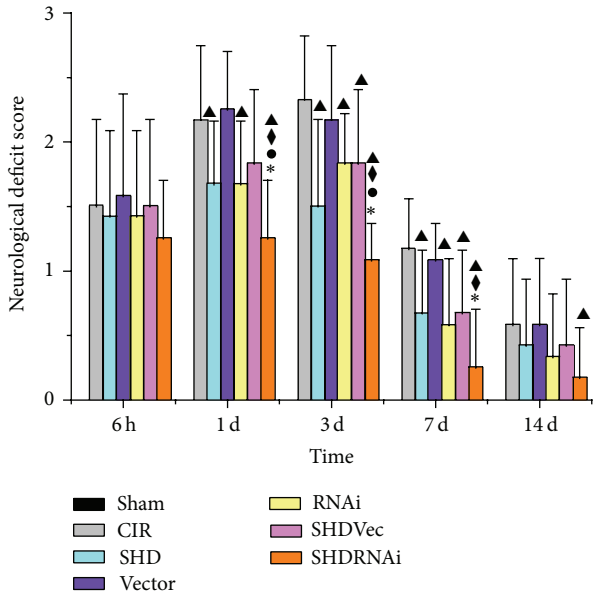

Figure 2: Neurological deficits after ischemia/reperfusion in rats ($\overline{x} \pm s, n = 8$). $^{\blacktriangle}P < 0.05$, compared with CIR group; $^{\blacklozenge}P < 0.05$, compared with SHD group; $^{*}P < 0.05$, compared with SHD + Vec group; $^{\bullet}P < 0.05$, compared with RNAi group. CIR, cerebral ischemia/reperfusion group; Sham, sham-operated group; SHD, Sanhua decoction-treated group; SHD + RNAi, Sanhua decoction plus AQP4-siRNA-treated group; SHD + Vec, Sanhua decoction plus vector-treated group; RNAi, AQP4-siRNA-treated group; Vector, vector-treated group.

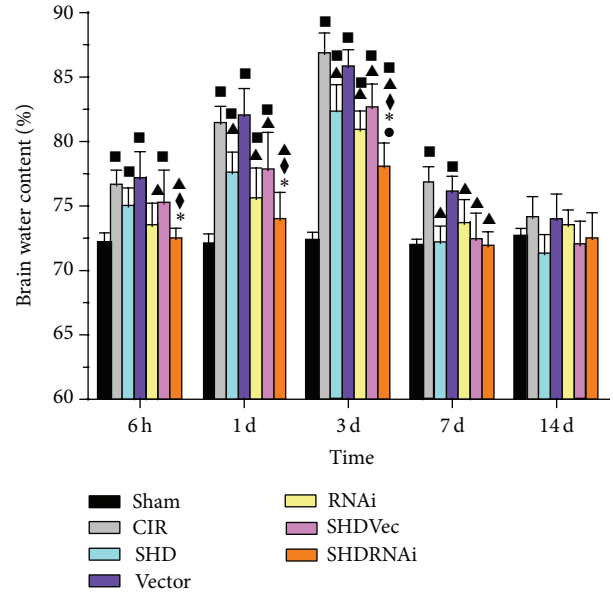

Figure 3: Brain water content of the ipsilateral side after ischemia/reperfusion in rats ($\overline{x} \pm s, n = 4$). $^{\blacksquare}P < 0.05$, compared with Sham group; $^{\blacktriangle}P < 0.05$, compared with CIR group; $^{\blacklozenge}P < 0.05$, compared with SHD group; $^{*}P < 0.05$, compared with SHD + Vec group; $^{\bullet}P < 0.05$, compared with RNAi group. CIR, cerebral ischemia/reperfusion group; Sham, sham-operated group; SHD, Sanhua decoction-treated group; SHD + RNAi, Sanhua decoction plus AQP4-siRNA-treated group; SHD + Vec, Sanhua decoction plus vector-treated group; RNAi, AQP4-siRNA-treated group; Vector, vector-treated group.

protein signals was normalized to the corresponding GAPDH intensity and was quantified by densitometric analysis with the use of Quantity One software (Bio-Rad Laboratories, USA).

2.9. Statistical Analysis. All experimental data were presented as mean ± standard deviation. Neurologic deficit score data were analyzed using a nonparametric Mann-Whitney U test. Paired t-test was used for the significant difference of brain water content between ipsilateral and contralateral hemispheres. Comparisons between multiple groups were done by one-way analysis of variance (ANOVA) followed by LSD-t-test. Statistical analyses were performed with SPSS 13.0 for Windows (Chicago, IL, USA). Statistical significance was set at $P < 0.05$.

3. Results

3.1. SHD Alleviated Neurological Deficits. Neurological scores increased at 6 h after ischemia/reperfusion and peaked at 3 d and then descended gradually but remained higher than normal at 14 d (Figure 2). Compared with Sham group, I/R group showed significant differences at the time points of 6 h, 1 d, 3 d, and 7 d ($P < 0.05$). Compared with I/R group, SHD + Vec group has significant differences at 3 d and 7 d ($P < 0.05$), SHD group and RNAi group both showed significances at 1 d, 3 d, and 7 d ($P < 0.05$), and SHD + RNAi group presented statistical differences at 1 d, 3 d, 7 d, and 14 d ($P < 0.05$). Compared with SHD group or SHD + Vec group, SHD + RNAi group had significant differences at 1 d, 3 d, and 7 d after I/R ($P < 0.05$). There were also statistical differences between RNAi group and SHD + RNAi group at the time points of 1 d and 3 d ($P < 0.05$). However, there was no significant difference between SHD group and RNAi group, Vector group and I/R group, SHD group and SHD + Vec group, and RNAi group and SHD + Vec group, at all the time points of 6 h, 1 d, 3 d, and 7 d ($P > 0.05$). Thus, SHD can alleviate neurological deficits and its effect was amplified by combination of AQP4-siRNA.

3.2. SHD Reduced Brain Water Content. Brain water content of contralateral hemisphere had no difference between groups ($P > 0.05$). In ipsilateral hemisphere, it increased at 6 h after I/R and peaked at 3 d and then descended gradually but remained higher than normal at 14d (Figure 3). Compared with Sham group, I/R group and Vector group both had significant differences at the time points of 6 h, 1 d, 3 d, and 7 d ($P < 0.05$), RNAi group had significant differences at 1 d and 3 d ($P < 0.05$), and SHD + RNAi group had significant differences at 3 d ($P < 0.05$). Compared with I/R group, SHD group and SHD + Vec group both had differences at 1 d, 3 d, and 7 d ($P < 0.05$), and RNAi group and SHD + RNAi group both showed significances at 6 h, 1 d, 3 d, and 7 d ($P < 0.05$). Compared with SHD group

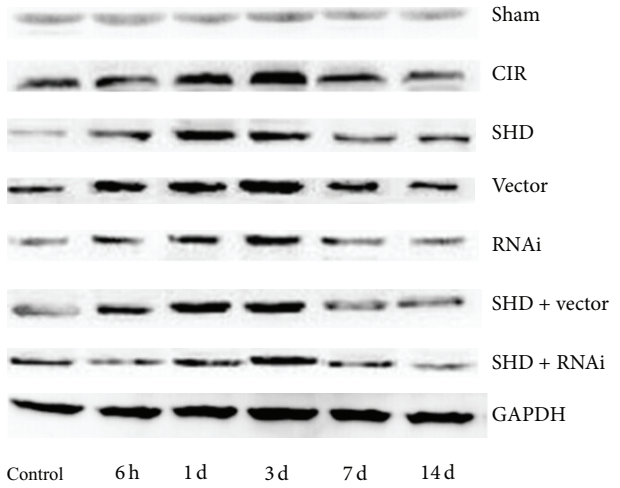

Figure 4: Aquaporin 4 (AQP4) expression in the ipsilateral hippocampus by western blot. CIR, cerebral ischemia/reperfusion group; Sham, sham-operated group; SHD, Sanhua decoction-treated group; SHD + RNAi, Sanhua decoction plus AQP4-siRNA-treated group; SHD + Vec, Sanhua decoction plus vector-treated group; RNAi, AQP4-siRNA-treated group; Vector, vector-treated group.

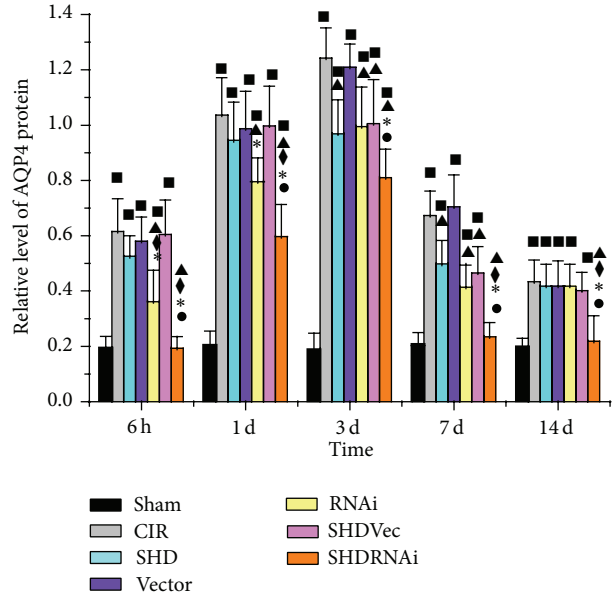

Figure 5: Western blot analyses of AQP4 expression in the ipsilateral hippocampus after ischemia/reperfusion in rats ($\overline{x} \pm s, n = 4$). $^{\blacksquare}P < 0.05$, compared with Sham group; $^{\blacktriangle}P < 0.05$, compared with CIR group; $^{\blacklozenge}P < 0.05$, compared with SHD group; $^{*}P < 0.05$, compared with SHD + Vec group; $^{\bullet}P < 0.05$, compared with RNAi group. CIR, cerebral ischemia/reperfusion group; Sham, sham-operated group; SHD, Sanhua decoction-treated group; SHD + RNAi, Sanhua decoction plus AQP4-siRNA-treated group; SHD + Vec, Sanhua decoction plus vector-treated group; RNAi, AQP4-siRNA-treated group; Vector, vector-treated group.

or SHD + Vec group, SHD + RNAi group had statistical differences at 6 h, 1 d, and 3 d ($P < 0.05$). There was statistical significance between RNAi group and SHD + RNAi group at the time point of 3 d ($P < 0.05$) (Figure 3). Thus, SHD can reduce brain water content and it was remarkable in combination with AQP4-siRNA.

3.3. SHD Downregulated the Expression of AQP4. Expression of AQP4 was detected by WB analyses. The expression of AQP4 in the ipsilateral hippocampus increased at 6 h after ischemia/reperfusion and peaked at 3 d and then descended gradually but remained higher than normal at 14 d (Figure 4). Compared with Sham group, SHD + RNAi group had statistical significances at 1 d and 3 d after I/R ($P < 0.05$), and the other 5 groups all showed differences at each time point after I/R ($P < 0.05$). Compared with I/R group, SHD group and SHD + Vec group both had significant differences at the time points of 3 d and 7 d ($P < 0.05$), RNAi group had differences at 6 h, 1 d, 3 d, and 7 d ($P < 0.05$), and SHD + RNAi group showed significance at each time point ($P < 0.05$). SHD + RNAi group showed significant differences at each time point after I/R when compared with SHD group, SHD + Vec group, or RNAi group ($P < 0.05$) (Figure 5). Thus, SHD can downregulate AQP4 expression in rat brain tissue and it was more notable when combined with AQP4-siRNA.

4. Discussion

In the present study, we demonstrated that SHD treatment could alleviate neurological deficit, reduce the brain water content, and decline AQP4 expression in peripheral ischemic lesions after I/R. Furthermore, neurobehavioral function and brain edema after I/R were significantly attenuated via downregulation of AQP4 expression when combined with AQP4-siRNA technology.

Transient suture-occluded MCAO method in rats is the most common and preferred focal I/R injury model for imitating human ischemic stroke [14]. Evaluation of neurological function impairment after cerebral ischemia according to Longa test with 5-point scale, which is highly recommended worldwide, was set up by the same author who created transient MCAO with the suture [13]. In the present study, this neurologic grading scale was applied to assess the degree of neurological deficits following suture-occluded MCAO for 2 h in rats. We found that SHD treatment notably reduced neurological deficit scores in rats with MCAO. More remarkable improvement for neurological deficits was shown when combining SHD with AQP4-siRNA technology. These findings suggest that SHD treatment promotes behavioral functional recovery after ischemic stroke. With AQP4-siRNA technology, SHD had stronger and more stable effect on the functional recovery.

Brain edema is detrimental because of its increasing volume occupied consequences having a swelling effect on adjacent tissues, and these effects were magnified by the fixed volume of the skull. The tissues were compromised with capillary inflow, leading to ischemia and edema formation in reverse, causing a secondary injury in brain [17]. It is broadly acknowledged that brain water content is practicable

for evaluating brain edema using dry and wet method. In the present study, we applied this weighing method with Bolliot formula to assess the extent of brain edema after cerebral ischemia. The data showed that brain water content increased immediately after MCAO in rats, SHD treatment could effectively inhibit the increase of water content, and the combined effect of SHD treatment with AQP4-siRNA had promoted decrease of water content more significantly. These results suggested that brain edema rapidly formed in the acute stage of I/R injury, which was obviously alleviated by SHD treatment and more prominently attenuated by SHD treatment integrated with AQP4-siRNA.

Although bumetanide [18], acetazolamide [19], and erythropoietin [20] were proposed to decrease AQP4 expression, there are no specific therapeutic blockers to inhibit the AQP4 channel at present and such agents are vital to evaluating the role and treatment of edema. In the present study, we investigated the effect of SHD on expression levels of AQP4 in hippocampus of I/R injured rats. Basically consistent with the result of brain water content, the data showed that AQP4 was upregulated and markedly expressed in the ipsilateral hemisphere after I/R, SHD treatment significantly inhibited the expression of AQP4, and such downregulated expression was magnified by the combination of SHD with AQP4-siRNA. Analyses of these results revealed that AQP4 was involved in the formation of brain edema after cerebral ischemia, and SHD treatment reduced AQP4 expression corresponding to its protective effect against brain edema. With the AQP4-siRNA technology, it provided further evidence that SHD treatment likely exerts neuroprotective effects following cerebral ischemia mainly via blocking AQP4 channel [21].

SiRNA, a short 21–23-nucleotide double-stranded RNA molecule that mediates sequence-specific gene silencing, was performed in several animal studies as potential therapeutics in acute brain injury, such as brain ischemia, brain hemorrhage, and traumatic brain injury [22–24]. Applying siRNA to stroke patient in the near future, a very promising method of therapy, is expected to lead to a global breakthrough in improving functional recovery [21]. Direct transfection of chemically synthetic siRNA and intracellular generation of siRNA from plasmid or viral vectors which drive expression of the precursor shRNA can both achieve RNAi that has been widely used in gene research and therapy. Because of active infection on dividing as well as resting and differentiated cells, viral DNA incorporated in the host genome, and relatively low immunogenicity, lentiviruses are particularly suited for long-term shRNA expression and gene silencing [25]. The present experimental results showed that AQP4-siRNA with intracerebroventricular injection could effectively reduce neurologic deficit scores, as well as brain water content in MCAO rats, and such benefits were amplified by the combination of siRNA with SHD treatment. The amelioration of neurological functional recovery and reduction of brain edema with AQP4-siRNA after brain injury was consistent with that in the study by Fukuda et al. [26]. Thus, the neuroprotection effect of SHD against I/R injury was mainly carried out by AQP4 blocking. However, the specific pathway of downregulating AQP4 expression involved in SHD deserves further exploration. In addition, vascular protection is the key for development of therapeutic agents for stroke [27]. Thus, whether SHD impacts the vascular factors related to ischemic brain damage is worthy of further study.

In conclusion, the present study demonstrated that SHD can improve neurological function deficits and reduce brain water content after focal cerebral ischemia. The mechanism of this neuroprotection by SHD after cerebral I/R mainly targets downregulation of AQP4 expression.

Conflict of Interests

The authors have declared that no conflict of interests exists.

Authors' Contribution

Lin Lu, Hui-qin Li, and Ji-huang Li contributed equally to this work.

Acknowledgments

This work was supported by the Grant of the National Natural Science Foundation of China (81173395/H2902) and the Young and Middle-Aged University Discipline Leaders of Zhejiang Province, China (2013277).

References

[1] V. L. Feigin, M. H. Forouzanfar, R. Krishnamurthi et al., "Global and regional burden of stroke during 1990–2010: findings from the global burden of disease study 2010," *The Lancet*, vol. 383, no. 9913, pp. 245–254, 2014.

[2] E. C. Jauch, J. L. Saver, H. P. Adams et al., "Guidelines for the early management of patients with acute ischemic stroke: a guideline for healthcare professionals from the American Heart Association/American Stroke Association," *Stroke*, vol. 44, no. 3, pp. 870–947, 2013.

[3] B. M. Demaerschalk and T. R. Yip, "Economic benefit of increasing utilization of intravenous tissue plasminogen activator for acute ischemic stroke in the United States," *Stroke*, vol. 36, no. 11, pp. 2500–2503, 2005.

[4] J. M. Wardlaw, V. Murray, E. Berge, and G. J. Del Zoppo, "Thrombolysis for acute ischaemic stroke," *Cochrane Database of Systematic Reviews*, no. 4, Article ID CD000213, 2009.

[5] C.-F. Tsai, B. Thomas, and C. L. M. Sudlow, "Epidemiology of stroke and its subtypes in Chinese vs white populations," *Neurology*, vol. 81, no. 3, pp. 264–272, 2013.

[6] Y. Wang, X.-M. Lin, and G.-Q. Zheng, "Traditional Chinese medicine for Parkinson's disease in china and beyond," *Journal of Alternative and Complementary Medicine*, vol. 17, no. 5, pp. 385–388, 2011.

[7] J. H. Liu, "Observation on treating acute ischemic stroke for 28 cases with Sanhua Decoction," *Western Journal of Traditional Chinese Medicine*, vol. 24, no. 7, pp. 61–63, 2011.

[8] Z. Z. Yang, Y. K. Sun, and M. D. Tian, "Clinical study on integrative medicine in treatment of 40 cases of acute cerebral infarction," *Jiangsu Journal of Traditional Chinese Medicine*, vol. 41, no. 7, pp. 33–34, 2009.

[9] S. Nielsen, E. A. Nagelhus, M. Amiry-Moghaddam, C. Bourque, P. Agre, and O. R. Ottersen, "Specialized membrane domains

for water transport in glial cells: high-resolution immunogold cytochemistry of aquaporin-4 in rat brain," *The Journal of Neuroscience*, vol. 17, no. 1, pp. 171–180, 1997.

[10] M. C. Papadopoulos and A. S. Verkman, "Aquaporin water channels in the nervous system," *Nature Reviews Neuroscience*, vol. 14, no. 4, pp. 265–277, 2013.

[11] Z. Zador, S. Stiver, V. Wang, and G. T. Manley, "Role of aquaporin-4 in cerebral edema and stroke," *Handbook of Experimental Pharmacology*, vol. 190, pp. 159–170, 2009.

[12] G. T. Manley, M. Fujimura, T. Ma et al., "Aquaporin-4 deletion in mice reduces brain edema after acute water intoxication and ischemic stroke," *Nature Medicine*, vol. 6, no. 2, pp. 159–163, 2000.

[13] E. Z. Longa, P. R. Weinstein, S. Carlson, and R. Cummins, "Reversible middle cerebral artery occlusion without craniectomy in rats," *Stroke*, vol. 20, no. 1, pp. 84–91, 1989.

[14] Y. Zhou, H. Q. Li, L. Lu et al., "Ginsenoside Rg1 provides neuroprotection against blood brain barrier disruption and neurological injury in a rat model of cerebral ischemia/reperfusion through downregulation of aquaporin 4 expression," *Phytomedicine*, vol. 21, no. 7, pp. 998–1003, 2014.

[15] G. Paxinos and C. Watson, *The Rat Brain in Stereotaxic Coordinates, Compact*, Academic Press, San Diego, Calif, USA, 3rd edition, 1997.

[16] W. Young, Z. H. Rappaport, D. J. Chalif, and E. S. Flamm, "Regional brain sodium, potassium, and water changes in the rat middle cerebral artery occlusion model of ischemia," *Stroke*, vol. 18, no. 4, pp. 751–759, 1987.

[17] J. M. Simard, T. A. Kent, M. Chen, K. V. Tarasov, and V. Gerzanich, "Brain oedema in focal ischaemia: molecular pathophysiology and theoretical implications," *The Lancet Neurology*, vol. 6, no. 3, pp. 258–268, 2007.

[18] E. Migliati, N. Meurice, P. DuBois et al., "Inhibition of aquaporin-1 and aquaporin-4 water permeability by a derivative of the loop diuretic bumetanide acting at an internal pore-occluding binding site," *Molecular Pharmacology*, vol. 76, no. 1, pp. 105–112, 2009.

[19] Y. Tanimura, Y. Hiroaki, and Y. Fujiyoshi, "Acetazolamide reversibly inhibits water conduction by aquaporin-4," *Journal of Structural Biology*, vol. 166, no. 1, pp. 16–21, 2009.

[20] E. Gunnarson, Y. Song, J. M. Kowalewski et al., "Erythropoietin modulation of astrocyte water permeability as a component of neuroprotection," *Proceedings of the National Academy of Sciences of the United States of America*, vol. 106, no. 5, pp. 1602–1607, 2009.

[21] A. M. Fukuda and J. Badaut, ""A Sword-in-the-Stone" for acute brain injuries," *Genes*, vol. 4, no. 3, pp. 435–456, 2013.

[22] Z. He, R. P. Ostrowski, X. Sun et al., "CHOP silencing reduces acute brain injury in the rat model of subarachnoid hemorrhage," *Stroke*, vol. 43, no. 2, pp. 484–490, 2012.

[23] J. Zhang, Y. Wang, P. Zhu, X. Wang, M. Lv, and H. Feng, "SiRNA-mediated silence of protease-activated receptor-1 minimizes ischemic injury of cerebral cortex through HSP70 and MAP2," *Journal of the Neurological Sciences*, vol. 320, no. 1-2, pp. 6–11, 2012.

[24] L.-J. Niu, R.-X. Xu, P. Zhang, M.-X. Du, and X.-D. Jiang, "Suppression of Frizzled-2-mediated Wnt/Ca^{2+} signaling significantly attenuates intracellular calcium accumulation in vitro and in a rat model of traumatic brain injury," *Neuroscience*, vol. 213, pp. 19–28, 2012.

[25] N. Manjunath, H. Wu, S. Subramanya, and P. Shankar, "Lentiviral delivery of short hairpin RNAs," *Advanced Drug Delivery Reviews*, vol. 61, no. 9, pp. 732–745, 2009.

[26] A. M. Fukuda, A. Adami, V. Pop et al., "Posttraumatic reduction of edema with aquaporin-4 RNA interference improves acute and chronic functional recovery," *Journal of Cerebral Blood Flow and Metabolism*, vol. 33, no. 10, pp. 1621–1632, 2013.

[27] Y. Bu, K. Lee, H. S. Jung, and S. K. Moon, "Therapeutic effects of traditional herbal medicine on cerebral ischemia: a perspective of vascular protection," *Chinese Journal of Integrative Medicine*, vol. 19, no. 11, pp. 804–814, 2013.

Hindawi Publishing Corporation
Evidence-Based Complementary and Alternative Medicine
Volume 2015, Article ID 927160, 8 pages
http://dx.doi.org/10.1155/2015/927160

Research Article

Chinese Herbal Medicine in the Treatment of Chronic Heart Failure: Three-Stage Study Protocol for a Randomized Controlled Trial

Liangtao Luo,[1,2] Jianxin Chen,[1] Shuzhen Guo,[1] Juan Wang,[1] Kuo Gao,[1] Peng Zhang,[1,3] Chan Chen,[1,4] Huihui Zhao,[1] and Wei Wang[1]

[1] *School of Preclinical Medicine, Beijing University of Chinese Medicine, No. 11, Beisanhuan Donglu, Chaoyang District, Beijing 100029, China*
[2] *School of Traditional Chinese Medicine, Capital Medical University, No. 10, Youanmenwai, Xitoutiao, Fengtai District, Beijing 100069, China*
[3] *Wuhan Hospital of Traditional Chinese Medicine, No. 49, Li Huang Po Lu, Han Kou Jiang An District, Wuhan, Hubei 430014, China*
[4] *Hangzhou Xiaoshan District Hospital of Traditional Chinese Medicine, 156 Yu Cai Lu, Xiaoshan District, Zhejiang 311201, China*

Correspondence should be addressed to Huihui Zhao; hh686@126.com and Wei Wang; wangwei26960@163.com

Received 10 July 2014; Accepted 1 December 2014

Academic Editor: Qunhao Zhang

Background. Chinese herbal medicine (CHM) has been used in the treatment of chronic heart failure (CHF) for a long time. Treatment based on syndrome differentiation and the main characteristic of TCM is the fundamental principle of TCM practice. In this study protocol, we have designed a trial to assess the efficacy and safety of CHM on CHF based on syndrome differentiation. *Methods/Design*. This is a three-stage trial of CHM in the treatment of CHF. The first stage is a literature review aiming to explore the common syndromes of CHF. The second is a multicentral, randomized, placebo-controlled trial to evaluate the efficacy and safety of CHM for the treatment of CHF. The third is a multicentral, randomized controlled clinical trial aiming to make cost-effectiveness analysis and evaluate the feasibility, compliance, and universality of CHM on CHF. *Discussion*. This trial will evaluate the efficacy, safety, feasibility, compliance, and universality of CHM on CHF. The expected outcome is to provide evidence-based recommendations for CHM on CHF and develop a prescription of CHM in the treatment of CHF. This trial is registered with NCT01939236 (Stage Two of the whole trial).

1. Background

Heart failure, as the final stage of cardiac diseases, is an abnormality of cardiac structure or function. This would lead to the failure of the heart to deliver oxygen at a rate commensurate with the requirements of the metabolizing tissues, despite the normal filling pressures or increased filling pressures [1]. In addition, according to the character of the clinical manifestation, HF is divided into acute and chronic HF. In 2003, a random sample survey of 15,518 urban or rural residents from 35 to 74 years old was made in China: the prevalence rate of heart failure was 0.9%, and according to the result there were approximately 4 million HF targets in China [2]. The diagnosis and treatment of cardiovascular disease (CVD) have developed quickly in the past several decades. The mortality of CVD has fallen down, except for HF. Annual hospital discharge in subjects with a primary diagnosis of HF has been rising steadily since 1975. And now it has exceeded 1 million discharges per year, though they may at last be leveling off in the United States [3, 4]. It can be expected that the incidence of HF in China will be in a significantly increasing trend, and the number of CHF patients will increase in the future.

According to the guideline, the conventional therapeutic approaches in HF management are angiotensin-converting enzyme inhibitors (ACEIs), β-adrenergic blockers, and diuretics [5]. However, side effects, such as electrolyte, fluid

Table 1: Databases search strategies.

Databases	Search terms
CNKI	[(Mesh terms = heart failure) OR (Title = chronic heart failure) OR (Keywords = chronic heart failure)] AND [(Mesh terms = syndrome) OR (Keywords = syndrome)]
CBM	(Mesh terms = chronic heart failure OR Mesh terms = CHF OR Mesh terms = chronic congestive heart failure OR Mesh terms = chronic cardiac insufficiency) and ((Mesh terms = syndrome) or (Mesh terms = traditional Chinese medicine))
VIP	((Title or keywords: chronic cardiac insufficiency) OR (Title or keywords: CHF) OR (Title or keywords: chronic heart failure) OR (Title or keywords: chronic congestive heart failure)) AND (Title or keywords: syndrome) AND (Title or keywords: symptom) AND (Medicine and health) AND (All Periodicals) AND (Year: 1994–2008)

depletion, and hypotension, are common during the treatment with western medicine [6]. Therefore, CHM, as an alternative medicine, has been considered the treatment of CHF with lower cost and fewer side effects.

In China, CHM has been used in the treatment of diseases for thousands of years. Treatment based on syndrome differentiation is the main characteristic and therapeutic rule of TCM. Syndrome differentiation is the comprehensive analysis of the clinical information gained by the four main diagnostic TCM procedures—observation, listening, interrogation, and pulse-taking, and it is used to guide the choice of treatment by CHM. Many clinical studies [7–9] have shown the efficacy of CHM on CHF. But in these studies, the syndrome of the CHF patients was stationary, and the formulation of CHM was in the form of capsule or injection. They may not completely reflect the efficacy of CHM in the treatment of CHF based on syndrome differentiation. This trial aims to evaluate the efficacy and safety of CHM in the treatment of CHF based on syndrome differentiation.

2. Objectives

The objective of this trial is to assess the efficacy and safety of CHM on CHF based on syndrome differentiation and to develop a prescription of CHM in the treatment of CHF which could be generally used in community health service centers.

3. Methods

3.1. Design. This is a three-stage, multicentral clinical trial in the treatment of CHF. The first stage is a literature study and aims to explore the common syndromes of CHF. The second stage is a multicentral, randomized controlled clinical trial with double-blinded method and aims to evaluate the efficacy and safety of CHM based on syndrome differentiation. The third stage is a multicentral, randomized controlled clinical trial and aims to make cost-effectiveness analysis and evaluate the feasibility, compliance, and universality of CHM on CHF based on syndrome differentiation.

3.1.1. Stage One. The first stage was to analyze the most common syndromes of CHF. A flowchart of Stage One is shown in Figure 1.

Inclusion Criteria for the Literature. The literatures included should focus on clinical research of CHM or integrative medicine on CHF.

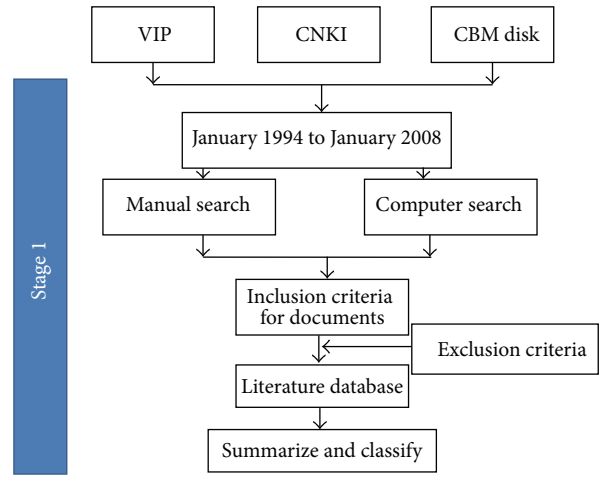

Figure 1: The flowchart of Stage One trial design.

The literatures should have integral data with exact data information about CHF syndromes.

Exclusion Criteria for the Literature. If the content of articles was identical and the study was identified to be the same one, we select one article with the most complete information:

literature reviews,

case reports,

export advice,

the literature focusing on the analysis of pathogenesis or the syndromes substantive,

the source of the literature being unknown or the actual situation being clearly incompatible with the clinical literature.

Search Range for Articles. We searched the China National Knowledge Infrastructure Database (CNKI), the China Biology Medicine Database (CBM), and the Chinese Science and Technology Periodical Database (VIP) from January 1994 to January 2008. Databases search strategies are shown in Table 1.

Search Methods. The literature search work was carried out by 2 students independently in the same search terms. After all work was accomplished, we checked the search result and resolved the differences through discussion. If

Table 2: The distribution of symptoms in 176 literatures.

Symptom	Frequency	Rate (%)
Palpitation	233	5.6
Shortness of breath	160	3.9
Edema	159	3.8
Lassitude	153	3.7
Thread pulse	146	3.5
Dyspnea	126	3.0
Wheeze	117	2.8
Pale tongue	111	2.7
Intermittent pulse	110	2.7
Knotted pulse	110	2.7
Oliguria	101	2.4
Sweating	100	2.4

the disagreements still could not be resolved, we invited related experts for identification.

Selecting the Content of Related Literatures. We selected records of CHF and syndromes and related information.

The Processing Methods of Selected Records. We picked out TCM syndromes, symptoms, and signs in records and attached the related information, such as paper title, journal name, issue number, page count, and author.

All data were input into database established with Epidata 3.0. The frequency of common syndromes and symptoms was analyzed. We encoded these common syndromes and symptoms and regulated the related TCM terms. We unified the TCM names or aliases with the same meaning but different expression into uniform names.

Summarizing and Classifying the Findings of Literatures. We summarized the clinical characteristics and distribution of CHF common syndromes from the results of searched records. There were 1432 literatures with full text search in three databases. According to inclusion and exclusion criteria, we selected 176 literatures from the three literature databases. According to Clinical Terminology of Diagnosis and Treatment for Traditional Chinese Medicine—Syndrome Section and Pharmacy Terminology of Traditional Chinese Medicine, with the suggestion of experts, we standardized all symptoms and syndromes of CHF. There were twelve symptoms with more than 100 repetitions after standardization, which were shown in Table 2. The top six symptoms are yang deficiency, qi deficiency, blood stasis, water retention, yin deficiency, and turbid phlegm, which were shown in Table 3 [10]. Combined with the literature review and experts' suggestions, we decided to make qi deficiency, blood stasis, yang deficiency, and water retention as objects for the further trial of Stages Two and Three.

3.1.2. Stage Two. The second stage of this trial was a multicentral, randomized clinical trial with placebo-controlled and double-blind methods. Figure 2 shows the trial flowchart.

Table 3: The distribution of syndromes in 176 literatures.

Syndrome	Frequency	Rate (%)
Yang deficiency	6489	18.57
Qi deficiency	6377	18.25
Blood stasis	5731	16.40
Water retention	3445	9.86
Phlegm syndrome	973	2.78

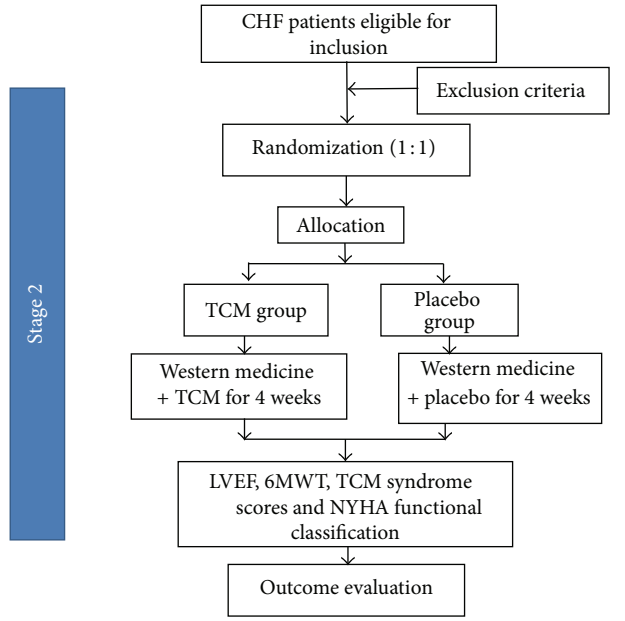

Figure 2: The flowchart of Stage Two trial design.

Diagnostic Criteria

Diagnostic Criteria for CHF. Diagnostic criteria were as follows: (1) diagnostic criteria of CHF: *2007 China Guideline for the Diagnosis and Treatment of CHF* [5]; (2) heart function standard: *The Criteria for Diagnosis and Treatment of Heart Disease* first published by the New York Heart Association (NYHA) [11].

Diagnostic Criteria for TCM Syndrome Differentiation. Diagnostic criteria were as follows: TCM differentiation standard: according to the *Guiding Principles for the Clinical Study of New Drugs in Traditional Chinese Medicine* released in 2002 [12].

Inclusion Criteria for Participants. Patients who accorded with diagnostic criteria were potentially eligible for the study if they met the following criteria.

(i) The primary heart disease is CHD (with diagnosis for CHD confirmed by coronary angiography, coronary computed tomography, history of acute myocardial infarction, limb-salvage Q wave for electrocardiogram (ECG), ECG test, radionuclide examination support, etc.). The included patients should have no

history of hypertension or taking antihypertensive drugs, with a blood pressure under 160/100 mmHg.

(ii) With a history of CHD, the following symptoms and signs were observed: difficult breathing, fatigue, fluid retention (edema), left ventricular enlargement, systolic volume of left ventricular increase with LVEF ≤ 40%, and NYHA functional classification II or III.

(iii) Male or female patients should be between 40 and 75 years old.

If there was any violation of those criteria, the subject could not participate in this research.

Exclusion Criteria for Participants. Patients would be excluded if they met one of the following criteria.

(i) Patients with one of the following diseases: (1) acute valvular heart disease; (2) pericardial disease; (3) cardiomyopathy; (4) congenital heart disease; (5) acute myocardial infarction (AMI) within four weeks; (6) cardiac shock; (7) acute myocarditis or serious arrhythmia with variation in hemodynamics.

(ii) Patients who suffer from pulmonary artery hypertension caused by cor pulmonale, pulmonary embolism, or stroke within a half year.

(iii) Patients who suffer from serious hepatic insufficiency (the index of liver function being 2 times the normal one), renal insufficiency (Ccr > 20%, Scr > 3 mg/dL, or 265 μmol/L), diseases of blood system, malignant tumor, diabetes mellitus with serious complications, hyperthyrea, or hypothyrea.

(iv) Patients who suffer from infection, fever, or patients meeting one of the following criteria: the numeration of leukocyte being more than 10×10^9/L, the percentage of neutrophil granulocyte being more than 85%; patchy shadows in X-ray of chest.

(v) Pregnant women and women in lactation.

(vi) Patients with mental disorders or related infections.

(vii) Patients who took part in other trials within two months before the present study.

Sample Size. The sample size calculation is based on prophase clinical study (31 cases, 13 in CHM group and 18 in placebo group), standard deviation of experimental group (S_e) = 25.84718, standard deviation of control group (S_c) = 32.54499, mean of experimental group ($\overline{x}_e$) = 39.07692, mean of control group ($\overline{x}_c$) = 32.54499, and the number of control group (c) = 1. The following formula is used to calculate the sample size:

$$n = \frac{\left(\upsilon_\alpha + \upsilon_\beta\right)^2 (1 + 1/c)\,\sigma^2}{\delta^2}$$
$$\sigma^2 = S^2 = \frac{S_e^2 + cS_c^2}{1 + c}\delta^2 = \left|\overline{x}_e - \overline{x}_c\right|^2. \quad (1)$$

The estimated number of subjects in each group was 98.18012, and 196.36024 subjects are needed in two groups. The number was increased to 215.18012 assuming a maximum dropout rate of less than or equal to 10%, and a total of 220 subjects were included (110 subjects in each group).

Randomization. A total number of 220 participants were randomly assigned with a ratio of 1 : 1 to CHM or placebo group according to random number sequence. Stratified blocked randomization was taken to insure the balance of two groups.

Blinding. In this stage, the double-blind design was used. Drugs for CHM and placebo groups were prepared and provided by Beijing Kangren Tang Pharmaceutical Co., Ltd. (Beijing, China). In CHM group, drugs of four syndromes (qi deficiency, blood stasis, water retention, and yang deficiency) were prepared, while the placebo was provided in the same character, smell, and weight as the drugs for CHM group. Drugs of each syndrome were prepared as granules without decoction. The CHM drugs and placebo were numbered according to a random figure table which was blinded to both the doctors and the patients. Participants were provided with CHM or placebo based on their syndrome differentiation at the beginning and two weeks later. They took CHM or placebo twice per day for four weeks.

Setting. In this stage, participants were admitted into seven hospitals of four provinces in China: (1) Dongfang Hospital Affiliated to Beijing University of Chinese Medicine; (2) The Affiliated Hospital to Changchun University of TCM; (3) Guang'anmen Hospital Affiliated to China Academy of Chinese Medicine Sciences; (4) Hubei Provincial Hospital of TCM; (5) Wuhan Hospital of TCM; (6) Yichang Hospital of TCM; (7) Zhengzhou Hospital of TCM.

Interventions. According to the guideline for chronic heart failure [5], standardized western medicine treatment, such as angiotensin-converting enzyme inhibitors (ACEIs) or angiotensin-receptor blockers (ARBs), β-blockers, and diuretics, could be used for patients in CHM and placebo groups as basic therapy. The dosages of all medicines used are following the guideline for CHF [5].

The recipe for qi deficiency was composed of *Astragalus membranaceus* (Fisch.) Bge. var. *mongholicus* (Bge.) Hsiao (huangqi, 60 g) and *Codonopsis pilosula* (Franch.) Nannf. (dangshen, 15 g).

The recipe for blood stasis was composed of *Salvia miltiorrhiza* Bge. (danshen, 15 g), *Paeonia lactiflora* Pall. (chishao, 15 g), *Prunus davidiana* (Carr.) Franch. (taoren, 10 g), and *Carthamus tinctorius* L (honghua, 10 g).

The recipe for water retention was composed of *Alisma orientalis* (Sam.) Juzep. (zexie, 10 g), *Polyporus umbellatus* (Pers.) Fries (zhuling, 15 g), *Plantago asiatica* L. (cheqianzi, 10 g), and *Descurainia sophia* (L.) Webb. ex Prantl (tinglizi, 10 g).

The recipe for yang deficiency was composed of *Cinnamomum cassia* Presl (rougui, 4.5 g) and *Aconitum carmichaelii* Debx. (zhifuzi, 10 g).

Table 4: The timeline of participants' course through Stage Two.

Items	Baseline	Treatment	
	Visit 1	Visit 2	Visit 3
	0 weeks	2 weeks	4 weeks
Inclusion/exclusion	•		
Informed consent	•		
Grouping	•		
Medical history collection	•		
General information	•		
Medication history	•		
Physical examination	•		
Complicating diseases	•		
Drug release	•	•	
TCM syndrome scores	•	•	•
NYHA functional classification	•	•	•
6-minute walk test	•	•	•
LVEF	•	•	•
X-ray	•		
Routine urine test	•		•
Liver function test	•		•
Renal function test	•		•
Electrolytes	•		•
Electrocardiogram	•	•	•
Side effect		•	•

Table 6 lists the names of the CHM drugs in Chinese and English. All CHM herbs were verified by high-performance liquid chromatography (HPLC).

Patients in placebo group received placebo which was the same in shape, size, taste, weight, and package as CHM granules. CHM drugs and placebo were prepared as granules. Granules quality met internal control standards of Beijing Kangren Tang Pharmaceutical Co., Ltd. (Beijing, China), and complied with GMP (Good Manufacturing Practice) standards. Patients were treated with CHM or placebo granules twice per day for four weeks based on syndrome differentiation.

Participants were prohibited from taking other Chinese medicine during the treatment period.

The drugs for the treatment of hypertension (HBP), diabetes mellitus, dyslipidemia, and other diseases could be used reasonably. And the reason, name, and dosage should be recorded in detail.

Outcome Measurements. The primary outcome measure was left ventricular ejection fraction (LVEF). Secondary outcome measurements were 6-minute walk test (6MWT), traditional Chinese medicine syndrome scores, and New York Heart Association (NYHA) functional classification. Side effects were to be monitored during the trial period. Many biological indicators (blood routine examination, liver function, kidney function, and ECG) were tested before and after the treatment. The timeline of participants through Stage Two is shown in Table 4.

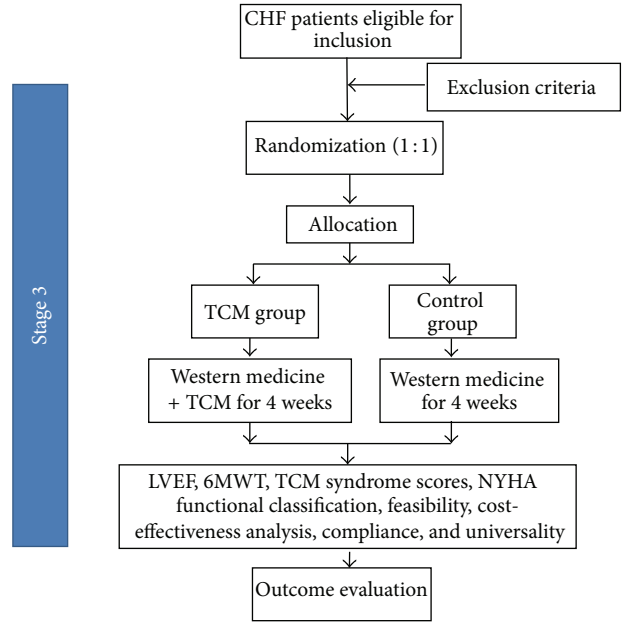

Figure 3: The flowchart of Stage Three trial design.

Statistical Analysis. Data were analyzed on the Intention-to-Treat (ITT) analysis and the per-protocol set (PPS) for coherence. The basic characteristics were compared with independent samples t-test for continuous variables and chi-square analyses for categorical variables. Repeated-measure ANOVA was used for the evaluation of the primary and secondary outcomes. The measurement data were expressed as mean ± standard deviation for us to check the data of all groups with normal test and homogeneity of variance test. Results were shown with 95% confidence intervals (CIs). The level of significance was set at 0.05. If $P < 0.05$, there were statistical differences. All tests were 2-tailed.

3.1.3. Stage Three. If the efficacy of CHM on CHF is better than placebo in Stage Two, we will conduct Stage Three to evaluate the feasibility, compliance, and universality and make cost-effectiveness analysis of CHM on CHF based on syndrome differentiation. A flowchart of the third stage is shown in Figure 3.

Diagnostic Criteria

Diagnostic Criteria for CHF. Diagnostic criteria are the same as those of Stage Two.

Diagnostic Criteria for TCM Syndrome Differentiation. Diagnostic criteria were the same as those of Stage Two.

Inclusion Criteria for Participants. Patients who accorded with diagnostic criteria were potentially eligible for the study if they met the following criteria.

(i) The primary heart disease is CHD (with diagnosis for CHD confirmed by coronary angiography, coronary computed tomography, history of acute myocardial

infarction, limb-salvage Q wave for electrocardiogram (ECG), ECG test, radionuclide examination support, etc.). The included patients also had no history of hypertension or taking antihypertensive drugs, with a blood pressure under 160/100 mmHg.

(ii) With a history of CHD, the following symptoms and signs were observed: difficult breathing, fatigue, and fluid retention (edema), with left ventricular enlargement, along with increasing of left ventricular end systolic volume and LVEF ≤ 50%, with NYHA cardiac function II or III.

(iii) Male or female patients should be between 40 and 75 years old.

If there is any violation of those criteria, the subject could not participate into this research.

Exclusion Criteria for Participants. Exclusion criteria were the same as those in Stage Two.

Sample Size. This design in this stage is to show the superiority of TCM based on syndrome differentiation. The ratio in this stage is 1 : 1. The sample size calculation is based on LVEF of Stage Two. To calculate the sample size, we will use the following formula ($\delta = 2$):

$$n = \frac{\left(\left(Z_{1-a/2} + Z_{1-\beta}\right)^2 * \left(\sigma_1^2 + \sigma_2^2\right)\right)}{(\varepsilon - \delta)^2}. \quad (2)$$

And the maximum dropout is 10%.

Randomization. All participants in this stage will be randomly distributed to CHM or placebo group according to random number sequence.

Setting. In this stage, five or more centers will take part in the trial.

Interventions. Besides standardized western medicine treatment, participants in CHM group will receive CHM based on syndrome differentiation. Control Group will receive standardized western medicine only.

CHM granules will be prepared as in Stage Two.

Outcome Measurements. In this stage, the primary outcome measurement is LVEF. Secondary outcome measurements are 6MWT, TCM syndrome scores, and NYHA functional classification. Meanwhile, the feasibility, cost-effectiveness analysis, compliance, and universality will be evaluated or performed. Feasibility and universality investigation of this research will be executed by the questionnaire of doctors and patients; compliance evaluation will be executed by the ratio between the actual amount of medication and the supposed amount in CHM group; cost effectiveness will be conducted by the ratio between the different improved condition of LVEF and treatment costs. Side effects will be monitored during the trial period. Biological indicators (blood routine examination, liver function, kidney function, and ECG) will be tested before and after the treatment. The timeline of participants through Stage Three is shown in Table 5.

Table 5: The timeline of participants' course through Stage Three.

Items	Baseline	Treatment	
	Visit 1	Visit 2	Visit 3
	0 weeks	2 weeks	4 weeks
Inclusion/exclusion	•		
Informed consent	•		
Grouping	•		
Medical history collection	•		
General information	•		
Medication history	•		
Physical examination	•		
Complicating diseases	•		
Drug release	•	•	
TCM syndrome scores	•		•
NYHA functional classification	•		•
6-minute walk test	•		•
LVEF	•		•
X-ray	•		
Routine urine test	•		•
Liver function test	•		•
Renal function test	•		•
Electrolytes	•		•
Electrocardiogram	•		•
Feasibility			•
Cost-effectiveness analysis			•
Compliance			•
Universality			•
Side effect		•	•

Table 6: List of CHMs used in the study.

Syndrome differentiation	English translation of CHM	Chinese script
Qi deficiency	Huangqi	黄芪
	Dangshen	党参
Blood stasis	Danshen	丹参
	Chishao	赤芍
	Taoren	桃仁
	Honghua	红花
Water retention	Zexie	泽泻
	Zhuling	猪苓
	Cheqianzi	车前子
	Tinglizi	葶苈子
Yang deficiency	Zhifuzi	制附子
	Rougui	肉桂

Statistical Analysis. Data will be analyzed on the Intention-to-Treat (ITT) analysis and the per-protocol set (PPS) for coherence. The basic characteristics will be compared with

independent samples t-test for continuous variables and chi-square analyses for categorical variables. The measurement data will be expressed as mean ± standard deviation for us to check the data of all groups with normal test and variance homogeneity test. The changes in measurement data between baseline and the assessment for four weeks will be performed with independent samples t-test. The categorical variables will be compared with chi-square analyses. Safety analysis will be conducted. Results will be shown with 95% confidence intervals (CIs). The level of significance will be set at 0.05. If $P < 0.05$, there will be statistical differences. All tests will be 2-tailed.

3.2. Ethical Issue of Stages Two and Three. The trial is conducted according to the guidelines of the Declaration of Helsinki and is approved by the Ethics Committee of Dongfang Hospital Affiliated to Beijing University of Chinese Medicine (number 201002102). All participants have been asked to provide informed consent before participating in the trial.

3.3. Quality Control of Stages Two and Three. Research workbook will be formulated. Before the beginning of this stage, all investigators will be trained and tested according to conformance standard. Drugs in this trial will be identified by pharmaceutical manufacturing sector and prepared in accordance with national technical standards procedures. Drugs will be marked only for clinical trial, which cannot be sold. The investigators in clinical centers will take charge of the usage of drugs. The usage record of drugs should include the following information: quantity, shipment, delivery, acceptance, distribution, recycling, and destruction.

In order to achieve the same detection methods, the physicians for 6MWT evaluation and echocardiography will be trained together. Clinical research associates will test the research progress of all clinical centers.

4. Discussion

CHF is a major public health problem all over the world. Western medicine has been used widely but has many common side effects [6]. In China, the integrated traditional and western medicine has been used for the treatment of CHF for a long time, and its efficacy has been seen in many clinical trials [13]. However, there is insufficient evidence to support the efficacy of CHM based on syndrome differentiation.

In TCM, patients are treated with different therapies based on their syndrome differentiations. Therefore, the key factor of this trial is to find out the common syndromes of CHF patients. At the first stage, we searched the most common syndromes.

This is the first randomized clinical trial on CHF with CHM based on syndrome differentiation. The aim of this trial is to develop a prescription of CHM in the treatment of CHF which could be used in community health service centers. So in Stage Two, we tested the efficacy and safety of CHM on CHF with a double-blind, randomized, placebo-controlled clinical trial. In Stage Three, we will test the feasibility, cost-effectiveness analysis, compliance, and universality of those CHMs, which have showed positive sign in efficacy and safety in Stage Two. And finally, according to the result of Stages Two and Three, we will decide whether this CHM treatment proposal for CHF should be generalized in community health service centers or not in the future.

In conclusion, we want to evaluate the efficacy, safety, feasibility, cost-effectiveness analysis, and universality of CHM treatment on CHF based on syndrome differentiation with three stages. The achievement of this trial will provide evidence-based data for CHM, which is helpful for the application of CHM on CHF.

Trial Status. Stages One and Two of this trial have been accomplished. Stage Three will be started in November 2013 and will be completed in September 2014.

Abbreviations

6MWT: 6-minute walk test
ACEI: Angiotensin-converting enzyme inhibitors
AMI: Acute myocardial infarction
CBM: China Biology Medicine Database
CHD: Coronary heart disease
CHF: Chronic heart failure
CHM: Chinese herbal medicine
CIs: Confidence intervals
CNKI: China National Knowledge Infrastructure Database
CVD: Cardiovascular disease
ECG: Electrocardiogram
GMP: Good Manufacturing Practice
HBP: Hypertension
ITT: Intention-to-Treat
LVEF: Left ventricular ejection fraction
NYHA: New York Heart Association
PPS: Per-protocol set
RCT: Randomized controlled trial
TCM: Traditional Chinese medicine
VIP: Chinese Science and Technology Periodical Database.

Conflict of Interests

The authors declare that there is no conflict of interests regarding the publication of this paper.

Authors' Contribution

Liangtao Luo, Jianxin Chen, and Shuzhen Guo drafted the paper and made revisions. Peng Zhang, Juan Wang, Kuo Gao, and Chan Chen were responsible for the development of the preceding two-stage protocol. Jianxin Chen provided suggestions for statistical data analysis. Huihui Zhao was responsible for the development of the last stage protocol. Wei Wang conceived this trial project and took charge of drafting the whole trial protocol. All authors have read and approved

the final paper. Liangtao Luo, Jianxin Chen, Shuzhen Guo, and Juan Wang are equal contributors.

Acknowledgments

This study is supported by the National Basic Research Program of China (no. 2011CB505106); the National Natural Science Foundation of China (nos. 81173463, 81102730, 81302914, 81473521, and 81303152); New Century Excellent Talent Support Plan of the Ministry of Education (NCET-12-084 and NCET-11-0607); Beijing Nova Program (Grant nos. xx2013032 and 2011069); Innovation Team of Wei Wang in Beijing University of Chinese Medicine; Project of Beijing Young Talents (YETP0821 by Xing Zhai); Special Project of Chinese Administration of Traditional Chinese Medicine (537/01204, 200807007 by Wei Wang).

References

[1] K. Dickstein, A. Cohen-Solal, G. Filippatos et al., "ESC Guidelines for the diagnosis and treatment of acute and chronic heart failure 2008: the Task Force for the Diagnosis and Treatment of Acute and Chronic Heart Failure 2008 of the European Society of Cardiology. Developed in collaboration with the Heart Failure Association of the ESC (HFA) and endorsed by the European Society of Intensive Care Medicine (ESICM)," *European Journal of Heart Failure*, vol. 10, pp. 933–989, 2008.

[2] D. F. Gu, G. Y. Huang, J. He et al., "Investigation of prevalence and distributing feature of chronic heart failure in Chinese adult population," *Chinese Journal of Cardiology*, vol. 1, pp. 3–6, 2003.

[3] V. L. Roger, A. S. Go, D. M. Lloyd-Jones et al., "Heart disease and stroke statistics—2012 update: a report from the American Heart Association," *Circulation*, vol. 125, no. 1, pp. e2–e220, 2012.

[4] National Institutes of Health and National Heart-Lung-and Blood Institute, *Morbidity & Mortality: 2012 Chart Book on Cardiovascular, Lung, and Blood Diseases*, 2012.

[5] Chinese Society of Cardiology of Chinese Medical Association and Editorial Board of Chinese Journal of Cardiology, "Guidelines for the diagnosis and management of chronic heart failure," *Chinese Journal of Cardiology*, vol. 12, pp. 1076–1095, 2007.

[6] C. W. Yancy, M. Jessup, B. Bozkurt et al., "2013 ACCF/AHA guideline for the management of heart failure: a report of the American college of cardiology foundation/american heart association task force on practice guidelines," *Journal of the American College of Cardiology*, vol. 62, no. 16, pp. e147–e239, 2013.

[7] Y. L. Wu, C. H. Gu, G. C. Xu, C. Wei, and X. D. Gao, "Clinical observation of randomized double-blind and multicenter trial on Qiliqiangxin capsule in the treatment of chronic heart failure," *Chinese Journal of Difficult and Complicated Cases*, vol. 5, pp. 263–266, 2007.

[8] Y.-Z. Hou, J.-Y. Mao, X.-L. Wang, J. Li, and C.-X. Liu, "Shenfu injection for patients with heart failure: a systematic review," *Chinese Journal of Evidence-Based Medicine*, vol. 11, no. 3, pp. 292–299, 2011.

[9] Y. Z. Hou, J. Y. Mao, X. L. Wang, C. X. Liu, and C. Zhang, "Shenmai injection in heart failure patients: a systematic review and meta-analysis," *Chinese Journal of Evidence-Based Medicine*, vol. 10, no. 8, pp. 939–945, 2010.

[10] Z. Peng, *Study of Distribution Regularities of Common Traditional Chinese Medicine Syndromes and Syndrome Factors in Patients with Chronic Heart Failure Caused by Coronary Heart Disease*, Beijing University of Chinese Medicine, Beijing, China, 2011.

[11] Association NYH, *Diseases of the Heart and Blood Vessels: Nomenclature and Criteria for Diagnosis*, Little, Brown, 1964.

[12] X. Y. Zheng, *The Guiding Principles for the Clinical Study of New Drugs for Use in Traditional Chinese Medicine (In Trying)*, Chinese Medical Science and Technology Press, 2002.

[13] X. Li, J. Zhang, J. Huang et al., "A multicenter, randomized, double-blind, parallel-group, placebo-controlled study of the effects of qili qiangxin capsules in patients with chronic heart failure," *Journal of the American College of Cardiology*, vol. 62, no. 12, pp. 1065–1072, 2013.

Hindawi Publishing Corporation
Evidence-Based Complementary and Alternative Medicine
Volume 2015, Article ID 869894, 7 pages
http://dx.doi.org/10.1155/2015/869894

Research Article

Extraction of Clinical Indicators That Are Associated with the Heat/Nonheat and Excess/Deficiency Patterns in Pattern Identifications for Stroke

Ju Ah Lee,[1] Mi Mi Ko,[1] Jungsup Lee,[2] Byoung-Kab Kang,[1] Terje Alraek,[3,4] Stephen Birch,[3] and Myeong Soo Lee[1]

[1] *Medical Research Division, Brain Disease Research Center, Korea Institute of Oriental Medicine, 1672 Yuseongdae-ro, Yuseong-gu, Daejeon 305-811, Republic of Korea*
[2] *Korean National Rehabilitation Center, Seoul, Republic of Korea*
[3] *University College of Health Sciences, Institute of Acupuncture, 0855 Oslo, Norway*
[4] *National Research Center in Complementary and Alternative Medicine (NAFKAM), Department of Community Medicine, Faculty of Health Sciences, UiT The Arctic University of Norway, Tromsø, Norway*

Correspondence should be addressed to Myeong Soo Lee; drmslee@gmail.com

Received 27 August 2014; Accepted 29 September 2014

Academic Editor: Keji Chen

The aim of this study is to extract indicators that are associated with the heat/nonheat and excess/deficiency patterns in stroke pattern identification through the large-scale analysis of clinical data. Two experts, who had more than three years of clinical experience with stroke, independently performed the pattern identification. We analyzed indicators of clinical data with two doctors' concurrent diagnoses on the patient's pattern identification. To verify heat/nonheat and excess/deficiency patterns, which are the basic elements of pattern identification, we grouped 960 patients diagnosed as the fire-heat pattern, the Yin deficiency pattern, and the Qi deficiency pattern in to two groups, the heat/nonheat group and the excess/deficiency group. We then extracted significant indicators using univariate and multivariate analysis. As a result of the comparison of 65 indicators, we were able to extract 10 indicators for the heat pattern, 6 for the nonheat pattern, 9 for the excess pattern, and 10 for the deficiency pattern. Extracted indicators in this study can be used for pattern identification in the context of stroke. These are positive indicators from large-scale clinical studies and are greatly expected to be crucial discriminant indicators in individual pattern identification henceforth.

1. Introduction

In Korea, many stroke patients receive traditional medical care because the country has its own system of traditional alternative medicine called traditional Korean medicine (TKM), the role of which has been emphasized in stroke management [1]. In TKM and traditional Chinese medicine (TCM), disease is defined as a condition with collapsed equilibrium. TKM doctors make it a rule to restore the imbalance to treat diseases. Pattern identification, a unique diagnostic system of TKM and TCM [2], is the process of overall analysis of clinical data to determine the location, cause, and nature of a patient's disease with an integrative viewpoint that involves the etiology, pathology, and treatment method [3]. There are many classifications in stroke pattern identification, including organ pattern identification, eight-pattern identification, and qi-blood identification. However, the basic elements of pattern identification, such as the discrimination of excessive/deficiency and heat/nonheat patterns, are the same. There were several previous studies on pattern identification, such as a study that diagnosed IBS with the excess/deficiency pattern [4], a study on the period of menstruation [5], and study on traditional Chinese medicine syndromes in women with a frequently recurring cystitis [6]. However, these studies have many limitations because they did not use validated criteria for their TCM diagnoses and hence the reliability of the work. And there are 2 studies that examined reliability of 8-principle diagnosis [7]. However, no study was

found to evaluate actual clinical data and extract meaningful indicators. These studies focused only on pattern of disease. Therefore, we adopted an alternative approach, which is to group research subjects into broad categories based on essential patterns of the TCM diagnosis, such as heat/nonheat and excess/deficiency patterns, rather than a detailed TCM diagnosis. First, we made indicators of pattern identification for stroke using Delphi process that is a practical way of generating consensus from a group of expert practitioners [8]. Next, based on the clinical data from a multicenter, large population, the Korean Standard Differentiation of the Symptoms and Signs of Stroke involved 5 categories: the fire-heat pattern, the damp-phlegm pattern, the Yin deficiency pattern, the Qi deficiency pattern, and the blood stasis pattern [9, 10]. Blood stasis pattern was excluded due to rare diagnosis ($n = 89$). Therefore, we extract significant clinical indicators, which affect two pairs of distinct patterns of TCM diagnosis in stroke through data of four patterns: the fire-heat pattern, the damp-phlegm pattern, the Yin deficiency pattern, and the Qi deficiency pattern.

2. Participants and Methods

2.1. Participants. This study was a community-based multicenter trial. We collected data on stroke patients who had been hospitalized in fifteen oriental medicine university hospitals nationwide from November 2006 to February 2010. Inclusion criteria included having acute stroke with a neurological deficit that persisted for over 24 hours; being finally diagnosed as stroke by imaging, including computerized tomography and magnetic resonance imaging; and agreeing to participate within 30 days of stroke onset. In addition, there were exclusion criteria. Exclusion criteria included traumatic stroke, including epidural hemorrhage and subdural hemorrhage; degenerative brain disease; a stroke concomitant with a brain tumor; and patients unable to communicate symptoms.

2.2. Data Collection and Gold Standard for Inclusion. We utilized the case report form (CRF) with a high reliability, collected data on the symptoms and signs, and recorded the score on the 3-point Likert scale for the standardization of stroke diagnosis that had been developed by an expert committee organized by the Korean Institute of Oriental Medicine (KIOM). The principle of symptoms and signs of each patterns extraction was as follows. First, we reflected the characteristic of stroke symptoms to exclude its own symptoms such as hemiparesis, dysphagia, dysarthria, and facial palsy. Second, we identified stroke patterns based on the present state of TKM clinically. Also we considered the association with the previous studies. Finally, we reflected the recent trend of stroke in TKM literature. And two independent physicians conducted this pattern identification. The gold standard was set up as two physicians' concurrent diagnosis which is an identical pattern as a result of diagnostic decision of two TKM physicians. The physicians had at least three years of clinical experiences with stroke and identified the PI of each participating patient. We used data from 960 patients who were diagnosed as the fire-heat pattern, the Yin deficiency pattern, or the Qi deficiency pattern. All of the involved researchers received formal training with standard operation procedures (SOPs) twice a year to exclude all of the possible individual differences.

2.3. Assumption for the Extraction of Clinical Indicators of the Heat/Nonheat Pattern and the Excess/Deficiency Pattern. We assumed that the three patterns (the fire-heat pattern, the Yin deficiency pattern, and the Qi deficiency pattern) lie on either side of the space that consists of two axes: the excess/deficiency axis and the heat/nonheat axis. As coldness is mentioned in neither the classical literatures nor the common opinion from the experts, we assumed only the existence and nonexistence of heat. However, this assumption only focused on stroke. We thought normal heat/cold pattern discrimination was replaced by heat/absence of heat signs because cold is not a recognized feature in PI for stroke, while heat is a common pattern and a method is needed to discriminate heat signs.

With the exception of the damp-phlegm pattern and blood stagnation pattern, which are taken as pathological products, we suppose that the fire-heat pattern involves the excess and heat patterns, the Qi deficiency pattern involves deficiency and nonheat patterns, and the Yin deficiency pattern involves deficiency and heat patterns.

2.4. Set-Up of an Independent Variable and a Dependent Variable. Among 65 clinical indicators, those with an appearance of less than 5% of the frequency were excluded. Each indicator was established as an independent variable after conversion to the binary form (existence and nonexistence of symptoms or signs). Dependent variables were grouped into two (heat/nonheat and excess/deficiency patterns): the fire-heat pattern and the Yin deficiency pattern to the heat pattern; the fire-heat pattern to the excess pattern; and the Yin deficiency pattern and the Qi deficiency pattern to the deficiency pattern.

2.5. Statistical Analysis. A univariate cross tabulation was performed for all of the independent variables and the binary dependent variables. We adopted multilogistic regression analysis for the indicators that showed a significant difference after univariate analysis. The analysis was performed using SAS, version 5.1.

3. Results

3.1. Number of Participants. The patients included consisted of 444 patients with the fire-heat pattern, 207 with the Yin deficiency pattern, and 313 with the Qi deficiency pattern (Table 1).

3.2. Selection of Variables to Be Involved in an Analysis. Six clinical indicators of the 65 indicators on the CRF that appeared at a frequency of less than 5% were found: darkish complexion, headache like flush, headache with nausea, stabbing headache, bluish purple tongue, and purple spots on the tongue. This clinical consideration was generally executed prior to multivariate analysis.

Table 1: Demographic parameters of enrolled participants.

Characteristics	QD	YD	FH	*P*
N	313	207	440	
Sex (M/F)	107/206	91/116	334/106	<0.0001
Age (year)	67.37 ± 11.53	69.27 ± 12.37	65.75 ± 11.98	0.0019
Smoking (none/stop/active)	41/40/232	40/32/135	170/107/163	<0.0001
Drinking (none/stop/active)	68/31/214	58/19/130	214/55/171	<0.0001
Weight (kg)	56.66 ± 9.19	56.97 ± 11.25	64.97 ± 10.78	<0.0001
BMI (kg/m^2)	22.74 ± 2.99	22.87 ± 4.43	24.16 ± 3.0	<0.0001
Waist circumference (cm)	84.57 ± 8.81	82.77 ± 9.16	88.33 ± 9.34	<0.0001
WHR	0.93 ± 0.11	0.93 ± 0.15	0.95 ± 0.10	NS
TOAST classification				
LAA	51	47	117	0.0073
CE	20	15	34	
SVO	182	95	199	
SOE	7	7	5	
SUE	14	10	22	
Medical history				
TIA (*n*, %)	26 (8.31)	20 (9.66)	35 (7.99)	NS
Hypertension (*n*, %)	180 (57.51)	123 (59.42)	258 (58.77)	NS
Hyperlipidemia (*n*, %)	35 (11.18)	18 (8.70)	54 (12.33)	NS
Diabetes (*n*, %)	82 (26.20)	47 (22.71)	116 (26.48)	NS
Heart disease (*n*, %)	17 (5.43)	12 (5.80)	26 (5.92)	NS

Data was expressed as frequencies for categorical variables and expressed as mean ± standard deviation for continuous variables. YD: Yin deficiency; QD: Qi deficiency; FH: fire-heat; NS: not significant. *P* values were calculated by chi-square test or ANOVA.

3.3. Univariate and Multivariate Analysis to Extract Clinical Indicators for the Heat Pattern and the Nonheat Pattern. After performing a multivariate analysis on the clinical indicators that had a significant difference in univariate analysis, we determined nine important clinical indicators: reddened complexion, blood-shot eyes, aphtha or tongue sore, fetid mouth odor, yellow fur, strong purse, surging purse, heat vexation and aversion to heat, and obesity. These factors displayed odds ratios greater than 1.0. Ten important clinical indicators were as follows: drowsiness, like to lie down, feeling powerless and lazy, pale complexion, pale face and malar flush, pale tongue, teeth-marked tongue, mirror tongue, weak purse, fine purse, and frequent urination. These factors displayed odds ratios of less than 1.0 (Table 2). Whole results of univariate and multivariate analysis to extract clinical indicators for the heat pattern and the nonheat pattern were shown in Supplemental Table 1 available online at http://dx.doi.org/10.1155/2014/869894.

3.4. Univariate and Multivariate Analyses to Extract Clinical Indicators in the Excessive Pattern and Deficiency Pattern. After performing a multivariate analysis on clinical indicators that displayed a significant difference on univariate analysis, we identified nine important clinical indicators: pale face and malar flush, reddened complexion, red eye, aphtha or tongue sore, fetid mouth odor, red tongue, dry fur, rapid purse, heat in the palms and soles, and gauntness (odds ratio > 1.0). We identified ten important clinical indicators: looking powerless and lazy, pale complexion, low voice, white fur, teeth-marked tongue, and weak purse (odds ratio < 1.0) (Table 3). Whole results of univariate and multivariate analysis to extract clinical indicators for the excessive pattern and deficiency pattern were shown in Supplemental Table 2.

3.5. Comparison of the Clinical Indicators That Explain the Heat/Nonheat Pattern and Excess/Deficiency Pattern. Comparing the results of the heat/nonheat pattern with those of the excess/deficiency pattern, four indicators were found for both heat and excess patterns: reddened complexion, red eye, aphtha or tongue soreness, and fetid mouth odor. Three indicators (pale complexion, teeth-marked tongue, and weak purse) were found in both nonheat and the deficiency patterns (Table 4).

4. Discussion

We provide important information for treatment by extracting clinical indicators that have reasonable and objective access to the heat/nonheat pattern and excess/deficiency pattern in acute stroke patients and present the relative risk. There are many diagnostic systems (e.g., organ pattern identification, eight-pattern identification, and qi-blood identification) in TKM [11], but they share certain features. The distinction between excessive/deficiency and heat/nonheat patterns are fundamental to pattern identification. Thus, it is indispensable for the identification of the heat/nonheat pattern and the excess/deficiency pattern. The potential advantages of this approach are the following: it may be easier

Table 2: Results of multivariate analysis in excessive pattern and deficiency pattern.

Clinical indicator	Deficiency	Excessive	[c]OR (95% CI)	*P*	[a]OR (95% CI)	*P*
q01_2	46 (8.85)	70 (15.91)	0.615 (0.286, 1.322)	NS	0.721 (0.236, 2.198)	NS
q01_3	146 (28.08)	58 (13.18)	2.346 (1.222, 4.507)	0.0104	2.881 (1.007, 8.243)	0.0485
q02_1	308 (59.23)	133 (30.23)	1.689 (0.94, 3.032)	NS	1.888 (0.713, 4.995)	NS
q02_2	345 (66.35)	125 (28.41)	1.382 (0.762, 2.507)	NS	1.073 (0.386, 2.984)	NS
q03_1_1	179 (34.42)	22 (5)	2.947 (1.178, 7.375)	0.0209	2.826 (0.622, 12.835)	NS
q03_1_2	123 (23.65)	64 (14.55)	1.179 (0.537, 2.587)	NS	0.754 (0.23, 2.467)	NS
q03_1_3	14 (2.69)	3 (0.68)	2.772 (0.42, 18.321)	NS	0.759 (0.055, 10.523)	NS
q03_1_4	90 (17.31)	32 (7.27)	2.646 (1.09, 6.425)	0.0315	2.302 (0.58, 9.135)	NS
q03_1_5	60 (11.54)	284 (64.55)	0.2 (0.094, 0.424)	<0.0001	0.103 (0.03, 0.353)	0.0003
q03_2	79 (15.19)	39 (8.86)	1.33 (0.622, 2.842)	NS	0.461 (0.142, 1.493)	NS
q04_3_2	15 (2.88)	31 (7.05)	0.139 (0.046, 0.42)	0.0005	0.157 (0.023, 1.05)	NS
q05_1	275 (52.88)	190 (43.18)	1.279 (0.78, 2.099)	NS	1.169 (0.538, 2.54)	NS
q06_1	74 (14.23)	90 (20.45)	0.859 (0.466, 1.585)	NS	2.504 (0.899, 6.973)	NS
q06_2	207 (39.81)	71 (16.14)	1.623 (0.858, 3.07)	NS	1.552 (0.505, 4.774)	NS
q07_1_1	23 (4.42)	37 (8.41)	0.306 (0.119, 0.79)	0.0144	0.133 (0.03, 0.584)	0.0075
q07_1_2	59 (11.35)	111 (25.23)	0.439 (0.228, 0.844)	0.0135	0.331 (0.122, 0.9)	0.0304
q07_4	157 (30.19)	182 (41.36)	0.515 (0.314, 0.842)	0.0082	0.679 (0.323, 1.429)	NS
q08_1_1	138 (26.54)	38 (8.64)	3.625 (1.229, 10.692)	0.0196	4.806 (0.962, 24.009)	NS
q08_1_2	221 (42.5)	147 (33.41)	2.079 (0.806, 5.364)	NS	1.703 (0.402, 7.222)	NS
q08_1_3	140 (26.92)	224 (50.91)	0.81 (0.319, 2.054)	NS	0.626 (0.149, 2.626)	NS
q08_2_1	101 (19.42)	216 (49.09)	0.281 (0.14, 0.563)	0.0003	0.487 (0.159, 1.488)	NS
q08_2_2	244 (46.92)	136 (30.91)	0.809 (0.437, 1.498)	NS	1.466 (0.553, 3.883)	NS
q08_3_1	102 (19.62)	201 (45.68)	0.56 (0.32, 0.98)	0.0422	0.439 (0.188, 1.026)	NS
q08_4_1	102 (19.62)	110 (25)	2.073 (1.178, 3.647)	0.0114	2.011 (0.841, 4.808)	NS
q08_5_1	85 (16.35)	40 (9.09)	2.317 (1.122, 4.784)	0.0231	4.518 (1.616, 12.632)	0.004
q08_5_4	34 (6.54)	15 (3.41)	4.956 (1.61, 15.257)	0.0053	15.977 (1.97, 129.6)	0.0095
q10_1	128 (24.62)	150 (34.09)	0.657 (0.389, 1.108)	NS	1.572 (0.672, 3.679)	NS
q11_1	205 (39.42)	146 (33.18)	1.799 (1.1, 2.941)	0.0193	2.598 (1.166, 5.788)	0.0195
q11_3	115 (22.12)	125 (28.41)	0.927 (0.543, 1.581)	NS	0.92 (0.412, 2.052)	NS
q12_4	73 (14.04)	86 (19.55)	0.683 (0.369, 1.262)	NS	1.262 (0.463, 3.446)	NS
q13_1	47 (9.04)	18 (4.09)	1.403 (0.532, 3.695)	NS	2.322 (0.443, 12.154)	NS
q14_1_1	116 (22.31)	189 (42.95)	0.957 (0.517, 1.772)	NS	0.398 (0.148, 1.068)	NS
q14_1_2	232 (44.62)	94 (21.36)	1.726 (0.934, 3.189)	NS	1.318 (0.508, 3.419)	NS
q14_2_1	127 (24.42)	38 (8.64)	1.097 (0.525, 2.294)	NS	1.619 (0.504, 5.204)	NS
q14_2_2	137 (26.35)	199 (45.23)	0.637 (0.371, 1.095)	NS	0.668 (0.285, 1.564)	NS
q14_3_1	108 (20.77)	297 (67.5)	0.494 (0.271, 0.9)	0.0212	0.441 (0.176, 1.104)	NS
q14_3_2	298 (57.31)	55 (12.5)	2.026 (1.037, 3.957)	0.0388	2.024 (0.726, 5.642)	NS
q14_4	229 (44.04)	23 (5.23)	6.098 (3.055, 12.172)	<0.0001	3.416 (1.208, 9.659)	0.0205
q14_5	90 (17.31)	161 (36.59)	0.912 (0.544, 1.528)	NS	0.755 (0.334, 1.71)	NS
q14_7	13 (2.5)	96 (21.82)	0.093 (0.034, 0.254)	<0.0001	0.087 (0.02, 0.38)	0.0012
q15_1	208 (40)	292 (66.36)	0.503 (0.308, 0.821)	0.006	0.341 (0.156, 0.744)	0.0069
q15_2_1	49 (9.42)	74 (16.82)	1.411 (0.68, 2.927)	NS	0.782 (0.272, 2.249)	NS
q15_2_2	35 (6.73)	69 (15.68)	0.423 (0.192, 0.931)	0.0327	0.853 (0.256, 2.848)	NS
q15_2_3	85 (16.35)	29 (6.59)	2.074 (0.959, 4.484)	NS	2.55 (0.781, 8.33)	NS
q16_1_1	76 (14.62)	125 (28.41)	0.44 (0.246, 0.786)	0.0056	0.391 (0.138, 1.113)	NS

Data was expressed as yes (%). Excessive: fire-heat pattern; deficiency: Qi deficiency pattern and Yin deficiency Pattern; [c]OR means crude odds ratio and [a]OR means odds ratio adjusted by sex, age, BMI, WHR, smoking, and drinking status. NS: not significant.

for physicians to agree on the fundamental pattern types than on complex pattern types; it captures the important and essential factors for stroke pattern identifications; and it can be applied to herbal formulas based on herbal pharmacology. We tried to find clinical data that could identify the heat/nonheat pattern and excess/deficiency pattern by using the Korean Standard Differentiation of the Symptoms and Signs for Stroke that grouped similar patterns into 5 patterns in the context of stroke at TKM. Dissimilar to the previous pattern identification (PI) with 5 patterns agreed upon by stroke experts, we adopted PI with 3 patterns, in which the Damp-phlegm pattern and Blood stagnation pattern were eliminated [12].

To extract indicators that can distinguish heat/nonheat based on this model, we set up Fire-heat/Yin deficiency versus Qi deficiency as independent variables. To extract indicators

Table 3: Results of multivariate analysis in heat pattern and nonheat pattern.

Clinical indicator	Heat	Nonheat	[c]OR (95% CI)	*P*	[a]OR (95% CI)	*P*
q01_2	97 (14.99)	19 (6.07)	2.891 (1.119, 7.464)	0.0283	1.471 (0.369, 5.868)	NS
q01_3	103 (15.92)	101 (32.27)	0.74 (0.416, 1.319)	NS	0.63 (0.259, 1.532)	NS
q02_1	233 (36.01)	208 (66.45)	0.729 (0.397, 1.337)	NS	0.579 (0.235, 1.43)	NS
q02_2	229 (35.39)	241 (77)	0.409 (0.219, 0.764)	0.005	0.516 (0.213, 1.249)	NS
q03_1_1	43 (6.65)	158 (50.48)	0.205 (0.112, 0.375)	<0.0001	0.279 (0.112, 0.694)	0.006
q03_1_4	105 (16.23)	17 (5.43)	5.985 (2.764, 12.961)	<0.0001	4.776 (1.591, 14.335)	0.0053
q03_1_5	321 (49.61)	23 (7.35)	4.581 (2.402, 8.735)	<0.0001	6.929 (2.589, 18.547)	0.0001
q03_2	69 (10.66)	49 (15.65)	0.801 (0.419, 1.531)	NS	1.025 (0.372, 2.824)	NS
q04_3_2	40 (6.18)	6 (1.92)	2.034 (0.487, 8.495)	NS	1.854 (0.267, 12.87)	NS
q05_1	288 (44.51)	177 (56.55)	0.916 (0.52, 1.614)	NS	1.022 (0.436, 2.394)	NS
q06_1	130 (20.09)	34 (10.86)	1.191 (0.618, 2.292)	NS	0.946 (0.316, 2.83)	NS
q06_2	131 (20.25)	147 (46.96)	0.496 (0.279, 0.88)	0.0165	0.361 (0.141, 0.921)	0.0329
q07_1_1	48 (7.42)	12 (3.83)	2.203 (0.796, 6.096)	NS	2.863 (0.572, 14.328)	NS
q07_1_2	138 (21.33)	32 (10.22)	2.727 (1.324, 5.614)	0.0065	2.713 (0.917, 8.023)	NS
q07_4	250 (38.64)	89 (28.43)	0.958 (0.583, 1.576)	NS	0.794 (0.388, 1.624)	NS
q08_1_1	62 (9.58)	114 (36.42)	0.425 (0.145, 1.25)	NS	0.974 (0.197, 4.817)	NS
q08_1_2	228 (35.24)	140 (44.73)	0.657 (0.24, 1.8)	NS	1.516 (0.337, 6.814)	NS
q08_1_3	318 (49.15)	46 (14.7)	3.119 (1.102, 8.826)	0.0321	9.338 (1.918, 45.477)	0.0057
q08_2_1	269 (41.58)	48 (15.34)	2.023 (0.987, 4.148)	NS	2.688 (0.952, 7.588)	NS
q08_2_2	205 (31.68)	175 (55.91)	0.436 (0.239, 0.795)	0.0067	0.478 (0.202, 1.132)	NS
q08_3_1	235 (36.32)	68 (21.73)	0.812 (0.452, 1.461)	NS	0.633 (0.27, 1.48)	NS
q08_4_1	178 (27.51)	34 (10.86)	2.175 (1.151, 4.111)	0.0167	4.771 (1.71, 13.318)	0.0028
q08_5_1	61 (9.43)	64 (20.45)	0.46 (0.242, 0.877)	0.0182	0.264 (0.106, 0.662)	0.0045
q08_5_4	41 (6.34)	8 (2.56)	3.018 (0.902, 10.102)	NS	6.052 (1.018, 35.979)	0.0478
q09_1	131 (20.25)	44 (14.06)	1.829 (0.715, 4.68)	NS	1.151 (0.303, 4.368)	NS
q09_3	99 (15.3)	26 (8.31)	0.81 (0.254, 2.575)	NS	1.356 (0.277, 6.639)	NS
q10_2	140 (21.64)	45 (14.38)	1.164 (0.632, 2.143)	NS	1.455 (0.571, 3.709)	NS
q11_3	184 (28.44)	56 (17.89)	1.199 (0.679, 2.12)	NS	1.356 (0.607, 3.031)	NS
q14_1_1	241 (37.25)	64 (20.45)	0.971 (0.502, 1.876)	NS	1.336 (0.503, 3.551)	NS
q14_1_2	162 (25.04)	164 (52.4)	0.472 (0.26, 0.855)	0.0133	0.491 (0.202, 1.191)	NS
q14_2_1	70 (10.82)	95 (30.35)	1.376 (0.704, 2.691)	NS	1.619 (0.582, 4.504)	NS
q14_2_2	285 (44.05)	51 (16.29)	3.207 (1.763, 5.833)	0.0001	3.874 (1.625, 9.235)	0.0022
q14_3_1	350 (54.1)	55 (17.57)	1.34 (0.679, 2.644)	NS	1.049 (0.387, 2.846)	NS
q14_3_2	149 (23.03)	204 (65.18)	0.434 (0.231, 0.816)	0.0096	0.365 (0.144, 0.921)	0.0328
q14_4	114 (17.62)	138 (44.09)	0.933 (0.532, 1.636)	NS	2.03 (0.847, 4.86)	NS
q14_5	201 (31.07)	50 (15.97)	1.503 (0.82, 2.755)	NS	2.104 (0.887, 4.993)	NS
q14_7	101 (15.61)	8 (2.56)	2.97 (1.003, 8.795)	0.0495	2.55 (0.554, 11.732)	NS
q15_1	390 (60.28)	110 (35.14)	1.446 (0.885, 2.364)	NS	1.517 (0.7, 3.112)	NS
q15_2_1	107 (16.54)	16 (5.11)	4.983 (1.857, 13.37)	0.0014	6.95 (1.646, 29.345)	0.0083
q15_2_2	87 (13.45)	17 (5.43)	0.988 (0.417, 2.341)	NS	0.502 (0.146, 1.727)	NS
q15_2_3	54 (8.35)	60 (19.17)	0.51 (0.253, 1.027)	NS	0.569 (0.204, 1.586)	NS
q15_3	85 (13.14)	22 (7.03)	1.61 (0.675, 3.84)	NS	1.383 (0.384, 4.986)	NS
q16_1_1	161 (24.88)	40 (12.78)	1.597 (0.799, 3.191)	NS	1.877 (0.626, 5.63)	NS
q16_1_2	140 (21.64)	47 (15.02)	1.731 (0.83, 3.61)	NS	1.06 (0.362, 3.102)	NS

Data was expressed as yes (%). Heat: fire-heat pattern and Yin deficiency pattern; Nonheat: Qi deficiency pattern; [c]OR means crude odds ratio and [a]OR means odds ratio adjusted by sex, age, BMI, WHR, smoking, and drinking status. NS: not significant.

that could distinguish the excessive/deficiency pattern, Yin deficiency/Qi deficiency and fire-heat patterns were used as independent variables. Clinical data that did not show a significant difference on the chi-square test or that had a total frequency less than 5% were excluded. The others were set as the independent variables in a logistic regression analysis and verified the statistical influence of independent variables on dependent variables.

As a result of the logistic regression analysis, 5 signs and 1 symptom in the excess/deficiency pattern and 8 signs and 6 symptoms in the heat/nonheat pattern were extracted as significant clinical data. This is because the signs like pulse

Table 4: Comparison of clinical indicators that explain heat/nonheat pattern and excess/deficiency.

	Excess	Deficiency
Heat	Reddened complexion Red eye Aphtha or tongue-sore Fetid mouth odor	
Nonheat		Pale complexion, Teeth-marked tongue Weak purse

and the tongue indicators were mainly weighted by physicians [13–15]. Physicians diagnose the heat/nonheat pattern and the excess/deficiency pattern by inspecting the existence and nonexistence of these indications. The mere extraction of indicators has certain limitations. It would be beneficial for providing the standardization of TKM in stroke and for evidence-based medicine if we made it possible to assess these factors quantitatively and qualitatively in further studies.

In conclusion, this is the first study aimed to extract objective indicators to differentiate the heat/nonheat pattern and excess/deficiency pattern on the basis of clinical data. This demonstrates how to establish major patterns on a specific disease, how to divide the groups for comparison according to their components, and how to extract significant clinical indicators using a multivariate analysis. Although this study relates to stroke only, this approach has the potential to be applicable to other diseases because it adopts pattern identification, which is an essential diagnostic procedure in TKM treatment.

This study enables us to obtain clinical evidence on pattern diagnosis, which was entirely dependent on the previous literature or expert opinions, and makes it possible to execute evidence-based diagnosis. It is highly likely that we will be able to use more obvious diagnostic evidence from systematic clinical trials in the future as fundamental studies evolve and treatment results accumulate. However, there are some limitations. This study shows only 5 patterns among the various possible patterns of TKM. It does not systematically reflect basic elements in PI from its inception but rather applied a Delphi technique to conventional PI. In this study, we analyzed only the cases that were not assessed to have accompanying patterns. Many physicians, however, understand the possibility of more than 2 patterns during PI and apply it to the clinical field [16, 17]. However, these accompanying patterns are complex. For that reason, this study excluded the accompanying patterns from the analysis and extracted important indicators of each pattern preferentially. Another limitation lies in the variation among raters, which is referred to frequently in TKM research. We made a great effort to minimize error by preparing SOPs and allowed raters to consult more than two SOPs.

Ethical Approval

This study was approved by the Institutional Review Board of each hospital and KIOM. Informed consent of all of the study patients was obtained after a thorough explanation of the study details.

Conflict of Interests

The authors declare that there is no conflict of interests regarding the publication of this paper.

Acknowledgment

This research was supported by a grant from the Korea Institute of Oriental Medicine (K13130 and K14281).

References

[1] W. S. Jung, H. J. Kim, H. S. Bae, S. U. Park, S. K. Moon, and J. M. Park, "Clinical approach to the standardization of oriental medical diagnostic pattern identification in stroke patients," *Evidence-based Complementary and Alternative Medicine*, vol. 2011, Article ID 768492, 7 pages, 2011.

[2] G. G. Zhang, B. Bausell, L. Lao, B. Handwerger, and B. M. Berman, "Assessing the consistency of traditional Chinese medical diagnosis: an integrative approach," *Alternative Therapies in Health and Medicine*, vol. 9, no. 1, pp. 66–71, 2003.

[3] N. Wiseman and F. Ye, *A Practical Dictionary of Chinese Medicine*, Paradigm Publications, Brookline, Mass, USA, 2nd edition, 1998.

[4] S. Tan, K. Tillisch, R. Bolus et al., "Traditional Chinese medicine based subgrouping of irritable bowel syndrome patients," *The American Journal of Chinese Medicine*, vol. 33, no. 3, pp. 365–379, 2005.

[5] N. Mantani, T. Kogure, S. Sakai, Y. Shimada, and K. Tarasawa, "Reexamination of the relation between menstrual cycle and Kampo diagnosis, Yin-yang," *American Journal of Chinese Medicine*, vol. 31, no. 1, pp. 137–140, 2003.

[6] T. Alræk, A. Aune, and A. Baerheim, "Traditional Chinese medicine syndromes in women with frequently recurring cystitis: frequencies of syndromes and symptoms," *Complementary Therapies in Medicine*, vol. 8, no. 4, pp. 260–265, 2000.

[7] K. A. O'Brien, E. Abbas, J. Zhang et al., "An investigation into the reliability of Chinese medicine diagnosis according to eight guiding principles and Zang-Fu theory in Australians with hypercholesterolemia," *The Journal of Alternative and Complementary Medicine*, vol. 15, no. 3, pp. 259–266, 2009.

[8] A. Flower, G. T. Lewith, and P. Little, "Seeking an oracle: using the Delphi process to develop practice guidelines for the treatment of endometriosis with Chinese herbal medicine," *The Journal of Alternative and Complementary Medicine*, vol. 13, no. 9, pp. 969–976, 2007.

[9] J. K. Kim, I. C. Seol, I. Lee, K. Oh, B. C. Yu, and S. M. Choi, "Report on the Korean standard differentiation of the symptoms and signs for the stoke-1," *Korean Journal of Oriental Physiology & Pathology*, vol. 20, pp. 229–234, 2006.

[10] H. Y. Go, Y. K. Kim, B. K. Kang et al., "Report on the Korean standard differentiation of the symptoms and signs for the stoke-2," *Korean Journal of Oriental Physiology & Pathology*, vol. 20, pp. 1789–1791, 2006.

[11] WHO, *WHO International Standard Terminologies on Traditional Medicine in the Western Pacific Region*, WHO, Geneva, Switzerland, 2007.

[12] J. Lee, S. Kim, B. Kang et al., "A review of static blood pattern in stroke pattern diagnosis," *The Korean Journal of Internal Medicine*, vol. 30, no. 4, pp. 813–820, 2009.

[13] S. Park, K. W. Kang, and B. G. Kang, "Study of tongue diagnosis for pattern identification in stroke patients," *Korean Journal of Oriental Physiology & Pathology*, vol. 22, pp. 262–266, 2008.

[14] J. Lee, M. Ko, S. Kim et al., "Study on the basic purse indicator for pattern identification in stroke," *Korean Journal of Oriental Internal Medicine*, vol. 23, no. 5, pp. 964–968, 2012.

[15] M. Kim, D. Cobbin, and C. Zaslawski, "Traditional Chinese medicine tongue inspection: an examination of the inter- and intrapractitioner reliability for specific tongue characteristics," *Journal of Alternative and Complementary Medicine*, vol. 14, no. 5, pp. 527–536, 2008.

[16] G. G. Zhang, W. L. Lee, L. Lao, B. Bausell, B. Berman, and B. Handwerger, "The variability of TCM pattern diagnosis and herbal prescription on rheumatoid arthritis patients," *Alternative Therapies in Health and Medicine*, vol. 10, no. 1, pp. 58–63, 2004.

[17] G. G. Zhang, B. Singh, W. Lee, B. Handwerger, L. Lao, and B. Berman, "Improvement of agreement in TCM diagnosis among TCM practitioners for persons with the conventional diagnosis of rheumatoid arthritis: Effect of training," *Journal of Alternative and Complementary Medicine*, vol. 14, no. 4, pp. 381–386, 2008.

Hindawi Publishing Corporation
Evidence-Based Complementary and Alternative Medicine
Volume 2015, Article ID 143145, 7 pages
http://dx.doi.org/10.1155/2015/143145

Review Article

Cardiovascular Disease, Mitochondria, and Traditional Chinese Medicine

Jie Wang,[1,2] Fei Lin,[2] Li-li Guo,[1] Xing-jiang Xiong,[1] and Xun Fan[2]

[1]*Department of Cardiology, Guang'anmen Hospital, China Academy of Chinese Medical Sciences, Beijing 100053, China*
[2]*Clinical Medical College, Hubei University of Chinese Medicine, Wuhan 430065, China*

Correspondence should be addressed to Fei Lin; linfeixixi@aliyun.com

Received 22 May 2014; Revised 6 September 2014; Accepted 14 September 2014

Academic Editor: Keji Chen

Recent studies demonstrated that mitochondria play an important role in the cardiovascular system and mutations of mitochondrial DNA affect coronary artery disease, resulting in hypertension, atherosclerosis, and cardiomyopathy. Traditional Chinese medicine (TCM) has been used for thousands of years to treat cardiovascular disease, but it is not yet clear how TCM affects mitochondrial function. By reviewing the interactions between the cardiovascular system, mitochondrial DNA, and TCM, we show that cardiovascular disease is negatively affected by mutations in mitochondrial DNA and that TCM can be used to treat cardiovascular disease by regulating the structure and function of mitochondria via increases in mitochondrial electron transport and oxidative phosphorylation, modulation of mitochondrial-mediated apoptosis, and decreases in mitochondrial ROS. However further research is still required to identify the mechanism by which TCM affects CVD and modifies mitochondrial DNA.

1. Introduction

At present, the anatomical paradigm of medicine and the Mendelian paradigm of genetics have failed to interpret anticipated genetic causes of common age-related diseases that include diabetes and metabolic syndrome, Alzheimer's disease, Parkinson's disease, cardiovascular disease (CVD), and cancer [1]. Nevertheless, with the development of medicine, mitochondrial biology and genetics have become excellent candidates for expanding these anatomical and Mendelian paradigms to reveal the complexities of CVDs that have become a worldwide problem [2]. Thus, the mitochondrial paradigm (a complementary concept to Mendelian genetics) is a paradigm of CVD susceptibility and cellular function [3].

Mitochondria are linked to the cardiovascular system. The heart is highly dependent for its function on oxidative energy generated in mitochondria, primarily by fatty acid beta-oxidation, the respiratory electron chain, and oxidative phosphorylation. The ability to utilize oxygen drives the development and evolution of the cardiovascular system in multicellular organisms [4]. Mitochondria are evolutionary endosymbionts derived from bacteria and contain DNA similar to bacterial DNA. Restructuring of the protomitochondrial genome included the transfer of virtually all 1500 genes of the mitochondrial genome into chromosomal nuclear DNA; mitochondrial DNA (mtDNA) retains 13 polypeptide-encoding genes, 2 rRNA genes, and 22 tRNA genes [5]. For those mtDNA-encoded proteins is either an electron or a proton carrier of oxidative phosphorylation. Mitochondria are recognizing sensors of oxygen and fuel and producers of heat and ATP. They generate reactive oxygen species, acting as signaling hubs with their redox-based signals reaching the cell membrane and the nucleus, and they regulate calcium and effective inducers of cell death (apoptosis) [5]. Notably, mtDNA deletion is significantly associated with loss of atrial adenine nucleotides. Atrial concentrations of ATP, ADP, AMP, and total adenine nucleotides were significantly lower in patients with deletions than those in patients without deletions [6].

Mutations of mtDNA are associated with several clinical manifestations affecting different systems. By virtue of the functional role of mitochondria in energy metabolism and

reactive oxygen species production, mutations in mtDNA are potential candidate risk factors for cardiovascular disorders. This has led to the mitochondrial paradigm in which it has been proposed that mtDNA sequence variation contributes to susceptibility to CVD. In addition, defects in mitochondrial structure and function are associated with CVDs, such as dilated and hypertrophy cardiomyopathy, cardiac conduction defects and sudden death, ischemic and alcoholic cardiomyopathy, and myocarditis [7].

Traditional Chinese medicine (TCM) has been in use for over 2500 years and has historically established itself as a system of holistic medical care in China [8]. What is more, Chinese medicine and integrative medicine health provision in conventional medical clinics and hospital settings have emerged worldwide [9–11]. TCM is known to efficiently prevent and cure CVD and other illnesses, as well as have a habilitative, strengthening effect on the body. However, the mechanisms by which TCM alleviates CVD are not clearly understood. Now unrecognized mitochondrial pathways and new therapeutic strategies for the treatment of CVD by TCM are systematic survey. If this strategy proves successful, it may have been prescient that a major concept in the parlance of Mitochondria is chi, which loosely translates as vital force or energy [5].

2. Coronary Artery Disease

Coronary artery disease (CAD) is one of the most widespread and common causes of death in the world. It is a multifactorial process that appears to be caused by the interaction of environmental risk factors with multiple predisposing genes. An increase in oxidative stress in CVD may be responsible for the accumulation of mtDNA damage in CAD patients. Reactive oxygen species (ROS) can damage mtDNA and this may cause tissue dysfunctionality, leading to early events in CVD.

Recent evidence suggests that a specific mtDNA deletion of 4977 bp, 3243A>G, and 16189T>C is associated with myocardial dysfunction and bioenergetic deficits. In numerous studies, a significant higher incidence of mtDNA 4977 was observed in CAD patients than in healthy subjects, and the relative degree of deletion was higher in CAD patients than in the control group [12]. Relative quantifications showed that the amount of mtDNA (4977) deletion was greater and that telomere length was shorter in CAD patients [13]. Of the most conventional risk factors, smoking and dyslipidemia have the strongest association with the degree of mtDNA (4977) deletion and significantly correlate with telomere attrition [13]. In addition, cardiac diseases are frequently detected among sudden natural deaths, with mtDNA 4977-deletion present more frequently in victims of sudden natural death than in subjects who died of unnatural causes [14].

In other studies, mitochondrial dysfunction may affect autonomic regulatory systems more directly; the A3243G mitochondrial DNA mutation [15] and individuals with the 3243A>G mutation in mtDNA have abnormalities in the spectral and fractal characteristics of heart rate variability, which suggest altered cardiac autonomic regulation [16]. The mitochondrial DNA variant 16189T>C is also associated with CAD and myocardial infarction in Saudi Arabs. The impact of mtDNA polymorphism on CAD manifestation is influenced by important confounders, particularly the presence of myocardial infarction, hypertension, and age [17].

3. Hypertension

Essential hypertension (EH), a polygenic, multifactorial, and highly heterogeneous disorder of unknown etiology, is the most common CVD in the world. Several studies have noted that mtDNA variation has become an additional target in the investigation of potential EH heritability. To assess the contribution of the mitochondrial genome to EH, researchers performed a systematic, extended screening of hypertensive individuals to identify potentially pathogenic mtDNA mutations. Of these mtDNA mutations, mt-transfer RNA (tRNA) was a mutational hotspot for pathogenic mutations associated with EH. Mutant mtDNA aggravates mitochondrial dysfunction, critically contributing to clinical phenotypes [18]. Moreover, the sequence of the entire mitochondrial genome in probands from 20 pedigrees was recently analyzed. Comparison with the reference "Cambridge" sequence revealed a total of 297 base changes, including 24 in ribosomal RNA (rRNA) genes, 15 in transfer RNA (tRNA) genes, and 46 amino acid substitutions [19]. The presence of the m.14484T>C mutation was reported in a Chinese family with maternally inherited EH. Mitochondrial respiration rate and membrane potential were reduced in lymphoblastoid cell lines established from affected members carrying m.14484T>C. There was a compensatory increase in mitochondrial mass in these mutant cell lines [20]. In addition, the 4435A>G mutation may act as an inherited risk factor for the development of hypertension in this Chinese pedigree. A failure in mitochondrial tRNA metabolism, caused by the 4435A>G mutation, led to an approximately 30% reduction in the rate of mitochondrial translation [21]. Furthermore, uncommon/rare variants were identified by sequencing the entire mitochondrial genome of 32 unrelated individuals with extreme hypertension and genotyping 40 mitochondrial single nucleotide polymorphisms in 7219 individuals. The nonsynonymous mitochondrial single nucleotide polymorphism 5913G>A in the cytochrome c oxidase subunit 1 of respiratory complex IV was significantly associated with blood pressure and fasting blood glucose levels [22]. In addition, the data provide support for a maternal effect on hypertension status and quantitative systolic hypertension, which is consistent with a mitochondrial influence. The estimated fraction of hypertensive pedigrees that were potentially the result of mitochondrial effects was 35.2%. Mitochondrial heritabilities for multivariable-adjusted long-term average systolic hypertension and diastolic hypertension were 5% and 4%, respectively [23].

4. Cardiomyopathy

Dilated cardiomyopathy (DCM) is one of the most frequent forms of primary myocardial disease and the third most

common cause of heart failure. Recent studies suggest that mtDNA mutations and mitochondrial abnormalities may be contributing factors for the development of DCM. Defects in mtDNA, both deletions and tRNA point mutations, are associated with cardiomyopathies [24]. In a study some patients had heteroplasmic mtDNA mutations [24]. Research also suggests that TNF-alpha-induced heart failure may be associated with reduced mtDNA repair activity [25]. A novel duplication in the mitochondrially encoded tRNA proline gene was found in a patient with dilated cardiomyopathy. Part of this duplication is localized within the tRNA proline gene that can act against oxidative stress and regulate the balance of reactive oxygen species within cells. The patient was described as having DCM and a novel mtDNA duplication. Sequencing of the mtDNA control region was performed, and a 15 bp duplication was observed between nucleotides 16,018 and 16,032 [26]. Five patients with CM shared a novel homoplasmic point mutation, and all of them demonstrated the evolutionarily related D-loop sequence of mitochondria [27]. At present, 13 types of mutations in subunits of the mitochondrial respiratory chain complexes are associated with cardiomyopathy and they include Cyt b 14927A>G, Cyt b 15236A>G, Cyt b 15452A>G, Co I 6521C>G, Co II 7673A>G, ND I 3394T>C, ND 6 13258A>T, and ND 6 14180T>C [28].

Additionally, left ventricular noncompaction cardiomyopathy (LVNC) is a rare congenital cardiomyopathy that is associated with mutations in mtDNA, as mtDNA copy number and mtDNA content were lower in the myocardium of LVNC patients, with abnormal mitochondrial morphology, suggesting that mitochondrial dysfunction may be associated with the etiology of LVNC [29]. In addition, mtDNA mutations in patients with beta myosin heavy chain- (beta MHC-) linked hypertrophic cardiomyopathy (HCM) are present in individuals who develop congestive heart failure. Although beta MHC gene mutations may be determinants of HCM and both of the mtDNA mutations in these patients are known prerequisites for pathogenicity. Coexistence of other genetic abnormalities in beta MHC-linked HCM, including mtDNA mutations, may contribute to variable phenotypic expression and explain the heterogeneous behavior of HCM [30]. Therefore, mtDNA is a key player in the pathogenesis of cardiomyopathy and has provided new mechanism-based approaches to therapy [31].

5. Heart Failure

Heart failure (HF) is the end stage of various types of CVDs whose mortality rate is considerably high. The advent of the mitochondrial paradigm has provided important insights into the mechanisms underlying HF. Results of studies show an intimate link between ROS, TNF-alpha, mtDNA damage, and defects in electron transport function, which may lead to the additional generation of ROS and might also play an important role in the development and progression of left ventricle remodeling and HF [32].

Excessive ROS produced by electron leaks from mitochondria in failing myocardium play an important role in the development and progression of HF and cardiac remodeling [33]. Mitochondrial electron transport is an enzymatic source of oxygen radical generation and is also a target of oxidant-induced damage [34]. Chronic increases in oxygen radical production in the mitochondria can possibly lead to a catastrophic cycle of mtDNA damage as well as functional decline, further oxygen radical generation, and cellular injury. ROS directly impair contractile functions by modifying proteins central to excitation-contraction coupling and activate a broad variety of hypertrophy signaling kinases and transcription factors and mediate apoptosis. Moreover, ROS stimulate cardiac fibroblast proliferation and activate matrix metalloproteinases, leading to extracellular matrix remodeling. ROS also play an important role in the pathophysiology of cardiac remodeling and heart failure [34–36]. Another study using Southern blot analysis showed that mtDNA copy number relative to a nuclear gene (18S rRNA) preferentially decreases by 44% after myocardial infarction, which was associated with a parallel decrease in the mtDNA-encoded gene transcripts, including subunits of complex I (ND1, 2, 3, 4, 4L, and 5), complex III (cytochrome b), complex IV (cytochrome c oxidase), and rRNA (12S and 16S) [32].

Therefore, oxidative stress and mtDNA damage are excellent therapeutic targets. Overexpression of peroxiredoxin-3 (Prx-3), mitochondrial antioxidants, or mitochondrial transcription factor A (TFAM) could ameliorate the decline in the mtDNA copy number in failing hearts. Consistent with alterations in mtDNA, the decrease in oxidative capacity may also be prevented [36].

ROS can damage mtDNA and thus lead to mitochondrial dysfunction and additional generation of ROS. Overexpression of TFAM, which is essential for mtDNA transcription and replication, ameliorates cardiac remodeling and failure [33]. Overexpression of TFAM attenuates the decrease in mtDNA copy number after myocardial infarction, ameliorates pathological hypertrophy, and markedly improves the chances of survival. TFAM also protects the heart from mtDNA deficiencies and attenuates left ventricular remodeling and failure after myocardial infarction created by ligating the left coronary artery [37]. Recombinant human TFAM protein increases mtDNA and abolishes the activation of nuclear factor of activated T cells (NFAT), which is well known to attenuate pathological hypertrophy of cardiac myocytes [38]. Furthermore, there are the intimate links between TNF-alpha, ROS, and mtDNA damage that might play an important role in myocardial remodeling and failure [39].

6. Atherosclerosis

Atherosclerotic plaques, which contain vascular and inflammatory cells, lipids, cholesterol crystals, and cellular debris, restrict lumen size and often rupture, causing infarctions [4]. Atherosclerosis is the major risk factor for development of CVD based on arterial endothelial dysfunction and is caused by the impairment of endothelial-dependent dilation. Recent findings have shown that the level of heteroplasmy of some somatic mtDNA is associated with coronary atherosclerosis and impaired mitochondrial function. Structural and qualitative changes in mitochondrial components such as

mtDNA may be directly involved in the development of multiple atherogenic mechanisms, including advanced oxidative stress, abnormalities in glucose and fat metabolism, and altered energy homeostasis [40]. Atherosclerotic vascular disease is typically a disease of aging. In accordance with the ROS theory of aging [41], accumulated data point to a key role of ROS in the pathogenesis of atherosclerosis. mtDNA, owing to electron transport chain proximity and the relative lack of mtDNA repair mechanisms, is the most vulnerable target of mitochondrial ROS. Greater mtDNA damage is present in human aorta atherosclerosis samples than in those of age-matched transplant donors [42]. Mitochondria have been recognised as critical regulators of cell death, generation of ATP, and the generation of reactive oxygen species (ROS), and mtDNA damage leads to mitochondrial dysfunction and promotes atherosclerosis directly [43]. Damage of mtDNA in the vessel wall and circulating cells is widespread and causative, indicates a higher risk of atherosclerosis, promotes atherosclerosis independently of ROS through effects on smooth muscle cells and monocytes, and correlates with higher-risk plaques in humans [44].

7. Summary

At present, modes for diagnosis and treatment of CVD differentiation used by modern medicine combined with syndrome differentiation from TCM have become a main method of treatment of CVD in China and other nations [45–47]. For example, *Radix Salviae miltiorrhizae*, *Radix et Rhizoma Notoginseng*, *Rhizoma Chuanxiong*, *Radix Astragali*, and others have been used for the treatment of CVDs [48], showing a remarkable curative effect however, mechanisms remain unknown.

Human mtDNA mutations cause a large spectrum of clinically important cardiovascular events. Research suggests that if mitochondrial ROS production becomes excessive, it is possible for mitochondria and mtDNA to be damaged [5]. To detect mitochondrially active compounds, Wallace assembled a mitochondrial cDNA expression array, the MITOCHIP, which interrogates ~1000 genes involved in mitochondrial energy production, ROS biology, and apoptosis. TCM might target mitochondrial function with a serial action aimed at treating CVDs. For example, restoratives are all medicinal herbs for replenishing qi and blood, nourishing yin and yang, improving the functions of the internal organs and body immunity, and relieving the various symptoms of weakness. Historically Chinese have been taking Astragali Radix as a natural invigorant in nourishing life. Astragali Radix injection can reverse mitochondrial dysfunction and abnormal structure in myocardial cells during myocardial cell hypertrophy, caused by angiotensin II. Reversion of myocardial cell hypertrophy and the restructuring of myocardial cells help improve energy metabolism in myocardial cells [49].

A yang-invigorating Chinese herb formula treatment increased red blood cell Cu-Zn-SOD (superoxide dismutase) activity and mitochondrial ATP generation capacity and reduced glutathione and alpha-tocopherol levels. It has been suggested that yang-invigorating herbs might promote ATP generation by increasing mitochondrial electron transport and induce increases in mitochondrial antioxidant capacity in various tissues as evidenced by a reduction in the extent of ROS generation in vitro. Red cell Cu-Zn-SOD activities correlated positively with mitochondrial antioxidant component tissue levels/activity. By contrast, yin-nourishing herbs either did not stimulate or decrease myocardial ATP generation capacity [50, 51]. *Herba Cistanche* belongs to the A class of yang-invigorating herbs and increases mitochondrial glutathione activity.

It increases mitochondrial ATP content, decreases mitochondrial Ca^{2+} content, and increases mitochondrial membrane potential [52]. *Ganoderma lucidum* increases the activity of cardiac mitochondrial enzymes and respiratory chain complexes in aged rats [53].

Moreover, Sini Decoction (SND) increases the activity and mRNA expression of Mn-SOD and the activity of Na^+-K^+ ATPase and Ca^{2+}-ATPase, while the degree of mitochondrial swelling and the content of malondialdehyde (MDA) were reduced in SND-treated rats [53]. Sodium tanshinone IIA sulfonate (STS) stimulates mitochondrial NADH oxidation dose dependently and partly restores NADH oxidation in the presence of a respiratory inhibitor (rotenone, antimycin A, or potassium cyanide) [54].

DaBu-Yin-Wan and QianZheng-San ameliorate behavior induced by administration of 1-methyl-4-phenyl-1,2,3,6-tetrahydropyridine (MPTP) and synergistically prevent decreases in tyrosine hydroxylase (TH) expression but also increase monoaminergic content and activity, improve ultrastructural changes, decrease mtDNA damage, and synergistically upregulate the expression of ND1 mRNA [55].

In addition, Guan-Xin-Er-Hao (GXEH) attenuates postischemia myocardial apoptosis. The antiapoptotic mechanisms of GXEH may involve mitochondrial cytochrome c-mediated caspase-3 activation in cardiomyocytes after the occurrence of acute myocardial infarction. GXEH adjusts the balance of Bax and Bcl-2 toward an antiapoptotic state, decreases mitochondrial cytochrome c release, reduces caspase-9 activation, and attenuates subsequent caspase-3 activation and postischemic myocardial apoptosis in rats [56]. Furthermore, Ginkgo biloba leaf extract alters mitochondrial gene expression, possibly by modulating mitochondrial-associated apoptosis [57]. Danshen-Gegen (DG) decoction treatment activates both ERK/Nrf2- and PKC epsilon-mediated pathways, presumably through ROS arising from CYP-catalyzed processes, with resultant inhibition of hypoxia/reoxygenation-induced apoptosis immediately after DG treatment, or even after an extended time interval following DG treatment [58]. In addition, the derivative deoxysppanone B was found to act through microtubules to increase oxidative phosphorylation and decrease mitochondrial ROS [59].

The mitochondrial paradigm for CVD susceptibility and cellular function may become a complementary concept to Mendelian genetics. In this regard, Wallace suggests that mitochondria are Qi (Chi), which loosely translates as vital force or energy, according to its TCM interpretation. The fact that TCM uses a variety of mitochondrial functional readouts may reveal previously unrecognized mitochondrial pathways

and new therapeutic strategies to manipulate them, and these could then be applied to treating CVD. It is therefore important to consider how we might initiate a search for a TCM method to regulate the function of mitochondria and the effects of mtDNA to treat CVD.

Conflict of Interests

The authors declare that there is no conflict of interests regarding the publication of this paper.

Acknowledgments

The current work was partially supported by the ministry of a national science and technology major project and dedicated funds for "significant new drugs creation" (no. 2012ZX09102-201-006). The corresponding author and third author contributed equally to this paper.

References

[1] D. C. Wallace, "A mitochondrial paradigm of metabolic and degenerative diseases, aging, and cancer: a dawn for evolutionary medicine," *Annual Review of Genetics*, vol. 39, pp. 359–407, 2005.

[2] D. C. Wallace, "Mitochondrial genetics: a paradigm for aging and degenerative diseases?" *Science*, vol. 256, no. 5057, pp. 628–632, 1992.

[3] D. M. Krzywanski, D. R. Moellering, J. L. Fetterman, K. J. Dunham-Snary, M. J. Sammy, and S. W. Ballinger, "The mitochondrial paradigm for cardiovascular disease susceptibility and cellular function: a complementary concept to Mendelian genetics," *Laboratory Investigation*, vol. 91, no. 8, pp. 1122–1135, 2011.

[4] P. Dromparis and E. D. Michelakis, "Mitochondria in vascular health and disease," *Annual Review of Physiology*, vol. 75, pp. 95–126, 2013.

[5] D. C. Wallace, "Mitochondria as chi," *Genetics*, vol. 179, no. 2, pp. 727–735, 2008.

[6] Y. Tomikura, I. Hisatome, M. Tsuboi et al., "Coordinate induction of AMP deaminase in human atrium with mitochondrial DNA deletion," *Biochemical and Biophysical Research Communications*, vol. 302, no. 2, pp. 372–376, 2003.

[7] J. Marín-García and M. J Goldenthal, "The mitochondrial organelle and the heart," *Revista Española de Cardiología*, vol. 55, no. 12, pp. 1293–1310, 2002.

[8] N. Robinson, "Integrative medicine: traditional Chinese medicine, a model?" *Chinese Journal of Integrative Medicine*, vol. 17, no. 1, pp. 21–25, 2011.

[9] H. R. Schumacher, "West meets East—observations on integrative medicine in rheumatology from the USA," *Chinese Journal of Integrative Medicine*, vol. 14, no. 3, pp. 165–166, 2008.

[10] S. Grace and J. Higgs, "Integrative medicine: enhancing quality in primary health care," *Journal of Alternative and Complementary Medicine*, vol. 16, no. 9, pp. 945–950, 2010.

[11] H. S. Boon and N. Kachan, "Integrative medicine: a tale of two clinics," *BMC Complementary and Alternative Medicine*, vol. 8, no. 1, article 32, 2008.

[12] N. Botto, S. Berti, S. Manfredi et al., "Detection of mtDNA with 4977 bp deletion in blood cells and atherosclerotic lesions of patients with coronary artery disease," *Mutation Research/Fundamental and Molecular Mechanisms of Mutagenesis*, vol. 570, no. 1, pp. 81–88, 2005.

[13] L. Sabatino, N. Botto, A. Borghini, S. Turchi, and M. G. Andreassi, "Development of a new multiplex quantitative real-time PCR assay for the detection of the mtDNA4977 deletion in coronary artery disease patients: a link with telomere shortening," *Environmental and Molecular Mutagenesis*, vol. 54, no. 5, pp. 299–307, 2013.

[14] E. Y. Polisecki, L. E. Schreier, J. Ravioli, and D. Corach, "Common mitochondrial DNA deletion associated with sudden natural death in adults," *Journal of Forensic Sciences*, vol. 49, no. 6, pp. 1335–1338, 2004.

[15] C. Harrison-Gómez, A. Harrison-Ragle, A. Macías-Hernández, and V. Guerrero-Sánchez, "A3243G mitochondrial DNA mutation and heterogeneous phenotypic expression," *Revista Médica del Instituto Mexicano del Seguro Social*, vol. 47, no. 2, pp. 219–225, 2009.

[16] K. Majamaa-Voltti, K. Majamaa, K. Peuhkurinen, T. H. Mäkikallio, and H. V. Huikuri, "Cardiovascular autonomic regulation in patients with 3243A>G mitochondrial DNA mutation," *Annals of Medicine*, vol. 36, no. 3, pp. 225–231, 2004.

[17] K. K. Abu-Amero, O. M. Al-Boudari, A. Mousa et al., "The mitochondrial DNA variant 16189T>C is associated with coronary artery disease and myocardial infarction in Saudi Arabs," *Genetic Testing and Molecular Biomarkers*, vol. 14, no. 1, pp. 43–47, 2010.

[18] Y. Ding, B. Xia, J. Yu, J. Leng, and J. Huang, "Mitochondrial DNA mutations and essential hypertension (Review)," *International Journal of Molecular Medicine*, vol. 32, no. 4, pp. 768–774, 2013.

[19] F. Schwartz, A. Duka, F. Sun, J. Cui, A. Manolis, and H. Gavras, "Mitochondrial genome mutations in hypertensive individuals," *The American Journal of Hypertension*, vol. 17, no. 7, pp. 629–635, 2004.

[20] Q. Yang, S. K. Kim, F. Sun et al., "Maternal influence on blood pressure suggests involvement of mitochondrial DNA in the pathogenesis of hypertension: the Framingham Heart Study," *Journal of Hypertension*, vol. 25, no. 10, pp. 2067–2073, 2007.

[21] Y. Liu, R. Li, Z. Li et al., "Mitochondrial transfer RNA met 4435a>g mutation is associated with maternally inherited hypertension in a chinese pedigree," *Hypertension*, vol. 53, no. 6, pp. 1083–1090, 2009.

[22] C. Liu, Q. Yang, S.-J. Hwang et al., "Association of genetic variation in the mitochondrial genome with blood pressure and metabolic traits," *Hypertension*, vol. 60, no. 4, pp. 949–956, 2012.

[23] H. Guo, X.-Y. Zhuang, A.-M. Zhang et al., "Presence of mutation m.14484T > C in a Chinese family with maternally inherited essential hypertension but no expression of LHON," *Biochimica et Biophysica Acta: Molecular Basis of Disease*, vol. 1822, no. 10, pp. 1535–1543, 2012.

[24] E. Arbustini, M. Diegoli, R. Fasani et al., "Mitochondrial DNA mutations and mitochondrial abnormalities in dilated cardiomyopathy," *The American Journal of Pathology*, vol. 153, no. 5, pp. 1501–1510, 1998.

[25] Y. Y. Li, D. Chen, S. C. Watkins, and A. M. Feldman, "Mitochondrial abnormalities in tumor necrosis factor-α-induced heart failure are associated with impaired DNA repair activity," *Circulation*, vol. 104, no. 20, pp. 2492–2497, 2001.

[26] M. M. S. G. Cardena, A. J. Mansur, A. D. C. Pereira, and C. Fridman, "A new duplication in the mitochondrially encoded

tRNA proline gene in a patient with dilated cardiomyopathy," *Mitochondrial DNA*, vol. 24, no. 1, pp. 46–49, 2013.

[27] W. S. Shin, M. Tanaka, J.-I. Suzuki, C. Hemmi, and T. Toyooka, "A novel homoplasmic mutation in mtDNA with a single evolutionary origin as a risk factor for cardiomyopathy," *The American Journal of Human Genetics*, vol. 67, no. 6, pp. 1617–1620, 2000.

[28] J. J. Liu and X. M. Wang, *The Medicine and Health of Mitochondria*, vol. 129, Science Press, Beijing, China, 2012.

[29] S. Liu, Y. Bai, J. Huang et al., "Do mitochondria contribute to left ventricular non-compaction cardiomyopathy? New findings from myocardium of patients with left ventricular non-compaction cardiomyopathy," *Molecular Genetics and Metabolism*, vol. 109, no. 1, pp. 100–106, 2013.

[30] E. Arbustini, R. Fasani, P. Morbini et al., "Coexistence of mitochondrial DNA and β myosin heavy chain mutations in hypertrophic cardiomyopathy with late congestive heart failure," *Heart*, vol. 80, no. 6, pp. 548–558, 1998.

[31] F. M. Santorelli, A. Tessa, G. D'amati, and C. Casali, "The emerging concept of mitochondrial cardiomyopathies," *American Heart Journal*, vol. 141, no. 1, pp. 5A–12A, 2001.

[32] T. Ide, H. Tsutsui, S. Hayashidani et al., "Mitochondrial DNA damage and dysfunction associated with oxidative stress in failing hearts after myocardial infarction," *Circulation Research*, vol. 88, no. 5, pp. 529–535, 2001.

[33] S. Kinugawa and H. Tsutsui, "Oxidative stress and heart failure," *Nippon Rinsho. Japanese Journal of Clinical Medicine*, vol. 64, no. 5, pp. 848–853, 2006.

[34] H. Tsutsui, T. Ide, and S. Kinugawa, "Mitochondrial oxidative stress, DNA damage, and heart failure," *Antioxidants and Redox Signaling*, vol. 8, no. 9-10, pp. 1737–1744, 2006.

[35] H. Tsutsui, S. Kinugawa, and S. Matsushima, "Oxidative stress and heart failure," *The American Journal of Physiology—Heart and Circulatory Physiology*, vol. 301, no. 6, pp. H2181–H2190, 2011.

[36] H. Tsutsui, S. Kinugawa, and S. Matsushima, "Oxidative stress and mitochondrial DNA damage in heart failure," *Circulation Journal*, vol. 72, pp. A31–A37, 2008.

[37] M. Ikeuchi, H. Matsusaka, D. Kang et al., "Overexpression of mitochondrial transcription factor A ameliorates mitochondrial deficiencies and cardiac failure after myocardial infarction," *Circulation*, vol. 112, no. 5, pp. 683–690, 2005.

[38] T. Fujino, T. Ide, M. Yoshida et al., "Recombinant mitochondrial transcription factor A protein inhibits nuclear factor of activated T cells signaling and attenuates pathological hypertrophy of cardiac myocytes," *Mitochondrion*, vol. 12, no. 4, pp. 449–458, 2012.

[39] N. Suematsu, H. Tsutsui, J. Wen et al., "Oxidative stress mediates tumor necrosis factor-α-induced mitochondrial DNA damage and dysfunction in cardiac myocytes," *Circulation*, vol. 107, no. 10, pp. 1418–1423, 2003.

[40] I. A. Sobenin, D. A. Chistiakov, Y. V. Bobryshev, A. Y. Postnov, and A. N. Orekhov, "Mitochondrial mutations in atherosclerosis: new solutions in research and possible clinical applications," *Current Pharmaceutical Design*, vol. 19, no. 33, pp. 5942–5953, 2013.

[41] D. Harman, "Aging: a theory based on free radical and radiation chemistry," *The Journal of Gerontology*, vol. 11, no. 3, pp. 298–300, 1956.

[42] S. W. Ballinger, C. Patterson, C. A. Knight-Lozano et al., "Mitochondrial integrity and function in atherogenesis," *Circulation*, vol. 106, no. 5, pp. 544–549, 2002.

[43] E. P. Yu and M. R. Bennett, "Mitochondrial DNA damage and atherosclerosis," *Trends in Endocrinology and Metabolism*, vol. 25, no. 9, pp. 481–487, 2014.

[44] E. Yu, P. A. Calvert, J. R. Mercer et al., "Mitochondrial DNA damage can promote atherosclerosis independently of reactive oxygen species through effects on smooth muscle cells and monocytes and correlates with higher-risk plaques in humans," *Circulation*, vol. 128, no. 7, pp. 702–712, 2013.

[45] X. J. Xiong, F. Borrelli, A. S. Ferreira, T. Ashfaq, and B. Feng, "Herbal medicines for cardiovascular diseases," *Evidence-Based Complementary and Alternative Medicine*, vol. 2014, Article ID 809741, 2014.

[46] X. J. Xiong, X. C. Yang, Y. M. Liu, Y. Zhang, P. Q. Wang, and J. Wang, "Chinese herbal formulas for treating hypertension in traditional Chinese medicine: perspective of modern science," *Hypertension Research*, vol. 36, pp. 570–579, 2013.

[47] J. Wang and X. J. Xiong, "Current situation and perspectives of clinical study in integrative medicine in China," *Evidence-Based Complementary and Alternative Medicine*, vol. 2012, Article ID 268542, 11 pages, 2012.

[48] F. Lin, J. Wang, L. L. Guo, and Q. Y. He, "Composition law of proprietary Chinese medicine for coronary heart disease in Chinese pharmacopoeia," *Journal of Traditional Chinese Medicine*, vol. 54, no. 18, pp. 1596–1599, 2013.

[49] Y. Yu, S. Wang, B. Nie, Y. Sun, Y. Yan, and L. Zhu, "Effect of Astragali Radix injection on myocardial cell mitochondrial structure and function in process of reversing myocardial cell hypertrophy," *Zhongguo Zhong Yao Za Zhi*, vol. 37, no. 7, pp. 979–984, 2012.

[50] H. Y. Leung, P. Y. Chiu, M. K. T. Poon, and K. M. Ko, "A Yang-invigorating Chinese herbal formula enhances mitochondrial functional ability and antioxidant capacity in various tissues of male and female rats," *Rejuvenation Research*, vol. 8, no. 4, pp. 238–247, 2005.

[51] K. M. Ko, T. Y. Y. Leon, D. H. F. Mak, P. Y. Chiu, Y. Du, and M. K. Poon, "A characteristic pharmacological action of "Yang-invigorating" Chinese tonifying herbs: enhancement of myocardial ATP-generation capacity," *Phytomedicine*, vol. 13, no. 9, pp. 636–642, 2006.

[52] A. H.-L. Siu and K. M. Ko, "Herba Cistanche extract enhances mitochondrial glutathione status and respiration in rat hearts, with possible induction of uncoupling proteins," *Pharmaceutical Biology*, vol. 48, no. 5, pp. 512–517, 2010.

[53] N. P. Sudheesh, T. A. Ajith, and K. K. Janardhanan, "Ganoderma lucidum (Fr.) P. Karst enhances activities of heart mitochondrial enzymes and respiratory chain complexes in the aged rat," *Biogerontology*, vol. 10, no. 5, pp. 627–636, 2009.

[54] M. Zhao, W. Wu, X. Duan et al., "The protective effects of sini decoction on mitochondrial function in adriamycin-induced heart failure rats," *Zhong Yao Cai*, vol. 28, no. 6, pp. 486–489, 2005.

[55] Y. Zhang, H.-M. Sun, X. He et al., "Da-Bu-Yin-Wan and Qian-Zheng-San, two traditional Chinese herbal formulas, up-regulate the expression of mitochondrial subunit NADH dehydrogenase 1 synergistically in the mice model of Parkinson's disease," *Journal of Ethnopharmacology*, vol. 146, no. 1, pp. 363–371, 2013.

[56] H.-W. Zhao, F. Qin, Y.-X. Liu, X. Huang, and P. Ren, "Antiapoptotic mechanisms of Chinese medicine formula, Guan-Xin-Er-Hao, in the rat ischemic heart," *Tohoku Journal of Experimental Medicine*, vol. 216, no. 4, pp. 309–316, 2008.

[57] J. V. Smith, A. J. Burdick, P. Golik, I. Khan, D. Wallace, and Y. Luo, "Anti-apoptotic properties of Ginkgo biloba extract EGb 761 in differentiated PC12 cells," *Cellular and Molecular Biology*, vol. 48, no. 6, pp. 699–707, 2002.

[58] P. Y. Chiu, H. Y. Leung, P. K. Leong et al., "Danshen-Gegen decoction protects against hypoxia/reoxygenation-induced apoptosis by inhibiting mitochondrial permeability transition via the redox-sensitive ERK/Nrf2 and PKCε/mK ATP pathways in H9c2 cardiomyocytes," *Phytomedicine*, vol. 19, no. 2, pp. 99–110, 2012.

[59] B. K. Wagner, T. Kitami, T. J. Gilbert et al., "Large-scale chemical dissection of mitochondrial function," *Nature Biotechnology*, vol. 26, no. 3, pp. 343–351, 2008.

Hindawi Publishing Corporation
Evidence-Based Complementary and Alternative Medicine
Volume 2015, Article ID 508029, 6 pages
http://dx.doi.org/10.1155/2015/508029

Research Article

In Vivo Antioxidant and Hypolipidemic Effects of Fermented Mung Bean on Hypercholesterolemic Mice

Swee Keong Yeap,[1] Boon Kee Beh,[2] Wan Yong Ho,[3] Hamidah Mohd Yusof,[4] Nurul Elyani Mohamad,[4] Norlaily Mohd Ali,[4] Indu Bala Jaganath,[5] Noorjahan Banu Alitheen,[4] Soo Peng Koh,[6] and Kamariah Long[6]

[1] *Institute of Bioscience, Universiti Putra Malaysia, 43400 Serdang, Selangor, Malaysia*
[2] *Department of Bioprocess Technology, Faculty of Biotechnology and Biomolecular Sciences, Universiti Putra Malaysia, 43400 Serdang, Selangor, Malaysia*
[3] *School of Biomedical Sciences, The University of Nottingham, Malaysia Campus, Jalan Broga, 43500 Semenyih, Selangor, Malaysia*
[4] *Department of Cell and Molecular Biology, Faculty of Biotechnology and Biomolecular Sciences, Universiti Putra Malaysia, 43400 Serdang, Selangor, Malaysia*
[5] *Biotechnology Research Centre, Malaysian Agriculture Research Development Institute, 43400 Serdang, Selangor, Malaysia*
[6] *Department of Bioprocess Biotechnology, Malaysian Agriculture Research Development Institute, 43400 Serdang, Selangor, Malaysia*

Correspondence should be addressed to Kamariah Long; amai@mardi.gov.my

Received 7 April 2014; Accepted 21 July 2014

Academic Editor: Qunhao Zhang

Legumes have previously been reported with hypolipidemic effect caused by the presence of flavonoid. This study was carried out to evaluate the antioxidant and hypolipidemic effects of fermented mung bean on hypercholesterolemic mice. Blood from all mice was collected and subjected to serum lipid and liver profiles biochemical analysis and quantitative RT-PCR for atherosclerosis related gene expressions. Besides, livers were collected for antioxidant assays and histopathology evaluation. Fermented mung bean was found to reduce the level of serum lipid and liver enzyme profiles of hypercholesterolemic mice. Furthermore, liver antioxidant and nitric oxide levels were also significantly restored by fermented mung bean in a dosage dependent manner. The gene expression study indicated that *Apoe* and *Bcl2a1a* were upregulated while *Npy* and *Vwf* expressions were downregulated after the treatment. The effects of fermented mung bean were greater than nonfermented mung bean. These results indicated that fermented mung bean possessed antioxidants that lead to its hypolipidemic effect on hypercholesterolemic mice.

1. Introduction

Hypercholesterolemia is generally caused by high-cholesterol diet and the lack of physical exercise. High income or developed countries such as USA and Western Europe have recorded higher incidence of hypercholesterolemia in their population due to the prevalence of raised cholesterol levels [1, 2]. This has been correlated to higher risk of cardiovascular disease and stroke. Besides, high cholesterol diet also contributed to steatohepatitis, which is often characterized by inflammation and mitochondria glutathione depletion [3]. Nowadays, the trend to reduce hypercholesterolemia through consuming functional foods has gained more acceptances.

Legumes such as soybean and mung bean have been identified as potential functional foods for the prevention of chronic diseases including cancer and cardiovascular diseases. For example, soy protein and isoflavones have been approved by the US Food and Drug Administration to be used as health foods for control of triglyceride (TG) and total cholesterol levels [4]. Mung bean (*Vigna radiata*) is a legume that contains large amounts of protein, essential amino acids, and metabolites such as γ-amino butyric acid (GABA) [5]. In Chinese medicine, mung bean has been widely used to prepare mung bean soup for cooling and detoxification of the body [6]. Moreover, mung bean was found to be a potent antioxidant and hepatoprotective agent [5]. Our

earlier research has reported the potential of fermentation in improving these effects shown by the mung bean [5]. Besides, fermented mung bean was also found to be a good source of GABA [5], while GABA enriched foods including tempeh (fermented soy) [7] and brown rice bran [8] have been recognized as good sources of functional foods to reduce high lipid profiles. To date, the hypolipidemic and hepatoprotective effects of fermented mung bean on hypercholesterolemic mice are still unknown. In this study, we evaluated its hypolipidemic and hepatoprotective effects through *in vivo* serum biochemical profiles, liver antioxidant level, and blood atherosclerosis related gene expressions of fermented mung bean treated hypercholesterolemic mice.

2. Materials and Methods

2.1. Materials. Cholesterol, phosphate buffer saline (PBS), Folin-Ciocalteu reagent, aluminium chloride, sodium nitrate, hypoxanthine, xanthine oxidase, and superoxide dismutase were purchased from Sigma (USA). Positive control red yeast rice (HypoCol) containing 2% monacolin k/100 mg of capsule was purchased from AsiaPharm Biotech (Singapore). Total cholesterol, triglyceride, low density lipoprotein, and high density lipoprotein assay kits were purchased from Biovision (USA), Griess reagent was purchased from Invitrogen (USA), and RNeasy mini kit was purchased from Qiagen (USA), while cDNA first-strand synthesis kit and atherosclerosis RT^2 PCR array were purchased from SABiosciences (USA).

2.2. Preparation of Fermented Mung Bean. Fermented mung bean was prepared using *Monascus purpureus* strains (Malaysian Agricultural Research and Development Institute, Malaysia) based on our previous publication. Briefly, mung bean (*Vigna radiata*) was dehulled and soaked in water for 18 h at room temperature. Then, the mung bean was washed, steamed (40 minutes), chilled to room temperature, and mixed with Mardi *Rhizopus* sp. strain of 5351 inoculums for 48 h at 30°C. After the inoculation, the fermented mung bean was dried and both fermented and nonfermented mung beans were extracted with deionized water (1 : 20 ratio) at 25°C for 1 h. The water extract was then subjected to freeze drying (at ~−50°C) to yield 25% w/w of extract powder. The GABA concentration in 100 g of dried fermented mung bean extract powder was 0.122 g while the nonfermented mung bean did not contain any GABA [5]. The total phenolic content of fermented and nonfermented mung bean was 38.39 and 11.62 mg gallic acid equivalent/g extract dry weight with protocatechuic acid as the main detected soluble phenolic acid in fermented mung bean (201.32 μg/g extract) and p-coumaric acid in nonfermented mung bean (8.97 μg/g extract) (results not shown). Both freeze-dried fermented and nonfermented mung bean powders were dissolved in normal saline at a concentration of 1 g/mL for feeding use in the following *in vivo* experiment.

2.3. Animals and In Vivo Experiment. Eight-week-old male Balb/c mice ($n = 48$) were purchased from the Institute of Bioscience, Universiti Putra Malaysia, and housed under 22°C (12 hours light/dark) with standard pellet and drinking water *ad libitum* according to the guidelines from National Institute of Health for Care and Use of Laboratory Animals. This work was approved by the Animal Care and Use Committee, Faculty of Veterinary Medicine (UPM/FPV/PS/3.2.1.551/AUP-R168). Mice were randomly assigned into six groups ($n = 8$) with mice from groups 2 to 6 being fed p.o. with cholesterol (1 g/kg body weight) while group 1 was fed with PBS for 10 weeks. Treatments were started on week 8 where mice from group 3 were fed orally with 60 mg/kg body weight of Hypocol; groups 4 and 5 were fed orally with 200 mg/kg and 1000 mg/kg body weight of fermented mung bean; group 6 was fed orally with 1000 mg/kg body weight of nonfermented mung bean until week 10. Group 2 (negative control) was fed with PBS until week 10. At the end of the experiments, the mice were anesthetized with ether and sacrificed by cervical dislocation. Blood was collected for gene expressions study and serum was obtained for biochemical analysis. Livers were harvested and either fixed for histopathological evaluation or homogenated in PBS for antioxidant quantifications. Serum total cholesterol, TG, LDL, HDL, AST, ALT, and ALP levels were quantified according to the standard protocols from the kits (Biovision, USA) and were measured using a Hitachi 902 Automatic Biochemical Analyzer (Roche, German). On the other hand, SOD, MDA, FRAP, and NO levels from liver homogenates were quantified according to [5]. Furthermore, livers were harvested, fixed, stained with haematoxylin and eosin (H&E), and viewed under bright-field microscopy (Nikon, Japan) according to [5].

Total RNA was isolated from whole blood of groups 2, 3, 5, and 6 using the RNeasy mini kit (Qiagen, USA). cDNA was synthesized using first-strand kit (SABiosciences, USA) and expression of atherosclerosis related genes was profiled using mouse atherosclerosis RT^2 Profiler PCR array (SABiosciences, USA) according to the manufacturer's protocol using an iCycler iQ real-time PCR system (Bio-Rad, USA). The results were analyzed using the comparative Cq method with normalization of the results with five housekeeping genes included in this PCR array kit. The relative expression (fold change) was calculated by dividing the normalized data of the genes from samples of group 3 or group 5 with the normalized data of the genes from samples of the untreated group 2. Only fold expression changes larger than ±2 were recorded as significant.

2.4. Statistical Analysis. The data were presented as mean ± S.D. Significant levels ($P < 0.05$) of treatment and control were analysed using one-way ANOVA followed by Duncan test.

3. Results

After 8 weeks of administration with cholesterol (1 g/kg body weight), mice from groups 2–6 were observed with similar body weights and cholesterol levels (body weight = group 2: 36.41 ± 2.75 g; group 3: 35.84 ± 1.77 g; group 4: 36.11 ±

2.34 g; group 5: 35.16 ± 2.54 g; group 6: 35.66 ± 3.24 g; serum cholesterol level = group 2: 201.13 ± 11.87 mg/dL; group 3: 208.14 ± 10.27 mg/dL; group 4: 206.23 ± 12.99 mg/dL; group 5: 205.86 ± 15.74 mg/dL; group 6: 209.61 ± 17.21 mg/dL) while control mice free from cholesterol were observed with body weights of 29.39 ± 1.88 g and serum cholesterol level of 99.54 ± 10.31 mg/dL. At week 10 of cholesterol feeding, untreated mice (group 2) were recorded with higher serum lipid profile (total cholesterol, TG, and LDL) and liver enzyme (AST, ALT, and ALP) levels than normal control mice (group 1). Overall, after 2 weeks of treatment, positive control (group 3) treated groups showed better lipid profile regulation than fermented mung bean. Nonetheless, fermented mung bean was able to regulate the lipid profile of hypercholesterolemic mice in a dosage dependent manner where 1000 mg/kg of fermented mung bean showed higher reduction percentage of cholesterol, TG, and LDL level than 200 mg/kg of fermented mung bean. Unlike the trend observed in the serum lipid profile, the mice liver profiles showed a reversed trend where fermented mung bean treated groups improved better as compared to both the untreated and the Hypocol treated groups. Nonfermented mung bean at 1000 mg/kg showed similar effect as the low concentration of fermented mung bean in lowering of serum lipid and liver profiles.

Hypercholesterolemic mice were recorded with lower antioxidant levels but elevated lipid peroxidation and nitric oxide levels as compared to normal mice. Hypocol and fermented mung bean were able to reduce liver lipid peroxidation levels and improve the antioxidant levels. On the other hand, Hypocol was found to increase the antioxidant levels better than fermented mung bean. However, fermented mung bean was able to reduce the NO level more significantly than the Hypocol group in a dosage dependent manner. Low concentration of fermented mung bean showed similar antioxidant effect to the 1000 mg/kg of nonfermented mung bean.

Histopathology examinations showed that lipid inclusion and ballooning in liver was observed in untreated hypercholesterolemic mice (Figure 1). Lipid inclusion and ballooning were not observed in Hypocol treated, 1000 mg/kg fermented mung bean treated, and healthy normal groups (Figure 1). However, small loci of necrotic cells were still observed in Hypocol and 200 mg/kg body weight of fermented mung bean groups. Furthermore, the loss of cellular boundary was observed in the Hypocol treated group. Comparatively, treatment with 1000 mg/kg body weight of fermented mung bean gave the best recovery.

To evaluate gene regulation after treatment with Hypocol and fermented mung bean, the expression of atherosclerosis related genes of blood from groups 2, 3, and 5 was tested using mouse atherosclerosis RT^2 Profiler PCR array (Figure 2). Only 4 genes (*Apoe*, *Bcl2a1a*, *Npy*, and *Vwf*) were positively regulated (>2 fold) in Hypocol and fermented mung bean treatment groups as compared to the untreated hypercholesterolemic mice. Hypocol downregulated high fold changes of *Npy* and *Vwf* genes but similarly upregulated the *Apoe* gene when compared to fermented mung bean. On the other hand, only fermented mung bean treatment groups were able to upregulate *Bcl2a1a* expression in blood.

4. Discussion

Increased incidences of cardiovascular diseases globally have been correlated with the burgeoning population with hypercholesterolemia [1]. The consumption of natural foods such as oat-based and fermented products including red yeast rice has been proposed as an alternative method to reduce high cholesterol levels in subjects [9]. However, most of the currently available supplements such as red yeast rice products are not properly standardized and may contain contaminants such as citrinin [10]. Thus, there is a need to identify potential new lipid lowering agents without side effect. Fermented mung bean has been previously reported as antioxidant, hepatoprotective [5], and antihyperglycemic agent [11]. In this study, we have evaluated the hypolipidemic and antioxidant effects of fermented mung bean on hypercholesterolemic mice. Feeding mice with cholesterol has resulted in increased concentrations of serum cholesterol and TG of the untreated mice (Table 1). Previously, we have reported the potential of fermented mung bean to reduce lipid profiles in alloxan-induced diabetic mice [11]. Similar results were obtained in this study where Hypocol and fermented mung bean were found to reduce the level of serum cholesterol, TG, and LDL better than nonfermented mung bean.

Hepatic steatosis is a type of nonalcohol induced fatty liver that is related to hyperlipidemia and obesity [12]. Our results have shown that feeding mice with high cholesterol was associated with ballooning and lipid inclusion in liver histopathology (Figure 2) and drastic increases in AST, ALT, and ALP levels (Table 1). Red yeast rice is not recommended to be consumed by patients with liver problems because it was found to associate with symptomatic hepatitis [13]. In this study, we found that red yeast rice treatment did not improve the liver enzyme profiles and caused abnormal liver histopathology. On the other hand, fermented mung bean which was previously reported as a potential hepatoprotective agent [5] was able to improve the liver enzyme levels and liver histopathology in a dosage dependent manner. Other than hepatic steatosis, high cholesterol was also associated with reduced liver antioxidant levels [14] and increased inflammation in liver, which might subsequently lead to induced hepatocellular death [3]. SOD is the antioxidant enzyme present in liver while FRAP measures the total antioxidant capacity of liver homogenate. MDA is the product of lipid peroxidation while NO is the inflammation mediator found in the liver [5]. In this study, the SOD, FRAP, MDA, and NO levels in liver homogenates were measured. The untreated hypercholesterolemic mice were observed with reducing antioxidant levels and accumulation of inflammatory mediator level (Table 2) in liver homogenates. Red yeast rice was able to increase the antioxidant levels and reduce the lipid peroxides in liver. However, this treatment did not alter the NO level in the liver. The results of liver enzyme profile, liver histology, and liver NO level indicated that inflammation still occurred in the liver of red yeast rice treated mice. Conversely, GABA and fermented mung bean were able to enhance liver's antioxidant activities and reduce lipid peroxidation and inflammatory mediator levels concurrently. This effect in fermented mung bean treated group may be caused by

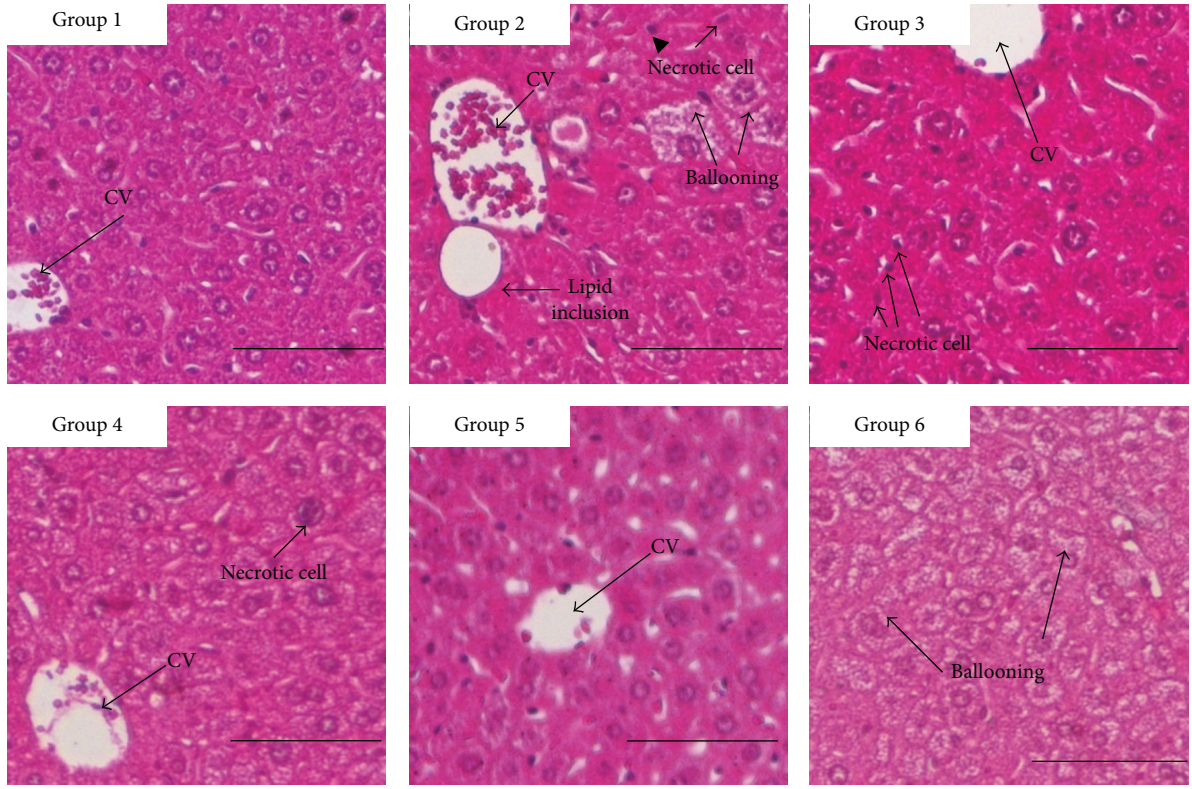

Figure 1: Liver histopathology of group 1 (normal control), 2 (untreated hypercholesterolemic), 3 (hypocol 60 mg/kg body weight), 4 (fermented mung bean 200 mg/kg body weight), and 5 (fermented mung bean 1000 mg/kg body weight) (100x). CV: centrilobular vein.

Table 1: Blood serum lipid and liver profiles of hypercholesterolemic mice after 2 weeks of treatments.

Treatment	Cholesterol (mg/dL)	Triglyceride (mg/dL)	LDL (mg/dL)	HDL (mg/dL)	ALT (U/L)	ALP (U/L)	AST (U/L)
Group 1 ($n = 8$)	103.71 ± 9.13*	101.52 ± 14.38*	39.00 ± 2.39*	57.86 ± 4.25*	62.50 ± 2.54*	90.13 ± 3.23*	120.42 ± 11.05*
Group 2 ($n = 8$)	216.73 ± 12.99	201.14 ± 12.52	86.18 ± 2.93	58.52 ± 3.19	277.20 ± 8.71	127.83 ± 5.21	320.13 ± 13.82
Group 3 ($n = 8$)	152.72 ± 7.36*	155.41 ± 9.84*	57.16 ± 1.38*	74.51 ± 3.42*	263.58 ± 4.18	137.00 ± 2.74	424.42 ± 14.07*
Group 4 ($n = 8$)	168.22 ± 5.41*	142.10 ± 11.85*	66.14 ± 6.48*	69.03 ± 5.65*	190.05 ± 2.81*	109.00 ± 2.77*	303.16 ± 9.11
Group 5 ($n = 8$)	163.41 ± 7.02*	133.20 ± 9.27*	59.46 ± 4.86*	71.51 ± 7.72*	162.50 ± 4.00*	102.75 ± 1.50*	186.72 ± 16.29*
Group 6 ($n = 8$)	181.75 ± 5.21*	172.13 ± 8.15*	71.11 ± 3.74*	66.28 ± 4.11*	181.58 ± 5.32*	110.36 ± 2.89*	294.61 ± 5.62*

*Significant difference ($P < 0.05$) among treated or normal group comparing with untreated hypercholesterolemic group was determined using ANOVA followed by Duncan's multiple range test.

the high phenolic content and the volatile antioxidant present in fermented mung bean [5]. GABA is a nonprotein amino acid that works as a neurotransmitter inhibitor [5]. Previous research has reported GABA as the major component that contributed to the hypocholesterolemic effect of germinated brown rice [15]. On top of that, GABA was also reported to have hepatoprotective effect towards ethanol induced damage [16]. Thus, the presence of GABA in the fermented mung bean [5] may contribute to both the hypocholesterolemic and hepatoprotective effects. Thus GABA present in fermented mung bean may also contribute to reducing the lipid and protecting the liver damage in fermented mung bean treated hypercholesterolemia mice.

The expressions of atherosclerosis related genes in blood were evaluated using real time PCR array (SABiosciences, USA). Only expressions with fold changes greater than 2 (comparing groups 3, 5, and 6 with the untreated group 2) are presented in Figure 1. The hypocholesterolemic effect of

Table 2: Liver homogenate antioxidant and nitric oxide levels of hypercholesterolemic mice after 2 weeks of treatments.

Treatment	MDA (nM MDA/mg sample)	FRAP (μM Fe(II)/mg of protein)	SOD (unit SOD/mg sample)	NO (μM/mg of protein)
Group 1 ($n = 8$)	$0.72 \pm 0.15^*$	$2.03 \pm 0.51^*$	$0.90 \pm 0.12^*$	$7.52 \pm 1.13^*$
Group 2 ($n = 8$)	2.21 ± 0.13	3.80 ± 0.31	0.60 ± 0.01	21.37 ± 0.53
Group 3 ($n = 8$)	$0.86 \pm 0.01^*$	$2.56 \pm 0.44^*$	$0.90 \pm 0.15^*$	$18.72 \pm 1.62^*$
Group 4 ($n = 8$)	$1.19 \pm 0.55^*$	$1.36 \pm 0.15^*$	$0.66 \pm 0.13^*$	$17.45 \pm 0.89^*$
Group 5 ($n = 8$)	$1.06 \pm 0.34^*$	$2.05 \pm 0.56^*$	$0.78 \pm 0.04^*$	$13.11 \pm 1.74^*$
Group 6 ($n = 8$)	$1.23 \pm 0.27^*$	$1.42 \pm 0.57^*$	$0.64 \pm 0.36^*$	$18.21 \pm 2.10^*$

*Significant difference ($P < 0.05$) among treated or normal group comparing with untreated hypercholesterolemic group was determined using ANOVA followed by Duncan's multiple range test.

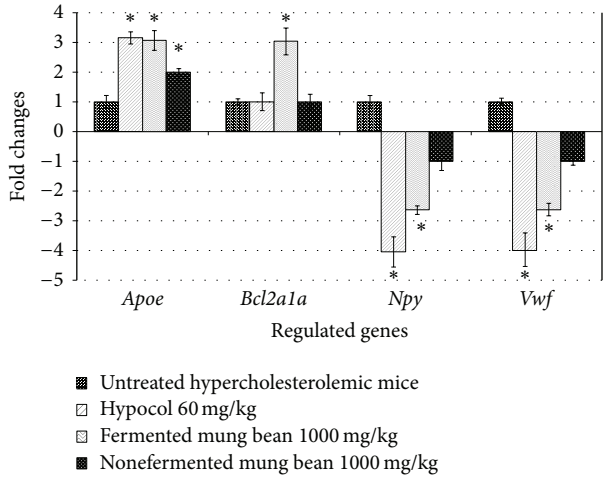

Figure 2: Fold changes of hypocol (60 mg/kg body weight) ($n = 4$) or fermented mung bean (1000 mg/kg body weight) ($n = 4$) positively regulated genes in blood compared to untreated hypercholesterolemic mice ($n = 4$) quantified by real time PCR. The data represent mean and S.D. of 3 independent experiments. Only fold expression changes greater than ±2 were recorded as significant. *Significant difference ($P < 0.05$) among treated or normal group comparing with untreated hypercholesterolemic group was determined using ANOVA followed by Duncan's multiple range test.

fermented mung bean was found to be associated with upregulation of the genes *ApoE* and *Bcl2a1a* but downregulation of *Npy* and *Vwf* in the blood of fermented mung bean treated mice. Apolipoprotein-E (*ApoE*) is a carrier for HDL that removes cholesterol from cell to liver. *ApoE* deficiency was associated with increase of blood cholesterol level and risk of atherosclerosis [17]. The results from the gene expression studies also indicated that red yeast rice and fermented mung bean treatments upregulated *ApoE* to transport cholesterol to liver, which resulted in the reduction of total cholesterol in the blood serum. *Bcl2a1a* is a member of *Bcl2* family that functions as an antiapoptotic protein [18]. The expression of *Bcl2a1a* was only significant in fermented mung bean treated mice. This phenomenon indicated that fermented mung bean may contribute to the protective effect of hepatocyte via upregulation of this antiapoptotic gene that was not observed in red yeast rice treated mice. Neuropeptide Y (*Npy*) is a 36-amino-acid peptide that is highly produced in obese mice [19]. Stimulation of *Npy* increases the appetite and reduces energy expenditure which ends up with promoting more energy storage [20]. Suppression of *Npy* by red yeast rice and fermented mung bean may reduce food intake and increase energy expenditure which indirectly improve the lipid profile of the hypercholesterolemic mice. Von Willebrand factor (*Vwf*) is a procoagulant glycoprotein that promotes platelet adhesion during vascular injury. Feeding mice with cholesterol was found to elevate the plasma level of *Vwf* which is now being used as one of the indicators of endothelial damage in vascular disease [21]. Suppression of *Vwf* expression was observed in red yeast rice and fermented mung bean treated hypercholesterolemic mice. These indicate that both treatments successfully reduced cholesterol levels in mice and subsequently reduced the level of endothelial damage and the risk of vascular disease.

In conclusion, fermented mung bean showed comparable hypolipidemic effect as red yeast rice through upregulation of *ApoE* and downregulation of *Npy* expressions. Moreover, its antioxidant activities were also able to reduce the high cholesterol associated hepatic steatosis and inflammation through upregulation of the *Bcl2a1a* antiapoptotic gene. However, further studies are needed on the genes that regulate anti-inflammation (e.g., *NFkB*), antioxidant (e.g., *Nrf2*), antiapoptotic (*Bcl2a1a*), and antiatherosclerosis (*Npy* and *ApoE*) mechanisms using Western blot in short- and long-term fermented mung bean treated hypercholesterolemic mice to validate its hypolipidemic effects and its ability to reduce the high cholesterol associated hepatic steatosis and inflammation.

Conflict of Interests

The authors declare that they have no conflict of interests.

Acknowledgments

The authors would like to thank MARDI for providing research funding. The authors also would like to thank Professor Tan Soon Guan for proof reading this paper.

References

[1] Global Health Observatory (GHO), "Raised cholesterol," 2013, http://www.who.int/gho/ncd/risk_factors/cholesterol_text/en/index.html.

[2] J. H. Wu, Q. H. Wang, F. Li et al., "Suppression of diet-induced hypercholesterolemia by turtle jelly, a traditional Chinese functional food, in rats," *Evidence-Based Complementary and Alternative Medicine*, vol. 2012, Article ID 320304, 15 pages, 2012.

[3] M. Marí, F. Caballero, A. Colell et al., "Mitochondrial free cholesterol loading sensitizes to TNF- and Fas-mediated steatohepatitis," *Cell Metabolism*, vol. 4, no. 3, pp. 185–198, 2006.

[4] E. de Mejia and B. O. de Lumen, "Soybean bioactive peptides: a new horizon in preventing chronic diseases," *Sexuality, Reproduction and Menopause*, vol. 4, no. 2, pp. 91–95, 2006.

[5] N. M. Ali, H. M. Yusof, K. Long et al., "Antioxidant and hepatoprotective effect of aqueous extract of germinated and fermented mung bean on ethanol-mediated liver damage," *BioMed Research International*, vol. 2013, Article ID 693613, 9 pages, 2013.

[6] D. Cao, H. Li, J. Yi et al., "Antioxidant properties of the mung bean flavonoids on alleviating heat stress," *PLoS ONE*, vol. 6, no. 6, Article ID e21071, 2011.

[7] N. Watanabe, Y. Endo, K. Fujimoto, and H. Aoki, "Tempeh-like fermented soybean (GABA-tempeh) has an effective influence on lipid metabolism in rats," *Journal of Oleo Science*, vol. 55, pp. 391–396, 2006.

[8] S. Roohinejad, A. Omidizadeh, H. Mirhosseini et al., "Effect of hypocholesterolemic properties of brown rice varieties containing different gamma aminobutyric acid (GABA) levels on Sprague-Dawley male rats," *Journal of Food, Agriculture and Environment*, vol. 7, no. 3-4, pp. 197–203, 2009.

[9] O. Mårtensson, M. Biörklund, A. M. Lambo et al., "Fermented, ropy, oat-based products reduce cholesterol levels and stimulate the bifidobacteria flora in humans," *Nutrition Research*, vol. 25, no. 5, pp. 429–442, 2005.

[10] R. Y. Gordon, T. Cooperman, W. Obermeyer, and J. Becker, "Marked variability of monacolin levels in commercial red yeast rice products," *JAMA Internal Medicine*, vol. 170, pp. 1722–1727, 2010.

[11] S. K. Yeap, N. Mohd Ali, H. Mohd Yusof et al., "Antihyperglycemic effects of fermented and nonfermented mung bean extracts on alloxan-induced-diabetic mice," *Journal of Biomedicine and Biotechnology*, vol. 2012, Article ID 285430, 7 pages, 2012.

[12] S. Zheng, L. Hoos, J. Cook et al., "Ezetimibe improves high fat and cholesterol diet-induced non-alcoholic fatty liver disease in mice," *European Journal of Pharmacology*, vol. 584, no. 1, pp. 118–124, 2008.

[13] H. Roselle, A. Ekatan, J. Tzeng, M. Sapienza, and J. Kocher, "Symptomatic hepatitis associated with the use of herbal red yeast rice," *Annals of Internal Medicine*, vol. 149, no. 7, pp. 516–517, 2008.

[14] M. Y. Kim, S. H. Cheong, J. H. Lee, M. J. Kim, D. Sok, and M. R. Kim, "Spirulina improves antioxidant status by reducing oxidative stress in rabbits fed a high-cholesterol diet," *Journal of Medicinal Food*, vol. 13, no. 2, pp. 420–426, 2010.

[15] S. Roohinejad, A. Omidizadeh, H. Mirhosseini et al., "Effect of pre-germination time of brown rice on serum cholesterol levels of hypercholesterolaemic rats," *Journal of the Science of Food and Agriculture*, vol. 90, no. 2, pp. 245–251, 2010.

[16] T. Norikura, A. Kojima-Yuasa, D. Opare Kennedy, and I. Matsui-Yuasa, "Protective effect of gamma-aminobutyric acid (GABA) against cytotoxicity of ethanol in isolated rat hepatocytes involves modulations in cellular polyamine levels," *Amino Acids*, vol. 32, no. 3, pp. 419–423, 2007.

[17] D. Kothapalli, S. L. Liu, Y. H. Bae et al., "Cardiovascular protection by ApoE and ApoE-HDL linked to suppression of ECM gene expression and arterial stiffening," *Cell Reports*, vol. 2, no. 5, pp. 1259–1271, 2012.

[18] J. Métais, T. Winkler, J. T. Geyer et al., "Bcl2a1a over-expression in murine hematopoietic stem and progenitor cells decreases apoptosis and results in hematopoietic transformation," *PLoS ONE*, vol. 7, no. 10, Article ID e48267, 2012.

[19] S. Dryden, L. Pickavance, H. M. Frankish, and G. Williams, "Increased neuropeptide Y secretion in the hypothalamic paraventricular nucleus of obese (fa/fa) Zucker rats," *Brain Research*, vol. 690, no. 2, pp. 185–188, 1995.

[20] F. Kokot and R. Ficek, "Effects of neuropeptide Y on appetite," *Mineral and Electrolyte Metabolism*, vol. 25, no. 4–6, pp. 303–305, 1999.

[21] M. Ghayour-Mobarhan, D. J. Lamb, S. Tavallaie, and G. A. A. Ferns, "Relationship between plasma cholesterol, von Willebrand factor concentrations, extent of atherosclerosis and antibody titres to heat shock proteins-60, -65 and -70 in cholesterol-fed rabbits," *International Journal of Experimental Pathology*, vol. 88, no. 4, pp. 249–255, 2007.

Hindawi Publishing Corporation
Evidence-Based Complementary and Alternative Medicine
Volume 2015, Article ID 101904, 9 pages
http://dx.doi.org/10.1155/2015/101904

Research Article

Wenxin Keli versus Sotalol for Paroxysmal Atrial Fibrillation Caused by Hyperthyroidism: A Prospective, Open Label, and Randomized Study

Zhaowei Meng,[1] Jian Tan,[1] Qing He,[2] Mei Zhu,[2] Xue Li,[1] Jianping Zhang,[1] Qiang Jia,[1] Shen Wang,[1] Guizhi Zhang,[1] and Wei Zheng[1]

[1] *Department of Nuclear Medicine, Tianjin Medical University General Hospital, Anshan Road No. 154, Heping District, Tianjin 300052, China*
[2] *Department of Endocrinology, Tianjin Medical University General Hospital, Tianjin 300052, China*

Correspondence should be addressed to Zhaowei Meng; jamesmencius@163.com and Jian Tan; tanposta@163.com

Received 27 June 2014; Revised 5 October 2014; Accepted 12 October 2014

Academic Editor: Myeong Soo Lee

We aimed to compare effectiveness of Wenxin Keli (WK) and sotalol in assisting sinus rhythm (SR) restoration from paroxysmal atrial fibrillation (PAF) caused by hyperthyroidism, as well as in maintaining SR. We randomly prescribed WK (18 g tid) or sotalol (80 mg bid) to 91 or 89 patients. Since it was not ethical not to give patients antiarrhythmia drugs, no control group was set. Antithyroid drugs were given to 90 patients (45 in WK group, 45 in sotalol group); ^{131}I was given to 90 patients (46 in WK group, 44 in sotalol group). Three months later, SR was obtained in 83/91 or 80/89 cases from WK or sotalol groups ($P = 0.762$). By another analysis, SR was obtained in 86/90 or 77/90 cases from ^{131}I or ATD groups ($P = 0.022$). Then, we randomly assigned the successfully SR-reverted patients into three groups: WK, sotalol, and control (no antiarrhythmia drug was given) groups. After twelve-month follow-up, PAF recurrence happened in 1/54, 2/54, and 9/55 cases, respectively. Log-Rank test showed significant higher PAF recurrent rate in control patients than either treatment ($P = 0.06$). We demonstrated the same efficacies of WK and sotalol to assist SR reversion from hyperthyroidism-caused PAF. We also showed that either drug could maintain SR in such patients.

1. Introduction

Atrial fibrillation is the most common cardiac rhythm disturbance, increasing in prevalence with age. By definition, atrial fibrillation is a supraventricular tachyarrhythmia characterized by uncoordinated atrial activation with consequent deterioration of atrial mechanical function [1–3]. Clinicians should distinguish a first-detected episode of atrial fibrillation, whether or not it is symptomatic or self-limited. Patients with atrial fibrillation have markedly reduced survival rate compared with subjects without atrial fibrillation. In paroxysmal atrial fibrillation (PAF), sudden repeated changes in rhythm cause symptoms which most patients find very debilitating. In addition, PAF carries an increasing risk of thromboembolic events, when compared with chronic atrial fibrillation [4, 5]. Therefore, the effective treatment and prevention of this kind of arrhythmia has important clinical significance [1–3, 6, 7]. Atrial fibrillation occurs in 10% to 25% of patients with hyperthyroidism, more commonly in men and elderly patients [2, 8, 9]. Mainstay treatment is restoration of euthyroid state, which can be accomplished by antithyroid drugs, ^{131}I, and surgery. Successful management of hyperthyroidism could result in restoration of sinus rhythm (SR) in up to two-thirds of patients [10]. Mechanism of hyperthyroidism-induced atrial fibrillation has been proposed [10–12]. It is generally agreed that shortening of action potential duration and effective refractory period play key roles in this electrophysiological abnormality.

Wenxin Keli (WK) is a pure Chinese herb medicine. It has been reported to be useful in the treatment of atrial fibrillation [13–15], ventricular arrhythmia [16, 17], myocardial infarction-induced arrhythmia, heart failure, Brugada syndrome [18], and so forth. WK extract is composed of 5

components: *Nardostachys chinensis* Batal. extract (NcBe), *Codonopsis*, notoginseng, amber, and rhizoma polygonati. Burashnikov and colleagues [13] recently presented a fascinating electrophysiological investigation of WK on atrial fibrillation. This study showed that WK, as a novel atrial-selective sodium-channel blocking agent, could prolong action potential duration and effective refractory period. This investigation was hailed in the same issue's editorial commentary as an emblematic milestone of integrating traditional Chinese medicine into Western medical practices [14]. In fact, WK monotherapy or in a combined antiarrhythmic regimen has been widely used for arrhythmia management in China. Chen and colleagues [15] recently conducted a meta-analysis and found solid evidence to prove WK as an effective drug to improve P-wave dispersion as well as to maintain SR in patients with PAF and its complications. However, the effect of WK on hyperthyroidism-induced atrial fibrillation has never been studied so far.

Therefore, in this open label and randomized study, we aimed to prospectively compare the effectiveness between WK and sotalol in assisting SR reversion from hyperthyroidism-caused PAF. We also intended to study their effectiveness in the maintenance of SR. Sotalol was chosen as a comparing drug, because it was proven to have efficacy to restore and maintain SR from atrial fibrillation. And sotalol possessed both class II and class III antiarrhythmic effects [2, 3].

2. Patients and Methods

2.1. Patients. From January 2011 till January 2013, a series of 180 hyperthyroidism patients (diagnosed as Graves' disease), who came to either Nuclear Medicine Department or Endocrinology Department, were consecutively enrolled in this prospective study. All of the patients had symptomatic PAF. There were 98 males (55.48 ± 12.02 years old) and 82 females (56.12 ± 9.98 years old). Entry criteria included PAF due to hyperthyroidism; electrocardiographic evidence of atrial fibrillation; symptoms such as palpitations, light headedness, chest pain, and dyspnoea in association with PAF; good compliance. Exclusion criteria were PAF due to other reasons, recent myocardial infarction, heart failure, inflammation such as pneumonia and diarrhea, unstable hepatic or renal function, poor compliance, and other major medical problems that would leave the patient with a life expectancy of less than two years. All enrolled patients gave their informed consent. This study was approved by the Institutional Review Board of Tianjin Medical University General Hospital (approval number #20101207A).

2.2. Definition. The diagnosis of PAF was made according to the American College of Cardiology Foundation/American Heart Association Task Force guideline definition; briefly, PAF had episodes that were generally less than 7 days (most less than 24 h), yet it was usually recurrent [1, 2].

2.3. Protocol. This study was designed as a prospective, open label, and randomized investigation. Generally, patients eligible for the study were allocated to one of the treatments using a computer generated random number algorithm. As reported [15], the clinical applications of WK against PAF include two aspects: restoration of SR from PAF and maintenance of SR afterwards. Therefore, we divided our study into two stages of sinus restoration and maintenance, in order to determine WK's effects on these two aspects.

Initially, baseline demographic data were obtained from the subjects. Relevant symptoms, cardiac diagnoses, and medical history were noted. Physical examination, 24-hour ambulatory electrocardiograph and/or regular 12-lead electrocardiograph, and serum biochemical tests (including electrolytes and renal and liver function) were carried out. All electrocardiographic recordings were reviewed by at least two experienced observers.

In the first part of the study, we randomly prescribed WK (18 g tid) or sotalol (80 mg bid) to 91 patients (49 males, 42 females) or 89 patients (49 males, 40 females), respectively. This part of the study compared the effectiveness of WK and sotalol to restore SR from PAF. In this investigation, it was not ethical not to give the patients any antiarrhythmia drugs. So, we did not design control; we just compared WK and sotalol. Antithyroid drugs (ATD) were given to 90 patients (45 in WK group, 45 in sotalol group), and ^{131}I was also given to 90 patients (46 in WK group, 44 in sotalol group). Due to the similar ethical reason, no control group was set. ATD-treated patients were given methimazole (initial dose 30 mg per day). ^{131}I therapeutic procedure was performed according to our protocol [19, 20]. Thyroid radioiodine uptake value was measured at 6, 24, 48, and 72 hours after an oral tracer dose uptake of ^{131}I (about 74 kBq) by a nuclear multifunctional instrument (MN-6300XT Apparatus, Technological University, China). Then ^{131}I effective half-life time ($T_{1/2\text{eff}}$) and maximum uptake in thyroid were calculated. Thyroid ultrasonography was performed by using a color doppler ultrasound machine (GE Vingmed Ultrasound Vivid Five, Horten, Norway). Thyroid volume was calculated with the following formula: volume (cm^3) = (width × length × thickness of left lobe) + (width × length × thickness of right lobe). Thyroid weight (g) = 0.479 × volume (cm^3). Serum thyroid hormones were tested by an immunofluorometric assay, including free triiodothyronine (FT3, reference 3.50–6.50 pmol/L), free thyroxine (FT4, reference 11.50–23.50 pmol/L), and thyroid stimulating hormone (TSH, reference 0.20–5.00 μIU/mL). The therapeutic dose of ^{131}I was calculated as the following formula [19, 20]: dose (37 MBq) = (thyroid weight (g) × absorption dose (Gy/g) × 0.67)/($T_{1/2\text{eff}}$ (days) × maximum uptake (%)). Absorption dose = 100 Gy/g thyroid tissue; 0.67 is a rectified factor. Participants visited our outpatient department every month. At each scheduled follow-up visit, physical examination and routine laboratory tests were done. And, at the end of the third month, ambulatory electrocardiograph and/or regular 12-lead electrocardiograph were repeated; all relevant symptoms were documented. Disappearing of PAF was defined as restoration of SR.

In the second part of the study, we randomly assigned the successfully SR-reverted patients into one of the following three groups: 54 cases were given WK (9 g tid), 54 cases were given sotalol (40 mg bid), and 55 cases served as control.

Table 1: Baseline information of all participants.

Parameters	WK* treatment (91 cases)	Sotalol treatment (89 cases)	t value (P value)**
Hyperthyroidism history (years)	8.374 ± 2.619	8.551 ± 2.680	0.448 (0.655)
PAF* history (years)	4.099 ± 1.599	4.213 ± 1.675	0.469 (0.639)
FT3* (pmol/L)	24.613 ± 5.059	24.405 ± 5.006	−0.278 (0.781)
FT4* (pmol/L)	118.697 ± 29.213	116.132 ± 28.266	−0.598 (0.550)
TSH* (μIU/mL)	0.007 ± 0.010	0.009 ± 0.015	1.191 (0.235)

*WK: Wenxin Keli, PAF: paroxysmal atrial fibrillation, FT3: free triiodothyronine, FT4: free thyroxine, and TSH: thyroid stimulating hormone; **analyzed by independent samples t-test.

In this part of the study, the control patients did not take any antiarrhythmia drug. Since patients recruited at this stage had much better improved thyroid status, and all of them were in SR when entering this investigation, it was ethically approved by our Institutional Review Board not to give the control patients any antiarrhythmia drugs. If patients were still in hyperthyroidism status, appropriate dose of methimazole was given to maintain euthyroidism. If the patients were in posttherapeutic hypothyroidism status, appropriate dose of levothyroxine was given to maintain euthyroidism. For hypothyroid patients who had already restored SR, WK and sotalol were stopped. Participants were asked to visit our outpatient department every three months. At each scheduled or sometimes unscheduled follow-up visit, physical examination and routine laboratory tests were repeated. And, at the end of the twelfth month, ambulatory electrocardiograph and/or regular 12-lead electrocardiograph were done; all relevant symptoms were documented. Time-point of PAF recurrence, its frequency, and related symptoms were collected as well.

Participant flow chart was presented in Figure 1 to illustrate the whole study process for better understanding.

2.4. Statistical Analysis. All data were presented as mean ± SD. Statistics were performed with SPSS 17.0 (SPSS Incorporated, IL, USA). Differences between two groups were analyzed by independent samples t-test. Differences between multiple groups were analyzed by one-way analysis of variance (ANOVA), and then least significant difference (LSD) test was used for multiple comparisons among the groups. χ^2 test was adopted to determine case number changes of patients after different treatments. χ^2 test was also used to check whether sex had a significant influence on the intergroup differences. Kaplan-Meier analysis by Log-Rank χ^2 test was used to estimate the cumulative recurrent rate of PAF in different groups. P value not exceeding 0.05 was considered statistically significant.

3. Results

3.1. Sinus Rhythm Restoration by Different Therapies. First, baseline information revealed no significant differences of hyperthyroidism history, PAF history, or thyroid hormone levels between the groups (Table 1). Data in this investigation were analyzed by two ways. In the first analysis, three months after treatment of WK or sotalol, SR was obtained in 83/91 cases (91.209%) or 80/89 cases (89.888%); χ^2 test showed no significant differences, indicating equal efficacies of the two drugs for assisting SR reversion (Table 2). Sex did not cause significant differences between the groups (Table 2). Thyroid hormones also demonstrated no differences before or after treatments (Table 3). In the second analysis, after treatment of ^{131}I or ATD, SR was obtained in 86/90 cases or 77/90 cases; χ^2 test showed significant differences, indicating better effects of ^{131}I treatment (Table 4). Thyroid hormones displayed no differences before treatment, yet significant differences existed after treatment (Table 5). A typical case showing successful converted SR from PAF was presented (Figure 2).

3.2. Sinus Rhythm Maintenance by Different Therapies. Data in the second investigation were analyzed by two methods. First, at the end of twelve-month follow-up, recurrent PAF happened in 1/54 (1.852%), 2/54 (3.704%), and 9/55 (16.364%) cases in WK, sotalol, or control groups, respectively. We found no differences of thyroid hormones at any follow-up time-point among the groups (Table 6). However, χ^2 test showed significant differences between WK and control groups and significant differences between sotalol and control groups, while there were no differences between WK and sotalol groups (Table 7). Second, Kaplan-Meier curves were drawn to determine the cumulative recurrent rate of PAF in different groups (Figure 3). Log-Rank test showed significant higher PAF recurrent rate in control patients compared with either treatment ($\chi^2 = 10.229$, $P = 0.06$). Therefore, we proved that both WK and sotalol could successfully maintain SR.

3.3. Side Effects. Since there is always an inherent bitter taste in Chinese medicine, some patients would unavoidably complain about the gastrointestinal discomfort or related symptoms after taking WK. Altogether, there were 10/91 cases (10.989%) in the first investigation and 6/54 (11.111%) in the second investigation who reported various degrees of nausea and dizziness after taking WK. However, all patients showed endurance and continued with the medication. For sotalol groups, the gastrointestinal discomfort was far less frequent; there were only 3/89 cases (3.371%) in the first investigation and 2/54 (3.704%) in the second investigation who reported mild stomach discomfort. However, after taking sotalol, 2/89 cases (2.247%) in the first investigation developed symptomatic bradycardia, whose PAF disappeared though. The problems completely dissolved after dose reduction from 80 mg bid to 40 mg bid for one patient and from 80 mg bid to 40 mg qd for the other patient. These two patients'

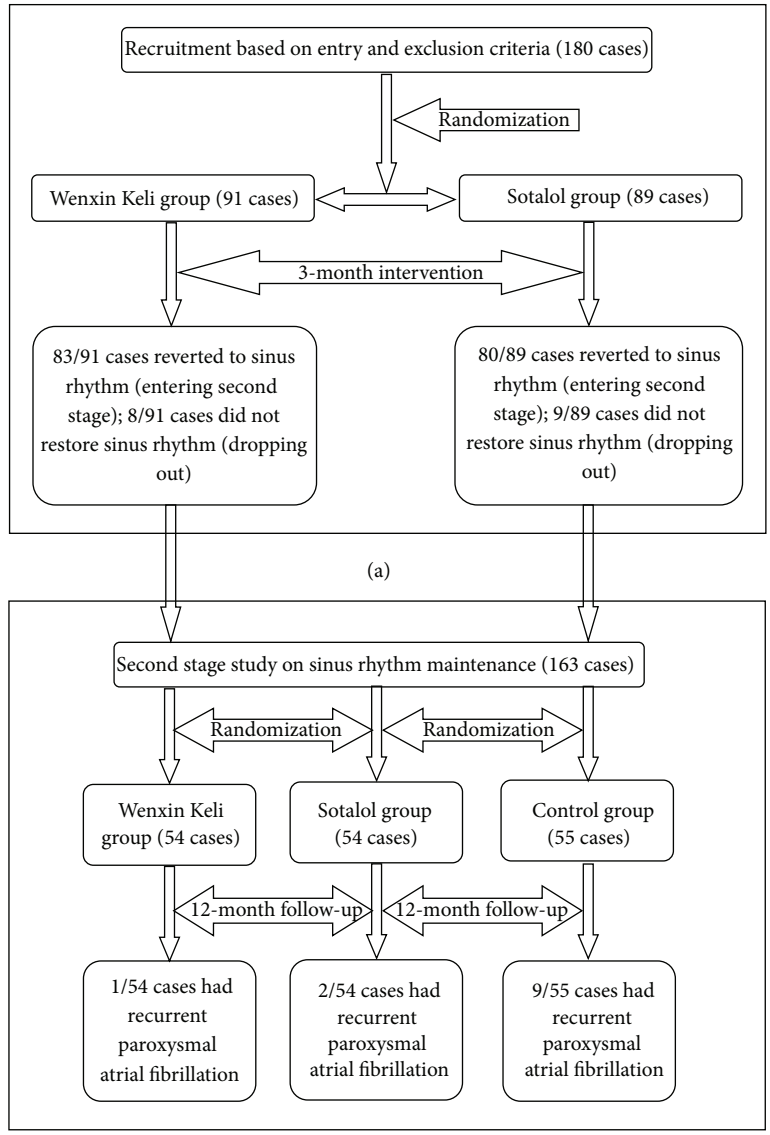

Figure 1: Participant flow chart. Initially, in the first stage of the study (a), 180 eligible hyperthyroidism patients with paroxysmal atrial fibrillation were randomized into either Wenxin Keli (91 cases) or sotalol (89 cases) treatment for sinus rhythm restoration. At the end of the first stage intervention, 83/91 cases and 80/89 cases were reverted to sinus rhythm, respectively. There were 8/91 cases and 9/89 cases who did not restore sinus rhythm. These 17 patients (still with atrial fibrillation) were not eligible for the second part of the study, and they were dropped out. In the second stage of the study (b), all sinus rhythm reverted patients (163 cases) were randomized into one of the following three groups: WK (54 cases), sotalol (54 cases), and control (55 cases) groups. The purpose is to observe drug's sinus rhythm maintenance effect. At the end of the second stage intervention, 1/54 cases, 2/54 cases, and 9/55 cases had recurrent paroxysmal atrial fibrillation, respectively.

Table 2: Case number distribution of patients after WK* or sotalol treatments in the first investigation.

Groups (case number)	Male		Female	
	Total number	SR* restored number	Total number	SR* restored number
WK* treatment (91 cases)	49	45	42	38
Sotalol treatment (89 cases)	49	44	40	36
χ^2 value (P value)$_{(WK):(sotalol)}$**	0.092 (0.762)			
χ^2 value (P value)$_{(male):(female)}$**	0.017 (0.896)			

*WK: Wenxin Keli; SR: sinus rhythm; **analyzed by χ^2 test.

Table 3: Comparisons of thyroid hormones in patients before and after WK* or sotalol treatments in the first investigation.

	Before treatments		
	WK* treatment (91 cases)	Sotalol treatment (89 cases)	t value (P value)**
FT3* (pmol/L)	24.613 ± 5.059	24.405 ± 5.006	−0.278 (0.781)
FT4* (pmol/L)	118.697 ± 29.213	116.132 ± 28.266	−0.598 (0.550)
TSH* (μIU/mL)	0.007 ± 0.010	0.009 ± 0.147	1.191 (0.235)
	Three months after treatments		
	WK* treatment (91 cases)	Sotalol treatment (89 cases)	t value (P value)**
FT3* (pmol/L)	6.495 ± 3.713	6.596 ± 3.740	0.182 (0.855)
FT4* (pmol/L)	21.447 ± 11.727	21.655 ± 10.612	0.125 (0.901)
TSH* (μIU/mL)	6.210 ± 10.002	5.752 ± 8.915	−0.324 (0.746)

*WK: Wenxin Keli, FT3: free triiodothyronine, FT4: free thyroxine, and TSH: thyroid stimulating hormone; **analyzed by independent samples t-test.

Table 4: Case number distribution of patients after ^{131}I or ATD* treatments in the first investigation.

Groups (case number)	Male		Female	
	Total number	SR* restored number	Total number	SR* restored number
^{131}I treatment (90 cases)	49	47	41	39
ATD* treatment (90 cases)	49	42	41	35
χ^2 value (P value)$_{(^{131}\text{I}):(\text{ATD})}$**	5.262 (0.022)			
χ^2 value (P value)$_{(\text{male}):(\text{female})}$**	0.017 (0.896)			

*ATD: antithyroid drugs; SR: sinus rhythm; **analyzed by χ^2 test.

heart rhythm maintained SR during the rest of the study. WK showed no bradycardia side effect. No other unwanted incidences were recorded.

4. Discussion

The risk of developing atrial fibrillation in patients with hyperthyroidism is approximately 6-fold of the euthyroidism population, which aggravates the overall conditions of such patients [9]. Successful treatment of hyperthyroidism with either ^{131}I or ATD is associated with a reversion to SR in a majority of patients [10, 21, 22]. However, pharmacological management of atrial fibrillation in patients with hyperthyroidism is still an issue lacking in comprehensive analysis. In general, rate control is very important to reduce the mortality rate of patients with atrial fibrillation [6, 7]. Selective or nonselective β-blockers can provide rapid symptom relief by reducing the ventricular rate, but these agents are unlikely to convert PAF to SR. Pharmacotherapy of atrial fibrillation has an advantage over electrical cardioversion and the catheter ablation methods, because it can be used on an outpatient basis [23]. However, the optimal pharmacological means to restore and maintain SR in patients with hyperthyroidism-caused atrial fibrillation remains controversial.

WK is identified as a novel drug against atrial fibrillation. Its mechanism has been elucidated recently. Burashnikov and colleagues [13] have implemented an isolated canine perfused right atrial preparation and recorded atrial and ventricular transmembrane action potentials and pseudoelectrograms before and after intracoronary perfusion of various concentrations of WK. Interestingly, WK produced effects more noticeable in atrial tissue than in ventricular tissue, as it caused action potential duration shortening and prolongation of effective refractory periods in an atrial-selective manner. In addition, WK produced a greater reduction in the maximum rate of rise of the action potential upstroke and a larger increase in the diastolic threshold for excitation in atrial cells, suggestive of sodium-channel current blockade. This was confirmed in HEK293 cells expressing the sodium ion channel protein SCN5A, in which WK decreased the peak sodium-channel current, in both dose-dependent and use-dependent fashions. Finally, antiarrhythmic properties of WK were illustrated by the prolongation of the P-wave duration and both the prevention and termination of acetylcholine-mediated atrial fibrillation. The above mechanism of WK acts directly against the electrophysiological changes in hyperthyroidism-induced atrial fibrillation [10–12].

Contrary to the relatively new discovery of the MK mechanisms, traditional Chinese medicines were first documented about 2500 years ago by Confucian scholars and are now still being used by tens of millions in China as well as around the world [14, 24, 25]. Clinical evidence of WK is based on results of clinical trials being carried out in Chinese hospitals for years. These studies have shown that WK can significantly improve heart palpitations, chest tightness, shortness of breath, fatigue, insomnia, and other symptoms of atrial fibrillation [15]. Currently, WK monotherapy or combined therapy with antiarrhythmic drugs has been recommended as an effective method for atrial fibrillation in China. In fact, WK is the first Chinese-developed antiarrhythmic medicine to be approved by the Chinese state. Besides antiarrhythmic property, clinical trials have also confirmed that WK can increase coronary blood low, reduce myocardial oxygen consumption, enhance myocardial compliance, improve myocardial hypoxia tolerance, relieve anterior and posterior cardiac

Table 5: Comparisons of thyroid hormones in patients before and after ^{131}I or ATD* treatments in the first investigation.

	Before treatments		
	^{131}I treatment (90 cases)	ATD* treatment (90 cases)	t value (P value)**
FT3* (pmol/L)	24.056 ± 5.321	24.964 ± 4.685	1.215 (0.226)
FT4* (pmol/L)	117.633 ± 29.225	117.225 ± 28.322	−0.095 (0.924)
TSH* (μIU/mL)	0.007 ± 0.011	0.009 ± 0.014	0.757 (0.450)
	Three months after treatments		
	^{131}I treatment (90 cases)	ATD* treatment (90 cases)	t value (P value)**
FT3* (pmol/L)	5.837 ± 2.830	7.252 ± 4.330	2.595 (0.010)
FT4* (pmol/L)	19.378 ± 8.292	23.722 ± 13.120	2.655 (0.009)
TSH* (μIU/mL)	6.427 ± 9.702	5.539 ± 9.237	−0.629 (0.530)

*ATD: antithyroid drugs, FT3: free triiodothyronine, FT4: free thyroxine, and TSH: thyroid stimulating hormone; **analyzed by independent samples t-test.

Table 6: Comparisons of thyroid hormones at any follow-up time-points in the second investigation.

	Baseline			
	WK* treatment (54 cases)	Sotalol treatment (54 cases)	Control (55 cases)	F value (P value)**
FT3* (pmol/L)	5.532 ± 2.372	5.752 ± 2.608	5.680 ± 2.486	0.110 (0.896)
FT4* (pmol/L)	18.469 ± 7.182	19.351 ± 7.577	19.046 ± 7.576	0.195 (0.823)
TSH* (μIU/mL)	7.126 ± 10.449	5.859 ± 8.668	6.832 ± 10.110	0.249 (0.780)
	Three months			
	WK* treatment (54 cases)	Sotalol treatment (54 cases)	Control (55 cases)	F value (P value)**
FT3* (pmol/L)	5.035 ± 0.934	5.129 ± 0.908	5.098 ± 0.965	0.140 (0.870)
FT4* (pmol/L)	15.664 ± 3.112	16.061 ± 3.336	15.994 ± 3.465	0.222 (0.801)
TSH* (μIU/mL)	4.683 ± 4.211	4.083 ± 3.456	4.352 ± 3.885	0.326 (0.722)
	Six months			
	WK* treatment (54 cases)	Sotalol treatment (54 cases)	Control (55 cases)	F value (P value)**
FT3* (pmol/L)	5.257 ± 0.930	5.373 ± 0.915	5.381 ± 1.057	0.277 (0.758)
FT4* (pmol/L)	16.446 ± 3.339	16.916 ± 3.727	16.955 ± 4.014	0.317 (0.729)
TSH* (μIU/mL)	4.032 ± 3.492	3.567 ± 2.885	3.756 ± 3.202	0.288 (0.750)
	Nine months			
	WK* treatment (54 cases)	Sotalol treatment (54 cases)	Control (55 cases)	F value (P value)**
FT3* (pmol/L)	5.367 ± 0.975	5.458 ± 0.958	5.590 ± 1.328	0.566 (0.569)
FT4* (pmol/L)	17.184 ± 3.208	17.760 ± 4.131	18.084 ± 4.833	0.668 (0.514)
TSH* (μIU/mL)	2.912 ± 1.730	2.701 ± 1.666	2.785 ± 1.719	0.211 (0.810)
	Twelve months			
	WK* treatment (54 cases)	Sotalol treatment (54 cases)	Control (55 cases)	F value (P value)**
FT3* (pmol/L)	5.562 ± 0.969	5.740 ± 1.302	5.874 ± 1.406	0.866 (0.422)
FT4* (pmol/L)	17.830 ± 3.485	18.532 ± 5.113	18.901 ± 5.388	0.716 (0.490)
TSH* (μIU/mL)	2.519 ± 1.420	2.388 ± 1.423	2.409 ± 1.488	0.129 (0.879)

*WK: Wenxin Keli, FT3: free triiodothyronine, FT4: free thyroxine, and TSH: thyroid stimulating hormone; **analyzed by one-way analysis of variance and least significant difference test.

Table 7: Cumulative recurrent PAF* at the end of follow-up in the second investigation.

Groups (case number)	Male		Female	
	Total number	Cumulative recurrent PAF	Total number	Cumulative recurrent PAF
WK* treatment (54 cases)	27	0	27	1
Sotalol treatment (54 cases)	27	2	27	0
Control (55 cases)	35	4	20	5
χ^2 value (P value)$_{(WK):(control)}$**		6.886 (0.009)		
χ^2 value (P value)$_{(sotalol):(control)}$**		4.813 (0.028)		
χ^2 value (P value)$_{(WK):(sotalol)}$**		0.343 (0.558)		

*WK: Wenxin Keli; PAF: paroxysmal atrial fibrillation; **analyzed by χ^2 test.

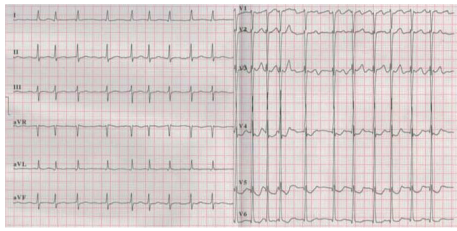

(a)

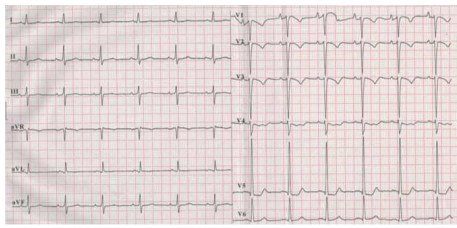

(b)

Figure 2: A typical case of successful sinus rhythm restoration from paroxysmal atrial fibrillation. A 64-year-old male patient was diagnosed with Graves' disease for eight years. He had paroxysmal atrial fibrillation for three years (a). He was given 6 mCi of ^{131}I for the treatment of Graves' disease. And Wenxin Keli (18 g tid) was prescribed during and after the ^{131}I treatment. Baseline free triiodothyronine, free thyroxine, and thyroid stimulating hormone were 21.46 pmol/L, 104.8 pmol/L, and 0.011 μIU/mL, respectively. One month later, when sinus rhythm was restored (b), free triiodothyronine, free thyroxine, and thyroid stimulating hormone were 3.35 pmol/L, 12.89 pmol/L, and 4.52 μIU/mL, respectively. At the three-month end-point of the first investigation, thyroid hormones were still normal. After entering the second investigation, Wenxin Keli (9 g tid) was prescribed during the follow-up. His thyroid function maintained normal level, and his heart rhythm maintained sinus rhythm during the rest of the study.

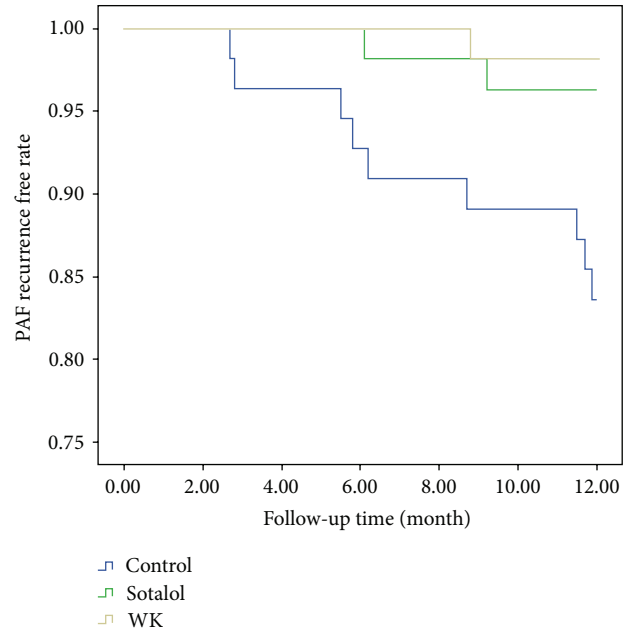

Figure 3: The cumulative recurrent rate of paroxysmal atrial fibrillation during the follow-up in different groups. In the second part of the study, we randomly assigned the successfully sinus rhythm reverted patients into one of the following three groups: 54 cases were given Wenxin Keli (9 g tid), 54 cases were given sotalol (40 mg bid), and 55 cases served as control. Kaplan-Meier analysis by Log-Rank χ^2 test was used to determine the cumulative recurrent rate of paroxysmal atrial fibrillation in different groups during the one-year-long follow-up. Vertical axle was PAF recurrence free rate and horizontal axle was the follow-up time (WK = Wenxin Keli, PAF = paroxysmal atrial fibrillation).

loading, and reduce myocardial tissue damage in patients with high blood pressure. These clinical evidences are in accordance with WK's basic mechanistic research findings recently [13, 16–18].

In the current investigation, we provided the first clinical evidence of WK as well as sotalol on the management of hyperthyroidism-induced PAF in two aspects. First, the drugs could assist SR reversion from PAF caused by hyperthyroidism. Second, the drugs could maintain SR afterwards. The second application seemed more important, since the first application was very dependent on the degree of thyroid hormone reduction. We showed that there were nearly the same efficacies of both WK and sotalol to assist SR restoration. However, ^{131}I was much more effective for hyperthyroidism management and thereafter to gain better SR reversion. We believed that this was largely due to better therapeutic results of ^{131}I to control thyroid hormones (Tables 4 and 5). In the latter investigation, we showed that both WK and sotalol could maintain SR with equal abilities in our cohort, who have already gained SR after treatments. The cumulative recurrent rate was significantly lower in the drug-treated patients than in the control cases (Figure 3). Our study proved the usefulness and effectiveness of WK as well as sotalol on the long-term maintenance management of such patients, which is indeed very important for clinical purposes.

Although WK's effect on hyperthyroidism-related atrial fibrillation has never been reported before, WK's anti-atrial-fibrillation ability is not new discovery. All of WK's clinical studies are published in Chinese language so far; however, after considering their relevancy to the current study, further comments are deserved. Chen and colleagues [15] compiled and evaluated all available randomized controlled trials regarding WK's therapeutic effects against PAF (complicated with diseases other than hyperthyroidism) according to the PRISMA systematic review standard. There were nine trials analyzing therapeutic effectiveness of WK alone or combined with Western medicine, compared with no medicine or Western medicine alone, in patients with PAF [26–34]. Most of the trials used amiodarone as the Western medicine, which cannot be used for hyperthyroidism-related atrial fibrillation. These trials were not homogeneous, requiring the use of the random effects model for statistical analysis. Meta-analysis results demonstrated a significant difference between the two therapeutic groups (the WK combination therapy was much better). Seven trials used the maintenance rate of SR at six months following treatment as an outcome measurement [33–39]. These seven trials compared the combination of WK plus Western medicine with Western medicine alone (mostly

amiodarone). These trials were homogeneous, requiring the use of the fixed effects model for statistical analysis. The rate of maintenance of SR in the former group was greater than the latter group. Meta-analysis results showed that there was a significant beneficial effect in the WK combination regimens compared with the Western medicine monotherapy. The above literature is in conformity with our findings in that WK is an effective drug for the management of PAF, not only for initial SR reversion therapy but also for the long-term maintenance therapy.

In conclusion, we demonstrated the same efficacies of WK and sotalol to assist SR reversion from hyperthyroidism-related PAF. ^{131}I was better to control thyroid hormone and to gain SR reversion. We also showed that both WK and sotalol could maintain SR with equal abilities in those PAF hyperthyroidism patients who had already gained SR after treatments. Therefore, WK is a useful drug that should be advocated in the initial treatment of PAF caused by hyperthyroidism, as well as in the follow-up management strategy.

Conflict of Interests

The authors declare that there is no conflict of interests regarding the publication of this paper.

Acknowledgments

This investigation was supported by the National Key Clinical Specialty Project (awarded to the Departments of Nuclear Medicine and Radiology). This study was also supported by Tianjin Medical University New Century Excellent Talent Program, Young and Middle-aged Innovative Talent Training Program from Tianjin Education Committee, and Talent Fostering Program (the 131 Project) from Tianjin Human Resources and Social Security Bureau (awarded to Zhaowei Meng). The authors wish to thank Buchang Pharma Co. Ltd. for providing the drug of Wenxin Keli.

References

[1] L. S. Wann, A. B. Curtis, C. T. January et al., "2011 ACCF/AHA/HRS focused update on the management of patients with atrial fibrillation (updating the 2006 guideline): a report of the American College of Cardiology Foundation/American Heart Association Task Force on Practice Guidelines," *Journal of the American College of Cardiology*, vol. 57, no. 2, pp. 223–242, 2011.

[2] V. Fuster, L. E. Rydén, D. S. Cannom et al., "2011 ACCF/AHA/HRS focused updates incorporated into the ACC/AHA/ESC 2006 Guidelines for the management of patients with atrial fibrillation: a report of the American College of Cardiology Foundation/American Heart Association Task Force on Practice Guidelines developed in partnership with the European Society of Cardiology and in collaboration with the European Heart Rhythm Association and the Heart Rhythm Society," *Journal of the American College of Cardiology*, vol. 57, no. 11, pp. e101–e198, 2011.

[3] G. Y. Lip and H.-F. Tse, "Management of atrial fibrillation," *The Lancet*, vol. 370, no. 9587, pp. 604–618, 2007.

[4] R. P. Steeds, A. S. Birchall, M. Smith, and K. S. Channer, "An open label, randomised, crossover study comparing sotalol and atenolol in the treatment of symptomatic paroxysmal atrial fibrillation," *Heart*, vol. 82, no. 2, pp. 170–175, 1999.

[5] T. Sanna and V. Di Lazzaro, "Thromboembolic risk management in paroxysmal atrial fibrillation after brain haemorrhage," *International Journal of Stroke*, vol. 6, no. 1, pp. 92–93, 2011.

[6] M. E. Cain and A. B. Curtis, "Rhythm control in atrial fibrillation—one setback after another," *The New England Journal of Medicine*, vol. 358, no. 25, pp. 2725–2727, 2008.

[7] D. Roy, M. Talajic, S. Nattel et al., "Rhythm control versus rate control for atrial fibrillation and heart failure," *The New England Journal of Medicine*, vol. 358, no. 25, pp. 2667–2677, 2008.

[8] C. T. Sawin, A. Geller, P. A. Wolf et al., "Low serum thyrotropin concentrations as a risk factor for atrial fibrillation in older persons," *The New England Journal of Medicine*, vol. 331, no. 19, pp. 1249–1252, 1994.

[9] I. Klein and S. Danzi, "Thyroid disease and the heart," *Circulation*, vol. 116, no. 15, pp. 1725–1735, 2007.

[10] A. Bielecka-Dabrowa, D. P. Mikhailidis, J. Rysz, and M. Banach, "The mechanisms of atrial fibrillation in hyperthyroidism," *Thyroid Research*, vol. 2, no. 1, article 4, 2009.

[11] K. Wustmann, J. P. Kucera, A. Zanchi et al., "Activation of electrical triggers of atrial fibrillation in hyperthyroidism," *The Journal of Clinical Endocrinology & Metabolism*, vol. 93, no. 6, pp. 2104–2108, 2008.

[12] N. Komiya, S. Isomoto, K. Nakao, M. Hayano, and K. Yano, "Electrophysiological abnormalities of the atrial muscle in patients with paroxysmal atrial fibrillation associated with hyperthyroidism," *Clinical Endocrinology*, vol. 56, no. 1, pp. 39–44, 2002.

[13] A. Burashnikov, A. Petroski, D. Hu, H. Barajas-Martinez, and C. Antzelevitch, "Atrial-selective inhibition of sodium-channel current by Wenxin Keli is effective in suppressing atrial fibrillation," *Heart Rhythm*, vol. 9, no. 1, pp. 125–131, 2012.

[14] J. Kalifa and U. M. R. Avula, "The Chinese herb extract Wenxin Keli: atrial selectivity from the Far East," *Heart Rhythm*, vol. 9, no. 1, pp. 132–133, 2012.

[15] Y. Chen, S. Nie, H. Gao et al., "The effects of Wenxin Keli on P-wave dispersion and maintenance of sinus rhythm in patients with paroxysmal atrial fibrillation: a meta-analysis of randomized controlled trials," *Evidence-Based Complementary and Alternative Medicine*, vol. 2013, Article ID 245958, 9 pages, 2013.

[16] X. Wang, Y. Gu, T. Wang, and C. Huang, "Wenxin Keli attenuates ischemia-induced ventricular arrhythmias in rats: involvement of L-type calcium and transient outward potassium currents," *Molecular Medicine Reports*, vol. 7, no. 2, pp. 519–524, 2013.

[17] X. Xue, D. Guo, H. Sun et al., "Wenxin Keli suppresses ventricular triggered arrhythmias via selective inhibition of late sodium current," *Pacing and Clinical Electrophysiology*, vol. 36, no. 6, pp. 732–740, 2013.

[18] Y. Minoura, B. K. Panama, V. V. Nesterenko et al., "Effect of Wenxin Keli and quinidine to suppress arrhythmogenesis in an experimental model of Brugada syndrome," *Heart Rhythm*, vol. 10, no. 7, pp. 1054–1062, 2013.

[19] R. F. Wang, J. Tan, G. Z. Zhang, Z. W. Meng, and W. Zheng, "A comparative study of influential factors correlating with early and late hypothyroidism after 131I therapy for graves' disease," *Chinese Medical Journal*, vol. 123, no. 12, pp. 1528–1532, 2010.

[20] W. Zheng, T. Jian, Z. Guizhi, M. Zhaowei, and W. Renfei, "Analysis of 131I therapy and correlation factors of Graves' disease patients: a 4-year retrospective study," *Nuclear Medicine Communications*, vol. 33, no. 1, pp. 97–101, 2012.

[21] H. Nakazawa, D. A. Lythall, J. Noh et al., "Is there a place for the late cardioversion of atrial fibrillation? A long-term follow-up study of patients with post-thyrotoxic atrial fibrillation," *European Heart Journal*, vol. 21, no. 4, pp. 327–333, 2000.

[22] Z. H. Zhou, L. L. Ma, and L. X. Wang, "Risk factors for persistent atrial fibrillation following successful hyperthyroidism treatment with radioiodine therapy," *Internal Medicine*, vol. 50, no. 24, pp. 2947–2951, 2011.

[23] Y. Kunii, T. Uruno, M. Matsumoto et al., "Pharmacological conversion of atrial fibrillation in the patients of Graves' disease," *Tokai Journal of Experimental and Clinical Medicine*, vol. 37, no. 4, pp. 107–112, 2012.

[24] E. Chan, M. Tan, J. Xin, S. Sudarsanam, and D. E. Johnson, "Interactions between traditional Chinese medicines and Western therapeutics," *Current Opinion in Drug Discovery & Development*, vol. 13, no. 1, pp. 50–65, 2010.

[25] X. J. Li and H. Y. Zhang, "Western healers in traditional Chinese medicine," *EMBO Reports*, vol. 9, no. 2, pp. 112–113, 2008.

[26] J. D. Cheng, "Clinical observation of Wenxin Keli for the treatment of paroxysmal atrial ibrillation," *Chinese Journal of Information on Traditional Chinese Medicine*, vol. 14, no. 8, pp. 55–56, 2007.

[27] Y. Dong, L. F. Xing, B. M. Li, and C. J. Tong, "Effect of Wenxin particle combine with fluvastatin on atrial remodelling in essential hypertension patients with atrial fibrillation," *Chinese Journal of Difficult and Complicated Cases*, vol. 9, no. 8, pp. 566–568, 2010.

[28] S. R. Jin, "The effect of Wenxin Keli on P wave dispersion and the treatment for the paroxysmal atrial fibrillation," *Chinese Journal of Modern Drug Application*, vol. 5, no. 12, pp. 92–93, 2011.

[29] N. Lv, D. Lin, and P. Lin, "Wenxin granule and low dose amiodarone in treating 60 cases of senile paroxysmal atrial fibrillation," *Fujian Journal of Traditional Chinese Medicine*, vol. 41, no. 3, pp. 7–8, 2010.

[30] C. J. Zhang, "Effect of Wenxin granule treatment for paroxysmal atrial fibrillation patients," *Practical Pharmacy and Clinical Remedies*, vol. 15, no. 11, pp. 737–739, 2012.

[31] M. L. Zhang, S. X. Jing, and H. Y. Zhang, "The effect of Buchangwenxin particle on dispersion of P wave in elder patients with diastolic cardiac dysfunction and paroxysmal atrial fibrillation," *Chinese Journal of Primary Medicine and Pharmacy*, vol. 18, no. 20, pp. 2756–2758, 2011.

[32] Z. M. Zhang, P. Bai, and J. Z. Lin, "Wenxin Keli combined with ethylamine iodine skin ketone in treating senile hypertension paroxysmal atrial fibrillation," *Chinese Journal of Hypertension*, vol. 16, no. 12, pp. 1134–1135, 2008.

[33] J. L. Lu, Y. Dong, and L. F. Xing, "The maintenance of sinus rhythm in patients with elderly hypertensive paroxysmal atrial fibrillation and the intervention of Wenxin Keli combined with fluvastatin," *Hebei Medical Journal*, vol. 32, no. 24, pp. 3483–3484, 2010.

[34] Y.-J. Yan, Y.-M. Zhang, Y. Lu, S.-Y. Wang, and H.-D. Cui, "Effect of Wenxin-Keli combined with amiodarone on dispersion of P wave and C-reactive protein in patients with paroxysmal atrial fibrillation," *Chinese Journal of New Drugs*, vol. 20, no. 15, pp. 1432–1434, 2011.

[35] B. Gao, "Clinical observation of Wenxin Keli combined with valsartan on the maintenance of sinus rhythm in patients with hypertension with paroxysmal atrial fibrillation," *Chinese Community Doctors*, vol. 14, no. 7, p. 54, 2012.

[36] F. C. Li, J. J. Tong, W. Hao, and Z. Ma, "The effect of Wenxin Keli combined with amiodarone for the treatment of paroxysmal atrial fibrillation in 32 cases," *Shanxi Journal of Traditional Chinese Medicine*, vol. 29, no. 7, pp. 839–840, 2008.

[37] P.-Y. Xie and S.-H. Shen, "Effect of combination of Chinese and Western medicines on sinus rhythm maintenance in patients with auricular fibrillation after conversion," *Chinese Journal of Integrated Traditional and Western Medicine*, vol. 26, no. 7, pp. 644–646, 2006.

[38] S. Z. Xu, "The study of prevention and curative effect of the Valsartan and Wenxin Keli on the paroxysmal atrial fibrillation," *Practical Clinical Journal of Integrated Traditional Chinese and Western Medicine*, vol. 8, no. 4, pp. 6–7, 2008.

[39] Q. H. Zheng and X. B. Zhang, "The effect of Wenxin Keli combined with amiodarone on the maintenance of sinus rhythm and serum MMP-9 in patients with paroxysmal atrial fibrillation," *Guiding Journal of Traditional Chinese Medicine and Pharmacology*, vol. 19, no. 2, pp. 36–37, 2013.

Hindawi Publishing Corporation
Evidence-Based Complementary and Alternative Medicine
Volume 2015, Article ID 639450, 11 pages
http://dx.doi.org/10.1155/2015/639450

Research Article

Effects of Qili Qiangxin Capsule on AQP2, V2R, and AT1R in Rats with Chronic Heart Failure

Xiangning Cui,[1] Jian Zhang,[2] Yubo Li,[3] Yuxiu Sun,[2] Jian Cao,[1] Mingjing Zhao,[4] Yizhou Zhao,[4] Xin Zhao,[1] Yaoyao He,[1] and Anbang Han[1]

[1]*Department of Cardiology, Guang'anmen Hospital, China Academy of Chinese Medical Sciences, Beijing 100053, China*
[2]*Beijing University of Chinese Medicine, Beijing 100029, China*
[3]*Institute of Basic Theory, China Academy of Traditional Chinese Medicine, Beijing 100700, China*
[4]*The Key Laboratory of Chinese Internal Medicine of the Ministry of Education, Dongzhimen Hospital Affiliated to Beijing University of Chinese Medicine, Beijing 100700, China*

Correspondence should be addressed to Xiangning Cui; cuixiangning@126.com

Received 2 April 2014; Revised 21 July 2014; Accepted 11 August 2014

Academic Editor: Hao Xu

Qili qiangxin capsule (QL), a traditional Chinese herbal compound, has been proved to be effective and safe for the treatment of chronic heart failure (CHF). Upregulation of aquaporin-2 (AQP2) accounts for the water retention in CHF. The aim of the present study was to evaluate the effects of QL on the expression of AQP2 in rats with CHF induced by acute myocardial infarction and to investigate the underlying mechanisms. The urine output of all rats was quantified and collected every day at the first week and the 4th week after administration of QL or Valsartan. The expression of AQP2, vasopressin type 2 receptor (V2R), and angiotensin II type 1 receptor (AT1R) were examined after treatment for 4 weeks. Urinary output increased significantly after administration of QL. Importantly, the protein expression of AQP2 and AQP2 phosphorylated at serine 256 (pS256-AQP2) was downregulated after administration of QL and Valsartan to CHF rats. Furthermore, QL reduced plasma arginine vasopressin (AVP) and angiotensin II (AngII) level and downregulated V2R and AT1R protein expression. Thus, QL exerts its diuretic effect and improves cardiac function in CHF rats by reversing the increases in both AQP2 and pS256-AQP2 expression. The possible mechanisms may involve inhibition of V2R and AT1R.

1. Introduction

Chronic heart failure (CHF) is now recognized as a major and escalating public health problem. The prevalence of CHF is 1-2% and appears to be increasing, in part because of ageing of the population [1]. It has an annual hospitalisation rate of 2% with subsequent 1-year mortality of 30% [2]. CHF has become a major public health burden in the world that is associated with high morbidity, mortality, and cost [3, 4].

Water retention, the hallmark feature of HF, not only causes signs and symptoms of congestion, but also impacts myocardial remodeling and HF progression [5]. Thus, improving congestion is a cornerstone of HF management. Although loop diuretics are among the most commonly prescribed drugs in this setting, there are some adverse drug reactions associated with their use. Moreover, up to 30% of the patients with decompensated HF present with loop-diuretic resistance [6]. Therefore, novel and safe therapeutic approaches for the treatment of congestion have been of interest in recent research.

Water retention in HF is primarily due to the defects in renal handling of sodium and water, resulting in the increasing of water reabsorption. A number of studies have proved that aquaporin-2 (AQP2), a channel that is exclusively selective for water molecules and never allows permeation of ions or other small molecules, primarily expressed in the collecting duct of the kidney, plays an important role in the regulation of urinary concentration and control of fluid and electrolyte homeostasis. In rat models of CHF, there was a significant increase in AQP2 mRNA and protein levels and

the targeting of AQP2 to the apical membrane, both of which elevate the water permeability of the collecting duct cells, resulting in the promotion of water reabsorption from the urinary tubule [7, 8]. Therefore, AQP2 impairment is an important cause of water retention that exacerbates the prognosis of congestive heart failure, which is now attracting considerable attention as a novel therapeutic target for water balance disorders which commonly occur in CHF.

The renin-angiotensin system and the nonosmotic release of arginine vasopressin (AVP) are increased in cardiac failure. Recent experimental evidence suggested that, in addition to the interaction between angiotensin AT1 and AVP V1 receptors on systemic and renal vasculature, there may be an important interaction between AVP and angiotensin II (AngII) in the regulation of AQP2 [9–11].

Qili qiangxin capsule is a traditional Chinese medicine that was approved by China Food and Drug Administration for the treatment of heart failure in 2004. Recently, a double-blind, multicenter, placebo-controlled, prospective, randomized clinical trial of qili qiangxin capsules in more than 500 patients with chronic heart failure was finished; it has proved qili qiangxin's efficacy and safety [12]. Previous studies showed that qili qiangxin capsule can improve cardiac function, inhibit the development of cardiac hypertrophy and remodeling, and regulate the inflammatory responses [13–15]. QL also inhibited $I_{Ca\text{-}L}$, I_{Na}, and multi-K^+ channels of ventricular myocytes [16, 17]. QL has been shown to have protective effects on energy metabolism and myocardial mitochondria in pressure overload heart failure rats [18]. However, little is known about whether qili qiangxin has a role in improving water retention in CHF. Therefore, using a postmyocardial infarction heart failure model, the present study was carried out to determine (1) whether QL can reduce volume overload and improve cardiac function in the late phase of infarction, (2) whether AQP2 and pS256-AQP2 are involved in the effects of QL, and (3) whether QL can regulate AVP-V2R-AQP2 and AngII-AT1R-AQP2 signaling in the renal medulla. The effects of QL were also compared with Valsartan, a commonly used AT1R blocker in clinical practice, which is known to have cardioprotective effects in the treatment of HF.

2. Materials and Methods

2.1. Vegetal Material. Qili qiangxin consists of Ginseng, Radix Astragali, Aconite Root, Salvia miltiorrhiza, Semen Lepidii Apetali, Cortex Periplocae Sepii Radicis, Rhizoma Alismatis, Carthamus tinctorius, Polygonatum Odorati, Seasoned Orange Peel, and Ramulus Cinnamomi (Yiling Pharmaceutical Corporation, Shijiazhuang, China). The drug powder was dissolved with sterile water at the concentration of 0.1 g/mL Qili qiangxin was prepared for the study. Valsartan (batch number X1428) was manufactured by Beijing Novartis Pharmaceutical Co. Ltd and dissolved with sterile water.

2.2. Animal Model and Administration. Normal male Sprague-Dawley rats (body weight 220~250 g) were provided by Beijing Vital River Laboratory Animal Technology Co. Ltd (Animal license number: SCXK (Beijing) 2012-0001). The animals were fed with standard diet and water and were subject to a 12 h light and 12 h dark cycle, a temperature of $20 \pm 2^{\circ}$C, and a humidity of $50 \pm 2\%$. All animal experimental protocols were approved by Animal Care and Use Committee of Beijing University of Chinese Medicine and complied with laboratory animal management and use regulations. HF was induced by myocardial infarction following ligation of the left anterior descending artery (LAD). Sodium pentobarbital 1% (50 mg/kg) was administered by intraperitoneal injection. The procedures performed included endotracheal intubation, ventilator positive pressure ventilation, preoperative recording of 12-lead ECG, local skin disinfection, chest opening, thoracotomy device setup, and opening of the pericardium, the pulmonary cone, and the left atrial appendage 2~3 mm from the bottom of the left anterior descending coronary artery ligation. For the rats assigned to the sham group, the same operation was performed without ligation of the left coronary artery. Twelve-lead ECG was recorded after the experiments. MI rats were fed normally for 4 weeks. According to transthoracic echocardiography results (Table 1), the survival rats were randomly assigned to the following groups: Model group (CHF, $n = 12$), Sham group (Sham, $n = 10$), QL group (QL, $n = 9$), and Valsartan group (Valsartan, $n = 9$). QL 1.0 g/kg and Valsartan 10 mg/kg were administered, respectively, by gavage once a day during the 4 weeks. Equal volume of distilled water was used for model and sham group. The urine of all rats was collected for 24 h. The urine volume was determined daily.

Table 1: Echocardiographic ejection fraction level in different groups before treatment with qili qiangxin ($\bar{x} \pm s$).

Group	n	EF (%)
Sham	10	84.490 ± 7.3354
CHF	12	44.708 ± 8.4369*
QL	9	47.933 ± 9.1211*
Valsartan	9	47.911 ± 9.1068*

*$P > 0.05$.

2.3. Transthoracic Echocardiography Measurements. A noninvasive transthoracic echocardiography method was used to evaluate the morphology and function of left ventricle. Echocardiography was performed in anesthetized animals. It consisted of a two-dimensional mode, that is, time-motion (TM) mode and blood flow measurements in pulsed Doppler mode.

2.4. Sample Preparation and Histological Examination. At the end of 4 weeks after treatment, rats were anesthetized. A blood sample from the aorta was centrifuged and plasma was collected for AVP and AngII measurements. Rat hearts were rapidly removed and rinsed with cold physiological saline, and water was adsorbed by filter paper. The excess tissues around the hearts were removed, and hearts were weighed and then were fixed in 4% paraformaldehyde and embedded in paraffin. Rat heart samples were cut into transverse

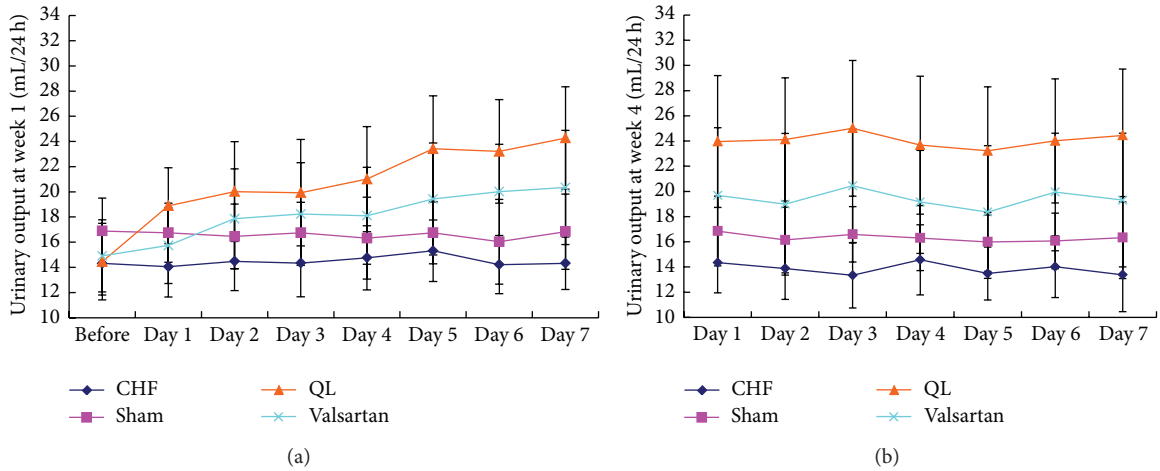

FIGURE 1: Both QL and Valsartan increased urinary output in CHF rats. (a) Urinary output was significantly increased in the rats treated with QL ($n = 9$) for 1 week compared with the CHF group ($n = 12$). Urinary output was slightly increased in Valsartan treatment group ($n = 9$). (b) Urinary output was increased in the rats treated with QL or Valsartan at the 4th week compared with the CHF group.

sections and stained with haematoxylin and eosin (H&E). Weight index was calculated using the following formula: index = heart weight (HW)/body weight (BW).

2.5. Preparation of Tissue for Immunocytochemistry. Rats were perfused and fixed with 4% PFA after anesthetizing with 10% chloral hydrate. The kidneys were stripped off and soaked in 4% PFA for 14 h. The fixed kidneys were dehydrated by 30% sucrose for 24 h and embedded in OCT medium after cryoprotection function. Frozen kidneys were cut into 30 μm coronal sections prelocated at caudate putamen by a refrigerated microtome. Endogenous peroxidase activity was blocked with 0.1% H_2O_2 in absolute methanol for 10 min at room temperature. To expose antigens, kidney sections were boiled in a target retrieval solution (1 mmol/l Tris, pH 9.0 with 0.5 mM EGTA) for 10 min. After cooling, incubate the tissue sections in 50 mM NH_4Cl in PBS for 30 min to prevent nonspecific binding, followed by blocking in PBS containing 1% BSA, 0.05% saponin, and 0.2% gelatin. Sections were incubated with primary antibodies diluted in PBS with 0.1% BSA and 0.3% Triton X-100 overnight at 4°C. After being washed for 3~10 min with PBS supplemented with 0.1% BSA, 0.05% saponin, and 0.2% gelatin, the sections were incubated with HRP-conjugated secondary antibody for 1 h at room temperature. After rinsing with PBS wash buffer, the sites of antibody-antigen reactions were visualized with 0.05% 3, 3′-diaminobenzidine tetrachloride dissolved in distilled water with 0.1% H_2O_2. Then light microscopy was carried out.

2.6. Western Blot Analysis. All animals were euthanized after 4 weeks of drug administration, and their hearts were immediately harvested and stored in liquid nitrogen until Western blot analyses were performed. The following antibodies were used: rabbit polyclonal Anti-Aquaporin 2 (1 : 2000, ABcam, Inc.), rabbit polyclonal Anti-Aquaporin 2 (phospho S256) (1 : 1000, ABcam, Inc.), rabbit polyclonal Anti-V2R (1 : 2000, ABcam, Inc.), and rabbit polyclonal Anti-AT1R (1 : 2000, ABcam, Inc.). Proteins were separated by 10% SDS-PAGE and transferred to nitrocellulose membranes, which were then incubated with antibodies at 4°C. The membranes were further incubated with horseradish peroxidase-conjugated anti-rabbit IgG (1 : 2,000) for 2 hours at room temperature. ECL visualisation was performed and the Gene Gnome Gel Imaging System (Syngene Co.) was used to capture the resulting images. Image J (NIH image, Bethesda, MD) was used to analysis the gel images.

2.7. Statistical Methods. All experimental data were presented as mean ± SD, single factor analysis of variance (ANOVA) was performed with the statistical software SPSS17.0, Dunnett's T3 was used for unequal variances, and A probability of $P < 0.05$ was considered as statistically significant.

3. Result

3.1. Effects of QL on Urinary Output at 1 or 4 Weeks after Treatment. To determine whether QL has diuretic effect, we measured urinary volume in rats in every group before and after treatment with QL or Valsartan for 1 or 4 weeks. We found that urinary volume was markedly increased after treatment with QL from week 1 to week 4. However urinary volume was slightly increased in Valsartan treatment group (Figures 1(a) and 1(b)). Therefore, QL has a diuretic action, and can reduce extracellular volume in CHF rats by increasing urinary volume.

3.2. Effects of QL on Survival Rate and Heart Weight/Body Weight Ratio at the 4th Week after Treatment. After treatment for 4 weeks, deaths had occurred, and the survival rates of the sham group ($n = 10$), the CHF group ($n = 11$), the QL group ($n = 8$), and the Valsartan group ($n = 8$) were therefore 100%, 92%, 89%, and 89%, respectively. As shown in Figures 2(a) and 2(b), long-term treatment with either QL or

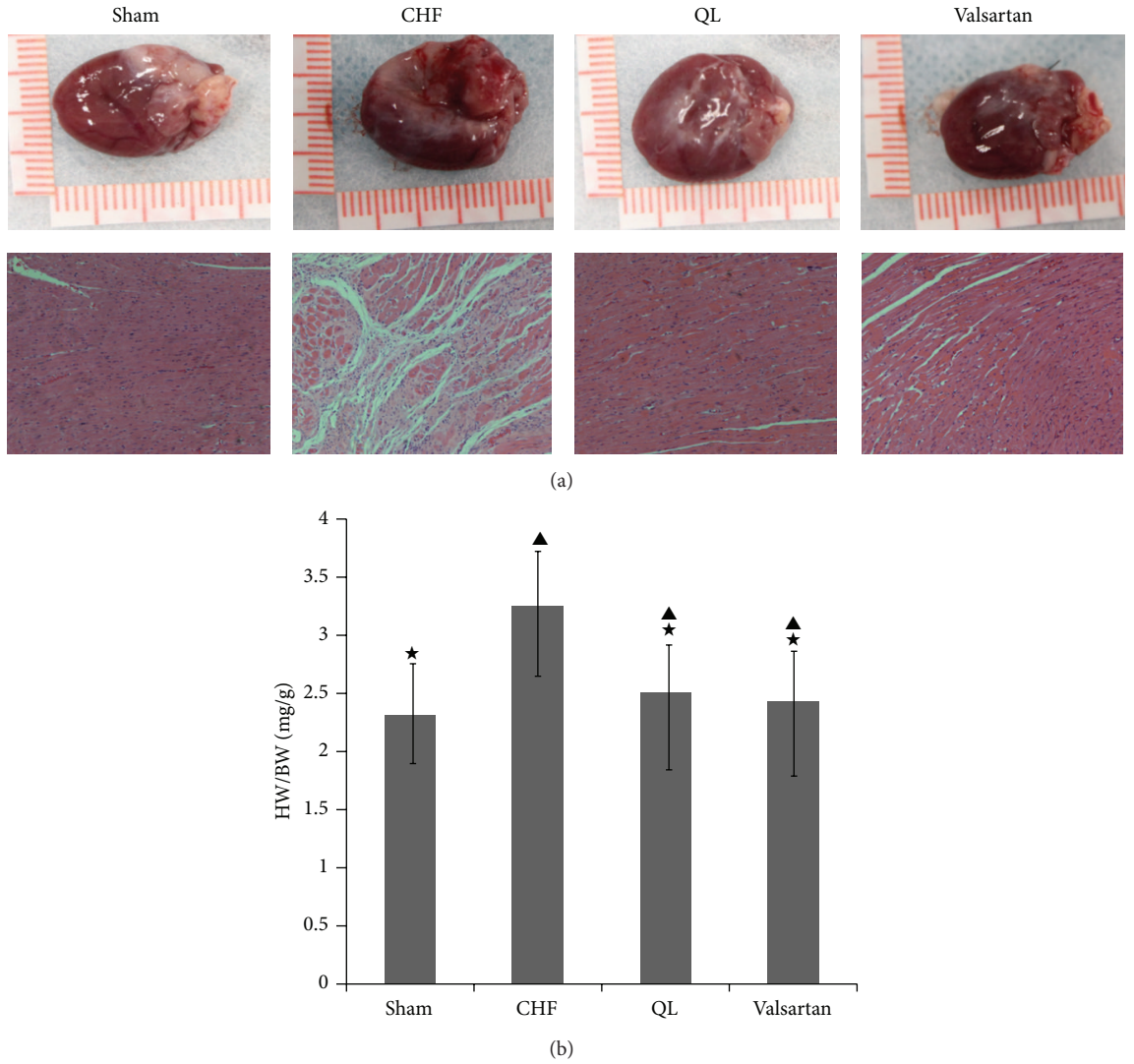

FIGURE 2: Heart preparation and pathological sections from normal and CHF rats. (a) Heart preparations [top (1~4)] and pathological sections [bottom (5~8)] from the sham group, the CHF group, the QL group, and the Valsartan group. (b) HW (heart weight)/BW (body weight) ratios in the sham group ($n = 10$), the CHF group ($n = 11$), the QL group ($n = 8$), and the Valsartan group ($n = 8$). ($^{\star}P < 0.05$, versus the CHF group, $^{\blacktriangle}P < 0.05$, versus the sham group).

Valsartan significantly reduced the heart weight/body weight ratio ($P < 0.05$).

3.3. Posttreatment Assessment of Cardiac Structure and Function by Echocardiography. Compared with the CHF group ($n = 11$), the ejection fraction (EF) and fractional shortening (FS) measurements were elevated in the QL group ($n = 8$) and the Valsartan group ($n = 8$) ($P < 0.05$), while the end-systolic volume (ESV) and left ventricular end-systolic dimension (LVIDs) measurements were lowered ($P < 0.05$). Although the measurements obtained for end-diastolic volume (EDV) and left ventricular end-diastolic dimension (LVIDd) displayed a decreasing trend in both the QL group and the Valsartan group versus the CHF group, the difference was not statistically significant ($P > 0.05$). Compared with those of the sham group, the EF and FS measurements obtained from the CHF group, the QL group, and the Valsartan group were reduced ($P < 0.05$), while the ESV and LVIDs measurements were increased ($P < 0.05$) (Figures 3(a) and 3(b)).

3.4. Effects of QL on the Expression of Total AQP2 in CHF Rats. Semiquantitative immunoblotting (Figures 4(a) and 4(b)) revealed that AQP2 protein abundance was significantly increased in the CHF rats compared with sham-operated rats ($P < 0.05$). Compared with the CHF group, the AQP2 protein abundance was reduced in both the QL group and the Valsartan group ($P < 0.05$), while no significant differences were observed in AQP2 protein abundance between QL group and Valsartan group ($P > 0.05$).

Consistent with this, immunohistochemical analysis (Figure 5) showed a much stronger labeling of anti-AQP2 antibody that was detected in principal cells in the collecting

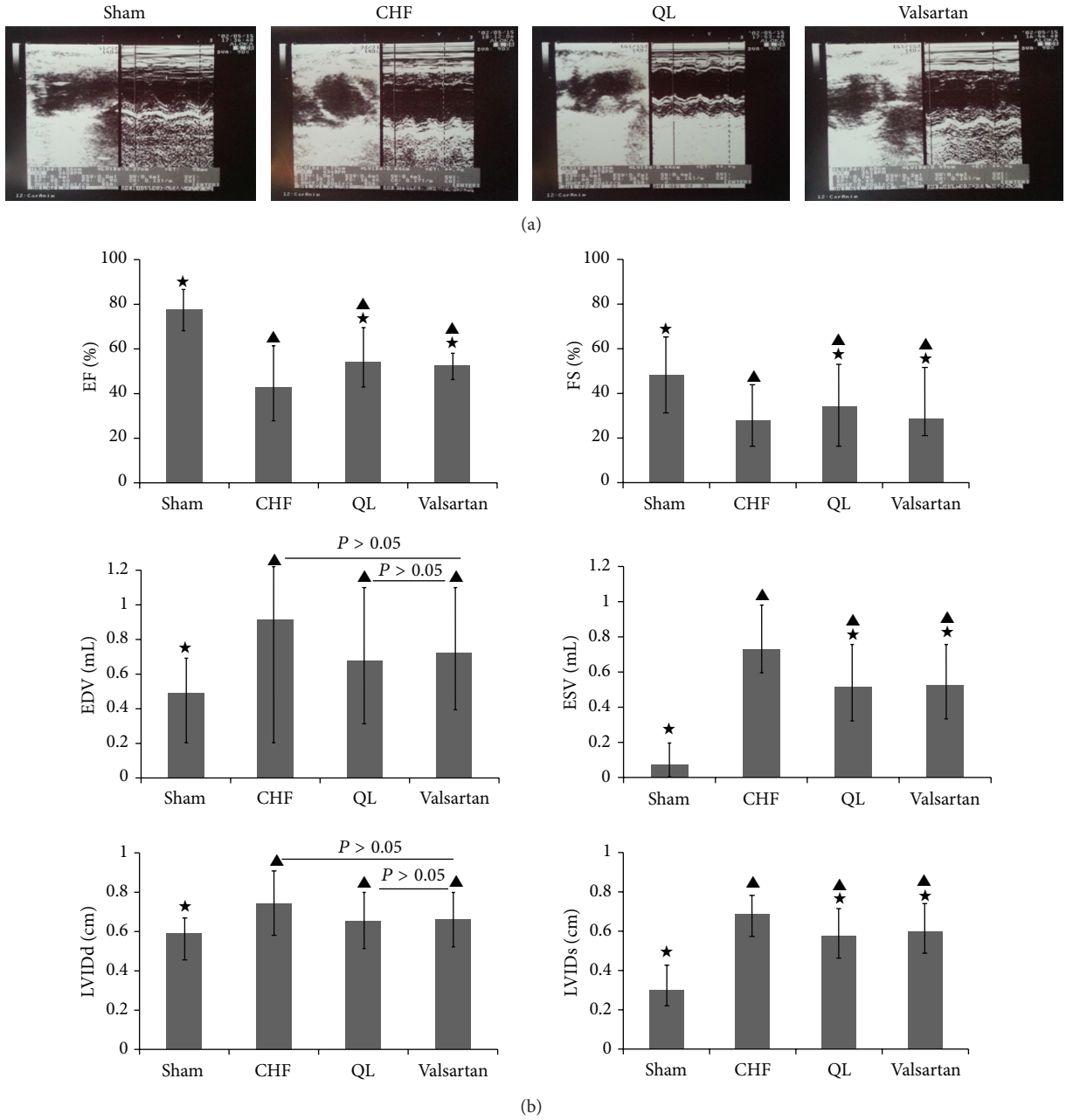

Figure 3: Typical echocardiography images from the sham group, the CHF group, the QL group, and the Valsartan group. At the 4th week of QL and Valsartan administration, cardiac structure and function were measured in each group by echocardiography. We evaluated cardiac systolic and diastolic functions by measuring the following variables: ejection fraction (EF), fractional shortening (FS), end-diastolic volume (EDV), end-systolic volume (ESV), left ventricular end-diastolic dimension (LVIDd), and left ventricular end-systolic dimension (LVIDs). Treatment with either QL or Valsartan improved systolic function. ($^{\star}P < 0.05$, versus the CHF group, $^{\blacktriangle}P < 0.05$, versus the sham group).

ducts in the CHF rats compared with sham-operated control rats, and labeling was much weaker in rats of QL group and the Valsartan group.

3.5. Effects of QL on the Expression of pS256-AQP2 in HF Rats. pS256-AQP2 protein (Figures 6(a) and 6(b)) was significantly upregulated in CHF rats; the level of pS256-AQP2 protein was significantly suppressed not only by valsartan but also by QL treatment.

Consistent with this, immunohistochemistry (Figure 7) showed an increased labeling of pS256-AQP2 at the apical membrane of the IMCD principal cells in CHF animals compared with sham-operated rats. There was a markedly weaker labeling at the apical membrane and a more pronounced

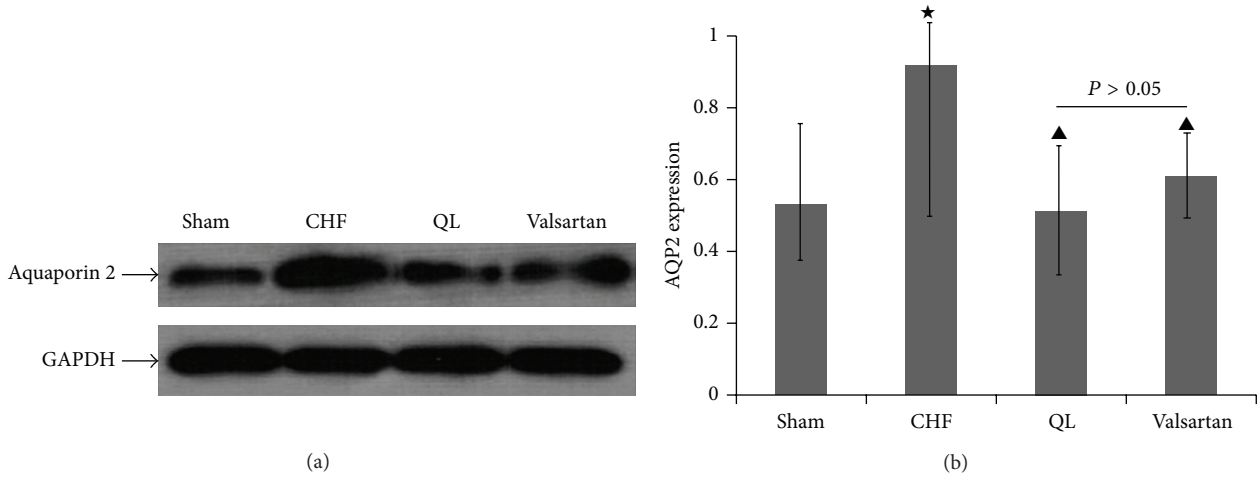

Figure 4: QL reduces renal AQP2 expression in CHF rats. (a) Representative images show that treatment with QL markedly attenuated AQP2 protein expression in CHF rats. (b) Densitometric analysis of the data demonstrated a significantly decreased AQP2 protein abundance in QL and Valsartan treatment rats compared with CHF rats. ($^{\star}P < 0.05$, versus the sham group, $^{\blacktriangle}P < 0.05$, versus the CHF group).

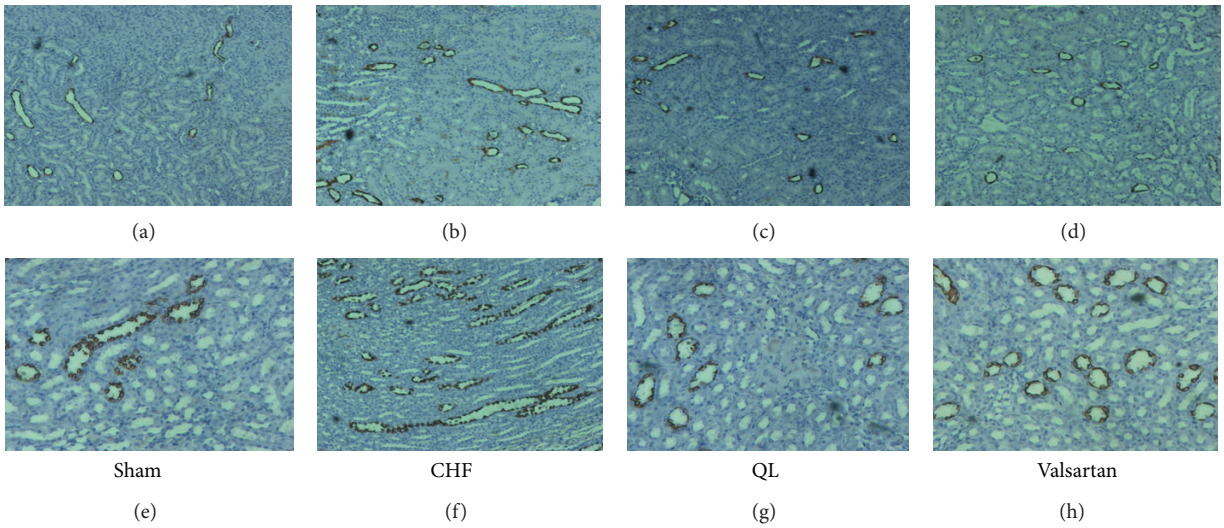

Figure 5: Immunohistochemistry for AQP2 expression in the groups: sham ((a) and (e)), CHF ((b) and (f)), QL ((c) and (g)), and valsartan ((d) and (h)) at different magnifications. AQP2 expression was detected in principal cells in the collecting ducts, and labeling was much stronger in rats with CHF than in sham rats; labeling was much weaker in QL and Valsartan rats.

intracellular distribution of the protein in rats of QL group and the Valsartan group.

3.6. Effects of QL on Plasma AVP and Renal V2R Expression in HF Rats. To investigate whether QL regulates plasma levels of AVP, we examined plasma AVP levels after treatment for 4 weeks. The levels of AVP in plasma were increased after treatment for 4 weeks in CHF rats. Treatment with QL had minor effect on the attenuation of the elevated levels of AVP in plasma in CHF rats at 4 weeks. In contrast, treatment with Valsartan had no effect on plasma AVP in CHF rats. To determine whether QL could alter the expression of renal V2R, we examined V2R protein expression in medulla at 4 weeks after treatment. We found that CHF rats expressed higher levels of renal V2R than sham rats. After treatment with QL for 4 weeks, V2R protein was significantly decreased (Figures 8(a) and 8(b)).

3.7. Effects of QL on Plasma AngII and Renal AT1R Expression in HF Rats. To investigate whether QL regulates plasma levels of AngII, we examined plasma AngII levels after treatment for 4 weeks. The levels of AngII in plasma were increased in CHF rats. Treatment with QL and Valsartan had significant effects on the attenuation of the elevated levels of AngII in plasma in CHF rats at 4 weeks. To determine whether QL could alter the expression of renal AT1R, we examined AT1R protein expression in medulla. We found that CHF rats expressed higher levels of renal AT1R than sham rats. After

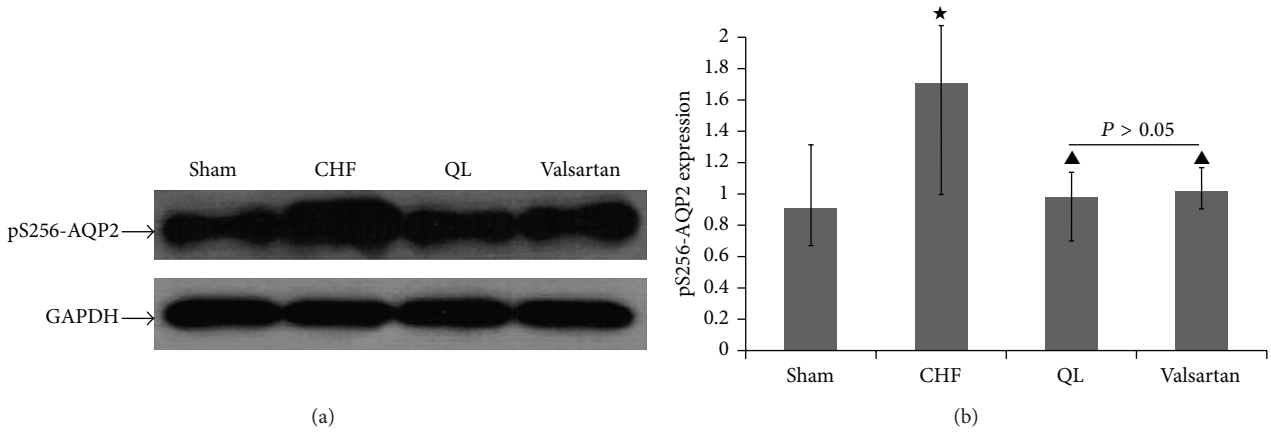

Figure 6: QL reduces renal pS256-AQP2 protein expression in CHF rats. (a) Representative images show that treatment with QL markedly attenuated pS256-AQP2 protein expression in CHF rats. (b) Densitometric analyses of the data demonstrated a significantly increased abundance of AQP2 phosphorylated at ser256 in CHF, rats compared with sham rats. Compared with the CHF rats, the abundance of AQP2 phosphorylated at ser256 was reduced in both QL and Valsartan rats. ($^{\star}P < 0.05$, versus the CHF group, $^{\blacktriangle}P < 0.05$, versus the sham group).

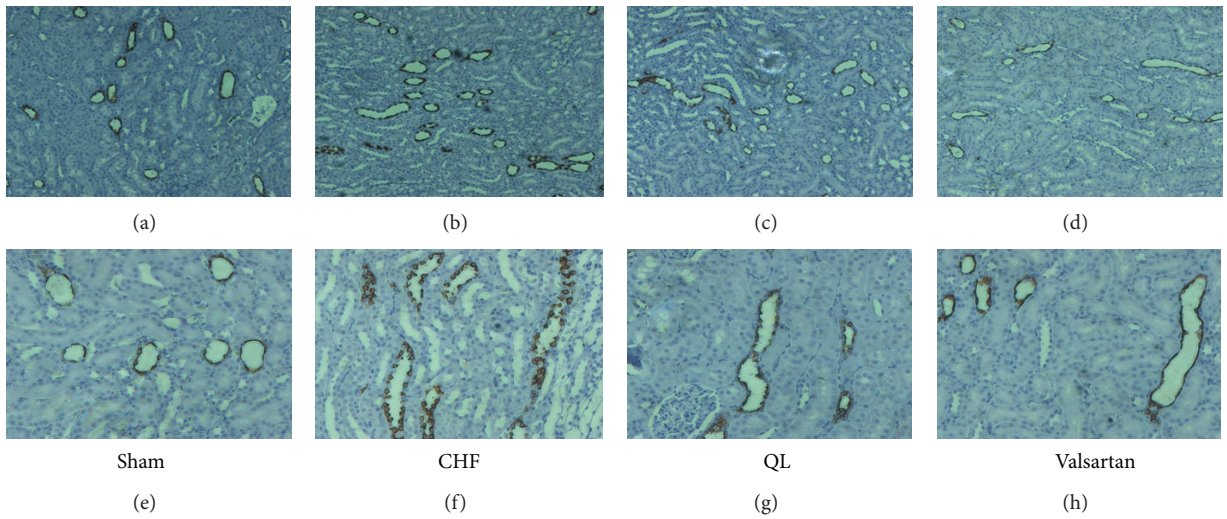

Figure 7: Immunohistochemistry for AQP2 phosphorylated at ser256 in sham ((a) and (e)) and CHF ((b) and (f)), QL ((c) and (g)), and Valsartan ((d) and (h)) at different magnifications. pS256-AQP2 immunoreactivity was detected apically in principal cells in the collecting ducts, and labeling was much stronger in CHF rats than in sham rats, while labeling was much weaker in QL and valsartan rats than in CHF rats.

treatment with QL and Valsartan for 4 weeks, AT1R protein was decreased (Figures 9(a) and 9(b)).

4. Discussion

We can draw the following conclusions from the present study. (1) QL has diuretic effect. (2) QL also could improve cardiac function in CHF rats. (3) QL could significantly reduce the protein expression of AQP2, pS256-AQP2, V2R, and AT1R in the renal medulla in CHF rats. (4) QL could reduce plasma AVP and AngII level in CHF rats.

From the perspective of traditional Chinese medicine (TCM), the fundamental problem in heart failure is the prolonged deficiency of heart qi and yang, which causes the heart to become too weak to move blood and transport fluid, leading to blood "stasis" and excessive fluid retention [19]. Qili qiangxin capsules are a specific TCM extract obtained from 11 types of herbs, including Ginseng, Radix Astragali, Aconite Root, Salvia miltiorrhiza, Semen Lepidii Apetali, Cortex Periplocae Sepii Radicis, Rhizoma Alismatis, Carthamus tinctorius, Polygonatum Odorati, Seasoned Orange Peel, and Ramulus Cinnamomi, which are well known to have effects on invigorating the heart qi and warming yang, accelerating blood circulation, disinhibiting water, dispersing swelling, and relieving congestion. Pharmacological studies have found that QL contains a number of active substances such as ginseng saponin, astragalus saponin, flavonoid, cardenolide, and phenolic acid which have been proved to have positive inotropic, vasodilation, anti-inflammation, and diuretic

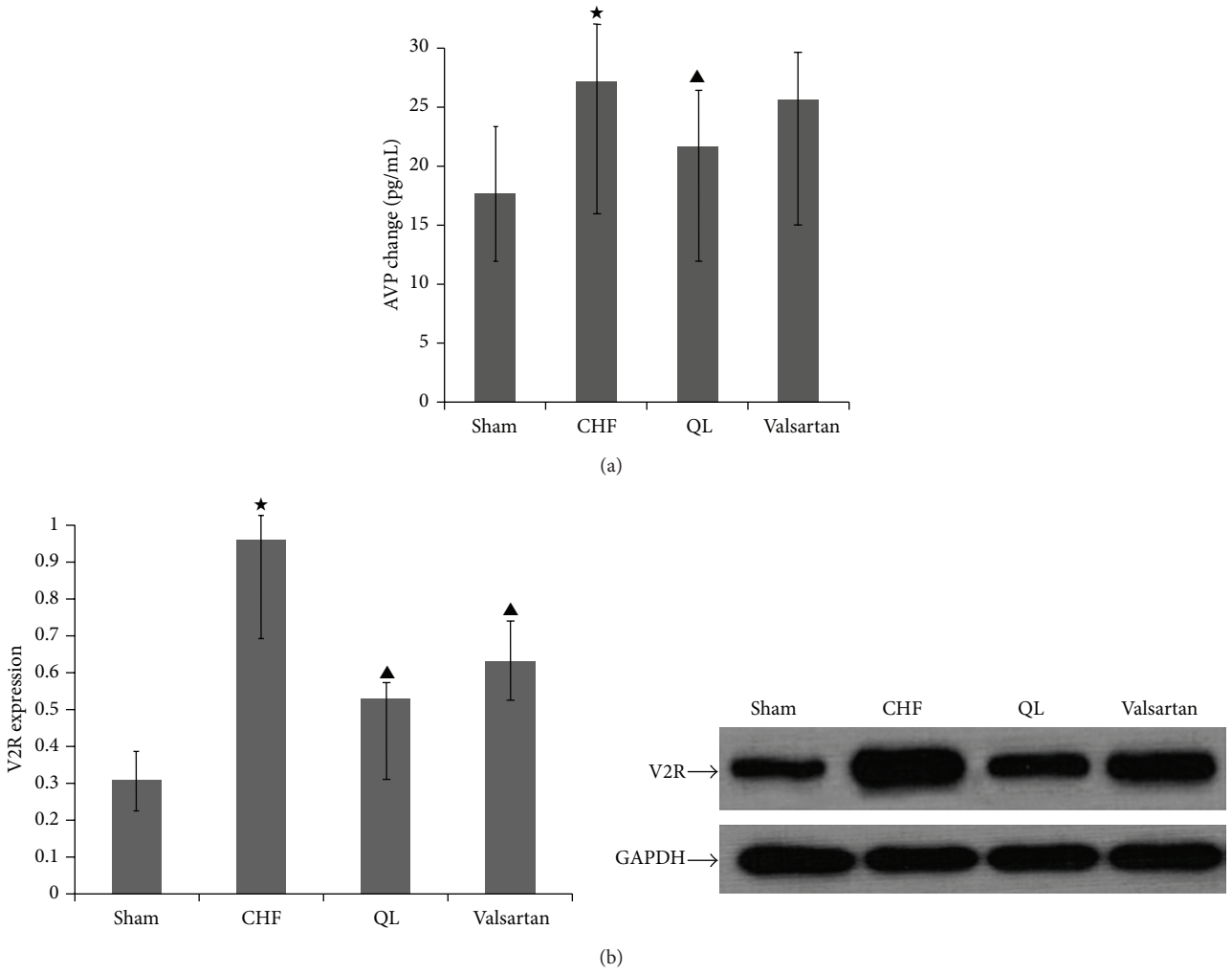

Figure 8: QL reduces the levels of plasma AVP and renal V2R protein expression in CHF rats. (a) AVP levels in plasma were elevated in CHF rats; treatment with QL decreased AVP levels in plasma; however treatment with Valsartan had no effect on plasma AVP in CHF rats. (b) Renal V2R protein increased in CHF rats; treatment with QL significantly attenuated renal V2R protein in CHF rats. ($^{\star}P < 0.05$, versus the CHF group, $^{\blacktriangle}P < 0.05$, versus the sham group).

effects. In this study, we confirmed that QL treatment has a significant effect to increase urinary output in CHF. QL could also reduce the heart/body weight ratio and the ESV and LVIDs measurements, while it elevates the EF and FS measurements to relieve congestion and improve cardiac function in rats with CHF.

AQP2 is the most important aquaporin, and plays a critical role in chronic heart failure and some diseases [7, 8, 20, 21]. The regulation of AQP2 expression was mainly by AVP signaling. Previous studies demonstrated that circulating AVP levels and V2 receptor mRNA expression are elevated in HF [22, 23]. The binding of AVP to its V2 receptor on the basolateral membrane of principal collecting duct cells initiates a signal transduction cascade that consists of activation of adenylate cyclase via the stimulatory G protein, an increase in intracellular cAMP and intracellular Ca^{2+} levels, and activation of protein kinase A. Subsequently, AQP2 are phosphorylated and translocated from cytosolic storage vesicles to the apical membrane, rendering this membrane permeable to water, thereby increasing water reabsorption. This is called short-term regulation, which occurs within a few minutes after a rise in circulating AVP levels. In the long term, AVP controls AQP2 gene expression through a cAMP response element on the AQP2 promoter [24]. AQP2 contains four serine residues in the C terminal, namely, ser256, ser261, ser264, and ser269. Recent studies demonstrated the view that phosphorylation of ser256 is necessary and sufficient to induce trafficking of AQP2 to the apical membrane [25–27]. In this study, we confirmed that QL treatment significantly reversed the increased protein abundance of AQP2 and phosphorylated AQP2 water channel in the renal medullary collecting duct; immunocytochemistry showed a weaker apical membrane labeling of AQP2 and phosphorylated AQP2 in QL treatment rats compared with model rats. This result suggests that QL exerts its diuretic effect mainly by a mechanism involving suppression of the increased AQP2 trafficking and abundance. At the same

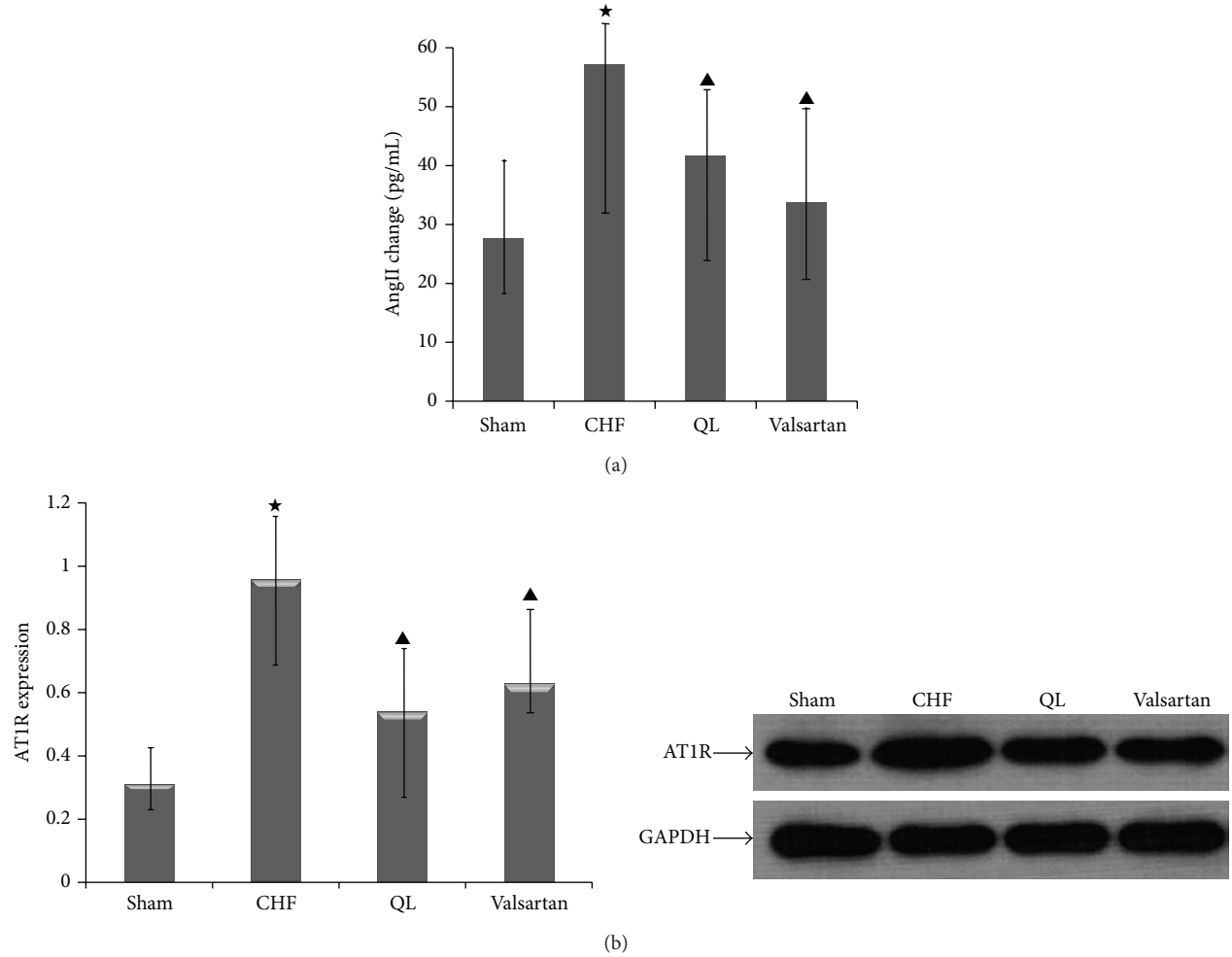

Figure 9: QL reduces the levels of plasma AngII and renal AT1R expression in CHF rats. (a) AngII levels in plasma were elevated in CHF rats; treatment with QL and Valsartan decreased AngII levels in plasma. (b) Renal AT1R protein increased in CHF rats, treatment with QL and Valsartan attenuated renal AT1R protein in CHF rats. ($^{\star}P < 0.05$, versus the CHF group, $^{\blacktriangle}P < 0.05$, versus the sham group).

time, the result showed that circulating AVP level and V2R protein expression in the renal medulla are decreased in QL treatment rats compared with model rats. In contrast, treatment with Valsartan had no effect on plasma AVP and slight effect on V2R protein expression. This result suggested that QL inhibits free water reabsorption through downregulation of V2R and AQP2 expression. Thus, reducing the effects of AVP and the AVP pathways of V2R-induced upregulation AQP2 and water retention appear to be an attractive therapeutic strategy to promote free water clearance. So far, several vasopressin antagonists are under development. In patients hospitalized with heart failure, oral tolvaptan, a V2 receptor antagonist, improved many, though not all, heart failure signs and symptoms, but without serious adverse events. However, tolvaptan initiated for acute treatment of patients hospitalized with heart failure had no effect on long-term mortality or heart failure-related morbidity [28, 29]. It is possible that QL may have similar therapeutic efficacy to V2 receptor antagonist, and this needs to be addressed in future studies.

In CHF, the renin-angiotensin-aldosterone system has also been demonstrated to play a critical role in the regulation of renal sodium and water metabolism through a variety of physiological pathways. In particular, AngII has known effects on the regulation of renal hemodynamics, glomerular filtration rate. Moreover, several recent studies have demonstrated that angiotensin II could play a role in the regulation of renal water reabsorption by changing intracellular AQP2 targeting and/or AQP2 abundance through inducing vasopressin V2-receptor mRNA expression, in addition to the AVP [30]. This potentiated the effects of vasopressin-modulated AQP2 trafficking and expression [9]. Blockade of the AngII AT1 receptor in rats cotreated with dDAVP and dietary NaCl-restriction (to induce high plasma endogenous AngII) resulted in an increase in urine production and blunted the AVP-induced upregulation of AQP2 [11]. AT1R blocker candesartan has been shown to decrease increased apical targeting of AQP2 and p-AQP2 in inner medulla of HF [8]. Thus, inhibiting AngII and the AngII pathways of AT1R-induced upregulation of AQP2 and water retention may be another important pathway to promote water clearance. Our study proved that QL and another type AT1R blocker Valsartan had the similar effects. Meanwhile, the result showed

that plasma AngII level and AT1R protein expression in the renal medulla are decreased in treatment rats compared with model rats, suggesting that QL inhibits water reabsorption through downregulation of AT1R and AQP2 expression.

5. Conclusion

In conclusion, the present study provided evidences for the 4 weeks use of QL for diuretics and cardiac function improvement in CHF rat model. Based on our results, we conclude that QL carries out its effects mainly by reversing abundance AQP2 and pS256-AQP2 protein as well as redistribution of AQP2 and pS256-AQP2 from apical to intracellular domains. The possible mechanisms may involve inhibition of V2R and AT1R. However, Valsartan carries out its effects mainly by AngII signaling regulating. Therefore, QL has multiple effects on chronic heart failure. Further studies should explore the deeper mechanism through which QL improves water metabolism to ultimately offer new avenues for the prevention and treatment of this and other related diseases.

Conflict of Interests

The authors declare that there is no conflict of interests regarding the publication of this paper.

Authors' Contribution

Xiangning Cui and Jian Zhang are co-first authors.

Acknowledgment

This work was supported by the National Science Foundation of China (Grant no. 81273945).

References

[1] C. Berry, D. R. Murdoch, and J. J. V. McMurray, "Economics of chronic heart failure," *European Journal of Heart Failure*, vol. 3, no. 3, pp. 283–291, 2001.

[2] J. Chen, S. L. Normand, Y. Wang, and H. M. Krumholz, "National and regional trends in heart failure hospitalization and mortality rates for Medicare beneficiaries, 1998–2008," *The Journal of the American Medical Association*, vol. 306, no. 15, pp. 1669–1678, 2011.

[3] J. J. V. Mcmurray, S. Adamopoulos, S. D. Anker et al., "ESC guidelines for the diagnosis and treatment of acute and chronic heart failure 2012: The Task Force for the Diagnosis and Treatment of Acute and Chronic Heart Failure 2012 of the European Society of Cardiology: developed in collaboration with the Heart Failure Association (HFA) of the ESC," *European Journal of Heart Failure*, vol. 14, no. 8, pp. 803–869, 2012.

[4] A. S. Go, D. Mozaffarian, V. L. Roger et al., "Heart disease and stroke statistics—2013 update: a report from the American Heart Association," *Circulation*, vol. 127, no. 1, pp. e6–e245, 2013.

[5] R. P. Morrissey, L. Czer, and P. K. Shah, "Chronic heart failure: current evidence, challenges to therapy, and future directions," *The American Journal of Cardiovascular Drugs*, vol. 11, no. 3, pp. 153–171, 2011.

[6] D. Shchekochikhin, F. Al Ammary, J. Lindenfeld, and R. Schrier, "Role of diuretics and ultrafiltration in congestive heart failure," *Pharmaceuticals*, vol. 6, no. 7, pp. 851–866, 2013.

[7] S. Nielsen, J. Terris, D. Andersen et al., "Congestive heart failure in rats is associated with increased expression and targeting of aquaporin-2 water channel in collecting duct," *Proceedings of the National Academy of Sciences of the United States of America*, vol. 94, no. 10, pp. 5450–5455, 1997.

[8] S. C. Lütken, S. W. Kim, T. Jonassen et al., "Changes of renal AQP2, ENaC, and NHE3 in experimentally induced heart failure: response to angiotensin II AT1 receptor blockade," *The American Journal of Physiology—Renal Physiology*, vol. 297, no. 6, pp. F1678–F1688, 2009.

[9] W. Wang, C. Li, S. Summer, S. Falk, and R. W. Schrier, "Interaction between vasopressin and angiotensin II in vivo and in vitro: effect on aquaporins and urine concentration," *American Journal of Physiology: Renal Physiology*, vol. 299, no. 3, pp. F577–F584, 2010.

[10] R. W. Schrier, "Interactions between angiotensin II and arginine vasopressin in water homeostasis," *Kidney International*, vol. 76, no. 2, pp. 137–139, 2009.

[11] T.-H. Kwon, J. Nielsen, M. A. Knepper, J. Frøkiær, and S. Nielsen, "Angiotensin II AT_1 receptor blockade decreases vasopressin-induced water reabsorption and AQP2 levels in NaCl-restricted rats," *American Journal of Physiology—Renal Physiology*, vol. 288, no. 4, pp. F673–F684, 2005.

[12] X. Li, J. Zhang, J. Huang et al., "A multicenter, randomized, double-blind, parallel-group, placebo-controlled study of the effects of qili qiangxin capsules in patients with chronic heart failure," *Journal of American College of Cardiology*, vol. 62, no. 12, pp. 1065–1072, 2013.

[13] H. Xiao, Y. Song, Y. Li, Y. H. Liao, and J. Chen, "Qiliqiangxin regulates the balance between tumor necrosis factor-α and interleukin-10 and improves cardiac function in rats with myocardial infarction," *Cellular Immunology*, vol. 260, no. 1, pp. 51–55, 2009.

[14] W. Liu, J. Chen, T. Xu et al., "Qiliqiangxin improves cardiac function in spontaneously hypertensive rats through the inhibition of cardiac chymase," *American Journal of Hypertension*, vol. 25, no. 2, pp. 250–260, 2012.

[15] Y. Zou, L. Lin, Y. Ye et al., "Qiliqiangxin inhibits the development of cardiac hypertrophy, remodeling, and dysfunction during 4 weeks of pressure overload in mice," *Journal of Cardiovascular Pharmacology*, vol. 59, no. 3, pp. 268–280, 2012.

[16] Y. Wei, X. Liu, L. Hou, W. Che, E. The, and M. V. Jhummon, "Qiliqiangxin affects L type Ca^{2+} current in the normal and hypertrophied rat heart," *Evidence-Based Complementary and Alternative Medicine*, vol. 2012, Article ID 131830, 4 pages, 2012.

[17] Y. D. Wei, X. Y. Liu, H. D. Wei et al., "The electrophysiological effects of qiliqiangxin on cardiac ventricular myocytes of rats," *Evidence-Based Complementary and Alternative Medicine*, vol. 2013, Article ID 213976, 4 pages, 2013.

[18] J. F. Zhang, C. Wei, H. T. Wang et al., "Protective effect of qiliqiangxin capsule on energy metabolism and myocardial mitochondria in pressure overload heart failure rats," *Evidence-Based Complementary and Alternative Medicine*, vol. 2013, Article ID 378298, 9 pages, 2013.

[19] D. Liang and M. Zhang, "The thinking on TCM differential treatment of congestive heart failure," *Journal of Traditional Chinese Medicine*, vol. 20, no. 1, pp. 44–47, 2000.

[20] Y. Noda, "Dynamic regulation and dysregulation of the water channel aquaporin-2: a common cause of and promising

therapeutic target for water balance disorders," *Clinical and Experimental Nephrology*, vol. 18, no. 4, pp. 558–570, 2013.

[21] T. Imamura, K. Kinugawa, T. Fujino et al., "Increased urine aquaporin-2 relative to plasma arginine vasopressin is a novel marker of response to tolvaptan in patients with decompensated heart failure," *Circulation Journal*, vol. 78, no. 9, pp. 2240–2249, 2014.

[22] S. R. Goldsmith, G. S. Francis, A. W. Cowley Jr., T. B. Levine, and J. N. Cohn, "Increased plasma arginine vasopressin levels in patients with congestive heart failure," *Journal of the American College of Cardiology*, vol. 1, no. 6, pp. 1385–1390, 1983.

[23] N. L. Wong and J. K. Tsui, "Upregulation of vasopressin V2 and aquaporin 2 in the inner medullary collecting duct of cardiomyopathic hamsters is attenuated by enalapril treatment," *Metabolism*, vol. 51, no. 8, pp. 970–975, 2002.

[24] S. Nielsen, J. Frøkiær, D. Marples, T.-H. Kwon, P. Agre, and M. A. Knepper, "Aquaporins in the kidney: from molecules to medicine," *Physiological Reviews*, vol. 82, no. 1, pp. 205–244, 2002.

[25] S. Nielsen, C.-L. Chou, D. Marples, E. I. Christensen, B. K. Kishore, and M. A. Knepper, "Vasopressin increases water permeability of kidney collecting duct by inducing translocation of aquaporin-CD water channels to plasma membrane," *Proceedings of the National Academy of Sciences of the United States of America*, vol. 92, no. 4, pp. 1013–1017, 1995.

[26] T. Katsura, C. E. Gustafson, D. A. Ausiello, and D. Brown, "Protein kinase A phosphorylation is involved in regulated exocytosis of aquaporin-2 in transfected LLC-PK1 cells," *The American Journal of Physiology*, vol. 272, no. 6, part 2, pp. 817–822, 1997.

[27] B. W. M. van Balkom, P. J. M. Savelkoul, D. Markovich et al., "The role of putative phosphorylation sites in the targeting and shuttling of the aquaporin-2 water channel," *The Journal of Biological Chemistry*, vol. 277, no. 44, pp. 41473–41479, 2002.

[28] M. Gheorghiade, M. A. Konstam, J. C. Burnett Jr. et al., "Short-term clinical effects of tolvaptan, an oral vasopressin antagonist, in patients hospitalized for heart failure: the EVEREST clinical status trials," *Journal of the American Medical Association*, vol. 297, no. 12, pp. 1332–1343, 2007.

[29] M. A. Konstam, M. Gheorghiade, J. C. Burnett et al., "Effects of oral tolvaptan in patients hospitalized for worsening heart failure: the EVEREST out come trial," *The Journal of the American Medical Association*, vol. 297, no. 12, pp. 1319–1331, 2007.

[30] N. L. M. Wong and J. K. C. Tsui, "Angiotensin II upregulates the expression of vasopressin V_2 mRNA in the inner medullary collecting duct of the rat," *Metabolism: Clinical and Experimental*, vol. 52, no. 3, pp. 290–295, 2003.

Hindawi Publishing Corporation
Evidence-Based Complementary and Alternative Medicine
Volume 2015, Article ID 918384, 10 pages
http://dx.doi.org/10.1155/2015/918384

Research Article

Apple Peel Supplemented Diet Reduces Parameters of Metabolic Syndrome and Atherogenic Progression in ApoE−/− Mice

Jaime Gonzalez,[1,2] Wendy Donoso,[3,4] Nathalie Sandoval,[1] María Reyes,[1] Priscila Gonzalez,[1] Monica Gajardo,[1] Erik Morales,[5] Amalia Neira,[6] Iván Razmilic,[4] José A. Yuri,[6,7,8] and Rodrigo Moore-Carrasco[1,7,8]

[1] *Departamento de Bioquímica Clínica e Inmunohematología, Facultad de Ciencias de la Salud, Universidad de Talca, P.O. Box 747, Talca, Chile*
[2] *Programa de Magister en Ciencias Biomédicas, Facultad de Ciencias de la Salud, Universidad de Talca, Chile*
[3] *Departamento de Estomatología, Facultad de Ciencias de la Salud, Universidad de Talca, Chile*
[4] *Instituto de Química y Recursos Naturales, Universidad de Talca, Chile*
[5] *Facultad de Medicina, Universidad Católica del Maule, Avenida San Miguel 3605, 3480112 Talca, Chile*
[6] *Centro de Pomáceas, Facultad de Ciencias Agrarias, Universidad de Talca, Chile*
[7] *Centro de Estudios en Alimentos Procesados (CEAP), Conicyt-Regional, Gore Maule, R09I2001, Avenida San Miguel 3425, 3480137 Talca, Chile*
[8] *Programa Investigación de Excelencia Interdisciplinario en Envejecimiento Saludable PIEI-ES, Universidad de Talca, Avenida Lircay s/n, Talca, Chile*

Correspondence should be addressed to Rodrigo Moore-Carrasco; rmoore@utalca.cl

Received 29 May 2014; Revised 3 October 2014; Accepted 4 October 2014

Academic Editor: Myeong Soo Lee

Cardiovascular Diseases (CVD) represent about 30% of all causes of death worldwide. The development of CVD is related in many cases with the previous existence of metabolic syndrome (MS). It is known that apple consumption has a cardiovascular protecting effect, containing phenolic compounds with antioxidant effect, which are concentrated in the fruit peel. The objective of this study was to test the effect of apple peel consumption in a murine model of MS and apoE−/− mice. Apple supplemented diets reduced the biochemical parameters (glycaemia, total cholesterol, HDL-cholesterol, LDL-cholesterol, ureic nitrogen, triglycerides, insulin, and asymmetric dimethylarginine (ADMA)) of MS model in CF1 mice significantly. The model apoE−/− mouse was used to evaluate the capacity of the apple peel to revert the progression of the atherogenesis. FD with HAP reverts cholesterol significantly and slows down the progression of the plate diminishing the cholesterol accumulation area. With these results, it can be concluded that the consumption of apple peel reduces several MS parameters and the atherogenic progression in mice.

1. Introduction

Cardiovascular diseases (CVD) are the main cause of death in the world [1] and there are several associated risk factors, among them, metabolic syndrome (MS), characterized by hyperglycemia, dyslipidemia, arterial hypertension, and obesity of central distribution.

The rate of atherothrombotic progression is influenced by the exposition to risk factors which increase the probability to suffer from a cardiovascular event. Such factors can be classified as modifiable (smoking, hypertension, diabetes, dyslipidemia, and sedentarism) and nonmodifiable (sex, age, and genetic). For this reason, genetically modified experimental animals have been generated which have contributed to the knowledge of the atherothrombotic phenomenon: the formation of the atheroma plaque, the induction of its formation, and the cellular elements involved [2].

Epidemiologic studies have demonstrated that fruit and vegetable consumption contributes to decreasing the cardiovascular risk [3]. For instance, apple consumption has

been inversely associated with acute myocardial infarction [4]. It has been described that the protecting effect of apple consumption has different levels and mechanisms of action: body weight loss and reduction in glycemia [5, 6], protective against low density lipoprotein oxidation (LDL) *in vitro* [7, 8], antiadipogenic, hypocholesterolemic, and antiatherogenic effects [9, 10], and inhibition of cholesteryl ester transfer protein activity, improving the distribution of cholesterol in lipoproteins [11]. Studies *in vitro* have demonstrated that apple flavonoids improve the availability of nitric oxide and protect the endothelial cells from apoptosis preventing the process of endothelial dysfunction and *in vivo* reduces blood pressure and oxidative stress [12]. Furthermore, flavonoids interfere with the proliferation and migration of smooth muscle cells preventing the association of them with others that will initiate the atherothrombotic process [13]. In the apple, polyphenols content and the level of antioxidant activity are about five times higher in peel than in pulp [14].

The ApoE deficient mice are an idoneous experimental model for the study of atherosclerosis [15], because it is unable to carry out the reverse cholesterol transport, since it lacks the gene coding for apolipoprotein E. The lack of this gene involves accumulation of lipids at the luminal level in blood vessels, developing lesions in the microvasculature and showing total blood cholesterol levels ≥500 mg/dL, mostly VLDL and remaining chylomicrons, after administering a normal diet [16]. The atherogenic process can be accelerated or induced in this model through the administration of high fat diets, allowing studying the process in a model different from human, with significant similarities [17]. In this study, we aimed to evaluate different forms of consumed apple skin: fresh skin, which is the primary product, dehydrated skin, representing a useful alternative in the conservation and transport of this product, and sunburned skin, which contains a higher amount of antioxidants, but its potential effect has not been demonstrated in biological assays [18]. For this reason we used CF1 mice fed a high fat diet, a model of early stage of CVD, and ApoE knockout mice, a model of atherosclerosis, to study the impact of apple peel consumption.

2. Materials and Methods

2.1. Animals. Four-week male CF-1 mice and C57BL6 mice obtained from the Public Health Institute, Santiago, Chile, and ApoE−/− mice (donated by Dr. Atilio Rigotti, Pontificia Universidad Católica de Chile) were used in the experiments. Animals were maintained at 22 ± 2°C, at a regular darkness-light 12:12 h cycle (light 08:00 to 20:00 h). Weight, food intake, and water consumption were measured daily. Animal handling was carried out in conformity with the regulation for the use of laboratory animals of the National Commission for Scientific and Technologic Research (CONICYT), Chile. The protocol was approved by the bioethics committee of Universidad de Talca. After an adaptation period of 10 days, animals were randomized into 5 groups.

2.2. Anesthesia and Euthanasia. At the end of the experimental period, mice were anesthetized with an intraperitoneal injection of ketamine 50 mg/kg (Ketostop; DrogasPharma-Invetec, Santiago, Chile) and xylazine 5 mg/kg (Xylavet; Alfasan International BV, Holland). Animals were euthanatized by blood collection from the abdominal aorta and later rupture of the diaphragm. Plasma and tissues were harvested and stored at −70°C until the analysis.

Initial and final weight of each animal, as well as systolic arterial blood pressure (SAP) at the tip of the mice tails, were obtained by using ultrasound equipment (Ultrasonic Doppler Flow 811-B, Aloha, Oregon, USA).

2.3. Diets. CF-1 mice were administered five types of diet: normal diet (ND), fat diet (FD), fat diet plus healthy apple peel (FD + HAP), fat diet plus dehydrated healthy apple peel (FD + DAP), and fat diet plus sun damaged apple peel (FD + SDAP) coming from Fuji apples, during 43 days.

ApoE−/− mice were administered ND, FD, and FD + HAP during 10 weeks using peel from Granny Smith apples as a supplement. C57BL6 mice were administered ND. Ingredients used and the preparation of different diets were performed as described by Moore-Carrasco et al., 2008 [19]. Different types of apple peel were added to ND and FD in 20% w/w. For the analysis of diet components, three pellets from each of them were selected at random and submitted to the Institute of Chemistry of Universidad de Talca for chemical analysis according to official methods of analysis of the Association of Official Analytical Chemists [20]. The lipid content of fat fraction was determined by mass spectrometry/gas chromatography (Perkin Elmer Turbo Mass and Autosystem XL Gas Chromatograph). Antioxidant capacity was determined measuring free radical traps 2,2-diphenyl-1-picrylhydrazyl by the method described by Von Gadow et al. (1997) [21] with modifications, using chlorogenic acid as standard. Glycoside quercetins were determined by High Performance Liquid Chromatography/Diode Array Detector (Merck Hitachi, LaChrom, Tokyo, Japan).

2.3.1. Determination of Total Phenolics Concentration. Total phenolics were determined by the Folin-Ciocalteu method [22]. Briefly, 0.1 mL of extract was mixed with 0.5 mL of the Folin-Ciocalteu phenol reagent (Merck, Darmstadt, Germany). The mixture was incubated for 5 min and then 0.5 mL of sodium carbonate (Na2CO3; 10%, w/v) was added and incubated for 15 min at room temperature. Absorbance was measured at 640 nm in a spectrophotometer. Total phenolic concentrations in the peel and diets were expressed as mg of chlorogenic acid equivalents (CAE) g-1 FW.

2.3.2. Determination of Antioxidant Activity. The capture of the free radical 2,2-diphenyl-1-picrylhydrazyl (DPPH; Fluka Chemie, Buchs, Switzerland) was measured by the method described by Von Gadow et al., [21] with modifications. Briefly, 0.1 mL extracts were mixed with 2 mL of 8×10^{-5} M DPPH solution and incubated for eight min at room temperature and the absorbance measured at 515 nm. Ethanol was used as blank. Chlorogenic acid in different concentrations was used as a standard and the capture of the DPPH free radicals was expressed as mg of chlorogenic acid equivalents (CAE) g-1 FW.

2.3.3. Determination of Specific Phenolics by HPLC. Specific phenolics (quercetins glycosides) and lipid profile in the samples (diets) were determined using a HPLC-DAD Merck Hitachi (LaChrom, Tokyo, Japan) equipment consisting of a LaChrom L-7100 pump and a diode array detector, L-7455 LaChrom, and a 100-5 C18 Kromasil column of 259 mm × 4.6 mm with a precolumn of the same characteristics, maintained at 20°C. Briefly, 0.02 mL previously filtered (0.45 μm filter) extracts were injected. To identify the compounds, different standards of specific phenolics were used with the UV-VIS spectra. The chromatogram was monitored at 256 nm. The solvents of the mobile phase were A: 1% formic acid in H_2O quality HPLC, B: 40% acetonitrile in H_2O, and C: acetonitrile. The elution parameters were time 0–10 min: A (70), B (30), and C (0) flow 1 mL min^{-1}; time 45 min: A (25), B (75), and C (0) flow 0.5 mL min^{-1}; time 52 min: A (0), B (0), and C (100) flow 1 mL min^{-1}; and time 55 min: A (70), B (30), and C (0) flow 1 mL min^{-1}. The results were expressed in μg of samples in g of FW-1.

2.4. Biochemical Parameters. Total cholesterol, HDL cholesterol, triglycerides, transaminase GOT, and glucose were determined by enzymatic and standardized colorimetric methods.

2.5. ELISAs. Plasmatic concentrations of insulin (ELISA Kit Rat/Mouse Insulin, Millipore) and asymmetric dimethylarginine, ADMA (ADMA Direct (mouse/rat) ELISA Kit, Immundiagnostik), were determined by ELISA. Measurements were obtained following the instructions of each manufacturer.

2.6. Histology. Thoracic aorta obtained from ApoE−/− and C57BL6 (Wild Type, WT) mice were fixed in 10% formalin at pH 7.4. Once the samples were fixed, the dehydration, clarification, and inclusion protocol were carried out. After blocks were obtained, sections were obtained using a microtome (Microm HM325), with a thickness of 5 μm. Sections of hydrated and deparaffinized tissues were stained with hematoxylin and eosin (HE) and Masson's Trichrome, following the appropriate methods for histologic observation. From each aorta description, 10 sections were analyzed by 3 independent observers (J.M., E.M., and R.MC.).

2.7. Image Processing. After the staining procedures, photographs (40x) were obtained with a Primo Star Carl Zeiss trinocular microscope used for this purpose and a Canon EOS Rebel XSI camera with the software EOS Utility (version 2.4, Copyright© CANON INC, USA, 2008) was used for image capturing. Later, they were quantified to determine the indirect presence of lipids as well as the degree of inflammation of the lesions, in terms of the presence of inflammatory cells; determining representative areas in each artery lesion with a dimension of 50 μm^2, the software AxioVision Release 4.8.1 (Carl Zeiss version 11. 2008) was used for this purpose, and the software Micrometrics SE Premium (version 2,8; ACCU-SCOPE Inc., Commack, NY, USA, 2008) was used for counting inflammatory cells. The lesion surface was quantified by using the ImageJ software (version 1,46j; National Institute of Health, USA, 2006) to determine the degree of fibrosis. Each image was analyzed through the Colour Deconvolution Plugin, selecting the vector for Masson's Trichrome, determining the quotient (density/area), and allowing the characterization of each lesion [23]. From each of the image analyses, 10 sections were measured by 2 independent operators (J.M. and W.D.).

2.8. Statistical Analysis. The results are presented as means ± standard deviation (SD). Comparisons between groups were done by the analysis of variance (ANOVA) using Graphpad software. A statistical difference was evaluated using a confidence interval of 95%, with Dunnett's and Newman-Keuls as post hoc tests.

3. Results

3.1. Nutritional Composition of Diets. First, we prepared diets supplemented with apple products. Table 1 shows the analysis of each diet administered to mice, in which, according to the results, ND can be homologated to a human diet since they have similar percentage of several components, while the rest of the diets have higher content of fat. These, except FD + HAP, present low percentage of myristic acid. While all diets have high content of oleic, linoleic, and palmitic acids and low contents of stearic, palmitoleic, and myristic acids, ND and FD do not have palmitoleic acid methyl ester (Table 1). Table 1 shows the content of total phenols and antioxidant activity of different diets. A low (nondetectable) content of phenols in ND and FD is observed compared with higher content of phenols and antioxidant activity in FD + HAP, FD + DAP, and FD + SDAP. Table 1 shows the quercetin content (Q); in general, a higher content of different Q in FD + HAP, FD + DAP, and FD + SDAP is observed. Diet supplemented with SDAP shows the highest content of all evaluated quercetins, except Q. rutinoside (Table 1).

3.2. Impact of Apple Consumptions in CF-1 Mice: A MS Model. Next, we tested our diets in an animal model of MS, for 43 days. Table 2 shows the body weight of mice, at the beginning and at the end of the experimental period. Mice subjected to FD present a higher weight gain (7.49 ± 0.35 g) than the ND group (6.90 ± 0.12 g, $P < 0.01$). On the other hand, mice subjected to FD + HAP, FD + DAP, and FD + SDAP presented a lower weight gain when compared to the FD group.

Regarding blood pressure, the group of mice that received FD presented significantly higher SAP (111 ± 1.4 mmHg, $P < 0.01$) than mice subjected to ND (79.14±10.1 mmHg) (Figure 1(a)). On the other hand, mice subjected to FD + HAP, FD + DAP, and FD + SDAP presented a significantly lower SAP than mice subjected to FD. The FD + HAP group was the one which presented lower SAP ($P < 0.01$).

Mice that received FD presented high levels of blood cholesterol (164 ± 17 mg/dL, $P < 0.05$ versus ND), triglycerides (171 ± 3 mg/dL, $P < 0.01$), and glycemia (343 ± 2.0 mg/dL, $P < 0.01$) when compared to mice subjected to ND (102 ± 3.0; 106 ± 6.0; 311 ± 5.5 mg/dL, resp.) (Table 2). Mice subjected to FD + HAP, FD + DAP, and FD + SDAP

Table 1: Nutritional report in percentage of lipid composition, total phenols, antioxidant content, and quercetin content of the different diets employed.

Component	ND	FD	FD + HAP	FD + SDAP	FD + DAP
Carbohydrates (%)	69.4	57.0	59.8	57.6	56.2
Proteins (%)	21.0	17.6	12.5	18.2	17.3
Lipids (%)	1.8	16.8	20.2	16.4	17.5
Water (%)	6.0	15.3	19.4	18.3	12.2
Ash (%)	6.0	5.1	4.8	4.8	5.1
Fiber (%)	2.8	3.5	2.8	3.0	3.9
Myristic acid (14:0)	1.6	0.1	1.1	0.0	0.1
Palmitoleic acid (16:1)	0.0	0.0	1.5	4.6	1.4
Palmitic acid (16:0)	40.0	14.0	14.1	38.9	29.7
Linoleic acid (18:2)	11.6	34.0	31.5	15.5	28.2
Oleic acid (18:1)	29.8	44.4	39.4	32.0	19.0
Stearic acid (18:0)	9.7	7.5	6.5	9.0	7.3
Total phenols	0.0	0.0	1.6 ± 0.5	2.0 ± 0.1	1.8 ± 0.1
Antioxidant activity	0.0	0.0	0.2 ± 0.02	0.3 ± 0.1	0.2 ± 0.02
Q. rutinoside	0.0	0.0	16.4 ± 7.2	19.2 ± 4.3	29.0 ± 1.4
Q. galactoside	0.0	0.0	55.9 ± 9.1	93.8 ± 16.8	46.0 ± 4.5
Q. glucoside	0.0	0.0	10.6 ± 5.8	29.9 ± 5.0	10.2 ± 0.4
Q. xyloside	0.0	0.0	7.9 ± 4.4	16.3 ± 2.8	8.9 ± 0.2
Q. arabinoside	0.0	0.0	15.6 ± 4.6	29.7 ± 5.7	20.9 ± 1.1
Q. rhamnoside	0.0	0.0	10.2 ± 3.4	14.5 ± 3.3	14.1 ± 0.9

ND, normal diet; FD, fat diet; HAP, healthy apple peel; SDAP, sun damaged apple peel; DAP, dehydrated apple peel. All lipid components have a methyl ester conjugation. Total phenols and antioxidant capacity expressed with mg eq. chlorogenic acid/sample g. The quercetin glycoside expressed with μg/sample g.

Table 2: Biochemical parameters and initial and final weight and weight gain of the different groups of CF-1 mice subjected to different diets.

Biochemical component	ND	FD	FD + HAP	FD + SDAP	FD + DAP
Total cholesterol (mg/dL)	102 ± 5	$164 \pm 30^{*}$	$101 \pm 9^{\&}$	$103 \pm 3^{\&}$	$112 \pm 7^{\&}$
HDL cholesterol (mg/dL)	56 ± 7	66 ± 13	53 ± 6	50 ± 4	61 ± 9
Total/HDL cholesterol (mg/dL)	1.8 ± 0.1	1.5 ± 0.1	2 ± 0.1	1.8 ± 0.3	1.9 ± 0.1
Triglyceridemia (mg/dL)	106 ± 8	$171 \pm 5^{***}$	$81 \pm 9^{*\&\&\&}$	$74 \pm 8^{*\&\&\&}$	$80 \pm 7^{*\&\&\&}$
Glycemia (mg/dL)	311 ± 10	343 ± 4	$134 \pm 30^{***\&\&\&}$	278 ± 28	294 ± 28
GOT (UI/L)	166 ± 48	144 ± 21	94 ± 19	116 ± 16	94 ± 33
Uric acid (mg/dL)	1.8 ± 0.2	2.7 ± 1.0	$0.8 \pm 0.6^{\&}$	1.2 ± 0.4	1.2 ± 0.6
Initial weight (g)	37.3 ± 1.3	38.0 ± 0.9	37.0 ± 1.4	36.4 ± 1.3	36.5 ± 1.1
Final weight (g)	44.3 ± 0.9	45.1 ± 1.1	45.2 ± 1.3	43.3 ± 1.5	43.2 ± 1.5
Gain (g)	6.9 ± 0.12	$7.5 \pm 0.35^{**}$	$6.2 \pm 0.55^{*\&\&\&}$	$6.0 \pm 0.58^{*\&\&\&}$	$6.7 \pm 0.60^{*}$

ND, normal diet; FD, fat diet; HAP, healthy apple peel; SDAP, sun damaged apple peel; DAP, dehydrated apple peel.
HDL: high density lipoprotein and GOT: glutamic-oxaloacetic transaminase.
The results are expressed as the ±SD average. Statistical significance: $^{*}P < 0.05$, $^{**}P < 0.01$, and $^{***}P < 0.001$ are compared with the ND group and $^{\&}P < 0.05$ and $^{\&\&\&}P < 0.001$ are compared with the FD group.

presented lower levels in these parameters when compared to the FD group. The FD + HAP group (134 ± 30 mg/dL, $P < 0.001$) was the one that presented lower levels of glycemia and the group FD + SDAP apple was the one which presented lower levels of triglyceridemia (74 ± 8.3 mg/dL, $P < 0.001$), when compared to FD group.

The group of mice that received FD (2.34 ± 0.37 ng/mL) presented significantly higher insulin levels than mice fed with ND (1.23±0.25 ng/mL) (Figure 1(b)). On the other hand, mice subjected to FD + SDAP presented significantly lower insulinemia values (1.53±0.32 ng/mL) when compared to FD group.

The group of mice subjected to FD presented higher serum ADMA levels than mice subjected to ND ($P < 0.001$) (Figure 1(c)), while mice fed with FD + HAP, FD + DAP, and FD + SDAP presented lower concentrations than FD group ($P < 0.001$; $P < 0.01$; $P < 0.01$, resp.), the FD + HAP group being the one that presented the lower ADMA levels.

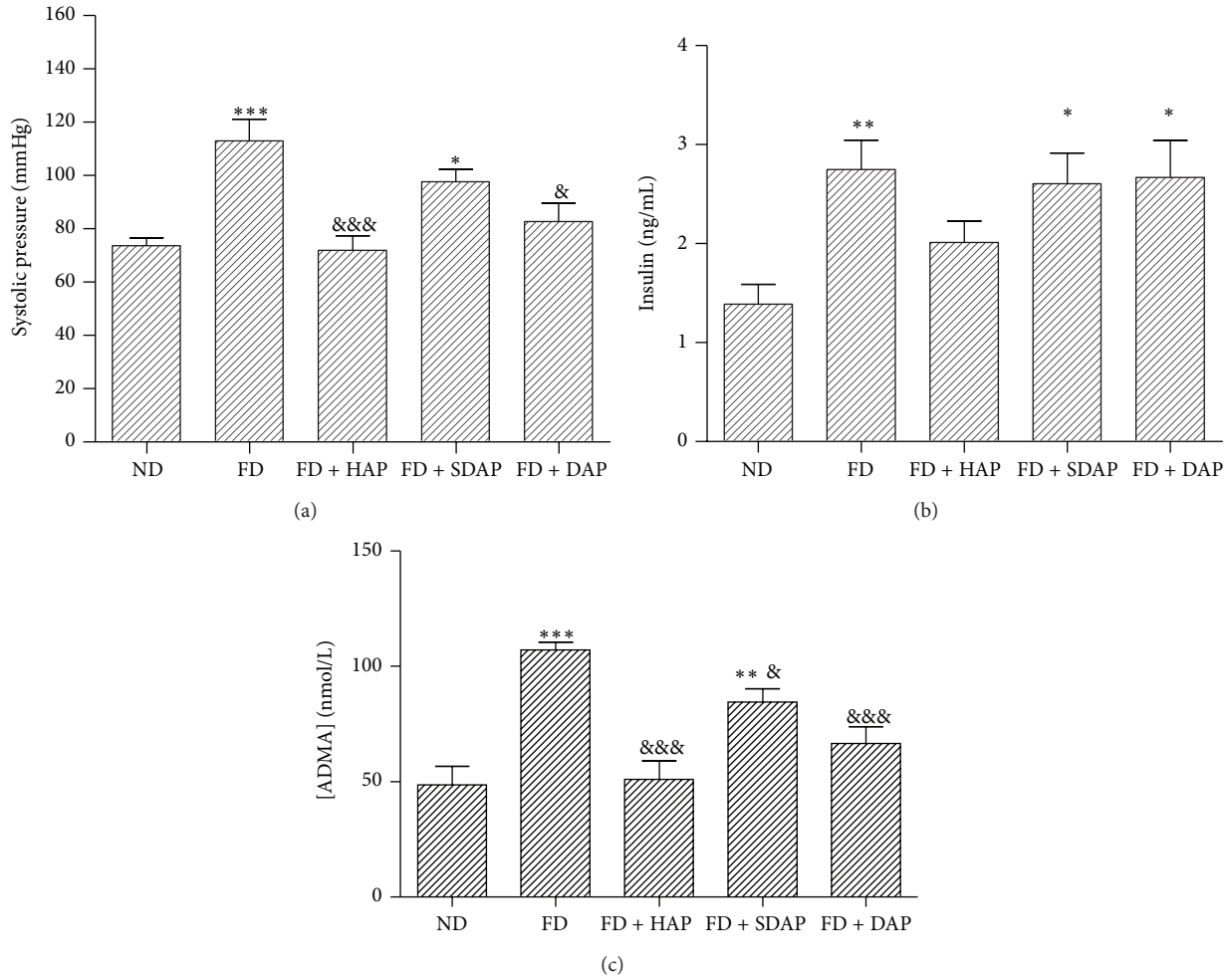

Figure 1: (a) Systolic blood pressure of mice subjected to different diets. ND, normal diet; FD, fat diet; HAP, healthy apple peel; SDAP, sun damaged apple peel; DAP, dehydrated apple peel. Statistical significance: $^{*}P < 0.05$, $^{***}P < 0.001$ versus normal diet. Statistical significance: $^{\&}P < 0.05$, $^{\&\&\&}P < 0.001$ versus fat diet. All groups have a minimum of 4 mice. (b) Average insulinemia in mice fed with different diets. Statistical significance: $^{*}P < 0.05$, $^{**}P < 0.01$ versus normal diet. Statistical significance: $^{\&}P < 0.05$ versus fat diet. All groups have a minimum of 4 individuals. (c) Serum ADMA of mice fed with different diets. $^{**}P < 0.01$, $^{***}P < 0.001$ versus normal diet. Statistical significance: $^{\&}P < 0.05$ versus fat diet. All groups have a minimum of 4 individuals.

3.3. Impact of Apple Consumptions in ApoE−/− Mice: A Model of Atherosclerosis. Next, we tested our diet with apple peel supplement in the ApoE−/− mouse, a model of dyslipidemia and atherosclerosis. Total cholesterol, triglycerides, and basal glycemia were determined in mice fed with the three types of diets, and control group of C57BL6 (WT) mice were incorporated for this analysis. Total cholesterol of ApoE−/− mice fed on a ND ($P < 0.01$), FD ($P < 0.001$), and FD + HAP ($P < 0.001$) was higher than control group (WT). Only glycemia of FD group had a significant increase with respect to the control group ($P < 0.05$).

Total cholesterol of the FD group and the FD + HAP group had statistically significant increase with respect to the ND group ($P < 0.01$), and only basal glycemia of the FD group had a statistically significant difference compared to the ND group ($P < 0.05$) (Table 3).

The final weight was higher in FD group than in FD + HAP group, with a value of $P < 0.05$ (Table 3).

Besides, using ANOVA to compare the initial and final body weight of all groups, it could be determined that the increase in body weight of mice on FD and mice on FD + HAP compared to the initial body weight of mice on ND was statistically significant ($P < 0.0001$). Also, mice on FD had higher body weight than mice on FD + HAP ($P < 0.05$).

3.4. Atherosclerosis. Finally, we analysed the progress of the atherosclerosis process in ApoE−/− mice fed with apple peel supplemented diets for 20 weeks. For this, we collected the thoracic aorta from animals treated and untreated and they were processed for HE and collagen staining. Figure 2 depicts representative histologic sections of HE and Masson's Trichrome from ApoE−/− mice.

Figures 2(a1) and 2(a2), as well as Figures 2(b1) and 2(b2), correspond to control groups (wild type (WT) and ApoE−/− fed with ND) showing histological sections corresponding

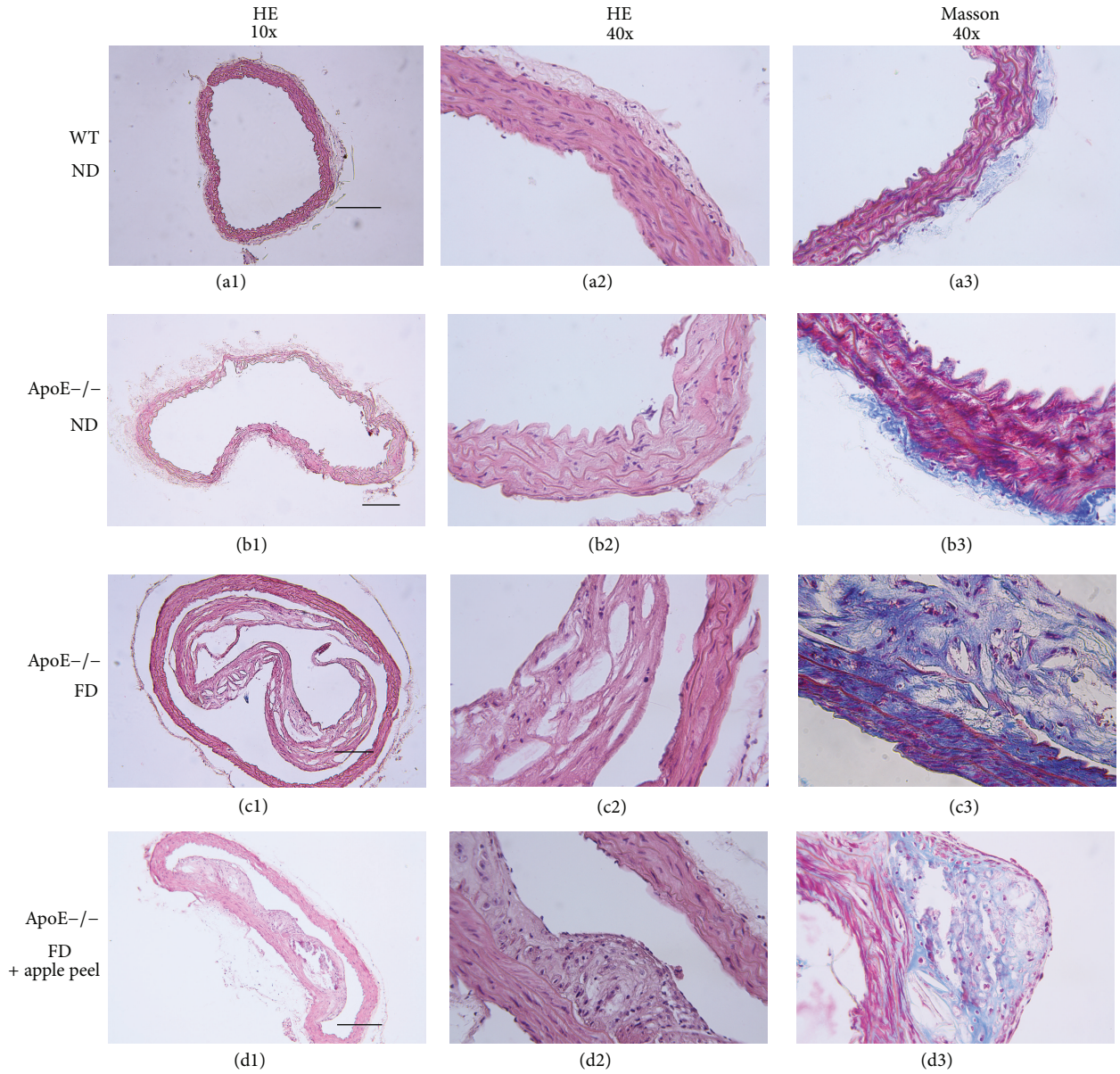

Figure 2: Aorta histochemical staining in mice: (a1) to (a3) control group C57BL6WT; (a1): Hematoxylin and eosin (HE) staining, magnification 10x; (a2): HE staining, magnification 40x; (a3): Masson's Trichrome staining, magnification 40x. (b1) to (b3): ApoE−/− normal diet group: (b1): HE staining, magnification 10x; (b2): HE staining, magnification 40x; (b3): Masson's Trichrome staining, magnification 40x. (c1) to (c3): ApoE−/− fat diet group: (c1): HE staining, magnification 10x; (c2): HE staining, magnification 40x; (c3): Masson's Trichrome staining, magnification 40x. (d1) to (d3): ApoE−/− fat diet plus apple peel group: (d1): HE staining, magnification 10x; (d2): HE staining, magnification 40x; (d3): Masson's Trichrome staining, magnification 40x. Scale bar: 200 μm.

to thoracic aorta, in which a vascular wall of conserved histoarchitecture is observed, with inner, middle, and adventitia layers without morphological evidence of lesion.

Figures 2(a3) and 2(b3) show histological sections of control groups WT and ApoE−/− with ND, corresponding to thoracic aorta, stained with Masson's Trichrome technique. A vascular wall of conserved histoarchitecture is observed, with inner, middle, and adventitia layers without morphological evidence of lesion.

Figures 2(c1), 2(c2), and 2(c3) are histological sections of aorta artery of ApoE−/− mice fed with FD corresponding to an elastic artery wall. Figures 2(c1) and 2(c2) were stained with HE technique and Figure 2(c3) was stained with Masson's Trichrome technique. A vascular wall presenting a high degree of histoarchitecture distortion, significant expansion, and partial detachment of the inner layer is observed. Figure 2(c2) highlights the composition of the histoarchitecture distortion, with abundant foam cells, some

Table 3: Biochemical parameters and initial and final weight in different groups of ApoE−/− mice subjected to different diets.

Biochemical component	WT	ApoE−/− ND	ApoE−/− FD	ApoE−/− FD + HAP
Total cholesterol (mg/dL)	86 ± 9	317 ± 67	533 ± 154**	515 ± 132**
Triglyceridemia (mg/dL)	55 ± 4	141 ± 16	185 ± 42	146 ± 55
Glycemia (mg/dL)	157 ± 44	161 ± 58	324 ± 128*	231 ± 107
Initial weight (g)	29.1 ± 1.8	32.5 ± 1.9	34.0 ± 2.2	34.1 ± 1.6
Final weight (g)	32.1 ± 1.8	35.1 ± 1.2	43.4 ± 4.3***	40.1 ± 1.9$^{**,\&}$

ND, normal diet; FD, fat diet; HAP, healthy apple peel.
The results are expressed as the ±SD average.
Statistical significance: $^{**}P < 0.01$, $^{***}P < 0.001$ final weight compared with the ND group and $^{\&}P < 0.05$ compared with the FD group.
Statistical significance $^{*}P < 0.05$.

inflammatory cells, and abundant optically empty spaces compatible with cholesterol crystals. Figure 2(c3) highlights degenerative changes of the extracellular matrix at the level of the distortion area.

The image analysis is presented in Figure 3 for the FD and FD + HAP groups. With the images obtained by HE staining, areas of 50 μm^2 were delimited and the empty area compatible with cholesterol accumulation was measured. The results show that animals fed with a fat diet supplemented with apple peel developed lower size plaques with lower cholesterol content than controls which consume only FD. In the same groups of images and sections, the amount of inflammatory cell nuclei and the intensity of blue colouring in Masson's Trichrome staining were measured. These results show that animals receiving apple peel supplement developed lower degree of fibrosis than animals on fat diet.

4. Discussion

4.1. MS Mice Model. Murine models for MS research are widely used. Moore-Carrasco et al. standardized a MS model in CF-1 mice fed with a high fat diet and developed metabolic alterations similar to those observed in human MS [19].

MS corresponds to a series of metabolic alterations that double the risk of suffering CVD [24]. The alteration of parameters, such as glycemia, insulin, triglycerides, and arterial pressure, in addition to the increase of prothrombotic molecules such as TNFα, ADMA, and P-selectin, contributes to the development of this pathology. The consumption of flavonoids as those present in apples might contribute to the decrease in cardiovascular risk factors. To evaluate this hypothesis, the development of MS was induced in CF-1 mice with a fat-rich diet for a period of 43 days [19] and the effect of different types of Fuji apple peel was determined. Here we showed that the consumption of a hyper caloric diet supplemented with fresh, dehydrated, or sunburned apple peel prevents the metabolic and hormonal alterations triggered by the MS. For instance, apple peel supplemented diets reduced blood glucose levels while they also reduced insulin levels in CF-1 mice. These results suggest a role in glucose metabolism. The mechanism for this improvement remains to be determined but may involve improved insulin sensitivity, decreased intestinal glucose absorption, or decreased hepatic glucose output.

The composition of lipids present in the different types of diets used for this study is very similar to other diets used in previous studies [25]. The murine model developed by our group [19] was validated in this study; when subjecting CF-1 mice to a diet rich in fat (17%) for a 43-day period, they developed MS.

Mice fed with FD presented a significantly higher weight gain when compared to mice subjected to ND. Mice fed with FD + HAP, FD + DAP, and FD + SDAP presented a lower weight gain than the group fed only with FD. These results agree with a study by Conceição de Oliveira et al. (2003) [26].

Mice that received FD show higher SAP than mice fed with ND. Mice subjected to FD+ HAP showed lower SAP compared to FD. These results are in agreement with other *in vivo* studies that have demonstrated that flavonoids present in apple decrease blood pressure [12] and with a study in a model of hypertensive rats in which antioxidants, such as the quercetins present in apples, decrease arterial pressure [27]. Recently, the capacity of a beverage prepared from fruits (cranberry, apple, and blueberry juices at the portions of 12.5%, 37.5%, and 50%, resp.) was described to reduce blood pressure in rats [28].

Mice that consumed a FD showed an increase in glycemia, triglycerides, and cholesterol when compared to the ND group, while mice subjected to FD + HAP, FD + DAP, and FD + SDAP showed significantly lower levels of these parameters compared to the FD group. These results agree with the study by Zhao et al. (2004) [29], using transgenic mice for type II diabetes. They demonstrated that the treatment with phloridzin, a component which is present in apple peel, reduced significantly the hyperglycemia in these mice. Aprikian et al. [30] evidenced a significant decrease of cholesterol levels in rats fed with a high fat diet complemented with lyophilized apple; the same was observed in obese Zucker rats [30]: the consumption of apples decreased the plasmatic LDL cholesterol [31].

The group of mice that received FD showed insulin levels significantly higher than the control group, and mice with FD + HAP showed insulin values significantly lower compared to the FD group. Gao et al. (2010) [32] demonstrated that mice fed with a high fat diet developed obesity and hyperinsulinemia, in only two weeks.

Studies have shown that the intake of polyphenol-rich foods influences cardiovascular health and decreases the

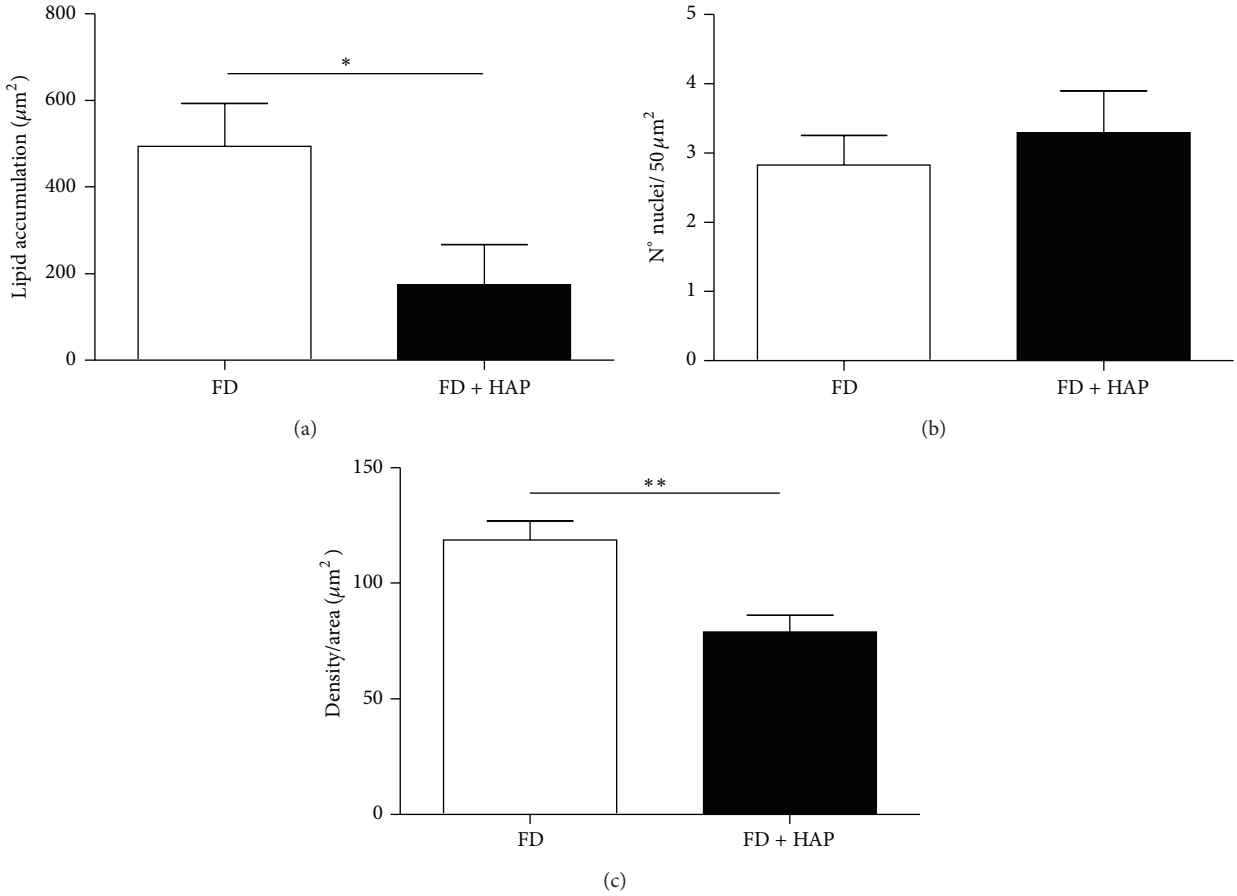

Figure 3: Image analysis of atherosclerotic lesions in ApoE−/− mice. (a) shows the area of cholesterol expressed as μm^2 of the lesion. In (b), the degree of infiltration expressed as number of cores in the lesion is shown. (c) illustrates the degree of infiltration expressed by the color intensity of the area. Statistical significance: $^{*}P < 0.05$, $^{**}P < 0.01$ versus fat diet.

expression of P-selectin [33]. Also, it has been observed that quercetins reduce significantly the concentrations of this adhesion molecule [34]. However, in this study, we did not find significant differences of P-selectin levels among groups (data not shown). It is known that platelet activation followed by inflammatory stimuli leads to the expression of surface receptors as P-selectin. Endothelial dysfunction, an early characteristic in atherosclerosis, is associated with the low degree inflammation inside the vascular wall [35]. This might explain partly the results obtained in this study in regard to P-selectin, insomuch as mice developed MS which causes a low degree of inflammation appearing usually in early stages of atherosclerosis.

We found that mice subjected to FD showed higher ADMA levels when compared to the ND group, which indicates that endothelial dysfunction is associated with MS. Mice subjected to FD + HAP, FD + DAP, and FD + SDAP showed lower plasma concentrations of ADMA compared with the FD group, specially the FD + HAP group. Some authors have stated that there is a reciprocal relation between ADMA and insulin resistance, suggesting that when there are metabolic alterations leading to insulin resistance, plasma levels of ADMA increase and vice versa [36, 37]. In this study, mice with FD showed high plasmatic levels of both ADMA and insulin. A study of a group of young adults evidenced a positive association between ADMA plasma levels, obesity, arterial pressure, and glycemia and it was observed that those individuals that consume diets with high content of antioxidants showed significantly lower levels of ADMA [38].

With the data obtained in this study, it can be concluded that an apple peel enriched diet decreased significantly several MS criteria in CF-1 mice.

4.2. Atherosclerosis Model. It is well established that raw or processed fruit and vegetable consumption decreases the incidence of CVD [39]. The mechanisms by which apple consumption decreases the CV risk is unknown; however, there is evidence that relates its favourable effect to a high antioxidant content, mostly flavonoids, with peel the main presenting antioxidant activity [14], in which its protecting effect would be related to its capacity to decrease serum cholesterol [40].

In the advanced atherosclerosis model obtained in ApoE−/− mice fed with FD + HAP, we observed a significant decrease of the fat content at the atheroma plaque, expressed as a lipid infiltration area. With these results, we

can postulate that the apple peel supplement in diet may have a protecting effect in the advance of the atherosclerotic disease, directly at the fat content level of the plaque, reducing endothelial dysfunction and serum cholesterol. This effect is possibly due to stimulation of cholesterol catabolism, or inhibition of its intestinal absorption, correlating with previous reports in ApoE−/− mice [41], and Sprague-Dawley rats [42]. Flavonoids, mainly from wine, also present in apples have been related to a decrease in migration and proliferation of smooth muscle cells as a response to a decrease of LDL [43]. In our study we observe a significant decrease of fibrosis in ApoE−/− FD + HAP mice, compared to the control group, confirming the results observed with wine flavonoids. However, this is the first time that this characteristic is proved with apple peel. Finally, the data of inflammation level expressed by the number of inflammatory cells infiltrating the plaque were not statistically significant compared with the control group, maybe because the beneficial effects of flavonoids present in apple peel are mainly related to stopping the progression of plaque formation, by reducing cholesterol accumulation, compared with its effect of improving endothelial dysfunction, corroborating the results mentioned above.

As a conclusion, apple peel consumption improves metabolic alterations associated with a fat-rich diet and also slowed the atherogenesis development, one of the most lethal consequences of a hypercaloric diet. Our results contribute to the concept of having a functional food from apple products with beneficial effects on risk factors for cardiovascular disease [44].

Conflict of Interests

The authors declare that there is no conflict of interests regarding the publication of this paper.

Acknowledgments

This work is supported by FONDECYT grant for initial research no. 11090027 and Project FONDEF Cod. AF1OI1022 from CONICYT-CHILE. The authors thank Dr. Daniel Gonzalez, Universidad de Talca, for helping in discussion and writing of this paper.

References

[1] R. H. Eckel, S. M. Grundy, and P. Z. Zimmet, "The metabolic syndrome," *The Lancet*, vol. 365, no. 9468, pp. 1415–1428, 2005.

[2] L. Badimón, G. Vilahur, and T. Padró, "Lipoproteins, platelets and atherothrombosis," *Revista Espanola de Cardiologia*, vol. 62, no. 10, pp. 1161–1178, 2009.

[3] J. Salmerón, F. B. Hu, J. E. Manson et al., "Dietary fat intake and risk of type 2 diabetes in women," *The American Journal of Clinical Nutrition*, vol. 73, no. 6, pp. 1019–1026, 2001.

[4] R. Hirano, W. Sasamoto, A. Matsumoto, H. Itakura, O. Igarashi, and K. Kondo, "Antioxidant ability of various flavonoids against DPPH radicals and LDL oxidation," *Journal of Nutritional Science and Vitaminology*, vol. 47, no. 5, pp. 357–362, 2001.

[5] M. Najafian, M. Z. Jahromi, M. J. Nowroznejhad et al., "Phloridzin reduces blood glucose levels and improves lipids metabolism in streptozotocin-induced diabetic rats," *Molecular Biology Reports*, vol. 39, no. 5, pp. 5299–5306, 2012.

[6] K.-D. Cho, C.-K. Han, and B.-H. Lee, "Loss of body weight and fat and improved lipid profiles in obese rats fed apple pomace or apple juice concentrate," *Journal of Medicinal Food*, vol. 16, no. 9, pp. 823–830, 2013.

[7] D. A. Pearson, C. H. Tan, J. B. German, P. A. Davis, and M. E. Gershwin, "Apple juice inhibits human low density lipoprotein oxidation," *Life Sciences*, vol. 64, no. 21, pp. 1913–1920, 1999.

[8] S. Zhao, J. Bomser, E. L. Joseph, and R. A. DiSilvestro, "Intakes of apples or apple polyphenols decease plasma values for oxidized low-density lipoprotein/beta2-glycoprotein I complex," *Journal of Functional Foods*, vol. 5, no. 1, pp. 493–497, 2013.

[9] K. Nakazato, H. Song, and T. Waga, "Effects of dietary apple polyphenol on adipose tissues weights in Wistar rats," *Experimental Animals*, vol. 55, no. 4, pp. 383–389, 2006.

[10] S. H. Thilakarathna, Y. Wang, H. P. V. Rupasinghe, and K. Ghanam, "Apple peel flavonoid- and triterpene-enriched extracts differentially affect cholesterol homeostasis in hamsters," *Journal of Functional Foods*, vol. 4, no. 4, pp. 963–971, 2012.

[11] C. K. Lam, Z. Zhang, H. Yu, S. Y. Tsang, Y. Huang, and Z. Y. Chen, "Apple polyphenols inhibit plasma CETP activity and reduce the ratio of non-HDL to HDL cholesterol," *Molecular Nutrition and Food Research*, vol. 52, no. 8, pp. 950–958, 2008.

[12] F. Perez-Vizcaino, J. Duarte, and R. Andriantsitohaina, "Endothelial function and cardiovascular disease: effects of quercetin and wine polyphenols," *Free Radical Research*, vol. 40, no. 10, pp. 1054–1065, 2006.

[13] M. R. Negrão, E. Keating, A. Faria, I. Azevedo, and M. J. Martins, "Acute effect of tea, wine, beer, and polyphenols on ecto-alkaline phosphatase activity in human vascular smooth muscle cells," *Journal of Agricultural and Food Chemistry*, vol. 54, no. 14, pp. 4982–4988, 2006.

[14] J. A. Yuri, A. Neira, A. Quilodran, Y. Motomura, and I. Palomo, "Antioxidant activity and total phenolics concentration in apple peel and flesh is determined by cultivar and agroclimatic growing regions in Chile," *Journal of Food, Agriculture and Environment*, vol. 7, no. 3-4, pp. 513–517, 2009.

[15] M. Buzello, J. Törnig, J. Faulhaber, H. Ehmke, E. Ritz, and K. Amann, "The apolipoprotein E knockout mouse: a model documenting accelerated atherogenesis in uremia," *Journal of the American Society of Nephrology*, vol. 14, no. 2, pp. 311–316, 2003.

[16] S. H. Zhang, R. L. Reddick, J. A. Piedrahita, and N. Maeda, "Spontaneous hypercholesterolemia and arterial lesions in mice lacking apolipoprotein E," *Science*, vol. 258, no. 5081, pp. 468–471, 1992.

[17] J. Jawien, P. Nastalek, and R. Korbut, "Mouse models of experimental atherosclerosis," *Journal of Physiology and Pharmacology*, vol. 55, no. 3, pp. 503–517, 2004.

[18] I. Palomo, J. A. Yuri, R. Moore-Carrasco, A. Quilodrán, and A. Neira, "El consumo de manzanas contribuye a prevenir el desarrollo de enfermedades cardiovasculares y cáncer: antecedentes epidemiológicos y mecanismos de acción," *Revista Chilena de Nutrición*, vol. 37, no. 3, pp. 377–385, 2010.

[19] R. Moore-Carrasco, C. Aranguez-Arellano, I. Razmilic et al., "A high fat diet in CF-1 mice: an experimental model for metabolic syndrome," *Molecular Medicine Reports*, vol. 1, no. 3, pp. 401–405, 2008.

[20] K. Helrich, *Official Method of Analysis of the A.O.A.C.*, Association of Official Analytical Chemists, Arlington, Va, USA, 15th edition, 1990.

[21] A. Von Gadow, E. Joubert, and C. F. Hansmann, "Comparison of the antioxidant activity of aspalathin with that of other plant phenols of rooibos tea (*Aspalathus linearis*), α-tocopherol, BHT, and BHA," *Journal of Agricultural and Food Chemistry*, vol. 45, no. 3, pp. 632–638, 1997.

[22] M. Y. Coseteng and C. Y. Lee, "Changes in apple polyphenoloxidase and polyphenol concentrations in relation to degree of browning," *Journal of Food Science*, vol. 52, no. 4, pp. 985–989, 1987.

[23] T. Vrekoussis, V. Chaniotis, I. Navrozoglou et al., "Image analysis of breast cancer immunohistochemistry-stained sections using imageJ: an RGB-based model," *Anticancer Research*, vol. 29, no. 12, pp. 4995–4998, 2009.

[24] R. Zaliunas, R. Slapikas, D. Luksiene et al., "Prevalence of metabolic syndrome components in patients with acute coronary syndromes," *Medicina (Kaunas, Lithuania)*, vol. 44, no. 3, pp. 182–188, 2008.

[25] C. K. Roberts, N. D. Vaziri, K. Hui Liang, and R. J. Barnard, "Reversibility of chronic experimental syndrome X by diet modification," *Hypertension*, vol. 37, no. 5, pp. 1323–1328, 2001.

[26] M. Conceição de Oliveira, R. Sichieri, and A. Sanchez Moura, "Weight loss associated with a daily intake of three apples or three pears among overweight women," *Nutrition*, vol. 19, no. 3, pp. 253–256, 2003.

[27] M. Romero, R. Jiménez, B. Hurtado et al., "Lack of beneficial metabolic effects of quercetin in adult spontaneously hypertensive rats," *European Journal of Pharmacology*, vol. 627, no. 1–3, pp. 242–250, 2010.

[28] K. D. P. P. Gunathilake, Y. Wang, and H. P. V. Rupasinghe, "Hypocholesterolemic and hypotensive effects of a fruit-based functional beverage in spontaneously hypertensive rats fed with cholesterol-rich diet," *Journal of Functional Foods*, vol. 5, no. 3, pp. 1392–1401, 2013.

[29] H. Zhao, S. Yakar, O. Gavrilova et al., "Phloridzin improves hyperglycemia but not hepatic insulin resistance in a transgenic mouse model of type 2 diabetes," *Diabetes*, vol. 53, no. 11, pp. 2901–2909, 2004.

[30] O. Aprikian, J. Busserolles, C. Manach et al., "Lyophilized apple counteracts the development of hypercholesterolemia, oxidative stress, and renal dysfunction in obese zucker rats," *Journal of Nutrition*, vol. 132, no. 7, pp. 1969–1976, 2002.

[31] M. Leontowicz, S. Gorinstein, E. Bartnikowska, H. Leontowicz, G. Kulasek, and S. Trakhtenberg, "Sugar beet pulp and apple pomace dietary fibers improve lipid metabolism in rats fed cholesterol," *Food Chemistry*, vol. 72, no. 1, pp. 73–78, 2001.

[32] S. Gao, L. He, Y. Ding, and G. Liu, "Mechanisms underlying different responses of plasma triglyceride to high-fat diets in hamsters and mice: roles of hepatic MTP and triglyceride secretion," *Biochemical and Biophysical Research Communications*, vol. 398, no. 4, pp. 619–626, 2010.

[33] A. R. Rechner and C. Kroner, "Anthocyanins and colonic metabolites of dietary polyphenols inhibit platelet function," *Thrombosis Research*, vol. 116, no. 4, pp. 327–334, 2005.

[34] W. M. Loke, J. M. Proudfoot, J. M. Hodgson et al., "Specific dietary polyphenols attenuate atherosclerosis in apolipoprotein e-knockout mice by alleviating inflammation and endothelial dysfunction," *Arteriosclerosis, Thrombosis, and Vascular Biology*, vol. 30, no. 4, pp. 749–757, 2010.

[35] C. Antoniades, C. Bakogiannis, D. Tousoulis, M. Demosthenous, K. Marinou, and C. Stefanadis, "Platelet activation in atherogenesis associated with low-grade inflammation," *Inflammation and Allergy—Drug Targets*, vol. 9, no. 5, pp. 334–345, 2010.

[36] K. Sydow, C. E. Mondon, J. Schrader, H. Konishi, and J. P. Cooke, "Dimethylarginine dimethylaminohydrolase overexpression enhances insulin sensitivity," *Arteriosclerosis, Thrombosis, and Vascular Biology*, vol. 28, no. 4, pp. 692–697, 2008.

[37] I. Palomo, A. Contreras, L. M. Alarcón et al., "Elevated concentration of asymmetric dimethylarginine (ADMA) in individuals with metabolic syndrome," *Nitric Oxide—Biology and Chemistry*, vol. 24, no. 4, pp. 224–228, 2011.

[38] B. Puchau, M. A. Zulet, G. Urtiaga, Í. Navarro-Blasco, and J. A. Martínez, "Asymmetric dimethylarginine association with antioxidants intake in healthy young adults: a role as an indicator of metabolic syndrome features," *Metabolism: Clinical and Experimental*, vol. 58, no. 10, pp. 1483–1488, 2009.

[39] L. M. Oude Griep, J. M. Geleijnse, D. Kromhout, M. C. Ocké, and W. M. Monique Verschuren, "Raw and processed fruit and vegetable consumption and 10-year coronary heart disease incidence in a population-based cohort study in the Netherlands," *PLoS ONE*, vol. 5, no. 10, Article ID e13609, 2010.

[40] H. Leontowicz, S. Gorinstein, A. Lojek et al., "Comparative content of some bioactive compounds in apples, peaches and pears and their influence on lipids and antioxidant capacity in rats," *The Journal of Nutritional Biochemistry*, vol. 13, no. 10, pp. 603–610, 2002.

[41] S. Auclair, M. Silberberg, E. Gueux et al., "Apple polyphenols and fibers attenuate atherosclerosis in apolipoprotein E-deficient mice," *Journal of Agricultural and Food Chemistry*, vol. 56, no. 14, pp. 5558–5563, 2008.

[42] K. Osada, T. Suzuki, Y. Kawakami et al., "Dose-dependent hypocholesterolemic actions of dietary apple polyphenol in rats fed cholesterol," *Lipids*, vol. 41, no. 2, pp. 133–139, 2006.

[43] P. Ouyang, W.-L. Peng, W.-Y. Lai, and A.-L. Xu, "Green tea polyphenols inhibit low-density lipoprotein-induced proliferation of rat vascular smooth muscle cells," *Di Yi Jun Yi Da Xue Xue Bao*, vol. 24, no. 9, pp. 975–979, 2004.

[44] R. K. Baboota, M. Bishnoi, P. Ambalam et al., "Functional food ingredients for the management of obesity and associated comorbidities—a review," *Journal of Functional Foods*, vol. 5, no. 3, pp. 997–1012, 2013.

Hindawi Publishing Corporation
Evidence-Based Complementary and Alternative Medicine
Volume 2015, Article ID 518926, 11 pages
http://dx.doi.org/10.1155/2015/518926

Research Article

Huangzhi Oral Liquid Prevents Arrhythmias by Upregulating Caspase-3 and Apoptosis Network Proteins in Myocardial Ischemia-Reperfusion Injury in Rats

Xu Ran,[1] Jian Xin Diao,[2] Xue Gang Sun,[2] Ming Wang,[3] Hui An,[1] Guo Qiang Huang,[1] Xiao Shan Zhao,[2] Wen Xiao Ma,[2] Feng Hua Zhou,[2] Yun Gao Yang,[2] and Can Ming Miao[1]

[1]*Zhongshan Hospital of Traditional Chinese Medicine Affiliated to Guangzhou University of TCM, Zhongshan, Guangdong 528400, China*
[2]*The Key Laboratory of Molecular Biology, State Administration of Traditional Chinese Medicine, School of Traditional Chinese Medicine, Southern Medical University, Guangzhou 510515, China*
[3]*ZhuJiang Hospital of Southern Medical University, Guangdong, Guangzhou 510515, China*

Correspondence should be addressed to Yun Gao Yang; yangyungao@263.net and Can Ming Miao; miaocm1030@163.com

Received 5 April 2014; Accepted 7 July 2014

Academic Editor: Myeong Soo Lee

To study the effect of Huangzhi oral liquid (HZOL) on I/R after 2 h and 4 h and determine its regulatory function on caspase-3 and protein networks. 70 SD male rats were randomly divided into seven groups and established myocardial I/R injury model by ligating the left anterior descending coronary artery. Myocardial infarction model was defined by TTC staining and color of the heart. The levels of CK-MB, CTnI, C-RPL, SOD, and MDA were tested at 2 h and 4 h after reperfusion. HE staining and ultramicrostructural were used to observe the pathological changes. The apoptotic index (AI) of cardiomyocyte was marked by TUNEL. The expression levels of caspase-3, p53, fas, Bcl-2, and Bax were tested by immunohistochemistry and western blot. HZOL corrected arrhythmia, improved the pathologic abnormalities, decreased CK-MB, CTnI, C-RPL, MDA, AI, caspase-3, p53, fas, and Bax, and increased SOD ans Bcl-2 with different times of myocardial reperfusion; this result was similar to the ISMOC ($P > 0.05$). HZOL could inhibit arrhythmia at 2 and 4 h after I/R and ameliorate cardiac function, which was more significant at 4 h after reperfusion. This result may be related to decreased expression of caspase-3, p53, and fas and increased Bcl-2/Bax ratio.

1. Introduction

The function of apoptosis in cardiovascular disease is gaining recognition. Necrosis is a myocardial cell injury caused by myocardial ischemia. Recent studies demonstrated that oxidative stress and ischemia/reperfusion (I/R) injury not only cause myocardial necrosis but also induce cardiomyocyte apoptosis. The degree of myocardial cell apoptosis is associated with the I/R time [1]. Apoptosis is controlled by a series of pathological processes that mediate the signaling pathway; blocking the signaling pathway helps block apoptosis, thereby preventing myocardial apoptosis and improving heart function [2]. Increasing evidence has indicated that traditional Chinese medicine (TCM) significantly influences the protection of myocardial apoptosis [3]. TCM provides alternative options for preventing myocardial apoptosis to ameliorate the prognosis of I/R. Huangzhi prescription is a TCM that has long been used in China. Previous literature indicated that Huangzhi can improve blood viscosity and hyperlipidemia in patients [4]. Huangzhi oral liquid (HZOL) consists of Huangzhi prescription boiled and alcohol sunk. HZOL ameliorates coronary heart disease by promoting blood circulation and removing blood stasis and turbidity for gasification [5]. However, the effects of HZOL on I/R have been rarely explored. In one of our previous prospective animal studies [6], we found that HZOL can significantly improve cardiac and coagulation functions. The mechanism involved in apoptosis has not been reported. To confirm the effects of HZOL on I/R and explore its potential mechanism, this study was performed.

2. Materials and Methods

2.1. Preparation of HZOL. HZOL consists of leech, rhubarb, and Fructus arctii, which were mixed at a ratio of 5 : 3 : 3, with a concentration of 2.2 g/mL. HZOL was purchased from the Affiliated Zhongshan Hospital of Traditional Chinese Medicine for Guangzhou University of Chinese Medicine (Guangzhou, China). The quality of HZOL was controlled by thin layer chromatography analysis. The solution was stored in aliquots (10 mL/vase) at −20°C.

2.2. Preparation of Rat I/R Model. Male Wistar rats (SPF, no. 0099755, 200 g to 240 g) were purchased from the Experimental Animal Center of Southern Medical University, housed individually in clear plastic cages at a temperature- and humidity-controlled environment with a 12 h light/dark cycle (23 ± 1°C; 12 h light/dark cycle, light on at 7 a.m.) and given ad libitum access to rodent chow and water. Animals were handled in accordance with the Guidelines of Animal Care at Southern Medical University.

A total of 70 rats were randomly divided into seven groups, namely, the Model-2 h group (reperfusion for 2 h after 30 min of myocardial ischemia), Model-4 h group (reperfusion for 4 h after 30 min of myocardial ischemia), HZOL-2 h group (application of HZOL before Model-2 h), HZOL-4 h group (application of HZOL before Model-4 h), isosorbide mononitrate capsule- (ISMOC-) 2 h group (application of ISMOC before Model-2 h), ISMOC-4 h group (application of ISMOC before Model-4 h), and sham group (subjected to the same surgical procedure in the absence of left anterior descending (LAD) coronary artery). Rats in the HZOL-2 h, HZOL-4 h, ISMOC-2 h, and ISMOC-4 h groups were intragastrically administered with HZOL (2 g/kg/d) and ISMOC (3.6 mg/kg/d) at 1 h before surgery. This procedure was performed for seven consecutive days. Normal saline was used as control. Rats were anesthetized with pentobarbital sodium (80 mg/kg, Fluka), intubated, and ventilated artificially using a rodent ventilator (SAR-830, IITC, USA). Ischemia-reperfusion made mould method as mentioned in the paper [7]. Coronary artery occlusion was confirmed by epicardial cyanosis, ST-segment elevation, and an increase in R-wave amplitude. Reperfusion was achieved by releasing the snare and confirmed by recovery from cyanosis and reversal of ECG changes [8]. Rats in the sham group were subjected to the same surgical procedure in the absence of LAD coronary artery. We not only observed cyanosis of the left ventricle using ECG, but also performed 30 min of myocardial ischemia in four rats randomly selected from the sham (two rats) and model groups (two rats). After ischemia, the suture around the LAD coronary artery was retightened, and 1 mL of 1% triphenyl tetrazolium chloride (TTC) stain was injected via the thoracic aorta. After 10 min, the heart was cut into five to six transverse slices, which were 2 mm thick and parallel to the atrioventricular groove. The infarct area was confirmed as the unstained part in the risk area following TTC.

2.3. Assessment of Arrhythmias. The incidence of arrhythmias was determined and diagnosed based on the criteria of the Lambeth Conventions [9], including ventricular tachycardia (VT), ventricular fibrillation (VF), and other types of arrhythmias (single extrasystoles, bigeminy, and salvos).

An arrhythmia score was used to evaluate the severity of arrhythmias by giving a grade to each animal as follows: 0 = no arrhythmias; 1 = less than 10 s of VT or other arrhythmias, no VF; 2 = 11 s to 30 s of VT or other arrhythmias, no VF; 3 = 31 s to 90 s of VT or other arrhythmias, no VF; 4 = 91 s to 180 s of VT or other arrhythmias, and/or less than 10 s of reversible VF; 5 = more than 180 s of VT or other arrhythmias, and/or more than 10 s of reversible VF; 6 = irreversible VF [10].

2.4. Exclusion Criteria. Experiments were terminated or excluded from the final data analysis if any of the following conditions occurred: absence of signs of successful coronary artery occlusion, severe arrhythmias prior to LAD occlusion and reperfusion, or severe atrioventricular block during the first 5 min of ischemia [11]. Four rats were unsuccessful (Model-2 h, Model-4 h,HZOL-2 h, and ISMOC-4 h groups).

2.5. Sample Preparation after Reperfusion. 5 mL of blood was collected through the abdominal aorta of live rats to detect levels of serum creatine kinase mb isoenzyme (CK-MB), cardiac troponin I (CTnI), C reactive protein (CRP), superoxide dismutase (SOD), and malondialdehyde (MDA). The AAR of the left ventricle of rats in the sham, Model-2 h, Model-4 h, HZOL-2 h, HZOL-4 h, ISMOC-2 h, and ISMOC-4 h groups was removed and divided into four parts. One part was fixed in 10% formalin, another was fixed in 0.1 M phosphate buffer containing 2.5% glutaraldehyde and 2% paraformaldehyde, and the other two parts were flash-frozen in liquid nitrogen and stored at −80°C for use.

2.6. Serum Examination. Serum CK-MB, CTnI, CRP, SOD, and MDA determination. The serum biochemical parameters CK-MB, CTnI, and CRP, which closely reflect cardiac function [12], were analyzed by the clinical laboratory of Nanfang Hospital Affiliated to Southern Medical University (Guangzhou, China). The serum levels of SOD and MDA were determined using an SOD and MDA detection kit (Jiancheng, Nanjing, China). The assay was performed according to the manufacturer's instructions.

2.7. Histological and Transmission. Electron microscopy (TEM) examination part of the AAR of the left ventricle was fixed in 10% formalin, embedded in paraffin, cut into 4 μm sections, and mounted on slides. The samples were stained with hematoxylin and eosin (HE) for histopathological examination. For TEM examination, samples containing a 2 mm portion from the edge of the incision were immediately fixed in 0.1 M phosphate buffer containing 2.5% glutaraldehyde and 2% paraformaldehyde for 4 h. The samples were then fixed with 1% osmium tetroxide for 2 h, dehydrated through a graded ethanol series, and embedded in epoxy resin. Resin-embedded blocks were cut into 60 nm to 80 nm ultrathin sections with an ultramicrotome (PT-XL, RMC, USA).

The ultrathin sections were placed on carbon-coated nickel grids and examined with an H-7500 transmission electron microscope (H-7500, Tokyo, Japan) operating at 80 kV.

2.8. Apoptosis Assay. We purchased a terminal deoxynucleotidyl transferase dUTP nick end labeling (TUNEL) apoptosis assay kit for paraffin sections from Nanjing KeyGen Biotech. Inc. (Nanjing, Jiangsu, China). Based on the manufacturer's instructions, all the procedures were performed. Cells were defined as apoptotic if the entire nuclear area of the cell was positively labeled. The apoptotic cells and bodies were counted in five high-power fields. The apoptotic index (AI) was calculated as the percentage of positively stained cells using the following equation: AI = number of apoptotic cells/total number of nucleated cells [13].

2.9. Immunohistochemistry. Immunohistochemical staining for caspase-3, p-53, fas, Bcl-2, and Bax was performed using routine immunohistochemistry streptavidin peroxidase method. This method contained a rabbit polyclonal IgG antibody against caspase-3 (1 : 100; Cell Signaling Technology Inc., no. 9662, USA), p-53 (1 : 50; Bioworld Technology Inc., BS3736, Louis Park, USA), fas (1 : 100; Assay Designs, ADI-AAP-221D, USA), Bcl-2 (1 : 50; Bioworld Technology Inc., BS1511, Louis Park, USA) (Cell Signaling Technology, no. 2876, USA), and Bax (1 : 50; Bioworld Technology Inc., BS2538, Louis Park, USA) (Cell Signaling Technology, no. 2772, USA). Nuclear counterstaining was performed using hematoxylin. Five randomly selected fields from each section were examined at a magnification of ×200 and analyzed using Image-Pro Plus 6.0. The positive content (PC) was calculated using the following formula: PC = mean optical density × positive area [10].

2.10. Western Blot. Aliquots of heart tissue (50 mg) were homogenized in liquid nitrogen and dissolved in lysis buffer. Protein concentrations were determined by BCA protein quantitative assay. The protein lysates were loaded onto 10% SDS-polyacrylamide gel for separation, electrotransferred to PVDF membranes, and blocked in 5% nonfat milk in Tris-buffered saline, Membranes were incubated overnight using primary antibodies, (caspase-3 (Cell Signaling Technology Inc., no. 9662, USA) diluted to 1 : 1000, p-53 (Bioworld Technology Inc., BS3736, Louis Park, USA) diluted to 1 : 500, fas (Assay Designs, ADI-AAP-221D, USA) diluted to 1 : 500, Bcl-2 (Cell Signaling Technology, no. 2876, USA) diluted to 1 : 1000, and Bax (Cell Signaling Technology, no. 2772, USA) diluted to 1 : 1000) at 4°C. This step was followed by secondary antibodies, which were conjugated using horseradish peroxidase. We performed enhanced chemiluminescence (Merck-Millipore, Germany) detection. The images were captured and documented using a CCD system (image station 2000MM, Kodak, Rochester, NY, USA). Quantitative analysis of these images was performed using Molecular Imaging Software Version 4.0, which was provided by Kodak 2000MM System. The optical density was normalized against actin [10].

2.11. Statistical Analysis. Each experiment was repeated at least three times. Data were represented in the form of means ± SD. Data were analyzed using SPSS statistical package (version 13.0, Armonk, NY, USA). Mean values were compared using one-way ANOVA, and multiple comparisons were performed. Data were analyzed using a homogeneity test for variance. If the variances were homogeneous, mean values were compared through ANOVA. The differences between two groups were analyzed based on least significant difference test. If the variances were not homogeneous, mean values were compared using Welch's test. The differences between two groups were analyzed by Games-Howell. Statistical significance was set at $P < 0.05$.

3. Results

3.1. Effects of HZOL for I/R 2 h- and I/R 4 h-Induced Arrhythmias and Infarct Size. Naked eye observations showed that the heart color from the model group was paler than that of the sham group (Figure 1(a)). Effects of different treatments on I/R-induced arrhythmias are shown in Figure 1(c). In the sham group, neither VT nor VF was observed, and only a few ventricular premature beats appeared during the entire procedure. By contrast, almost all rats in the Model-2 h and Model-4 h groups experienced obvious ST-segment elevation, VT occurrence, and high VF frequency. Furthermore, the frequency of arrhythmias was significantly reduced in the Model-2 h and Model-4 h groups. During reperfusion, malignant arrhythmias were observed in the rats of the I/R group. Pretreatment with HZOL and ISMOC markedly reduced the mean duration of VT ($P < 0.05$), VF ($P < 0.05$), and arrhythmia score compared with those of the I/R group (Figure 1(d)).

3.2. Effects of HZOL for I/R 2 h and I/R 4 h on the Serum Levels of CK-MB, CTnI, CRP, SOD, and MDA. The serum levels of CK-MB, CTnI, CRP, SOD, and MDA after treatment are shown in Figure 2. Results show that CK-MB, CTnI, CRP, and MDA significantly increased, whereas SOD significantly decreased after Model-2 h and Model-4 h ($P < 0.05$). All these parameters indicate severe myocardial ischemia. However, the HZOL-2 h, ISMOC-2 h, HZOL-4 h, and ISMOC-4 h groups could improve cardiac function by decreasing CK-MB, CTnI, CRP, and MDA and increasing SOD levels ($P < 0.01$). The effects were more significant in the HZOL-4 h and ISMOC-4 h groups. Compared with the HZOL-2 h group, the HZOL-4 h group showed more significant effects by decreasing CK-MB and CTnI and increasing SOD levels ($P < 0.05$).

3.3. Effects of HZOL for I/R 2 h and I/R 4 h on the Histological and Ultrastructural Changes in the Myocardium. Results of HE staining of AAR are shown in Figure 3(a). Massive necroses were found in the myocardial tissues of the Model-2 h and Model-4 h groups. The necroses were reduced in the HZOL-2 h, HZOL-4 h, ISMOC-2 h, and ISMOC-4 h groups, but the effects were more significant in the HZOL-4 h and ISMOC-4 h groups. TEM images of ultrathin sections of

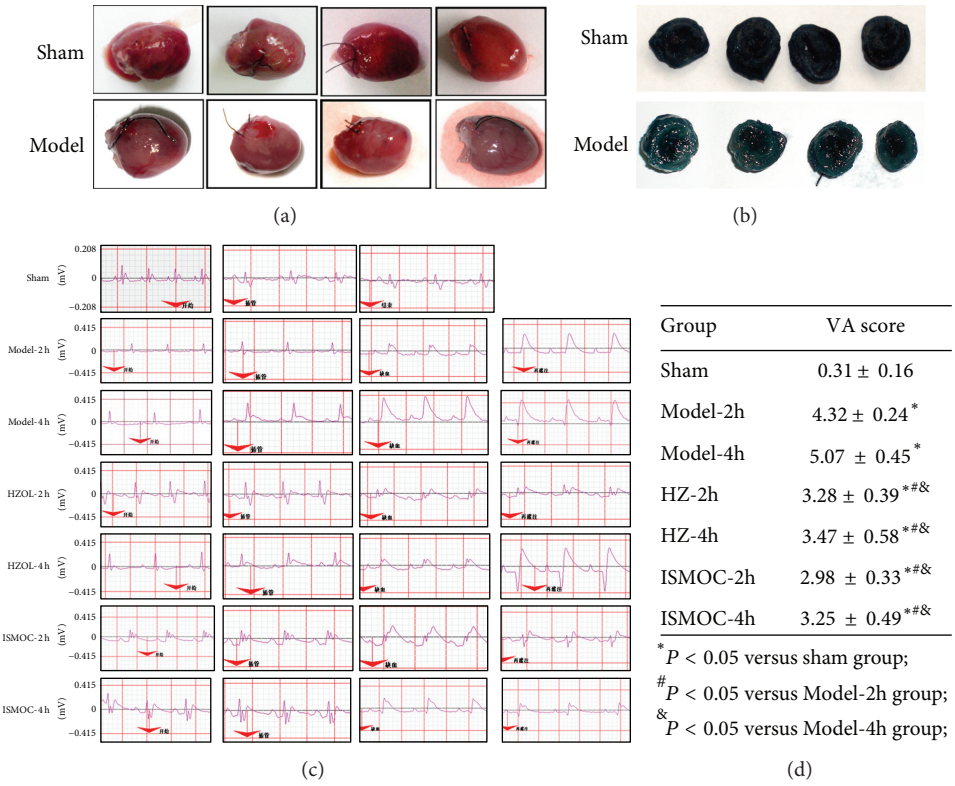

Group	VA score
Sham	0.31 ± 0.16
Model-2h	4.32 ± 0.24 *
Model-4h	5.07 ± 0.45 *
HZ-2h	3.28 ± 0.39 *#&
HZ-4h	3.47 ± 0.58 *#&
ISMOC-2h	2.98 ± 0.33 *#&
ISMOC-4h	3.25 ± 0.49 *#&

(d)

* $P < 0.05$ versus sham group;
# $P < 0.05$ versus Model-2h group;
& $P < 0.05$ versus Model-4h group;

Figure 1: Histological and electrocardiography (ECG) parameters. (a) Representative gross images of whole hearts. (b) Representative of 1% triphenyl tetrazolium chloride (TTC) staining results. (c) Representative of 2-lead electrocardiogram results. (d) Arrhythmia was scored according to 2-lead electrocardiogram. Model-2 h group (after 30 min of myocardial ischemia, reperfusion 2 h), Model-4 h group (reperfusion for 2 h after 30 min of myocardial ischemia), Model-4 h group (reperfusion for 4 h after 30 min of myocardial ischemia), HZOL-2 h group (application of HZOL before Model-2 h), HZOL-4 h group (application of HZOL before Model-4 h), isosorbide mononitrate capsule (ISMOC)-2 h group (application of ISMOC before Model-2 h), ISMOC-4 h group (application of ISMOC before Model-4 h), and sham group (subjected to the same surgical procedure in the absence of left anterior descending coronary artery). $^{\#}P < 0.05$ versus sham group; $^{\&}P < 0.05$ versus Model-2 h group; $^{*}P < 0.05$ versus Model-4 h group.

myocardial tissues are shown in Figure 3(b)A. We observed cardiomyocytes in a well-arranged myofilament and intercalated disc manner, as well as abundant normal mitochondria with no swelling, normal matrix density, and intact cristae, in the sham group (Figure 3(b)). However, in the I/R 2 h and I/R 4 h groups, myocardial I/R produced remarkable ultrastructural damages associated with irregularities and edematous separation of myofilaments and shortening of sarcomeres. Large areas of cytoplasmic vacuolization and mitochondrial swelling were evident with decreasing matrix density and cristae distortion (Figures 3(b)B and 3(b)C). HZOL treatment showed clear protection with relatively parallel arrangement of myofilaments and normal sarcomeres. Mitochondria were normal with mild swelling, normal matrix density, and slightly damaged cristae. However, mild cytoplasmic rarefaction with mild edema could still be observed (Figures 3(b)D and 3(b)E). These results were consistent with those of ISMOC (Figures 3(b)F and 3(b)G).

3.4. Effects of HZOL Pretreatment for I/R 2 h and I/R 4 h on Myocardial Apoptosis and Caspase-3 Expression. TUNEL staining suggested that more brown stained cells were found in the Model-2 h and Model-4 h groups than those in the sham group ($P < 0.05$). Compared with the Model-2 h and Model-4 h groups, HZOL significantly decreased the number of apoptotic cells ($P < 0.05$) (Figure 4(a)).

Western blot showed that caspase-3 expression ($P < 0.05$) (Figure 4(c)) in the Model-2 h and Model-4 h groups significantly increased than that in the sham group. Compared with the Model-2 h and Model-4 h groups, the HZOL-2 h, HZOL-4 h, ISMOC-2 h, and ISMOC-4 h groups significantly decreased caspase-3 expression ($P < 0.05$). The effects were more significant in the HZOL-4 h and ISMOC-4 h groups. Compared with the HZOL-4 h group, the HZOL-2 h group significantly decreased caspase-3 expression ($P < 0.05$). The immunohistochemical results were similar to those of western blot (Figure 4(b)).

3.5. Effects of HZOL Pretreatment for Expression Levels of p53, Fas, and Bcl-2/Bax in I/R 2 h and I/R 4 h. The expression levels of p53, fas, and Bcl-2/Bax are shown in Figure 5. The immunohistochemical results show that p53 and fas significantly increased, whereas Bcl-2/Bax significantly decreased in the Model-2 h and Model-4 h groups than

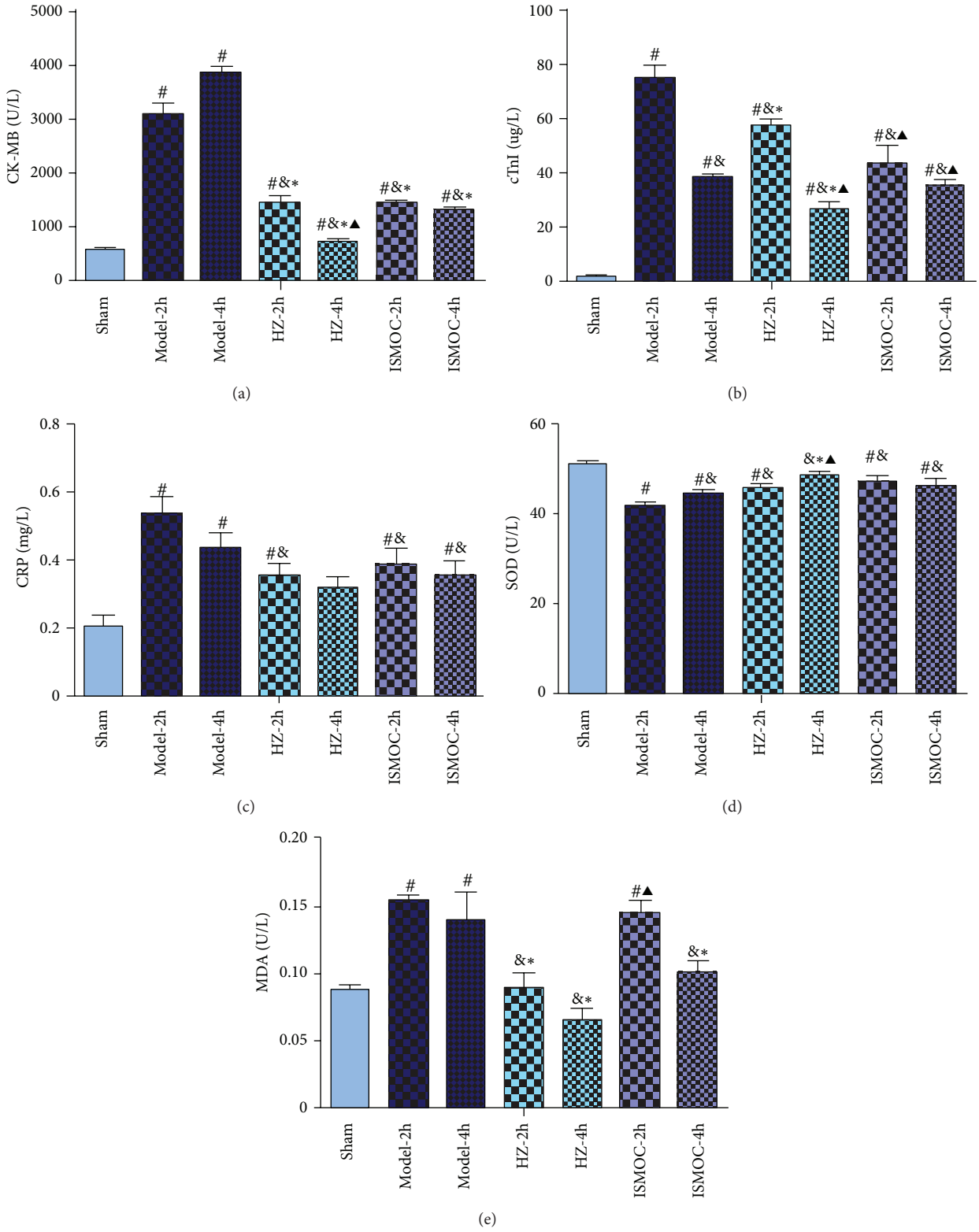

Figure 2: The serum levels of CK-MB, CTnI, CRP, SOD, and MDA after treatment. (a) CK-MB; (b) CTnI; (c) CRP; (d) SOD; (e) MDA; Model-2 h group (after 30 min of myocardial ischemia, reperfusion 2 h), Model-4 h group (reperfusion for 2 h after 30 min of myocardial ischemia), Model-4 h group (reperfusion for 4 h after 30 min of myocardial ischemia), HZOL-2 h group (application of HZOL before Model-2 h), HZOL-4 h group (application of HZOL before Model-4 h), isosorbide mononitrate capsule (ISMOC)-2 h group (application of ISMOC before Model-2 h), ISMOC-4 h group (application of ISMOC before Model-4 h), and sham group (subjected to the same surgical procedure in the absence of left anterior descending coronary artery). $^{\#}P < 0.05$ versus sham group; $^{\&}P < 0.05$ versus Model-2 h group; $^{*}P < 0.05$ versus Model-4 h group; $^{\blacktriangle}P < 0.05$ versus HZOL-2 h group.

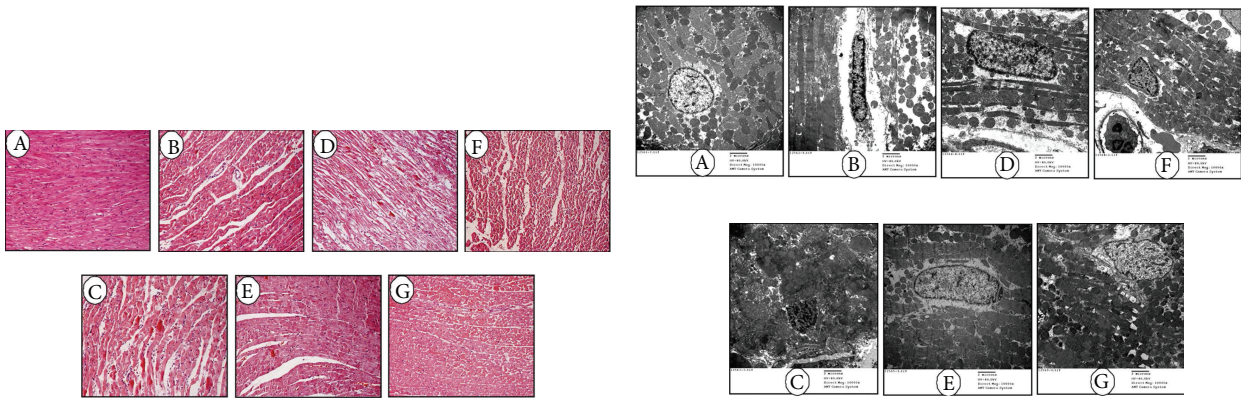

(a) HE (b) EMT

Figure 3: The effects of HZOL for I/R 2 h and I/R 4 h on the histological and ultrastructural changes in the myocardium (a) representative microscopic images of HE stain. (b) TEM images of ultrathin sections of myocardial tissue are changed. A: sham group; B: Model-2 h group; C: Model-4 h group; D: HZOL-2 h group; E: HZOL-4 h group; F: ISMOC-2 h group; G: ISMOC-4 h group.

those in the sham group ($P < 0.01$). However, the HZOL-2 h, ISMOC-2 h, HZOL-4 h, and ISMOC-4 h groups could improve myocardial apoptosis by decreasing p53 and fas and increasing Bcl-2/Bax expression ($P < 0.01$). The effects were more significant in the HZOL-4 h and ISMOC-4 h groups ($P < 0.01$). Compared with the HZOL-2 h group, the HZOL-4 h group was more significant in decreasing p53 and fas and increasing Bcl-2/Bax expression ($P < 0.01$) (Figures 5(a) to 5(c)). Western blot results were similar to those of immunohistochemical analysis (Figure 5(d)).

4. Discussion

Our results indicate that the activation of HZOL at the beginning of reperfusion produced a protective effect in I/R injury and participated in a cascade of events that resulted in apoptosis. This study is the first to demonstrate the protective effect of HZOL inhibition against apoptosis caused by I/R injury.

The effects of HZOL prevented arrhythmias in rats by myocardial I/R for 2 and 4 h. Naked eye observations showed that the color of the heart in the model group was paler than that in the sham group. Almost all rats in the Model-2 h and Model-4 h groups experienced obvious ST-segment elevation, VT occurrence, and high VF frequency, which was the frequency of arrhythmias. By contrast, neither VT nor VF was observed in the sham group, and only a few ventricular premature beats appeared during the entire procedure. The serum results illustrate that CK-MB, CTnI, CRP, and MDA significantly increased, whereas SOD significantly decreased in the Model-2 h and Model-4 h groups ($P < 0.05$). All these parameters indicate severe myocardial ischemia. However, the HZOL-2 h, ISMOC-2 h, HZOL-4 h, and ISMOC-4 h groups could improve cardiac function by decreasing CK-MB, CTnI, CRP, and MDA and increasing SOD levels ($P < 0.01$). These effects were more notable in the HZOL-4 h and ISMOC-4 h groups. CK-MB, CTnI, and CRP are important indicators of cardiac function. MDA is an unsaturated fatty acid in free radical and lipid peroxidation metabolites. The content of MDA, which is an indirect marker of cellular damage, reflects the extent of systemic lipid peroxidation. The antioxidant SOD protects cells by reducing free radical-induced injury. SOD levels reflect the body's capacity to scavenge oxygen free radicals [11–13]. In the present study, myocardial SOD activity was attenuated in the Model-2 h and Model-4 h groups, combined with increased MDA content in the Model-2 h and Model-4 h groups. Our data suggest that myocardial oxidative stress may exacerbate I/R injury. The HZOL-2 h and HZOL-4 h groups could improve cardiac function by decreasing MDA and increasing SOD levels ($P < 0.01$). HZOL prevented arrhythmias by improving both cardiac function and resistance to oxidative stress.

The use of HZOL has been practiced for many years in the Affiliated Hospital of Zhongshan University of Traditional Chinese Medicine and is highly effective in relieving hypertension and hyperlipidemia [5]. This TCM includes leech, rhubarb, and Fructus arctii in its recipe. Leech secretions include vasodilation, bacteriostatic, analgesic, anti-inflammatory, anticoagulant, and antiedematous effects, which eliminate microcirculatory disorders, restore the damaged vascular permeability of tissues and organs, eliminate hypoxia, reduce blood pressure, and increase immune system activity [14–16]. Rhubarb has antioxidant, antiplatelet, and anticoagulant activities and can treat experimental jaundice in rats [17, 18]. Arctiin is one of the major lignans in Fructus Arctii that can enhance immunological function and acts as an anti-inflammatory agent [19], platelet-activating factor antagonist [20], Ca^{2+} antagonist, and antihypertensive agent [21, 22]. Moreover, arctiin can be metabolized into arctigenin by human intestinal bacteria [23]. Thus, the direct protective effects of HZOL on ischemia-induced arrhythmias can be assumed. Our research is related to these active constituents, especially those associated with the antiapoptotic components of HZOL.

Apoptosis typically proceeds through one of two signaling cascades, known as extrinsic and intrinsic pathways, both

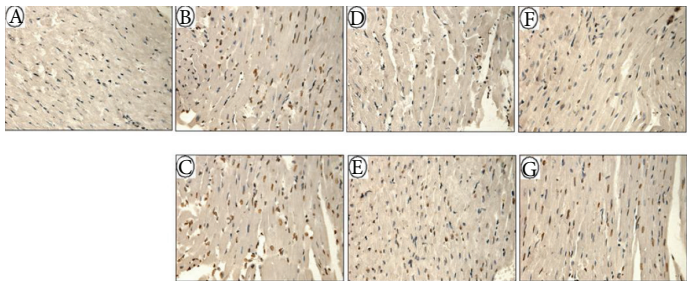

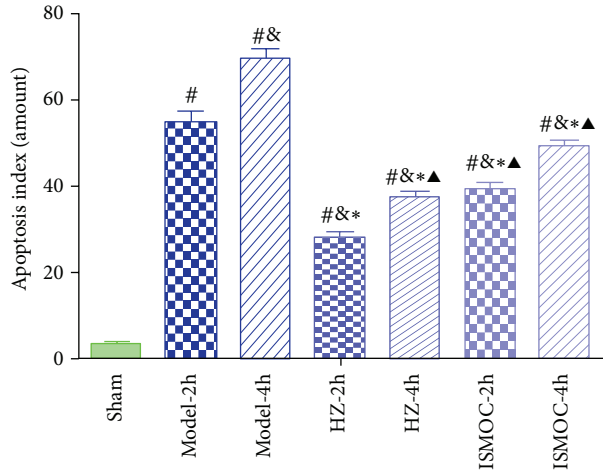

(a)

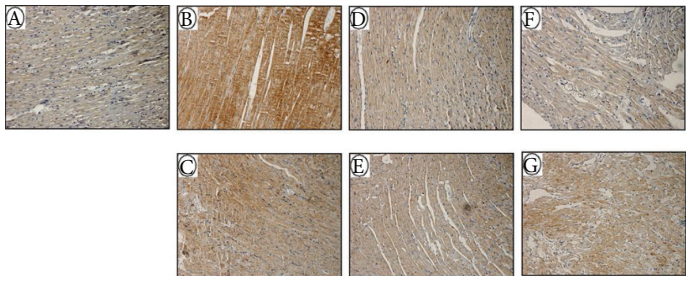

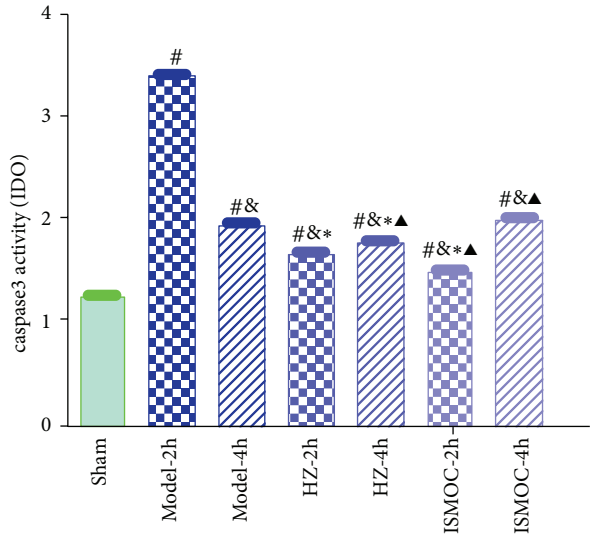

(b)

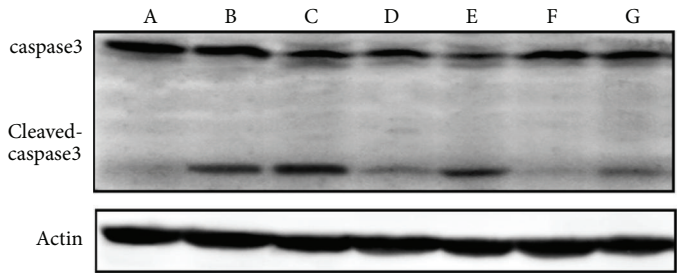

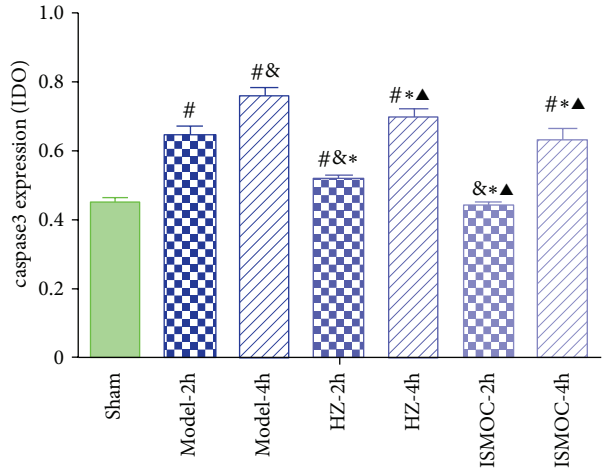

(c)

Figure 4: Effects of HZOL on apoptosis and expression of caspase-3. (a) TUNEL analysis of apoptosis in left ventricular AAR. (b) Immunohistochemical assay of caspase-3 expression. (c) Western blotting assay of caspase-3 expression. A: sham group; B: Model-2 h group; C: Model-4 h group; D: HZOL-2 h group; E: HZOL-4 h group; F: ISMOC-2 h group; G: ISMOC-4 h group; $^{\#}P < 0.05$ versus sham group; $^{\&}P < 0.05$ versus Model-2 h group; $^{*}P < 0.05$ versus Model-4 h group; $^{\blacktriangle}P < 0.05$ versus HZOL-2 h group.

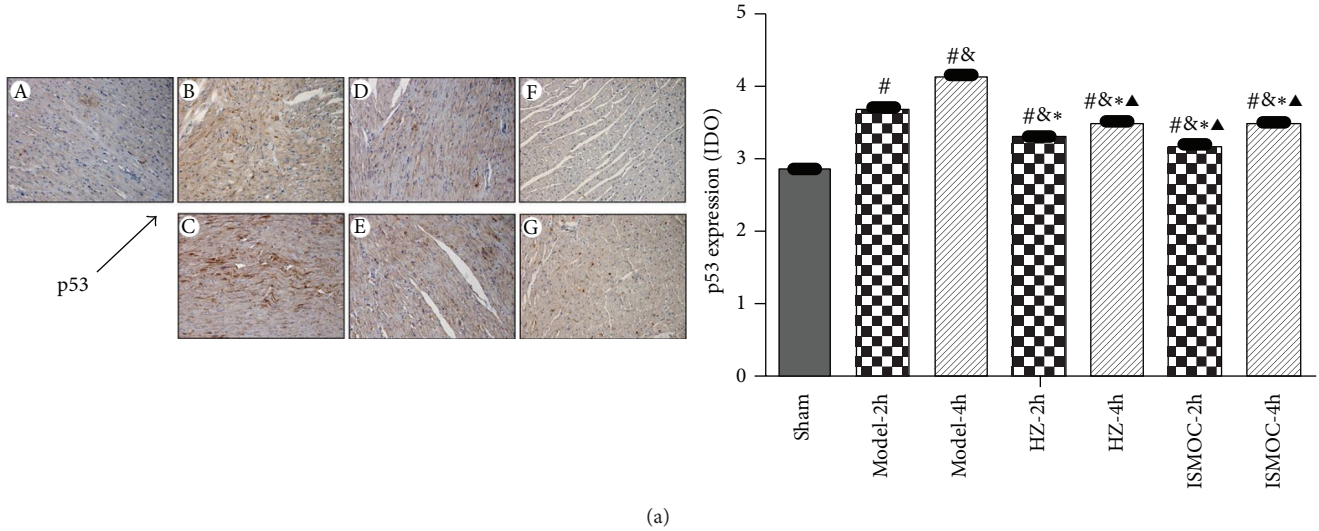

(a)

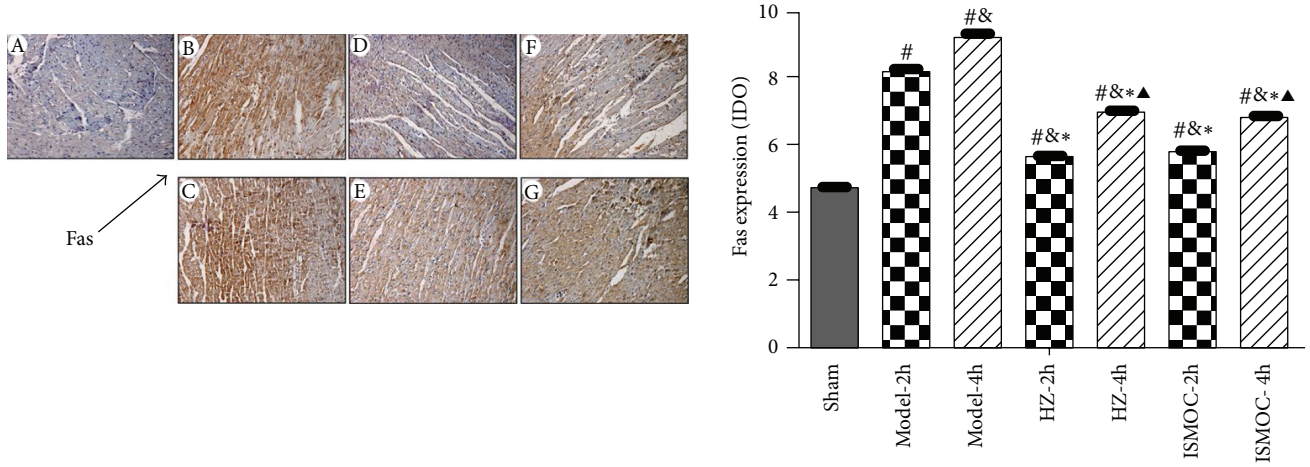

(b)

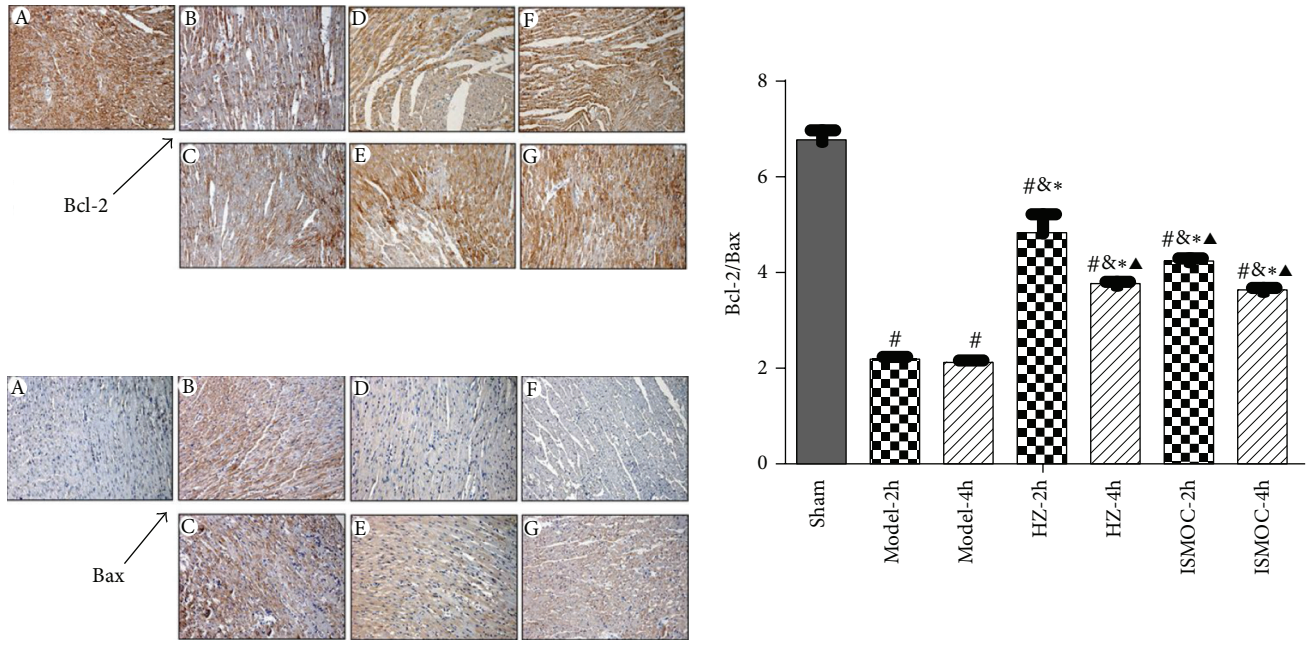

(c)

Figure 5: Continued.

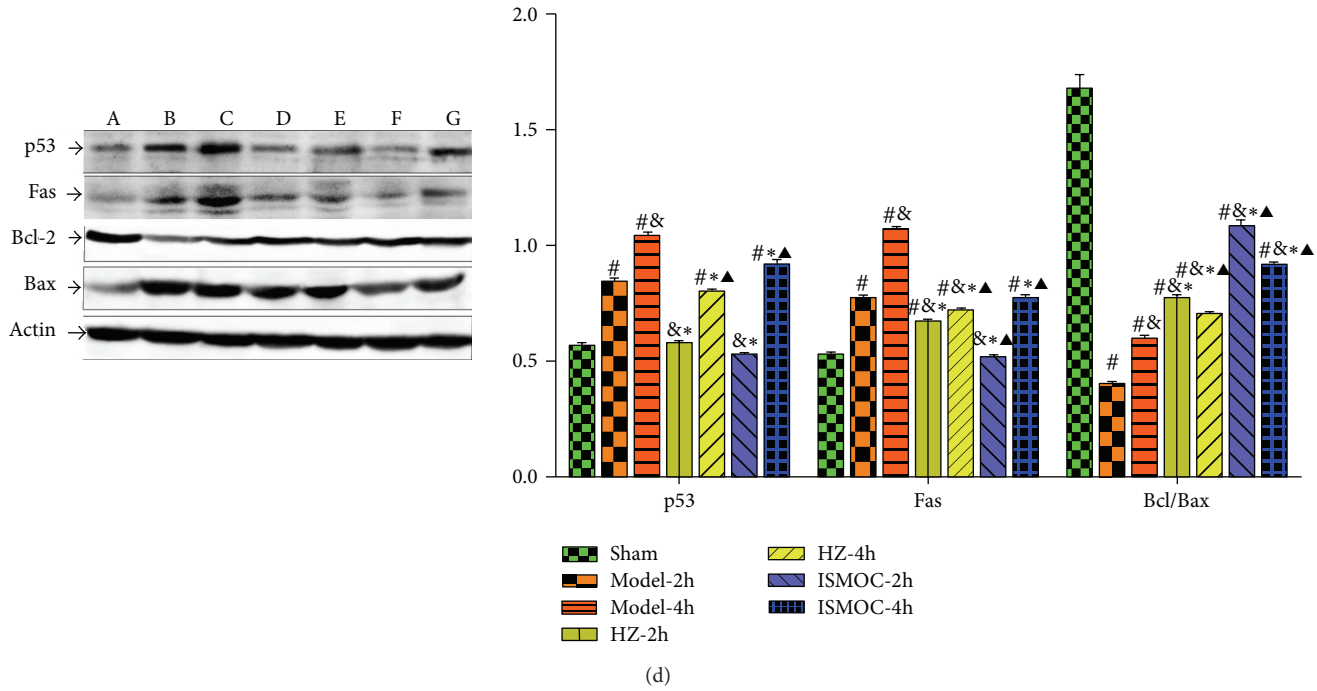

Figure 5: Effects of HZOL on apoptosis proteins expression. (a) Immunohistochemical assay of p53 expression. (b) Immunohistochemical assay of Fas expression. (c) Immunohistochemical assay of Bcl-2 and Bax expression. (d) Western blotting assay of p53, Fas, Bcl-2, and Bax expression. A: sham group; B: Model-2 h group; C: Model-4 h group; D: HZOL-2 h group; E: HZOL-4 h group; F: ISMOC-2 h group; G: ISMOC-4 h group; $^{\#}P < 0.05$ versus sham group; $^{\&}P < 0.05$ versus Model-2 h group; $^{*}P < 0.05$ versus Model-4 h group; $^{\blacktriangle}P < 0.05$ versus HZOL-2 h group.

of which converge to activate the executioner caspase-3 [24]. The results in Figure 4 show that caspase-3 expression significantly increased in the Model-2 h and Model-4 h groups than that in the sham group. The HZOL-2 h, HZOL-4 h, ISMOC-2 h, and ISMOC-4 h groups significantly decreased caspase-3 expression and the number of apoptotic cells ($P < 0.05$). The extrinsic pathway is initiated by binding of death receptors, such as fas or tumor necrosis factor (TNF), with their respective ligands (fas ligand and TNF-α). These proteins further bind initiator procaspase-8 (or procaspase-10) and form the death-inducing signaling complex (DISC), thereby enabling their autoactivation [25–27]. Depending on the efficiency of DISC formation, activated caspase-8 can either directly activate the downstream executioner caspase-3 [28] or initiate the cleavage of the proapoptotic BH3-interacting domain death agonist (Bid), which subsequently engages the mitochondrial apoptotic cascade [29, 30]. The intrinsic (mitochondrial) pathway is activated by stimuli that trigger the permeabilization of the outer mitochondrial membrane followed by the release of proapoptotic proteins from the mitochondrial intermembrane space, leading to executioner caspase activation [31, 32]. This pathway is regulated by members of the Bcl-2 family of proteins that contain one or more Bcl-2 homology (BH) domains [33–35]. By contrast, the proapoptotic proteins Bax and Bak contain BH domains 1 to 3 [36, 37]. A larger group of proapoptotic proteins, including Bcl-2-associated death promoter, Bcl-2-interacting mediator of cell death, and Bid, contains only the BH3 domain. The Bcl-2 and Bax protein levels are directly related to apoptosis regulation. The increase in Bax levels promotes cell apoptosis, whereas Bcl-2 increases the inhibition of cell apoptosis; the Bcl-2/Bax ratio determines the viability of cells after apoptotic stimulation [38, 39]. The activation of p53 triggers apoptosis by transcriptional activation of proapoptotic genes and transcription-independent mechanisms. p53 can mediate apoptosis by inducing the expression of Bax [40] and other proapoptotic proteins. p53 induced by transient ischemia possibly switches off Bcl-2 expression and switches on Bax expression within the discrete area [38]. In this context, apoptosis of myocardial I/R in myocardial cells may be commonly regulated by endogenous and exogenous apoptosis mechanisms, thereby initiating the apoptotic factor caspase-3, which results in apoptosis of myocardial cells. Results show that HZOL increased the Bcl-2/Bax ratio and decreased the activities of p53, fas, and caspase-3. HZOL reduced the apoptosis rate induced by ischemia through decreased caspase-3 expression. This result occurred in association with heart failure and apoptosis of experimental animals [41]. In TEM, a large area of cytoplasmic vacuolization and mitochondrial swelling was evident with decreasing matrix density and cristae distortion in the I/R 2 h and I/R 4 h groups. Results of HZOL treatment showed normal mitochondria with mild swelling, normal matrix density, and slightly damaged cristae. HZOL ameliorated myocardial I/R through multiple apoptosis-related signal pathways that decreased p53, fas, and caspase-3 and increased the Bcl-2/Bax ratio. The regulation of these factors on apoptosis will

be instrumental in defining novel therapeutic approaches to ischemic injury.

Conflict of Interests

The authors declare that there is no conflict of interests regarding the publication of this paper.

Authors' Contribution

Xu Ran and Jian Xin Diao equally contributed to this work.

References

[1] M. Vila-Petroff, M. A. Salas, M. Said et al., "CaMKII inhibition protects against necrosis and apoptosis in irreversible ischemia-reperfusion injury," *Cardiovascular Research*, vol. 73, no. 4, pp. 689–698, 2007.

[2] R. Q. Xie, W. Cui, Y. M. Hao et al., "Effects of remote preconditioning induced by skeletal muscle ischemia on myocardial cells apoptosis and roles of opioid receptors in pigs," *Chinese Journal of Applied Physiology*, vol. 22, no. 4, pp. 474–478, 2006.

[3] Y. C. Zhou, B. Liu, Y. J. Li et al., "Effects of buyang huanwu decoction on ventricular remodeling and differential protein profile in a rat model of myocardial infarction," *Evidence-based Complementary and Alternative Medicine*, vol. 2012, Article ID 385247, 11 pages, 2012.

[4] C. Y. Zeng, Y. Li, Y. Wan, Y. Zhang, and S. Liang, "Preparation and clinical efficacy of Huangzhi Oral liquid," *Chinese Journal of Hospital Pharmacy*, no. 05, pp. P669–P670, 2007.

[5] X. S. Li, C. Miao, K. Lin, L. Gan, G. Huang, and Y. Zheng, "Clinical Studies of hypertension and left ventricular hypertrophy on the blood rheology," *Jouranl of New Chinese Medicine*, no. 07, pp. 23–24, 2004.

[6] Y. Q. Gao, D. Su, H. Lin, and Q. Mei, "Effect of Huangzhi Oral liquid. on platelet aggregation," *Chinese Journal of Pharmacy*, no. 15, pp. p1129–p1130, 2008.

[7] Y. Jia, L. Yu, and Y. Chen, "Effect of dingxin recipe on arrhythmia and injury induced by ischemia and reperfusion in rabbits," *Zhongguo Zhong Xi Yi Jie He Za Zhi*, vol. 19, no. 11, pp. 678–681, 1999.

[8] N. Himori and A. Matsuura, "A simple technique for occlusion and reperfusion of coronary artery in conscious rats," *The American Journal of Physiology—Heart and Circulatory Physiology*, vol. 256, no. 6, pp. H1719–H1725, 1989.

[9] M. J. A. Walker, M. J. Curtis, D. J. Hearse et al., "The Lambeth conventions: guidelines for the study of arrhythmias in ischaemia, infarction, and reperfusion," *Cardiovascular Research*, vol. 22, no. 7, pp. 447–455, 1988.

[10] H. B. Cai, X. G. Sun, Z. F. Liu et al., "Effects of dahuangzhechong pills on cytokines and mitogen activated protein kinase activation in rats with hepatic fibrosis," *Journal of Ethnopharmacology*, vol. 132, no. 1, pp. 157–164, 2010.

[11] J. Chen, H. Zhao, Y. Yang, B. Liu, J. Ni, and W. Wang, "Lipid-lowering and antioxidant activities of Jiang-Zhi-Ning in traditional chinese medicine," *Journal of Ethnopharmacology*, vol. 134, no. 3, pp. 919–930, 2011.

[12] E. M. El-Sayed, O. M. Abo-Salem, H. A. Aly, and A. M. Mansour, "Potential antidiabetic and hypolipidemic effects of propolis extract in streptozotocin-induced diabetic rats," *Pakistan Journal of Pharmaceutical Sciences*, vol. 22, no. 2, pp. 168–174, 2009.

[13] P. Jyothi, N. Riyaz, G. Nandakumar, and M. Binitha, "A study of oxidative stress in paucibacillary and multibacillary leprosy," *Indian Journal of Dermatology, Venereology and Leprology*, vol. 74, no. 1, p. 80, 2008.

[14] A. Godekmerdan, S. Arusan, B. Bayar, and N. Sağlam, "Medicinal leeches and hirudotherapy," *Türkiye Parazitolojii Dergisi*, vol. 35, no. 4, pp. 234–239, 2011.

[15] J. Hildebrandt and S. Lemke, "Small bite, large impact-saliva and salivary molecules in the medicinal leech, *Hirudo medicinalis*," *Naturwissenschaften*, vol. 98, no. 12, pp. 995–1008, 2011.

[16] I. P. Baskova and L. L. Zavalova, "Polyfunctionality of destabilase, a lysozyme from a medicinal leech," *Bioorganicheskaia khimiia*, vol. 34, no. 3, pp. 337–343, 2008.

[17] J. Lv, S. Fu, J. Guo, Y. Liu, H. Yuan, and X. Xiao, "Primary research on daily administration times of rhubarb used to treat experimental jaundice in rats," *Zhongguo Zhongyao Zazhi*, vol. 36, no. 24, pp. 3506–3510, 2011.

[18] R. Hu, Y. Lu, X. Dai, and Y. Pan, "Screening of antioxidant phenolic compounds in Chinese Rhubarb combining fast countercurrent chromatography fractionation and liquid chromatography/mass spectrometry analysis," *Journal of Separation Science*, vol. 33, no. 11, pp. 1595–1603, 2010.

[19] E. Sohn, S. Jang, H. Joo et al., "Anti-allergic and anti-inflammatory effects of butanol extract from Arctium Lappa L," *Clinical and Molecular Allergy*, vol. 9, no. 1, article 4, 2011.

[20] S. Iwakami, J.-B. Wu, Y. Ebizuka, and U. Sankawa, "Platelet activating factor (PAF) antagonists contained in medicinal plants: lignans and sesquiterpenes," *Chemical and Pharmaceutical Bulletin*, vol. 40, no. 5, pp. 1196–1198, 1992.

[21] L. H. Xie, E. Ahn, T. Akao, A. A. Abdel-Hafez, N. Nakamura, and M. Hattori, "Transformation of arctiin to estrogenic and antiestrogenic substances by human intestinal bacteria," *Chemical & Pharmaceutical Bulletin*, vol. 51, no. 4, pp. 378–384, 2003.

[22] B. G. Sun, Z. Chen, S. Zhang, Y. Liu, H. Huang, and L. Yin, "Study of antitumous effect of the complex prescription of Chinese crude drug in athymic mice with HCC," *Zhong Yao Cai*, vol. 30, no. 11, pp. 1417–1421, 2007.

[23] X. Han, W. Wang, R. Tan, and D. Dou, "Determination of plasma protein binding rate of arctiin and arctigenin with ultrafiltration," *Zhongguo Zhongyao Zazhi*, vol. 38, no. 3, pp. 432–434, 2013.

[24] A. Almeida, "Genetic determinants of neuronal vulnerability to apoptosis," *Cellular and Molecular Life Sciences*, vol. 70, no. 1, pp. 71–88, 2013.

[25] M. Okouchi, O. Ekshyyan, M. Maracine, and Y. A. Tak, "Neuronal apoptosis in neurodegeneration," *Antioxidants & Redox Signaling*, vol. 9, no. 8, pp. 1059–1096, 2007.

[26] G. Chen and D. V. Goeddel, "TNF-R1 signaling: a beautiful pathway," *Science*, vol. 296, no. 5573, pp. 1634–1635, 2002.

[27] H. Wajant, "The Fas signaling pathway: more than a paradigm," *Science*, vol. 296, no. 5573, pp. 1635–1636, 2002.

[28] M. E. Peter and P. H. Krammer, "The CD95(APO-1/Fas) DISC and beyond," *Cell Death and Differentiation*, vol. 10, no. 1, pp. 26–35, 2003.

[29] R. Singh, S. Pervin, and G. Chaudhuri, "Caspase-8-mediated BID cleavage and release of mitochondrial cytochrome c during Nω-hydroxy-L-arginine-induced apoptosis in MDA-MB-468 cells: antagonistic effects of L-ornithine," *Journal of Biological Chemistry*, vol. 277, no. 40, pp. 37630–37636, 2002.

[30] L. P. Billen, A. Shamas-Din, and D. W. Andrews, "Bid: a Bax-like BH3 protein," *Oncogene*, vol. 27, supplement 1, pp. S93–S104, 2008.

[31] J. P. Bolaños, M. A. Moro, I. Lizasoain, and A. Almeida, "Mitochondria and reactive oxygen and nitrogen species in neurological disorders and stroke: therapeutic implications," *Advanced Drug Delivery Reviews*, vol. 61, no. 14, pp. 1299–1315, 2009.

[32] S. W. G. Tait and D. R. Green, "Mitochondria and cell death: outer membrane permeabilization and beyond," *Nature Reviews Molecular Cell Biology*, vol. 11, no. 9, pp. 621–632, 2010.

[33] J. Yuan and B. A. Yankner, "Apoptosis in the nervous system," *Nature*, vol. 407, no. 6805, pp. 802–809, 2000.

[34] T. Chittenden, C. Flemington, A. B. Houghton et al., "A conserved domain in Bak, distinct from BH1 and BH2, mediates cell death and protein binding functions," *The EMBO Journal*, vol. 14, no. 22, pp. 5589–5596, 1995.

[35] J. Martinou and R. J. Youle, "Mitochondria in apoptosis: Bcl-2 family members and mitochondrial dynamics," *Developmental Cell*, vol. 21, no. 1, pp. 92–101, 2011.

[36] T. Kuwana, M. R. Mackey, G. Perkins et al., "Bid, Bax, and lipids cooperate to form supramolecular openings in the outer mitochondrial membrane," *Cell*, vol. 111, no. 3, pp. 331–342, 2002.

[37] S. N. Willis, J. I. Fletcher, T. Kaufmann et al., "Apoptosis initiated when BH3 ligands engage multiple Bcl-2 homologs, not Bax or Bak," *Science*, vol. 315, no. 5813, pp. 856–859, 2007.

[38] Z. Xie, T. Koyama, J. Suzuki et al., "Coronary reperfusion following ischemia: different expression of Bcl-2 and bax proteins, and cardiomyocyte apoptosis," *Japanese Heart Journal*, vol. 42, no. 6, pp. 759–770, 2001.

[39] D. S. McClintock, M. T. Santore, V. Y. Lee et al., "Bcl-2 family members and functional electron transport chain regulate oxygen deprivation-induced cell death," *Molecular & Cellular Biology*, vol. 22, no. 1, pp. 94–104, 2002.

[40] C. C. Harris, "1995 Deichmann lecture—p53 tumor suppressor gene: at the crossroads of molecular carcinogenesis, molecular epidemiology and cancer risk assessment," *Toxicology Letters*, vol. 82-83, pp. 1–7, 1995.

[41] N. Guttenplan, C. Lee, and W. H. Frishman, "Inhibition of myocardial apoptosis as a therapeutic target in cardiovascular disease prevention: focus on caspase inhibition," *Heart Disease*, vol. 3, no. 5, pp. 313–318, 2001.

Hindawi Publishing Corporation
Evidence-Based Complementary and Alternative Medicine
Volume 2015, Article ID 171306, 6 pages
http://dx.doi.org/10.1155/2015/171306

Research Article

Ginsenoside-Rb1 Protects Hypoxic- and Ischemic-Damaged Cardiomyocytes by Regulating Expression of miRNAs

Xu Yan,[1,2,3] Jinrong Xue,[4] Hongjin Wu,[1] Shengqi Wang,[5] Yuna Liu,[3] Sidao Zheng,[3] Chengying Zhang,[3] and Cui Yang[3]

[1] *Beijing Haidian Hospital, Haidian Section of Peking University Third Hospital, 29 Zhongguancun Dajie, Haidian District, Beijing 100080, China*
[2] *Postdoctoral Workstation of the Zhongguancun Haidian Science Park, No. 6 Sijiqing Road, Haidian District, Beijing 100195, China*
[3] *Beijing Hospital of Integrated Traditional Chinese and Western Medicine, Dongjie 3, Yongding Road, Haidian District, Beijing 100039, China*
[4] *Department of Cardiovascular Surgery, Beijing Aortic Disease Center, Beijing Anzhen Hospital, Capital Medical University, No. 2 Anzhen Road, Chaoyang District, Beijing 100029, China*
[5] *Beijing Institute of Radiation Medicine, Beijing 100850, China*

Correspondence should be addressed to Hongjin Wu; whjyuanzhang@aliyun.com

Received 9 July 2014; Revised 25 September 2014; Accepted 2 October 2014

Academic Editor: Hao Xu

Ginsenoside (GS-Rb1) is one of the most important active compounds of ginseng, with extensive evidence of its cardioprotective properties. However, the miRNA mediated mechanism of GS-Rb1 on cardiomyocytes remains unclear. Here, the roles of miRNAs in cardioprotective activity of GS-Rb1 were investigated in hypoxic- and ischemic-damaged cardiomyocytes. Neonatal rat cardiomyocytes (NRCMs) were first isolated, cultured, and then incubated with or without GS-Rb1 (2.5–40 μM) *in vitro* under conditions of hypoxia and ischemia. Cell growth, proliferation, and apoptosis were detected by MTT and flow cytometry. Expressions of various microRNAs were analyzed by real-time PCR. Compared with that of the control group, GS-Rb1 significantly decreased cell death in a dose-dependent manner and expressions of mir-1, mir-29a, and mir-208 obviously increased in the experimental model groups. In contrast, expressions of mir-21 and mir-320 were significantly downregulated and GS-Rb1 could reverse the differences in a certain extent. The miRNAs might be involved in the protective effect of GS-Rb1 on the hypoxia/ischemia injuries in cardiomyocytes. The effect might be based on the upregulation of mir-1, mir-29a, and mir-208 and downregulation of mir-21 and mir-320. This might provide us a new target to explore the novel strategy for ischemic cardioprotection.

1. Introduction

MicroRNAs (miRNAs) are a kind of conservative single stranded noncoding RNA molecules found in animals, plants, virus, and other organisms and regulate proliferation, differentiation, apoptosis and metabolism, and other cellular processes [1, 2]. In recent years, investigations found that miRNAs play an important role in the development of cardiovascular diseases and may become a possible new target in the treatment of cardiovascular diseases [3].

Myocardial ischemic injury resulting from severe impairment of the coronary blood supply is a severe stress that leads to the loss of cardiomyocytes by apoptosis and necrosis. MicroRNAs have been proved to be potential biomarkers for ischemic heart disease, such as mir-1, mir-133, mir-208, and mir-499 [4–6]. Several studies also demonstrated that miRNAs dysregulation has a key role in the ischemic heart disease process. Various miRNAs can regulate gene expression at the posttranscriptional level by either translational repression of a target mRNA or degradation of myocardial death induced mir expression in the genome of most eukaryotes. Many studies have revealed that microRNAs could be the therapeutic targets for common used drugs or new drug design, which could be potentially used as complementary and alternative interventions for the treatment of ischemic heart disease.

Ginseng, the root of *Panax ginseng* C.A. Meyer, has been widely used in traditional Chinese medicine for several thousand years [7]. Ginseng plays critical roles in the endocrine, immune, central nervous, and especially the cardiovascular systems [8]. Ginsenoside-Rb1 (GS-Rb1), a major pharmacological extract, is one of the most important active compounds of ginseng, with extensive evidence of its cardioprotective properties. Numerous studies have indicated that the cardioprotective effect of GS-Rb1 was affected by multiple pathways [9]. However, regulatory roles of GS-Rb1 in miRNA during cardiomyocytes apoptosis are rarely studied. In the present investigation, rat myocardial cells were first isolated, cultured, and incubated with GS-Rb1 *in vitro* under conditions of hypoxia and ischemia. The protective roles of GS-Rb1 were explored, and five circulation-related microRNAs' expression change in each group was then analyzed by poly(A) tailing SYBR Green real-time PCR.

2. Materials and Methods

2.1. Materials. GS-Rb1 (catalog number 110704) purchased from National Institutes for Food and Drug Control was dissolved in phosphate-buffered saline (PBS) to create a stock solution for subsequent dilution. miRNA extracting kit (CW0627), reverse transcription kit (CW2141), and fluorescent quantitation PCR (CW2142) kit were all purchased from BeiJing Cowin Biotech Co., Ltd. Annexin V-FITC/PI kit was purchased from Kaiji Biological Engineering Institute.

2.2. Isolation and Culture of Neonatal Rat Cardiomyocytes. All experiments were approved by the Beijing Ethics Committee for the Use of Experimental Animals. Primary cultures of NRCMs from 12–24-hour-old Sprague Dawley rats (Vital River Laboratories, Beijing, China) were prepared by means of gentle serial trypsinization as described before with slight modification [10]. Briefly, the ventricular myocardium was removed and cut into small pieces (1-2 mm^3). The ventricles obtained were washed three times in cold PBS and digested 5 times for 5 min each at 37°C with 0.18% (w/v) trypsin and 0.01% EDTA. Addition of an equal volume of cold Dulbecco's modified Eagle's medium (DMEM) containing 10% (v/v) newborn calf serum was used to terminate the digestion. Then, cells were collected by centrifugation for 10 min at 1000 g/min at room temperature. Cells were then resuspended in DMEM with 20% (v/v) FCS for 60 min to facilitate separation of ventricular myocytes from the faster-attaching nonmyocytes. The NRCMs were then collected and plated in collagen-coated 96- or 6-well plates and maintained at 37°C in a 5% CO_2/95% air humidified incubator in DMEM containing 10% (v/v) fetal bovine serum, 100 U/mL penicillin, and 100 mg/mL streptomycin. The following experiments used spontaneously beating cardiomyocytes 48–72 h after plating.

2.3. Hypoxia/Ischemia Treatment. To generate hypoxic/ischemic conditions, culture medium was replaced with DMEM (no glucose) (Gibco, Grand Island, USA) with serum free. NRCMs with or without GS-Rb1 were then placed in a W-Zip package (an0010, Oxide Anaerobe Pouch System), which was capable of depleting the concentration of O_2 down to 10% in 2 h. The sealed package was subsequently placed into a 37°C incubator for 12 h after pretreatment with GS-Rb1 for 6 h. The control plates were kept in normoxic conditions for the corresponding times.

2.4. MTT Assay. NRCMs viability was determined using the MTT assay. Cardiomyocytes were plated on 96-well dishes at 2 × 104 cells/well. MTT at 5 mg/mL was added to each well immediately after 12 h of hypoxia/ischemia. Plates were incubated for 4 h at 37°C. The medium was aspirated from each well and 100 μL of DMSO was added to dissolve the formazan crystals. The optical density of each well was read at 492 nm using a Microplate Reader (Bio-Rad, Hercules, CA). Results are given as percentages of the control group taken as 100%.

2.5. Apoptosis Assay by Annexin V/PI Staining. NRCMs with different concentration of GS-Rb1 exposed to hypoxia/ischemia conditions were harvested and washed with PBS. The percentage of normal nonapoptotic cells was measured by double supravital staining with Annexin V and PI, using an Annexin V Apoptosis Detection kit (KeyGen, Nanjing, China). Flow cytometric analysis used a Cytomics FC500 flow cytometer with CXP software (Beckman Coulter, Fullerton, USA), the operator being blind to the group assignment.

2.6. Detection of miRNA Expression Using Poly(A) Tailing SYBR Green Real-Time PCR. Total RNA (5 μg) was treated with DNase I for 15 minutes at 22°C (Invitrogen) and then poly(A)-tailed using poly(A) polymerase (NEB) at 37°C for 1 hour. The final reaction mixture was extracted with phenol/chloroform, precipitated with isopropanol, and redissolved in 25 μL of diethylpyrocarbonate-treated water. Poly(A)-tailed RNA (6 μL) was reverse-transcribed into first-strand cDNA using a miRNA cDNA kit (cw2141, BeiJing Cowin Biotech Co., Ltd.). For PCR, 30 ng of cDNA was used as a template in each reaction using miRNA Real-Time PCR Assay Kit (cw2142, BeiJing Cowin Biotech Co., Ltd.). The forward primer for each miRNA was

mir-1: 5′-GCGTGGAATGTAAAGAAGTGTGTAT AAA-3′;

mir-29a: 5′-TAGCACCATCTGAAATCGGTT AAAA-3′;

mir-208: 5′-ATAAGACGAGCAAAAAGCAAAAA AAA-3′;

mir-21: 5′-GCTAGCTTATCAGACTGATGTTG AAAA-3′;

mir-320: 5′-AAGCTGGGTTGAGAGGGCGA-3′; U6 small noncoding RNA sequence was amplified as an internal control using the primers 5′-CTCGCTTCGGCAGCACA-3′ (forward) and 5′-AACGCTTCACGAATTTGCGT-3′ (reverse).

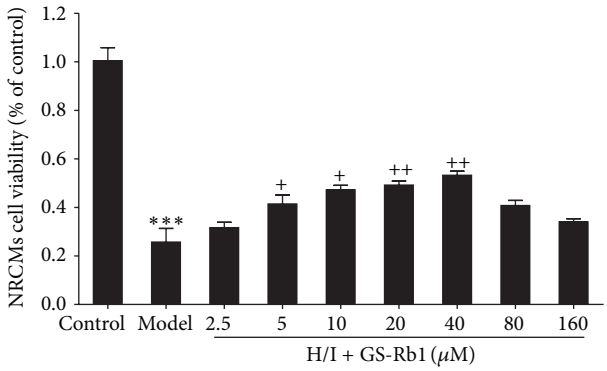

Figure 1: Protective effect of GS-Rb1 on H/I-induced NRCMs death. NRCMs were copretreated with or without GS-Rb1 during H/I condition for 12 h. Cell viability was determined by MTT assay. Error bars represent mean ± SD. Error bars represent mean ± SD. $^{***}P < 0.001$ versus control, $^{+}P < 0.05$, and $^{++}P < 0.01$ versus H/I group ($n = 3$).

The anneal temperature was 63°C. The SYBR Green-based real-time PCR was performed using ABI 7500 Real-Time PCR System (Applied Biosystems). The relative expression of miRNA was calculated based on the formula: $2^{-(\Delta CtmiR - \Delta CtU6)}$.

2.7. Statistical Analysis. The data obtained were presented as the mean ± SEM of 3 independent experiments. The relationship between two factors was analyzed by Pearson correlation analysis. Bootstrap was used in paired samples tests. Group results were analysed for variance using ANOVA. Two groups were compared by Student's t-test. All analyses used GraphPad Prism 5.0 software. A $P < 0.05$ indicated that the difference was statistically significant. A $P < 0.01$ indicated that the difference was extremely and statistically significant.

3. Results

3.1. Effects of GS-Rb1 on Hypoxic- and Ischemic-Induced Damaged Cardiomyocytes. Ginsenoside plays important roles in physiological and pathological conditions of various cells. In this research, neonatal rat cardiomyocytes were treated under hypoxia and ischemic conditions in the presence or absence of GS-Rb1. As shown in Figure 1, addition of GS-Rb1 significantly decreased cell death in a dependent manner at an optimal concentration of 40 μM, indicating that GS-Rb1 has a protective role in hypoxic- and ischemic-induced damaged myocardial cells.

3.2. Effects of GS-Rb1 on Cell Apoptosis of Cardiomyocytes. To examine the effect of GS-Rb1 on the cell death induced by H/I, Annexin V-FITC /propidium iodide (PI) double-staining assay of cells was analyzed by flow cytometry (Figure 2). The percentage of apoptotic cells (including early and late apoptotic cells) markedly increased in H/I group compared to the control group. With GS-Rb1, apoptosis accounted for 31.0 ± 1.8% at 40 μM GS-Rb1, with the surviving cells increasing 52.8 ± 3.1%. These data indicate that GS-Rb1 can inhibit hypoxic- and ischemic-induced cell apoptosis of neonatal rat cardiomyocytes.

3.3. Expression of MicroRNAs in Hypoxic- and Ischemic-Treated Cardiomyocytes. The level of microRNAs was detected by real-time RT-PCR assay. The expression level of mir-1, mir-29a, and mir-208 was increased in the H/I group (5.9-, 3.4-, and 9.3-fold versus control, relatively), while that of mir-21 and mir-320 was significantly decreased (0.35- and 0.41-fold versus control, relatively). With the treatment of GS-Rb1, the expression change of miRNAs in H/I group could be reversed in a certain extent (Figure 3).

4. Discussion

GS-Rb1 is one of the most important active compounds of ginseng, and it has multiple pharmacological actions [11–14] and the protective effects of different organs [15–20]. Furthermore, GS-Rb1 has been proved to have cardiovascular protective effect by considerable research.

MicroRNAs (miRNAs) are a kind of conservative single stranded noncoding RNA molecules found in animals, plants, virus, and other organisms and are important regulators of gene expression and fundamentally impact on cardiovascular functions. In recent years, investigations found that miRNAs play an important role in the development of cardiovascular diseases and may become a possible new target in the treatment of cardiovascular diseases. Some researchers have revealed that the miRNAs could be the targets of traditional Chinese medicine to protect cardiovascular system. Tanshinone IIA, a lipid-soluble pharmacologically active compound extracted from the rhizome of traditional Chinese herb *Salvia miltiorrhiza*, has been reported to improve hypoxic cardiac myocytes and postinfarction rat cardiomyocytes by regulating mir-133 and mir-1 and MAPK pathways [21, 22]. In the present research, we have found that GS-Rb1 could protect primary cardiomyocytes from hypoxia and ischemia injuries by reducing cell apoptosis and modulating circulation of miRNAs. Compared with that of the control group, expressions of mir-1, mir-29a, and mir-208 obviously increased in the experimental model groups. In contrast, expressions of mir-21 and mir-320 were significantly downregulated and GS-Rb1 incubation in model group could reverse the differences in a certain extent.

Specifically, mir-1 is skeletal and cardiac muscle specific microRNA necessary for postmitotic muscle proliferation and differentiation [23]. Many researchers have proved that mir-1 plays an important part during cardiac apoptosis [24, 25]. Overexpression of mir-1 could exacerbate cardiac injury; on the contrary, knockdown of mir-1 significantly attenuated cardiac ischemia/reperfusion injury [26]. Mir-29 has shown relationship with cancer cell apoptosis by activating p53 [27]. Downregulation of mir-29 (mir-29a and mir-29c) by antisense inhibitor also protected H9c2 cardiomyocytes from simulated IR injury. Antagomirs against mir-29a or mir-29c significantly reduced myocardial infarct size and apoptosis in

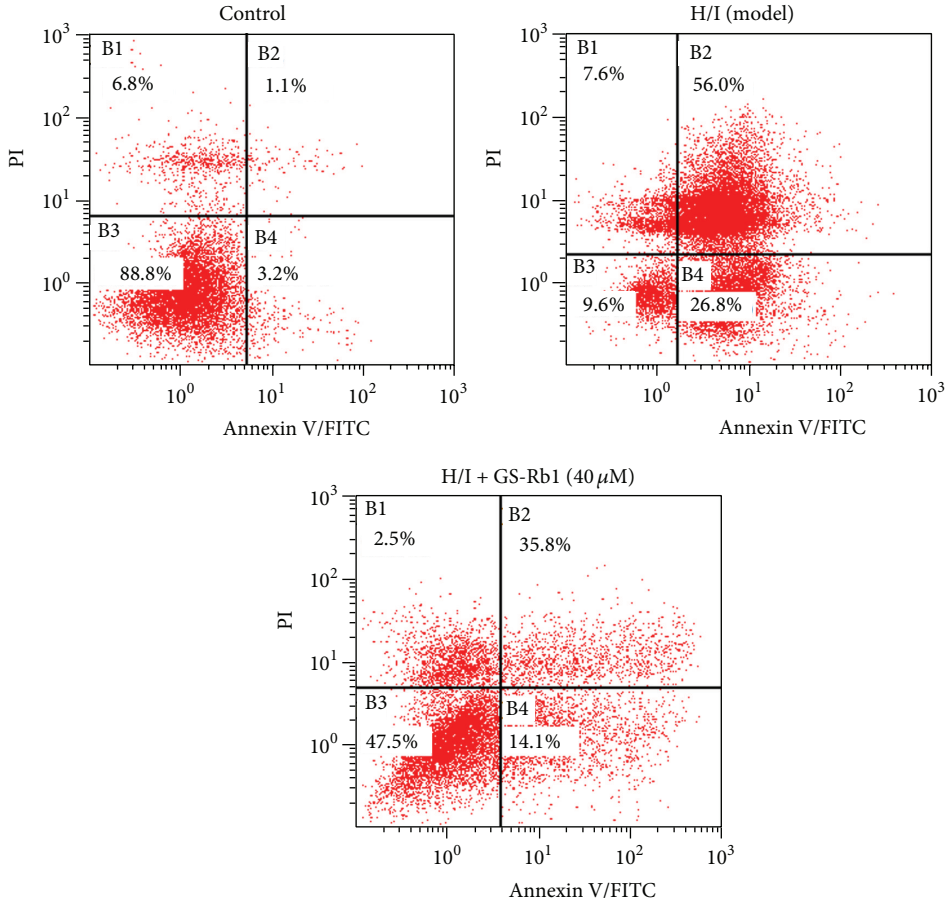

(a)

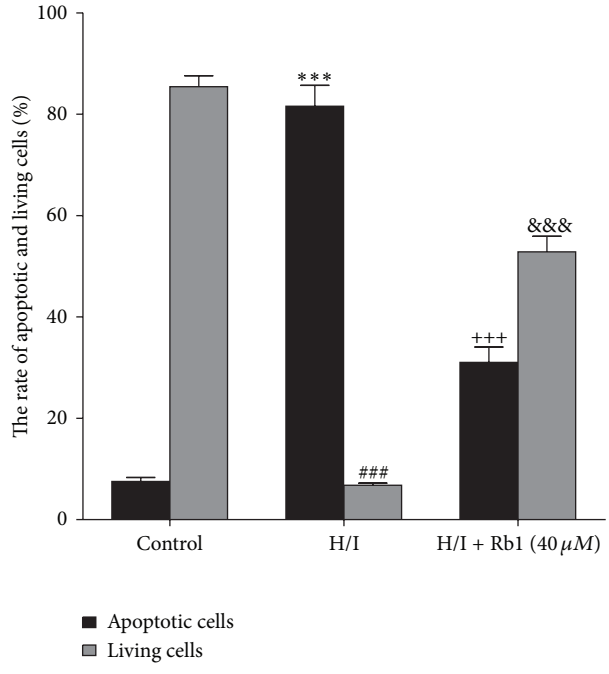

(b)

Figure 2: Flow cytometry analysis of GS-Rb1 on cell death induced by H/I. (a) NRCMs were cotreated with or without GS-Rb1 (40 μM) during H/I for 12 h and stained with Annexin V-FITC/PI. (b) Quantification of the percent of apoptotic and living cells in each group. Error bars represent mean ± SD. $^{***}P < 0.001$ versus apoptotic cells in control group; $^{\#\#\#}P < 0.001$ versus living cells in control group; $^{+++}P < 0.001$ versus apoptotic cells in H/I group; $^{\&\&\&}P < 0.001$ versus living cells in H/I group ($n = 3$).

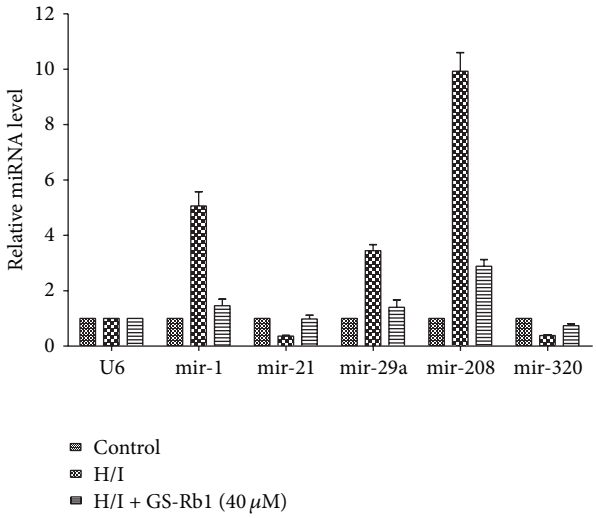

Figure 3: Real-time PCR analysis of GS-Rb1 on miRNAs expression change induced by H/I. NRCMs were cotreated with or without GS-Rb1 (40 μM) during H/I for 12 h. Detection of miRNA expression was performed using poly(A) tailing SYBR Green real-time PCR. The relative expression of miRNA was calculated based on the formula: $2^{-(\Delta CtmiR-\Delta CtU6)}$. Error bars represent mean ± SD.

hearts subjected to IR injury [28]. Our results demonstrated that GS-Rb1 suppressed the expression of mir-1 and mir-29a in the model group, which might be the microRNA targets of GS-Rb1 to protect cardiomyocytes from H/I injuries.

Mir-21 is another cardiac enriched microRNA, which has been proved to be involved in ischemic heart disease, myocardial remodeling, and vascular proliferative diseases [29]. Overexpression of mir-21 plays an important role during cardiomyocytes apoptosis and ischemia/reperfusion- (I/R-) induced heart damages [30, 31]. Mir-320 has the familiar function with mir-21. Mir-320 expression was significantly decreased in the hearts on ischemia/reperfusion *in vivo* and *in vitro*. Overexpression of mir-320 enhanced cardiomyocyte apoptosis and increased extent of apoptosis and infarction size in the hearts. Conversely, *in vivo* treatment with antagomir-320 reduced infarction size and showed cytoprotective [32]. Our results showed that mir-21 and mir-320 significantly decreased in the H/I injured cardiomyocytes and increased by GS-Rb1 treatment following H/I, which suggested that mir-21 and mir-320 might be the potential microRNA targets of GS-Rb1 to protect cardiomyocytes.

Mir-208 is produced exclusively in the heart. A growing number of studies have demonstrated that mir-208 could be selected as a possible biomarker of myocardial injury and myocardial infarction [33, 34]. Plasma mir-208 increased significantly after isoproterenol-induced myocardial injury and showed a similar time course to the concentration of cTnI [35]. Therapeutic inhibition of mir-208a by systemic delivery of antisense oligonucleotide could improve cardiac function and survival during hypertension-induced heart failure [36]. But there was no enough evidence shown that overexpression or knockdown mir-208 was related to the hypoxia/ischemia injuries and cardiomyocytes apoptosis. Our results showed that GS-Rb1 could suppress the expression of mir-208 in model group. The relationship of mir-208 and cardiomyocytes injury or cell apoptosis needs to be further studied.

In conclusion, GS-Rb1 protects hypoxic- and ischemic-induced damaged myocardial cells by regulating expression of miRNAs, which not only is important in uncovering mechanism of GS-Rb1 in hypoxic- and ischemic-induced damage of myocardial cells, but also may provide a new method for treating myocardial diseases in clinical applications.

Conflict of Interests

The authors declare that they have no conflict of interests.

Authors' Contribution

Xu Yan and Jinrong Xue contributed equally to this work.

Acknowledgments

This work was supported by Grants from the National Natural Science Foundation of China (nos. 81273890 and 81173367) and Postdoctoral Science Foundation of Beijing (2013ZZ-57).

References

[1] A. Kozomara and S. Griffiths-Jones, "MiRBase: integrating microRNA annotation and deep-sequencing data," *Nucleic Acids Research*, vol. 39, supplement 1, pp. D152–D157, 2011.

[2] B. K. Dey, K. Pfeifer, and A. Dutta, "The H19 long noncoding RNA gives rise to microRNAs miR-675-3p and miR-675-5p to promote skeletal muscle differentiation and regeneration," *Genes & Development*, vol. 28, no. 5, pp. 491–501, 2014.

[3] T. Baars, A. Skyschally, L. Klein-Hitpass et al., "microRNA expression and its potential role in cardioprotection by ischemic postconditioning in pigs," *Pflügers Archiv*, vol. 466, no. 10, pp. 1953–1961, 2014.

[4] J. Ai, R. Zhang, Y. Li et al., "Circulating microRNA-1 as a potential novel biomarker for acute myocardial infarction," *Biochemical and Biophysical Research Communications*, vol. 391, no. 1, pp. 73–77, 2010.

[5] G.-K. Wang, J.-Q. Zhu, J.-T. Zhang et al., "Circulating microRNA: a novel potential biomarker for early diagnosis of acute myocardial infarction in humans," *European Heart Journal*, vol. 31, no. 6, pp. 659–666, 2010.

[6] G. W. Dorn, S. J. Matkovich, W. H. Eschenbacher, and Y. Zhang, "A human 3′ miR-499 mutation alters cardiac mRNA targeting and function," *Circulation Research*, vol. 110, no. 7, pp. 958–967, 2012.

[7] Z. Liu, J. Chen, W. Huang, Z. Zeng, Y. Yang, and B. Zhu, "Ginsenoside Rb1 protects rat retinal ganglion cells against hypoxia and oxidative stress," *Molecular Medicine Reports*, vol. 8, no. 5, pp. 1397–1403, 2013.

[8] L. Jia, Y. Zhao, and X.-J. Liang, "Current evaluation of the millennium phytomedicine—ginseng (II): collected chemical entities, modern pharmacology, and clinical applications emanated from traditional chinese medicine," *Current Medicinal Chemistry*, vol. 16, no. 22, pp. 2924–2942, 2009.

[9] S.-D. Zheng, H.-J. Wu, and D.-L. Wu, "Roles and mechanisms of ginseng in protecting heart," *Chinese Journal of Integrative Medicine*, vol. 18, no. 7, pp. 548–555, 2012.

[10] P. Simpson and S. Savion, "Differentiation of rat myocytes in single cell cultures with and without proliferating nonmyocardial cells. Cross-striations, ultrastructure, and chronotropic response to isoproterenol," *Circulation Research*, vol. 50, no. 1, pp. 101–116, 1982.

[11] S. Tan, F. Zhou, N. Li et al., "Anti-fatigue effect of ginsenoside Rb1 on postoperative fatigue syndrome induced by major small intestinal resection in rat," *Biological and Pharmaceutical Bulletin*, vol. 36, no. 10, pp. 1634–1639, 2013.

[12] L. Shen, Y. Xiong, D. Q.-H. Wang et al., "Ginsenoside Rb1 reduces fatty liver by activating AMP-activated protein kinase in obese rats," *The Journal of Lipid Research*, vol. 54, no. 5, pp. 1430–1438, 2013.

[13] N. Lin, D.-L. Cai, D. Jin, Y. Chen, and J.-J. Shi, "Ginseng panaxoside Rb1 reduces body weight in diet-induced obese mice," *Cell Biochemistry and Biophysics*, vol. 68, no. 1, pp. 189–194, 2014.

[14] T. H. Kang, H. M. Park, Y.-B. Kim et al., "Effects of red ginseng extract on UVB irradiation-induced skin aging in hairless mice," *Journal of Ethnopharmacology*, vol. 123, no. 3, pp. 446–451, 2009.

[15] D. Liu, H. Zhang, W. Gu, Y. Liu, and M. Zhang, "Neuroprotective effects of ginsenoside Rb1 on high glucose-induced neurotoxicity in primary cultured rat," *PLoS ONE*, vol. 8, no. 11, Article ID e79399, 2013.

[16] Z. Liu, J. Chen, W. Huang, Z. Zeng, Y. Yang, and B. Zhu, "Ginsenoside Rb1 protects rat retinal ganglion cells against hypoxia and oxidative stress," *Molecular Medicine Reports*, vol. 8, no. 5, pp. 1397–1403, 2013.

[17] W. Cheng, D. Wu, Q. Zuo, Z. Wang, and W. Fan, "Ginsenoside Rb1 prevents interleukin-1 beta induced inflammation and apoptosis in human articular chondrocytes," *International Orthopaedics*, vol. 37, no. 10, pp. 2065–2070, 2013.

[18] J. Wang, L. Qiao, S. Li, and G. Yang, "Protective effect of ginsenoside Rb1 against lung injury induced by intestinal ischemia-reperfusion in rats," *Molecules*, vol. 18, no. 1, pp. 1214–1226, 2013.

[19] J. Wang, L. Qiao, Y. Li, and G. Yang, "Ginsenoside Rb1 attenuates intestinal ischemia-reperfusion-induced liver injury by inhibiting NF-κB activation," *Experimental and Molecular Medicine*, vol. 40, no. 6, pp. 686–698, 2008.

[20] Q. Sun, Q.-T. Meng, Y. Jiang, and Z.-Y. Xia, "Ginsenoside Rb1 attenuates intestinal ischemia reperfusion induced renal injury by activating Nrf2/ARE pathway," *Molecules*, vol. 17, no. 6, pp. 7195–7205, 2012.

[21] Y. Zhang, L. Zhang, W. Chu et al., "Tanshinone IIA inhibits miR-1 expression through p38 MAPK signal pathway in post-infarction rat cardiomyocytes," *Cellular Physiology and Biochemistry*, vol. 26, no. 6, pp. 991–998, 2010.

[22] L. Zhang, Y. Wu, Y. Li et al., "Tanshinone IIA improves miR-133 expression through MAPK ERK1/2 pathway in hypoxic cardiac myocytes," *Cellular Physiology and Biochemistry*, vol. 30, no. 4, pp. 843–852, 2012.

[23] Y. Zhao, J. F. Ransom, A. Li et al., "Dysregulation of cardiogenesis, cardiac conduction, and cell cycle in mice lacking miRNA-1-2," *Cell*, vol. 129, no. 2, pp. 303–317, 2007.

[24] Z.-X. Shan, Q.-X. Lin, C.-Y. Deng et al., "MiR-1/miR-206 regulate Hsp60 expression contributing to glucose-mediated apoptosis in cardiomyocytes," *FEBS Letters*, vol. 584, no. 16, pp. 3592–3600, 2010.

[25] B. He, J. Xiao, A.-J. Ren et al., "Role of miR-1 and miR-133a in myocardial ischemic postconditioning," *Journal of Biomedical Science*, vol. 18, no. 1, article 22, 2011.

[26] Z. Pan, X. Sun, J. Ren et al., "miR-1 exacerbates cardiac ischemia-reperfusion injury in mouse models," *PLoS ONE*, vol. 7, no. 11, Article ID e50515, 2012.

[27] S.-Y. Park, J. H. Lee, M. Ha, J.-W. Nam, and V. N. Kim, "miR-29 miRNAs activate p53 by targeting p85α and CDC42," *Nature Structural & Molecular Biology*, vol. 16, no. 1, pp. 23–29, 2009.

[28] Y. Ye, Z. Hu, Y. Lin, C. Zhang, and J. R. Perez-Polo, "Downregulation of microRNA-29 by antisense inhibitors and a PPAR-γ agonist protects against myocardial ischaemia–reperfusion injury," *Cardiovascular Research*, vol. 87, no. 3, pp. 535–544, 2010.

[29] Y. Cheng and C. Zhang, "MicroRNA-21 in cardiovascular disease," *Journal of Cardiovascular Translational Research*, vol. 3, no. 3, pp. 251–255, 2010.

[30] C. Yin, X. Wang, and R. C. Kukreja, "Endogenous microRNAs induced by heat-shock reduce myocardial infarction following ischemia-reperfusion in mice," *FEBS Letters*, vol. 582, no. 30, pp. 4137–4142, 2008.

[31] C. Wei, L. Li, I. K. Kim, P. Sun, and S. Gupta, "NF-κB mediated miR-21 regulation in cardiomyocytes apoptosis under oxidative stress," *Free Radical Research*, vol. 48, no. 3, pp. 282–291, 2014.

[32] X.-P. Ren, J. Wu, X. Wang et al., "MicroRNA-320 is involved in the regulation of cardiac ischemia/reperfusion injury by targeting heat-shock protein 20," *Circulation*, vol. 119, no. 17, pp. 2357–2366, 2009.

[33] E. Boštjančič, N. Zidar, D. Štajer, and D. Glavač, "MicroRNAs miR-1, miR-133a, miR-133b and miR-208 are dysregulated in human myocardial infarction," *Cardiology*, vol. 115, no. 3, pp. 163–169, 2010.

[34] Y. Cheng, X. Wang, J. Yang et al., "A translational study of urine miRNAs in acute myocardial infarction," *Journal of Molecular and Cellular Cardiology*, vol. 53, no. 5, pp. 668–676, 2012.

[35] X. Ji, R. Takahashi, Y. Hiura, G. Hirokawa, Y. Fukushima, and N. Iwai, "Plasma miR-208 as a biomarker of myocardial injury," *Clinical Chemistry*, vol. 55, no. 11, pp. 1944–1949, 2009.

[36] Y. Cheng, X. Wang, J. Yang et al., "A translational study of urine miRNAs in acute myocardial infarction," *Journal of Molecular and Cellular Cardiology*, vol. 53, no. 5, pp. 668–676, 2012.

Hindawi Publishing Corporation
Evidence-Based Complementary and Alternative Medicine
Volume 2014, Article ID 497836, 8 pages
http://dx.doi.org/10.1155/2014/497836

Research Article

Effects of an Aqueous Extract of Dangguijagyagsan on Serum Lipid Levels and Blood Flow Improvement in Ovariectomized Rats

In Sil Park, Hye Won Lee, Jin Ah Ryuk, and Byoung Seob Ko

Korean Medicine Based Herbal Drug Development Group, Herbal Medicine Research Division, Korea Institute of Oriental Medicine, 1672, Yuseong-daero, Daejeon 305-811, Republic of Korea

Correspondence should be addressed to Byoung Seob Ko; bsko@kiom.re.kr

Received 26 July 2014; Revised 12 August 2014; Accepted 12 August 2014; Published 7 September 2014

Academic Editor: Myeong Soo Lee

Dangguijagyagsan (DJS), a traditional herbal prescription, has long been used to treat menopause-related symptoms. We identified the cardioprotective effects of an aqueous extract of DJS using an ovariectomized (OVX) and ferric chloride- (FeCl-) induced carotid thrombosis rat model. Female Sprague-Dawley (SD) rats were ovariectomized or Sham-operated (Sham-control). The ovariectomized rats were divided into three groups: OVX with saline (OVX-control), aspirin 30 mg/kg/day (OVX-ASA), and DJS 100 mg/kg/day (OVX-DJS). The treatments were administered for 5 weeks. Then, blood samples were collected to analyze the serum lipid levels and platelet aggregation. The topical application of 40% $FeCl_3$ induced intravascular thrombosis, which was used to test thrombotic occlusion and for histological examination. Body weight and the levels of total cholesterol (TC), triglyceride (TG), and LDL-cholesterol (LDL-C) increased in the OVX rats. These effects were reduced by ASA and DJS treatment. In addition, ASA and DJS treatment significantly inhibited platelet aggregation. These treatments also increased time to occlusion and decreased both thrombus size and the presence of collagen fibers in surrounding vessel walls compared with the Sham-control and OVX-control groups. These results suggest that DJS has beneficial effects in terms of preventing cardiovascular disease in menopausal woman because it can reduce the serum lipid levels and improve blood flow by inhibiting platelet aggregation and thrombus formation.

1. Introduction

The incidence of cardiovascular disease (CVD) remains the leading cause of death, with high morbidity and mortality after menopause. Estrogen deficiency may cause an increase in cardiovascular risks by affecting lipoprotein metabolism, platelet aggregation ability, and vessel resistance. It is well established that the incidence of CVD is due to hyperlipidemia, a condition characterized by significant increases in total cholesterol (TC), triglycerides (TG), and low-density lipoprotein cholesterol (LDL-C) and a reduction in high-density cholesterol (HDL-C) [1, 2]. Platelets from hypercholesterolemic patients were more reactive to aggregating reagents such as epinephrine and adenosine diphosphate (ADP) than were platelets from normal individuals, and platelets from hypercholesterolemic patients showed hyperactivity and shortened platelet survival *ex vivo* [3]. Estrogen deficiency in OVX animals and menopausal woman can cause activated platelet aggregation and thrombosis by affecting platelet agonist hydrolysis and nitric oxide production in blood vessels. An atherosclerotic plaque rupture releases collagen, lipids, and smooth muscle cells and leads to platelet activation and occlusive thrombosis, thereby stimulating the coagulation cascade system. Thus, abnormal platelet activation plays a key role in interrupting blood flow, for which antiplatelet drugs are available to prevent intravascular thrombosis [4]. Hormone replacement therapy (HRT) is the combination treatment with estrogen or progestin. As a primary therapy, HRT has been observed to exert a protective effect against menopausal cardiovascular disease by modulating the serum lipid profiles and augmenting the response to atherosclerosis [5]. However, HRT studies in menopausal women have reported side effects such as breast cancer, thromboembolic disease, and ischemic stroke [6].

Table 1: Composition of DJS aqueous extract and ingredients.

Ingredients	Contents (g)
Paeonia lactiflora Pallas	93.75
Cnidium officinale Makino	56.25
Alisma orientale Juzepzuk	56.25
Angelica gigas Nakai	28.13
Poria cocos Wolf	28.13
Atractylodes japonica Koidzumi	28.13
Total	290.00

Considering the negative side effects, herbal medicines have been given further attention as candidates for alternative therapy for safe and effective HRT [7]. Dangguijagyagsan (DangQui-Shaoyao-San in Chinese; Tokishakuyakusan in Japanese) is a traditional medicinal prescription that has long been used for the treatment of menopause-related symptoms in East Asia. Previous gynecologic reports related to DJS have documented its improvement of ovarian hormones [8], estrogenic action [9], and neurotoxicity effects of DJS under postmenopausal conditions [10]. However, no studies have investigated the effectiveness of DJS in restoring blood flow. In this study, aspirin was used as a positive control. Aspirin is a widely used anti-thrombosis drug, and low-dose aspirin has been shown to have a preventive effect on thrombus formation in animal testing [11]. Thus, we aimed to investigate the oral administration of DJS (100 mg/kg/day) for 5 weeks to determine the beneficial effects on serum lipid levels and blood flow improvement in OVX and thrombosis-induced rat models in comparison with a Sham-control group.

2. Materials and Methods

2.1. Chemicals and Reagents. Acetonitrile (100%), formic acid (99.9%), and distilled water were purchased from J.T. Baker (HPLC grade, USA). Reference compounds of albiflorin and paeoniflorin were purchased from Wako (Japan). *z*-Ligustilide was purchased from ChromaDex (USA). Nodakenin and decursin were divided from Ministry of Food and Drug Safety (Korea).

2.2. Plant Extracts. The formula of DJS consists of 6 herbs, including *Paeonia lactiflora* (93.75 g), *Cnidium officinale* (56.25 g), *Alisma orientale* (56.25 g), *Angelica gigas* (28.13 g), *Poria cocos* (28.13 g), and *Atractylodis rhizoma alba* (28.13 g). Briefly, 290 g of the 6-herb mixture was boiled in 6 L of distilled water for 4 h at 100°C and filtered using filter paper (Whatman, Maidstone, UK). After filtration, the extract was evaporated and lyophilized. The DJS product (KIOM PH 130005) was stored at Korea Institute of Oriental Medicine (KIOM, Daejeon, Korea) until used in this experiment. The composition of DJS extract and contents of ingredients are shown in Table 1.

2.3. Chromatographic Conditions of HPLC-DAD. The contents albiflorin, paeoniflorin, *z*-ligustilide, decursin, and nodakenin in the DJS water extract were analyzed using an HPLC instrument (Agilent Technologies, USA) with a Atlantis dC_{18} column (4.6 × 250 mm, 5 μm; Waters, USA). The mobile phase consisted of the solvents, distilled water (A) and acetonitrile with 0.1% formic acid (B). The following gradient was used: 0 min, A : B 90 : 10 (v/v); 20 min, A : B 75 : 25; 25 min, A : B 75 : 25; 30 min, A : B 50 : 50; 45 min, A : B 20 : 80; and 60 min, A : B 0 : 100. The mobile phase flow rate was 1.0 mL/min, the column temperature was 30°C, the injection volume was 10 μL, and UV detection was at 230 and 330 nm.

2.4. Animals. Seven-week-old female Sprague-Dawley rats (180–200 g) were purchased from Orient Bio (Seongnam, Gyeonggi, Korea). Animals were maintained at a regular 12 h light/dark cycle, at 21 ± 2°C, with a relative humidity of 50 ± 5%, and were fed a commercial diet (Ralston-Purina, St. Louis, MO, USA). After 1 week of acclimation, rats were Sham-operated (saline; Sham-control group), or bilateral ovariectomies were performed under general anesthesia. The ovariectomized rats were randomly divided into 3 groups: (A) vehicle control (saline; OVX-control group) (B) aspirin 30 mg/kg/day (OVX-ASA group); (C) DJS 100 mg/kg/day (OVX-DJS group). The rats were orally administered the drugs for 5 weeks. Food intake was recorded daily, and the body weight was recorded weekly. The animals used in this study were treated in accordance with the Guide for Care and Use of Laboratory Animals by the Institutional Animal Care and Use Committee (IACUC) of Institute of Oriental Medicine (approval number: 14-003, 14-021).

2.5. Serum Lipid Levels. At the end of the experiment, rats were fasted for 12 h, anesthetized with Zoletil (1 mL/kg intraperitoneally), and sacrificed. Blood samples were collected from the inferior vena cava and centrifuged at 3000 rpm for 10 min to collect the serum. Measurements of TC, TG, and HDL-C levels were performed enzymatically using a Roche Modular P Autoanalyzer (Roche Diagnostics, Indianapolis, IN). The concentration of LDL-C was calculated using the Friedewald equation [12].

2.6. Measurement of Platelet Aggregation. Platelet-rich plasma (PRP) was separated from the blood using an anticoagulant citrate dextrose (ACD) solution that contained 0.8% citric acid, 2.2% sodium citrate, and 2% dextrose at a concentration of 3×10^8 cells/mL. Platelet aggregation in response to collagen (2.5 μg/mL) was performed in PRP using an aggregometer (Chrono-Log Co., Harbortown, CA, USA). The extent of aggregation was expressed as a percentage of the Sham-control stimulated with collagen.

2.7. $FeCl_3$-Induced Carotid Artery Thrombosis Models. Saline or test compounds were administered 4 h before the initiation of thrombotic occlusion. During operative procedures, body temperature was maintained at 37.0 ± 0.2°C using a heating pad. After isoflurane anesthesia, one of the carotid arteries was exposed and a Doppler flow probe (Powerlab/8SP, ADInstruments Pty Ltd, Castle Hill, NSW, Australia) was placed on it. After stabilization for 3 min, vascular injuries were induced

Table 2: Effect of DJS administration on body weight gain and food intake in OVX rats.

Group	Final body weight (g)	Body weight gain (g/day)	Food intake (g/day)
Sham	306.83 ± 19.04^{a}	3.74 ± 2.67^{a}	17.02 ± 2.12^{a}
OVX-control	341.15 ± 21.85^{b}	5.72 ± 2.43^{b}	17.72 ± 2.84^{a}
OVX-ASA	345.91 ± 19.93^{b}	5.39 ± 2.43^{b}	19.14 ± 3.71^{b}
OVX-DJS	346.54 ± 23.62^{b}	5.11 ± 2.18^{b}	19.39 ± 3.22^{b}

Results are mean ± S.D. ($n = 15$). Means of letters recorded as a and b within a column indicated the same level of body weight and food intake within the values determined by one-way ANOVA. OVX: ovariectomized; ASA: aspirin; DJS: Dangguijagyagsan.

by a topical application of a $FeCl_3$-saturated filter paper (2 × 2 mm). The filter paper was removed and the common carotid artery was washed with saline. A Doppler flow probe was placed on the exposed artery and blood flow was measured continuously with Laser Doppler Flowmetry (LDF; BFL21, Transonic Instrument, USA) for 30 min. To determine the time to occlusion (TTO), arterial occlusion was determined by decreased blood flow, and complete occlusion was defined as cessation of the carotid artery blood flow for 10 minutes.

2.8. Histology. The injured artery of rats was fixed in 4% paraformaldehyde and embedded in paraffin for histological analysis. These were sectioned longitudinally into 4 μm slices and stained with hematoxylin-eosin (H&E) and Masson's trichrome. The thrombus for each animal was imaged using a light microscope (Axio Imager D2; Carl Zeiss Microimaging, Oberkochen, Germany) and the Zeiss AxioVision software (AxioVs40V4.8.1.0; Carl Zeiss imaging Solution) to obtain an image slice that represented the largest part of the thrombus.

2.9. Statistical Analysis. The results are presented as a mean ± standard deviation (SD). Statistical significance was analyzed using SPSS (version 20.0, SPSS Inc., Chicago, IL, USA). Differences among groups were compared with a one-way ANOVA test, followed by Tukey's post hoc test. P values less than 0.05 were considered significant.

3. Results

3.1. HPLC Analysis of Reference Compounds in DJS. The standard curves for the five components containing albiflorin, paeoniflorin, z-ligustilide, decursin, and nodakenin were $y = 13.026x + 70.072$ (R^2 1.000), $y = 13.446x + 124.71$ (R^2 0.999), $y = 25.841x + 40.72$ (R^2 1.000), $y = 38.995x + 31.219$ (R^2 0.999), and $y = 19.043x + 108.95$ (R^2 1.000), respectively. HPLC analysis of DJS and standard mixtures was carried out at 230 and 330 nm. The retention time of each compound was 15.6 min (albiflorin), 17.1 min (paeoniflorin), 22.3 min (nodakenin), 42.9 min (z-ligustilide), and 43.8 min (decursin). The contents of each component in DJS aqueous extract were albiflorin 2.97 ± 0.065 mg/g and paeoniflorin 16.17±0.120 mg/g at 230 nm, nodakenin 3.63±0.005 mg/g, z-ligustilide 0.11 ± 0.004 mg/g, and decursin 0.020 ± 0.001 mg/g at 330 nm, respectively (Figure 1).

3.2. Effects of DJS on Body Weight Gain and Food Intake. The final body weights after 5-week treatments increased significantly in the OVX-control compared with that in the Sham-control group ($P < 0.05$). OVX-ASA and OVX-DJS groups showed similar body weight with OVX-control group. In the OVX-control group, treatment with saline demonstrated a significant increase in body weight gain compared to the Sham-control group (5.7 ± 2.4 g/day versus 3.7 ± 2.7 g/day, $P < 0.001$). The body weight gain was slightly decreased in the OVX-ASA (5.4 ± 2.4 g/day) and OVX-DJS groups (5.1 ± 2.2 g/day) compared with OVX-control group, although not significantly compared with the Sham-control group ($P > 0.05$). When animals were allowed free access to food following an experimental period, the food intake was the same in the Sham-control (17.02 ± 2.12 g/day) and OVX-control groups (17.72 ± 2.84 g/day). Food intake was increased in the OVX-ASA (19.14 ± 3.71 g/day) and OVX-DJS groups (19.39 ± 3.22 g/day) compared with the Sham-control ($P < 0.001$) and OVX-control groups ($P < 0.01$) (Table 2).

3.3. Effects of DJS on Serum Lipid Levels. Ovariectomy caused a substantial increase in the TC, TG, and LDL-C levels compared with the Sham-control group ($P < 0.001$, $P < 0.05$, and $P < 0.01$). In OVX rats, treatment with 30 mg/kg/day of ASA (OVX-ASA group) and 100 mg/kg/day of DJS (OVX-DJS group) significantly attenuated the increase in the TC, TG and LDL-C levels but did not affect HDL-C levels compared with the OVX-control group ($P < 0.05$, resp.). Additionally, the OVX-ASA and OVX-DJS groups exhibited no significant changes in the HDL-C levels compared with the Sham-control and OVX-control groups ($P > 0.05$) (Figure 2).

3.4. Effects of DJS on Platelet Aggregation. There was no difference in the inhibition of platelet aggregation between the OVX-control and Sham-control groups (79.5% ± 7.4% versus 74.5% ± 9.0%, $P > 0.05$). Treatment with 30 mg/kg/day of ASA markedly suppressed platelet aggregation (32.3% ± 4.7%, $P < 0.001$), as did treatment with 100 mg/kg/day of DJS (47.3% ± 2.6%, $P < 0.001$) compared with the OVX-control group (74.5% ± 9.0%) (Figure 3).

3.5. Effects of DJS in OVX Rats with $FeCl_3$-Induced Thrombosis. The mean time to occlusion in the OVX-control group was significantly decreased (7.80 ± 0.84 min) compared with that of the Sham-control group (30.00 ± 0.00 min). Therefore, the application of 40% $FeCl_3$ to the external surface of the carotid artery for 3 min induced a rapid decrease in blood flow and was considered optimal for measuring blood flow. In comparison, treatment with either 30 mg/kg of ASA

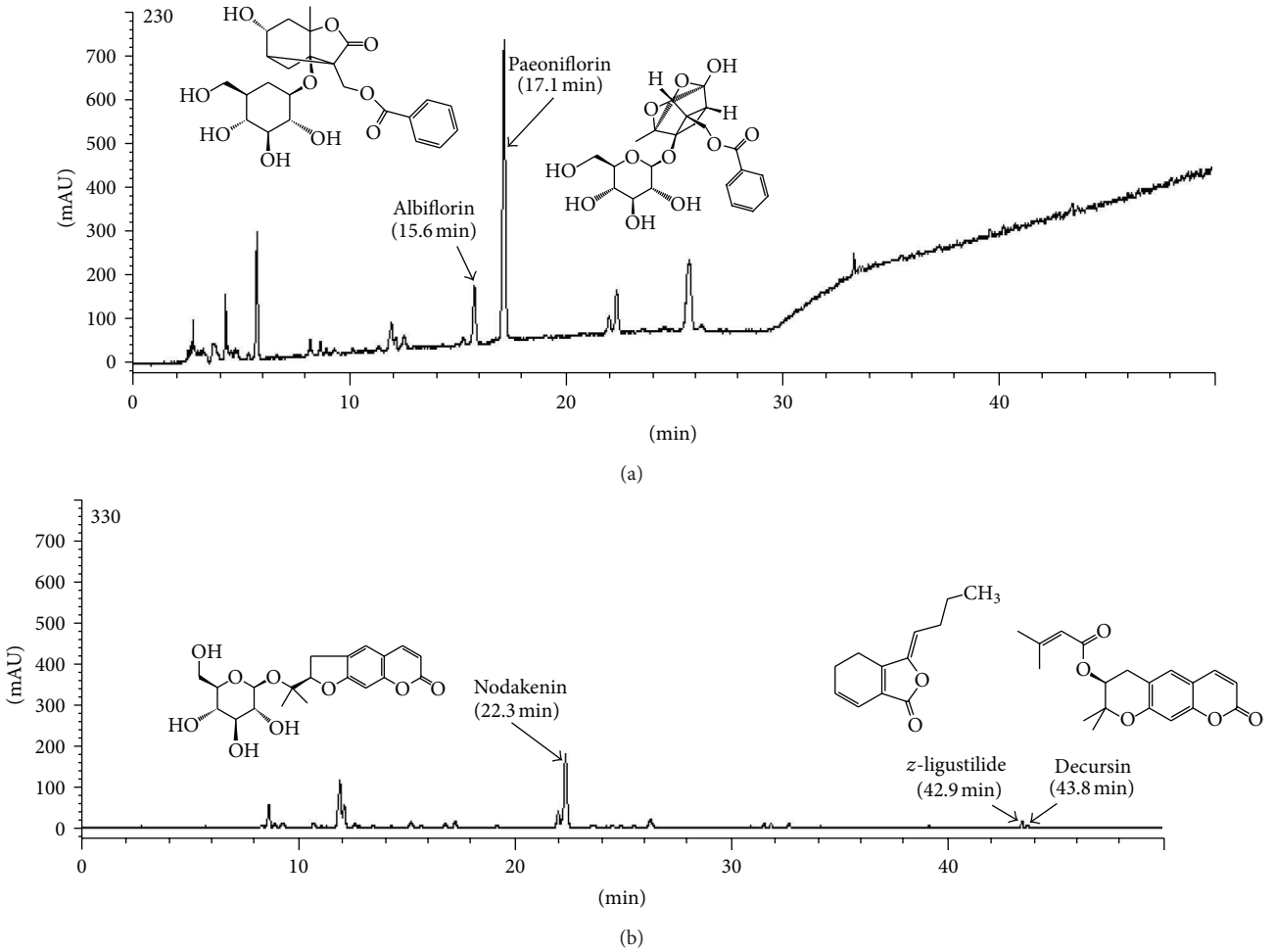

Figure 1: HPLC-DAD chromatogram of five reference compounds in DJS detected at 230 nm (albiflorin, paeoniflorin) and 330 nm (nodakenin, *z*-ligustilide, and decursin). DJS: Dangguijagyagsan aqueous extract (29.28 mg/mL).

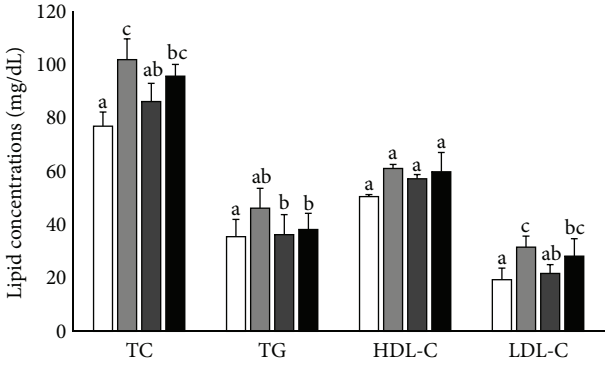

Figure 2: Effects of ASA (30 mg/kg/day) and DJS (100 mg/kg/day) on serum lipid profiles in SD rats compared with their corresponding controls: serum total cholesterol (TC), triglyceride (TG), high-density lipoprotein cholesterol (HDL-C), low-density lipoprotein cholesterol (LDL-C) levels in Sham (white bar) and OVX SD rats after 5 weeks of oral demonstration with saline (grey bar), ASA (dark grey bar, 30 mg/kg/day), or DJS (black bar, 100 mg/kg/day). Values of the same measured parameter that are not followed by the same alphabetical letter are significantly different (n = 5–7 in each group).

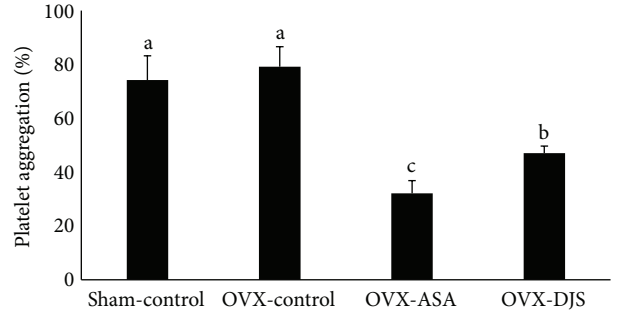

Figure 3: Inhibition by ASA (30 mg/kg/day) and DJS (100 mg/kg/day) of platelet aggregation induced by collagen (2.5 μg/mL). Values of the same measured parameter that are not followed by the same alphabetical letter are significantly different (n = 5 in each group).

(OVX-ASA group) (16.80 ± 1.30 min) and 100 mg/kg of DJS (OVX-DJS group) (13.20 ± 0.84 min) also prolonged time to occlusion by 2.49 ± 0.33 ratio and 1.94 ± 0.08 ratio, respectively (Figure 4).

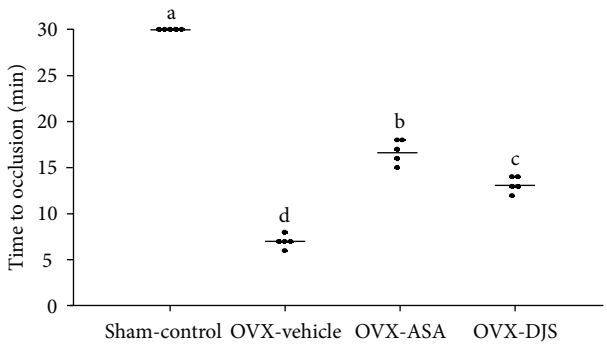

Figure 4: Time to occlusion of DJS in a carotid arterial thrombosis model. The horizontal lines represent the mean of the displayed values for time to occlusion in each group. Values of the same measured parameter that are not followed by the same alphabetical letter are significantly different ($n = 5$ in each group).

3.6. Histology of the Carotid Artery with Thrombotic Occlusion after $FeCl_3$ Treatment. Complete occlusion was defined as the absence of blood flow for 10 minutes after the application of $FeCl_3$. We collected those arteries and processed them with H&E and Masson's Trichrome for collagen fiber staining. In this study, histological changes were observed in the carotid arteries after $FeCl_3$-induced thrombosis. In these images, the type I collagen fiber stained blue, the nuclei stained black, and the background stained red. Thrombotic occlusion and collagen fiber damage were observed in the carotid artery of the OVX-control group after $FeCl_3$ treatment. However, treatment with ASA and DJS provided an excellent recovery of collagen fiber in the thrombotic vessels induced by $FeCl_3$ (Figure 5).

4. Discussion

Postmenopausal women frequently experience weight gain and are thus vulnerable to obesity-related diseases, which lead to an increased risk of cardiovascular diseases (CVD) such as coronary heart disease, hypertension, and non-insulin-dependent diabetes mellitus [13, 14]. In the present study, body weight gain was significantly increased in OVX-control group compared to Sham-control group for five-week treatment and there were no significant weight gain differences in OVX-ASA and OVX-DJS groups compared to OVX-control group. However, food intake in OVX-ASA and OVX-DJS group had much consumption compared to OVX-control group and these results suggest that administration of DJS could have beneficial effect on obesity in menopause.

Large number of pharmacological studies were carried out on the influence of the menopause on serum lipids and lipoproteins profiles. Menopausal statement increases the incidence of CVD due to hyperlipidemia, which is characterized by increases in total cholesterol (TC), triglycerides (TG), and low-density lipoprotein cholesterol (LDL-C) and a reduction in high-density lipoprotein cholesterol (HDL-C) [15–18]. Many attempts have been made to use herbal extracts to improve serum lipid levels in postmenopausal women suffering from hyperlipidemia associated with CVD [19–21]. In the present study, DJS treatment significantly reduced the TC, TG, and LDL-C levels ($P < 0.05$). Contrary to the conventional studies, HDL-C level of OVX-control did not appear to be significantly increased ($P > 0.05$). These results indicate that the rodent model for studying lipid metabolism physiology may have limitations, but it still provides a good model for studying the effects on serum lipid levels. Therefore, it is suggested that the effects of the DJS on serum lipid levels are very complex and should be investigated further. It has been reported that ovariectomy caused an elevation of TC and LDL-C in serum, leading to the development of atherosclerosis and coronary heart disease [22]. Furthermore, we further investigated the antithrombosis activity based on the serum lipid level changes of DJS treatment.

We also determined the effect of DJS on thrombus formation. Endothelial dysfunction is considered the first step in the atherosclerotic process, and our experimental approach was based on endothelial injury and platelet aggregation being key events in the pathogenesis of thrombus formation [23, 24]. Intravascular thrombosis is involved a series of complex events including platelet adhesion, activation, aggregation, granule release, and coagulation cascade activation, is likely to platelets contribute to thrombosis in several ways [25]. Platelets provide the membrane surface required for the generation of thrombin and express surface receptors that affect platelet-platelet and platelet-vessel wall interactions [26]. As a positive control, we used aspirin, one of the most widely used blood thinning agents, is used long-term in low doses to prevent heart attacks, strokes and blood clot formation in people at high risk for these events [27, 28]. In this study, although the cardiovascular protective effects of DJS treatment were not as strong as ASA, DJS treatment was successful in inhibiting platelet aggregation and thrombus formation. Previous studies have reported that biochanin A, a phytoestrogen that acts as a weak estrogen receptor agonist, restored endothelial function in an animal model of vascular injury [29]. This study showed the possibility that DJS treatment can restore endothelial function in an animal model of carotid artery injury, an effect similar to the vascular effects of estrogen.

Measurement of platelet aggregation has been a useful method to examine inhibition of thrombus formation. Furthermore, $FeCl_3$-induced thrombosis model method in rats is the optimal technique as it exhibits simplicity and reproducibility. In a previous test, we demonstrated the arterial response to various concentrations (10–50%) of $FeCl_3$ and found that filter paper saturated with a 40% concentration of $FeCl_3$resulted in fast, effective recanalization. $FeCl_3$ triggers an oxidative vascular endothelial matrix. Then, platelets interact with collagen and vWF in the matrix via their respective platelet surface receptors, leading to platelet adhesion [30]. According to the *in vitro* results, the *in vivo* antithrombotic efficacy of DJS was anticipated. Indeed, the oral administration of DJS delayed the occlusion time in a $FeCl_3$-induced artery thrombosis model. Notably, DJS doubled the occlusion time at 100 mg/kg compared with the OVX-control group. In this study, we did not design the Sham-vehicle and OVX-control groups to measure time to

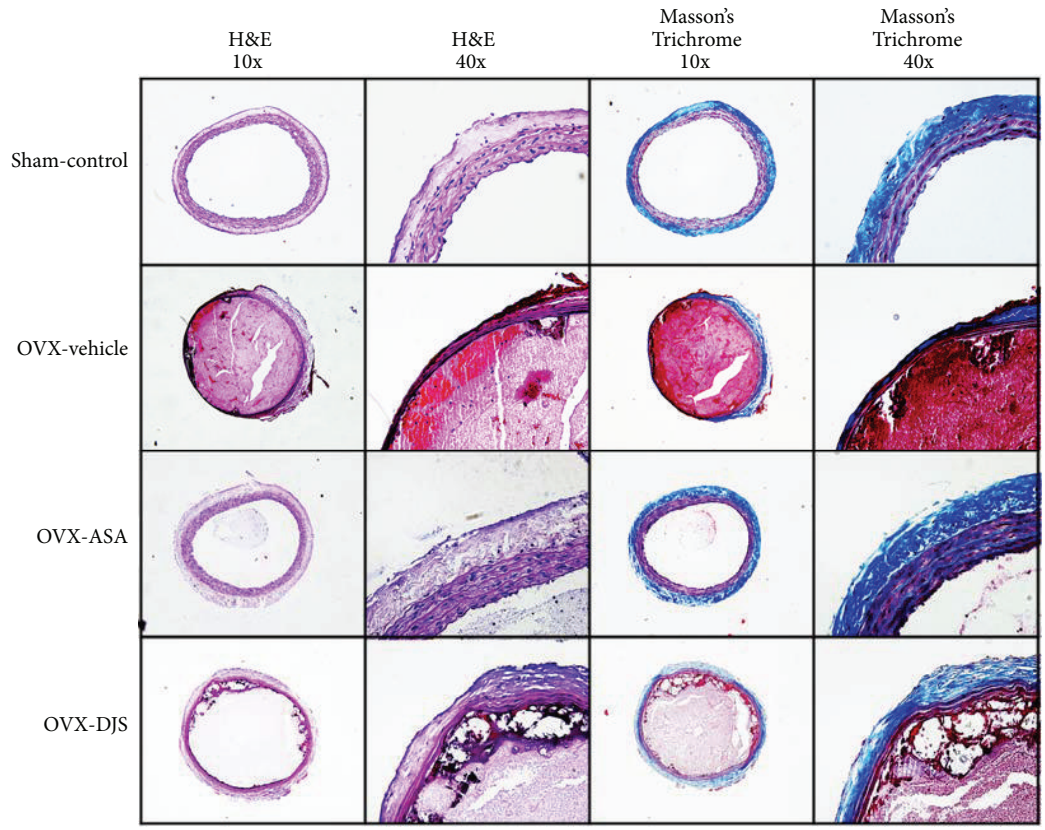

FIGURE 5: Histological examination of a $FeCl_3$-induced thrombus from the Sham-control group, OVX-vehicle group, OVX-ASA group, and OVX-DJS group. All sections were stained with hematoxylin and eosin (H&E, two left columns, and magnification ×100, 400) and Masson's trichrome (MT, two right columns, and magnification ×100, 400).

occlusion after the $FeCl_3$ topical application. Our previous study investigated the effects of saline administration on rats following Sham operation and ovariectomy, which is similar to the Sham-control and OVX-control groups. In support of our hypothesis, the histological staining methods also demonstrated that DJS inhibited arterial thrombus formation and damage of collagen fiber in arterial vessel wall.

Various clinical studies have shown that herbal extraction components have significant association antioxidant effects; it leads to antithrombotic properties by increase of platelet NO release and radical scavenging activity [31, 32]. DJS consists of 6 herbs and each herb also has antioxidant effects [33–37]. We hypothesize that antioxidant effects are responsible for the results from above antithrombotic studies.

Female sex appears to be associated with cardioprotection and menopauses are major risk factors for cardiovascular disease. In fact, the ideal postmenopausal cardiovascular protective therapy is expected to reproduce the beneficial effects of blood flow without producing any adverse effects. Although the exact mechanism of action remains to be clarified, we have demonstrated the beneficial effects of DJS on the improvement of plasma lipid profiles and restoration of blood flow. These beneficial effects may be caused by (1) decreased TC, TG, and LDL-C; (2) inhibition of platelet aggregation; or (3) inhibition of thrombus formation. In conclusion, DJS could be a candidate for inhibiting the development of cardiovascular risk factors.

Conflict of Interests

The authors declare that there is no conflict of interests regarding the publication of this paper.

Authors' Contributions

In Sil Park and Hye Won Lee contributed equally. In Sil Park and Byoung Seob Ko conceived and designed the experiments. In Sil Park, Hye Won Lee, and Jin Ah Ryuk performed the experiments and wrote the paper. Byoung Seob Ko monitored the experiments and discussed the results. Hye Won Lee and Byoung Seob Ko analyzed the data and reviewed the manuscript. All authors have read and approved the paper.

Acknowledgment

This work was supported by a grant from the Korea Institute of Oriental Medicine (Grant no. K14080).

References

[1] L. Wroblewski Lissin and J. P. Cooke, "Phytoestrogens and cardiovascular health," *Journal of the American College of Cardiology*, vol. 35, no. 6, pp. 1403–1410, 2000.

[2] R. Rossi, T. Grimaldi, G. Origliani, G. Fantini, F. Coppi, and M. G. Modena, "Menopause and cardiovascular risk," *Pathophysiology of Haemostasis and Thrombosis*, vol. 32, no. 5-6, pp. 325–328, 2002.

[3] T. M. Quinton, S. Kim, J. Jin, and S. P. Kunapuli, "Lipid rafts are required in $G\alpha_i$ signaling downstream of the P2Y12 receptor during ADP-mediated platelet activation," *Journal of Thrombosis and Haemostasis*, vol. 3, no. 5, pp. 1036–1041, 2005.

[4] Y. Nakano, T. Oshima, H. Matsuura, G. Kajiyama, and M. Kambe, "Effect of 17β-estradiol on inhibition of platelet aggregation in vitro is mediated by an increase in NO synthesis," *Arteriosclerosis, Thrombosis, and Vascular Biology*, vol. 18, no. 6, pp. 961–967, 1998.

[5] F. Grodstein, M. J. Stampfer, J. E. Manson et al., "Postmenopausal estrogen and progestin use and the risk of cardiovascular disease," *The New England Journal of Medicine*, vol. 335, no. 7, pp. 453–461, 1996.

[6] E. Barrett-Connor, L. Mosca, P. Collins et al., "Effects of raloxifene on cardiovascular events and breast cancer in postmenopausal women," *The New England Journal of Medicine*, vol. 355, no. 2, pp. 125–137, 2006.

[7] H. J. Kang, R. Ansbacher, and M. M. Hammoud, "Use of alternative and complementary medicine in menopause," *International Journal of Gynecology and Obstetrics*, vol. 79, no. 3, pp. 195–207, 2002.

[8] S. Usuki, T. Nakauchi, S. Higa, and K. Someya, "The improvement of luteal insufficiency in fecund women by Tokishakuyakusan treatment," *American Journal of Chinese Medicine*, vol. 30, no. 2-3, pp. 327–338, 2002.

[9] M. H. Chung, S. Suzuki, T. Nishihara, and M. Hattori, "Estrogenic effects of a Kampo formula, Tokishakuyakusan, in parous ovariectomized rats," *Biological and Pharmaceutical Bulletin*, vol. 31, no. 6, pp. 1145–1149, 2008.

[10] J. Lee, D. Hwang, H. G. Kim, C. Lee, and M. S. Oh, "Dangguijakyak-san protects dopamine neurons against 1-methyl-4-phenyl-1,2, 3,6-tetrahydropyridine-induced neurotoxicity under postmenopausal conditions," *Journal of Ethnopharmacology*, vol. 139, no. 3, pp. 883–888, 2012.

[11] F. W. Peter, R. J. P. M. Franken, W. Z. Wang et al., "Effect of low dose aspirin on thrombus formation at arterial and venous microanastomoses and on the tissue microcirculation," *Plastic and Reconstructive Surgery*, vol. 99, no. 4, pp. 1112–1121, 1997.

[12] W. T. Friedewald, R. I. Levy, and D. S. Fredrickson, "Estimation of the concentration of low-density lipoprotein cholesterol in plasma, without use of the preparative ultracentrifuge.," *Clinical Chemistry*, vol. 18, no. 6, pp. 499–502, 1972.

[13] M. E. Mendelsohn and R. H. Karas, "The protective effects of estrogen on the cardiovascular system," *The New England Journal of Medicine*, vol. 340, no. 23, pp. 1801–1811, 1999.

[14] R. W. Robinson, N. Higano, and W. D. Cohen, "Increased incidence of coronary heart disease in women castrated prior to the menopause," *AMA Archives of Internal Medicine*, vol. 104, no. 6, pp. 908–913, 1959.

[15] G. A. Colditz, W. C. Willett, M. J. Stampfer, B. Rosner, F. E. Speizer, and C. H. Hennekens, "Menopause and the risk of coronary heart disease in women," *The New England Journal of Medicine*, vol. 316, no. 18, pp. 1105–1110, 1987.

[16] J. Jensen, L. Nilas, and C. Christiansen, "Influence of menopause on serum lipids and lipoproteins," *Maturitas*, vol. 12, no. 4, pp. 321–331, 1990.

[17] M. G. Shlipak, J. A. Simon, E. Vittinghoff et al., "Estrogen and progestin, lipoprotein(a) and the risk of recurrent coronary heart disease events after menopause," *The Journal of the American Medical Association*, vol. 283, no. 14, pp. 1845–1852, 2000.

[18] C. Bonithon-Kopp, P.-Y. Scarabin, B. Darne, A. Malmejac, and L. Guize, "Menopause-related changes in lipoproteins and some other cardiovascular risk factors," *International Journal of Epidemiology*, vol. 19, no. 1, pp. 42–48, 1990.

[19] E. A. Lucas, D. A. Khali, B. P. Daggy, and B. H. Arjmandi, "Ethanol-extracted soy protein isolate does not modulate serum cholesterol in golden syrian hamsters: a model of postmenopausal hypercholesterolemia," *The Journal of Nutrition*, vol. 131, no. 2, pp. 211–214, 2001.

[20] S. Hidaka, Y. Okamoto, and M. Arita, "A hot water extract of Chlorella pyrenoidosa reduces body weight and serum lipids in ovariectomized rats," *Phytotherapy Research*, vol. 18, no. 2, pp. 164–168, 2004.

[21] Y. Park, H. Kwon, M. K. Shimi, M. Rhyu, and Y. Lee, "Improved lipid profile in ovariectomized rats by red ginseng extract," *Pharmazie*, vol. 66, no. 6, pp. 450–453, 2011.

[22] M. Liu, X. Xu, W. Rang, Y. Li, and H. Song, "Influence of ovariectomy and 17β-estradiol treatment on insulin sensitivity, lipid metabolism and post-ischemic cardiac function," *International Journal of Cardiology*, vol. 97, no. 3, pp. 485–493, 2004.

[23] P. M. Vanhoutte, "Endothelial dysfunction and atherosclerosis," *European Heart Journal*, vol. 18, no. 5, pp. E19–E29, 1997.

[24] U. Rauch, J. I. Osende, V. Fuster, J. J. Badimon, Z. Fayad, and J. H. Chesebro, "Thrombus formation on atherosclerotic plaques: pathogenesis and clinical consequences," *Annals of Internal Medicine*, vol. 134, no. 3, pp. 224–238, 2001.

[25] B. Furie and B. C. Furie, "Mechanisms of thrombus formation," *New England Journal of Medicine*, vol. 359, no. 9, pp. 938–949, 2008.

[26] G. Davì and C. Patrono, "Platelet activation and atherothrombosis," *The New England Journal of Medicine*, vol. 357, no. 24, pp. 2482–2494, 2007.

[27] D. L. Bhatt, K. A. A. Fox, W. Hacke et al., "Clopidogrel and aspirin versus aspirin alone for the prevention of atherothrombotic events," *New England Journal of Medicine*, vol. 354, no. 16, pp. 1706–1717, 2006.

[28] A. O. Maree and D. J. Fitzgerald, "Variable platelet response to aspirin and clopidogrel in atherothrombotic disease," *Circulation*, vol. 115, no. 16, pp. 2196–2207, 2007.

[29] S. Schrepfer, T. Deuse, T. Münzel, H. Schäfer, W. Braendle, and H. Reichenspurner, "The selective estrogen receptor-β agonist biochanin A shows vasculoprotective effects without uterotrophic activity," *Menopause*, vol. 13, no. 3, pp. 489–499, 2006.

[30] A. Eckly, B. Hechler, M. Freund et al., "Mechanisms underlying $FeCl_3$-induced arterial thrombosis," *Journal of Thrombosis and Haemostasis*, vol. 9, no. 4, pp. 779–789, 2011.

[31] O. Vitseva, S. Varghese, S. Chakrabarti, J. D. Folts, and J. E. Freedman, "Grape seed and skin extracts inhibit platelet function and release of reactive oxygen intermediates," *Journal of Cardiovascular Pharmacology*, vol. 46, no. 4, pp. 445–451, 2005.

[32] J. E. Tanus-Santos, M. Desai, L. R. Deak et al., "Effects of endothelial nitric oxide synthase gene polymorphisms on platelet function, nitric oxide release, and interactions with estradiol," *Pharmacogenetics and Genomics*, vol. 12, no. 5, pp. 407–413, 2002.

[33] S. Wu, L. Ng, and C. Lin, "Antioxidant activities of some common ingredients of traditional chinese medicine, *Angelica sinensis*, *Lycium barbarum*and *Poria cocos*," *Phytotherapy Research*, vol. 18, no. 12, pp. 1008–1012, 2004.

[34] J. B. Jeong, S. Y. Ju, J. H. Park et al., "Antioxidant activity in essential oils of Cnidium officinale makino and Ligusticum chuanxiong hort and their inhibitory effects on DNA damage and apoptosis induced by ultraviolet B in mammalian cell," *Cancer Epidemiology*, vol. 33, no. 1, pp. 41–46, 2009.

[35] H. J. Kim, E. J. Chang, S. H. Cho, S. K. Chung, H. D. Park, and S. W. Choi, "Antioxidative activity of resveratrol and its derivatives isolated from seeds of Paeonia lactiflora," *Bioscience, Biotechnology and Biochemistry*, vol. 66, no. 9, pp. 1990–1993, 2002.

[36] C. W. Han, E. S. Kang, S. A. Ham, H. J. Woo, J. H. Lee, and H. G. Seo, "Antioxidative effects of Alisma orientale extract in palmitate-induced cellular injury," *Pharmaceutical Biology*, vol. 50, no. 10, pp. 1281–1288, 2012.

[37] C. Wang, K. Wang, L. Chen, D. Chou, and W. Liang, "Antioxidative abilities of essential oils from atractylodes ovata rhizome," *Evidence-Based Complementary and Alternative Medicine*, vol. 2011, Article ID 204892, 8 pages, 2011.

Hindawi Publishing Corporation
Evidence-Based Complementary and Alternative Medicine
Volume 2014, Article ID 521602, 11 pages
http://dx.doi.org/10.1155/2014/521602

Review Article

The Usefulness of Xuefu Zhuyu Tang for Patients with Angina Pectoris: A Meta-Analysis and Systematic Review

Guo-zhong Yi,[1] Yu-qin Qiu,[2] Ya Xiao,[2,3] and Li-xia Yuan[2]

[1] *The First College of Clinical Medicine, Southern Medical University, Guangzhou, Guangdong 510515, China*
[2] *College of Traditional Chinese Medicine, Southern Medical University, Guangzhou, Guangdong 510515, China*
[3] *Department of Traditional Chinese Medicine, Nanfang Hospital, Southern Medical University, Guangzhou, Guangdong 510515, China*

Correspondence should be addressed to Li-xia Yuan; yiguozhong09@126.com

Received 7 April 2014; Revised 10 August 2014; Accepted 10 August 2014; Published 31 August 2014

Academic Editor: Myeong Soo Lee

Objective. To evaluate the efficacy of Xuefu Zhuyu Tang (XFZYT) for treating angina pectoris (AP). *Methods.* Six databases were searched (up to December, 2013). Eligible randomized controlled trials (RCTs) evaluating the efficiency of XFZYT plus traditional antianginal medications (TAMs) compared with TAMs alone in patients with AP were included. The outcomes were relief of anginal symptoms (RAS) and improvement of electrocardiogram (ECG) and blood high-density lipoprotein cholesterol (HDL-C) level. *Result.* Finally 14 RCTs were included. There were evidences that XFZYT combined with TAMs was more effective in improving RAS (RR = 1.29; 95% CI = [1.20, 1.38]), ECG (RR = 1.37; 95% CI = [1.22, 1.54]), and blood HDL-C level (MD = 0.29 mmol/L; 95% CI = [0.23, 0.35]) compared with TAMs alone. Our meta-analysis also showed the pooled number needed to treat (NNT) of the group with stable angina pectoris (SAP) was smaller in improving RAS (4.2 versus 5.7) and ECG (3.1 versus 5.5) compared with the group with both SAP and unstable angina pectoris (UAP). *Conclusion.* Combination therapy with XFZYT and TAMs is more effective in treating AP compared with TAMs alone. And XFZYT may be a more suitable choice for the treatment of SAP. However, the findings should be interpreted with caution due to the mediocre methodological quality of the included RCTs.

1. Introduction

Cardiovascular diseases are the number one cause of death globally [1]. According to the World Health Organization (WHO), an estimated 17.3 million people died from cardiovascular diseases in 2008, representing 30% of all global deaths. Of these deaths, an estimated 7.3 million deaths were due to coronary heart disease. Angina pectoris is the most prevalent manifestation of coronary artery diseases and has a major negative impact on the general health status and quality of life [2].

Angina pectoris is clinically classified into stable angina pectoris (SAP) and unstable angina pectoris (UAP). Both SAP and UAP can use traditional antianginal medications (TAMs) such as organic nitrates, antiplatelet drugs, antithrombotic drugs, and β blockers. Antiplatelet drugs include aspirin, platelet glycoprotein IIb/IIIa inhibitor, and clopidogrel, antithrombotic drugs include heparin and low-molecular-weight heparin, and β blockers included metoprolol tartrate [3, 4]. Despite the effectiveness of TAMs, episodes of angina may still persist or become even worse, and many patients cannot tolerate a combination of TAMs due to their many serious adverse effects, such as antithrombotic complications, decreasing heart rate or blood pressure, and other hemodynamic changes [5, 6]. Therefore, we need to research a new medication which is effective and tolerant in improving the symptoms of angina and will provide an alternative option for patients.

Xuefu Zhuyu Tang (XFZYT) originated from the "Corrections on the Errors of Medical Works" in Qing Dynasty. It is a very famous traditional Chinese formula in promoting Qi circulation and removing blood stasis according to traditional Chinese medicine (TCM) theory [7]. This formula consists of rehmannia root (shengdi), peach seed (taoren), safflower (honghua), Chinese angelica (danggui), red peony root (chishao), platycodon root (jiegeng), orange fruit (zhiqiao), hare's ear root (chaihu), sichuan lovage root (chuangxiong), two-toothed achyranthes root (niuxi), and prepared liquorice

root (gancao). Some pharmacological researches showed that XFZYT could improve blood rheology, reduce blood lipid level, and prevent antimyocardial ischemia [8, 9]. This Chinese herbal medicine (CHM) is commonly used for the treatment of patients with cardiovascular diseases [7, 10].

How about the efficacy of XFZYT in improving AP outcomes and the application of XFZYT in the treatment of different AP subtypes? We therefore conducted an updated systematic review and meta-analysis of published RCTs to answer these questions.

2. Materials and Methods

2.1. Search Strategy. Two authors (G. Z. Yi and Y. Q. Qiu) systematically searched the Medline database (1989–December 2013), Cochrane Library (1993–December 2013), Chinese National Knowledge Infrastructure database (CNKI, 1989–December 2013), Chinese Biomedical Literature database (CBM, 1990–December 2013), Wanfang database (1989–December 2013), and Chinese Scientific Journal database (VIP, 1989–December 2013). The following keywords were used: coronary heart disease, CHD, angina pectoris, AP, and Xuefu Zhuyu.

2.2. Eligibility Criteria. We included RCTs met criteria as follows: (1) involving patients who were diagnosed with SAP or UAP according to the American College of Cardiology Foundation/American Heart Association (ACCF/AHA) Guideline for the Diagnosis and Management of Patients with Unstable Ischemic Heart Disease [11], the International Society and Federation of Cardiology/World Health Organization (ISFC/WHO) guideline [12], or the Chinese Society of Cardiology (CSC) guidelines [13, 14]; (2) comparing XFZYT plus TAMs with TAMs alone for maintenance therapy for at least 4 weeks and the two groups were comparable on the basis of the characteristic of patients and studies, such as gender, age, and sample size; (3) using improvement of the relief of angina symptoms (RAS) and electrocardiogram (ECG) as the outcome measures [15] and quality of life (QL), blood lipid (HDL-C, LDL-C, TC, and TG) level, reduction of nitroglycerin use (RNU), and adverse events (AEs) were also included.

2.3. Data Extraction. Two researchers (G. Z. Yi and Y. Q. Qiu) independently extracted from each article the authors information, year of publication, types of AP, sample size, the number of participants in each group, percent of male and average age, criteria for inclusion and exclusion, method of randomization, details of blinding, interventions of each group, duration of treatment, criteria for outcome assessments, and data reported. Disagreements were resolved after discussion with a third researcher (Y. Xiao).

2.4. Statistical Analysis. Meta-analysis was carried out using Review Manager software (version 5.2), provided by the Cochrane Collaboration. Dichotomous data were presented as risk ratios (RRs) and continuous outcomes as mean difference (MD), both with 95% confidence interval (CI). The chi-squared test and I-squared statistic were performed to assess the heterogeneity, and heterogeneity was presented as significant when I^2 was over 25%. In the absence of statistical heterogeneity, a fixed-effect model was used to pool the result; otherwise, a random-effect model was used [16]. In subgroup analysis, we used the number needed to treat (NNT) to evaluate the usefulness of XFZYT plus TAMs for each subgroup with different AP subtypes; the NNT was calculated as 1/(Therapeutic Gain). And we also performed a funnel plot of the improvement of RAS between XFZYT plus TAMs group and TAMs group to assess the publication bias.

3. Results

3.1. Description of Included Trials. A total of 1044 studies were identified by computer search and manual search of cited references. After further reading, we excluded 1030 studies according to the eligibility criteria. Finally, a total of 14 studies [17–30] were included in the meta-analysis and systematic review, of which 4 studies [18, 21, 26, 28] included patients with SAP, 2 studies [23, 24] included patients with UAP, and 8 studies [17, 19, 20, 22, 25, 27, 29, 30] included patients with SAP or UAP. All these studies were published in Chinese. Figure 1 is a flow diagram of studies selection process.

All 14 studies included were RCTs, and all of them recruited participants for treatment with XFZYT combined with TAMs versus TAMs. Most of the studies used the improvement of RAS and ECG as the primary outcome measures; the reduction of nitroglycerin use (RNU) and blood lipid level were also reported in some studies. One study [23] used the Seattle Angina Questionnaire (SAQ) [31] and Short Form-36 (SF-36) [32] to evaluate the quality of life of patients after treatment. The characteristics of these original studies are presented in Table 1.

3.2. Methodological Quality of Included Trials. The methodological quality of the RCTs included in our study was assessed by the criteria in the Cochrane Handbook for Systematic Review [16]. The quality of trials was evaluated as having low risk of bias, uncertain risk of bias, and high risk of bias according to the risk of trials, including sequence generation, allocation concealment, blinding, incomplete outcome data, selective outcome reporting, and other potential sources of bias. All studies had described a correct randomization method, but only 2 [19, 23] mentioned allocation concealment. 5 studies [19, 20, 23, 25, 30] described blinding of participants and 4 RCTs [19, 23, 25, 28] mentioned withdrawal and dropout information. Among all these RCTs, the characteristics of participants in each study arm were similar at baseline (age, race, sex, and disease course). The details are shown in Table 2.

3.3. The Effect of XFZYT in Patients with AP. All the 14 RCTs tested XFZYT plus TAMs versus TAMs alone, and we analyzed the following outcomes: RAS (12 trials), ECG (9 trials), blood lipid (HDL-C, LDL-C, TC, and TG) level (3 trials), reduction of nitroglycerin use (2 trials), and quality of life (1 trial).

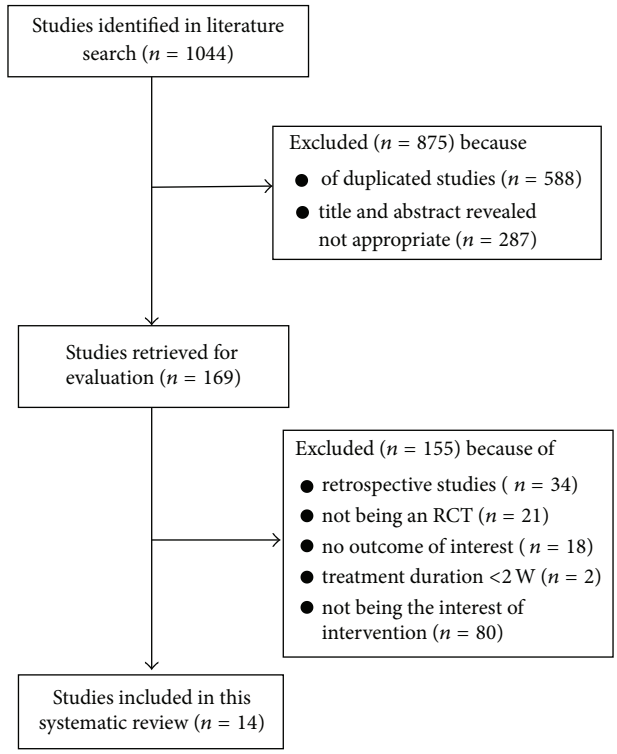

Figure 1: The flow diagram of study selection process.

3.3.1. RAS. The improvement of RAS was reported in 12 RCTs [17–22, 25–30] involving 992 participants and results favored XFZYT combined with TAMs group (RR = 1.29; 95% CI = [1.20, 1.38]) without significant heterogeneity (χ^2 = 5.38; I^2 = 0%) (Figure 2).

3.3.2. ECG. After analyzing 9 RCTs [17, 18, 20, 22, 24, 26–28, 30] involving 683 participants, the result also indicated favoring XFZYT combined with TAMs group (RR = 1.37; 95% CI = [1.22, 1.54]) in the improvement of ECG and with significant homogeneity (χ^2 = 6.17; I^2 = 0%) (Figure 3).

3.3.3. Blood Lipid (HDL-C, LDL-C, TC, and TG) Level. 3 RCTs [17, 18, 29] involving 342 participants reported the improvement of blood lipid level. HDL-C was significantly increased in XFZYT combined with TAMs group (MD = 0.29 mmol/L; 95% CI = [0.23, 0.35]) and without significant heterogeneity (χ^2 = 1.05; I^2 = 0%) (Figure 4), while LDL-C, TG, and TC were significantly decreased in XFZYT combined with TAMs group (MD = 1.08 mmol/L, 0.98 mmol/L, and 1.27 mmol/L; 95% CI = [0.72,1.44], [−0.05, 2.02, 0.63, 1.91]) but with significant heterogeneity (χ^2 = 5.31, 88.48, and 11.48; I^2 = 62%, 98%, and 83%) (Figures 5, 6, and 7).

3.3.4. Reduction of Nitroglycerin Use. 2 RCTs [19, 24] involving 121 patients showed that the dosage of nitroglycerin can be significantly reduced after the treatment with XFZYT combined with TAMs. We did not perform a meta-analysis for the significant heterogeneity (χ^2 = 13.08; I^2 = 92%). Results of the two trials are as follows: the dosage of nitroglycerin decreased from 3.96 ± 1.27 to 1.15 ± 0.58 pills/day [19] and from 2.2 ± 0.6 to 2.0 ± 0.9 pills/day [24].

3.3.5. The Quality of Life. A randomized, double-blinded, double-dummy, and placebo controlled study [23] used Seattle Angina Questionnaire (SAQ) [31] and Short Form-36 (SF-36) [32] as the criteria to evaluate the efficacy of XFZYT combined with TAMs on patients with UAP after percutaneous coronary intervention (PCI). The SAQ results showed that the XFZYT combined with TAMs group could significantly improve ($P < 0.05$) the score of angina stability (AS), angina frequency (AF), and treating satisfaction (TS). And the score of body pain (BP), general health (GH), vitality (VT), social function (SF), and role emotional (RE) of the SF-36 was also significantly ($P < 0.05$) improved in the XFZYT combined with TAMs group.

3.3.6. Subgroup Analysis. For our key analysis of the add-on effect of XFZYT for treating different AP subtypes, 13 studies provided the data necessary to perform our evaluation. Of these RCTs, 1 RCT [24] involved participants with UAP, 4 RCTs [18, 21, 26, 28] involved participants with SAP, and the other 8 RCTs [17, 19, 20, 22, 25, 27, 29, 30] involved participants with SAP or UAP. Overall, (1) for patients with SAP, 94.3% reported RAS improvement after the treatment with XFZYT plus TAMs compared with 70.7% after the treatment with TAMs only (therapeutic gain = 23.6% with a number needed to treat (NNT) = 4.2) (Table 3), and 77.0%

Table 1: Characteristics of the included studies.

Study ID	AP subtypes	Criteria	Participants included (experimental/control)	Percent of male (%)	Mean age (years)	Interventional		Duration (weeks)	Outcome measures
						Experimental	Control		
Li, 2008 [21]	SAP	ISFC/WHO	40/40	67.5	63.5	XFZYT + TAMs	TAMs	4	RAS
Wang, 2011 [28]	SAP	ISFC/WHO	20/20	57.5	60.6	XFZYT + TAMs	TAMs	8	RAS, ECG, and AEs
Zhao, 2009 [26]	SAP	ISFC/WHO	30/30	45.0	58.8	XFZYT + TAMs	TAMs	4	RAS and ECG
Yang, 2010 [18]	SAP	ISFC/WHO	50/50	56.0	48.5	XFZYT + TAMs	TAMs	4	RAS, ECG, and HDL-C
Chu et al., 2009 [23]	UAP	ACCF/AHA	30/30	63.3	60.3	XFZYT + TAMs	TAMs + placebo	4	QL and AEs
Zheng and Wang, 2009 [24]	UAP	ISFC/WHO	30/30	66.7	65	XFZYT + TAMs	TAMs	8	ECG, RNU, and AEs
Lv, 2009 [22]	Both	CSC	32/30	69.4	60.9	XFZYT + TAMs	TAMs	4	RAS and ECG
Wang et al., 2000 [20]	Both	ISFC/WHO	34/27	66.7	58	XFZYT + TAMs	TAMs	4	RAS, ECG, and AEs
Du et al., 2013 [29]	Both	ISFC/WHO	92/50	62.7	65	XFZYT + TAMs	TAMs	6	RAS, HDL-C, and AEs
Wang and Jing, 2007 [19]	Both	ISFC/WHO	31/30	52.5	62.5	XFZYT + TAMs	TAMs + placebo	4	RAS, RNU, and AEs
Li and Zhang, 2011 [27]	Both	ISFC/WHO	60/60	72.5	56.3	XFZYT + TAMs	TAMs	4	RAS and ECG
Liu et al., 2007 [25]	Both	CSC	45/45	NA	NA	XFZYT + TAMs	TAMs	8	RAS and AEs
Zhang, 2012 [17]	Both	CSC	50/50	49	69.9	XFZYT + TAMs	TAMs	4	RAS, ECG, HDL-C, and AEs
Li, 2009 [30]	Both	ISFC/WHO	40/40	53.8	64.5	XFZYT + TAMs	TAMs	4	RAS, ECG, and AEs

SAP: stable angina pectoris; UAP: unstable angina pectoris; NA: not available; XFZYT: Xuefu Zhuyu Tang; TAMs: traditional antianginal medications; RAS: relief of anginal symptoms; ECG: electrocardiogram; RNU: reduction of nitroglycerin use; AEs: adverse effects; QL: quality of life; HDL-C: high-density lipoprotein cholesterol.

Table 2: Methodological quality of the included studies.

Study ID	Risk of bias for randomization	Risk of bias for concealment	Risk of bias for blinding	Risk of bias for incomplete data	Risk of bias for selective outcome reporting	Risk of bias for other problems
Li, 2008 [21]	Low risk	Uncertain	Uncertain	Low risk	Low risk	Low risk
Wang, 2011 [28]	Low risk	Uncertain	Uncertain	Low risk	Low risk	Low risk
Zhao, 2009 [26]	Low risk	Uncertain	Uncertain	Low risk	Low risk	Low risk
Yang, 2010 [18]	Low risk	Uncertain	Uncertain	Low risk	Low risk	Low risk
Chu et al., 2009 [23]	Low risk	Low risk	Low risk	Low risk	Low risk	Low risk
Zheng and Wang, 2009 [24]	Low risk	Uncertain	Uncertain	Low risk	Low risk	Low risk
Lv, 2009 [22]	Low risk	Uncertain	Uncertain	Low risk	Low risk	Low risk
Wang et al., 2000 [20]	Low risk	Uncertain	Low risk	Low risk	Low risk	Low risk
Du et al., 2013 [29]	Low risk	Uncertain	Uncertain	Low risk	Low risk	Low risk
Wang and Jing, 2007 [19]	Low risk	Low risk	Low risk	Low risk	Low risk	Low risk
Li and Zhang, 2011 [27]	Low risk	Uncertain	Uncertain	Low risk	Low risk	Low risk
Liu et al., 2007 [25]	Low risk	Low risk	Low risk	Low risk	Low risk	Low risk
Zhang, 2012 [17]	Low risk	Uncertain	Uncertain	Low risk	Low risk	Low risk
Li, 2009 [30]	Low risk	Uncertain	Low risk	Low risk	Low risk	Low risk

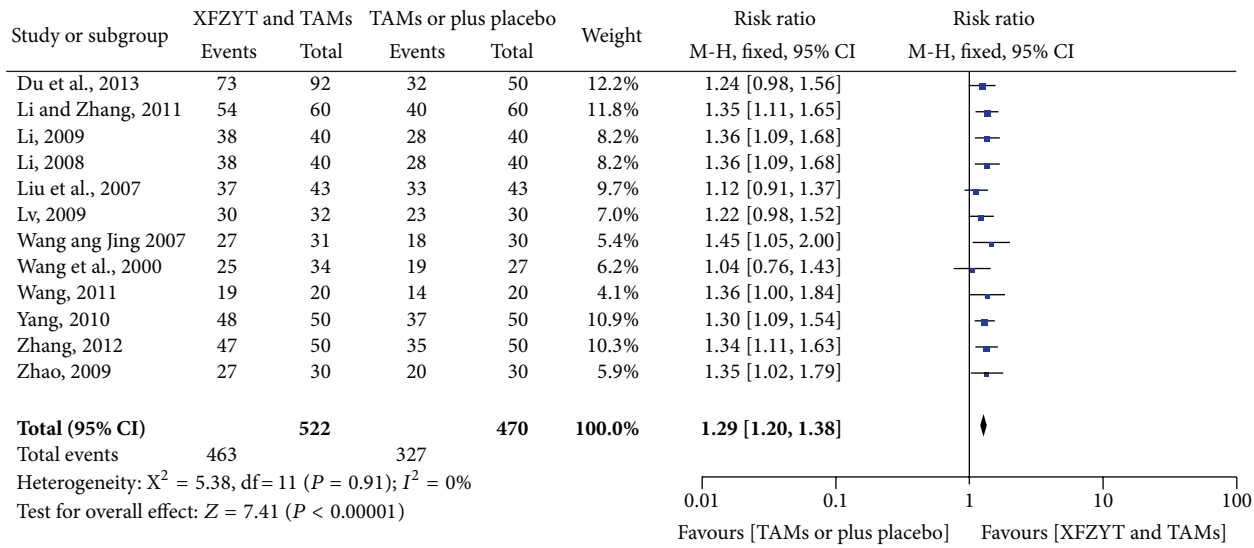

Figure 2: Forest plot of trials comparing XFZYT plus TAMs with TAMs, outcome = RAS.

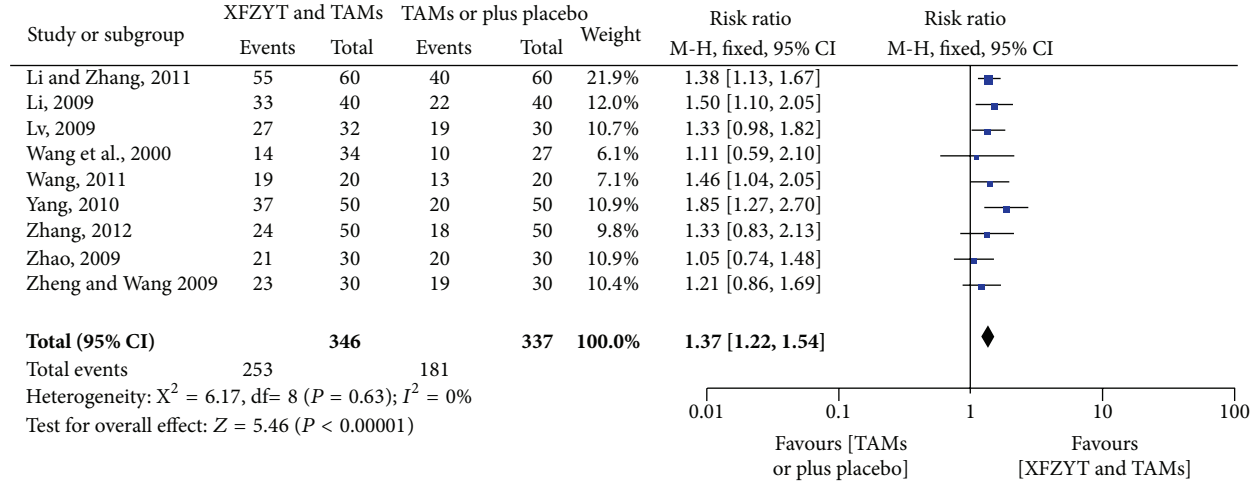

Figure 3: Forest plot of trials comparing XFZYT plus TAMs with TAMs, outcome = ECG.

compared with 45.0% in ECG improvement (therapeutic gain = 32.0% with an NNT = 3.1) (Table 4). (2) For patients with UAP, 76.7% reported ECG improvement in the experimental group compared with 63.3% in the control group (therapeutic gain = 13.4% with an NNT = 7.5) (Table 5). (3) For patients with diagnosis of either SAP or UAP, 86.6% reported RAS improvement in the experimental group compared with 69.1% in the control group (therapeutic gain = 17.5% with an NNT = 5.7) (Table 6), and ECG improvement was 70.8% versus 52.7% (therapeutic gain = 18.1% with an NNT = 5.5) (Table 7).

3.4. Publication Bias. We performed a funnel plot of the improvement of RAS between XFZYT plus TAMs group and TAMs group (Figure 8). Visual inspection suggested that there was no publication bias.

3.5. Safety. A total of 9 trials [17, 19, 20, 23–25, 28–30] mentioned the occurrence of adverse effects. 2 trials [23, 25] of these reported adverse effects in the experiment group (2%, 3/150), stomachache, dry mouth, and loose stool included. Other 2 trials [19, 24] reported adverse effects in the control group (3.3%, 4/121), including stomachache, dizziness, and headache. And the remaining 5 trials [17, 20, 28–30] reported that no adverse effects occurred. And no serious adverse effects were reported.

4. Discussions

We performed a series of meta-analyses involving 14 RCTs with a total of 1116 participants, and what we can get from this review are as follows: (1) XFZYT combined with TAMs was more effective than TAMs alone for treating patients diagnosed with AP. It could significantly improve ECG and the relief of AP symptoms. The combination therapy of XFZYT and TAMs could also reduce the nitroglycerin use, improve blood HDL-C level which benefits patients with cardiovascular diseases [33], and decrease blood LDL-C, TG,

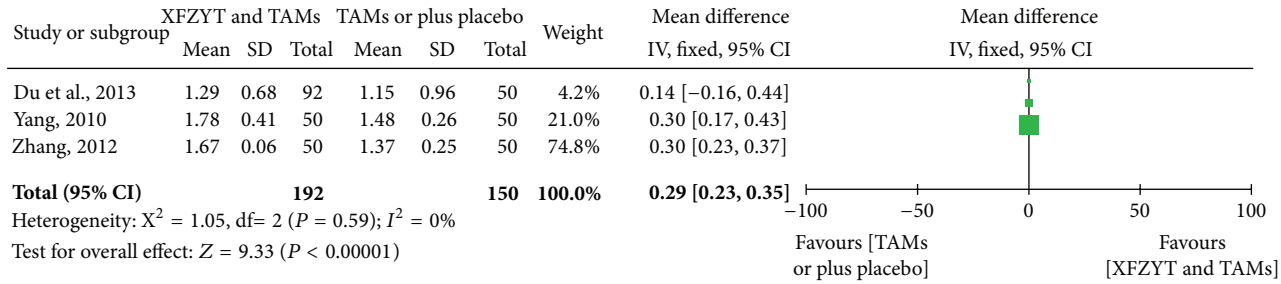

Figure 4: Forest plot of trials comparing XFZYT plus TAMs with TAMs, outcome = blood HDL-C level (mmol/L).

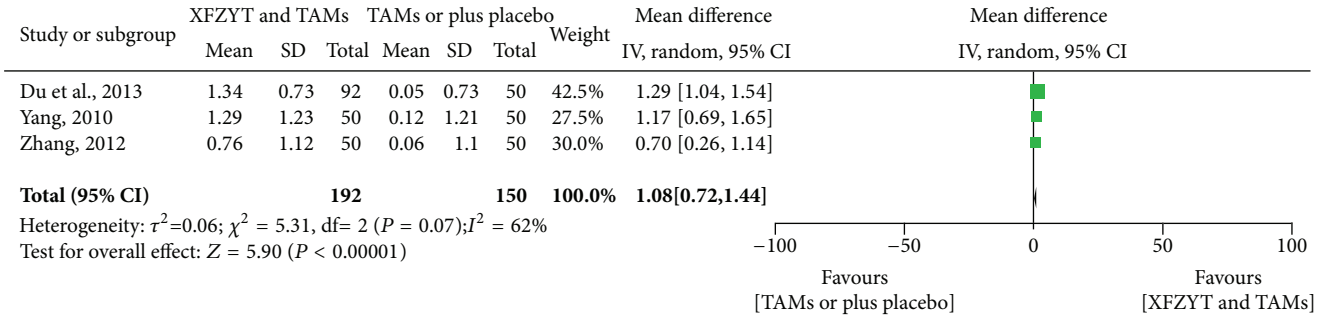

Figure 5: Forest plot of trials comparing XFZYT plus TAMs with TAMs, outcome = blood LDL-C level (mmol/L).

and TC level which seemed as risk factors of cardiovascular disease [34]. No significant differences were identified on the incidence of adverse effects between XFZYT plus TAMs and TAMs. (2) For patients with UAP, XFZYT combined with TAMs could improve ECG and quality of life in some aspects. The data of RAS was not reported, so we could not make a conclusion about the efficacy of XFZYT plus TAMs in improving RAS on patients with UAP. (3) The therapeutic gain and NNT showed that the SAP group could get more clinical benefits from the add-on effect of XFZYT than other groups. So XFZYT may be a more suitable choice for treating patients with SAP than those with UAP.

We are not able to make confident statements about the safety of XFZYT for reason of insufficient RCTs included and the short treatment duration, nor can we draw firm conclusion that XFZYT can benefit patients with UAP, for there was only one RCT [24] included into the meta-analysis and only the data of ECG improvement was reported; the NNT of the UAP group for ECG improvement (NNT = 7.5) was also larger compared with the other two groups. Although one RCT [23] with superior methodological quality showed that XFZYT can improve the quality of life of patients with UAP after PCI, more studies should be performed to confirm the efficacy of XFZYT for treating patients with UAP.

However, our meta-analysis showed that patients with SAP could get more clinical benefits such as RAS and ECG improvement from the add-on effect of XFZYT compared with the other two groups. We also found that the NNT varied from 3.7 to 32.3 for RAS improvement and from 3.6 to 23.8 for ECG improvement in the SAP and UAP group, which may be relevant to the variance in the percent of SAP of each study. But we failed to detect the correlation coefficient between the therapeutic gain and the percent of SAP, due to the fact that the number of patients with SAP in each included study was not reported. So the future studies should pay attention to the difference of the outcomes between SAP and UAP patients after the treatment with XFZYT, which may have important implication for clinical practice.

There are also limitations to this study. Visual inspection of the funnel plot revealed symmetry, so the publication bias may be minimized. But the methodological quality of the trials included was generally not high; only 3 [19, 23, 25] of these RCTs were scored as having superior quality. And only two RCTs [19, 23] mentioned allocation concealment process, so the potential selection bias may exist. A few trials mentioned the blinding and withdrawal/dropout, and no multicenter, large sample, and cooperative RCTs were included. Apart from the limitations on the mediocre methodological quality of included studies, for outcome measures of patients with UAP, only the quality of life and ECG improvement were reported, and the estimates of some outcomes, such as the blood lipid level and reduction of nitroglycerin use, were limited by relatively small sample size, which may influence the precision of estimates.

5. Conclusion

In summary, these data suggest that XFZYT combined with TAMs is more effective than TAMs alone at improving the clinical symptoms of patients with AP, especially with SAP. And there is no significant difference in the incidence of adverse effects. XFZYT combined with TAM may be an alternative option for patients suffering from AP. However, most

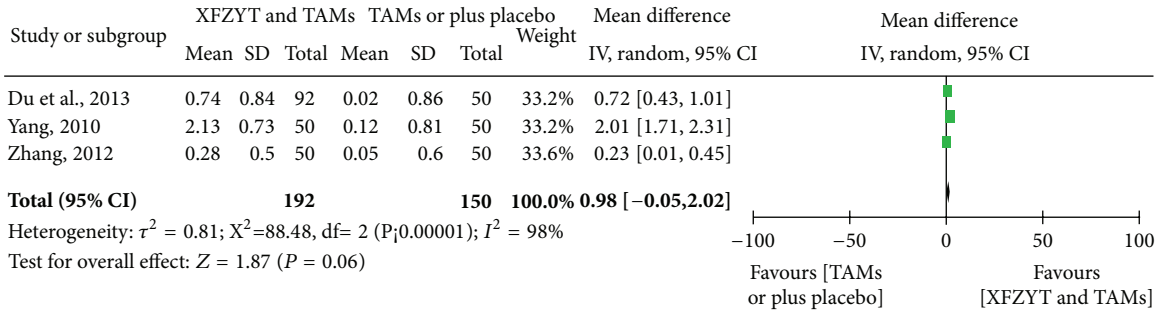

Figure 6: Forest plot of trials comparing XFZYT plus TAMs with TAMs, outcome = blood TG level (mmol/L).

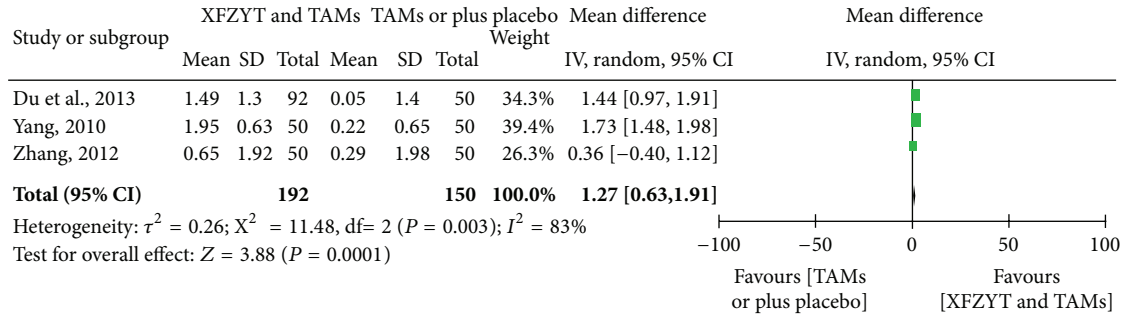

Figure 7: Forest plot of trials comparing XFZYT plus TAMs with TAMs, outcome = blood TC level (mmol/L).

Table 3: The effect of XFZYT for SAP group, outcome = RAS.

Study ID	Treatment duration	Response rate, %; (response/N)		Therapeutic gain, %	NNT	RR
		Experimental	Control			
Li, 2008 [21]	4 weeks	95.0 (38/40)	70.0 (28/40)	25.0	4.0	1.36
Wang, 2011 [28]	8 weeks	95.0 (19/20)	70.0 (14/20)	25.0	4.0	1.36
Zhao, 2009 [26]	4 weeks	90.0 (27/30)	66.7 (20/30)	23.3	4.3	1.35
Yang, 2010 [18]	4 weeks	96.0 (48/50)	74.0 (37/50)	22.0	4.5	1.30
Pooled RR	—	94.3 (132/140)	70.7 (99/140)	23.6	4.2	1.33

NNT: number needed to treat; RR: risk ratio.

Table 4: The effect of XFZYT for SAP group, outcome = ECG.

Study ID	Treatment duration	Response rate, %; (response/N)		Therapeutic gain, %	NNT	RR
		Experimental	Control			
Li, 2008 [21]	4 weeks	NA	NA	—	—	—
Wang, 2011 [28]	8 weeks	95.0 (19/20)	65.0 (13/20)	30.0	3.3	1.46
Zhao, 2009 [26]	4 weeks	70.0 (21/30)	40.0 (12/30)	30.0	3.3	1.75
Yang, 2010 [18]	4 weeks	74.0 (37/50)	40.0 (20/50)	34.0	2.9	1.85
Pooled RR	—	77.0 (77/100)	45.0 (45/100)	32.0	3.1	1.71

NNT: number needed to treat; NA: not available; RR: risk ratio.

Table 5: The effect of XFZYT for UAP group, outcome = ECG.

Study ID	Treatment duration	Response rate, %; (response/N)		Therapeutic gain, %	NNT	RR
		Experimental	Control			
Zheng and Wang, 2009 [24]	8 weeks	76.7 (23/30)	63.3 (19/30)	13.4	7.5	1.21
Pooled RR	—	76.7 (23/30)	63.3 (19/30)	13.4	7.5	1.21

NNT: number needed to treat; RR: risk ratio.

Table 6: The effect of XFZYT for SAP and UAP group, outcome = RAS.

Study ID	Treatment duration	Response rate, %; (response/N)		Therapeutic gain, %	NNT	RR
		Experimental	Control			
Lv, 2009 [22]	4 weeks	93.8 (30/32)	76.7 (23/30)	17.1	5.8	1.22
Wang et al., 2000 [18]	4 weeks	73.5 (25/34)	70.4 (19/27)	3.1	32.3	1.04
Du et al., 2013 [29]	6 weeks	79.3 (73/92)	64.0 (32/50)	15.3	6.5	1.24
Wang and Jing, 2007 [19]	4 weeks	87.1 (27/31)	60.0 (18/30)	27.1	3.7	1.45
Li and Zhang, 2011 [27]	4 weeks	90.0 (54/60)	66.7 (40/60)	23.3	4.3	1.35
Liu et al., 2007 [25]	8 weeks	86.0 (37/43)	76.7 (33/43)	9.4	10.6	1.12
Zhang, 2012 [17]	4 weeks	94.0 (47/50)	70.0 (35/50)	24.0	4.2	1.34
Li, 2009 [30]	4 weeks	95.0 (38/40)	70.0 (28/40)	25.0	4.0	1.36
Pooled RR	—	86.6 (331/382)	69.1 (228/330)	17.5	5.7	1.25

NNT: number needed to treat; RR: risk ratio.

Table 7: The effect of XFZYT for SAP and UAP group, outcome = ECG.

Study ID	Treatment duration	Response rate, %; (response/N)		Therapeutic gain, %	NNT	RR
		Experimental	Control			
Lv, 2009 [22]	4 weeks	84.4 (27/32)	63.3 (19/30)	21.1	4.7	1.33
Wang et al., 2000 [18]	4 weeks	41.2 (14/34)	37.0 (10/27)	4.2	23.8	1.11
Du et al., 2013 [29]	6 weeks	NA	NA	—	—	—
Wang and Jing, 2007 [19]	4 weeks	NA	NA	—	—	—
Li and Zhang, 2011 [27]	4 weeks	91.7 (55/60)	66.7 (40/60)	25.0	4.0	1.37
Liu et al., 2007 [25]	8 weeks	NA	NA	—	—	—
Zhang, 2012 [17]	4 weeks	48.0 (24/50)	36.0 (18/50)	12.0	8.3	1.33
Li, 2009 [30]	4 weeks	82.5 (33/40)	55.0 (22/40)	27.5	3.6	1.50
Pooled RR	—	70.8 (153/216)	52.7 (109/207)	18.1	5.5	1.34

NNT: number needed to treat; NA: not available; RR: risk ratio.

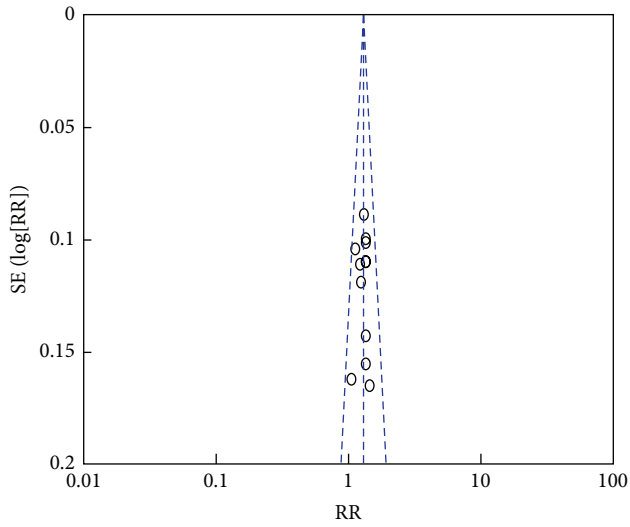

Figure 8: Funnel plot of trials comparing XFZYT plus TAMs with TAMs, outcome = RAS.

of included RCTs were scored as having mediocre methodological quality; the findings should be interpreted with caution. Hence, future studies of XFZYT in the treatment of AP are warranted in rigorously designed, multicentre, and large-scale trials worldwide.

Conflict of Interests

All the authors declare that there is no conflict of interests.

Authors' Contribution

L. X. Yuan contributed to the design of the study and analytic strategy; G. Z. Yi, Y. Q. Qiu, and Y. Xiao searched the literature and extracted the data; G. Z. Yi analyzed the data and wrote the paper.

Acknowledgment

All the authors are indebted to the authors of the primary studies.

References

[1] *Global Status Report on Noncommunicable Diseases 2010*, World Health Organization, Geneva, Switzerland, 2011, http://www.who.int/nmh/publications/ncd_report2010/en/.

[2] World Health Organization, *Global Atlas on Cardiovascular Disease Prevention and Control*, WHO, Geneva, Switzerland, 2011.

[3] H. H. Gray, R. A. Henderson, M. A. de Belder, S. R. Underwood, and A. J. Camm, "Early management of unstable angina and non-ST-segment elevation myocardial infarction: summary of NICE guidance," *Heart*, vol. 96, no. 20, pp. 1662–1668, 2010.

[4] R. A. Henderson and N. O'Flynn, "Management of stable angina: summary of NICE guidance," *Heart*, vol. 98, no. 6, pp. 500–507, 2012.

[5] R. Parikh and P. J. Kadowitz, "Angina pectoris: current therapy and future treatment options," *Expert Review of Cardiovascular Therapy*, vol. 12, no. 2, pp. 175–186, 2014.

[6] W. Hueb, P. R. Soares, B. J. Gersh et al., "The medicine, angioplasty, or surgery study (MASS-II): a randomized, controlled clinical trial of three therapeutic strategies for multivessel coronary artery disease: one-year results," *Journal of the American College of Cardiology*, vol. 43, no. 10, pp. 1743–1751, 2004.

[7] H. F. Wang, H. Shi, and Y. Xia, "Research progress of Xuefu Zhuyu decoction in the treatment of Cardiovascular and Cerebrovascular Disease," *China Journal of Chinese Medicine*, vol. 28, no. 11, pp. 1732–1734, 2013.

[8] D. Su and L. Yao, "Modern pharmacological research of xuefu zhuyu decoction," *Acta Chinese Medicine and Pharmacology*, vol. 41, no. 3, pp. 172–175, 2013.

[9] W. L. Shi, J. S. Zhang, Y. Q. Hu et al., "The research of clinical application and mechanism of Xuefu Zhuyu Tang in preventing and treating vascular disease," *Chinese Journal of Integrated Traditional and Western Medicine*, vol. 33, no. 5, pp. 712–716, 2013.

[10] X. Wu, "Progress of clinical and experimental study on the application of Xuefu Zhuyu Tang," *CJGMCM*, vol. 28, no. 3, pp. 635–637, 2013.

[11] E. Braunwald, E. M. Antman, J. W. Beasley et al., "ACC/AHA guidelines for the management of patients with unstable angina and non-ST-segment elevation myocardial infarction: executive summary and recommendations: a report of the American College of Cardiology/American Heart Association task force on practice guidelines (committee on the management of patients with unstable angina)," *Circulation*, vol. 102, no. 10, pp. 1193–1209, 2000.

[12] "Nomenclature and criteria for diagnosis of ischemic heart disease. Report of the Joint International Society and Federation of Cardiology/World Health Organization task force on standardization of clinical nomenclature," *Circulation*, vol. 59, no. 3, pp. 607–609, 1979.

[13] "Recommendations for the diagnosis and treatment of unstable angina pectoris," *Chinese Journal of Cardiology*, vol. 28, no. 6, pp. 8–11, 2000.

[14] "Guideline for the diagnosis and treatment of stable angina pectoris," *Chinese Journal of Cardiology*, vol. 28, no. 3, pp. 195–206, 2007.

[15] "The curative effect standard for angina pectoris symptoms and ECG (Symposium of integrated traditional Chinese and Western medicine for treatment of angina pectoris of coronary heart disease and arrhythmia, 1979,Shanghai)," *Chinese Pharmaceutical Affairs*, vol. 1, no. 2, pp. 17–20, 1987.

[16] J. Higgins and S. Green, *Cochrane Handbook for Systematic Reviews of Interventions*, Version 5.1.0, The Cochrane Collaboration, 2011, http://handbook.cochrane.org/.

[17] S. J. Zhang, "Comparative study of the efficacy of different formulations of traditional Chinese medicine in the treatment of blood stasis type of unstable angina," *China Modern Medicine*, vol. 19, no. 18, pp. 11–13, 2012.

[18] Y. J. Yang, "Shenqi Zhuyu Decoction: clinical observation of 50 cases with western medicine in the treatment angina pectoris of coronary heart disease," *Journal of Sichuan of Traditional Chinese Medicine*, vol. 28, no. 7, pp. 63–65, 2010.

[19] J. Wang and L. Jing, "Clinical research of compound Chinese medicine based on combination of disease and syndrome," *World Science and Technology Modernization of Traditional Chinese Medicine and Materia Medica*, vol. 9, no. 1, pp. 16–20, 2007.

[20] W. Wang, X. C. Ma, X. F. Wang et al., "Clinical observation on 30 cases of refined Xuefu Zhuyu Capsule in treatment of angina pectoris of coronary heart disease," *Journal of Traditional and Complementary Medicine*, vol. 41, no. 8, pp. 471–473, 2000.

[21] D. B. Li, "Clinical observation of combined with Xuefu Zhuyu Capsule in treatment of angina pectoris of coronary heart disease in 40 cases," *Beijing Journal of Traditional Chinese Medicine*, vol. 27, no. 10, pp. 810–811, 2008.

[22] G. Lv, "Combined with Zhuyu Decoction in treating stasis angina pectoris of coronary heart disease 32 cases," *Guangxi Journal of Traditional Chinese Medicine*, vol. 32, no. 6, pp. 35–36, 2009.

[23] F.-Y. Chu, J. Wang, X.-W. Sun et al., "A randomized double-blinded controlled trial of Xuefu Zhuyu Capsule on short-term quality of life in unstable anginal patients with blood-stasis syndrome after percutaneous coronary intervention," *Journal of Chinese Integrative Medicine*, vol. 7, no. 8, pp. 729–735, 2009.

[24] G.-L. Zheng and S.-H. Wang, "Clinical effect and mechanismn of xuefu zhuyu capsule in treating unstable angina pectoris," *CJITWM*, vol. 29, no. 1, pp. 65–68, 2009.

[25] J. G. Liu, H. Xu, G. J. Dong et al., "Effect of Xuefu Zhuyu oral liquid on expression of activation molecules of platelet in patients with coronary heart disease and angina pectoris," *Journal of Changchun University of Traditional Chinese Medicine*, vol. 23, no. 1, pp. 29–31, 2007.

[26] S. L. Zhao, "60 cases observation of Xuefu Zhuyu Tang on clinical curative effect and coagulation index of patients with angina pectoris," in *Proceedings of the 3rd Academic Conference on Thrombotic Disease of Traditional Chinese Medicine Association*, Thrombus Disease Branch of Chinese Medicine Association, 2009.

[27] J. L. Li and Q. M. Zhang, "The curative effect Xuefu Zhuyu Decoction in treating coronary heart disease and angina pectoris: observation of 60 cases," *Chinese Journal of Integrative Medicine on Cardio-/Cerebrovascular Disease*, vol. 9, no. 12, pp. 1412–1413, 2011.

[28] C. X. Wang, *The clinic study on curative effect of the Xuefu Zhuyu Decoction with isosorbide mononitrate in treating angina pectoris [Dissertation, thesis]*, Nanjing University of Chinese Medicine, 2011.

[29] Z. L. Du, D. L. Chen, and J. L. Chen, "Random Parallel Study of Xuefu Zhuyu Tang combined with Western Medicine in the treatment of coronary heart disease and angina pectoris," *Journal of Practical Traditional Chinese Internal Medicine*, vol. 27, no. 2, pp. 85–87, 2013.

[30] G. C. Li, "Observation of the curative effect of Xuefu Zhuyu Tang on treating coronary heart disease and angina pectoris," *Henan Traditional Chinese Medicine*, vol. 29, no. 12, pp. 1226–1227, 2009.

[31] J. A. Spertus, J. A. Winder, T. A. Dewhurst et al., "Development and evaluation of the Seattle Angina Questionnaire: a new functional status measure for coronary artery disease," *Journal of the American College of Cardiology*, vol. 25, no. 2, pp. 333–341, 1995.

[32] C. Jenkinson, L. Wright, and A. Coulter, "Criterion validity and reliability of the SF-36 in a population sample," *Quality of Life Research*, vol. 3, no. 1, pp. 7–12, 1994.

[33] G. Rajagopal, V. Suresh, and A. Sachan, "High-density lipoprotein cholesterol: how High," *Indian Journal of Endocrinology and Metabolism*, vol. 16, no. 2, pp. 236–238, 2012.

[34] J. Nuotio, M. Oikonen, C. G. Magnussen et al., "Cardiovascular risk factors in 2011 and secular trends since 2007: The Cardiovascular Risk in Young Finns Study," *Scandinavian Journal of Public Health*, 2014.

Hindawi Publishing Corporation
Evidence-Based Complementary and Alternative Medicine
Volume 2014, Article ID 149195, 10 pages
http://dx.doi.org/10.1155/2014/149195

Research Article

Ginsenoside Rb1 Protects Neonatal Rat Cardiomyocytes from Hypoxia/Ischemia Induced Apoptosis and Inhibits Activation of the Mitochondrial Apoptotic Pathway

Xu Yan,[1,2] Jinwen Tian,[3] Hongjin Wu,[1] Yuna Liu,[4] Jianxun Ren,[4] Sidao Zheng,[4] Chengying Zhang,[4] Cui Yang,[4] Yang Li,[3] and Shengqi Wang[5]

[1] *Beijing Haidian Hospital (Haidian Section of Peking University Third Hospital), 29 Zhongguancun Dajie, Haidian District, Beijing 100080, China*
[2] *Postdoctoral Workstation of the Zhongguancun Haidian Science Park, NO. 6, Sijiqing Road, Haidian District, Beijing 100195, China*
[3] *Institute of Geriatric Cardiology, The General Hospital of People's Liberation Army, 28 Fuxing Road, Beijing 100853, China*
[4] *Beijing Hospital of Integrated Traditional Chinese and Western Medicine, Dongjie 3, Yongding Road, Haidian District, Beijing 100039, China*
[5] *Beijing Institute of Radiation Medicine, Beijing 100850, China*

Correspondence should be addressed to Hongjin Wu; whjyuanzhang@aliyun.com

Received 1 April 2014; Revised 2 June 2014; Accepted 23 June 2014; Published 10 July 2014

Academic Editor: Ke-Ji Chen

Aim. To investigate the effect of Ginsenoside Rb1 (GS-Rb1) on hypoxia/ischemia (H/I) injury in cardiomyocytes *in vitro* and the mitochondrial apoptotic pathway mediated mechanism. *Methods*. Neonatal rat cardiomyocytes (NRCMs) for the H/I groups were kept in DMEM without glucose and serum, and were placed into a hypoxic jar for 24 h. GS-Rb1 at concentrations from 2.5 to 40 μM was given during hypoxic period for 24 h. NRCMs injury was determined by MTT and lactate dehydrogenase (LDH) leakage assay. Cell apoptosis, ROS accumulation, and mitochondrial membrane potential (MMP) were assessed by flow cytometry. Cytosolic translocation of mitochondrial cytochrome c and Bcl-2 family proteins were determined by Western blot. Caspase-3 and caspase-9 activities were determined by the assay kit. *Results*. GS-Rb1 significantly reduced cell death and LDH leakage induced by H/I. It also reduced H/I induced NRCMs apoptosis induced by H/I, in accordance with a minimal reactive oxygen species (ROS) burst. Moreover, GS-Rb1 markedly decreased the translocation of cytochrome c from the mitochondria to the cytosol, increased the Bcl-2/Bax ratio, and preserved mitochondrial transmembrane potential ($\Delta\Psi$m). Its administration also inhibited activities of caspase-9 and caspase-3. *Conclusion*. Administration of GS-Rb1 during H/I *in vitro* is involved in cardioprotection by inhibiting apoptosis, which may be due to inhibition of the mitochondrial apoptotic pathway.

1. Introduction

Myocardial ischemic injury resulting from severe impairment of the coronary blood supply is a severe stress that leads to the loss of cardiomyocytes by apoptosis and necrosis. Activation of the mitochondrial apoptotic pathway is seen as a common cause of cell death in numerous cardiac diseases [1, 2]. The mitochondrial apoptotic pathway is characterized by mitochondrial dysfunction with release of caspase activators, including mitochondrial permeability transition pore (mPTP) opening, loss of mitochondrial transmembrane potential ($\Delta\Psi$m), cytochrome c release, and changes in Bcl2/Bax ratio, which are followed by activation of caspase-9 and caspase-3 [3, 4]. Specific inhibition of the mitochondrial apoptotic pathway could protect cardiomyocytes from injuries, which implies that mitochondria could be a critical site for intervention [5, 6].

Ginseng, the root of *Panax ginseng* Meyer, has been widely used for more than 2,000 years in China. [7]. Its beneficial effects act on the endocrine, immune, central nervous and, especially, the cardiovascular systems [8]. Ginsenoside Rb1 (GS-Rb1), the major pharmacological extract, is one of

the most important active compounds of ginseng, with extensive evidence of its cardioprotective properties. GS-Rb1 can protect cardiomyocytes from H_2O_2 induced oxidative injury by suppressing JNK activation [9]. It can exert its cardioprotective effect against ischemia reperfusion (MI/R) injury in diabetic rats by activation of the phosphatidylinositol 3-kinase (PI3 K)/Akt pathway [10], and GS-Rb1 preconditioning can enhance eNOS expression and attenuate myocardial ischemia/reperfusion injury in diabetic rats [11]. However, the specific mechanisms of cardioprotective properties of GS-Rb1 in a hypoxic environment *in vitro* and the changes of the anti- and proapoptotic proteins involved need clarification.

In the present research, we have investigated the protective effect of GS-Rb1 and its impact on the mitochondrial apoptotic pathway, in neonatal rat cardiomyocytes (NRCMs) exposed to hypoxic/ischemic damage. It had antiapoptotic activity under the hypoxic/ischemic conditions *in vitro* and inhibited activation of the mitochondrial apoptotic pathway.

2. Materials and Methods

2.1. Materials. GS-Rb1 (catalog number #110704), purchased from National Institutes for food and drug Control, was dissolved in phosphate-buffered saline (PBS) to create a stock solution for subsequent dilution. Dulbecco's Modified Eagle Medium (DMEM) and fetal bovine serum (FBS) were obtained from Gibco (Grand Island, NY, USA). DMSO and 3-(4, 5-dimethyl-thiazol-2-yl)-2, 5-diphenyltetrazolium-bromide (MTT) were obtained from Sigma (St.Louis, MO, USA). Cell Lysis Buffer for Western blotting and IP and Enhanced BCA Protein Assay Kit were obtained from Beyotime (Haimen, China). The primary antibodies against Bcl-2 (catalog number #2870), Bax (catalog number #2772), cytochrome c (catalog number #4272), GAPDH (catalog number #2118), and horseradish peroxidase (HRP)-conjugated secondary antibodies were obtained from Cell Signaling Technology (Danvers, MA, USA). Enhanced chemiluminescence kit was obtained from Millipore (Billerica, MA, USA).

2.2. Culture of Neonatal Rat Cardiomyocytes. Primary cultures of NRCMs from 12 to 24 h old Sprague Dawley rats (Vital River Laboratories, Beijing, China) were prepared by means of gentle serial trypsinization as described before with slight modification [12]. All experiments were approved by the Beijing Ethics Committee for the Use of Experimental Animals. The NRCMs were plated in collagen-coated 96- or 6-well plates and maintained at 37°C in a 5% CO_2/95% air humidified incubator in DMEM containing 10% (v/v) fetal bovine serum, 100 U/mL penicillin, and 100 mg/mL streptomycin. The following experiments used spontaneously beating cardiomyocytes 48–72 h after plating.

2.3. Hypoxia/Ischemia Treatment. For hypoxic/ischemic protocol, hypoxia was achieved by using the MGC AnaeroPack System in a AnaeroPack jar (Mitsubishi Gas Chemical Co., Tokyo, Japan), which was capable of depleting the concentration of O_2 down to 10% in 2 h. Ischemic condition was achieved by replacing culture medium with DMEM without glucose (Gibco, Grand Island, USA) and serum. NRCMs with or without GS-Rb1 were placed in the AnaeroPack jar and then put into a 37°C incubator for 24 h. Control plates were kept in normoxic conditions for the corresponding times.

2.4. MTT Assay. NRCMs viability was determined using the MTT assay. Cardiomyocytes were plated on 96-well dishes at 2×10^4 cells/well. MTT at 5 mg/mL was added to each well immediately after 24 h of hypoxia/ischemia. Plates were incubated for 4 h at 37°C. The medium was aspirated from each well and 100 μL of DMSO was added to dissolve the formazan crystals. The optical density of each well was read at 492 nm using a Microplate Reader (Bio-Rad, Hercules, CA). Results are given as percentages of the control group taken as 100%.

2.5. Assay of LDH Activity. The extent of cellular injury was monitored by LDH leakage. Culture medium (120 μL) was taken to measure LDH activity using a commercial kit with a spectrophotometer (JianCheng Bioengineering Institute, Nanjing, China).

2.6. Apoptosis Assay by Annexin V/PI Staining. NRCMs with different concentration of GS-Rb1 exposed to hypoxia/ischemia conditions were harvested and washed with PBS. The percentage of normal nonapoptotic cells and apoptotic cells was measured by double supravital staining with Annexin-V and PI, using an Annexin V-FITC Apoptosis Detection kit (KeyGen, Nanjing, China). Flow cytometric analysis used a Cytomics FC500 flow cytometer with CXP software (Beckman Coulter, Fullerton, USA), the operator being blind of the group assignment.

2.7. Fluorescent Measurement of Intracellular ROS. Determination of ROS concentration was based on the oxidation of 2,7-dichlorodihydrofluorescein (DCFH) (JianCheng Bioengineering Institute, Nanjing, China). In brief, the cells were collected after hypoxia/ischemia and washed with DMEM without FBS and incubated with DCFH-DA at 37°C for 20 min. Dichlorofluorescein (DCF) fluorescence intensity was detected at 488 nm excitation and 525 nm emission by flow cytometry and the mean fluorescence intensity used to represent the amount of ROS.

2.8. Determination of $\Delta\Psi m$. The mitochondrial transmembrane potential ($\Delta\Psi$m) was estimated by monitoring fluorescence aggregates of 5,5′,6,6′-tetrachloro-1,1′,3,3′-tetraethyl benzimidazolo carbocyanine iodide (JC-1), (Beyotime, Haimen, China). Briefly, NRCMs were collected and incubated at 37°C for 30 min with JC-1 (1×), washed twice with PBS for detection of the fluorescent ratio by flow cytometry. JC-1 fluorescence was measured to assess the emission shift from green (530 nm) to red (590 nm) using 488 nm excitation. Data are given as the relative ratio of green to red fluorescence intensity, indicating the level of depolarization of the mitochondrial membrane potential.

2.9. Isolation of Mitochondria. Cytochrome c release from mitochondria was measured by Western blotting. The preparation of the mitochondrial and cytosolic protein fractions was done with a Cell Mitochondria Isolation Kit (Beyotime, Haimen, China). Briefly, cells were collected and resuspended

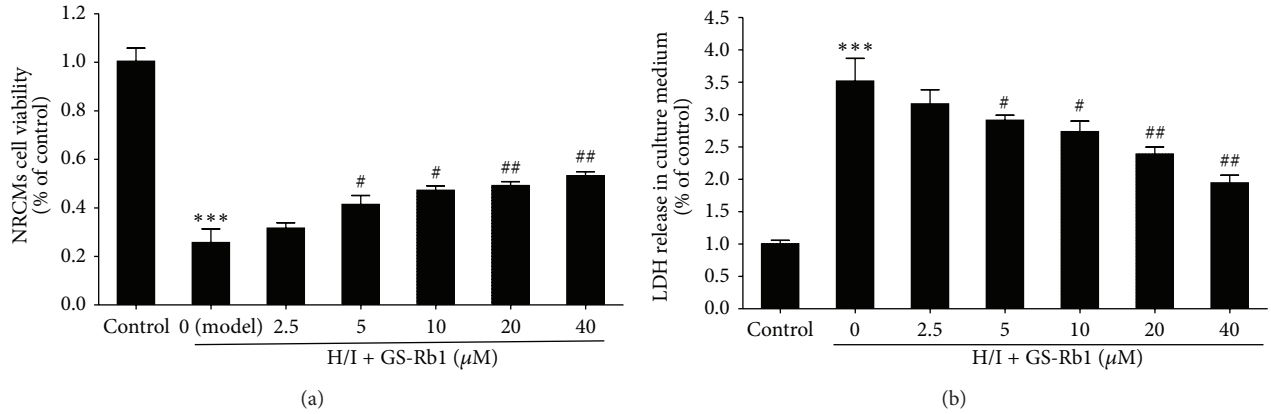

Figure 1: Protective effect of GS-Rb1 on H/I induced NRCMs death. NRCMs were copretreated with or without GS-Rb1 during H/I condition for 24 h. (a) Cell viability determined by MTT assay. (b) LDH release determined by the LDH activity kit. Error bars represent mean ± SD. $^{***}P < 0.001$ versus control; $^{\#}P < 0.05$ and $^{\#\#}P < 0.01$ versus H/I group ($n = 3$).

in mitochondrial isolation reagent containing PMSF and protease inhibitors, centrifuged at 600 ×g for 10 min at 4°C. The supernatant was transferred to a fresh 1.5 mL microcentrifuge tube and centrifuged at 11,000 ×g for 10 min at 4°C. The supernatant was collected as the cytosolic fraction and the pellet was resuspended in 0.1 mL mitochondrial lysis buffer, which was kept as the mitochondrial fraction.

2.10. Western Blotting. The mitochondria and NRCMs with under hypoxic and ischemic conditions treated with different concentrations of GS-Rb1 for 24 h were harvested and lysed with Cell Lysis Buffer for Western blotting and IP. Protein concentration was measured using a BCA Protein Assay Kit. Equal amounts of sample lysate were separated by sodium dodecyl sulfate polyacrylamide gel electrophoresis (SDS-PAGE) and transferred by electroblotting to a nitrocellulose membrane (Millipore). The membrane was blocked with 5% nonfat milk in TBST buffer (20 mM Tris-HCl, pH 7.4, 150 mM NaCl and 0.1% Tween 20) overnight at 4°C. The membrane was incubated with specific primary antibodies for 2 h and an IgG HRP conjugated specific secondary antibody for 1 h at room temperature. The signals were visualized with an enhanced chemiluminescence (ECL) kit (Pierce) on Syngene G: BOX Chemi gel documentation system (Syngene, Cambridge, UK). Densitometric values were normalized using GAPDH in each group as an internal control.

2.11. In Vitro Caspase-3 and Caspase-9 Activity Assay. Caspase activities was measured by Caspase-3 and Caspase-9 Activity Assay Kit (Beyotime, Haimen, China). Briefly, NRCMs lysates were prepared after treatment with different dose of GS-Rb1 for 24 h under hypoxia/ischemia conditions. Assays were performed on 96-well microtitre plates by incubating 10 μL protein cell lysate per sample in 80 μL reaction buffer containing 10 μL substrate (Asp-Glu-Val-Asp (DEVD)-p-nitroaniline (pNA) for caspase-3, and Leu-Glu-His-Asp (LEHD)-pNA for caspase-9, 2 mM). Lysates were incubated at 37°C for 4–6 h. Samples were measured with a Microplate Reader (Bio-Rad, Hercules, CA) at an absorbance of 405 nm. Caspase activity was expressed as the percentage relative to the control group.

2.12. Statistical Analysis. Data are expressed as the mean ± SD of at least three independent experiments. Group results were analysed for variance using ANOVA. Two groups were compared by Student's t-test. All analyses used GraphPad Prism 5.0 software. $P < 0.05$ was taken as statistically significant.

3. Results

3.1. Effect of GS-Rb1 on the Viability of NRCMs. The effect of GS-Rb1 on NRCMs viability was examined by the MTT assay (Figure 1(a)). Those given H/I accounted for 25% of the normal control cells ($P < 0.001$). Compared with the control group, GS-Rb1 from 2.5 to 40 μM incubation increased viability from 31.7%±1.3% to 53.3%±1.7%. GS-Rb1 alone had no effect on cell viability.

3.2. Effect of GS-Rb1 on the LDH Leakage Induced by H/I. H/I treatment increased LDH leakage from NRCMs by 3.5 ± 0.2-fold in comparison with the control group. GS-Rb1 incubation significantly reduced leakage induced to 1.9±0.12-fold (Figure 1(b)).

3.3. GS-Rb1 Reduced Apoptotic Cells Induced by H/I in NRCMs. To examine the effect of GS-Rb1 on the cell death induced by H/I, Annexin V-fitc/propidium iodide (PI) double-staining assay of cells was analyzed by flow cytometry (Figures 2(a) and 2(b)). The percentage of apoptotic cells (including early and late apoptotic cells) markedly increased in H/I group compared to the control group. With GS-Rb1, apoptosis accounted for 70.4 ± 2.4, 56.5 ± 1.7, and 31.0 ± 1.8% at 10, 20, and 40 μM GS-Rb1 for 24 h, respectively, with the surviving cells increasing from 6.8 ± 0.4 to 52.8 ± 3.1%.

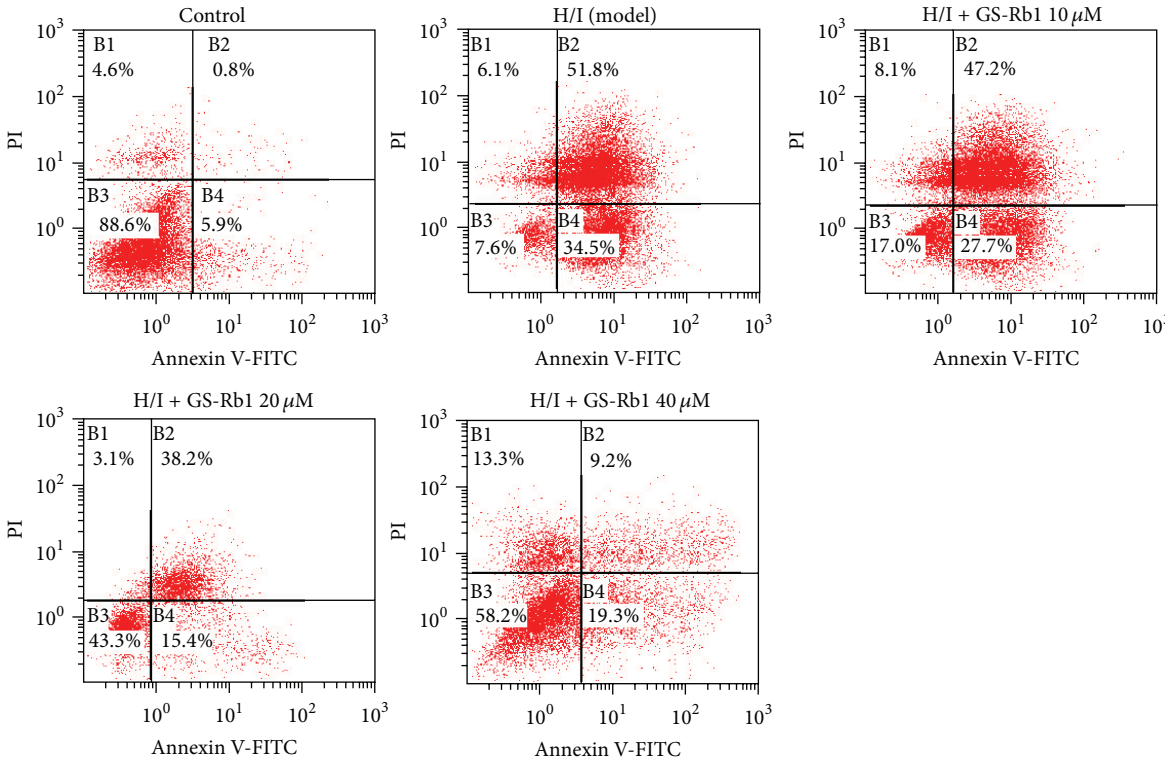

(a)

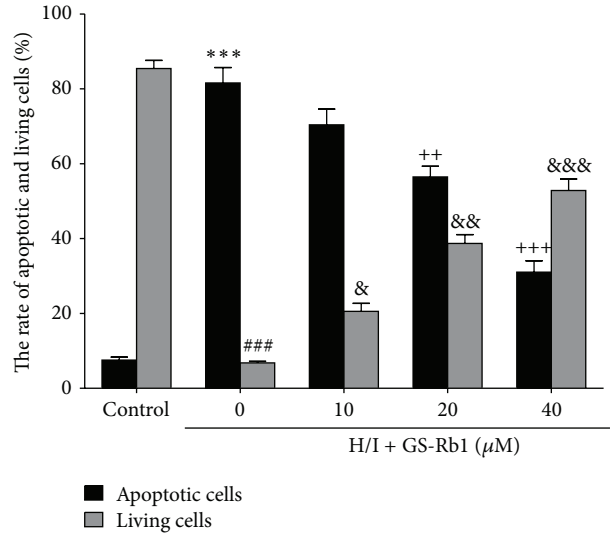

(b)

Figure 2: Flow cytometry analysis of GS-Rb1 on cell death induced by H/I. (a) NRCMs were cotreated with or without GS-Rb1 (10, 20, and 40 μM) during H/I, for 24 h, and stained with Annexin V-fitc/PI. (b) Quantification of the percent of apoptotic and living cells in each group. Error bars represent mean ± SD. $^{***}P < 0.001$ versus apoptotic cells in control group; $^{\#\#\#}P < 0.001$ versus living cells in control group; $^{++}P < 0.01$ and $^{+++}P < 0.001$ versus apoptotic cells in H/I group; $^{\&}P < 0.05$, $^{\&\&}P < 0.01$, and $^{\&\&\&}P < 0.001$ versus living cells in H/I group ($n = 3$).

3.4. Effect of GS-Rb1 on the Intracellular ROS Level in NRCMs. Cells in different groups were harvested and stained with fluorescent probe DCFH before being analyzed by flow cytometry. H/I treatment significantly increased the intracellular level of ROS, with the fluorescence intensity increasing from 9.3 ± 0.9 to 313.3 ± 11.9 (Figures 3(a) and 3(b)). Cotreatment with GS-Rb1 significantly inhibited the raised intracellular concentration of ROS induced by H/I. These results indicate that the cardioprotective effect of GS-Rb1 from H/I injury is associated with the inhibition of cellular ROS.

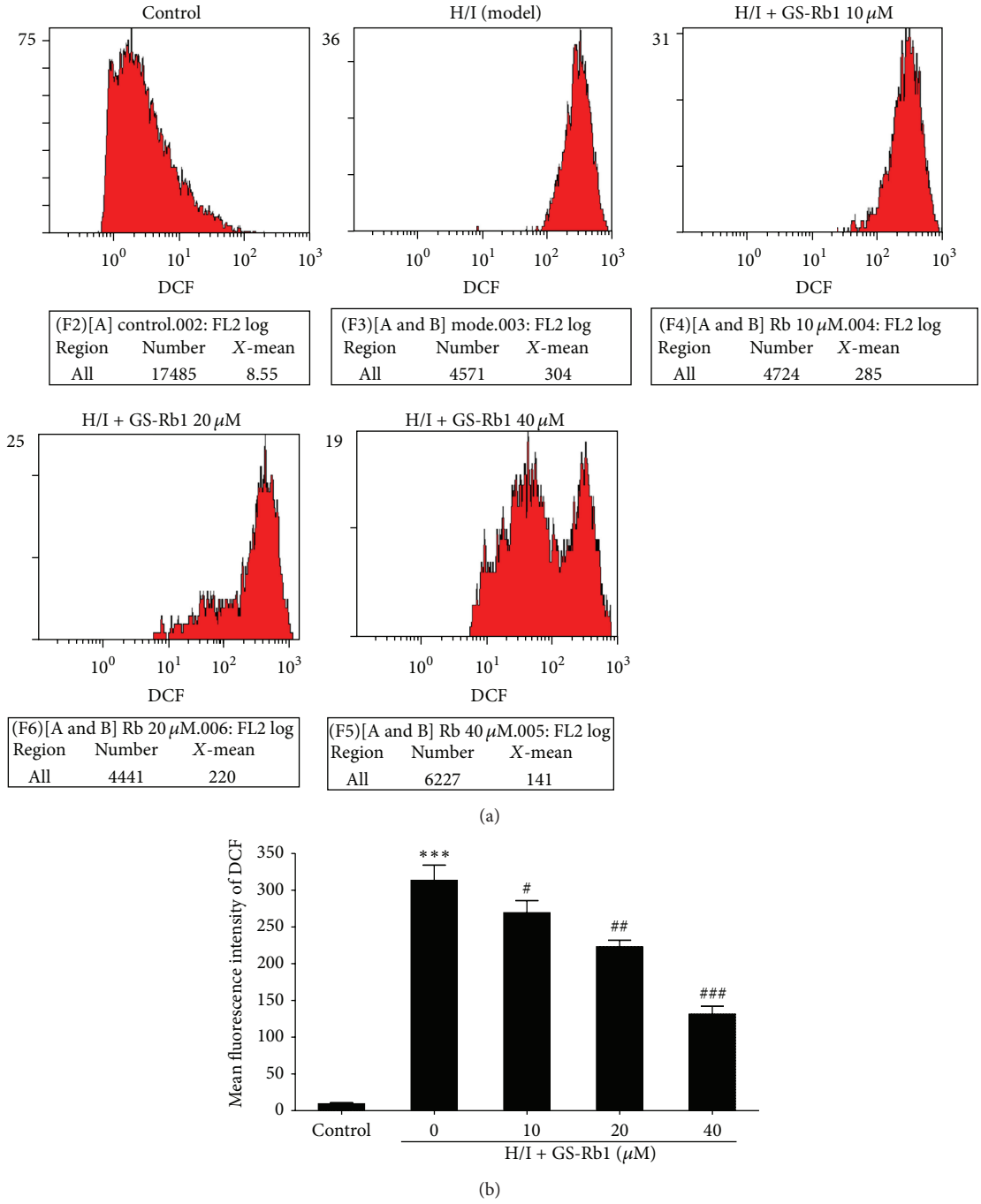

Figure 3: Flow cytometry analysis of GS-Rb1 on intracellular ROS induced by H/I. (a) NRCMs were cotreated with or without GS-Rb1 (10, 20, and 40 μM) during H/I for 24 h. The intracellular ROS level was measured by the fluorescent probe DCFH-DA. (b) Analysis of the mean fluorescence intensity of each group. Error bars represent mean ± SD. $^{***}P < 0.001$ versus control, $^{\#}P < 0.05$, $^{\#\#}P < 0.01$, and $^{\#\#\#}P < 0.001$ versus H/I group ($n = 3$).

3.5. Effect of GS-Rb1 on ΔΨm in NRCMs. Loss of ΔΨm indicates mitochondrial dysfunction that ultimately leads to apoptosis. JC-1 staining was carried out before flow cytometric analysis. NRCMs exposed to H/I condition for 24 h resulted in dissipation of ΔΨm compared with the control group (Figures 4(a) and 4(b)), seen as increased green fluorescence. Cotreatment with different concentrations of GS-Rb1 moderated the dissipation of ΔΨm, indicating its protective effect. The ratio of green and red fluorescence was used to demonstrate the mitochondrial membrane potential (ΔΨm) change induced by H/I treatment and the protective effect of GS-Rb1. In the control group, JC-1 aggregated in mitochondria with a ratio of 1.87 ± 0.065, that of the H/I group being 0.797 ± 0.018. The groups cotreated with 10,

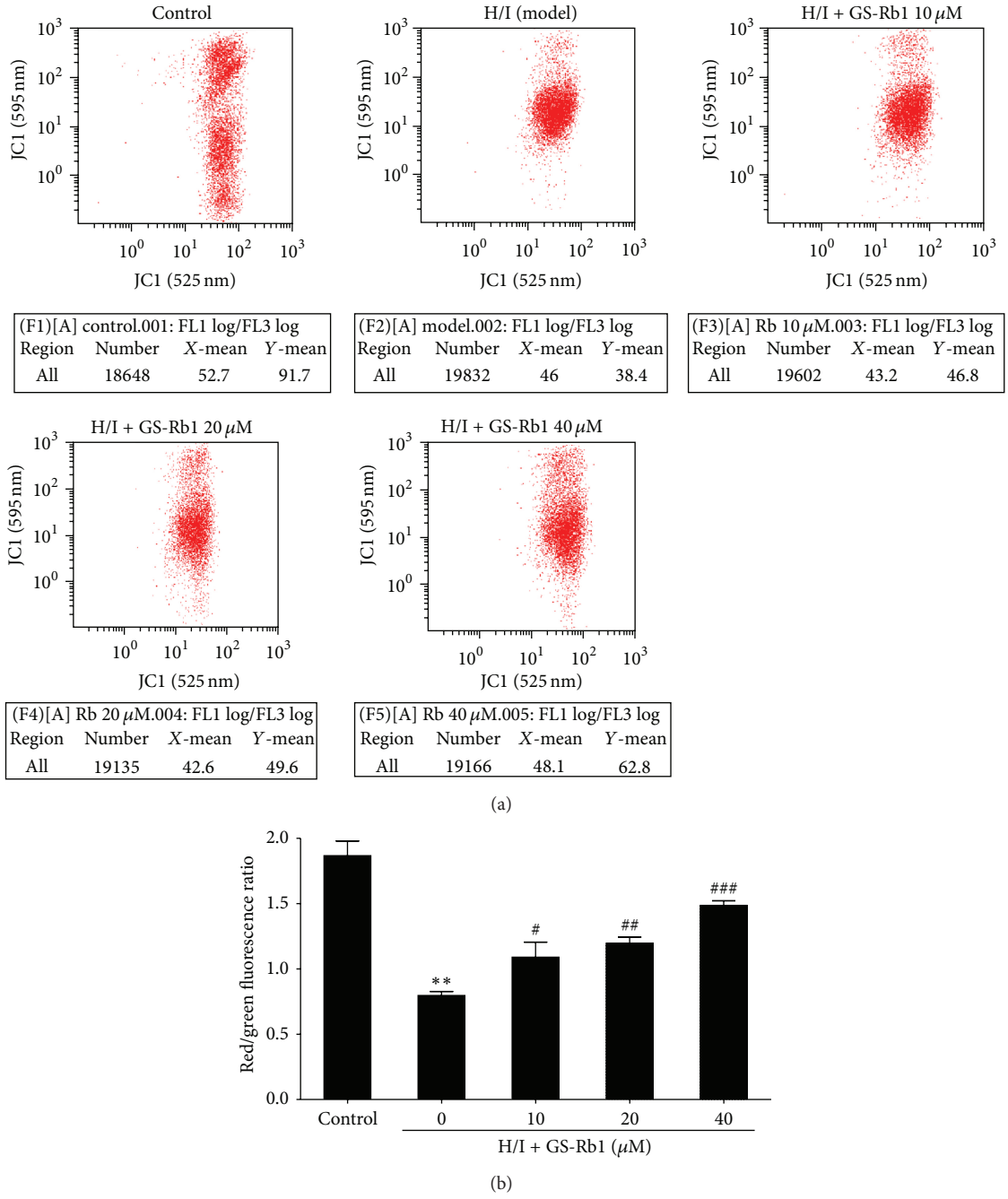

Figure 4: Flow cytometry analysis of GS-Rb1 on mitochondrial membrane potential (ΔΨm) induced by H/I. (a) NRCMs were cotreated with or without GS-Rb1 (10, 20, and 40 μM) during H/I for 24 h. ΔΨm was measured by JC-1 and analyzed by flow cytometry. (b) Analysis of the red/green fluorescence ratio of each group. Error bars represent mean ± SD. $^{***}P < 0.001$ versus control, $^{\#}P < 0.05$, $^{\#\#}P < 0.01$, and $^{\#\#\#}P < 0.001$ versus H/I group, ($n = 3$).

20, and 40 μM GS-Rb1 showed increases of 1.090 ± 0.067 to 1.487±0.020, which suggests that the mitochondria-mediated pathway was involved in the cardioprotective effect of GS-Rb1 on H/I injuries.

3.6. Effects of GS-Rb1 on the Release of Cytochrome c. The release of cytochrome c from mitochondria into cytosol is one of the early events leading to apoptosis. Increased mitochondrial membrane permeability was confirmed by the translocation of cytochrome c from the mitochondria to the cytosol. Few cytochromes c in the cytoplasm were found in the control group (Figures 5(a) and 5(b)) whereas an obvious increase of cytochrome c in cytosol occurred in H/I treated cells (348.2 ± 16.9). Compared with the H/I group, cytochrome c in cytosol in the GS-Rb1 treatment group decreased from 298.9 ± 6.3 to 139.6 ± 5.9. Gs-Rb1 cotreatment

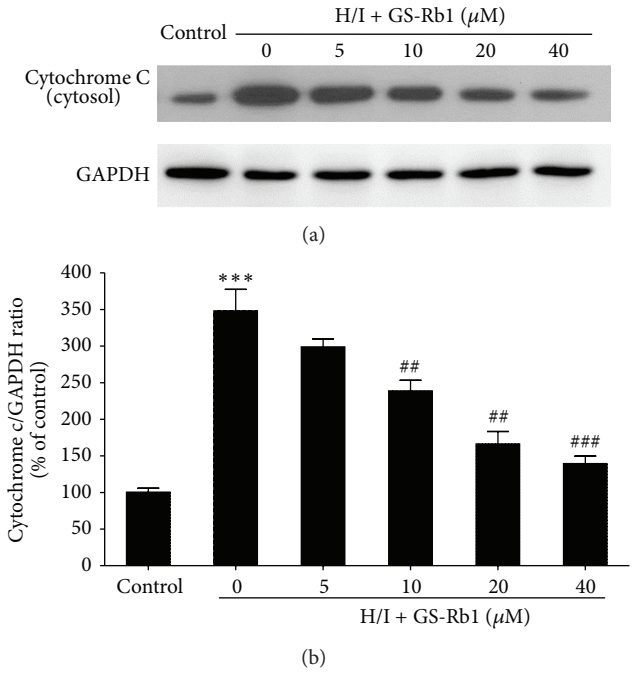

Figure 5: Effect of GS-Rb1 on cytosolic cytochrome c level change induced by H/I. NRCMs were cotreated with or without GS-Rb1 (5, 10, 20, and 40 μM) during H/I for 24 h. (a) Cytochrome c was measured by Western blot. (b) Quantitative data was analysed for each group. Error bars represent mean ± SD. $^{***}P < 0.001$ versus control; $^{\#\#}P < 0.01$ and $^{\#\#\#}P < 0.001$ versus H/I group ($n = 3$).

significantly inhibited H/I-induced cytochrome c release into the cytoplasm, which shows again that GS-Rb1 acts on the mitochondria mediated pathway in its cardioprotective effect.

3.7. Effect of GS-Rb1 on the Expression of Bax and Bcl-2 following H/R Injury. Bcl-2 family proteins have a function in mitochondria mediated apoptosis. Expression of antiapoptotic Bcl-2 and proapoptotic Bax proteins were analyzed by Western blot after H/I and GS-Rb1 treatment. Compared with the control group, H/I significantly increased Bax expression and decreased Bcl-2. The ratio of Bcl-2 to Bax decreased over 10-fold. With GS-Rb1 cotreatment, increased levels of Bcl-2 and a marked reduction in Bax were observed in a dose-dependent manner (Figures 6(a), 6(b), and 6(c)). Thus, GS-Rb1 inhibits apoptosis induced by H/I by upregulating the ratio of Bcl-2 to Bax.

3.8. Effect of GS-Rb1 on the Activation of Caspase 3 and Caspase 9. Activation of caspase-3 and caspase-9 is a key irreversible point in mitochondria mediated apoptosis. When compared with the controls (Figure 7), H/I significantly increased the activity of caspase-3 and caspase-9 by 355.3±6.0 and 286.2 ± 6.1%, respectively. When cotreated with different doses of GS-Rb1, activities of caspase-3 and caspase-9 were attenuated from 247.8 ± 7.0 to 153.7 ± 13.1 and 217.3 ± 7.8% to 97.8 ± 19.0%, respectively. These results indicated that GS-Rb1 could inhibit apoptosis induced by H/I by attenuating caspase-3 and caspase-9 activity.

4. Discussion

GS-Rb1 is one of the most important active compounds of ginseng, which has multiple pharmacological actions, including antifatigue [13], reducing fatty liver [14], antiobesity [15], antiskin aging [16], protective effects of central nervous system [17], retinal ganglion [18], lung [19], liver [20], and renal injury [21]. GS-Rb1 has an established cardiovascular protective effect. The protective effects of GS-Rb1 on neonatal rat cardiomyocytes (NRCMs) have been shown here by MTT combined with LDH leakage assay in increasing the viability of NRCMs when subjected in the H/I conditions in a dose-dependent manner. Flow cytometric analysis showed that cardioprotection in response to GS-Rb1 was due to inhibition of apoptosis, cellular ROS production, and prevention of $\Delta\Psi$m loss. Our novel finding is that GS-Rb1 significantly inhibited the release of cytochrome c from mitochondria into cytosol and maintained the ratio of Bcl-2 to Bax. It also regulated downstream both caspase-3 and caspase-9 activity.

Apoptosis is heavily involved in the development and progression of cardiovascular disease [22]. Blocking it can prevent the loss of contractile cells and minimize cardiac injury [23]. H/I induces NRCMs apoptosis (including early and late apoptosis). With H/I alone, GS-Rb1 attenuated cardiomyocyte apoptosis from 81.6 to 31.0%, while living cells rose from 6.78 to 52.8%. Therefore, cotreatment with GS-Rb1 mitigates H/I-induced apoptosis of cardiomyocytes.

Ischemia injuries provoke ROS generation in cardiomyocytes [24], and these have a secondary messenger function because of their ability to influence MMP and mitochondrial function, thereby activating the caspase cascade [25]. When ROSs reach a threshold level, opening of transition pores is triggered, which decreases $\Delta\Psi$m and induces the side leakage of caspase-activating proteins, that is, cytochrome c to the cytosol [26, 27]. GS-Rb1 is known to be protective to neonatal rat cardiomyocytes treated with from $CoCl_2$ to induce hypoxic injuries by inhibiting GSK-3β-mediated mPTP opening [28]. Our results demonstrate that H/I induce $\Delta\Psi$m loss and ROS accumulation and that GS-Rb1 significantly inhibits $\Delta\Psi$m depolarization and ROS production. These results suggest that the cardioprotective effects of GS-Rb1 might be related to the inhibition of ROS rather than the generation and preservation of the mitochondria.

It has been demonstrated that mitochondrial permeability and release of the apoptosome could be controlled by Bcl-2 family [29]. An increase of proapoptosis proteins (Bax and Bid) and/or a decrease in antiapoptosis proteins (Bcl-2 and Bcl-xL) could lead to a decrease in mitochondrial membrane potential and an opening of mitochondrial permeability transition pores, leading to cytochrome c release from mitochondria into cytosol [30]. The current research showed that ratio of Bcl-2 to Bax was increased by GS-Rb1 treatment following H/I, which suggested that Bcl-2 family was involved in the cardioprotection of GS-Rb1 in H/I.

Mitochondria play an important role in cardiomyocytes injuries by releasing cytochrome c and other apoptogenic proteins into the cytosol [31]. Cytochrome c in the cytosol forms a complex that is composed of apoptosis-activating factor-1 (Apaf-1), which recruits and activates the death

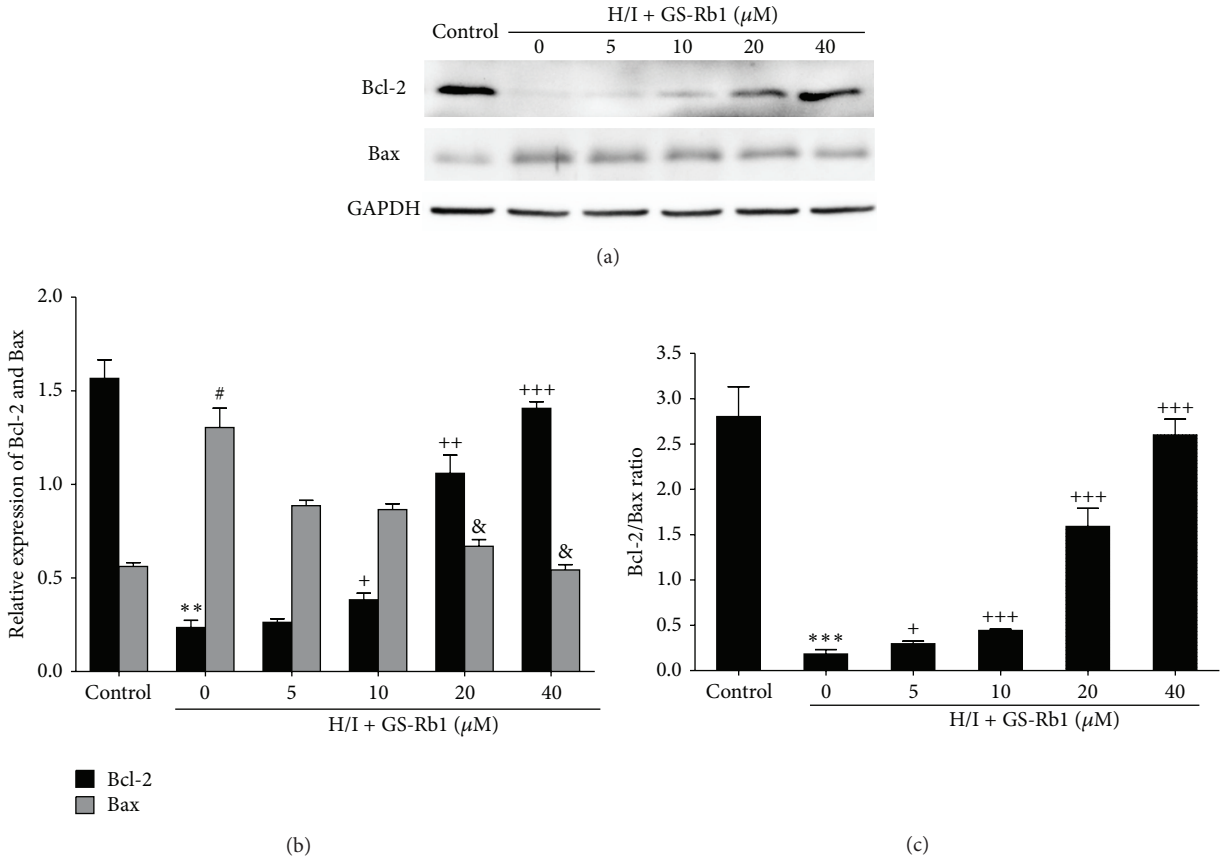

Figure 6: Effect of GS-Rb1 on Bcl-2 and Bax changes induced by H/I. NRCMs were cotreated with or without GS-Rb1 (5, 10, 20, and 40 μM) during H/I for 24 h. (a) The protein levels of Bcl-2 and Bax were quantified by Western blot. (b) Quantitative data analysis for each group. (c) Bcl-2/Bax protein expression ratio in each group. Error bars represent mean ± SD. $^{***}P < 0.001$ versus Bcl-2 in control group; $^{\#\#}P < 0.01$ versus Bax in control group; $^{+}P < 0.05$, $^{++}P < 0.01$, and $^{+++}P < 0.001$ versus Bcl-2 in H/I group; $^{\&}P < 0.05$ and $^{\&\&}P < 0.01$ versus Bax in H/I group.

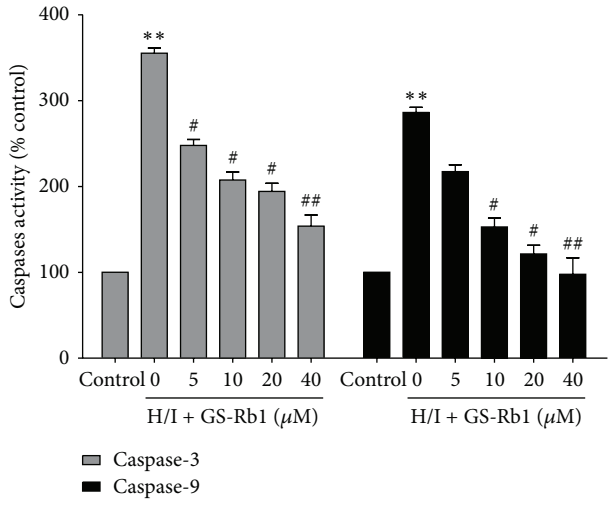

Figure 7: Effect of GS-Rb1 on caspase-3 and caspase-9 activities induced by H/I. NRCMs were cotreated with or without GS-Rb1 (5, 10, 20, and 40 μM) during H/I for 24 h. NRCMs were lysed and caspase-3 and caspase-9 activities were analyzed. Error bars represent mean ± SD. $^{**}P < 0.01$ versus control group; $^{\#}P < 0.05$ and $^{\#\#}P < 0.01$ versus H/I group ($n = 3$).

effector caspase-9 [32]. The activated caspase-9 subsequently activates caspase-3, which in turn activates the early apoptosis process [33]. Our results showed that GS-Rb1 significantly inhibited mitochondrial cytochrome c release and caspase-3 and caspase-9 activity following H/I, which suggested that cytochrome c release and the mitochondrial dependent pathway were involved in the cardioprotection of GS-Rb1 in H/I.

5. Conclusion

In conclusion, GS-Rb1 exerts a protective effect in hypoxia/ischemia-induced cell death, which may underlie the inhibition of the mitochondrial apoptotic pathway. The cardioprotective effect seems to act by decreasing cellular ROS production, restoring $\Delta\Psi$m, attenuating H/I-mediated mitochondrial cytochrome c release, reducing the ratio of Bax to Bcl-2, and thereby affecting caspase-3 and caspase-9 activity. Further work will be required to understand the beneficial role and the effect on other organs of GS-Rb1 in postischemic injury *in vivo*, with the hope that these benefits can be translated to clinical interventions in the treatment of ischemic heart diseases.

Conflict of Interests

No conflict of interests was declared in relation to this paper.

Authors' Contribution

Xu Yan and Jinwen Tian contributed equally to this work.

Acknowledgments

This work was supported by a Grant from the National Natural Science Foundation of China (no. 81273890, no. 81030002/H02, and no. 81173367) and Beijing Postdoctoral Research Foundation (2013ZZ-57).

References

[1] V. G. Sharov, A. Todor, S. Khanal, M. Imai, and H. N. Sabbah, "Cyclosporine A attenuates mitochondrial permeability transition and improves mitochondrial respiratory function in cardiomyocytes isolated from dogs with heart failure," *Journal of Molecular and Cellular Cardiology*, vol. 42, no. 1, pp. 150–158, 2007.

[2] Q. Li, L. Zhou, G. Gao, J. Jiao, and P. Li, "Mitochondrial network in the heart," *Protein and Cell*, vol. 3, no. 6, pp. 410–418, 2012.

[3] L. Bouchier-Hayes, L. Lartigue, and D. D. Newmeyer, "Mitochondria: pharmacological manipulation of cell death," *The Journal of Clinical Investigation*, vol. 115, no. 10, pp. 2640–2647, 2005.

[4] C. M. Schonhoff, B. Gaston, and J. B. Mannick, "Nitrosylation of cytochrome c during apoptosis," *Journal of Biological Chemistry*, vol. 278, no. 20, pp. 18265–18270, 2003.

[5] C. Guo, X. Zeng, J. Song et al., "A soluble receptor for advanced glycation end-products inhibits hypoxia/reoxygenation-induced apoptosis in rat cardiomyocytes via the mitochondrial pathway," *International Journal of Molecular Sciences*, vol. 13, no. 9, pp. 11923–11940, 2012.

[6] H. Huang, K. Wu, Q. You, R. Huang, and S. Li, "Naringin inhibits high glucose-induced cardiomyocyte apoptosis by attenuating mitochondrial dysfunction and modulating the activation of the p38 signaling pathway," *International Journal of Molecular Medicine*, vol. 32, no. 2, pp. 396–402, 2013.

[7] M. L. Xu, H.-J. Kim, Y.-R. Choi, and H.-J. Kim, "Intake of Korean red ginseng extract and saponin enhances the protection conferred by vaccination with inactivated influenza A virus," *Journal of Ginseng Research*, vol. 36, no. 4, pp. 396–402, 2012.

[8] L. Jia, Y. Zhao, and X. Liang, "Current evaluation of the millennium phytomedicine - Ginseng (II): Collected chemical entities, modern pharmacology, and clinical applications emanated from traditional chinese medicine," *Current Medicinal Chemistry*, vol. 16, no. 22, pp. 2924–2942, 2009.

[9] J. Li, Z. H. Shao, J. Z. Xie et al., "The effects of ginsenoside Rb1 on JNK in oxidative injury in cardiomyocytes," *Archives of Pharmacal Research*, vol. 35, no. 7, pp. 1259–1267, 2012.

[10] Y. Wu, Z. Y. Xia, J. J. Dou et al., "Protective effect of ginsenoside Rb1 against myocardial ischemia/reperfusion injury in streptozotocin-induced diabetic rats," *Molecular Biology Reports*, vol. 38, no. 7, pp. 4327–4335, 2011.

[11] R. Xia, B. Zhao, Y. Wu et al., "Ginsenoside Rb1 preconditioning enhances eNOS expression and attenuates myocardial ischemia/reperfusion injury in diabetic rats," *Journal of Biomedicine and Biotechnology*, vol. 2011, Article ID 767930, 8 pages, 2011.

[12] P. Simpson and S. Savion, "Differentiation of rat myocytes in single cell cultures with and without proliferating nonmyocardial cells. Cross-striations, ultrastructure, and chronotropic response to isoproterenol," *Circulation Research*, vol. 50, no. 1, pp. 101–116, 1982.

[13] S. Tan, F. Zhou, and N. Li, "Anti-fatigue effect of ginsenoside Rb1 on postoperative fatigue syndrome induced by major small intestinal resection in rat," *Biological & Pharmaceutical Bulletin*, vol. 36, pp. 1634–1639, 2013.

[14] L. Shen, Y. Xiong, D. Q. Wang et al., "Ginsenoside Rb1 reduces fatty liver by activating AMP-activated protein kinase in obese rats," *Journal of Lipid Research*, vol. 54, no. 5, pp. 1430–1438, 2013.

[15] N. Lin, D. Cai, D. Jin, Y. Chen, and J. Shi, "Ginseng panaxoside Rb1 reduces body weight in diet-induced obese mice," *Cell Biochemistry and Biophysics*, vol. 68, no. 1, pp. 189–194, 2014.

[16] T. H. Kang, H. M. Park, Y. Kim et al., "Effects of red ginseng extract on UVB irradiation-induced skin aging in hairless mice," *Journal of Ethnopharmacology*, vol. 123, no. 3, pp. 446–451, 2009.

[17] D. Liu, H. Zhang, W. Gu, Y. Liu, and M. Zhang, "Neuroprotective effects of ginsenoside rb1 on high glucose-induced neurotoxicity in primary cultured rat hippocampal neurons," *PLoS ONE*, vol. 8, no. 11, Article ID e79399, 2013.

[18] Z. Liu, J. Chen, W. Huang, Z. Zeng, Y. Yang, and B. Zhu, "Ginsenoside Rb1 protects rat retinal ganglion cells against hypoxia and oxidative stress," *Molecular Medicine Reports*, vol. 8, pp. 1397–1403, 2013.

[19] J. Wang, L. Qiao, S. Li, and G. Yang, "Protective effect of ginsenoside rb1 against lung injury induced by intestinal ischemia-reperfusion in rats," *Molecules*, vol. 18, no. 1, pp. 1214–1226, 2013.

[20] J. Wang, L. Qiao, Y. Li, and G. Yang, "Ginsenoside Rb1 attenuates intestinal ischemia-reperfusion-induced liver injury by inhibiting NF-κB activation," *Experimental and Molecular Medicine*, vol. 40, no. 6, pp. 686–698, 2008.

[21] Q. Sun, Q. Meng, Y. Jiang, and Z. Xia, "Ginsenoside Rb1 attenuates intestinal ischemia reperfusion induced renal injury by activating Nrf2/ARE pathway," *Molecules*, vol. 17, no. 6, pp. 7195–7205, 2012.

[22] Y. Lee and Å. B. Gustafsson, "Role of apoptosis in cardiovascular disease," *Apoptosis*, vol. 14, no. 4, pp. 536–548, 2009.

[23] J. Song, X. Teng, Y. Cai, C. Tang, and Y. Qi, "Activation of Akt/GSK-3β signaling pathway is involved in intermedin1–53 protection against myocardial apoptosis induced by ischemia/reperfusion," *Apoptosis*, vol. 14, no. 11, pp. 1299–1307, 2009.

[24] S. Cadenas, J. Aragonés, and M. O. Landázuri, "Mitochondrial reprogramming through cardiac oxygen sensors in ischaemic heart disease," *Cardiovascular Research*, vol. 88, no. 2, pp. 219–228, 2010.

[25] J. D. Ly, D. R. Grubb, and A. Lawen, "The mitochondrial membrane potential ($\delta\psi$m) in apoptosis; an update," *Apoptosis*, vol. 8, no. 2, pp. 115–128, 2003.

[26] D. B. Zorov, M. Juhaszova, and S. J. Sollott, "Mitochondrial ROS-induced ROS release: an update and review," *Biochimica et Biophysica Acta*, vol. 1757, no. 5-6, pp. 509–517, 2006.

[27] M. L. Circu and T. Y. Aw, "Reactive oxygen species, cellular redox systems, and apoptosis," *Free Radical Biology and Medicine*, vol. 48, no. 6, pp. 749–762, 2010.

[28] H. L. Kong, Z. Q. Li, Y. J. Zhao et al., "Ginsenoside Rb1 protects cardiomyocytes against CoCl2-induced apoptosis in neonatal rats by inhibiting mitochondria permeability transition pore opening," *Acta Pharmacologica Sinica*, vol. 31, no. 6, pp. 687–695, 2010.

[29] E. Yang and S. J. Korsmeyer, "Molecular thanatopsis: a discourse on the BCL2 family and cell death," *Blood*, vol. 88, no. 2, pp. 386–401, 1996.

[30] G. van Loo, X. Saelens, M. van Gurp, M. MacFarlane, S. J. Martin, and P. Vandenabeele, "The role of mitochondrial factors in apoptosis: a Russian roulette with more than one bullet," *Cell Death & Differentiation*, vol. 9, no. 10, pp. 1031–1042, 2002.

[31] H. M. Honda and P. Ping, "Mitochondrial permeability transition in cardiac cell injury and death," *Cardiovascular Drugs and Therapy*, vol. 20, no. 6, pp. 425–432, 2006.

[32] H. Yuanming, M. A. Benedict, L. Ding, and G. Núñez, "Role of cytochrome c and dATP/ATP hydrolysis in Apaf-1-mediated caspase-9 activation and apoptosis," *EMBO Journal*, vol. 18, no. 13, pp. 3586–3595, 1999.

[33] K. Nishida, O. Yamaguchi, and K. Otsu, "Crosstalk between autophagy and apoptosis in heart disease," *Circulation Research*, vol. 103, no. 4, pp. 343–351, 2008.

Hindawi Publishing Corporation
Evidence-Based Complementary and Alternative Medicine
Volume 2014, Article ID 707829, 7 pages
http://dx.doi.org/10.1155/2014/707829

Research Article

In Vivo Hypocholesterolemic Effect of MARDI Fermented Red Yeast Rice Water Extract in High Cholesterol Diet Fed Mice

Swee Keong Yeap,[1] Boon Kee Beh,[2] Joan Kong,[3] Wan Yong Ho,[4] Hamidah Mohd Yusof,[5] Nurul Elyani Mohamad,[5] Aminuddin bin Hussin,[6] Indu Bala Jaganath,[7] Noorjahan Banu Alitheen,[5] Anisah Jamaluddin,[6] and Kamariah Long[6]

[1] *Institute of Bioscience, Universiti Putra Malaysia, 43400 Serdang, Selangor, Malaysia*
[2] *Department of Bioprocess Technology, Faculty of Biotechnology and Biomolecular Sciences, Universiti Putra Malaysia, 43400 Serdang, Selangor, Malaysia*
[3] *Aning Biotech Corporation Sdn Bhd., 13G & 13-1, Jalan LJ3, Lembah Jaya Industrial Park, 68000 Ampang, Selangor, Malaysia*
[4] *School of Biomedical Sciences, The University of Nottingham, Malaysia Campus, Jalan Broga, 43500 Semenyih, Selangor, Malaysia*
[5] *Department of Cell and Molecular Biology, Faculty of Biotechnology and Biomolecular Sciences, Universiti Putra Malaysia, 43400 Serdang, Selangor, Malaysia*
[6] *Department of Bioprocess Biotechnology, Malaysian Agriculture Research Development Institute, 43400 Serdang, Selangor, Malaysia*
[7] *Biotechnology Research Centre, Malaysian Agriculture Research Development Institute, 43400 Serdang, Selangor, Malaysia*

Correspondence should be addressed to Kamariah Long; amai@mardi.gov.my

Received 1 March 2014; Accepted 21 May 2014; Published 16 June 2014

Academic Editor: Qunhao Zhang

Fermented red yeast rice has been traditionally consumed as medication in Asian cuisine. This study aimed to determine the *in vivo* hypocholesterolemic and antioxidant effects of fermented red yeast rice water extract produced using Malaysian Agricultural Research and Development Institute (MARDI) *Monascus purpureus* strains in mice fed with high cholesterol diet. Absence of monacolin-k, lower level of γ-aminobutyric acid (GABA), higher content of total amino acids, and antioxidant activities were detected in MARDI fermented red yeast rice water extract (MFRYR). *In vivo* MFRYR treatment on hypercholesterolemic mice recorded similar lipid lowering effect as commercial red yeast rice extract (CRYR) as it helps to reduce the elevated serum liver enzyme and increased the antioxidant levels in liver. This effect was also associated with the upregulation of apolipoproteins-E and inhibition of Von Willebrand factor expression. In summary, MFRYR enriched in antioxidant and amino acid without monacolin-k showed similar hypocholesterolemic effect as CRYR that was rich in monacolin-k and GABA.

1. Introduction

Red yeast rice, a product of *Monascus* fermentation, has traditionally been used as a medicine (to improve digestion and blood circulation), preservative (Chinese bean curd/cheese, meat, fish, etc.), and coloring agent and inoculant for alcoholic beverages (*Anchu*, *somsu*) in Asian countries since ancient time [1]. It can be produced through either the submerged or the solid state fermentation system. Rice is the common fermentation medium [2] to produce *Monascus* fermentation products [3] besides other agricultural products including dioscorea, cassava, sweet potato, potato [4], barley [5], mixture of rice and garlic [6], soybean [7], corn meal, peanut meal, coconut residue, and soybean meal. Monacolin-k (that is identical to lovastatin) was the most commonly standardized monacolin compound in fermented red yeast rice for its lipid lowering property via inhibition of the 3-hydroxy-3-methylglutaryl-coenzyme A reductase [8]. Other secondary metabolites including γ-aminobutyric acid (GABA), dimerumic acid, and monascin, which are potential hypotensive, antioxidant, and anti-inflammation agents, were also reported as being present in fermented red yeast rice [4, 9, 10].

Over the past decades, red yeast rice has gained drastic attention and sales due to its use as statin alternative therapy

for hyperlipidemia and dyslipidemia management [11]. Clinical studies have reported that red yeast rice can significantly reduce lipid level and prevent recurrence of coronary events in human subjects [12, 13]. However, the Food and Drug Administration (FDA, USA) issued a consumer warning to avoid online promotion of commercial red yeast rice products in August 2007 due to the presence of monacolin-k, which is biosimilar to the active pharmaceutical ingredient lovastatin [14]. Use of statin drug has been reported to cause some side effects such as headache, dizziness, rash, stomach discomfort, hepatic dysfunction, muscle weakness, or even rhabdomyolysis symptoms [15]. Although many studies have proven the potential lipid lowering properties of *Monascus* fermented red yeast rice, the effects of fermented red yeast rice water extract produced using the MARDI *Monascus purpureus* strains, which did not contain monacolin-k and their derivatives, are not yet to be determined and compared with fermented red yeast rice extract that contains monacolin-k. Hence, the aim of this study was to determine and compare the hypocholesterolemic and antioxidant effects of fermented red yeast rice water extract (MFRYR) produced from the MARDI *Monascus purpureus* strains with commercial red yeast rice extract (CRYR) in high cholesterol diet mice model *in vivo*.

2. Materials and Methods

2.1. Materials. Cholesterol, 94%, was purchased from Sigma Aldrich (USA). Commercial red yeast rice extract (CRYR) was purchased from the local pharmacy store. Hypoxanthine, xanthine oxidase, superoxide dismutase, Folin-Ciocalteu reagent, aluminium chloride, sodium nitrate, ascorbic acid, and gallic acid were obtained from Sigma Aldrich (USA). Griess reagent was from Invitrogen (USA). All solvents used were of analytical reagent or HPLC grade. *Monascus purpureus* strain inoculumwas obtained from MARDI's culture collection center.

2.2. Preparation of MARDI Fermented Red Yeast Rice Water Extract (MFRYR) Using Monascus purpureus Strains. Broken rice (1000 g) was washed 6 times and soaked in cold water at room temperature for 18 h. The soaked broken rice was washed, autoclaved at 121°C for 20 min, and cooled down to room temperature. The broken rice was then inoculated with MARDI *Monascus purpureus* strains and incubated aerobically at 32°C for 16 days. It was then harvested, oven-dried, ground into powder, and extracted with deionized water. The MARDI *Monascus purpureus* strains fermented red yeast rice water extract (MFRYR) was lyophilised using a Virtis BenchTop freeze dryer (SP Industries, Inc., USA) and stored in a 4°C chiller until analysis. Nonfermented rice, MFRYR, and commercial red yeast rice extract (CRYR) were subjected to monacolin-k and GABA quantification using the UPLC method. Monacolin-k analysis was conducted using the Acquity UPLC system (Waters Corp., USA) equipped with a RP-18 column (1.7 μm, 2.1 × 100 mm, Waters Acquity, USA) and gradient mobile phase of 100% acetonitrile (Eluent A) and 0.1% trifluoroacetic acid (Eluent B). The linear gradient mode was performed (flow rate at 0.2 mL/min) from 35% to 75% Eluent A for 7.8 min and maintained at 75% Eluent A for another 3.2 min before being reverted back to 35% Eluent A for 0.8 min. Total analysis time was set for 14 min with an injection volume of 1 μL and column temperature of 30°C. Monacolin-k was detected using a Photodiode array (PDA) detector at 237 nm with the detection range between 210 and 350 nm. On the other hand, the concentration of GABA and amino acids was determined according to Ali et al. [16]. The *in vitro* antioxidant effects of nonfermented rice, MFRYR, and CRYR were compared using total phenolic content and Ferric reducing power (FRAP) tests [17].

2.3. Hypocholesterolemic Study. Male Balb/c mice (8 weeks old, average body weight of 25 ± 2 g), obtained from the Animal Housing Department, Institute of Bioscience, Universiti Putra Malaysia, were used for the experiments below. The mice were kept in prebeded plastic cages in controlled conditions of 22 ± 3°C and standard 12 hours of day/dark light cycles with food and water *ad libitum*. The procedures for this study were carried out according to the guidelines of the National Institute of Health for the Care and Use of Laboratory Animals (ref.: UPM/FPV/PS/3.2.1.551/AUP-R2). Male Balb/c mice were randomly assigned into five groups with eight animals each, namely:

group 1: normal control, mice (p.o.) receiving normal saline daily only;

group 2: negative control, mice (p.o.) receiving cholesterol at 1000 mg/kg concentration and normal saline daily only;

group 3: MFRYR treated group, receiving cholesterol at 1000 mg/kg concentration and 6 mg/kg of body weight MFRYR daily;

group 4: MFRYR treated group, receiving cholesterol at 1000 mg/kg concentration and 60 mg/kg of body weight MFRYR daily;

group 5: CRYR treated group, receiving cholesterol at 1000 mg/kg concentration and 60 mg/kg of body weight CRYR daily.

All groups (except group 1) were preincubated with cholesterol 1000 mg/kg body weight (p.o.) for 8 weeks and continued with cholesterol and the respective extract treatments for another 2 weeks. On the last day of the experiment, the mice were sacrificed. Blood and liver were collected for the following analyses.

2.3.1. Biochemical Assays of Lipid and Liver Profiles in Serum. The lipid profile (total cholesterol, TAG, LDL, and HDL) and liver profile (ALT, ALP, and AST) in serum were measured using a biochemical analyzer (Hitachi 902 Automatic Analyzer) and adapted reagents from Roche (Germany) [16].

2.3.2. Liver Histopathological Evaluation. Liver was removed, fixed, and stained in haematoxylin and eosin (H&E) [16].

Table 1: Monacolin-k, GABA, total amino acid (free and essential), total phenolic content, and FRAP antioxidant activity of nonfermented rice, MARDI fermented red yeast rice water extract (MFRYR), and commercial red yeast rice extract (CRYR).

	Nonfermented rice	MFRYR	CRYR
Monacolin-k (μg/g sample)	ND	ND	182.61 ± 0.02
GABA (g/100 g sample)	ND	0.14 ± 0.01	0.48 ± 0.03
Total free amino acid (g/100 g sample)	ND	3.33 ± 0.54	0.03 ± 0.01
Total essential amino acid (g/100 g sample)	ND	1.32 ± 0.26	0.03 ± 0.01
Total phenolic content (μg GAE/mg sample)	7.60 ± 0.10	16.20 ± 0.10	0.81 ± 0.10
FRAP (mg ascorbic acid equivalent (AAE)/g sample)	29.80 ± 0.01	74.04 ± 0.02	5.40 ± 0.02

ND: not detected; values were mean ± standard deviation of three independent experiments.

The histopathological alterations of the liver from different groups were observed using a bright-field microscope (Nikon, Japan).

2.3.3. In Vivo Antioxidant Assays for Mice Liver Homogenate. Liver homogenates were prepared by meshing the harvested liver in ice-cold PBS followed by homogenization and centrifugation at 2000 rpm and 4°C for 5 minutes. The supernatants collected were subjected to superoxide dismutase (SOD) and malondialdehyde (MDA) assays [16]. One unit of SOD was calculated as the amount of protein needed to achieve 50% inhibition and was expressed as unit SOD/mg protein while MDA activity was expressed as nmol MDA/g protein.

2.3.4. PCR Array on Atherosclerosis Related Gene Expression in Blood. Blood from group 2, group 4, and group 5 was collected and subjected to RNA extraction using the RNeasy mini kit (Qiagen, USA). cDNA synthesis and mouse atherosclerosis RT^2 Profiler PCR array (SABiosciences, USA) were performed using an iCycler iQ real-time PCR system (Bio-Rad, USA) according to the manufacturer's protocols. The results were normalized with the five housekeeping genes which were included in the kit and the relative fold change was determined by dividing the normalized data of the genes from samples of groups 4 and 5 with the normalized data of the genes from the untreated group 2.

2.4. Statistical Analysis. All quantitative measurements were conveyed as mean ± S.D. Analyses were performed using one-way analysis of variance (ANOVA) and the group means were compared by Duncan test. P values < 0.05 were considered as statistically significant.

3. Results and Discussion

3.1. In Vitro Monacolin-k, GABA, Amino Acid, Total Phenolic Contents, and Antioxidant Effects (FRAP Activity) of MFRYR. Fermentation using *Monascus* spp. was recorded with enhanced levels of nutritious compounds including γ-aminobutyric acid (GABA) and monacolin-k. However, monacolin-k was found to be associated with several side effects including hepatotoxicity [15] and it was advised by the FDA for it is not to be present in commercial red yeast rice supplements [14]. A previous study has reported that alterations of fermentation conditions including fermentation temperature, aeration, and nutritional factors and method (submerged and solid state fermentations) were able to prevent the production of monacolin-k by *M. purpureus* without altering the hypocholesterolemic effect of this red yeast rice [18]. For example, Ajdari et al. [18] suggested that the hypocholesterolemic effect of this fermented product without monacolin-k was contributed by other bioactive compounds. In this study, we have evaluated the monacolin-k, GABA, total amino acid, and antioxidant levels in the water extract of MARDI's *Monascus purpureus* fermented red yeast rice (MFRYR). Chromatographic analyses showed that monacolin-k, GABA, and amino acid (both free and essential) were not detected in the nonfermented rice sample. The commercial fermented red yeast rice (CRYR) sample was detected to have high level of monacolin-k (182.61 ± 0.02 μg/g) but it was not found in the MFRYR sample. GABA content was recorded to be 3.4- fold higher in the CRYR sample as compared to MFRYR sample (Table 1). Wang et al. [19] had demonstrated that the alteration of the fermentation process could modulate the production of monacolin-k and GABA in a similar trend by using *M. purpureus*. Thus, it was not surprising to find that MFRYR which did not contain monacolin-k had a lower GABA concentration since these two compounds were always produced with similar trends during fermentation [19]. On the other hand, MFRYR recorded the highest total free and essential amino acids as compared to CRYR. Nevertheless, both nonfermented rice and MFRYR were recorded to have 2-fold higher phenolic content and antioxidant activities in the FRAP antioxidant test when compared to CRYR. These indicated that MARDI's *Monascus purpureus* strains were able to increase the antioxidant level during the fermentation process. The results showed that the MFRYR contained higher levels of total amino acid (free and essential) and antioxidants as compared to commercial red yeast rice extract (CRYR) and nonfermented rice (Table 1).

3.2. In Vivo Hypocholesterolemic and Antioxidant Effects of MFRYR. In this experiment, high cholesterol mice were induced by feeding cholesterol p.o. at concentration of 1000 mg/kg body weight daily for continuously 8 weeks before proceeding with cholesterol and extract treatments for another 2 weeks. The results showed significant reductions of total cholesterol, triglycerides (TAG), and low density

Table 2: Blood serum lipid and liver profile.

Treatment	Cholesterol (mg/dL)	Triglyceride (mg/dL)	LDL (mg/dL)	HDL (mg/dL)	ALT (U/L)	ALP (U/L)	AST (U/L)
Group 1 ($n = 8$)	115.05 ± 10.53*	177.11 ± 13.19*	39.00 ± 2.39*	47.19 ± 3.17*	62.50 ± 3.55*	90.13 ± 4.45*	120.42 ± 13.05*
Group 2 ($n = 8$)	230.47 ± 15.99	264.33 ± 23.40	113.85 ± 3.90	56.55 ± 4.29	277.20 ± 9.76	127.83 ± 4.29	320.13 ± 30.71
Group 3 ($n = 8$)	201.72 ± 24.57	202.03 ± 25.86	62.40 ± 1.56*	64.16 ± 1.95*	155.33 ± 9.73*	106.75 ± 4.69*	170.49 ± 31.69*
Group 4 ($n = 8$)	179.85 ± 10.12*	171.30 ± 12.60*	44.28 ± 4.33*	70.59 ± 6.17*	173.13 ± 5.58*	105.80 ± 1.08*	181.16 ± 17.59*
Group 5 ($n = 8$)	181.07 ± 11.06*	176.22 ± 24.08*	52.26 ± 3.12*	77.42 ± 4.29*	263.58 ± 5.08	137.00 ± 3.70	424.42 ± 43.07*

Values were mean ± standard deviation of 8 animals in each group and significant difference indicated by * ($P < 0.05$) was determined using ANOVA followed by Duncan's multiple range test.

lipoprotein (LDL) levels and significant increment of high density lipoprotein (HLD) among extract treatment groups as compared to the untreated control group 2 (Table 2). MFRYR had a dose-dependent hypocholesterolemic effect whereby hypercholesterolemic mice treated with higher concentration (60 mg/kg body weight) showed more significant reduction of serum lipid profiles (Table 2). Besides, MFRYR had comparable hypocholesterolemic properties comparing to CRYR where treatment with 60 mg/kg body weight of MFRYR and CRYR showed approximate 22% of total cholesterol, 30% of TAG, and 55% of LDL reduction. In terms of HDL level, the highest increment (~36%) was recorded in CRYR treatment group. Besides the serum lipid profile, liver histopathology observation was carried out in this experiment. Figure 1 showed the histology of the liver sections for groups 1, 2, 4, and 5. Lipid droplets were only observed in livers of untreated mice, which indicated that all treatments were able to reduce fat accumulation in the livers of the high cholesterol diet mice. Besides monacolin-k, GABA which was reported as one of the major active ingredients in germinated brown rice could also contribute to the hypocholesterolemic effect [20]. In this study, although monacolin-k was not detected and GABA was 3.4-fold lower, MFRYR recorded equally good hypocholesterolemic effect as CRYR in a dosage dependent manner (Table 2 and Figure 1). This effect may be contributed by the increased levels of phenolic content and total amino acids in MFRYR. Afonso et al. [21] and Børsheim et al. [22] reported the potential use of phenolic compounds and amino acid supplementation to reduce serum lipid profile which in turn complemented our observations in this study. More importantly, phenolic compounds have been reported as one of the most important dietary bioactive compounds that contributed to the antioxidant effect [21].

In general, consumption of a high fat diet could contribute to the formation of fatty liver and subsequently elevated the liver enzyme levels as observed in the untreated high cholesterol diet group (Table 2). All extract treatments showed different degrees of liver enzyme recoveries when compared to the untreated cholesterol control (group 2). MFRYR at both concentrations managed to recover the elevated liver enzymes to lower levels in the dosage dependent manner. Nonetheless, the elevated liver enzyme levels in the MFRYR treatment groups at both concentrations were still higher than the normal control (group 1). On the other hand, the CRYR group was found to have higher serum liver enzyme profile, which was close to the untreated cholesterol control (group 2). Recovery from liver damage was always correlated to the antioxidant, lipid peroxidation, and nitric oxide level in the liver [16]. Similar to the serum liver profile, liver homogenates from the untreated cholesterol control and CRYR treated group were recorded to have the higher lipid peroxidation and the lower SOD antioxidant enzyme level. On the other hand, MFRYR was able to reduce lipid peroxidation and increase SOD level in a dosage dependent manner (Table 3). Red yeast rice produced by *M. purpureus* via fermentation was also found to be associated with higher *in vitro* and *in vivo* antioxidant effects [23]. The degree of enhanced antioxidant level may differ based on the initial antioxidant level found in the raw material used [24]. In this study, nonfermented rice was found to contain higher antioxidant level (total phenolic content and FRAP antioxidant activity) than CRYR. Thus, it was not surprising to observe that MFRYR with further enriched antioxidants than the nonfermented rice had recorded much higher *in vitro* (Table 1) and *in vivo* (Table 3) antioxidant activities. Unlike MFRYR, higher level of serum liver enzyme profile and lower level of liver antioxidant in CRYR treated group

Table 3: Liver homogenate lipid peroxidation and SOD enzyme levels.

Treatment	MDA (nM MDA/mg sample)	SOD (unit SOD/mg sample)
Group 1 ($n = 8$)	0.72 ± 0.15*	0.90 ± 0.12*
Group 2 ($n = 8$)	2.21 ± 0.13	0.60 ± 0.01
Group 3 ($n = 8$)	1.11 ± 0.20*	0.72 ± 0.09*
Group 4 ($n = 8$)	0.90 ± 0.03*	0.83 ± 0.03*
Group 5 ($n = 8$)	1.46 ± 0.21*	0.70 ± 0.19*

Values were mean ± standard deviation of 8 animals in each group and significant difference indicated by * ($P < 0.05$) was determined using ANOVA followed by Duncan's multiple range test.

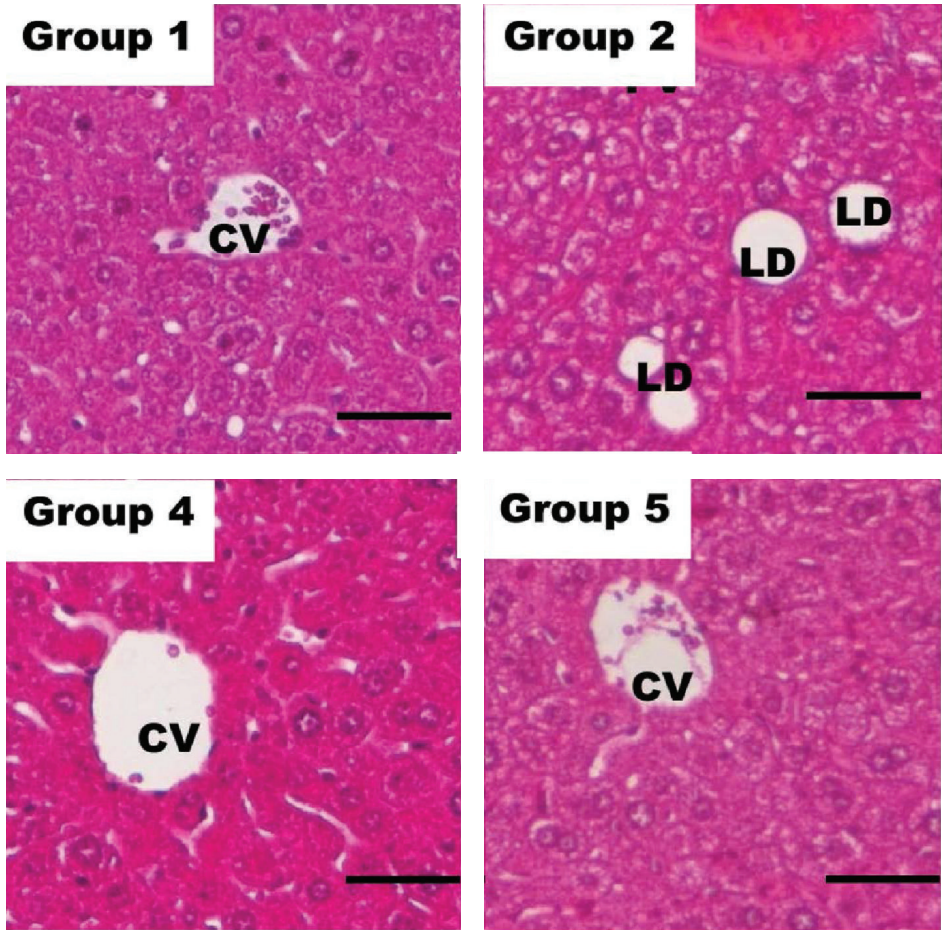

Figure 1: Representative histological micrograph of liver sections from groups 1, 2, 4, and 5 of 14-day treatment stained with H&E (×100, Bar = 50 μm). Only untreated group (group 2) showed lipid droplet in the histological section. CV = central vein, LD = lipid droplet, and PV = portal vein.

Table 4: Relative expression of atherosclerosis related gene in blood of 60 mg/kg body weight of MFRYR (group 4) and CRYR (group 5) treated mice as compared to the untreated mice (group 2).

Genes	Group 4 (MFRYR 60 mg/kg body weight)	Group 5 (CRYR 60 mg/kg body weight)
	Relative expression (fold change)	
ATP-binding cassette transporter 1 (Abca1)	N.S	2.00 ± 0.02
Apolipoproteins-E (ApoE)	**2.66 ± 0.11**	**3.68 ± 0.09**
Chemokine (C-C motif) ligand 2 (CCL2)	N.S	−2.00 ± 0.03
CD44	N.S	−2.01 ± 0.01
Fibronectin (Fn1)	N.S	−2.03 ± 0.01
Integrin, alpha 2 (ITGA2)	N.S	−2.00 ± 0.03
Lipoprotein lipase (LPL)	N.S	−2.00 ± 0.02
Macrophage scavenger receptor 1 (MSR1)	N.S	−2.01 ± 0.04
Neuropeptide Y (Npy)	N.S	−3.85 ± 0.01
Prostaglandin-endoperoxide synthase 1 (PTGS1)	N.S	−2.00 ± 0.03
Selectin P (SELP)	N.S	−2.00 ± 0.05
Transforming growth factor, beta 2 (TGFB2)	N.S	−2.01 ± 0.02
Tumor necrosis factor (TNF)	N.S	−2.00 ± 0.01
Vascular cell adhesion molecule 1 (Vcam1)	N.S	−2.00 ± 0.01
Von Willebrand factor (Vwf)	**−3.00 ± 0.13**	**−4.24 ± 0.12**

N.S.: not significant, only fold change greater than ±2 was recorded and presented as significant results.

might be due to the presence of the potentially hepatotoxic monacolin-k [15] and the lower level of antioxidant (Table 1) compared to MFRYR.

High level of serum cholesterol is often associated with increased risk of atherosclerosis [25]. To understand the possible mechanism of the hypocholesterolemic effect by MFRYR and CRYR, RNA was extracted from blood and subjected to PCR array for evaluation of atherosclerosis related gene expressions. Only fold changes greater than ±2 were recorded in Table 4 as significant regulated genes in comparison to the untreated cholesterol group (group 2). MFRYR only showed significant upregulation of *Apoe* and downregulation of *Vwf* gene expressions. On the other hand, CRYR was able to significantly upregulate *Abca1* and *Apoe* (~3-fold) while downregulating *Ccl2*, *Cd44*, *Fn1*, *Itga2*, *Lpl*, *Msr1*, *Npy* (~4-fold), *Ptgs1*, *Selp*, *Tgfb2*, *Tnf*, *Vcam1*, and *Vwf* (~4-fold). The regulations of *Apoe* and *Vwf* by MFRYR showed similar trends as CRYR but at lower magnitudes. Furthermore, MFRYR also showed regulations of *Abca1*, *Ccl2*, *Cd44*, *Fn1*, *Itga2*, *Lpk*, *Msr1*, *Npy*, *Ptgs1*, *Selp*, *Tgfb2*, *Tnf*, and *Vcam1* with similar trends as CRYR but with fold changes of less than 2 (results not shown). The deficiency of *ApoE* is related to the elevation of blood cholesterol level and subsequently leads to increased risk of atherosclerosis [26]. On the other hand, *Vwf* is a procoagulant glycoprotein which has been widely used as an indicator of endothelial damage during atherosclerosis [27]. These two genes have been significantly regulated by both MFRYR and CRYR. More atherosclerosis related genes were regulated in the CRYR treated mice indicating that MFRYR and CRYR which contained different types of active metabolites possessed hypocholesterolemic effects via different mechanisms. As indicated by Table 1, total phenolic contents of MFRYR were 20 times higher than CRYR. Previous study has reported that common polyphenol that is in grape seed, which were gallic acid and catechin, inhibited the pancreatic cholesterol esterase and reduced solubility of cholesterol in micelles thus slowing the adsorption of cholesterol [28]. Thus, polyphenols that are present in MFRYR may also utilize similar mechanism to reduce adsorption of cholesterol in this study. However, further detailed transcriptome analysis on the hypercholesterolemic mice treated with amino acid and phenolic compounds isolated from MFRYR is needed to have a better understanding of the different hypocholesterolemic regulations between MFRYR which does not and CRYR which does contain monacolin-k.

4. Conclusion

MFRYR contained higher free amino acid (111-fold) and total phenolic level (20 times) comparing to unfermented rice and CRYR. Furthermore, MFRYR reduced the cholesterol level similarly and more effectively enhanced the antioxidant level in hypercholesterol mice comparing to CRYR. Atherosclerosis related gene expression study proposed that MFRYR may differentially regulate hypocholesterolemic effect comparing to CRYR. These results concluded that MFRYR that is free from monacolin-k possesses good and comparable hypocholesterolemic properties as CRYR with better hepatoprotective effect contributed by the enhanced antioxidants present in MFRYR.

Abbreviations

CRYR: Commercial red yeast rice extract
MFRYR: MARDI *Monascus purpureus* strain fermented red yeast rice water extract
GABA: γ-aminobutyric acid
TAG: Triglycerides
LDL: Low density lipoprotein
HDL: High density lipoprotein
ALT: Alanine transaminase
ALP: Alkaline phosphatase
AST: Aspartate aminotransferase
ApoE: Apolipoproteins-E
Vwf: Von Willebrand factor.

Conflict of Interests

All authors declare that there is no conflict of interests.

Acknowledgments

This project was funded by Techno Fund Grant provided by the Ministry of Agriculture and Bio-Based Industry (MOA), Malaysia. The authors would like to thank Professor Tan Soon Guan for proofreading this paper.

References

[1] C. Arunachalam and D. Narmadhapriya, "MONASCUS fermented rice and its beneficial aspects: a new review," *Asian Journal of Pharmaceutical and Clinical Research*, vol. 4, no. 1, pp. 29–31, 2011.

[2] C. L. Lee, H. K. Hung, J. J. Wang, and T. M. Pan, "Red mold dioscorea has greater hypolipidemic and antiatherosclerotic effect than traditional red mold rice and unfermented dioscorea in hamsters," *Journal of Agricultural and Food Chemistry*, vol. 55, no. 17, pp. 7162–7169, 2007.

[3] P. Nimnoi and S. Lumyong, "Improving solid-state fermentation of *Monascus purpureus* on agricultural products for pigment production," *Food and Bioprocess Technology*, vol. 4, no. 8, pp. 1384–1390, 2011.

[4] C. L. Lee, J. J. Wang, S. L. Kuo, and T. M. Pan, "Monascus fermentation of dioscorea for increasing the production of cholesterol-lowering agent—monacolin K and antiinflammation agent—monascin," *Applied Microbiology and Biotechnology*, vol. 72, no. 6, pp. 1254–1262, 2006.

[5] H. Jun, Y. M. Choi, M. H. Hoang, Y. Jia, J. H. Lee, and S. J. Lee, "Red yeast barley reduces plasma glucose levels and activates AMPK phosphorylation in db/db mice," *Food Science and Biotechnology*, vol. 20, no. 5, pp. 1265–1270, 2011.

[6] H. J. Park and I. S. Kim, "Antioxidant activities and anticancer effects of red yeast rice grown in the medium containing garlic," *Food Science and Biotechnology*, vol. 20, no. 2, pp. 297–302, 2011.

[7] Y. H. Pyo and K. I. S. Seong, "Hypolipidemic effects of monascus-fermented soybean extracts in rats fed a high-fat and

-cholesterol diet," *Journal of Agricultural and Food Chemistry*, vol. 57, no. 18, pp. 8617–8622, 2009.

[8] Y. G. Li, F. Zhang, Z. T. Wang, and Z. B. Hu, "Identification and chemical profiling of monacolins in red yeast rice using high-performance liquid chromatography with photodiode array detector and mass spectrometry," *Journal of Pharmaceutical and Biomedical Analysis*, vol. 35, no. 5, pp. 1101–1112, 2004.

[9] Y. C. Su, J. J. Wang, T. T. Lin, and T. M. Pan, "Production of the secondary metabolites γ-aminobutyric acid and monacolin K by *Monascus*," *Journal of Industrial Microbiology and Biotechnology*, vol. 30, no. 1, pp. 41–46, 2003.

[10] J. I. Yamashiro, S. Shiraishi, T. Fuwa, and T. Horie, "Dimerumic acid protected oxidative stress-induced cytotoxicity in isolated rat hepatocytes," *Cell Biology and Toxicology*, vol. 24, no. 4, pp. 283–290, 2008.

[11] M. Klimek, S. Wang, and A. Ogunkanmi, "Safety and efficacy of red yeast rice (*Monascus purpureus*) as an alternative therapy for hyperlipidemia," *Pharmacy and Therapeutics*, vol. 34, no. 6, pp. 313–327, 2009.

[12] C. C. Lin, T. C. Li, and M. M. Lai, "Efficacy and safety of *Monascus purpureus* Went rice in subjects with hyperlipidemia," *European Journal of Endocrinology*, vol. 153, no. 5, pp. 679–686, 2005.

[13] Z. Lu, W. Kou, B. Du et al., "Effect of Xuezhikang, an extract from red yeast Chinese rice, on coronary events in a Chinese population with previous myocardial infarction," *The American Journal of Cardiology*, vol. 101, no. 12, pp. 1689–1693, 2008.

[14] FDA, "FDA warns consumers to avoid red yeast rice products promoted on Internet as treatments for high cholesterol," http://www.fda.gov/bbs/topics/NEWS/2007/NEW01678.html.

[15] Merck, "Mevacor (lovastatin)," package insert, http://www.merck.com/product/usa/pi_circulars/m/mevacor/mevacor_pi.pdf.

[16] N. M. Ali, H. M. Yusof, K. Long et al., "Antioxidant and hepatoprotective effect of aqueous extract of germinated and fermented mung bean on ethanol-mediated liver damage," *BioMed Research International*, vol. 2013, Article ID 693613, 9 pages, 2013.

[17] L. K. Beh, Z. Zakaria, B. K. Beh, W. Y. Ho, S. K. Yeap, and N. B. M. Alitheen, "Comparison of total phenolic content and antioxidant activities of freeze-dried commercial and fresh fruit juices," *Journal of Medicinal Plants Research*, vol. 6, pp. 5857–5862, 2012.

[18] Z. Ajdari, A. Ebrahimpour, M. Abdul Manan, M. Hamid, R. Mohamad, and A. B. Ariff, "Assessment of monacolin in the fermented products using *Monascus purpureus* FTC5391," *Journal of Biomedicine and Biotechnology*, vol. 2011, Article ID 426168, 9 pages, 2011.

[19] J. J. Wang, C. L. Lee, and T. M. Pan, "Improvement of monacolin K, γ-aminobutyric acid and citrinin production ratio as a function of environmental conditions of *Monascus purpureus* NTU 601," *Journal of Industrial Microbiology and Biotechnology*, vol. 30, no. 11, pp. 669–676, 2003.

[20] S. Roohinejad, A. Omidizadeh, H. Mirhosseini et al., "Effect of pre-germination time of brown rice on serum cholesterol levels of hypercholesterolaemic rats," *Journal of the Science of Food and Agriculture*, vol. 90, no. 2, pp. 245–251, 2010.

[21] M. S. Afonso, A. M. de O Silva, E. B. Carvalho et al., "Phenolic compounds from Rosemary (*Rosmarinus officinalis* L.) attenuate oxidative stress and reduce blood cholesterol concentrations in diet-induced hypercholesterolemic rats," *Nutrition and Metabolism*, vol. 10, no. 1, article 19, 2013.

[22] E. Børsheim, Q. U. T. Bui, S. Tissier et al., "Amino acid supplementation decreases plasma and liver triacylglycerols in elderly," *Nutrition*, vol. 25, no. 3, pp. 281–288, 2009.

[23] A. Rajasekaran and M. Kalaivani, "Hypolipidemic and antioxidant activity of aqueous extract of *Monascus purpureus* fermented indian rice in high cholesterol diet fed rats," *Turkish Journal of Medical Sciences*, vol. 41, no. 1, pp. 25–32, 2011.

[24] C. F. Kuo, C. C. Chyau, T. S. Wang, C. R. Li, and T. J. Hu, "Enhanced antioxidant and anti-inflammatory activities of *Monascus pilosus* fermented products by addition of turmeric to the medium," *Journal of Agricultural and Food Chemistry*, vol. 57, no. 23, pp. 11397–11405, 2009.

[25] J. Skogsberg, J. Lundström, A. Kovacs et al., "Transcriptional profiling uncovers a network of cholesterol-responsive atherosclerosis target genes," *PLoS Genetics*, vol. 4, no. 3, Article ID e1000036, 2008.

[26] J. Y. Métais, T. Winkler, J. T. Geyer et al., "BCL2A1a overexpression in murine hematopoietic stem and progenitor cells decreases apoptosis and results in hematopoietic transformation," *PLoS ONE*, vol. 7, no. 10, Article ID e48267, 2012.

[27] M. Ghayour-Mobarhan, D. J. Lamb, S. Tavallaie, and G. A. A. Ferns, "Relationship between plasma cholesterol, von Willebrand factor concentrations, extent of atherosclerosis and antibody titres to heat shock proteins-60, -65 and -70 in cholesterol-fed rabbits," *International Journal of Experimental Pathology*, vol. 88, no. 4, pp. 249–255, 2007.

[28] S. Ngamukote, K. Mäkynen, T. Thilawech, and S. Adisakwattana, "Cholesterol-lowering activity of the major polyphenols in grape seed," *Molecules*, vol. 16, no. 6, pp. 5054–5061, 2011.

Hindawi Publishing Corporation
Evidence-Based Complementary and Alternative Medicine
Volume 2014, Article ID 180965, 10 pages
http://dx.doi.org/10.1155/2014/180965

Research Article

Traditional Chinese Medicine Shuang Shen Ning Xin Attenuates Myocardial Ischemia/Reperfusion Injury by Preserving of Mitochondrial Function

Xueli Li,[1,2] Jianxun Liu,[2] Li Lin,[2] Yujie Guo,[2] Chengren Lin,[2] Cuixiang Zhang,[2] and Bin Yang[2]

[1] *Beijing University of Chinese Medicine, Beijing 100029, China*
[2] *Institute of Basic Medical Sciences, Xiyuan Hospital, China Academy of Chinese Medical Sciences, No. 1 Xiyuan Caochang, Haidian District, Beijing 100091, China*

Correspondence should be addressed to Jianxun Liu; liujx0324@sina.com

Received 26 February 2014; Revised 11 May 2014; Accepted 20 May 2014; Published 16 June 2014

Academic Editor: Ke-ji Chen

To investigate the potential cardioprotective effects of Shuang Shen Ning Xin on myocardial ischemia/reperfusion injury. Wistar rats were treated with trimetazidine (10 mg/kg/day, ig), Shuang Shen Ning Xin (22.5, 45 mg/kg/day, ig), or saline for 5 consecutive days. Myocardial ischemia/reperfusion injury was induced by ligation of the left anterior descending coronary artery for 40 min and reperfusion for 120 min on the last day of administration. It is found that Shuang Shen Ning Xin pretreatment markedly decreased infarct size and serum LDH levels, and this observed protection was associated with reduced myocardial oxidative stress and cardiomyocyte apoptosis after myocardial ischemia/reperfusion injury. In addition, further studies on mitochondrial function showed that rats treated with Shuang Shen Ning Xin displayed decreased mitochondrial swelling and cytosolic cytochrome c levels, which were accompanied by a preservation of complex I activities and inhibition of mitochondrial permeability transition. In conclusion, the mitochondrial protective effect of Shuang Shen Ning Xin could be a new mechanism, by which Shuang Shen Ning Xin attenuates myocardial ischemia/reperfusion injury.

1. Introduction

Myocardial ischemia/reperfusion (MI/R) has been shown to result in mitochondrial dysfunction, and the importance of mitochondria as both targets and mediators of MI/R injury is well recognized [1, 2]. The mitochondrion is a vital component in cellular energy metabolism and intracellular signaling cascades. As the high energy requirement of contracting cardiac myocytes, the mitochondria cover 30% of the cell's total volume providing energy via oxidative phosphorylation, and as a result these cells are particularly vulnerable to mitochondrial defects [3]. During myocardial ischaemia and reperfusion, mitochondria can quickly turn into death-promoting organelles by depressing respiratory chain complex activity, disrupting adenosine triphosphate synthesis, releasing pro-death proteins, producing reactive oxygen species, and inducing the mitochondrial permeability transition pore (mPTP) opening [4]. Thus, mitochondrial dysfunction is widely acknowledged as an important event in necrotic and apoptotic cell death and is emerging as a key mediator of MI/R injury. In this context, the preservation of mitochondrial integrity and function is a potential therapeutic strategy to limit MI/R injury and attenuate the disease process.

Traditional Chinese medicine (TCM) has unique theories of etiology, diagnosis, and treatment. According to TCM, the pathogenesis of MI/R injury is usually diagnosed as Qi stagnation and blood stasis [5, 6]. Shuang Shen Ning Xin (SSNX), a traditional Chinese medicine for invigorating Qi, activating blood circulation, and relieving pain, has been developed for the treatment of coronary heart diseases. The SSNX is composed of three kinds of effective fractions in certain proportion including total ginsenosides, total salvianolic acids, and total alkaloids which are isolated

from *Ginseng* Radix et Rhizoma, *Salviae miltiorrhizae* Radix et Rhizoma, and *Corydalis* Rhizoma, respectively, and the quality control of SSNX is satisfactory. Experimental studies have shown that SSNX can effectively inhibit myocardial infarction and preserve left ventricular structure and function in a porcine myocardial ischemia model [7–9]. Moreover, these beneficial effects can be partly attributed to improving cardiac energy metabolism during ischemia or reperfusion [10]. These results indicate that mitochondria may be a potential therapeutic target of SSNX to reduce cell damage during MI/R. Therefore, the aim of this study is to ascertain whether the mitochondrial protection was involved in the above cardioprotective effects of SSNX.

2. Materials and Methods

2.1. Drugs and Reagents. SSNX was provided by Institute of Basic Medical Sciences of Xiyuan Hospital (Beijing, China). In brief, three kinds of Chinese herbs including *Ginseng* Radix et Rhizoma, *Salviae miltiorrhizae* Radix et Rhizoma, and *Corydalis* Rhizoma were extracted by alcohol according to a standard method to obtain "full components" and were separated by macroporous resin column to isolate target effective fractions such as total ginsenosides (containing in % the following: 18.6 ginsenoside Rg_1; 6.2 ginsenoside Re; 14.6 ginsenoside Rb_1; 2.6 ginsenoside Rd; 7.7 ginsenoside Rc; 2.5 ginsenoside $Rb_{2/3}$; 3.7 ginsenoside Rf), total salvianolic acids (containing in % the following: 1.3 salvianolic acid A; 55.1 salvianolic acid B; 3.0 rosmarinic acid; 2.9 lithospermic acid), and total alkaloids (containing in % the following: 0.8 berberine; 3.5 tetrahydropalmatine; 5.0 palmatine; 17.4 dehydrocorydaline; 2.6 corydaline; 0.4 worenine; 3.1 protopine; 1.2 epiberberine; 2.0 tetrahydrocolumbamine; 3.4 coptisine; 2.2 A-allocryptopine; 3.6 glaucine; 3.0 Jatrorrhizine; 3.1 tetrahydrojatrorrhizine; 0.2 canadine), respectively. SSNX was composed of these three kinds of effective fractions in certain proportion.

Trimetazidine (TMZ) was produced by Servier Pharmaceutical Co., Ltd., Tianjin, China. Nitroblue tetrazolium (NBT) was purchased from Amresco (Solon, OH, USA). The in situ cell apoptosis detection kit was purchased from Boster Biological Technology (Wuhan, China). The assay kit of lactate dehydrogenase (LDH) was purchased from Hitachi High-Tech (Japan). The assay kits of malondialdehyde (MDA) and glutathione peroxidase (GSH-Px) were purchased from Nanjing Jiancheng Bioengineering Institute (Nanjing, China). The assay kits of Cytochrome c (Cyt c) Protein Quantity and Complex I Enzyme Activity Microplate were purchased from Abcam (Cambridge, UK). The rabbit anticleaved caspase-3 was purchased from Cell Signaling Technology (Beverly, MA, USA).

2.2. Animal Treatment. Wistar rats (SPF grade, male, 230–280 g) were purchased from the Vital River Laboratories (VRL, Beijing, China). The animals were kept in rooms maintained at $23 \pm 2^{\circ}$C in a 12 h light/dark cycle and were fed a rodent standard diet with free access to water following international recommendations. All animal experiments in this study were performed in accordance with China Academy of Chinese Medical Sciences Guide for Laboratory Animals that conforms to the Guide for the Care and Use of Laboratory Animals published by the U.S. National Institutes of Health (NIH Publications number 85-23, revised in 1996). Rats were randomly divided into five groups and treated as follows: (1) the sham group; (2) the I/R group; (3) the I/R group treated with TMZ solution at doses of 10 mg/kg TMZ; (4) the I/R group treated with SSNX solution at doses of 22.5, 45 mg/kg SSNX, respectively. TMZ or SSNX was given intragastrically one time a day for five consecutive days, while the sham and I/R groups were given normal saline.

One hour after the last treatment period, rats were anesthetized with chloral hydrate (350 mg/kg, ip) before operation. The surgical procedure for MI/R was performed as previously described [10]. Briefly, a parasternal incision was made by cutting the intercostal muscles between the left third and fourth ribs and the pericardium was excised to expose the heart. Then, myocardial ischemia was induced by ligation of the left anterior descending coronary artery at a point 1~2 mm inferior to the left auricle with a 6-0 silk suture. After 40 min of left coronary artery (LCA) ischemia the ligature was released to allow reperfusion for 2 h.

At the end of the reperfusion period, blood samples were drawn from the abdominal aorta and serum was separated by centrifugation at 1620 g for 10 min (Thermo Scientific IEC CL31R Multispeed Centrifuge) and analyzed for LDH activity. The hearts were subsequently excised and processed for biochemical, morphological, and molecular studies.

2.3. Assessment of Myocardial Infarct Size. At the end of the experiments, rat hearts were removed and irrigated with normal saline to wash out blood. The left ventricle was separated and sliced into 2 mm thick transverse sections which were incubated with 0.05% NBT solution (dissolved in phosphate buffer pH 7.2) at 37°C for 15 min to distinguish the viable myocardium from the necrotic myocardium. The viable tissue was stained dark blue by NBT, while the infarct portion without NBT staining remained red. Both sides of each section were photographed. The area measurement was performed by a computerized high-resolution pathological image analysis system (HPIAS-1000, Wuhan, China). Infarct size was calculated as a percentage of the left ventricle as follows: infarct size = total area of red tissue/area of the left ventricle × 100%.

2.4. Biochemical Studies. The 10% heart homogenate was prepared in ice-cold phosphate buffer (0.1 mol/L, pH 7.4) and centrifuged at 1620 g for 15 min at 4°C. The supernatant was used for determination of MDA levels and GSH-Px activities after the measurement of total protein content. Furthermore, the serum LDH levels were assayed spectrophotometrically with a commercial kit following the manufacturer's instructions.

2.5. Histological Analysis. Left ventricular heart tissues fixed in 10% phosphate-buffered formalin were embedded in paraffin, and serial sections (4 μm thick) were cut using microtome

(Leica RM 2125, Germany). Several sections were stained with hematoxylin and eosin (HE) and examined under a light microscope (Olympus BX51, Tokyo, Japan) for any histopathological changes. Other serial sections were used to determine myocardial apoptosis.

2.6. Determination of Myocardial Apoptosis by TdT-Mediated dUTP Nick End Labeling (TUNEL). A TUNEL assay was performed with the commercially available in situ cell apoptosis detection kit, according to the manufacturer's instructions. Proteinase K (100 μL) was added to each heart tissue slide for 15 min, and then slides were incubated with TdT and DIG-dUTP mixture labeling buffer at 37°C for 2 h. After the reactions were terminated, the slides were washed and incubated with hematoxylin to determine the number of nuclei. The TUNEL signals were observed with the Olympus BX51 microscope. In each slide, the TUNEL signals (brown signals) were mainly distributed around the border zone of the ischemic area in which five fields were randomly selected and the cells positive with TUNEL staining and hematoxylin staining (blue signals) were counted. Quantitative assessment of apoptosis was determined as a ratio of the number of TUNEL-positive cells to total nuclear number in each field.

2.7. Western Blot Analysis. Myocardium tissue samples were homogenized with ice-cold lysis buffer (Applygen Technologies Inc., Beijing, China). The lysates were centrifuged, and protein concentration was determined with BCA protein assay kit (Applygen Technologies Inc., Beijing, China). Protein extracts (10 μg) were separated by electrophoresis on 12% sodium dodecyl sulfate polyacrylamide gel (SDS-PAGE) and then transferred onto polyvinylidene difluoride (PVDF) membranes. Blots were first blocked in 5% dry milk for 30 min and then incubated overnight at 4°C with primary antibody (rabbit anticleaved caspase-3 at 1 : 1000 dilution). The membranes were subsequently washed five times in 1 × Tris-buffer saline Tween 20 (TBST) buffer and then incubated with horseradish peroxidase- (HRP-) conjugated goat anti-rabbit secondary antibodies (dilution 1 : 40000; Cell Signaling). The protein bands were visualized with an enhanced chemiluminescent substrate (Applygen Technologies Inc., Beijing, China). Glyceraldehyde-3-phosphate dehydrogenase (GADPH) was chosen as a loading control to further assure the same volume for all the samples.

2.8. Identification of Cardiac Mitochondria with Transmission Electron Microscope. Electron microscopy was used to identify isolated mitochondria from the hearts. Isolated cardiac mitochondria were fixed in 2.5% glutaraldehyde in phosphate buffer (0.1 mol/L, pH 7.4) at 4°C. After rinsing in cacodylate buffer, mitochondrial pellets were postfixed in 1% cacodylate-buffered osmium tetroxide for 2 h at room temperature and then dehydrated in a graded series of ethanol solutions. The specimens were then embedded in Epon Araldite to block tissue and ultrathin sections. The sections were stained with uranyl acetate and lead acetate and examined under a transmission electron microscope (Hitachi H-600, Japan).

2.9. Isolation of Mitochondria and Cytosol. The mitochondrial and cytosolic fractions were prepared with the mitochondria/cytosol isolation kit (Applygen Technologies Inc., Beijing, China) according to the manufacturer's instructions [11]. All isolation procedures were conducted at 4°C. Heart tissues were homogenized with the ice-cold mitochondria/cytosol buffer as described above. After the first spin, the supernatant was further centrifuged at 12,000 g for 10 min to obtain pure cytosolic fraction. The pellet was resuspended in mitochondria/cytosol buffer and centrifuged at 12,000 g for 10 min again, and the final pellet was resuspended and represented the mitochondrial fraction. Both mitochondrial and cytosolic fractions were stored at −80°C until they were used. Protein content was determined by the BCA method as described above.

2.10. Cyt c Release Assay. The cytosolic fraction samples were normalized for protein and subjected to enzyme linked immunosorbent assay (ELISA) for estimating Cyt c contents following the manufacturer's instructions. Cyt c contents were analyzed at 450 nm and the optical density normalized to total protein content.

2.11. Determination of Mitochondrial Complex I Activity. The mitochondrial fraction samples were normalized for protein, and the activity of complex I was determined with a multimode microplate reader (Bio-Tek, Synergy HT, USA). Mitochondrial complex I was immunocaptured and the activity was determined at 450 nm by following the oxidation of nicotinamide adenine dinucleotide (NADH) to NAD^+.

2.12. Measurement of Mitochondrial Swelling. The activation of the mPTP was determined by Ca^{2+}-induced swelling of isolated cardiac mitochondria. The intact mitochondria samples were resuspended in swelling buffer containing (in mmol/L) 120 KCl, 5 KH_2PO_4, 20 MOPS, and 10 Tris·HCl, with pH 7.4 to a final protein concentration of 0.5 g/L. Mitochondrial permeability transition causes mitochondrial swelling, which is measured spectrophotometrically as a decrease in absorbance at 520 nm followed by the addition of 200 μmol/L $CaCl_2$ [12, 13].

2.13. Statistical Analysis. All data were expressed as mean ± SD and were subjected to one-way ANOVA followed by Bonferroni's multiple comparisons test. All results with $P < 0.05$ were considered statistically significant.

3. Results

3.1. SSNX Reduces Myocardial Infarct Size and Oxidative Stress and Preserves Left Ventricular Structure. To examine whether SSNX treatment reduces the myocardial injury following I/R in rat hearts, myocardial infarct size was measured first. As shown in Figures 1(a) and 1(b), NBT staining of myocardium revealed that I/R challenged myocardium resulted in markedly increased percent infarct size (28.36 ± 4.96%). On the other hand, rats pretreatment with SSNX at dose of 22.5, 45 mg/kg, and TMZ at dose of 10 mg·kg^{-1}

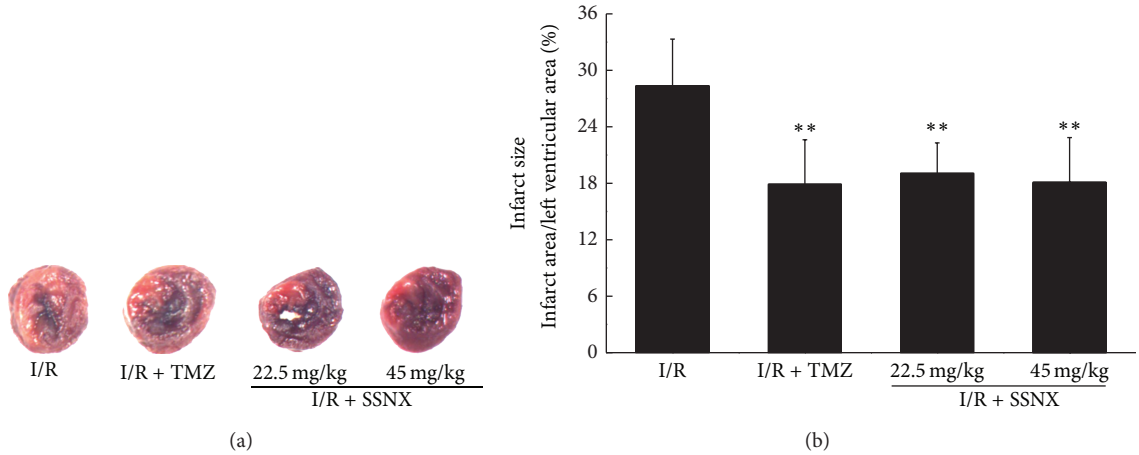

(a) (b)

Figure 1: The effect of SSNX on infarct size after MI/R injury. (a) Representative midmyocardial cross-sections of NBT-stained hearts. The viable myocardium was stained dark blue, and the infracted myocardium was not stained. (b) Bar chart of myocardial infarct size determined by NBT staining. Data are shown as mean ± SD, $n = 8$/group. $^{**}P < 0.01$ versus I/R group.

Table 1: Theeffect of SSNX on serum LDH levels, MDA contents and GSH-Px activities after MI/R injury.

Groups	Dose, mg/kg	LDH, U/L	MDA, nmol/mg protein	GSH-Px, U/mg protein
Sham	—	489 ± 96	1.58 ± 0.25	29.93 ± 6.11
I/R	—	$1843 \pm 787^{\#\#}$	$4.55 \pm 0.81^{\#\#}$	$16.14 \pm 2.32^{\#\#}$
I/R + TMZ	10	$911 \pm 416^{**}$	$1.89 \pm 0.26^{**}$	$24.77 \pm 3.91^{*}$
I/R + SSNX	22.5	$953 \pm 271^{*}$	$2.32 \pm 0.89^{**}$	22.14 ± 4.47
I/R + SSNX	45	$828 \pm 301^{**}$	$2.17 \pm 0.49^{**}$	$25.10 \pm 5.52^{*}$

Note: LDH, $n = 8$/group; MDA, $n = 6$/group; GSH-Px, $n = 6$/group; Date are shown as mean ± SD, $^{\#\#}P < 0.01$ versus Sham group, $^{*}P < 0.05$, $^{**}P < 0.01$ versus I/R group.

markedly reduced the infarct size as compared to I/R group (19.05 ± 3.24%, 18.10 ± 4.76%, and 17.89 ± 4.73%, respectively, versus I/R $P < 0.01$). The representative images of midventricular cross-sections from each group are shown in Figure 1(a).

Circulating plasma levels of LDH were evaluated as an additional marker of myocardial injury. As shown in Table 1, rats subjected to MI/R exhibited significant elevation of serum LDH activity as compared to the sham group (versus sham $P < 0.01$). However, as with the standard drug TMZ, pretreatment with SSNX dose dependently prevented the leakage of LDH from cardiomyocytes (versus I/R $P < 0.05$ or $P < 0.01$). Moreover, this preventative effect was associated with antioxidation. Table 1 also represents the effect of SSNX on the activity of antioxidant enzyme and lipid peroxidation marker in myocardial tissue. Rats in I/R group exhibited significant depletion in the activities of GSH-Px, with a concomitant increase in MDA levels as compared to the sham group (versus sham $P < 0.01$). However, pretreatment with SSNX for 5 days markedly reduced the production of MDA (versus I/R $P < 0.01$), and this preventive effect was partly associated with a significant increase in the GSH-Px activities (versus I/R $P < 0.05$), but pretreatment with SSNX at the dose of 22.5 mg/kg showed no significant effect on the GSH-Px activities.

Tissue sections were also stained with HE for the histopathological evaluation of hearts. As shown in Figure 2, I/R challenged hearts showed extensive myofibrillar degeneration, with infiltration of inflammatory cells and interstitial edema as compared with the sham group. TMZ and SSNX treated rats displayed a reduced degree of tissue edema, degenerative changes and disruption of myofibers, and inflammatory cell infiltration as compared to the sham group.

3.2. SSNX Reduces Cardiomyocyte Apoptosis after MI/R Injury. Since inhibition of the apoptotic processes has been shown to prevent the MI/R injury, we hereby studied the effect of SSNX on apoptotic markers including TUNEL positivity and cleaved caspase-3 expressions' levels. As shown in Figures 3(a) and 3(b), the percentage of TUNEL-positive myocyte nuclei was markedly increased in I/R rats compared with the sham group (34.53 ± 2.92%, versus sham $P < 0.01$). As with the standard drug TMZ (23.81 ± 2.06%, versus I/R $P < 0.01$), rats' pretreatment with SSNX markedly reduced TUNEL-positive cells (26.28±3.43% and 23.79±2.10% versus I/R $P < 0.01$).

To further investigate the effects of SSNX on caspase-3 activation, we measured cleaved caspase-3 expression levels by western blot assay in tissue lysates. As shown in Figure 3(c),

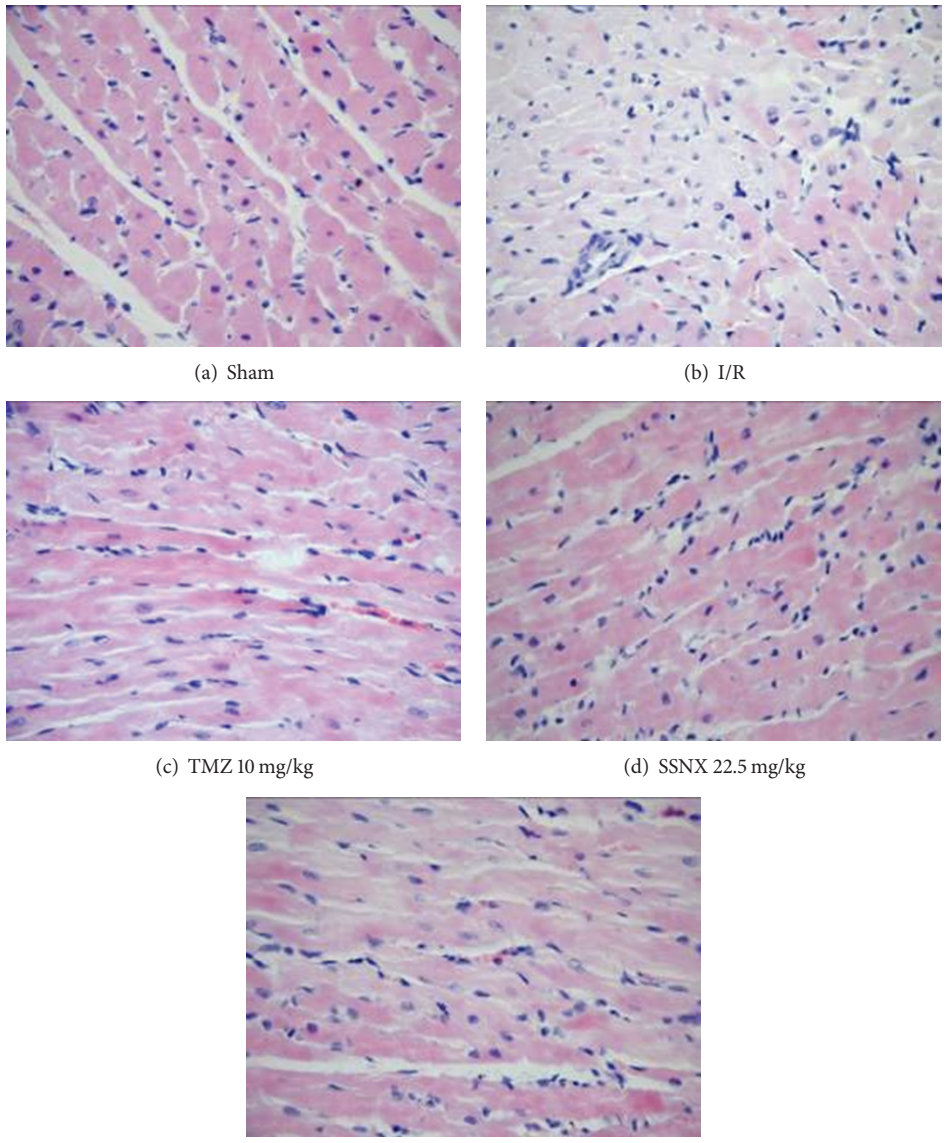

(a) Sham (b) I/R

(c) TMZ 10 mg/kg (d) SSNX 22.5 mg/kg

(e) SSNX 45 mg/kg

Figure 2: Representative HE-stained histological images after 40 min LCA ischemia and 2 h reperfusion (200x). $n = 5$/group.

I/R caused a significant increase in cleaved caspase-3 expression as compared with that in the sham group (versus sham $P < 0.01$). On the other hand, rats treated with TMZ and SSNX at the dose of 45 mg/kg were found to have a significant decrease in cleaved caspase-3 expression levels (versus I/R $P < 0.01$).

Mitochondrial dysfunction may initiate apoptosis by releasing proapoptotic factors, such as Cyt c, from the mitochondrial intermembrane space into the cytosol to trigger apoptosis via a caspase-3-dependent pathway [14, 15]. Thus, changes in cytosolic Cyt c levels were measured by ELISA with the data normalized to total protein. As shown in Figure 3(d), the ELISA analysis revealed I/R group rats to have a significant increase in cytosolic Cyt c levels as compared with the sham group rats (versus sham $P < 0.01$) which indicated the release of Cyt c from the mitochondria into the cytosol, while this subcellular shift of Cyt c was markedly inhibited by pretreatment with SSNX and TMZ (versus I/R $P < 0.01$).

3.3. SSNX Preserves Mitochondrial Function and Membrane Integrity after MI/R Injury. After 40 min of ischemia and 2 h reperfusion, myocardial samples were also qualitatively assessed by transmission electron microscopy for structural mitochondrial changes. As shown in Figure 4, longitudinal sections of the I/R group hearts displayed uniform mitochondrial swelling with disorganized cristae and decreased matrix density, and the presence of amorphous matrix densities in a number of mitochondria revealed a distinctive feature of irreversible myocardial cell injury after reperfusion. TMZ and SSNX-pretreated hearts displayed little change in mitochondrial structure. Generally, mitochondria seemed to be highly

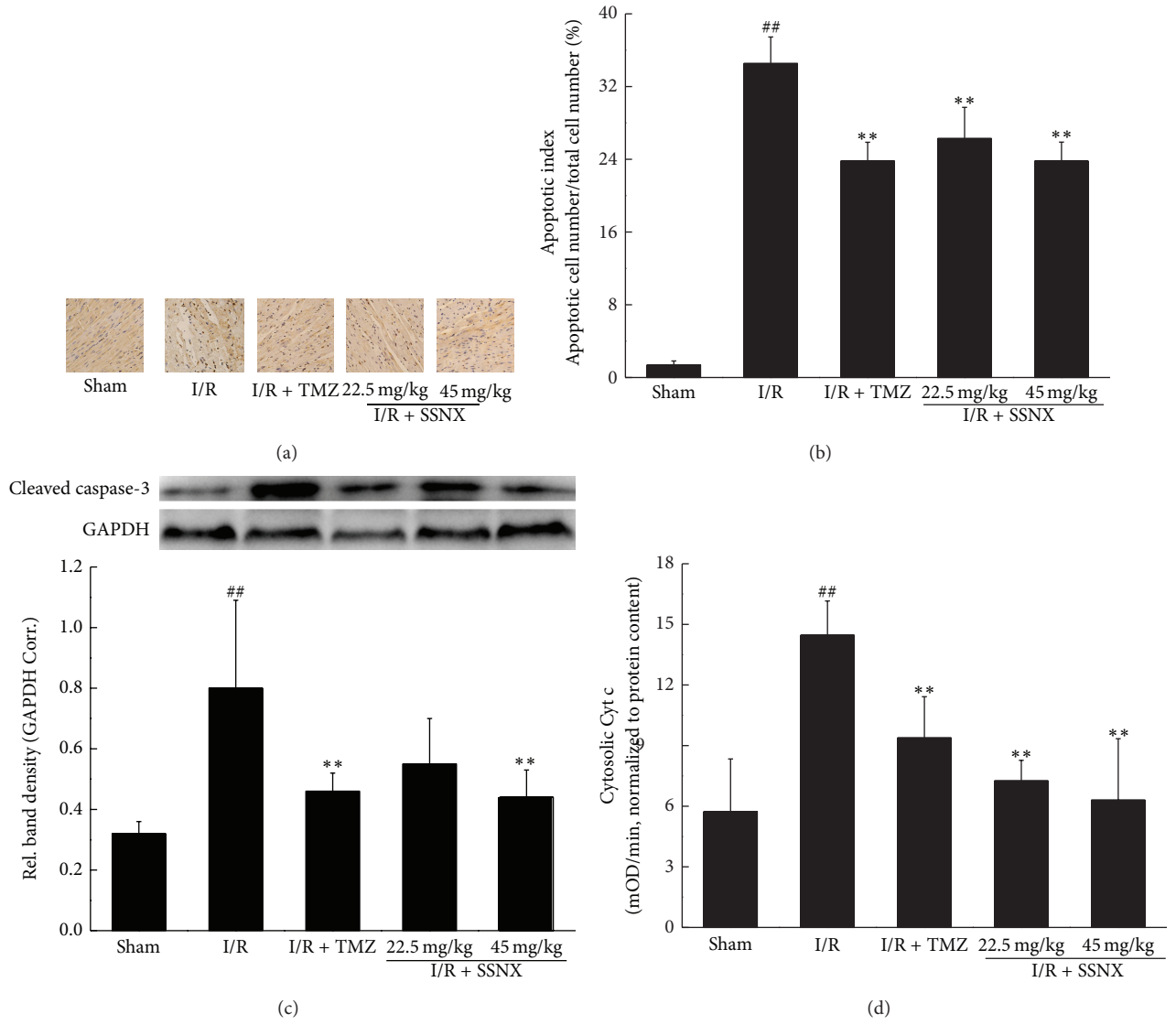

FIGURE 3: The effect of SSNX on cardiomyocyte apoptosis after MI/R injury. Representative photographs (a) and quantitative data (b) on cardiomyocyte apoptosis obtained by TUNEL staining, $n = 5$/group; (c) representative western blot images and densitometry analysis of immunoreactive bands of cleaved caspase-3, $n = 6$/group; (d) the effect of SSNX on cytosolic Cyt c levels after MI/R injury, $n = 6$/group. Data are shown as mean ± SD; $^{\#\#}P < 0.01$ versus sham group; $^{**}P < 0.01$ versus I/R group.

dense with well-organized cristae and a decreased mitochondrial swelling as compared with I/R group myocardium.

The complex I (NADH-CoQ reductase) activities were measured in all the above preparations of mitochondria. As shown in Figure 5, mitochondria from I/R group rat hearts exhibited a marked decrease of 42% in the activities of complex I, compared with the sham group hearts (versus sham $P < 0.01$). As with the standard drug TMZ (versus I/R $P < 0.05$), rats pretreatment with SSNX at dose of 22.5, 45 mg/kg, had a protective effect and actually attenuated the decline in the complex I activities (versus I/R $P < 0.05$ and $P < 0.01$, resp.).

3.4. SSNX Reduces Mitochondrial Permeability Transition Induced by MI/R Injury. Mitochondrial swelling is a hallmark of mitochondrial dysfunction and is an important indicator of the opening of mPTP [16, 17]. To test if SSNX modulates the mitochondrial permeability transition, the mitochondrial swelling following calcium addition was measured as changes in absorbance in isolated mitochondria. As shown in Figure 6, MI/R induced an increase in the swelling rate of mitochondria by 215% compared with the sham group (versus sham $P < 0.01$). In contrast, pretreatment with TMZ and SSNX showed a much smaller increase in the swelling rate of mitochondria, implying that SSNX can prevent the mitochondrial permeability transition (versus I/R $P < 0.05$ and $P < 0.01$, resp.).

4. Discussion

First, TMZ was used as a positive control drug because it was a known metabolic anti-ischemic agent [18–20], which had

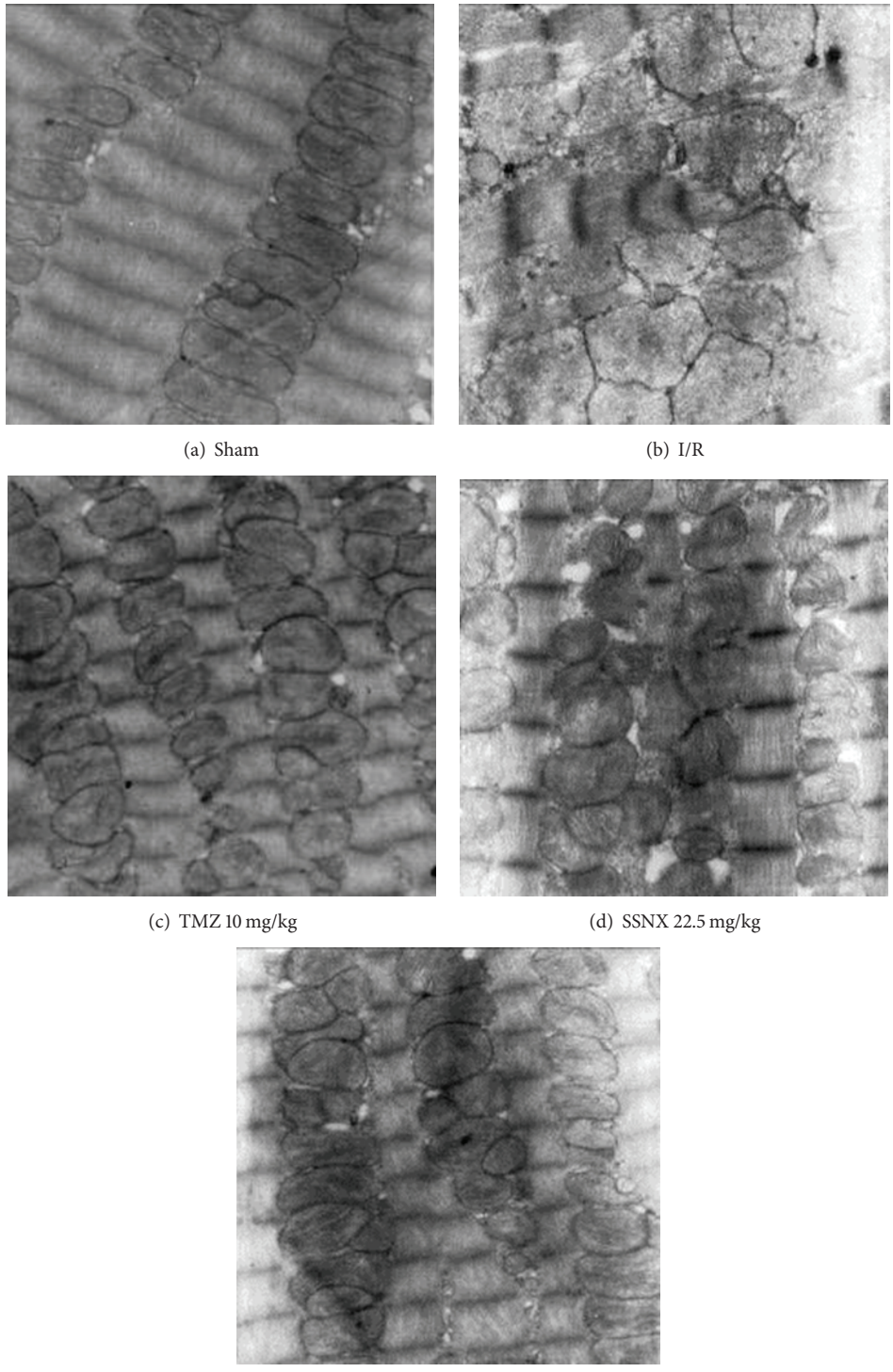

(a) Sham

(b) I/R

(c) TMZ 10 mg/kg

(d) SSNX 22.5 mg/kg

(e) SSNX 45 mg/kg

Figure 4: Representative electron micrographs of myocardial tissues after 40 min LCA ischemia and 2 h reperfusion (12,000x). $n = 2$/group.

a preferential action on mitochondrial function of ischemic hearts [21, 22]. In this study, we showed that pretreatment with SSNX for 5 days limited the extent of myocardial injury in a rat model in vivo. A dose-response study revealed that SSNX displayed a marked reduction in infarct size which had previously been reported by Liu et al. with a Chinese miniporcine myocardial ischemia model [7]. We also found that SSNX markedly reduced MI/R-induced cardiomyocyte

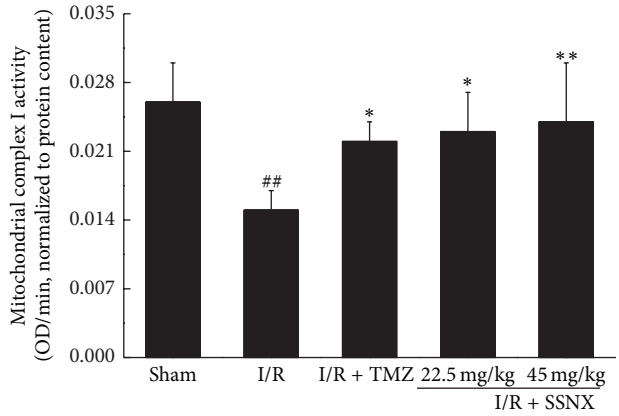

Figure 5: The effect of SSNX on mitochondrial complex I activity after MI/R injury. Data are shown as mean ± SD, $n = 6$/group. $^{\#\#}P < 0.01$ versus sham group; $^{*}P < 0.05$ and $^{**}P < 0.01$ versus I/R group.

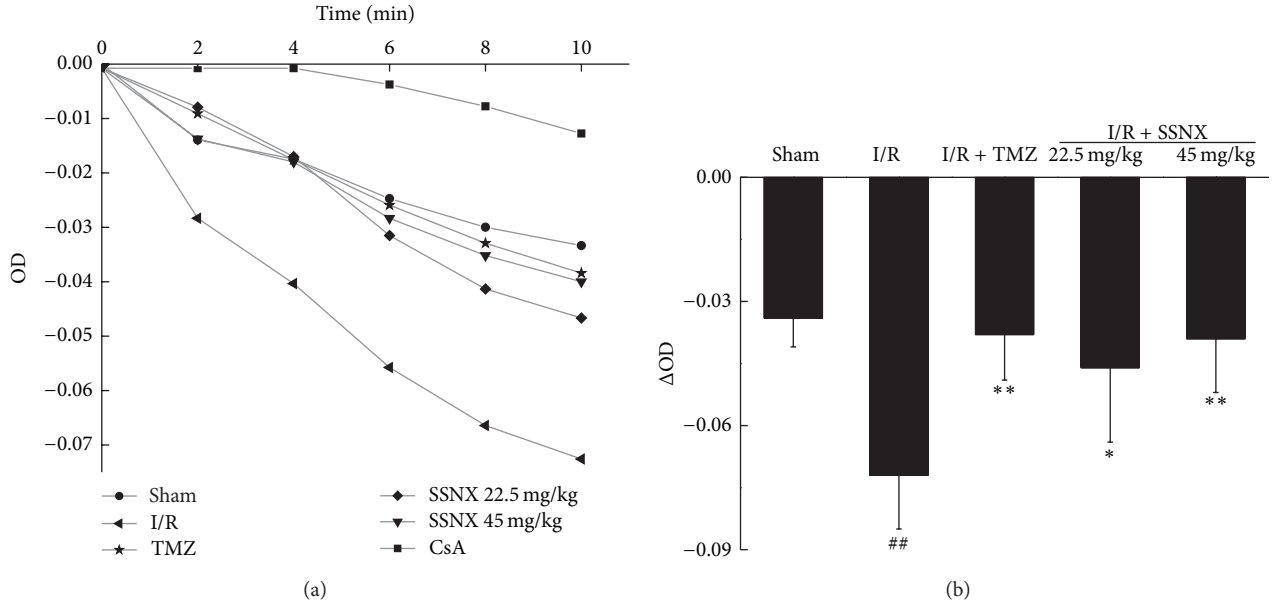

Figure 6: Effect of SSNX on mitochondrial permeability transition in cardiac tissue after MI/R injury. (a) Ca^{2+}-induced mitochondrial swelling measured as decrease in the initial optical density (OD520) within 10 min. Note: cyclosporin A (CsA) is an mPTP inhibitor. (b) Mean changes in the initial optical density (OD520) at 10 min. Data are shown as mean ± SD, $n = 6$/group. $^{\#\#}P < 0.01$ versus sham group; $^{*}P < 0.05$ and $^{**}P < 0.01$ versus I/R group.

apoptosis measured by TUNEL staining. Furthermore, the effects of SSNX against MI/R injury were confirmed by the improved histopathological changes and decreased intracellular LDH leakage. Importantly, the above protective effects were partly attributed to reduced oxidative stress in terms of decreasing MDA production and increasing GSH-Px activities.

Mitochondria play an important role in regulating the life and death of cells. They provide the cell with energy but can quickly switch from a supporter of life to a promoter of death in response to stress [23–25]. It is well established that myocardial ischemia and reperfusion are associated with mitochondrial dysfunction and cell death via both apoptosis and necrosis. Thus, another important research field in myocardial cytoprotection is the preservation of mitochondrial function [3, 4].

Complex I, also known as NADH-ubiquinone oxidoreductase, is a multisubunit integral membrane complex of the mitochondrial electron transport chain that catalyzes electron transfer from NADH to ubiquinone. Complex I is considered an important site of superoxide anion generation in mitochondria [26]. Moreover, it has been reported that MI/R injury resulted in a marked defect of complex I activities, of which the defect is the most important factor

responsible for ROS production by increasing the electron leak from the electron transport chain [27]. This study demonstrated that mitochondria isolated from rats given TMZ displayed a significant increase in complex I activities, which is consistent with previously reported results [22]. Compared with TMZ, rats pretreated with SSNX were found to have a better recovery of complex I activities. This finding indicates that the reduced MDA production by treatment with SSNX may be partly ascribed to preservation of complex I activities, resulting in a decreased production of ROS.

In addition, a key aspect of mitochondrial involvement in cell demise is responsible for the opening of the mPTP [28]. The mPTP is a highly dynamic, nonselective pore which is thought to mediate the lethal permeability changes of the outer mitochondrial membrane (OMM) and the inner mitochondrial membrane (IMM) that causes release of proapoptotic proteins and loss of membrane potential that may lead to apoptotic cell death [24, 29]. It is proposed that MI/R promotes mPTP opening, especially in reperfusion conditions such as increased matrix Ca^{2+}, Pi, and ROS which favor long-lasting pore opening, resulting in swelling and subsequent rupture of mitochondria [30]. In this study, electron microscopy revealed a striking reduction in mitochondrial swelling and increased matrix density in rats receiving SSNX, suggesting a prominent role for the preservation of mitochondrial function in the observed cytoprotection. Furthermore, mPTP displayed an increased sensitivity to calcium after MI/R, and pretreatment with SSNX largely delayed MI/R-induced mitochondrial permeability transition. As has been established, the permeabilization of the OMM results in the release of pro-death proteins, such as Cyt c, from the mitochondrial intermembrane space into the cytosol [28, 31]. Once it is released into the cytosol, Cyt c triggers the formation of Apaf-1/caspase-9 apoptosome and activation of caspases to initiate apoptosis [31], and caspase-3 has conventionally been considered one of the executioner caspases. A further exploration of the role of SSNX involved in apoptotic processes reveals that SSNX inhibits the activation of caspase-3, which is associated with lower cytosolic Cyt c levels. Although the precise mechanisms require further study, this study demonstrates that SSNX exerts an antiapoptotic effect by blocking the mitochondrial apoptotic pathway.

In conclusion, we have shown that pretreatment with SSNX limits the extent of myocardial injury. This protection is accompanied by a decrease in myocardial oxidative stress and cardiomyocyte apoptosis, and these are associated with preservation of mitochondrial function. Furthermore, the present results can also partly account for the improved cardiac energy metabolism of the SSNX treated rat heart after MI/R injury [10], which is reported in our previous studies. Thus, preservation of mitochondrial function may be a new mechanism by which SSNX exerts its cardioprotective effects. In addition, another important mechanism of cardiomyocyte protection by SSNX that we have found in previous studies is suppression of hypoxia/reoxygenation induced-calcium overload [32–34]. These studies confirm that the antimyocardial ischemia effect of SSNX is achieved through collectively modulating the multitargets of the body system by its active ingredients, which is one of the significant advantages of TCM in treating complex diseases.

Conflict of Interests

The authors declare that there is no conflict of interests regarding the publication of this paper.

Acknowledgments

The study was supported by Grants from the National Natural Science Foundation of China (no. 81102795) and the National Major Scientific and Technological Special Project for "Significant New Drugs Development" of China (no. 2012ZX09301002-004). The authors thank Professor Dan Zhu for critical comments regarding this paper.

References

[1] Q. Chen, A. K. Camara, D. F. Stowe, C. L. Hoppel, and E. J. Lesnefsky, "Modulation of electron transport protects cardiac mitochondria and decreases myocardial injury during ischemia and reperfusion," *American Journal of Physiology—Cell Physiology*, vol. 292, no. 1, pp. C137–C147, 2007.

[2] A. K. S. Camara, E. J. Lesnefsky, and D. F. Stowe, "Potential therapeutic benefits of strategies directed to mitochondria," *Antioxidants & Redox Signaling*, vol. 13, no. 3, pp. 279–347, 2010.

[3] S. B. Ong and A. B. Gustafsson, "New roles for mitochondria in cell death in the reperfused myocardium," *Cardiovascular Research*, vol. 94, no. 2, pp. 190–196, 2012.

[4] A. K. S. Camara, M. Bienengraeber, and D. F. Stowe, "Mitochondrial approaches to protect against cardiac ischemia and reperfusion injury," *Frontiers in Physiology*, vol. 2, article 13, 2011.

[5] Y. Q. Li, M. Jin, S. L. Qiu et al., "Effect of Chinese drugs for supplementing qi, nourishing Yin and activating blood circulation on myocardial perfusion in patients with acute myocardial infarction after revascularization," *Chinese Journal of Integrative Medicine*, vol. 15, no. 1, pp. 19–25, 2009.

[6] Z. G. Wu, "Therapeutic angiogenesis: the combination point of Chinese and Western medicine in prevention and treatment of ischemic heart disease," *Chinese Journal of Integrative Medicine*, vol. 15, no. 5, pp. 323–324, 2009.

[7] J. X. Liu, Z. Yu, and X. Z. Li, "Effects of shuangshen ningxin capsule on mini-porcine myocardial ischemia model induced by thrombosis via cardiac catheterization intervention," *Chinese Journal of Integrated Traditional and Western Medicine*, vol. 26, no. 8, pp. 728–731, 2006.

[8] Z. Yu, J. X. Liu, X. Z. Li, X. H. Shang, A. G. Yan, and X. Q. Feng, "Protective effects of Shuangshen Ningxin capsule on miniature swine after myocardial ischemia by intervention," *China Journal of Chinese Materia Medica*, vol. 32, no. 16, pp. 1695–1699, 2007.

[9] Z. Yu, J. X. Liu, X. Z. Li, X. H. Shang, and L. F. Yao, "Effects of Shuangshen Ningxin capsule on ventricular remodeling and wall motion in myocardial ischemic miniature swine induced by thrombus," *Chinese Pharmacological Bulletin*, vol. 24, no. 2, pp. 178–182, 2008.

[10] X. L. Li, J. X. Liu, and Y. J. Guo, "Effect of SSNX on myocardial energy metabolism in ischemia/reperfusion rat hearts," *China Journal of Chinese Materia Medica*, vol. 38, no. 17, pp. 89–92, 2013.

[11] Y. Wu, L. Y. Dong, W. An, and Y. Q. An, "Comparison between different methods to extract mitochondria and its effects on mitochondria content and activity," *Journal of Capital Medical University*, vol. 31, no. 2, pp. 241–244, 2010.

[12] J. B. Gong and L. J. Qian, "Measurement of rat myocardial mitochondria permeability transition with spectrophotometer," *Chinese Journal of Applied Physiology*, vol. 17, no. 1, pp. 97–99, 2001.

[13] G. Wang, D. A. Liem, T. M. Vondriska et al., "Nitric oxide donors protect murine myocardium against infarction via modulation of mitochondrial permeability transition," *American Journal of Physiology—Heart and Circulatory Physiology*, vol. 288, no. 3, pp. H1290–H1295, 2005.

[14] P. Li, D. Nijhawan, I. Budihardjo et al., "Cytochrome c and dATP-dependent formation of Apaf-1/caspase-9 complex initiates an apoptotic protease cascade," *Cell*, vol. 91, no. 4, pp. 479–489, 1997.

[15] T. Takatani, K. Takahashi, Y. Uozumi et al., "Taurine prevents the ischemia-induced apoptosis in cultured neonatal rat cardiomyocytes through Akt/caspase-9 pathway," *Biochemical and Biophysical Research Communications*, vol. 316, no. 2, pp. 484–489, 2004.

[16] M. Zoratti and I. Szabo, "The mitochondrial permeability transition," *Biochimica et Biophysica Acta—Reviews on Biomembranes*, vol. 1241, no. 2, pp. 139–176, 1995.

[17] P. Bernardi, R. Colonna, P. Costantini et al., "The mitochondrial permeability transition," *BioFactors*, vol. 8, no. 3-4, pp. 273–281, 1998.

[18] P. F. Kantor, A. Lucien, R. Kozak, and G. D. Lopaschuk, "The antianginal drug trimetazidine shifts cardiac energy metabolism from fatty acid oxidation to glucose oxidation by inhibiting mitochondrial long- chain 3-ketoacyl coenzyme A thiolase," *Circulation Research*, vol. 86, no. 5, pp. 580–588, 2000.

[19] P. G. Steg, G. Grollier, P. Gallay et al., "A randomized double-blind trial of intravenous trimetazidine as adjunctive therapy to primary angioplasty for acute myocardial infarction," *International Journal of Cardiology*, vol. 77, no. 2-3, pp. 263–273, 2001.

[20] L. Polodski, I. Dec, R. Wojnar, and K. Wilczek, "Trimetazidine limits the effects of myocardial ischaemia during percutaneous coronary angioplasty," *Current Medical Research and Opinion*, vol. 18, no. 7, pp. 389–396, 2002.

[21] P. Monteiro, A. I. Duartec, L. M. Goncalves, A. Moreno, and L. A. Providencia, "Protective effect of trimetazidine on myocardial mitochondrial function in an ex-vivo model of global myocardial ischemia," *European Journal of Pharmacology*, vol. 503, no. 1–3, pp. 123–128, 2004.

[22] L. Dehina, F. Vaillant, A. Tabib et al., "Trimetazidine demonstrated cardioprotective effects through mitochondrial pathway in a model of acute coronary ischemia," *Naunyn-Schmiedeberg's Archives of Pharmacology*, vol. 386, no. 3, pp. 205–215, 2013.

[23] D. R. Green and G. Kroemer, "The pathophysiology of mitochondrial cell death," *Science*, vol. 305, no. 5684, pp. 626–629, 2004.

[24] G. Kroemer, L. Galluzzi, and C. Brenner, "Mitochondrial membrane permeabilization in cell death," *Physiological Reviews*, vol. 87, no. 1, pp. 99–163, 2007.

[25] A. B. Gustafsson and R. A. Gottlieb, "Heart mitochondria: gates of life and death," *Cardiovascular Research*, vol. 77, no. 2, pp. 334–343, 2008.

[26] R. G. Hansford, B. A. Hogue, and V. Mildaziene, "Dependence of H_2O_2 formation by rat heart mitochondria on substrate availability and donor age," *Journal of Bioenergetics and Biomembranes*, vol. 29, no. 1, pp. 89–95, 1997.

[27] G. Paradies, G. Petrosillo, M. Pistolese, N. di Venosa, A. Federici, and F. M. Ruggiero, "Decrease in mitochondrial complex I activity in ischemic/reperfused rat heart: involvement of reactive oxygen species and cardiolipin," *Circulation Research*, vol. 94, no. 1, pp. 53–59, 2004.

[28] J. S. Armstrong, "The role of the mitochondrial permeability transition in cell death," *Mitochondrion*, vol. 6, no. 5, pp. 225–234, 2006.

[29] G. T. Kim, Y. S. Chun, J. W. Park, and M. S. Kim, "Role of apoptosis-inducing factor in myocardial cell death by ischemia-reperfusion," *Biochemical and Biophysical Research Communications*, vol. 309, no. 3, pp. 619–624, 2003.

[30] S. Javadov, M. Karmazyn, and N. Escobales, "Mitochondrial permeability transition pore opening as a promising therapeutic target in cardiac diseases," *The Journal of Pharmacology and Experimental Therapeutics*, vol. 330, no. 3, pp. 670–678, 2009.

[31] L. Galluzzi, E. Morselli, O. Kepp, and G. Kroemer, "Targeting post-mitochondrial effectors of apoptosis for neuroprotection," *Biochimica et Biophysica Acta—Bioenergetics*, vol. 1787, no. 5, pp. 402–413, 2009.

[32] J. X. Liu, X. Han, and Y. Y. Sun, "Effect of serum containing SSTG on calcium overload in cardiomyocytes injuryed by hypoxia and reoxygenation," *China Journal of Chinese Materia Medica*, vol. 31, no. 8, pp. 697–699, 2006.

[33] J. X. Liu, X. Han, Y. G. Xu, and R. Ma, "Mechanism of serum containing SSTG on calcium overload in cardiomyocytes injuryed by hypoxia and reoxygenation," *China Journal of Chinese Materia Medica*, vol. 31, no. 12, pp. 995–998, 2006.

[34] X. Han and J. X. Liu, "The effects of SSTG drug serum on Caclium-CaM-CaMPK II signal system in cardiomyocytes injury induced by hypoxia and reoxgyenization," *Chinese Pharmacological Bulletin*, vol. 22, no. 7, pp. 876–879, 2006.

Hindawi Publishing Corporation
Evidence-Based Complementary and Alternative Medicine
Volume 2014, Article ID 484269, 9 pages
http://dx.doi.org/10.1155/2014/484269

Research Article

Paeonol Inhibits Proliferation of Vascular Smooth Muscle Cells Stimulated by High Glucose via Ras-Raf-ERK1/2 Signaling Pathway in Coculture Model

Junjun Chen,[1] Min Dai,[1,2] and Yueqin Wang[1]

[1] *Key Laboratory of Xin'an Medicine, Ministry of Education, Anhui Province Key Laboratory of R&D of Chinese Medicine, Anhui University of Traditional Chinese Medicine, Hefei 230038, China*
[2] *School of Pharmacy, Anhui University of Traditional Chinese Medicine, Shihe Road 45, Hefei, Anhui 230031, China*

Correspondence should be addressed to Min Dai; daiminliao@163.com

Received 19 February 2014; Revised 29 April 2014; Accepted 18 May 2014; Published 5 June 2014

Academic Editor: Hao Xu

Paeonol (Pae) has been previously reported to protect against atherosclerosis (AS) by inhibiting vascular smooth muscle cell (VSMC) proliferation or vascular endothelial cell (VEC) injury. But studies lack how VSMCs and VECs interact when Pae plays a role. The current study was based on a coculture model of VSMCs and VECs to investigate the protective mechanisms of Pae on atherosclerosis (AS) by determining the secretory function of VECs and proliferation of VSMCs focusing on the Ras-Raf-ERK1/2 signaling pathway. VECs were stimulated by high glucose. Our data showed that high concentration (35.5 mM) of glucose induced damage in VECs. Injury of VECs stimulated VSMC proliferation in the coculture model. Pae (120 μM) decreased vascular endothelial growth factor (VEGF) and platelet derivative growth factor B (PDGF-B) release from VECs and inhibited overexpression of Ras, P-Raf, and P-ERK proteins in VSMCs. The results indicate that diabetes modulates the inflammatory response in VECs to stimulate VSMC proliferation and promote the development of AS. Pae was beneficial by inhibiting the inflammatory effects of VECs on VSMC proliferation. This study suggests the inhibitory mechanism of Pae due to the inhibition of VEGF and PDGF-B secretion in VECs and Ras-Raf-ERK1/2 signaling pathway in VSMCs.

1. Introduction

Atherosclerosis (AS) is a major pathological disease for cardiovascular and cerebrovascular problems and also the most common disease in the cardiovascular system [1]. AS is harmful to human health seriously and responsible for most of the deaths in the senior population [2]. Diabetes mellitus is considered as an important risk factor to the accelerated atherosclerosis [3–5]. High glucose has been shown to injure vascular endothelial cells (VECs) and vascular smooth muscle cells (VSMCs), which are two important cells of artery wall and responsible for AS progression [6]. Among them, VEC inflammatory injury and dysfunction are initial factors, and VSMC proliferation and migration are key pathological features [7–9]. In the native artery, VSMCs are tightly associated with VECs in structure and function. VECs dysfunction will release cytokines like VEGF, bFGF, TGF-β, and PDGF which have shown regulatory effects on VSMC proliferation and migration.

The mitogen activated protein kinase (MAPK) signaling pathway is one of the most important pathways for cellular stress response to injury. The MAPK signaling pathway consists of four subfamilies: p38 kinases, Jun-NH2-terminal kinases (JNK1/2), extracellular signal-regulated kinases (ERK1/2), and ERK5 [10]. Signaling through ERK1/2 is typically initiated by Ras, which can be activated by cytokines like VEGF and PDGF-B [11]. They activate Ras, which directly couples with the Raf (MAPK kinase kinase) and then combines with MEK1/2 (MAPK kinases). MEK1/2 functions as a dual specific kinase, which phosphorylates ERK1/2 directly. High concentrations of glucose (GS) have been shown to induce VEC membrane damage by increasing the release of inflammatory cytokines, such as vascular endothelial growth factor (VEGF) and platelet derived

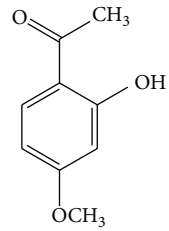

Figure 1: Chemical structure of paeonol.

growth factor-B (PDGF-B) which bind with VSMC membrane receptors and lead to the receptor phosphorylation [12–14]. The activated receptors stimulate downstream signal transduction pathways and eventually activate ERK1/2 protein which lead to VSMC proliferation and intimal thickening [15, 16]. Previous studies have shown that PDGF-B expression was increased when VECs were damaged [17]. PDGF-B then activates the ERK1/2 related signaling pathway, which mainly mediates growth factor-induced cell proliferation [14, 18, 19]. Statistical analysis also showed that VEGF increased in diabetics and associated with blood glucose concentration which can also activate signal pathway involved in ERK1/2 participate [20]. Accordingly, we hypothesise that high glucose induced VECs producing a series of biologically active substances which stimulated VSMC proliferation.

Paeonol (Pae, 2′-hydroxy-4′-methoxyacetophenone, Figure 1) is the major biologically active compound contained in *Cortex Moutan* (*Paeonia suffruticosa* Andrews, Ranunculaceae), which is a Chinese herbal remedy widely used in clinical treatment of inflammatory diseases such as atopic dermatitis, hyperlipidemia, and atherosclerosis [21, 22]. Our previous investigations suggested that Pae had a significant effect on different aspects of AS. *In vivo*, Pae prevented AS in our experimental model and protected against arterial endothelial cell hyperlipidemia [21, 23, 24]. *In vitro*, serum containing Pae significantly inhibited TNF-α-induced VSMC proliferation. Furthermore, our most current research confirmed that Pae significantly reduced the phosphorylation levels of JNK1/2, p38, and ERK1/2, which was activated by TNF-α, ox-LDL, and/or bacterial lipopolysaccharide in VECs [25]. Unfortunately, the previous *in vitro* studies were based only on a single cell type (VECs or VSMCs) and ignored the interactions between these two important cell types.

The current study was focused on a coculture model to determine essential crosstalk pathways between VECs and VSMCs. The coculture model is a novel method which could simulate the environment in native artery to study Pae action. The principal aim of this study was to investigate the effects of Pae on VECs cellular damage and its downstream effects on VSMC proliferation, which ultimately leads to the pathological feature observed in AS. In addition, this study worked to determine the relationship between the secretion function of damaged VECs and the Ras-Raf-ERK1/2 signaling pathway in VSMCs in order to clarify the therapeutic mechanisms of Pae. This experiment model provided a theoretical basis for Pae intervention in AS and optimized a technical platform to determine the cellular target of novel therapeutic compounds.

2. Materials and Methods

2.1. Chemicals and Reagents. The compound paeonol (99% purity) was obtained from Baicao Plants Biotech Co., Ltd. (Anhui, China). Dulbecco's modified Eagle's medium (DMEM), Transwell chamber, type I collagenase, and fetal bovine serum (FBS) were purchased from Gibco Life Technologies, Co., Ltd. (Paisley, UK). 3-(4,5-dimethylthiazolyl-2)-2,5-diphenyltetrazolium bromide (MTT) was obtained from Sigma Chemical Co. (St. Louis, MO, USA). Lactic dehydrogenase (LDH) reagent was purchased from Nanjing Jiancheng Bioengineering Institute (Nanjing, China). Antibodies against PDGF-B, Ras, Raf, phosphorylated Raf (P-Raf), ERK1/2, and phosphorylated ERK1/2 (P-ERK1/2) were obtained from Cell Signaling Technology (Beverly, MA, USA). PDGFR inhibitor (Sunitinib Malate) and ERK1/2 inhibitor (PD98059) were purchased from Santa Cruz Biotechnology Co. (Santa Cruz, CA, USA).

2.2. Animals. Sprague-Dawley (SD) rats (160 ± 10 g) were obtained from Shanghai Super-B&K Laboratory Animal Corp. Ltd. (license number: SCXK 2008-0016). All animal protocols were conducted in accordance with animal welfare protocols at the local institution Animal Care and Use Committee.

2.3. Cell Culture. VECs and VSMCs were isolated from rat thoracic aortas by primary explants techniques according to a previously published protocol [26, 27]. Briefly, the cells were incubated in a 50 mL culture flask at 37°C in a humidified atmosphere containing 5% CO_2. Culture medium was composed of DMEM supplemented with 20% FBS, $NaHCO_3$ (1.8 g/L), penicillin 100 kU/L, and gentamicin 100 kU/L. The culture media were changed every 3 d. Cells were grown to an 80% confluence state and subcultured using 0.2% trypsin. VECs and VSMCs at passages three to five were used in the current study.

2.4. VECs and VSMCs Coculture. The coculture model was created to investigate the effects of damaged VECs on VSMCs through polycarbonate filter membrane (Transwell chamber). The coculture model was created according to the methods of Fillinger et al. [28, 29]. VECs and VSMCs were diluted into cell suspension of 1×10^5 cells/mL. VECs were inoculated into the bottom of a 6-well chamber and pretreated with a high glucose (HG) concentration (35.5 mM) for 48 h, whereas 5.5 mM was considered as normal glucose concentration. Then, VSMCs were inoculated into the top of the Transwell plate. The Transwell chamber was then set into the 6-well chamber and cocultured. The two types of cells were not physically connected but were able to interact by secreting soluble factors through a polycarbonate filter membrane.

2.5. Cell Survival Rate Assay. The cytotoxic effects of glucose and Pae on VECs growth were determined through the 3-(4,5-dimethylthiazolyl-2)-2,5-diphenyltetrazolium bromide (MTT) assay. VECs were grown to 80% confluence and then seeded into a 96-well flat-bottom plate and incubated with DMEM supplemented with 20% FBS. Different concentrations of glucose (5.5, 15.5, 25.5, 35.5, and 45.5 mM) at multiple time points (0, 12, 24, 48, and 72 h) were used. Furthermore, to investigate the effects of Pae on VECs, cells were pretreated with different concentrations of Pae (7.5, 15, 30, 60, and 120 μM) for different time points (0.5, 6, 12, and 24 h) before being stimulated by glucose at a suitable concentration (35.5 mM) for 48 h. Cells were incubated with glucose at 5.5 mM, which is indicated as the normal glucose (NG) group. After treatment, cells were incubated with MTT (20 μL/well) (Sigma Chemical, USA) for 4 h at 37°C. The medium was then removed and DMSO (200 μL/well) was added to solubilize the precipitate. The absorbance then was measured at 490 nm on an absorbance microplate reader (Molecular Devices, USA).

2.6. Lactic Dehydrogenase (LDH) Release Assay. The LDH release was used to investigate the cytoprotective effects of Pae on VEC injury due to high glucose concentrations. VECs were centrifuged at 160 ×g for 8 min to obtain a supernatant comprised of extracellular VEC components. VECs were incubated with 2% Triton X-100, freezed and thawed three times, and centrifuged at 240 ×g for 5 min to obtain a supernatant comprised of intracellular components. LDH concentrations in the extracellular medium and intracellular medium were quantified through the LDH reagent for clinical diagnosis.

2.7. Immunocytochemistry Assay. VECs seeded on coverslips were rinsed with ultrapure water twice, fixed with acetone for 20 min, and then rinsed with phosphate-buffered saline (PBS). Cells were soaked in 3% H_2O_2 at room temperature for 30 min. After washing with PBS, blocking buffer containing 1% goat serum was added and incubated for 20 min. The primary antibody (1 : 200 diluted) against VEGF or PDGF-B was added and incubated at 4°C overnight. A biotinylated secondary antibody was incubated for 20 min; then Streptavidin/Peroxidase (SP) reagent was incubated for 20 min at room temperature. The slides were colored with DAB under a light microscope for 10 min before examination. Immunocomplexes were visualized by the DAB detection system. Brown or dark brown stained cells were considered positive cells. Ten randomly selected fields were visualized at 200x magnification.

2.8. Western Blotting Analysis. Cytoplasmic proteins were obtained using a cell lysis buffer (20 mM HEPES, 2 mM $MgCl_2$, 1 mM EDTA, 2 mM DTT, 1 mM PMSF, pH 7.4) and stored at −80°C. The protein concentrations were quantified by the BCA method. Aliquots (30 μL) were separated on a 10% SDS-PAGE and transferred to an equilibrated polyvinylidene difluoride membrane (PVDF) by electroblotting. Membranes were blocked in 5% fat-free milk for 2 h at room temperature and incubated at 4°C overnight with primary antibodies (rabbit anti-Ras, rabbit anti-Raf, rabbit anti-phospho-Raf, mouse anti-ERK1/2, and rabbit anti-phospho-ERK1/2). Horseradish peroxidase labeled secondary antibodies were added and incubated at room temperature for 2 h. Bands were detected by enhanced chemiluminescence (ECL) kit. Beta-actin protein levels were used as an endogenous control to allow the normalization of target proteins.

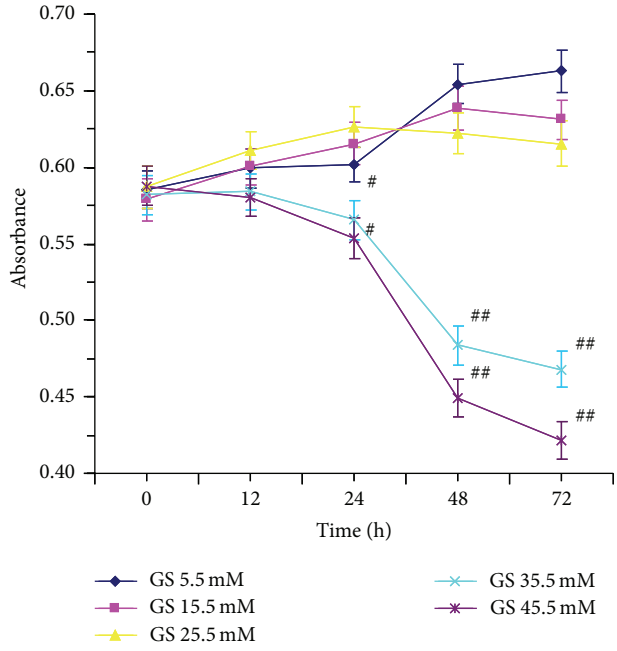

Figure 2: Effect of high glucose on VECs injury. VECs were induced by various concentrations (5.5, 15.5, 25.5, 35.5, and 45.5 mM) of glucose and incubated for different time points (0, 12, 24, 48, and 72 h) to explore the effect of glucose on VECs.

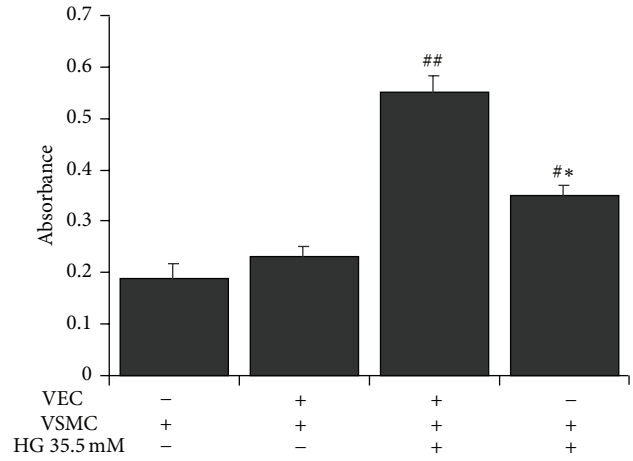

Figure 3: Effect of high glucose on VSMC proliferation in the coculture model. VECs were pretreated with high glucose concentration (35.5 mM) for 48 h and then cocultured with VSMCs for another 24 h to stimulate VSMC proliferation. $^{\#}P < 0.05$, $^{\#\#}P < 0.01$ versus NG (5.5 mM) coculture group; $^{*}P < 0.05$ versus HG (35.5 mM) coculture group.

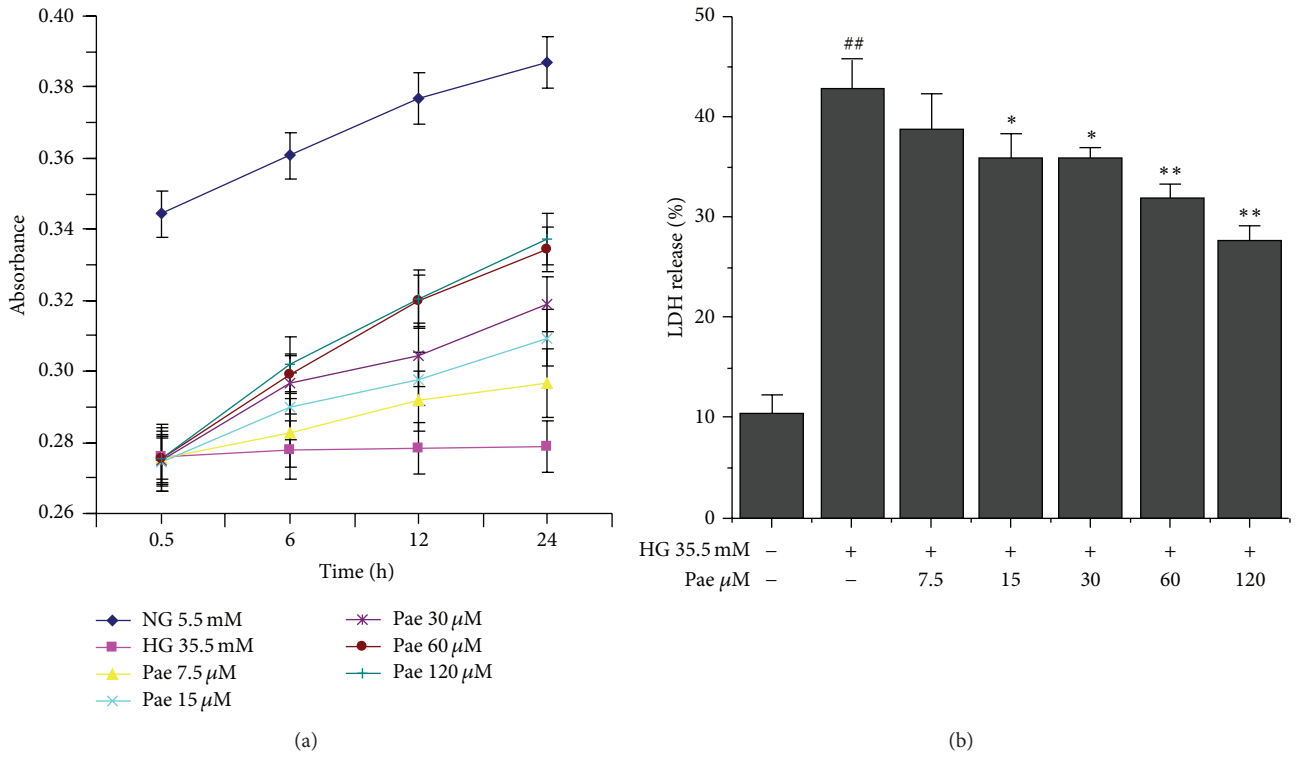

Figure 4: Effect of paeonol on survival and LDH release in VECs. VECs survival (a) and LDH release (b) induced by high glucose (35.5 mM) were determined by MTT assay. $^{\#\#}P < 0.01$ versus NG (5.5 mM) group; $^{*}P < 0.05$, $^{**}P < 0.01$ versus HG (35.5 mM) group.

The band intensity was quantified and analyzed with Quantity One software (Bio-Rad, USA). The results were quantified by using the integrated optical density of each band with the background subtracted.

2.9. Statistical Analysis. Data were analyzed by a one-way ANOVA or independent t-test. Data are presented as mean ± S.D. averaging three or more independent experiments. Significance was noted at a $P < 0.05$.

3. Results

3.1. High Glucose Injured VECs. VEC survival was measured by MTT assay. VEC survival rates in glucose concentrations of 5.5 and 15.5 mM increased in a dose- and time-dependent manner. When the concentration was up to 25.5 mM, VEC survival rate was a little inhibited after incubatation for 48 h. However, the rate was inhibited significantly in glucose concentrations of 35.5 and 45.5 mM even in 24 h incubation. VEC morphology changed into contraction, rounded and smaller in glucose concentrations of 35.5 and 45.5 mM. Moreover, cells cultured in glucose concentrations of 35.5 mM for 48 h showed the most significant inhibition (Figure 2).

3.2. High Glucose Induced VSMC Proliferation in the Coculture Model. VECs were pretreated with a high glucose (HG) concentration (35.5 mM) for 48 h and then cocultured with VSMCs for 24 h to induce VSMC proliferation. Glucose concentration of 5.5 mM was considered as normal group. VSMCs inoculated in the upper chamber alone and stimulated with 35.5 mM glucose were set as the single cultured group. Compared with the normal group, VSMCs proliferated significantly in the cocultured group ($P < 0.01$), as well as in the single cultured group ($P < 0.05$). Compared with the single cultured group, VSMCs in the coculture group also proliferated significantly ($P < 0.05$), which suggested that injured VECs stimulated VSMCs proliferation (Figure 3). These results showed that VSMC proliferation stimulated by high glucose injured VECs was even much stronger than that stimulated directly by high glucose.

3.3. Paeonol Partially Restored Survival and Reduced LDH Release in VECs. VECs were pretreated with Pae at 7.5, 15, 30, 60, and 120 μM for 24 h prior to being stimulated by high glucose. Compared with control group, VEC survival increased in a dose- and time-dependent manner. The effect of Pae was greatest ($P < 0.01$) when VECs were pretreated with Pae at 120 μM (Figure 4(a)). Additionally, the LDH level was increased by the stimulation of 35.5 mM glucose. LDH release was gradually reduced as the Pae concentration increased. At a final concentration of 15 μM Pae, LDH release was significantly decreased ($P < 0.05$). When the concentration of Pae was 60 μM and 120 μM, the difference in LDH release was highly significant ($P < 0.01$) (Figure 4(b)).

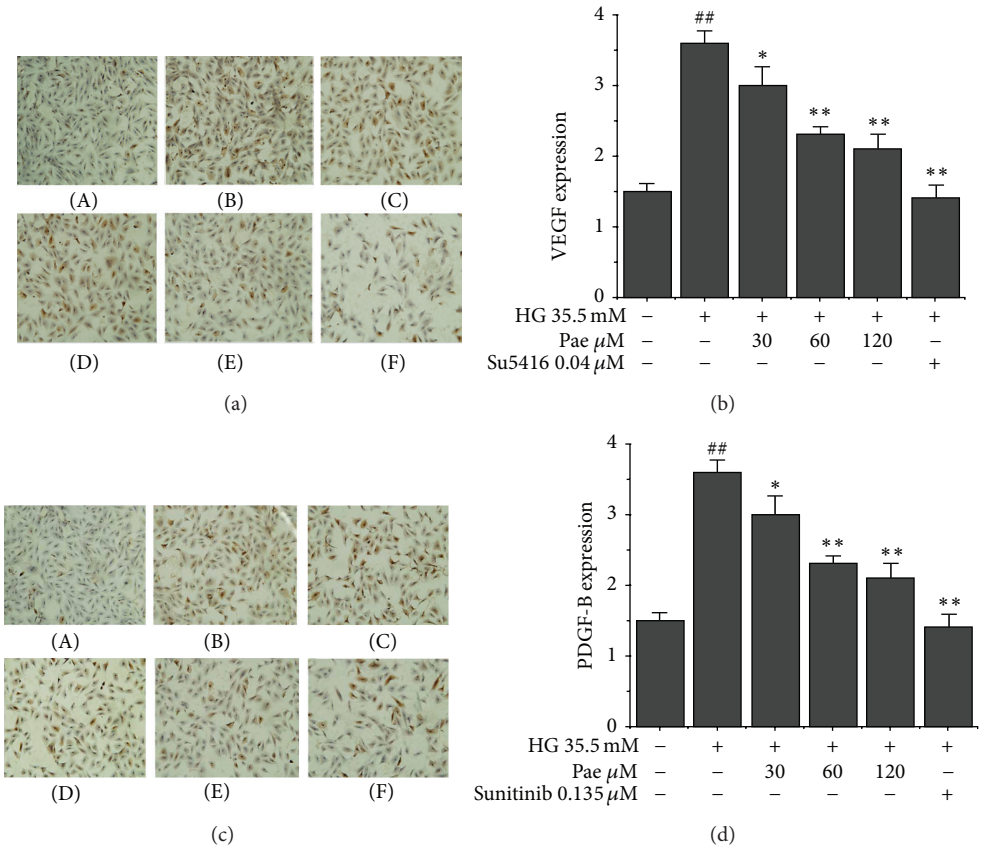

Figure 5: Effect of paeonol on VEGF and PDGF-B expression in VECs. VEGF (a and b) and PDGF-B (c and d) expression in VECs was performed through immunocytochemical staining as described in Section 2. (A) NG (5.5 mM); (B) HG (35.5 mM); (C) HG + Pae (30 μM); (D) HG + Pae (60 μM); (E) HG + Pae (120 μM); (F) HG + Sunitinib (0.135 μM). $^{\#\#}P < 0.01$ versus NG (5.5 mM) group; $^{*}P < 0.05$, $^{**}P < 0.01$ versus HG (35.5 mM) group.

3.4. Paeonol Inhibited VEGF and PDGF-B Overexpression in VECs. Through immunocytochemical staining, VEGF and PDGF-B expression were quantified inside VECs. Positive cytoplasm was brown. The positive rate of VEC was used to evaluate the effect of high glucose and Pae. High glucose resulted in increasing expression of VEGF and PDGF-B in vascular endothelial cells. The expression decreased with increasing concentrations of Pae (Figures 5(a) and 5(c)). Concentrations of 60 μM and 120 μM Pae decreased the expression of VEGF and PDGF-B significantly ($P < 0.01$). As shown in Figures 5(b) and 5(d), the VEGFR inhibitor, SU5416, not only decreased the expression of VEGF significantly ($P < 0.01$) but also decreased the number of cells with brown nuclei. The PDGFR inhibitor, Sunitinib, showed the same results. These results suggested that the proliferation of VSMC induced by high glucose may be achieved by upregulating VEGF and PDGF-B factors. And Pae reversed the effect of high glucose. Based on the results, we chose an appropriate signaling pathway to further explore how the cytokine mediates proliferation of VSMC.

3.5. Paeonol Blocked Ras-Raf-ERK1/2 Pathway in VSMCs in Coculture Model. One of the most important downstream signaling cascades of VEGF and PDGF-B is the Ras-Raf-ERK pathway [30]. To inhibit this signaling pathway initially, SU5416 and Sunitinib were used to inhibit the respective receptor and associated downstream proteins. In order to explore the cellular target of Pae, PD98059 was used to inhibit ERK1/2 protein expression. As shown in Figure 6, high glucose (35.5 mM) significantly induced the expression of Ras, P-Raf, and P-ERK1/2 in VSMCs ($P < 0.01$). Pae (120 μM) significantly inhibited the expression of Ras, P-Raf, and P-ERK1/2 ($P < 0.05$). For protein Ras and P-Raf, SU5416 and Sunitinib significantly reduced the expression ($P < 0.01$). Likewise, cells treated with SU5416, Sunitinib, or PD98059 showed significantly inhibitory effect on P-ERK1/2 expression. Moreover, the cotreatment of Pae (120 μM) with SU5416, Sunitinib, or PD98059 had a greater inhibitory effect than treating VSMCs with each individual compound. These results indicated that the effect of Pae to block Ras-Raf-ERK signaling pathway may be due to the ability to inhibit the expression of VEGF and PDGF-B.

3.6. Paeonol Inhibited VSMC Proliferation in Coculture Model. VECs were pretreated with different concentrations of

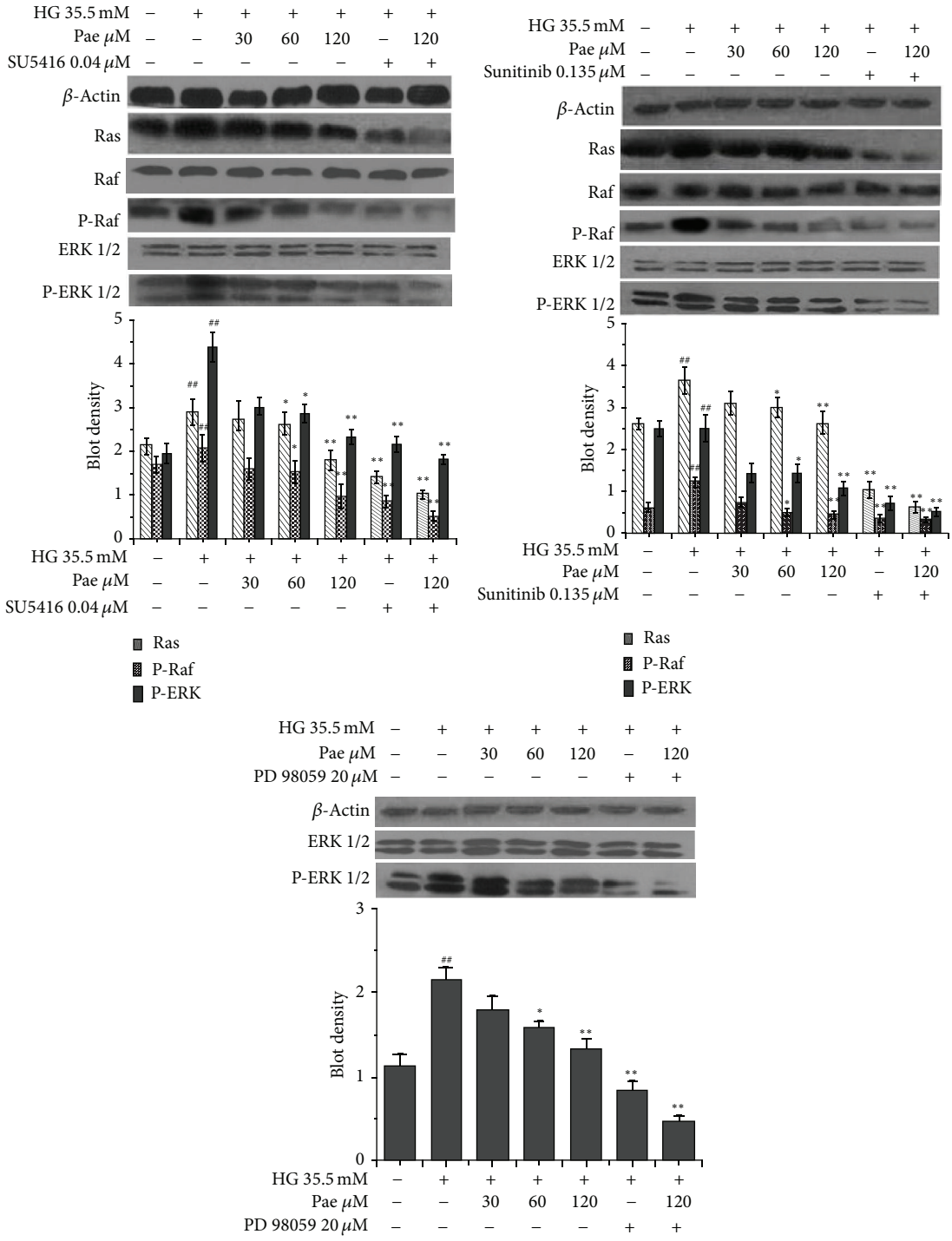

Figure 6: Effect of paeonol on Ras-Raf-ERK1/2 signaling pathway in VSMCs in the coculture model. VECs were pretreated with various concentrations of Pae for 24 h before being incubated with HG (final concentration of 35.5 mM) for another 48 h. Then VSMCs were inoculated into the top of the Transwell plate and cocultured with VECs for another 24 h. Protein concentrations were analyzed by Western blot. $^{\#\#}P < 0.01$ versus NG (5.5 mM) coculture group; $^{*}P < 0.05$, $^{**}P < 0.01$ versus HG (35.5 mM) coculture group.

Pae (30, 60, and 120 μM) before being stimulated by high glucose (35.5 mM) for 48 h. The results of MTT indicated that Pae (30, 60, and 120 μM) inhibited VSMC proliferation ($P < 0.01$) compared with high glucose group. The levels of VSMC proliferation were also inhibited with Pae plus Sunitinib or PD98059 group. The level of inhibition was greater than each single treatment group, but no significant difference was observed (Figure 7). The results proved the protective effect of Pae on VSMC proliferation which cocultured with VECs in high glucose.

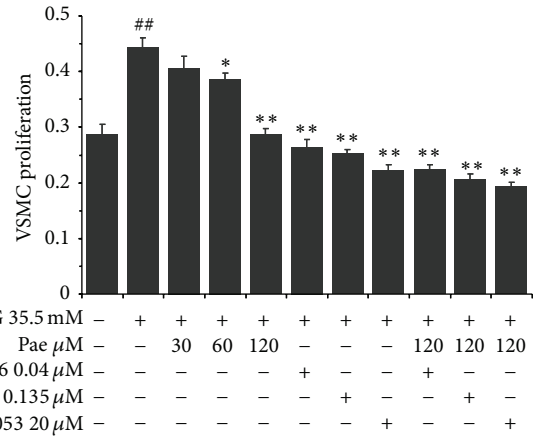

Figure 7: Effect of paeonol on VSMC proliferation in the coculture model. VECs and VSMCs cocultured model was established as described in Section 2. The effects of paeonol on VSMC proliferation were assayed by MTT. $^{\#\#}P < 0.01$ versus NG (5.5 mM) coculture group; $^{*}P < 0.05$, $^{**}P < 0.01$ versus HG (35.5 mM) coculture group.

4. Discussion

Diabetes is one of the main predisposing factors of atherosclerosis. Type 2 diabetic vascular complications are based on diabetes-induced arteriosclerosis [31]. High glucose concentrations exerted a harmful effect on VECs and VSMCs, which are important components of artery wall. Impaired VECs destroy the structure of the endothelial monolayer and lead to vascular barrier dysfunction [32]. Large numbers of damaged VECs have been shown to impact the vasodilatation function and VECs regeneration [33]. These effects may be an important mechanism of diabetic complication of AS [34]. Our present study indicated that high glucose concentrations increased membrane permeability and decreased VEC survival. VSMC proliferation and phenotypic transformation are critical pathological features of AS, which depend on growth factors, cytokines, and vasoactive substances. VEGF is the initial factor for early VEC angiogenesis and VSMC proliferation. However, a mature vascular system can not be generated alone. PDGF-B also had a strong effect on promoting inflammation in this study. Several reports support the hypothesis that PDGF-B plays a crucial role in the development of atherosclerotic plaques [35–37]. Our study demonstrated that VEGF and PDGF-B expression in VECs was increased significantly by high glucose. Treatment with Pae significantly attenuated VEGF and PDGF-B expression. Therefore, our results indicate that Pae may act against VEC injury by reducing VEGF and PDGF-B release as an anti-inflammatory and antithromboembolic effect.

Monolayer cell culture, in many cases, is difficult to simulate the interaction between various types of cells *in vivo*. Coculture model can simulate the internal *in vivo* environment to observe important interactions between cells [38]. In addition to the morphological changes, a variety of angiogenesis-related gene expression changes occur in VECs cocultured with VSMCs [39, 40]. Thus, the coculture model in this study not only retained the cellular microenvironment of material and structural basis *in vivo* but also showed the advantages of controllability and macroscopic visibility of the cell culture. The significant proliferation of VSMCs in the coculture model confirmed that damaged VECs could stimulate VSMC proliferation and also indicated that basic interaction between VECs and VSMCs can be carried out smoothly. Accordingly, the coculture model provides the necessary conditions to explore the pathogenesis of atherosclerosis.

Ras-Raf-ERK1/2 signaling pathway was activated by high glucose concentration in our coculture model. The phosphorylated proteins regulate the target gene expression which promote cell proliferation [41, 42]. Our study indicated that Pae protected the integrity and survival rate of VECs and reduced the VEGF and PDGF-B release of VECs into the cocultured model to inhibit VSMC proliferation. We also presume that the effect may relate to the downstream signaling pathway in VSMCs. For this reason, the study used the VEGFR and PDGFR inhibitor to explore the possible targets of Pae. The results showed that Pae in combination with SU5416 or Sunitinib could further reduce the Ras, P-Raf, and P-ERK1/2 expression levels. In order to further clarify whether Pae had effect on protein ERK1/2 as well, the ERK1/2 inhibitor, PD98059, was utilized. We found that ERK1/2 expression levels were reduced when treated with Pae and the inhibitor. These findings indicated that Pae may decrease the VEGF and PDGF-B expression, resulting in protecting the VEC and inhibiting the downstream signaling pathway. Otherwise, Pae may inhibit the VSMC proliferation due to the direct inhibition of Ras-Raf-ERK1/2 pathway.

Our findings confirmed that Pae can inhibit the proliferation of VSMC cocultured with VECs induced by high glucose concentration. One reason is that Pae decreased the release of inflammatory cytokines, VEGF and PDGF-B, in VECs which combined with VSMC membrane receptors and led to phosphorylation of the receptors. The inhibited receptors blocked downstream signaling pathways, Ras-Raf-ERK1/2, which are responsible for VSMC proliferation. The other is that Pae inhibited Ras-Raf-ERK1/2 activation directly to suppress VSMC proliferation. Based on our study, Pae appears to be a promising inhibitor to AS.

5. Conclusion

Taken together, our findings indicated that the mechanism of Pae effects on AS might involve its sequential inhibition of VEGF and PDGF-B in VECs and the Ras-Raf-ERK1/2 signaling pathways in VSMCs.

Conflict of Interests

The authors claim no conflict of interests involved in the study.

Acknowledgments

This work was supported by research Grants from the National Natural Science Foundation of China (81073090 and

81274134). The authors thank Dr. David J. Blake for critical reading of this paper.

References

[1] A. Didangelos, D. Simper, C. Monaco, and M. Mayr, "Proteomics of acute coronary syndromes," *Current Atherosclerosis Reports*, vol. 11, no. 3, pp. 188–195, 2009.

[2] J. C. Wang and M. Bennett, "Aging and atherosclerosis: mechanisms, functional consequences, and potential therapeutics for cellular senescence," *Circulation Research*, vol. 111, no. 2, pp. 245–259, 2012.

[3] J. A. Beckman, M. A. Creager, and P. Libby, "Diabetes and atherosclerosis epidemiology, pathophysiology, and management," *Journal of the American Medical Association*, vol. 287, no. 19, pp. 2570–2581, 2002.

[4] L. Piconi, L. Quagliaro, R. Assaloni et al., "Constant and intermittent high glucose enhances endothelial cell apoptosis through mitochondrial superoxide overproduction," *Diabetes/Metabolism Research and Reviews*, vol. 22, no. 3, pp. 198–203, 2006.

[5] S. M. Baumgartner-Parzer, L. Wagner, M. Pettermann, J. Grillari, A. Gessl, and W. Waldhausl, "High-glucose-triggered apoptosis in cultured endothelial cells," *Diabetes*, vol. 44, no. 11, pp. 1323–1327, 1995.

[6] S. Stintzing, M. Ocker, A. Hartner, K. Amann, L. Barbera, and D. Neureiter, "Differentiation patterning of vascular smooth muscle cells (VSMC) in atherosclerosis," *Virchows Archiv*, vol. 455, no. 2, pp. 171–185, 2009.

[7] A. R. Keramati, R. Singh, A. Lin et al., "Wild-type LRP6 inhibits, whereas atherosclerosis-linked LRP6R611C increases PDGF-dependent vascular smooth muscle cell proliferation," *Proceedings of the National Academy of Sciences of the United States of America*, vol. 108, no. 5, pp. 1914–1918, 2011.

[8] K. Sternberg, M. Gratz, K. Koeck et al., "Magnesium used in bioabsorbable stents controls smooth muscle cell proliferation and stimulates endothelial cells in vitro," *Journal of Biomedical Materials Research B, Applied Biomaterials*, vol. 100, no. 1, pp. 41–50, 2012.

[9] C. Qin and Z. Liu, "In atherogenesis, the apoptosis of endothelial cell itself could directly induce over-proliferation of smooth muscle cells," *Medical Hypotheses*, vol. 68, no. 2, pp. 275–277, 2007.

[10] T. P. Garrington and G. L. Johnson, "Organization and regulation of mitogen-activated protein kinase signaling pathways," *Current Opinion in Cell Biology*, vol. 11, no. 2, pp. 211–218, 1999.

[11] J. Huang, L.-S. Li, D.-L. Yang, Q.-H. Gong, J. Deng, and X.-N. Huang, "Inhibitory effect of ginsenoside Rg1 on vascular smooth muscle cell proliferation induced by PDGF-BB is involved in nitric oxide formation," *Evidence-Based Complementary and Alternative Medicine*, vol. 2012, Article ID 314395, 12 pages, 2012.

[12] L. Labrecque, S. Lamy, A. Chapus et al., "Combined inhibition of PDGF and VEGF receptors by ellagic acid, a dietary-derived phenolic compound," *Carcinogenesis*, vol. 26, no. 4, pp. 821–826, 2005.

[13] H. Shimizu, Y. Nakagawa, C. Murakami, N. Aoki, S. Kim-Mitsuyama, and H. Miyazaki, "Protein tyrosine phosphatase PTPεM negatively regulates PDGF β-receptor signaling induced by high glucose and PDGF in vascular smooth muscle cells," *The American Journal of Physiology—Cell Physiology*, vol. 299, no. 5, pp. C1144–C1152, 2010.

[14] M. Kernt, A. S. Neubauer, R. G. Liegl et al., "Sorafenib prevents human retinal pigment epithelium cells from light-induced overexpression of VEGF, PDGF and PlGF," *The British Journal of Ophthalmology*, vol. 94, no. 11, pp. 1533–1539, 2010.

[15] J. Ortmann, M. Veit, S. Zingg et al., "Estrogen receptor-α but not -β or GPER inhibits high glucose-induced human VSMC proliferation: potential role of ROS and ERK," *Journal of Clinical Endocrinology and Metabolism*, vol. 96, no. 1, pp. 220–228, 2011.

[16] M. G. Sirois, M. Simons, and E. R. Edelman, "Antisense oligonucleotide inhibition of PDGFR-β receptor subunit expression directs suppression of intimal thickening," *Circulation*, vol. 95, no. 3, pp. 669–676, 1997.

[17] W. Lederle, N. Linde, J. Heusel et al., "Platelet-derived growth factor-B normalizes micromorphology and vessel function in vascular endothelial growth factor-A-induced squamous cell carcinomas," *The American Journal of Pathology*, vol. 176, no. 2, pp. 981–994, 2010.

[18] S. M. Wilhelm, L. Adnane, P. Newell, A. Villanueva, J. M. Llovet, and M. Lynch, "Preclinical overview of sorafenib, a multikinase inhibitor that targets both Raf and VEGF and PDGF receptor tyrosine kinase signaling," *Molecular Cancer Therapeutics*, vol. 7, no. 10, pp. 3129–3140, 2008.

[19] A. Das, U. Shergill, L. Thakur et al., "Ephrin B2/EphB4 pathway in hepatic stellate cells stimulates Erk-dependent VEGF production and sinusoidal endothelial cell recruitment," *The American Journal of Physiology—Gastrointestinal and Liver Physiology*, vol. 298, no. 6, pp. G908–G915, 2010.

[20] S. Satofuka, A. Ichihara, N. Nagai et al., "(Pro)renin receptor-mediated signal transduction and tissue renin-angiotensin system contribute to diabetes-induced retinal inflammation," *Diabetes*, vol. 58, no. 7, pp. 1625–1633, 2009.

[21] H. Li, M. Dai, and W. Jia, "Paeonol attenuates high-fat-diet-induced atherosclerosis in rabbits by anti-inflammatory activity," *Planta Medica*, vol. 75, no. 1, pp. 7–11, 2009.

[22] J. Hu, Y.-L. Li, Z.-L. Li et al., "Chronic supplementation of paeonol combined with danshensu for the improvement of vascular reactivity in the cerebral basilar artery of diabetic rats," *International Journal of Molecular Sciences*, vol. 13, no. 11, pp. 14565–14578, 2012.

[23] M. Dai, Q. Y. Liu, C. G. Gu, and H. Y. Zhang, "Inhibitory effect of paeonol on lipid peroxidational reaction and oxidational decorate of low density lipoprotein," *China Journal of Chinese Materia Medica*, vol. 25, no. 10, pp. 625–627, 2000.

[24] M. Dai, X. Zhi, D. Peng, and Q. Liu, "Inhibitory effect of paeonol on experimental atherosclerosis in quails," *China Journal of Chinese Materia Medica*, vol. 24, no. 8, pp. 488–512, 1999.

[25] Y.-Q. Wang, M. Dai, J.-C. Zhong, and D.-K. Yin, "Paeonol inhibits oxidized low density lipoprotein-induced monocyte adhesion to vascular endothelial cells by inhibiting the mitogen activated protein kinase pathway," *Biological and Pharmaceutical Bulletin*, vol. 35, no. 5, pp. 767–772, 2012.

[26] L.-L. Pan, M. Dai, and W. Wang, "A new method for culturing endothelial cells from the rat aorta," *Chinese Pharmacological Bulletin*, vol. 23, no. 3, pp. 410–413, 2007.

[27] W. Wang, M. Dai, and L.-L. Pan, "A new method for culturing vascular smooth muscle cells from the rabbit aorta," *Chinese Pharmacological Bulletin*, vol. 24, no. 11, pp. 1534–1537, 2008.

[28] M. F. Fillinger, L. N. Sampson, J. L. Cronenwett, R. J. Powell, and R. J. Wagner, "Coculture of endothelial cells and smooth muscle cells in bilayer and conditioned media models," *Journal of Surgical Research*, vol. 67, no. 2, pp. 169–178, 1997.

[29] N. S. Roy, C. Cleren, S. K. Singh, L. Yang, M. F. Beal, and S. A. Goldman, "Functional engraftment of human ES cell-derived dopaminergic neurons enriched by coculture with telomerase-immortalized midbrain astrocytes," *Nature Medicine*, vol. 12, no. 11, pp. 1259–1268, 2006.

[30] H. Zhang, X. Jia, F. Han et al., "Dual-delivery of VEGF and PDGF by double-layered electrospun membranes for blood vessel regeneration," *Biomaterials*, vol. 34, no. 9, pp. 2202–2212, 2013.

[31] J. A. Beckman, F. Paneni, F. Cosentino, and J. A. Beckman, "Diabetes and vascular disease: pathophysiology, clinical consequences, and medical therapy: part II," *European Heart Journal*, vol. 108, no. 13, pp. 1527–1532, 2013.

[32] E. Stoyanova, M. Trudel, H. Felfly, W. Lemsaddek, D. Garcia, and G. Cloutier, "Vascular endothelial dysfunction in β-Thalassemia occurs despite increased eNOS expression and preserved vascular smooth muscle cell reactivity to NO," *PLoS ONE*, vol. 7, no. 6, Article ID e38089, 2012.

[33] J. S. Petrofsky, "The effect of type-2-diabetes-related vascular endothelial dysfunction on skin physiology and activities of daily living," *Journal of Diabetes Science Technology*, vol. 5, no. 3, pp. 657–667, 2011.

[34] S. Sartini, S. Cosconati, L. Marinelli et al., "Benzofuroxane derivatives as multi-effective agents for the treatment of cardiovascular diabetic complications. Synthesis, functional evaluation, and molecular modeling studies," *Journal of Medicinal Chemistry*, vol. 55, no. 23, pp. 10523–10531, 2012.

[35] J. Homsi and A. I. Daud, "Spectrum of activity and mechanism of action of VEGF/PDGF inhibitors," *Cancer Control*, vol. 14, no. 3, pp. 285–294, 2007.

[36] C. Ionescu, I. Berindan-Neagoe, C. Burz et al., "The clinical implications of platelet derived growth factor B, vascular endothelial growth factor and basic fibroblast growth factor in colorectal cancer," *Journal of Buon*, vol. 16, no. 2, pp. 274–276, 2011.

[37] N. Liu, J.-T. Liu, Y.-Y. Ji, and P.-P. Lu, "Effects and mechanisms of the functional parts of Dahuang Zhechong Pill containing serum on platelet-derived growth factor-stimulated proliferation of vascular smooth muscle cells," *Chinese Journal of Integrative Medicine*, vol. 19, no. 6, pp. 432–438, 2013.

[38] D. Ge, N. Meng, L. Su et al., "Human vascular endothelial cells reduce sphingosylphosphorylcholine-induced smooth muscle cell contraction in co-culture system through integrin B4 and Fyn," *Acta Pharmacologica Sinica*, vol. 33, no. 1, pp. 57–65, 2012.

[39] C. S. Wallace, J. C. Champion, and G. A. Truskey, "Adhesion and function of human endothelial cells co-cultured on smooth muscle cells," *Annals of Biomedical Engineering*, vol. 35, no. 3, pp. 375–386, 2007.

[40] T. Korff, S. Kimmina, G. Martiny-Baron, and H. G. Augustin, "Blood vessel maturation in a 3-dimensional spheroidal coculture model: direct contact with smooth muscle cells regulates endothelial cell quiescence and abrogates VEGF responsiveness," *The FASEB Journal*, vol. 15, no. 2, pp. 447–457, 2001.

[41] L.-M. Zhao, L.-J. Ma, L.-X. Zhang, and J.-Z. Wu, "Shenmai injection inhibiting the extracellular signal regulated kinase-induced human airway smooth muscle proliferation in asthma," *Chinese Journal of Integrative Medicine*, vol. 16, no. 4, pp. 331–336, 2010.

[42] Y. Mebratu and Y. Tesfaigzi, "How ERK1/2 activation controls cell proliferation and cell death is subcellular localization the answer?" *Cell Cycle*, vol. 8, no. 8, pp. 1168–1175, 2009.